2021

# ESTIMATING WOLF PREDATION METRICS, PATTERNS, AND DYNAMICS ACROSS TIME AND SPACE IN THE MULTI-PREY SYSTEM OF YELLOWSTONE NATIONAL PARK

Matthew Caldwell Metz

## Recommended Citation

Metz, Matthew Caldwell, "ESTIMATING WOLF PREDATION METRICS, PATTERNS, AND DYNAMICS ACROSS TIME AND SPACE IN THE MULTI-PREY SYSTEM OF YELLOWSTONE NATIONAL PARK" (2021). *Graduate Student Theses, Dissertations, & Professional Papers*. 11842.
https://scholarworks.umt.edu/etd/11842

# ESTIMATING WOLF PREDATION METRICS, PATTERNS, AND DYNAMICS ACROSS TIME AND SPACE IN THE MULTI-PREY SYSTEM OF YELLOWSTONE NATIONAL PARK

By

MATTHEW CALDWELL METZ

M.S., Michigan Technological University, Houghton, Michigan, 2010
B.S., University of Montana, Missoula, Montana, 2001

Dissertation

presented in partial fulfillment of the requirements
for the degree of

Doctor of Philosophy
in Fish and Wildlife Biology

The University of Montana
Missoula, MT

December 2021

Approved by:

Scott Whittenburg,
Graduate School Dean

Dr. Mark Hebblewhite, Chair
Department of Ecosystem and Conservation Science, Wildlife Biology Program

Dr. Douglas W. Smith
Department of Ecosystem and Conservation Science, Wildlife Biology Program

Dr. Angela D. Luis
Department of Ecosystem and Conservation Science, Wildlife Biology Program

Dr. Paul M. Lukacs
Department of Ecosystem and Conservation Science, Wildlife Biology Program

Dr. Douglas J. Emlen
Division of Biological Sciences

*Metz, Matthew, Ph.D., Fall 2021* *Fish and Wildlife Biology*

Estimating wolf predation metrics, patterns, and dynamics across time and space in the multi-prey system of Yellowstone National Park

Chairperson: Mark Hebblewhite

Predation is a fundamental driver in ecology, structuring ecosystems across the globe. However, understanding the effects of large carnivore predation is limited by both the observation process and the shorter duration of many studies. I used data from 23 years in Yellowstone National Park to disentangle both the importance of wolf predation on prey, and the imperfect observation process of studying predation. I first used field observations to test whether a sexually-selected trait, antlers in male elk, deterred wolf predation. I found that antlers reduced predation risk, emphasizing the selective nature of predation. Next, I used GPS data and ground-based observations to develop wolf sightability models to understand the nature of wolf sightings. I found forest cover, distance from road, topography, and wolf group size affected the probability of observing wolves. Next, I leveraged my sightability model to develop a Bayesian mark-recapture abundance model that estimated the number of ungulates fed on by wolf packs during study sessions. I built a model for carcass detection by ground-based observation, aerial-based observation, and GPS cluster searches. Overlooking all details, field methods found only 47% of the estimated occasions when wolf packs fed on ungulates. Using these detection-corrected estimates to evaluate how six wolf predation metrics differed through time as elk declined and stabilized and bison increased, I found that wolf predation on elk generally declined concurrent with the elk decline. I also found that wolf diet (niche) breadth expanded over time primarily by scavenging bison. Though generalizing was challenging, using the simple metric of predation rate, I found predation rate was inversely density dependent in winter on just the wintering elk population within northern Yellowstone National Park. However, wolf predation was conversely a stabilizing force when considering annual predation rate on the entire northern Yellowstone elk population. These observations are consistent with wolves acting as a stabilizing, regulating force on the northern Yellowstone elk population. Finally, I built theoretical models guided by my observations of the wolf-elk-bison system in northern Yellowstone to evaluate how scavenging affects predator-prey dynamics. I found that including scavenging fundamentally changes dynamics, generally increasing prey and predator populations.

## ACKNOWLEDGEMENTS

I begin my Acknowledgements by thanking the wolf population that has been radiomarked and studied as a part of my dissertation. I also acknowledge the special land where Yellowstone National Park now sits for providing a home to these and other animals. And I thank the people who have cared for this land, most significant of which are the at least 27 American Indian Tribes with connections to this land, including prior to its designation as a National Park.

My dissertation would not have been possible without the financial support from the Yellowstone Wolf Project (through Yellowstone Forever). Funders through this avenue included Valerie Gates, Annie and Bob Graham (Tapeats Fund), Frank and Kay Yeager, and many individual donors. This funding supported the majority of my dissertation and for that I am deeply grateful. I am also appreciative for the generous financial support provided through the Wesley M. Dixon Graduate Fellowship, Montana Institute on Ecosystems Graduate Enhancement Fellowship, Bertha Morton Scholarship (x2), Program of National Distinction Travel Award, and Zuuring/MAGIP Graduate GIS Scholarship.

Moreover, my dissertation research was fundamentally supported through the fieldwork of the Yellowstone Wolf Project. Funding for this program was also awarded through National Science Foundation (NSF) Long Term Research in Environmental Biology grants DEB-0613730 and DEB-1245373. I am also grateful for this funding.

At the University of Montana, I thank Jeanne Franz, Wendy Maltonic, and Taylor Haas for administrative support. For myself personally, it was special to be among the final couple students to who Jeanne administered comprehensive exams given that I had also frequented Jeanne’s office many years prior as an undergraduate student. Additionally, I thank Dr. Chad Bishop for his leadership of the Wildlife Biology Program.

I am eternally grateful for the support, wisdom, guidance, and friendship provided by my advisor, Dr. Mark Hebblewhite. Mark’s enthusiasm for conservation and his commitment to impactful science are inspiring. Equally inspiring is Mark’s passion to mentor. Mark says the best part about his job is working with his students, and there is no doubt that he means it. He even does it in the field sometimes, all while also being a fantastic role model as someone who balances the demands of academia with having a family. Relatedly, I am equally as grateful to Emily (Mark's wife) and his children for sharing the demands of Mark’s time with his students. I am also thankful to have had the chance to work and learn from Emily while developing the figures for my second chapter. It has been an honor to be your student Mark. Thanks for being a great mentor and friend, and for caring equally about your students, including myself, as people.

I was fortunate to also have Dr. Doug Smith as a committee-member plus. Thank you Doug as well for your support, wisdom, guidance, and friendship. When I finished my undergraduate degree twenty years ago, my dream position would have been fairly close to what I have done for the last two decades. What I did not know then, but know now, is that the person who leads the Yellowstone Wolf Project is superior to the science that comes out of it – which is saying quite a lot. Thank you Doug for your friendship, mentorship, and commitment to me. Thank you as well for your commitment and support to all of the other people who are fortunate to work with you and benefit from your leadership and management of the research in Yellowstone. It has been my great honor to work with and learn from you for two decades now.

I also thank the remainder of my committee: Dr. Doug Emlen, Dr. Angela Luis, and Dr. Paul Lukacs. At every turn, they each made themselves available to me as soon as they could. And their support and patience for me were unrelenting. I had the pleasure to work closely with each of these three committee members on at least one chapter, which I am especially grateful for. This provided me the opportunity to learn from each of them in unique ways, of which I just want to highlight a simple one. To Doug, I am grateful for learning how to better tell interesting stories in science (and will hope that another paper in my career excites me to write as much as the one we worked on together). To Paul, I am grateful for an improved ability to simplify problems to the parts that matter. To Angie, I am grateful for developing tools to mechanistically address complex scientific interactions.

To my entire committee, thank you for all the ways in that you improved me as an ecologist and as a person, and for caring about my well-being and development. I very much value the relationship I developed or furthered with each of you. For all of these reasons, I am beyond grateful to my advisor and committee.

I take great pleasure in thanking each of my lab mates. My PhD went a little longer than expected but the accompanying benefit was that I will likely lay claim to the most people to have been active lab mates with in the Heb lab. I thank Colby Anton, Ellen Brandell, Brenna Cassidy, T.J. Clark, Gabrielle Coulombe, Daniel Eacker, Libby Ehlers, Mateen Hessami, Mark Hurley, Andrew Jakes, Clayton Lamb, Hans Martin, Connor Meyer, Tara Meyer, Eric Palm, Wibke Peters, Derek Spitz, Robin Steenweg, Jeremy SunderRaj, Tshering Tempa, Scott Waller, Sara Williams, and Wenhong Xiao. I was fortunate to learn and develop friendships with the entire lab, and for that I am very grateful. I am even grateful for Zoom furthering my communication with the lab while living a few hours away. I also specifically thank Sara and T.J., each of whose expertise I benefited from in a manner in which we could also collaborate together in support of my dissertation. I also thank Colby for lending his Bayesian expertise to me on a few occasions prior to when he joined the lab.

From my time in Missoula, I thank current and former members of the nearby Lukacs lab. Thank you to Josh Nowak, Sara Williams, Anna Moeller, Jenny Helm, Charlie Henderson, and Molly McDevitt for occasional whiteboard chats and/or a bit of sanity. Josh, in particular, thank you for lending your knowledge in support of myself and numerous other graduate students at the University of Montana.

Additionally, I thank Libby, Nick, Bechler, and Taela Ehlers and Jim Napoli for kindly putting me up on numerous work trips to Missoula.

I thank with the deepest gratitude my coworkers at the Yellowstone Wolf Project. First, to my coworkers of at least fifteen years, Dan Stahler, Erin Stahler, and Kira Cassidy. Thank you for your leadership, insights, and commitment to the research we do in Yellowstone. The work that was accomplished during my dissertation could have not been done without each of your contributions. It is an honor to work with each of you. Additionally, I thank you Kira for providing various graphics for my dissertation. I have also been fortunate to work with a number of other individuals throughout my PhD, many of who directly supported my dissertation work. Here, I acknowledge the amazing contribution of the hundreds of individuals who I have worked with. I especially thank the amazing skills of Lisa Koitzsch, Ky Koitzsch, Quinn Harrison, Connor Meyer, Jack Rabe, Nikki Tatton, Brenna Cassidy, Rebecca Thomas-Kuzilik, Rick McIntyre, Jeremy SunderRaj, Maddy Jackson, Elise Loggers, Wes Binder, Ellen Brandell, and Elizabeth Cato, each of who were year-round employees during my PhD. Many of you managed significant components of the GPS cluster field work that was the backbone of much of my dissertation work, and your contribution is very much appreciated. The dedication of each of you cannot be overstated. Perhaps the greatest strength of the Yellowstone Wolf Project is the field work that each of you, and literally hundreds of other beyond dedicated individuals, are the driving force behind. I thank this amazing team for their work and am appreciative of the opportunities to have spent time in the field with many of you. Those field days were great fun, and also provided many wonderful conversations that strengthened my dissertation.

I thank Tom Drummer (deceased) for his vision and efforts in developing the double-count estimator with Doug. Their insights led to the evolution of the triple-count model that was the foundation of much of my dissertation and Tom's efforts here were critical.

At Yellowstone National Park, I thank P.J. White for his leadership and support, and also Chris Geremia for sharing inspiring conversations and data. I also thank key collaborators at (or formerly at) Utah State University, Dan MacNulty, Michel Kohl, and Aimee Tallian – each of who I got to extensively learn from while working on papers or just conversing. I also thank Brian Smith at Utah State University for sharing the snow data that I used in Chapter 4.

I next generally thank my family and friends who have supported me on this journey, and also to specifically thank a few groups of people. First, I thank close friends Brian, Marnie, Jackson, and Brenden Lancz who provided support for my family in various ways throughout my dissertation. Next, I thank our immediate families – Brian, Beverly, Cortlyne, and Ian Jones and Adam, Christina, Landon, and Miles Metz for support and laughs along the way. We certainly would not have kept our sanity without the support of our parents, Wayne and Cindy Jones and Howard and Emily Metz. Thank you for your unending encouragement and support, and babysitting! Additionally, I would be remiss to not specifically thank my parents for their support and encouragement, along with lots of patience, for me to follow my dreams and passions. I would have not taken this path to completing my PhD without that encouragement. Thank you.

Finally, I end with thanking my family – my wife Jenny, our son Mason, and our dog Ripple. I would not have wanted to take this journey with anyone else. It has been quite a journey – to think Jenny, we got married during this PhD. It has been an amazing six years of marriage so far, with many years together prior, and I look forward to having my PhD in the rearview mirror and continuing on new journeys – maybe even find the time to travel. Thank you for all your support along the way, even occasionally tolerating drawings on the whiteboard. And of course, our life at the beginning of my PhD did not include Mason. Mason, thank you for teaching me about the most important things in life. Being your Dad is simply the best part of my life. The best things I read during my PhD were definitely all board books! And even when I put on my Bose headphones (thanks Bose!) and turned up the Dead as loud as possible, it was not because I didn't want to hear you, it was so that I could be done and we could hang some more. I am happy to now be able to do that with my family.

### A note on authorship

Throughout my dissertation, I use the pronoun "we" to recognize the contribution of my coauthors and, moreover, to recognize the critical role of additional collaborators, coworkers, and field technicians who collected the associated data for nearly three decades.

# TABLE OF CONTENTS

# Chapter 1: Dissertation overview and introduction

Predation is simply one of the strongest forces in all of nature, shaping key ecological and evolutionary characteristics of organisms of all sizes across the globe (Darwin 1859). The presence and effects of predators are well appreciated to structure ecosystems, and conversely, their absence can lead to very different ecosystem states (Taylor 1984, Estes et al. 2011). Theory tells us, however, that predators sometimes have minimal impacts on prey, and in other cases, can exert strong reductions in prey abundance (Messier 1995). Matching theory with empirical data is often challenging. Thus, it is a bit unsatisfying that relatively little is often understood about how predators affect their prey, and therefore, structure ecosystems. This is especially true for large carnivores that hunt long-lived ungulates and range widely because of the difficulty of studying such secretive, wary, and wide-ranging mammals. Nonetheless, it is expected that the basic theoretical relationships should also drive predator-prey dynamics.

How predation is expected to drive predator-prey dynamics is rooted in the work of Solomon (1949) and Holling (1959), each of who further developed the ideas of how predation was density dependent. Holling (1959) provided perhaps the most significant advance to determining the effect of predation through unifying the density-dependent responses of the rate that predators kill prey (functional response) and predator abundance given prey abundance (numerical response) into the total predation rate, the proportion of the prey population removed through predation. These ideas were moved forward by future work (Sinclair 1989, Messier 1994, 1995) that evaluated how the product of various functional and numerical responses combined to form different predation rates that had different theoretical effects on whether predators regulated prey dynamics and also stabilized the predator-prey system. Messier (1994) used an empirical example of wolves preying on moose and found close correspondence to theoretical predictions from single prey, single predator models. Since that work, relatively little focus has existed for estimating predation rate for large carnivores, with the notable exceptions of work such as long-term studies on Isle Royale, Banff, and Yellowstone (Vucetich et al. 2011). In my dissertation I expand on that work while also considering various influences of prey vulnerability and the observation process.

My dissertation is well positioned to test classic predator-prey theory using the data collected about wolf-prey relationships in Yellowstone National Park (YNP). The predator-prey dynamics of this system have been historically well studied since the 1995 reintroduction of wolves. Indeed, one of the motivating ecological reasons to reintroduce wolves to Yellowstone was the restoration of the ecological process of predation by wolves on the intensely debated overabundant ungulate population (Huff and Varley 1999). Prior to reintroduction, the National Park Service conducted an Environmental Impact Statement (EIS) consisting of three different sets of predator-prey models to evaluate the potential impact of wolves on prey, especially elk, in YNP (Varley and Brewster 1992). Immediately prior to wolf reintroduction, leading predator-prey biologists presented advice to the NPS on how to monitor wolves and their prey to help advance predator-prey theory (Messier et al. 1995). Though there have been several studies to revisit these EIS predictions (Varley and Boyce 2006), none have done so using the long-term, empirical predator-prey data collected from the wolf population perspective following the recommendations of Messier et al. (1995). In my dissertation, I use data collected through both observation and global positioning system (GPS) radiocollars to test ideas related to why predators kill certain prey and how inferences may be affected by limitations in the observation process itself.

In Chapter 2, I test a long-held but rarely tested hypothesis of whether a sexually-selected weapon, antlers in male elk, affects predation dynamics. In this case, the antlers of cervids are unique in that many individuals, i.e., across species and individuals within populations, retain them long after their primary use during reproductive periods. Here, I used data collected from observations of wolf-elk encounters and the characteristics of both living and dead male elk to test whether benefits associated with antlers being a predatory deterrent may help explain why male elk retain their antlers for as many as six months following the reproductive period of elk. I primarily used measures of preference and binomial models to evaluate this question. I found evidence that antlers are indeed a strong predatory deterrent, and that the benefits of retaining them is one reason why individuals may keep them. The twist was that healthy individuals were the first to shed their antlers, thus both increasing their predation risk and chances for reproductive success. This work advanced understanding of how factors such as prey vulnerability might affect predator-prey dynamics.

In Chapter 3, I next developed sightability models to help inform management and development of my estimator of feeding events that depended on imperfect observations of predation in YNP. That is, the questions that I asked in Chapter 2 were largely dependent on observations from the field, observations that are influential in a wide variety of research questions about wolves in YNP. In Chapter 3, I leveraged many years of wolf GPS data and continuous observations and evaluated the factors that affected wolf sightability. I did so in a used-unused framework using binomial models and predicted wolf sightability over the ~1,000 $km^2$ of northern Yellowstone National Park. I showed that predictable factors such as forest cover, distance, and viewshed affected whether wolf groups were successfully observed, also finding that the probability of successful observation was affected by group size. In Chapter 3, I also developed covariates, such as viewshed, that were critical to Chapter 4.

In Chapter 4, I ultimately assessed the density-dependent nature of wolf predation metrics in Yellowstone using 23 years of data. However, building on results from Chapter 3 emphasizing the imperfect nature of wolf observations, I first developed a Bayesian abundance model(s) to estimate the number of ungulates that wolf packs fed on. I did so for 349 study sessions for wolf packs during the winter, along with 20 others during the summer. For example, during the winter, I estimated abundance through independent detections by ground observation, air observation, and GPS cluster searches. These methods were employed for wolf packs in a number of different combinations, and thus my estimator also incorporated whether a carcass was even available to be detected by each method. I successfully created this framework and then estimated the abundance of wolf feeding events. I then turned these estimates into those specific to species to test how wolf predation metrics have changed across time, concurrent to numerical changes in the elk and bison populations. Here, I developed a series of analyses that tested whether predation metrics changed through time, because time was a superior metric to anchor my analyses given the strong correlation between elk and bison abundance. My results in Chapter 4 indicated that predation metrics did change with time as expected by density-dependent predictions, but not consistently. Other results in the chapter suggest that wolves might not always exert a stabilizing impact on elk (especially) because of the influence of prey vulnerability and spatial structure in the prey population. Moreover, we also found significant evidence that the Yellowstone wolf-prey system had moved strongly away from being defined as a wolf-elk system, and is now best defined as a wolf-elk-bison system. But the bison component of wolf diet was largely acquired through facultative scavenging by wolves. Here, we ultimately found evidence that wolf predation, as indicated by predation rate, was destabilizing to winter elk dynamics, yet also a regulating, stabilizing factor when considering annual elk population dynamics. Combined, this work is consistent with the notion that wolf predation is at least helping regulate elk around a lower density stable equilibrium of about 10,000 elk in Northern YNP. However, one challenging part of Chapter 4 was the inability to fully evaluate the effects of wolf predation via classical approaches such as estimation of functional responses because of the correlation in elk and bison abundances, which I overcame in Chapter 5.

In Chapter 5, I developed dynamical mathematical models for a theoretical system that overcame the challenge associated with correlated elk and bison abundances in classic predator-prey models. I used these mathematical models of predator-prey dynamics to evaluate how scavenging affected the abundance and stability properties of a predator-prey system. I modeled this system using parameters that I largely estimated through data collected in northern YNP, and used my results from Chapter 4 to guide how I modeled the system. In Chapter 5, I found that scavenging generally tended to promote increased abundance in primary prey, while also increasing aspects of stability. These results support recent findings about the importance of scavenging, and highlight how scavenging may be the critical piece affecting wolf-elk dynamics in northern YNP, given the shifting predator-prey dynamics over time that I observed in Chapter 4.

## LITERATURE CITED

Darwin, C. 1859. On the origins of species by means of natural selection. John Murray, London.

Estes, J. A., J. Terborgh, J. S. Brashares, M. E. Power, J. Berger, W. J. Bond, S. R. Carpenter, T. E. Essington, R. D. Holt, J. B. C. Jackson, R. J. Marquis, L. Oksanen, T. Oksanen, R. T. Paine, E. K. Pikitch, W. J. Ripple, S. A. Sandin, M. Scheffer, T. W. Schoener, J. B. Shurin, A. R. E. Sinclair, M. E. Soule, R. Virtanen, and D. A. Wardle. 2011. Trophic downgrading of planet Earth. Science **333**:301-306.

Holling, C. S. 1959. The components of predation as revealed by a study of small-mammal predation of the European pine sawfly. The Canadian Entomologist **91**:293-320.

Huff, D. E., and J. D. Varley. 1999. Natural regulation in Yellowstone National Park's northern range. Ecological Applications **9**:17-29.

Messier, F. 1994. Ungulate population models with predation: a case study with the North American moose. Ecology **75**:478-488.

Messier, F. 1995. On the functional and numerical responses of wolves to changing prey density. Pages 187-198 *in* L. N. Carbyn, S. H. Fritts, and D. R. Seip, editors. Ecology and conservation of wolves in a changing world. Canadian Circumpolar Institute, Edmonton, Alberta.

Messier, F., W. C. Gasaway, and R. O. Peterson. 1995. Wolf-ungulate interactions in the Northern Range of Yellowstone: Hypotheses, research priorities, and methodologies. Fort Collins, CO.

Sinclair, A. R. E. 1989. Population regulation in animals. Pages 197–241 *in* J. Cherrett, editor. Ecological Concepts: The Contribution of Ecology to an Understanding of the Natural World. Blackwell, Melbourne.

Solomon, M. 1949. The natural control of animal populations. The Journal of Animal Ecology **18**:1-35.

Taylor, R. J. 1984. Predation. Springer, New York.

Varley, J. D., and W. G. Brewster. 1992. Wolves for Yellowstone? A report to the United States Congress. Volume IV Research and Analysis. National Park Service, Yellowstone National Park, WY.

Varley, N., and M. S. Boyce. 2006. Adaptive management for reintroductions: updating a wolf recovery model for Yellowstone National Park. Ecological Modelling **193**:315-339.

Vucetich, J. A., M. Hebblewhite, D. W. Smith, and R. O. Peterson. 2011. Predicting prey population dynamics from kill rate, predation rate and predator–prey ratios in three wolf-ungulate systems. Journal of Animal Ecology **80**:1236-1245.

## Chapter 2: Predation shapes the evolutionary traits of cervid weapons[1]

### ABSTRACT

Sexually-selected weapons evolved to maximize individual reproductive success of males in many polygynous breeding species. Many weapons are also retained outside of reproductive periods for secondary reasons, but the importance of these secondary functions is poorly understood. Here we leveraged a unique opportunity from the predator-prey system in northern Yellowstone National Park, USA to evaluate whether predation by a widespread, coursing predator (wolves) has influenced a specific weapon trait (antler retention time) in their primary cervid prey (elk). Male elk face a tradeoff: individuals casting antlers early begin regrowth before other males, resulting in relatively larger antlers in the following year, and thus greater reproductive success, as indicated by research with red deer. We show, however, that male elk that cast their antlers early are preferentially hunted and killed by wolves, despite early casters being in better nutritional condition than antlered individuals. Our results run counter to classic expectations of coursing predators preferring poorer-conditioned individuals, and in so doing, reveal a significant secondary function for an exaggerated sexually-selected weapon, predatory deterrence. We suggest this secondary function played a key evolutionary role in elk, uniquely among North American cervids, retaining their antlers long after they fulfill their primary role in reproduction.

### INTRODUCTION

---

[1] Paper published (and formatted as) as: Metz, M.C., D.J. Emlen, D.W. Smith, D.R. MacNulty, & M. Hebblewhite. 2018. *Nature Ecology and Evolution*, 2:1619-1625.

Intense competition for mates drives the evolution of sexually-selected traits that maximize individual reproductive success[1,2]. The associated arms race produced striking ornaments in some species, while in others it resulted in traits that provide tools (e.g., increased appendage size) to physically outcompete conspecifics for access to mates[3,4]. Developing and wielding such elaborate traits often carries a significant cost; more conspicuous individuals may be preferentially killed by predators[5-7], and individuals with large weapons may suffer from awkward and metabolically expensive locomotion[8]. Conversely, developing relatively more pronounced sexually-selected traits can provide secondary benefits to individuals. Larger claw size in fiddler crabs (genus *Uca*) also reduces predation risk[9,10], for example. The associated costs and benefits of sexually-selected traits highlight that selection also acts on these traits outside of the context of reproduction. Yet, only a limited understanding exists of how benefits provided through secondary functions have affected the evolution of sexually-selected traits.

Among the most impressive sexually-selected traits are ungulate weapons (horns or antlers). These weapons differ in that horns are permanent structures, while antlers, unique to and nearly ubiquitous among cervids, are annually cast and regrown. In many species with horns, both sexes have this weapon. In contrast, antlers are confined to males in all cervids except caribou/reindeer (*Rangifer tarandus*). Regardless, for both horns and antlers, competition for mates is the primary driver of weapon evolution in males. This is evidenced by larger weapon size among ungulate species with bigger breeding group sizes[11,12], and higher within-population annual reproductive success for males with larger weapons[13,14].

The timing of antler casting and regrowth is tied to the reproductive cycle of species and is triggered by changes in hormone levels and, for individuals living in temperate climates, photoperiod[15-17]. By annually re-growing antlers, males develop honest signals of fighting ability that track age-specific changes in quality and status[18-20]. Every adult male within a population casts its antlers each year, but they do not all do so at the same time, even in temperate climates where casting is generally synchronous. Some of this variation occurs at the population-level – all individuals may cast their antlers earlier when environmental conditions are less severe, for example[21]. Yet significant variation also exists between individual males within a population. Across cervid species, older, dominant males are the first to cast their antlers over the period of antler casting[21-24], which often spans multiple months[25]. For instance, like our study population of North American elk (*Cervus canadensis*), red deer (*Cervus elaphus*) cast their antlers over a 2 – 3 month period[21] (Fig. 2-1a). Elk and red deer, species so similar that whether their taxonomy differs is still debated[26,27], begin growing their next set of antlers immediately following casting. Individuals who start growth earlier benefit by growing larger antlers, as evidenced by research on red deer[21].

Why all individuals within a population do not cast their antlers as early as possible is unclear because weapons such as antlers are heavy and expensive to carry[28], and casting them sooner would minimize these costs. That some males within populations retain their antlers for months longer than others hints at significant benefits that accrue after the rut. One obvious possible benefit is protection from large carnivores[29]. Many adult males emerge from the rut exhausted, starved, and injured[18,30-32], and therefore especially vulnerable to predation[33]. Horns are a known predatory deterrent[34,35], and if antlers function similarly, then males should benefit from retaining their antlers longer following their breeding season, especially for species most preferred by predators.

Predator preference for various prey species, and individuals within each prey species, is generally driven by factors (e.g., body size, age, nutritional condition) that affect a prey's vulnerability to predators[36-41]. Here, we tested whether antlers functioned as a predatory deterrent using data from the wolf (*Canis lupus*)-prey system of northern Yellowstone National Park, USA, 2004 – 2016. We focused our analysis on wolf predation on adult male elk during March when individuals begin to cast their antlers (Fig. 2-1a). Eight ungulate species (all bearing horns or antlers) are available for wolves to kill, but elk are wolves' most used and preferred prey, especially during winter[42,43] (Fig. S2-1). We expected wolf predation to have been a strong evolutionary source of selection on adult male elk because wolves preferentially kill adult males during winter months[44,45] (Fig. S2-2a). Moreover, relative to other age-sex classes of elk, adult males often experience the highest per capita risk of dying due to wolf predation during winter months, especially in comparison to adult females (Fig. S2-2b). If antlers deter wolves, then wolves should prefer pedicled (i.e., individuals who have cast their antlers) to antlered individuals when they hunt adult males.

To test this prediction, we analyzed data about wolves hunting adult male elk (2005 – 2015), the composition (i.e., antlered or pedicled) of wolf-killed adult male elk (2004 – 2016), and the composition of the adult male elk population (2005 – 2008). Our results revealed that wolves strongly preferred to kill pedicled individuals despite these individuals often being in better nutritional condition, and thereby highlight that antlers are indeed an important predatory deterrent for elk. In fact, we now suspect that predation may help explain variation in post-rut antler retention time across cervid species living in temperate climates.

## RESULTS AND DISCUSSION

**Hunting encounters of wolves on adult male elk.** We first used data from 55 observations of wolves encountering adult male elk individuals and groups (≥ 2 male elk), characterizing each individual or group as ‘antlered’, ‘pedicled’, or ‘mixed’ (consisting of both antlered and pedicled individuals; Table S2-1 for model selection; Fig. S2-3 for beta coefficients; Fig. S2-4 for predictions). Individuals or groups that included pedicled individuals were 3.6 times more likely to be attacked by wolves (odds ratio: 3.6; 85% CI: 1.2 – 11.7). The presence of at least one pedicled individual appeared more influential on whether wolves attacked male elk, however, when wolves encountered groups of ≥ 2 male elk (*n* = 37 groups; Fig. 2-1b). For these encounters, wolves were almost ten times more likely to attack the group if a pedicled individual was present (odds ratio: 9.7; 85% CI: 2.2 – 60.3). Additionally, wolves tended to specifically target these pedicled individuals as encounters escalated in their predatory intensity (Fig. 2-1b).

**Wolf preference for pedicled and antlered adult male elk.** Our observations of wolf-male elk encounters suggested that wolves tended to preferentially attack male elk groups when they included pedicled individuals, although our ability to fully evaluate the effect of pedicled individuals being present was limited by our relatively small sample size (see also *Methods*). But if wolves preferentially attacked pedicled males, then this choice should be reflected in the characteristics of male elk killed by wolves. We therefore leveraged a much larger sample of wolf-killed adult (≥ 2 years old) male elk, and compared the frequency of pedicled males in this sample with that in the male elk population at large. We evaluated wolves’ preference for pedicled or antlered elk when pedicled individuals were rare (early March: 1 March – 15 March) and increasingly common (late March: 16 March – 30 March) in the population (Fig. S2-5). We measured use (i.e., killed) and availability (i.e., classified during surveys) of adult male elk with 216 detected wolf kills ($n_{early}$ = 103, $n_{late}$ = 113; Fig. S2-6; Table S2-2) and 460 classified individuals ($n_{early}$ = 194, $n_{late}$ = 266; Figs. S2-5, S2-6). We used these data to calculate preference ratios for pedicled and antlered elk. In both March periods, wolves preferred pedicled individuals (Fig. 2-2). That wolves strongly preferred to kill pedicled individuals indicates that antlers are indeed an important predatory deterrent for male elk.

**Characteristics of wolf-killed adult male elk.** Given that pedicled males are at higher risk of predation from wolves, why are some males then casting their antlers earlier than others? The timing of antler casting in red deer is known to be affected by an animal's age[21,46], and is thought to be influenced by their nutritional condition. We used generalized linear mixed-effect models (including a random effect for wolf pack) on our sample of wolf-killed male elk to evaluate the effect of these characteristics (age, femur marrow percent fat [a measure of nutritional condition[47,48]]) on whether a male had cast his antlers. We also included population-level factors known to affect the timing of casting (elk abundance, winter severity[21,46,49]) and the day in March when the animal died. We only included males that were at least 5 years old ($n$ = 139) because there were no pedicled individuals younger than age 5 in our data (Fig. S2-7).

Whether a wolf-killed male elk had cast its antlers or not was affected by the individual's nutritional condition, how long into the antler-casting season it was when the animal was killed by wolves, and how many elk were in the population (Fig. 2-3a; Table S2-3; Fig. S2-8). Other than date – males continue to drop their antlers as the antler-casting season progresses (Fig. 2-2b; Fig. S2-5), so wolf-killed males were more likely to be antlerless at the end of March than they were at the beginning of the month (Fig. 2-3a; Fig. S2-8) – the animal's nutritional condition most influenced the likelihood that an individual had cast its antlers (Fig. S2-8). Specifically, wolf-killed pedicled males tended to be in better nutritional condition than antlered males (Fig. 2-3; Fig. S2-8).

Male elk (≥ 5 years old) were more likely to get an early start on growing their antlers when they were in better nutritional condition. The odds of an individual having cast its antlers were 2.1 (85% CI: 1.6 – 2.7) times greater for every 20% increase in femur marrow percent fat, equivalent to an ~1% increase in total fat (for elk with femur marrow fat ≤ 90%[48]). Previous work on red deer showed that males casting their antlers earliest grew new antlers that were relatively heavier, leading to increased reproductive success during the subsequent breeding season[21]. Our research suggests that early casters can grow these heavier antlers because these individuals begin antler growth sooner due to their relatively better nutritional condition during the early portion of the antler-casting season. Presumably for these individuals the benefits of an early onset to antler growth outweigh the increased risk of predation.

Young male elk (i.e., ages 2 – 4) did not cast their antlers early (i.e., during March) in our study (Fig. S2-7), despite usually being in similar, or better, nutritional condition to old individuals that had cast their antlers (Fig. 2-3b). If these young individuals rarely successfully reproduce during the upcoming breeding season anyway, then delaying casting as long as possible makes sense (e.g., the mating strategy-effort hypothesis[50]). Studies of mating success on the Isle of Rum red deer population indicate that young males are unlikely to successfully defend a harem[18], and these young males delay antler casting until later than older males[21]. Interestingly, this introduced red deer population has not lived with wolves for centuries[51,52] (though red deer are often preferred by wolves in parts of their range where they overlap[53,54]), suggesting that there may be additional benefits to retaining one's antlers. For example, delaying the onset of new antler growth to better match the period when forage conditions are improving may be one such benefit. But other cervid species cast their antlers at times when forage is clearly not improving (i.e., winter), and young males in these other species such as moose (*Alces alces*) and caribou also cast their antlers relatively later than older individuals[15]. Our study highlights a secondary function of antlers that could help explain why these young individuals evolved to retain their antlers for an extended period of time.

**Comparing antler retention across ungulate species.** At the end of winter in Yellowstone National Park, wolves frequently encounter male elk within the population that are antlered and antlerless (pedicled). Wolves prefer to kill pedicled individuals (Fig. 2-2c), despite these individuals being in better nutritional condition than antlered males (Fig. 2-3). That these preferred individuals tend to be in better nutritional condition highlights that a prey's vulnerability to predators is affected by multiple factors, and often cannot be simply defined by a single characteristic such as nutritional condition. Nonetheless, this behavior runs counter to theory and numerous studies worldwide that demonstrate that coursing predators prefer to kill poorer-conditioned individuals, especially during periods of the year when prey are nutritionally constrained[37-39,55,56]. This striking finding is consistent with antlers being a formidable anti-predator weapon, and may help explain why elk retain their antlers for ≥ 5 months' post-rut. Predation risk is greatest post-rut through early spring for male elk, when individuals are in declining or poor nutritional condition (Fig. 2-1a), and this period coincides with their unusually long antler-retention time.

In fact, considering the post-rut, anti-predator function of antlers may help explain broader patterns in the timing of antler casting across ungulate species in temperate climates (Fig. 2-4). It is well-appreciated that predation risk for large ungulates varies across species and is also seasonally dynamic[33,40,42,57]. Elk and moose, both residents in our study system, provide a striking illustration. Elk, often strongly preferred by wolves in multi-prey systems[44,45,58], retain their antlers for ~3 months longer than moose whose large body size acts itself as a predatory deterrent[40,59]. This extreme difference in taking on the costs of carrying antlers occurs despite elk and moose both breeding at the same time (Fig. 2-4).

Similar to moose, male caribou also cast their antlers well before elk (Fig. 2-4). Many adult male caribou, in fact, begin casting their antlers shortly after the end of their rut[60]. The primary ways in which caribou avoid being killed by wolves include using their speed and spatially separating themselves from wolves during winter[59,61]. Lastly, both white-tailed and mule deer (*Odocoileus virginianus* and *O. hemionus*, respectively) retain their antlers throughout much of winter, which may be at least partially related to their later breeding seasons (Fig. 2-4). But these deer species still each cast their antlers 1 – 2 months prior to elk, resulting in a much shorter period of post-rut retention than elk. For deer, using their speed to flee is the primary way that they avoid wolf predation[59]. Conversely, male elk often stand their ground when encountered by wolves and are therefore more likely to benefit from a weapon[59].

That wolf predation was an important source of natural selection for a secondary weapon function (i.e., predatory deterrence) is possible because wolves were once the most widespread of any land mammal, ubiquitously spread across much of the northern hemisphere[52]. Our across-species comparison suggests that the evolution of antler retention times may have been affected by how vulnerable various species were to wolf predation, an idea similar in many respects to previous work proposing that large carnivore predation was a driving force on the evolution of horns in female African antelopes[34]. There, females of most medium-to-large species have straight, sharp horns that provide an effective weapon for predator defense. For males with antlers, sexual selection determined the general characteristics of their antlers (e.g., shape, number of tines)[62], as is also the case for bovids[34,62]. But the prolonged retention of antlers after the breeding season in elk, and possibly other medium-to-large species such as red deer that are also often preferred by predators[53,54], appears to have instead been influenced by selection for a predatory deterrent. Through keeping their antlers longer, males of these species may have reduced their risk of predation during the season of the year (e.g., winter) when their vulnerability to wolf predation was highest.

**Conclusions.** Our study highlights an evolutionary tension between the benefits and costs of an extreme, sexually-selected weapon. Casting antlers early rids male elk of heavy, awkward structures and permits them to begin regrowth ahead of rival males, increasing the relative size of the next year's antlers. But early casting comes at a cost, because the first males to drop their antlers are preferentially killed by wolves and thus experience greater risk of predation. For younger males not likely to breed in the upcoming rut anyway, this risk is too high, and these males are among the last to cast their antlers. Old males in better nutritional condition, on the other hand, stand to benefit the most from increased antler size, and it is these males who take the risk and cast their antlers first. Through identifying this tradeoff, our study reveals the largely unexplored importance of secondary functions of sexually-selected structures. We also suggest that the tradeoff associated with delayed casting of antlers differs across cervid species, helping explain species differences in weapon retention time.

Although cervids are unusual in regularly shedding and re-growing their weapons, and this means the specific trait we describe, antler retention time, will be specific to these animals, our study provides a new example of the many ways that secondary functions of sexually-selected weapons can influence the evolution of these structures.

## METHODS

### Data collection and preparation

*Wolf hunting behavior on adult male elk.* – We recorded 713 hunting encounters between wolves and their ungulate prey during March (2004 – 2016) through ground-based observations associated with our long-term monitoring of wolf predation dynamics[42,44,63] (see further details below). Of these, 446 encounters were of wolves hunting elk (Fig. S2-9). For each encounter, we characterized the elk encountered by wolves as 'Mixed age class' (consisting of adult females, yearlings, calves, and adult males; $n = 174$), 'Adult male' (only adult males; $n = 255$), or 'Unknown' ($n = 17$). From the 255 encounters with only adult males, we used a subset of 55 interactions, which mostly occurred from 2005 – 2008 (Fig. S2-9) and came from one wolf pack (i.e., 41 of the 55 observations were of the Leopold pack), where we recorded the antler condition of the adult male elk encountered by wolves. We observed the beginning of the encounter in 43 of 55 cases but included all 55 encounters, of which 37 involved wolves encountering a group of ≥ 2, and 18 an individual, adult male elk. We recorded whether an encounter included an attack (i.e., wolves pursued or harassed prey)[63], as well as the maximum number of wolves and elk participating during the prey encounter[63].

*Composition of wolf-killed adult male elk.* – We used data collected in northern Yellowstone as part of our long-term monitoring effort of wolf predation dynamics[42,44], but began our analysis with data from 2004 because antler condition of wolf-killed adult (≥ 2 years old) male elk was not routinely recorded prior to 2004 (Table S2-2). The general methods of our monitoring included daily aerial radio-tracking of all wolf packs in northern Yellowstone, weather permitting, for 30 days during the 1 – 30 of March each year. Additionally, we also used ground radio-tracking to monitor, and then observe for as much of daylight hours as possible, three wolf packs. For both aerial and ground-based radio-tracking, the primary goal of our monitoring was to detect any kills the wolves had made. During the 1 – 30 March periods from

2004 – 2016 included here, we conducted, on average, aerial telemetry flights on 14.2 ± 1.6 SE days and visually observed wolf packs on 23.5 ± 0.6 SE days. In addition to aerial and/or ground-based monitoring, we also detected wolf-killed ungulates through searching clusters of wolf Global Positioning System (GPS) locations[64] for 1 – 3 wolf packs during each March monitoring period since 2010. Wolves were captured and handled following guidelines of the American Society of Mammalogists[65] and approved under University of Montana IACUC protocol 043-15MHWB-121515.

We detected 223 adult male elk (of 596 total elk) killed by wolves during March in northern Yellowstone from 2004 – 2016, but restricted our data set to 216 wolf-killed adult male elk for which we recorded antler condition (Fig. S2-6). Rarely ($n$ = 3), a wolf-killed adult male elk had one antler; in these cases, we classified the individual as pedicled (Table S2-2). For these 216 individuals, we determined age (through cementum annuli analysis; Matson's Laboratory, Milltown, MT, USA) for 180 individuals and femur marrow percent fat[47] (an indicator of nutritional condition; see below) for 166 individuals. For our analysis where we evaluated the influence of individual characteristics on the probability of a wolf-killed adult male elk having cast his antlers (see below), we restricted our data set to individuals where we recorded both age and femur marrow percent fat. Initially, our data set included 157 individuals. However, we limited our analysis to include only individuals ≥ 5 years old ($n$ = 139) because we did not detect any wolf-killed individuals who were < 5 that had cast their antlers (Fig. S2-7). We likely did not detect any pedicled individuals that were between 2 – 4 years old because we sampled for wolf-killed elk only in March during the period of antler casting[44], and the youngest adult males in the population typically cast their antlers after March[21].

Note that femur marrow percent fat is an indicator of ungulate nutritional condition, but is most useful for individuals that are in poorer nutritional condition. Specific to elk, femur marrow fat is a reliable indicator of nutritional condition when femur marrow fat is ≤ 90%, which corresponds to body fat being ≤ 6%[48]. The ability of bone marrow fat to provide a reliable indication of nutritional condition was not limiting for our study because most individual ungulates are in fairly poor nutritional condition during late winter[66,67]. Specific to our data, 163 of the 166 femur marrow fat samples that we collected from wolf-killed male elk had femur marrow percent fat values ≤ 90%.

*Composition of adult male elk population.* – We classified the availability of adult male elk with and without antlers (i.e., 'antlered' and 'pedicled') during March 2005 – 2008. During each year, we conducted approximately weekly ground-based observational classification surveys on a 6.7 $\text{km}^2$ area in northern Yellowstone National Park, Wyoming, USA (44.9383, -110.5576; Fig. S2-6). Although we conducted surveys only in this one area of northern Yellowstone, proportional availability of pedicled and antlered adult male elk is relatively homogenous during March across the portion of northern Yellowstone National Park where we monitored wolf predation (Northern Yellowstone Cooperative Wildlife Working Group, unpublished data; see Fig. S2-6). In total, we classified 460 individuals during 19 surveys ($n_{2005} = 4$, $n_{2006} = 6$, $n_{2007} = 6$, $n_{2008} = 3$). On average, 24.2 ± 4.5 (mean ± SE; median = 22; range: 1 – 69) adult male elk were classified during each survey (Fig. S2-5).

## Data analysis

*Wolf hunting behavior on adult male elk.* – We used generalized linear models (binomial) to evaluate the influence of the number of wolves (defined as the maximum number participating in any foraging state within the prey encounter[63]; log-transformed to account for the previously demonstrated non-linear influence of the number of wolves involved in prey encounters[68]), the number of adult male elk, and adult male elk group type (Pedicled, Mixed, Antlered) on the probability of an encounter escalating to an attack. We did so in two ways. First, we included all encounters and next, only for encounters with adult male elk groups that included ≥ 2 elk. We evaluated encounters with groups separately because our data suggested that when wolves encountered a single adult male elk, the hunt was likely to include an attack, regardless of whether the antler condition of the individual was pedicled or antlered. We combined pedicled and mixed groups, as both of these groups included individuals without antlers. We did not evaluate models including interactions or use mixed-effect models to include a random effect for pack because of our relatively small sample size. We screened for collinearity and association among covariates; no covariates were highly correlated ($r \leq 0.26$) or showed evidence of being associated. All continuous covariates, here and in the following analysis, were standardized to facilitate comparison and estimation through subtracting the mean and dividing by the standard deviation. We also present beta coefficients from models where we did not standardize covariates, and use the non-standardized beta coefficients from the top model to calculate the odds ratio for the presence of pedicled individual(s) for all encounters and only encounters with ≥ 2 elk. For all analyses, we used AICc to evaluate relative support among models. We conducted all analyses in R version 3.3.1 (R Core Team 2016). We used the package 'AICcmodavg'[69] for AIC model evaluation and selection and the package 'oddsratio'[70] to estimate odds ratios and their 85% confidence intervals[71].

We did not evaluate what factors affected the probability of an encounter escalating to the attack of a specific individual because our relatively small sample size ($n = 27$ encounters that included an attack) was particularly limiting during this portion of wolf-elk encounters. This was because wolves sometimes attacked multiple individuals within the same wolf-prey encounter. Accordingly, the raw data that we present (Fig. 2-1b) included 32 predation attempts, but only 27 encounters.

*Wolf preference for pedicled and antlered adult male elk.* – We calculated a preference ratio[72] for pedicled and antlered adult male elk as:

$$\mathrm{LN}\left(\frac{proportion\ kills}{proportion\ available}\right) \quad \text{Eqn 1}$$

For the preference ratios calculated through Eqn 1, we used bootstrapping to estimate standard errors for the proportion of elk killed, available, and preferred. To do so, we sampled with replacement the kill and classification count data for early and late March 10,000 times. For each iteration, we calculated the proportion of pedicled and antlered adult male elk killed and available, as well as the preference ratio.

*Characteristics of wolf-killed adult male elk.* – We used generalized linear mixed-effect models (binomial; pedicled individuals = 1, antlered = 0; random effect for pack – see below), to evaluate the effect of age, femur marrow percent fat, day in March, winter severity, and elk abundance on predicting whether a wolf-killed adult male elk (≥ 5 years old; *n* = 139) had antlers, as each of these covariates may affect the precise timing of when an individual casts its antlers[21,46,49]. To characterize winter severity, we used spatially-explicit weekly predictions of Snow Water Equivalent (SWE)[73]. More specifically, we used the mean SWE value for a 3 km-buffered area around each kill (Fig. S2-6) for the week within which the observation occurred. Elk abundance was estimated via an annual winter count conducted by the Northern Yellowstone Cooperative Wildlife Working Group; years without a count were interpolated using a state-space model and each count was adjusted for imperfect detection[43].

In our full model set, we included all combinations of additive models and models that also considered 2-way interactions for *i*) femur marrow percent fat and age, winter severity, or elk abundance and *ii*) age and winter severity or elk abundance. We considered these 2-way interactions because we hypothesized (a priori) each could be important. We also included a random effect for pack (or lone wolf if the wolf was not a member of a pack; but see below). We identified the pack or lone wolf ($n = 23$) that made the kill for 137 of the 139 kills included in our analysis. Many packs existed during multiple monitoring periods and, on average, we detected adult male elk (≥ 5 years old) killed by a particular pack (or lone wolf) during 2.5 ± 0.3 SE study periods (range: 1 – 5). Because we did not detect many kills for some packs or lone wolves (median = 3 kills, range: 1 – 26), we grouped together all packs as 'Other' for any packs for which we detected fewer than the median number of kills. Within 'Other', we also included the two kills detected where we did not know which pack made the kill. We did not, however, ultimately include pack in our final set of candidate models because the random effect for pack was non-existent or trivial in our top models. No covariates were highly correlated ($r \leq 0.22$). As above, we present both non-standardized and standardized beta coefficient estimates, and used the non-standardized beta coefficients to estimate odds ratios.

**Data availability**

Data used for analyses is available at datadryad.org/resource/doi:10.5061/dryad.j72tt79.

## REFERENCES

1 Emlen, S. T. & Oring, L. W. Ecology, sexual selection, and the evolution of mating systems. *Science* **197**, 215-223 (1977).
2 Clutton-Brock, T. H. *Reproductive Success: Studies of Individual Variation in Contrasting Breeding Systems*. (University of Chicago Press, 1988).
3 Darwin, C. *The Descent of Man, and Selection in Relation to Sex*. (John Murray, 1871).
4 Andersson, M. B. *Sexual Selection*. (Princeton University Press, 1994).

5 Godin, J.-G. J. & McDonough, H. E. Predator preference for brightly colored males in the guppy: a viability cost for a sexually selected trait. *Behavioral Ecology* **14**, 194-200 (2003).

6 Johnson, S. & Candolin, U. Predation cost of a sexual signal in the threespine stickleback. *Behavioral Ecology* **28**, 1160-1165 (2017).

7 Stuart-Fox, D. M., Moussalli, A., Marshall, N. J. & Owens, I. P. F. Conspicuous males suffer higher predation risk: visual modelling and experimental evidence from lizards. *Animal Behaviour* **66**, 541-550 (2003).

8 Goyens, J., Dirckx, J. & Aerts, P. Costly sexual dimorphism in *Cyclommatus metallifer* stag beetles. *Functional Ecology* **29**, 35-43 (2015).

9 Bildstein, K. L., McDowell, S. G. & Brisbin, I. L. Consequences of sexual dimorphism in sand fiddler crabs, *Uca pugilator*: differential vulnerability to avian predation. *Animal Behaviour* **37**, 133-139 (1989).

10 McLain, D. K., Pratt, A. E. & Berry, A. S. Predation by red-jointed fiddler crabs on congeners: interaction between body size and positive allometry of the sexually selected claw. *Behavioral Ecology* **14**, 741-747 (2003).

11 Bro-Jørgensen, J. The intensity of sexual selection predicts weapon size in male bovids. *Evolution* **61**, 1316-1326 (2007).

12 Clutton-Brock, T. H., Albon, S. D. & Harvey, P. H. Antlers, body size and breeding group size in the Cervidae. *Nature* **285**, 565-567 (1980).

13 Coltman, D. W., Festa-Bianchet, M., Jorgenson, J. T. & Strobeck, C. Age-dependent sexual selection in bighorn rams. *Proceedings of the Royal Society of London B: Biological Sciences* **269**, 165-172 (2002).

14 Kruuk, L. E. B. *et al.* Antler size in red deer: heritability and selection but no evolution. *Evolution* **56**, 1683-1695 (2002).

15 Goss, R. J. *Deer antlers: regeneration, function and evolution*. (Academic Press, 1983).

16 Lincoln, G. A. Biology of antlers. *Journal of Zoology* **226**, 517-528 (1992).

17 Price, J. & Allen, S. Exploring the mechanisms regulating regeneration of deer antlers. *Philosophical Transactions of the Royal Society B: Biological Sciences* **359**, 809-822 (2004).

18 Clutton-Brock, T. H., Albon, S. D., Gibson, R. M. & Guinness, F. E. The logical stag: adaptive aspects of fighting in red deer (*Cervus elaphus L.*). *Animal Behaviour* **27**, 211-225 (1979).

19 Malo, A. F., Roldan, E. R. S., Garde, J., Soler, A. J. & Gomendio, M. Antlers honestly advertise sperm production and quality. *Proceedings of the Royal Society of London B: Biological Sciences* **272**, 149-157 (2005).

20 Vanpé, C. *et al.* Antler size provides an honest signal of male phenotypic quality in roe deer. *The American Naturalist* **169**, 481-493 (2007).

21 Clements, M. N., Clutton-Brock, T. H., Albon, S. D., Pemberton, J. M. & Kruuk, L. E. B. Getting the timing right: antler growth phenology and sexual selection in a wild red deer population. *Oecologia* **164**, 357-368 (2010).

22 Bartoš, L. The date of antler casting, age and social hierarchy relationships in the red deer stag. *Behavioural Processes* **5**, 293-301 (1980).

23 Bowyer, R. T. Antler characteristics as related to social status of male southern mule deer. *The Southwestern Naturalist* **31**, 289-298 (1986).

24 Van Ballenberghe, V. in *Antler development in Cervidae* (ed Brown, R.D.) 37-48 (Caesar Kleberg Wildlife Research Institute, 1983).
25 Chapman, D. I. Antlers–bones of contention. *Mammal Review* **5**, 121-172 (1975).
26 Polziehn, R. O. & Strobeck, C. A phylogenetic comparison of red deer and wapiti using mitochondrial DNA. *Molecular Phylogenetics and Evolution* **22**, 342-356 (2002).
27 Meiri, M. *et al.* Subspecies dynamics in space and time: A study of the red deer complex using ancient and modern DNA and morphology. *Journal of Biogeography* **45**, 367-380 (2018).
28 Allen, B. J. & Levinton, J. S. Costs of bearing a sexually selected ornamental weapon in a fiddler crab. *Functional Ecology* **21**, 154-161 (2007).
29 Clutton-Brock, T. H. The functions of antlers. *Behaviour* **79**, 108-125 (1982).
30 Bobek, B., Perzanowski, K. & Weiner, J. Energy expenditure for reproduction in male red deer. *Journal of Mammalogy* **71**, 230-232 (1990).
31 Rughetti, M. & Festa-Bianchet, M. Seasonal changes in sexual size dimorphism in northern chamois. *Journal of Zoology* **284**, 257-264 (2011).
32 Geist, V. New evidence of high frequency of antler wounding in cervids. *Canadian Journal of Zoology* **64**, 380-384 (1986).
33 Owen-Smith, N. Changing vulnerability to predation related to season and sex in an African ungulate assemblage. *Oikos* **117**, 602-610 (2008).
34 Packer, C. Sexual dimorphism: the horns of African antelopes. *Science* **221**, 1191-1193 (1983).
35 Clements, H. S., Tambling, C. J. & Kerley, G. I. H. Prey morphology and predator sociality drive predator prey preferences. *Journal of Mammalogy* **97**, 919-927 (2016).
36 Peterson, R. O. *Wolf ecology and prey relationships on Isle Royale*. (US Government Printing Office, 1977).
37 Fitzgibbon, C. D. & Fanshawe, J. H. The condition and age of Thomson's gazelles killed by cheetahs and wild dogs. *Journal of Zoology* **218**, 99-107 (1989).
38 Sinclair, A. R. E. & Arcese, P. Population consequences of predation-sensitive foraging: The Serengeti wildebeest. *Ecology* **76**, 882-891 (1995).
39 Husseman, J. S. *et al.* Assessing differential prey selection patterns between two sympatric large carnivores. *Oikos* **101**, 591-601 (2003).
40 Sinclair, A. R. E., Mduma, S. & Brashares, J. S. Patterns of predation in a diverse predator–prey system. *Nature* **425**, 288-290 (2003).
41 Wright, G. J., Peterson, R. O., Smith, D. W. & Lemke, T. O. Selection of northern Yellowstone elk by gray wolves and hunters. *Journal of Wildlife Management* **70**, 1070-1078 (2006).
42 Metz, M. C., Smith, D. W., Vucetich, J. A., Stahler, D. R. & Peterson, R. O. Seasonal patterns of predation for gray wolves in the multi-prey system of Yellowstone National Park. *Journal of Animal Ecology* **81**, 553-563 (2012).
43 Tallian, A. *et al.* Predator foraging response to a resurgent dangerous prey. *Functional Ecology* **31**, 1418-1429 (2017).
44 Smith, D. W., Drummer, T. D., Murphy, K. M., Guernsey, D. S. & Evans, S. B. Winter prey selection and estimation of wolf kill rates in Yellowstone National Park, 1995–2000. *Journal of Wildlife Management* **68**, 153-166 (2004).
45 Huggard, D. J. Prey selectivity of wolves in Banff National Park. II. Age, sex, and condition of elk. *Canadian Journal of Zoology* **71**, 140-147 (1993).

46 Clutton-Brock, T. H., Guinness, F. E. & Albon, S. D. *Red deer: behavior and ecology of two sexes*. (University of Chicago Press, 1982).

47 Neiland, K. A. Weight of dried marrow as indicator of fat in caribou femurs. *The Journal of Wildlife Management* **34**, 904-907 (1970).

48 Cook, R. C. *et al.* Development of predictive models of nutritional condition for Rocky Mountain elk. *The Journal of Wildlife Management* **65**, 973-987 (2001).

49 Watson, A. Climate and the antler-shedding and performance of red deer in north-east Scotland. *Journal of Applied Ecology* **8**, 53-67 (1971).

50 Yoccoz, N. G., Mysterud, A., Langvatn, R. & Stenseth, N. C. Age– and density–dependent reproductive effort in male red deer. *Proceedings of the Royal Society of London B: Biological Sciences* **269**, 1523-1528 (2002).

51 Nussey, D. H., Pemberton, J., Donald, A. & Kruuk, L. E. B. Genetic consequences of human management in an introduced island population of red deer (*Cervus elaphus*). *Heredity* **97**, 56-65 (2006).

52 Boitani, L. in *Wolves: behavior, ecology, and conservation* (eds Mech, L.D. & Boitaini, L.) 317-340 (University of Chicago Press, 2003).

53 Jędrzejewski, W. *et al.* Prey selection and predation by wolves in Białowieża Primeval Forest, Poland. *Journal of Mammalogy* **81**, 197-212 (2000).

54 Gazzola, A. *et al.* Predation by wolves (*Canis lupus*) on wild and domestic ungulates of the western Alps, Italy. *Journal of Zoology* **266**, 205-213 (2005).

55 Pole, A., Gordon, I. J. & Gorman, M. L. African wild dogs test the 'survival of the fittest' paradigm. *Proceedings of the Royal Society of London B: Biological Sciences* **270**, S57 (2003).

56 Atwood, T. C., Gese, E. M. & Kunkel, K. E. Comparative patterns of predation by cougars and recolonizing wolves in Montana's Madison Range. *Journal of Wildlife Management* **71**, 1098-1106 (2007).

57 Jędrzejewski, W. *et al.* Kill rates and predation by wolves on ungulate populations in Białowieża Primeval Forest (Poland). *Ecology* **83**, 1341-1356 (2002).

58 Carbyn, L. N. Wolf predation on elk in Riding Mountain National Park, Manitoba. *The Journal of Wildlife Management* **47**, 963-976 (1983).

59 Mech, L. D., Smith, D. W. & MacNulty, D. R. *Wolves on the hunt: the behavior of wolves hunting wild prey*. (University of Chicago Press, 2015).

60 Bergerud, A. The annual antler cycle in Newfoundland caribou. *Canadian Field-Naturalist* **90**, 449-463 (1976).

61 Seip, D. R. Factors limiting woodland caribou populations and their interrelationships with wolves and moose in southeastern British Columbia. *Canadian Journal of Zoology* **70**, 1494-1503 (1992).

62 Caro, T. M., Graham, C. M., Stoner, C. J. & Flores, M. M. Correlates of horn and antler shape in bovids and cervids. *Behavioral Ecology and Sociobiology* **55**, 32-41 (2003).

63 MacNulty, D. R., Mech, L. D. & Smith, D. W. A proposed ethogram of large-carnivore predatory behavior, exemplified by the wolf. *Journal of Mammalogy* **88**, 595-605 (2007).

64 Metz, M. C., Vucetich, J. A., Smith, D. W., Stahler, D. R. & Peterson, R. O. Effect of sociality and season on gray wolf (*Canis lupus*) foraging behavior: implications for estimating summer kill rate. *PLoS One* **6**, e17332 (2011).

65 Sikes, R. S., Gannon, W. L., Care, A. & the Animal Care and Use Committee of the American Society of Mammalogists. Guidelines of the American Society of

Mammalogists for the use of wild mammals in research. *Journal of Mammalogy* **92**, 235-253 (2011).
66 Mautz, W. W. Sledding on a bushy hillside: the fat cycle in deer. *Wildlife Society Bulletin* **6**, 88-90 (1978).
67 Parker, K. L., Barboza, P. S. & Gillingham, M. P. Nutrition integrates environmental responses of ungulates. *Functional Ecology* **23**, 57-69 (2009).
68 MacNulty, D. R., Smith, D. W., Mech, L. D., Vucetich, J. A. & Packer, C. Nonlinear effects of group size on the success of wolves hunting elk. *Behavioral Ecology* **23**, 75-82 (2012).
69 Mazerolle, M. J. AICcmodavg: model selection and multimodel inference based on (Q) AIC (c). *R package version* **2.1.1** (2017).
70 Schratz, P. R package 'oddsratio': Odds ratio calculation for GAM(M)s & GLM(M)s. *R package version* **1.0.2** (2017).
71 Arnold, T. W. Uninformative parameters and model selection using Akaike's Information Criterion. *Journal of Wildlife Management* **74**, 1175-1178 (2010).
72 Manly, B. F. L., McDonald, L., Thomas, D., McDonald, T. L. & Erickson, W. P. *Resource selection by animals: statistical design and analysis for field studies*. (Springer Science & Business Media, 2007).
73 Wockner, G., Singer, F., Coughenour, M. & Farnes, P. Yellowstone Snow Model. *Natural Resources Ecology Lab, Colorado State University, Fort Collins, CO,* http://www.nrel/*.colostate.edu/projects/yellowstone* (2006).
74 Martin, H. W. *et al.* Factors affecting gray wolf (*Canis lupus*) encounter rate with elk (*Cervus elaphus*) in Yellowstone National Park *Canadian Journal of Zoology*, doi:10.1139/cjz-2017-0220 (2018).
75 Kamischke, E. *Estimation of Kill Rates by Yellowstone Wolves*, Michigan Technological University, (2007).

## END NOTES

**Acknowledgements.** We thank all Yellowstone Wolf Project field technicians and Gallatin Flying Services for data collection and Erin Stahler, Kira Cassidy, Ky Koitzsch, and Jennifer Jones for discussions. This work was supported by Yellowstone Forever (Tapeats Foundation, Anonymous donor, Frank and Kay Yeager, many individual donors) and NSF LTREB grants DEB-0613770, DEB-1245373, and DEB-1556248. M.C.M. was also supported by the Wesley M. Dixon Graduate Fellowship and Bertha Morton Scholarship from the University of Montana and a Graduate Enhancement Fellowship from the Montana Institute on Ecosystems funded through NSF EPSCoR.

**Author contributions.** M.C.M. conceived of the study. M.C.M., D.R.S., and D.W.S. collected the data and coordinated the study. M.C.M. and M.H. developed the methods and M.C.M. analyzed the data. M.C.M., D.J.E., and M.H. wrote the paper with input from other authors.

**Author information.** Reprints and permissions information is available at www.nature.com/reprints. The authors declare no conflicts of interest. Correspondence and requests for materials should be addressed to M.C.M. (matthew.metz@umontana.edu).

**FIGURES.**

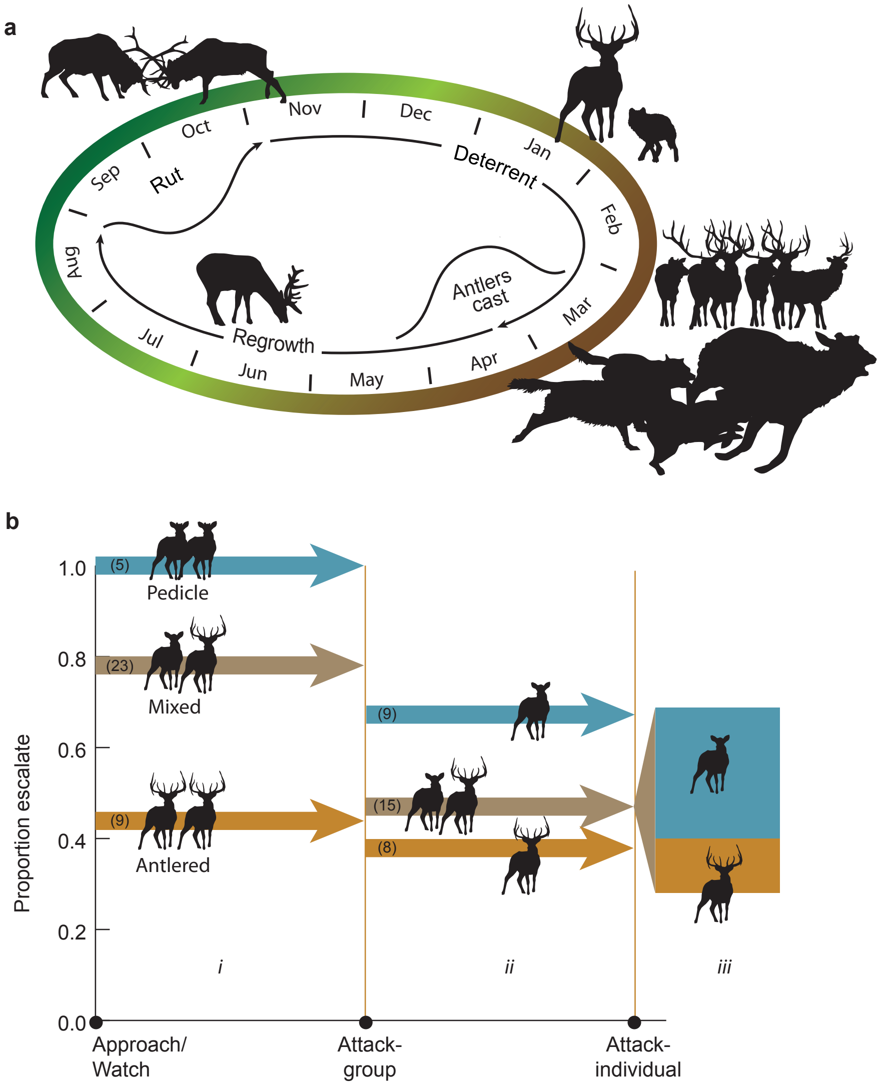

**Figure 2-1. The function of antlers and wolf-adult male elk encounters. a,** Adult male elk cast their antlers, over a 2 – 3 month period at the population-level, each spring to grow new antlers to use in competition for mates during the rut. Early casters trade the benefit of increased reproductive success[21] for the cost of losing a predatory deterrent. Shading of circle depicts elk nutritional condition (dark green = best, dark brown = poorest), which begins to decline during fall and improve during spring. **b,** Raw data from observations of wolf-adult male elk encounters (only for groups of ≥ 2 individuals), highlight the potential cost of being an early caster. Arrows represent the proportion of observations for pedicled, mixed, and antlered male elk that escalated from wolves ***i)*** encountering the group to attacking (e.g., pursuing) it and ***ii)*** attacking an individual, with the type of individual attacked for 'mixed' also displayed **(*iii*)**. Note that the antler condition above ***ii*** represents the antler condition for the group (or individual) being attacked (e.g., pursued) during ***ii***, and is not necessarily the same as ***i***. Also note that multiple attacks can occur during an encounter[63]. Numbers in parentheses indicate total number of observations. (Illustration by Emily Harrington, Missoula, MT)

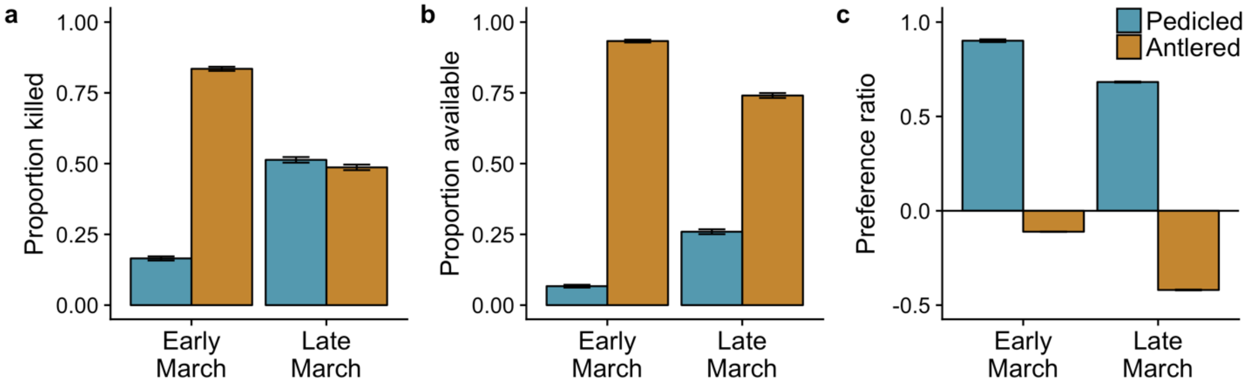

**Figure 2-2. Adult male elk antler condition and preference by wolves. a,** Use, **b,** availability and **c,** wolf preference for adult male elk, dependent on antler condition. Error bars represent 95% confidence intervals.

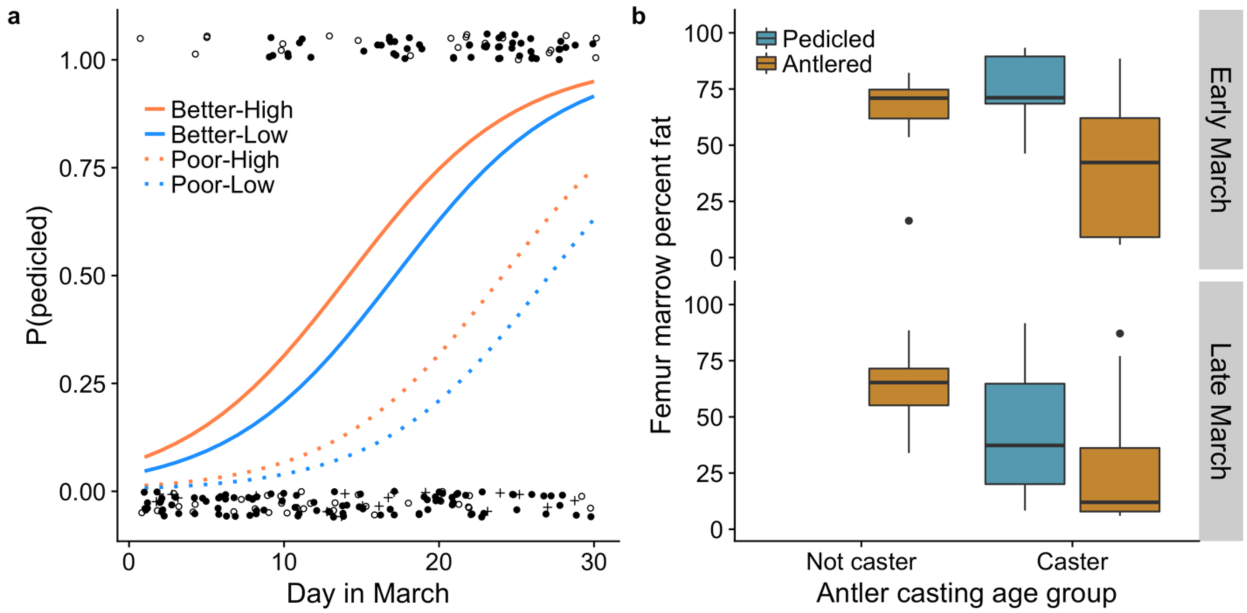

**Figure 2-3. Characteristics of wolf-killed male elk and antler condition. a,** Predicted probabilities, from our top model (Table S2-3; Fig. S2-8), of a wolf-killed adult male elk (≥ 5 years old) being a pedicled individual during March. Predicted probabilities are displayed for the first and third quartile of femur marrow percent fat (‘Poor’ = 12%; ‘Better’ = 63%) and elk abundance (‘Low’ = 7,601; ‘High’ = 10,192). Only the filled circles were used in the analysis (*n* = 139). Pluses indicate that the male was 2 – 4 years old (*n* = 18) and open circles indicate that we did not have data describing both the male’s age and nutritional condition (*n* = 59). **b,** Percent femur marrow fat for wolf-killed male elk in relation to March period and ‘antler casting age group’. For antler casting age group, ‘Not caster’ indicates the individual was 2 – 4 year old (pluses in **a**) and ‘Caster’ indicates the individual was ≥ 5 years old (filled circles in **a**). The box plot displays the median, as well as the first and third quartiles. Whiskers extend from the inter-quartile range to the largest value that is no further than 1.5 * inter-quartile range, in each direction. Filled circles represent outliers.

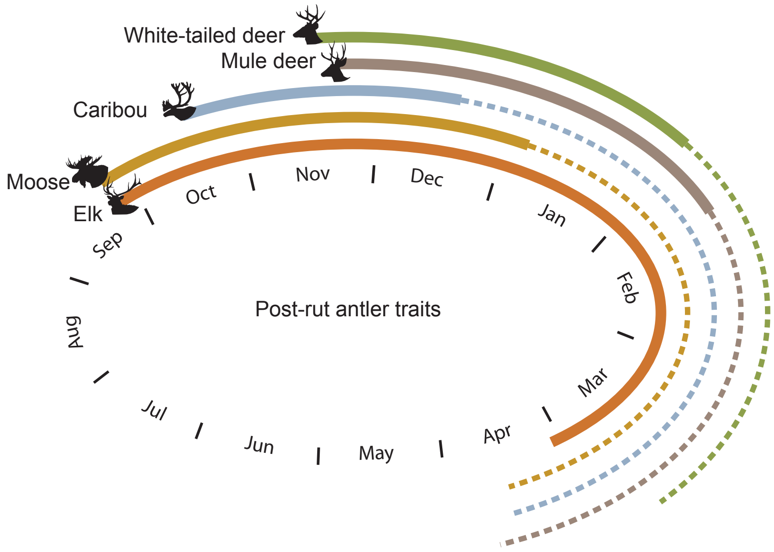

**Figure 2-4. Antler traits of adult male North American ungulate species.** For each species, the species symbol represents the peak of the rut, the solid portion of the line represents the period of antler retention following the peak of the rut, and the dashed portion represents the pedicled period when each species is without antlers until new growth commences. Independent of other traits (e.g., body size, speed), elk retain their antlers longer post-rut than any other species because of their effectiveness as a predatory deterrent. (Illustration by Emily Harrington, Missoula, MT)

# Chapter 3: Accounting for imperfect detection in observational studies: modeling wolf sightability in Yellowstone National Park [2]

## ABSTRACT

Imperfect detection is ubiquitous among wildlife research, and is therefore commonly included in abundance estimation. Yet, the factors that affect observation success are largely unknown for rare and elusive species, such as large carnivores. Here, we took advantage of intensive ground-based monitoring effort and an extensive GPS data set (2000 – 2018) and developed a winter sightability model for gray wolves (*Canis lupus*) in northern Yellowstone National Park, WY, USA. Our resulting sightability model indicated that observation success was positively affected by the topographic nature of where wolves were in relation to observer locations (viewshed), areas being less forested (openness), and wolf group size, and negatively affected by distance from observer locations. Of these, viewshed had the strongest effect on the probability of observing a wolf, with the odds of observing a wolf being four times more likely when wolves were in the predicted viewshed. Openness was the next most influential covariate, and group size was the least influential. We also tested whether a wolf being harvested from a pack when they were outside of Yellowstone National Park had an effect on wolf sightability. We did not, however, find support for human-induced mortality affecting wolf sightability inside of Yellowstone National Park. Our results indicate that the ability to observe wolves was greatly affected by ecological and landscape-level factors, a finding that is likely to generally extend to other large carnivores. As such, our sightability model highlights the importance of considering

---

[2] Paper published as: M.C. Metz, J. SunderRaj, D.W. Smith, D.R. Stahler, M.T. Kohl, K.A. Cassidy, & M. Hebblewhite. 2020. *Ecosphere*, 11:e03152.

landscape structure and variation in large carnivore use of the landscape when conducting observational-based studies.

**Keywords:** *Canis lupus; harvest; resource selection probability function; wildlife observation; wolves.*

## INTRODUCTION

Direct observations of wildlife provide foundational data for understanding how species are distributed across the globe and how these species use landscapes. This is even true in modern wildlife research where expensive Global Positioning System (GPS) data and camera traps are increasingly used to study wildlife populations (Kays et al. 2015, Steenweg et al. 2017) because of the importance of combining observational data with remote methods (e.g., Patzelt et al. 2014, Kohl et al. 2018). Observing wildlife is also a key form of nature-based tourism (Newsome et al. 2005), the economic consequences of which are significant for local economies (Naidoo and Adamowicz 2005). Moreover, observations collected by the general public (i.e., citizen or community science) are important for monitoring and research (Bonney et al. 2009, van Strien et al. 2013, Sun et al. 2019). Regardless of the purpose, wildlife observations are affected by many factors, and a great deal of variation therefore exists in the ‘success’ of attempts to observe wildlife.

Variation in observation success is driven by factors related to the species’ ecology and the observation process. For example, marine mammals such as whales spend much of their time underwater, surfacing only rarely, which affects their availability to be detected during surveys (Hain et al. 1999). Even upon surfacing, boat-based detection is affected by factors such as distance and group size (Williams et al. 2016). Similarly, for terrestrial species, distance from observers, vegetation characteristics (e.g., forest cover), and group size often affect detection (Samuel et al. 1987, Buckland et al. 2001, Peters et al. 2014). It is surprising then that detection is sometimes assumed to be perfect (Hutto 2016), with any consequences of imperfect detection therefore underestimated (Peters et al. 2014). The problem of imperfect detection generally permeates all wildlife studies, but is particularly severe for rare and elusive species.

A bit ironically, however, the observation of rare and elusive species, such as large carnivores, is often highly desired by both the general public and researchers. In the case of large carnivores, such observations, including those collected through citizen science efforts (Farhadinia et al. 2018), contribute information for estimating their distribution, abundance, and ecological effects (Ripple et al. 2014). Direct observations have also provided the backbone for many studies of large carnivores and their prey in African systems (Schaller 1972, Creel and Creel 2002). But conclusions from observational studies are affected by the relationship between large carnivore observations, the factors affecting the observation process, and how large carnivores use the landscape. Much of the initial research on cheetahs (*Acinonyx jubatus*), for example, focused on their use of open plains, and often overlooked their capacity to skillfully use woodland areas (Mills et al. 2004, Bissett and Bernard 2007). To date, we are aware of no studies that directly assessed the detection of large carnivores using only ground-based observations.

Perhaps nowhere else in North America is the desire to see large mammals, including gray wolves (*Canis lupus*), greater than it is in Yellowstone National Park (YNP). Opportunities to observe wolves have been uniquely abundant since their reintroduction in 1995, and wolf watching has, in turn, benefited local economies (Duffield et al. 2008) and wildlife research.

Observations of wolves during long-term behavioral studies have revealed heretofore unknown aspects of wolf ecology. For example, how wolf hunting success is affected by individual characteristics of predators (MacNulty et al. 2009) and prey (Metz et al. 2018), and how the social structure of wolf groups affects aggressive interactions between wolf packs (Cassidy et al. 2015). Such studies obviously rely on observations, but the degree to which wolves are successfully observed could vary through time as ecological conditions change. In fact, the number of summer wolf observations have recently declined, with the decline having been associated with the effects of human harvest of wolves outside of YNP (and Denali National Park; Borg et al. 2016). However, a comprehensive assessment of factors that affect the sightability of wolves has not yet occurred, although Borg et al. (2016) found that the number of wolf observations declined concurrently with declining wolf abundance. Smith et al. (2004) also previously showed how increased distance from park roads negatively affected the detection of wolf kills. The frequent observations of wolves in YNP provides a unique opportunity to identify the factors that affect large carnivore sightability.

Here, we employed a logistic regression framework to evaluate factors affecting the likelihood of successful ground-based observations of GPS-collared wolves in northern YNP during winter from 2000 – 2018. We hypothesized that wolf group sightability would be affected by wolves being in more or less forested areas, how far wolves were from observer locations, whether wolves were in areas where observers could physically view (i.e., whether the view was not obstructed by topographic features), and how many wolves were present in the group. We also evaluated the effect of human harvest on sightability by testing whether sightability of wolves in a pack declined following harvest. Finally, we predicted that the opportunity to successfully observe wolves may have changed over time due to changes in wolf and elk (*Cervus* *canadensis*) abundance. We therefore explored whether wolf use of ‘sightable’ locations, as determined through our initial analysis, has changed through time. Understanding sightability of large carnivores such as wolves will generally improve monitoring of these ecologically-important species, primarily through providing a tool that can account for spatial-temporal variation in sightability.

## METHODS

### STUDY AREA

Our study area was defined by the movements of 13 wolf packs that resided primarily within northern YNP during 17 winters (November 2000 – March 2018; Fig. 3-1, Fig. S3-A.1). The study area included much of Yellowstone’s well-known “Northern Range”, which is generally characterized by elevations between 1,500–2,400 meters (Houston 1982). Accordingly, snow generally covered the ground during our monitoring efforts. Lower elevations of northern Yellowstone are generally dominated by large open valleys and shrub steppe vegetation, while higher elevations are increasingly characterized by coniferous forests (Houston 1982). The portion of the study area inside YNP is protected from human harvest. Researchers and tourists do, however, observe wildlife and recreate within YNP, which also affects animal behavior (Cassirer et al. 1992). Outside of YNP, recreationists and hunters use the landscape for both non-consumptive and consumptive (hunting) use.

### WINTER STUDY

‘Winter study’ is a long-term (i.e., beginning in November 1995) research program that investigates wolf-prey relationships through visual observation of wolf packs feeding on carcasses (Smith et al. 2004). Elk, and more recently, bison (*Bison bison*) are the most important food sources for wolves in northern YNP (Metz et al. 2012, Metz et al. 2016). To observe wolves, wolf packs were monitored through aerial and ground-based radio-tracking for 30-day periods during an early (mid-November to mid-December) and late (March) winter period. Observations therefore rely on radiocollaring, accomplished through helicopter darting or netgunning. Wolf capture and handling conformed to National Park Service animal capture and handling policies, as well as University of Montana IACUC protocol AUP MH-043-15. Both Very High Frequency (VHF) and GPS collars were routinely deployed. Here, we used data only for packs that contained GPS-collared wolves during a 30-day period (but see Appendix S3-B for a complementary sightability model developed using VHF data).

Our study relied on ground-based observations collected by teams of 2-3 field technicians (hereafter, observation crew). Each observation crew was assigned to a single wolf pack and, together, they observed 1-3 GPS-collared wolf packs (Fig. S3-A.1) during each 30-day period. Daily, observation crews located their assigned wolf pack at daybreak using standard radio telemetry, and then used high-powered spotting scopes to observe the wolf pack for as much of daylight as possible (Smith et al. 2004, Martin et al. 2018). We visually observed GPS-collared wolf packs on 21.7 (± 0.6 SE) days, on average. Observation crews did not have access to real-time GPS locations.

### GPS DATA PREPARATION

Among included wolf packs, GPS data was available from 17 winters (27 30-day periods), 13 packs, and 45 wolves. We included wolves only if they were usually with other members of their pack, which was known from our aforementioned daily observations. Some packs contained multiple GPS-collared wolves, but we included only one wolf per pack for each 30-day period. We used a multi-step process to thin our data to a single wolf, stopping whenever a single wolf remained. First, we excluded wolves who only tangentially belonged to a pack. If multiple wolves were core members of their pack, we selected wolves whose collars acquired hourly locations. Then, we censored wolves that did not survive the 30-day period. Finally, when multiple wolves still remained, we randomly selected a wolf and removed the remaining individual(s). Such thinning of our data resulted in data from 33 wolves.

We further filtered the GPS data in two ways. First, we included GPS data only for days that observation crews attempted to monitor the wolf pack (i.e., rarely, severe weather events precluded ground-based monitoring for a day). Next, we included only daylight wolf GPS locations that occurred well after or before sunrise and sunset, respectively, by including GPS locations acquired only from the 09:00 – 16:00 hours during early winter (mid-month sunrise ≈ 07:40 and sunset ≈ 16:45) and the 08:00 – 18:00 hours during late winter (mid-month average of sunrise ≈ 06:30 and sunset ≈ 18:30). Data on sunrise and sunset were obtained from the United States Naval Observatory (http://aa.usno.navy.mil/data). GPS data was recorded at varying intervals, although most collars recorded a location each hour. On average, we included nine successfully acquired locations per wolf per day. Overall, GPS location fix success was high, with GPS collars successfully recording a location 98.0% of the time (11,999 of 12,243 possible locations). We determined whether the wolf group containing the GPS-collared wolf was observed or not observed when a GPS location was recorded through comparing our daily observations to each acquired wolf GPS location. Of the 11,999 included GPS locations, 3,082 were observed, and 8,917 were unobserved.

### WOLF SIGHTABILITY MODEL

For each GPS location, we included covariates that we hypothesized may affect the observation of the wolf group in a logistic regression framework (Hosmer and Lemeshow 2000).

The first covariate that we included was wolf group size (*group size*), which represented the number of wolves 'present', not necessarily the number of wolves seen at the precise time when the GPS collar recorded the spatial location. We did not record group size for 46 of 3,082 observed locations, and we were unable to observe group size for the 8,917 unobserved locations. For these 8,963 locations (i.e., the 46 observed and 8,917 unobserved locations), we assigned group size in the following manner. First, if the wolf group was both observed on the day and had only one group size recorded for the day, we assigned this group size. Next, if wolves were observed on the day but group size differed during the day (36 of 696 observed wolf group days), we assigned the mean group size. Finally, when we did not observe the wolf pack on a given day, we randomly sampled with replacement from the daily values of the single-daily and mean group sizes for that pack during that study period.

We also included covariates that described the distance from the nearest road or observation point [*distance*], openness [*openness*], and whether the location was "viewable" [*viewshed*]. These spatial covariates were extracted from Geographic Information System layers in Program R (version 3.4.1; R Core Team 2017) using the package raster (Hijmans et al. 2015; we converted all continuous covariates to rasters).

A road transecting the study area, and plowed during winter, was our main observation platform (Fig. 3-1). Observation crews occasionally used an additional section of the road, dependent on the specific movements of a pack and road conditions (Fig. S3-A.1). Additionally, observation crews took advantage of various higher-elevation observation points, typically located near the road (Fig. 3-1a). Some of these observation points were commonly used, while others were less commonly used because they were physically difficult to reach. For simplicity, we considered only the two roads (i.e., minimum or maximum; Fig. 3-1a) and the 17 common observation points (Fig. 3-1a; but see Appendix S3-B). Two of these 17 observation points were included only through the winter of 2008 – 2009 because observation crews did not use these after Montana wolf harvest seasons were implemented (see below). These roads and observation points affected the values of *distance* and *viewshed*.

For *distance*, we determined the minimum distance (measured in kilometers) to the road (i.e., minimum or maximum) used by the observation crew for a pack during a particular study period (hereafter, 'pack-road') or a common observation point. We similarly determined whether the wolf location was in (1) or out (0) of a model-predicted viewshed (Fig. 3-1a). We created our viewshed layers with the Viewshed 2 tool in ArcGIS version 10.3.1 and Digital Elevation Model layers of our study area (pixel size equal to ~9.7 meters). We set the observer offset to 2m (assuming an observer height of 2m), the vertical upper and lower angles to -90 to +90, respectively (assuming an observer could look up and down), and the maximum viewable distance to 6 miles (i.e., ~9.66 km), nearly equivalent to the maximum distance where wolves were observed.

Openness values ranged from 0 – 289 and characterized the openness of a 500 x 500 m window, with the pixel as the central location (0 = heavily forested, 289 = fully open; see Kohl et al. 2018; Fig. 3-1b). Vegetation data from the LANDFIRE program (landfire.gov) for all available years (2001, 2008, 2010, 2012, 2014) was used to create the openness layers (2001 for 1995–2005, 2008 for 2006–2009, 2010 for 2010–2011, 2012 for 2012–2013, and 2014 for 2014–2017).

Lastly, we included a covariate that described whether a wolf was harvested from the pack during the immediately preceding or ongoing hunting season because previous work has suggested that wolf harvest affects the number of wolf sightings in Yellowstone (Borg et al.

2016). Wolf harvest became seasonally legal in the autumn of 2009, and has been so since (with the exception of the winter of 2010-2011). Human harvest is permissible only outside of YNP, and was often limited by a quota in the relevant geographic area (see Fig. 3-1c and Smith et al. 2016). Most harvest that affected wolves in our study occurred in Montana, where the harvest season generally began in September and lasted through March, unless the quota was filled. The time and location of wolf harvest events were reported to the governing state wildlife agency, and, together with that agency, we used near daily observations of pack movements and counts to assign harvests as having occurred within a pack that commonly frequented Yellowstone National Park. We assigned harvest as having occurred in a pack beginning on the day after the initial harvest event for each pack, and allowed the potential effect of harvest to continue throughout winter.

We estimated wolf group sightability with the logistic link function in the package lme4 (Bates et al. 2014) using mixed-effect logistic regression models (binomial; observed = 1, unobserved = 0; random effect for ‘pack’ and ‘biological year’) through comparing GPS locations where wolf groups were observed to GPS locations where wolf groups were not observed (Gillies et al. 2006), akin to a true used-unused Resource Selection Probability Function (RSPF) design (Manly et al. 2002). Our specific model was:

$$P(\text{wolf group sighting}) = \text{logit}(\beta_{0i} + \beta_{1i}\,\textit{viewshed} + \beta_{2i}\,\textit{distance} + \beta_{3i}\,\textit{openness} + \beta_{4i}\,\textit{group size} + \beta_{5i}\,\textit{harvest} + \varepsilon_i). \quad \text{Eq. 1}$$

where $\beta_x$ is the effect of that covariate’s coefficient on the probability of observing the wolf group at wolf location $i = 1 \ldots n$, $\varepsilon$ is the error, and $\beta_0$ is the baseline probability of observing the wolf group containing the GPS-collared wolf independent of covariates because of the true used-unused (observed-unobserved) design (Manly et al. 2007).

We screened for association and collinearity among covariates, of which we found none (e.g., maximum $r = |0.19|$). We scaled continuous covariates to facilitate model convergence, evaluation of covariate effects, and comparison among models. We created a-priori candidate model sets based on the hypothesized importance of our covariates. We created all combinations of additive models using *viewshed*, *openness*, *distance*, *group size*, and *harvest*. We did not include models with interactions because they increased complexity without improving model-based predictions (*unpublished data*). We evaluated the models in the package 'AICcmodavg' (Mazerolle 2017) using Bayesian Information Criterion (BIC). We used BIC instead of AIC (Akaike Information Criterion) due to its superior performance in identifying the best model when data is abundant (Aho et al. 2014), as was the case with our GPS data.

We evaluated the performance of the top models using standard logistic regression diagnostics, and report overall classification success, sensitivity (probability of correctly classifying observed locations), specificity (probability of correctly classifying unobserved locations), and the Area Under the Curve (AUC) that measures overall model performance (values of 0.7 – 0.8 suggest acceptable discrimation, while values of 0.8 – 0.9 suggest excellent discrimination; Hosmer and Lemeshow 2000). Finally, we externally validated our top-ranked wolf sightability model. To do so, we predicted the response, p(sighting), for an "average" pack (i.e., re.form = NA) for 1,258 GPS locations from the winter of 2018–2019 ($n = 5$ packs; again limited to a single wolf per pack). We then used the optimal cutpoint to evaluate classification success, sensitivity, and specificity.

## RESULTS

### COVARIATES AFFECTING SIGHTABILITY

The 3,082 observed locations were, on average, 2.3 km (± 0.02 SE) from the closest road or common observation point, while the 8,917 unobserved locations were 3.3 km (± 0.03 SE) away (Fig. S3-A.2). Mean openness values were 215 (± 1.1 SE) and 156 (± 0.9 SE) for the observed and unobserved locations, respectively. Of the 3,082 observed locations, 2,671 (86.7%) were in "viewable" locations (i.e., *viewshed* = 1). Conversely, 4,897 of 8,917 (54.9%) unobserved locations were in "viewable" locations. Finally, of the 49 wolf pack-study periods in our observed-unobserved data set, 9 experienced a harvest event (Fig. S3-A.1).

### OBSERVED-UNOBSERVED WOLF SIGHTABILITY MODEL

The top wolf sightability model included viewshed, distance, openness, and group size, as well as the random effects for pack and biological year (i.e., winter). Harvest was not included in our top model. Among our candidate models, the top model was strongly supported, with 97% of the BIC weight (Table S3-A.1). The beta coefficients for the top model, all of which were significant (Fig. 3-2), indicated a positive effect of viewshed ($\beta = 1.37$; Odds Ratio [OR] = 3.95 [95% CI: 3.49, 4.47]), openness ($\beta = 0.81$; OR = 2.25 [2.13, 2.39]), and group size ($\beta = 0.23$; OR = 1.26 [1.19, 1.34]) on the probability of sighting a wolf group. Conversely, distance had the expected negative effect ($\beta = -0.56$; OR = 0.57 [0.52, 0.63]). The combined influence of these covariates resulted in, for example, the probability of seeing a group of 12 wolves that were in a location that was viewable, fairly open (openness = 242), and 500 m from the nearest observer location that was approximately 14 times greater than seeing a group of 6 wolves in a location that was non-viewable, fairly forested (openness = 112), and 3 km from the nearest observer location (Fig. 3-3).

### PREDICTIONS: THE CONFUSION MATRIX, SPACE, AND TIME

Our top model showed excellent discriminatory power as the AUC was 0.80 (Table 3-1). Using the optimal cutpoint (see Table 3-1), we predicted whether each observation in our data set was observed or unobserved (Fig. 3-4a). Upon doing so, 72% of wolf GPS locations were correctly predicted (Table 3-1). Sensitivity (i.e., the correct prediction of 1s) was 0.77, while specificity (i.e., the correct prediction of 0s) was 0.70 (Table 3-1).

Our external validation of the top model similarly suggested that this model did a good job of predicting whether a GPS-collared wolf group would be observed. Specifically, 76% of the 1,258 GPS locations were correctly predicted, with a sensitivity of 0.79 and a specificity of 0.74 (Table 3-1).

Of course, an end-product from our sightability model is a map of northern YNP that visualizes the variation in where wolves were most, and least, likely to be seen (Fig. 3-4b). But whether wolves were observed is the product of this sightability map (or a representation of it that varied across time; see Appendix S3-C) and the probability that a wolf group was in a sightable location. We therefore used the predictions from our observed-unobserved model to show how wolves were less likely, over time, to be in spatial locations where they were predicted to be observed (i.e., where the prediction for each wolf GPS location was greater than the optimal cutpoint; Table 3-1). This pattern was clearer if the data from the earliest years, when sample sizes were smallest, were ignored (Fig. 3-5).

## DISCUSSION

Our study showed how wolf group sightability was driven by both ecological (i.e., forest cover, group size) and landscape (i.e., topography, distance) factors (Figs. 3-2, 3-3, 3-4), but not human harvest (Table S3-A.1). Viewshed, followed by openness and then distance, most affected the success of our ground-based observation attempts (Fig. 3-2). In our case, the relative importance of distance was likely influenced by our use of high-powered spotting scopes. But our results nonetheless suggest that distance, most commonly employed in sightability models (Buckland et al. 2001), may not always be the most important factor affecting detection. Ultimately, our work highlights how sightability of large carnivores is substantially and intuitively affected by multiple factors, and that accounting for these factors may be important for reducing bias in observational-based studies.

Larger group sizes increase the search image for an observer, and while group size did have a positive effect on sightability, its importance was much less than other factors (Fig. 3-2). The relatively small effect of wolf group size tends to differ from previous work with other species. For example, even small changes in group size (i.e., from one to two individuals) may double boat-based detection of whales (Williams et al. 2016), and aerial detection has been estimated to be essentially one once group size reaches at least fifteen in elk (Samuel et al. 1987). Group size may more strongly influence large carnivore detection when snow is not commonly present in a study area or for a species such as the spotted hyena (*Crocuta crocuta*) that tends to live in much larger groups (Kruuk 1972). Determining whether group size does more substantially influence detection in other instances could be useful for other applications, such as estimating abundance from camera traps (Burton et al. 2015).

Our sightability model correctly classified 72% of wolf GPS locations in our original dataset as being observed or not, indicating strong predictive power (Table 3-1). This classification success occurred despite our model deriving the viewshed and distance covariates from fixed observer locations (Appendix S3-B). Further, observation success or failure was also affected by stochastic events such as heavy snowfall while the collar was recording a fix, which we could not include in our sightability model. Despite these limitations, our model performed similarly well during our external validation, correctly predicting 76% of the 1,258 locations. This strong validation of our model indicates its usefulness in predicting wolf sightability in northern YNP, and that models developed for other large carnivore populations could be similarly useful.

Factors that affected wolf sightings changed relatively little over time in our system (Fig. S3-A.3), but we observed a general temporal decline in wolf use of sightable locations (Fig. 3-5). At least three relevant changes during our study period could explain this pattern. The first two, declining wolf and elk abundance, are linked together through the numeric response of predator-prey dynamics (i.e., wolf abundance changes in response to prey abundance; Messier 1994). In turn, GPS-collared wolf territory sizes have increased over time in northern YNP (Fig. S3-A.4; Kittle et al. 2015), which results in many territories including more area further from the road and out of the viewshed. Any effect of elk on wolf use of sightable locations also likely resulted from changes in elk (and other prey) distribution across northern Yellowstone (White et al. 2012, White et al. 2015). Wolves' increased use of bison in northern YNP (Metz et al. 2016) further complicates wolf sightability in northern YNP.

The last relevant change was the implementation of a wolf harvest season outside of YNP (Smith et al. 2016). A harvest effect has been suggested by previous work evaluating wolf sightings during summer in YNP (Borg et al. 2016) and elsewhere where wolves are subject to harvest (Thurber et al. 1994, Hebblewhite and Merrill 2008, Borg et al. 2016). We, however, found no effect of human harvest on wolf sightability during winter, seemingly indicating that wolf packs did not display substantial behavioral changes following a harvest event that had any lasting (i.e., throughout winter) effect on wolf sightability when a wolf group was in a similar covariate space. Moreover, GPS-collared wolves used spatial locations outside of YNP more frequently in recent years (black dashes in Fig. 3-5), although we did not account for whether harvest seasons were ongoing. This pattern of increased use of locations outside of YNP, along with concurrent shifts in elk abundance (White et al. 2012), suggests elk abundance and distribution could in fact be the driving force behind the general temporal decline of wolf use of sightable spatial locations during winter. It is difficult, however, to tease apart these three effects (elk and wolf abundance, hunting) because each have occurred concurrently and, in the case of wolf and elk abundance, are clearly linked. We should also note that some of our results could be affected by the distribution of wolf GPS collars, although our inclusion of a random effect for the baseline sighting of a wolf pack minimized this potential effect. Similarly, the random effect for biological year also minimized the effect of other factors that likely affected wolf sightability, such as fine-scale temporal variation in snow cover.

In addition to our observed-unobserved logistic regression model, we developed a similar observed-available logistic regression model (Appendix S3-B), which is the model structure that researchers without GPS data would need. The top-ranked observed-available model was similar, but did not include group size (Table S3-B.1). The most important difference between the observed-unobserved and observed-available model was how the relative strengths of the remaining beta coefficients differed (Fig. S3-B.3). Likely due to the strength of viewshed being markedly different, the observed-unobserved model was far superior in its overall classification success (Table S3-B.2). Our results nonetheless suggest that other researchers could develop carnivore sightability models without concurrent GPS data, which could be useful in study areas where cost and/or sample size limit the use of GPS data.

Our observed-unobserved model was developed with data collected over a nearly two-decade period. During that time, hundreds of thousands of park visitors have viewed wolves. Our results show that the potential to successfully observe wolves has differed across time (Fig. 3-5), but where on the landscape wolves are most sightable is essentially ‘fixed’ by the covariates that most strongly affect sightability (Fig. 3-2). Our model could therefore be used to identify areas of future development that enhance visitor experience, while minimizing any negative visitor effect on wolves. Visitation to YNP to attempt to observe wolves is not trivial. In fact, a decade ago when there were ~3 millions visitors (2018: ~4.1 million visitors), Duffield et al. (2008) estimated that ~300,000 visitors observed wolves annually, and that these ~300,000 visitors (plus those who had hoped to observe wolves) brought ~35 million dollars annually to local economies (Duffield et al. 2008). These observations, however, often result in ‘wildlife jams’ that present significant management challenges to YNP staff (Haroldson and Gunther 2013); the use of our spatial predictions (Fig. 3-4b) would allow for easy identification of appropriate places to increase vehicle parking that could reduce these management challenges, for example.

Wolf group sightability was predictably affected by factors (viewshed, openness, distance) related to the study area and, to a lesser extent, the species’ ecology (group size). Previous work in our system identified that only distance affected ground-based detection of wolf-killed prey (Smith et al. 2004); but our sightability model suggests that distance would not necessarily be the most important covariate in an updated version of this kill-recovery model. Moreover, given that the potential to view wolves and their interactions with each other and other species varies through time (Fig. 3-5), our work also suggests that future work in our system may need to explicitly account for the imperfect observation process. Temporal evaluation of wolf-prey (Martin et al. 2018) or wolf-wolf (Cubaynes et al. 2014) interactions may be affected by temporal changes in observation success, for example. The importance of including sightability models in large carnivore observation-based studies would seemingly extend to other systems as well, such as African large carnivore-prey systems. Given the frequency with which GPS collars are now used, such work could similarly develop detection models such as ours to account for large carnivore sightability.

## ACKNOWLEDGEMENTS

We thank E. Stahler for data management, B. Cassidy for GIS assistance, and P. Mahoney for statistical advice. We also thank A. Nelson (Montana Fish Wildlife and Parks) and K. Mills (Wyoming Game and Fish) for their assistance in assigning pack affiliation for harvested wolves. Finally, we thank all of the Yellowstone winter study field technicians who dedicatedly collected the observational data that was the foundation of this work. Our work was supported by Yellowstone Forever (Tapeats Fund, Valerie Gates, Frank and Kay Yeager, many individual donors), National Science Foundation (NSF) Long Term Research in Environmental Biology grants DEB-0613730 (D.W.S) and DEB-1245373 (D.R.S and D.W.S.). M.C.M. was also supported by the Wesley M. Dixon Graduate Fellowship and Bertha Morton Scholarship from the University of Montana and a Graduate Enhancement Fellowship from the Montana Institute on Ecosystems funded through NSF Established Program to Stimulate Competitive Research (EPSCOR).

## LITERATURE CITED

Aho, K., D. Derryberry, and T. Peterson. 2014. Model selection for ecologists: the worldviews of AIC and BIC. Ecology **95**:631-636.

Bates, D., M. Maechler, B. Bolker, and S. Walker. 2014. lme4: Linear mixed-effects models using Eigen and S4. R package version **1**:1-23.

Bissett, C., and R. T. F. Bernard. 2007. Habitat selection and feeding ecology of the cheetah (Acinonyx jubatus) in thicket vegetation: is the cheetah a savanna specialist? Journal of Zoology **271**:310-317.

Bonney, R., C. B. Cooper, J. Dickinson, S. Kelling, T. Phillips, K. V. Rosenberg, and J. Shirk. 2009. Citizen science: a developing tool for expanding science knowledge and scientific literacy. Bioscience **59**:977-984.

Borg, B. L., S. M. Arthur, N. A. Bromen, K. A. Cassidy, R. McIntyre, D. W. Smith, and L. R. Prugh. 2016. Implications of harvest on the boundaries of protected areas for large carnivore viewing opportunities. Plos One **11**:e0153808.

Buckland, S. T., D. R. Anderson, K. P. Burnham, J. L. Laake, D. L. Borchers, and L. Thomas. 2001. Introduction to distance sampling: estimating abundance of biological populations. Oxford University Press, New York.

Burton, A. C., E. Neilson, D. Moreira, A. Ladle, R. Steenweg, J. T. Fisher, E. Bayne, and S. Boutin. 2015. Wildlife camera trapping: a review and recommendations for linking surveys to ecological processes. Journal of Applied Ecology **52**:675-685.

Cassidy, K. A., D. R. MacNulty, D. R. Stahler, D. W. Smith, and L. D. Mech. 2015. Group composition effects on aggressive interpack interactions of gray wolves in Yellowstone National Park. Behavioral Ecology **26**:1352-1360.

Cassirer, E. F., D. J. Freddy, and E. D. Ables. 1992. Elk responses to disturbance by cross-country skiers in Yellowstone National Park. Wildlife Society Bulletin **20**:375-381.

Creel, S., and N. M. Creel. 2002. The African wild dog: behavior, ecology, and conservation. Princeton University Press, Princeton.

Cubaynes, S., D. R. MacNulty, D. R. Stahler, K. A. Quimby, D. W. Smith, and T. Coulson. 2014. Density-dependent intraspecific aggression regulates survival in northern Yellowstone wolves (*Canis lupus*). Journal of Animal Ecology **83**:1344-1356.

Duffield, J. W., C. J. Neher, and D. A. Patterson. 2008. Wolf recovery in Yellowstone: park visitor attitudes, expenditures, and economic impacts. The George Wright Forum **25**:13-19.

Farhadinia, M. S., R. J. Moll, R. A. Montgomery, S. Ashrafi, P. J. Johnson, L. T. B. Hunter, and D. W. Macdonald. 2018. Citizen science data facilitate monitoring of rare large carnivores in remote montane landscapes. Ecological indicators **94**:283-291.

Gillies, C. S., M. Hebblewhite, S. E. Nielsen, M. A. Krawchuk, C. L. Aldridge, J. L. Frair, D. J. Saher, C. E. Stevens, and C. L. Jerde. 2006. Application of random effects to the study of resource selection by animals. Journal of Animal Ecology **75**:887-898.

Hain, J., S. Ellis, R. D. Kenney, and C. K. Slay. 1999. Sightability of right whales in coastal waters of the southeastern United States with implications for the aerial monitoring program. Pages 191-207 *in* G. Garner, S. Amstrup, J. Laake, B. Manley, L. McDonald, and D. Robertson, editors. Marine mammal survey and assessment methods. A.A. Balkema, Rotterdam, The Netherlands.

Haroldson, M. A., and K. A. Gunther. 2013. Roadside bear viewing opportunities in Yellowstone National Park: characteristics, trends, and influence of whitebark pine. Ursus **24**:27-41.

Harrell Jr, F. E. 2001. Regression modeling strategies: with applications to linear models, logistic regression and survival analysis. Springer, New York.

Hebblewhite, M., and E. Merrill. 2008. Modelling wildlife–human relationships for social species with mixed-effects resource selection models. Journal of Applied Ecology **45**:834-844.

Hijmans, R., J. van Etten, J. Cheng, M. Mattiuzzi, M. Summer, J. Greenberg, O. Lamigueiro, A. Bevan, E. Racine, and A. Shortridge. 2015. Package 'raster'. R package.

Hosmer, D. W., and S. Lemeshow. 2000. Applied Logistic Regression. Wiley, New York.

Houston, D. B. 1982. The Northern Yellowstone Elk: Ecology and Management. Macmillan Publishing, New York.

Hutto, R. L. 2016. Should scientists be required to use a model-based solution to adjust for possible distance-based detectability bias? Ecological Applications **26**:1287-1294.

Kays, R., M. C. Crofoot, W. Jetz, and M. Wikelski. 2015. Terrestrial animal tracking as an eye on life and planet. Science **348**:aaa2478.

Kittle, A. M., M. Anderson, T. Avgar, J. A. Baker, G. S. Brown, J. Hagens, E. Iwachewski, S. Moffatt, A. Mosser, and B. R. Patterson. 2015. Wolves adapt territory size, not pack size to local habitat quality. Journal of Animal Ecology **84**:1177-1186.

Kohl, M. T., D. R. Stahler, M. C. Metz, J. D. Forester, M. J. Kauffman, N. Varley, P. White, D. W. Smith, and D. R. MacNulty. 2018. Diel predator activity drives a dynamic landscape of fear. Ecological Monographs **88**:638-652.

Kruuk, H. 1972. The spotted hyena: a study of predation and social behavior. University of Chicago Press, Chicago.

MacNulty, D. R., D. W. Smith, L. D. Mech, and L. E. Eberly. 2009. Body size and predatory performance in wolves: is bigger better? Journal of Animal Ecology **78**:532-539.

Manly, B. F. L., L. McDonald, D. Thomas, T. L. McDonald, and W. P. Erickson. 2007. Resource selection by animals: statistical design and analysis for field studies. Springer Science & Business Media.

Martin, H. W., L. Mech, J. Fieberg, M. Metz, D. MacNulty, D. Stahler, and D. Smith. 2018. Factors affecting gray wolf (Canis lupus) encounter rate with elk (Cervus elaphus) in Yellowstone National Park. Canadian Journal of Zoology **96**:1032-1042.

Mazerolle, M. J. 2017. AICcmodavg: model selection and multimodel inference based on (Q) AIC (c). R package version **2.1.1**.

Messier, F. 1994. Ungulate population models with predation: a case study with the North American moose. Ecology **75**:478-488.

Metz, M. C., D. J. Emlen, D. R. Stahler, D. R. MacNulty, D. W. Smith, and M. Hebblewhite. 2018. Predation shapes the evolutionary traits of cervid weapons. Nature Ecology & Evolution **2**:1619-1625.

Metz, M. C., D. W. Smith, D. R. Stahler, J. A. Vucetich, and R. O. Peterson. 2016. Temporal variation in wolf predation dynamics in Yellowstone: lessons learned from two decades of research. Yellowstone Science **24**:55-60.

Metz, M. C., D. W. Smith, J. A. Vucetich, D. R. Stahler, and R. O. Peterson. 2012. Seasonal patterns of predation for gray wolves in the multi-prey system of Yellowstone National Park. Journal of Animal Ecology **81**:553-563.

Mills, M., L. S. Broomhall, and J. T. du Toit. 2004. Cheetah Acinonyx jubatus feeding ecology in the Kruger National Park and a comparison across African savanna habitats: is the cheetah only a successful hunter on open grassland plains? Wildlife Biology **10**:177-186.

Naidoo, R., and W. L. Adamowicz. 2005. Economic benefits of biodiversity exceed costs of conservation at an African rainforest reserve. Proceedings of the National Academy of Sciences **102**:16712-16716.

Newsome, D., R. K. Dowling, and S. A. Moore. 2005. Wildlife tourism. Channel View Publications, Clevedon.

Patzelt, A., G. H. Kopp, I. Ndao, U. Kalbitzer, D. Zinner, and J. Fischer. 2014. Male tolerance and male–male bonds in a multilevel primate society. Proceedings of the National Academy of Sciences **111**:14740-14745.

Peters, W., M. Hebblewhite, K. G. Smith, S. M. Webb, N. Webb, M. Russell, C. Stambaugh, and R. B. Anderson. 2014. Contrasting aerial moose population estimation methods and evaluating sightability in west-central Alberta, Canada. Wildlife Society Bulletin **38**:639-649.

Ripple, W. J., J. A. Estes, R. L. Beschta, C. C. Wilmers, E. G. Ritchie, M. Hebblewhite, J. Berger, B. Elmhagen, M. Letnic, and M. P. Nelson. 2014. Status and ecological effects of the world's largest carnivores. Science **343**:1241484.

Samuel, M. D., E. O. Garton, M. W. Schlegel, and R. G. Carson. 1987. Visibility bias during aerial surveys of elk in northcentral Idaho. The Journal of Wildlife Management **51**:622-630.

Schaller, G. B. 1972. The Serengetti lion: a study of predator-prey relations. University of Chicago, Chicago.

Smith, D. W., T. D. Drummer, K. M. Murphy, D. S. Guernsey, and S. B. Evans. 2004. Winter prey selection and estimation of wolf kill rates in Yellowstone National Park, 1995–2000. Journal of Wildlife Management **68**:153-166.

Smith, D. W., P. White, D. R. Stahler, A. Wydeven, and D. E. Hallac. 2016. Managing wolves in the Yellowstone area: Balancing goals across jurisdictional boundaries. Wildlife Society Bulletin **40**:436-445.

Steenweg, R., M. Hebblewhite, R. Kays, J. Ahumada, J. T. Fisher, C. Burton, S. E. Townsend, C. Carbone, J. M. Rowcliffe, and J. Whittington. 2017. Scaling-up camera traps: Monitoring the planet's biodiversity with networks of remote sensors. Frontiers in Ecology and the Environment **15**:26-34.

Sun, C. C., J. A. Royle, and A. K. Fuller. 2019. Incorporating citizen science data in spatially explicit integrated population models. Ecology **100**:e02777.

Thurber, J. M., R. O. Peterson, T. D. Drummer, and S. A. Thomasma. 1994. Gray wolf response to refuge boundaries and roads in Alaska. Wildlife Society Bulletin **22**:61-68.

van Strien, A. J., C. A. van Swaay, and T. Termaat. 2013. Opportunistic citizen science data of animal species produce reliable estimates of distribution trends if analysed with occupancy models. Journal of Applied Ecology **50**:1450-1458.

White, P., K. M. Proffitt, and T. O. Lemke. 2012. Changes in elk distribution and group sizes after wolf restoration. The American Midland Naturalist **167**:174-187.

White, P. J., R. L. Wallen, and D. E. Hallac. 2015. Yellowstone Bison: Conserving an American Icon in Modern Society, Yellowstone National Park.

Williams, S. H., S. M. Gende, P. M. Lukacs, and K. Webb. 2016. Factors affecting whale detection from large ships in Alaska with implications for whale avoidance. Endangered Species Research **30**:209-223.

## TABLES.

**Table 3-1. Classification success of wolf sightability model.** Row for ‘Model’ reports the classification success of the observed-unobserved data that was used to develop the wolf sightability model, while the row for ‘Validation’ reports the classification success for the external validation. ‘Locations’ indicates the total number of locations in the dataset, ‘Predict’ indicates the number of locations correctly predicted as a 1 (i.e., above the cutpoint), and ‘Prop. correct’ is the proportion of total locations correctly predicted. Specificity indicates the proportion of 0 (i.e., unobserved) locations correctly predicted, and, sensitivity, the same for 1 (i.e., observed) locations.

| Dataset | Locations | Predict | Prop. correct | AUC | Cutpoint | Specificity | Sensitivity |
|---|---|---|---|---|---|---|---|
| Model | 11999 | 8620 | 0.72 | 0.80 | 0.26 | 0.70 | 0.77 |
| Validation | 1258 | 955 | 0.76 | - | - | 0.74 | 0.79 |

**FIGURES.**

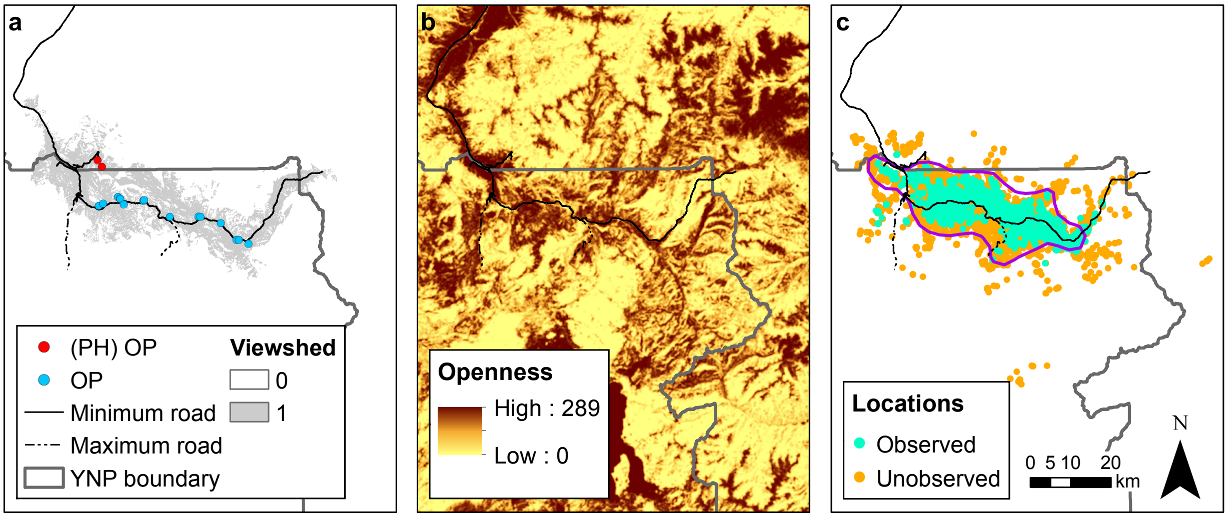

**Figure 3-1. Spatial distribution of observation points, covariates, and wolf GPS data.** Panels display (a) common observation points (OP; red circles indicate observation points used only before Montana wolf harvest season was implemented), the minimum and maximum road, viewshed (from the minimum road and all common observation points; 1 = viewshed-predicted viewable, 0 = viewshed-predicted not viewable), and the Yellowstone National Park boundary (roads and boundary shown in all panels), (b) openness (2001), and (c) wolf GPS locations (i.e., observed-unobserved wolf locations). Note that the purple line in panel (c) displays an 85% population-level utilization distribution that was used in Fig. 3-4.

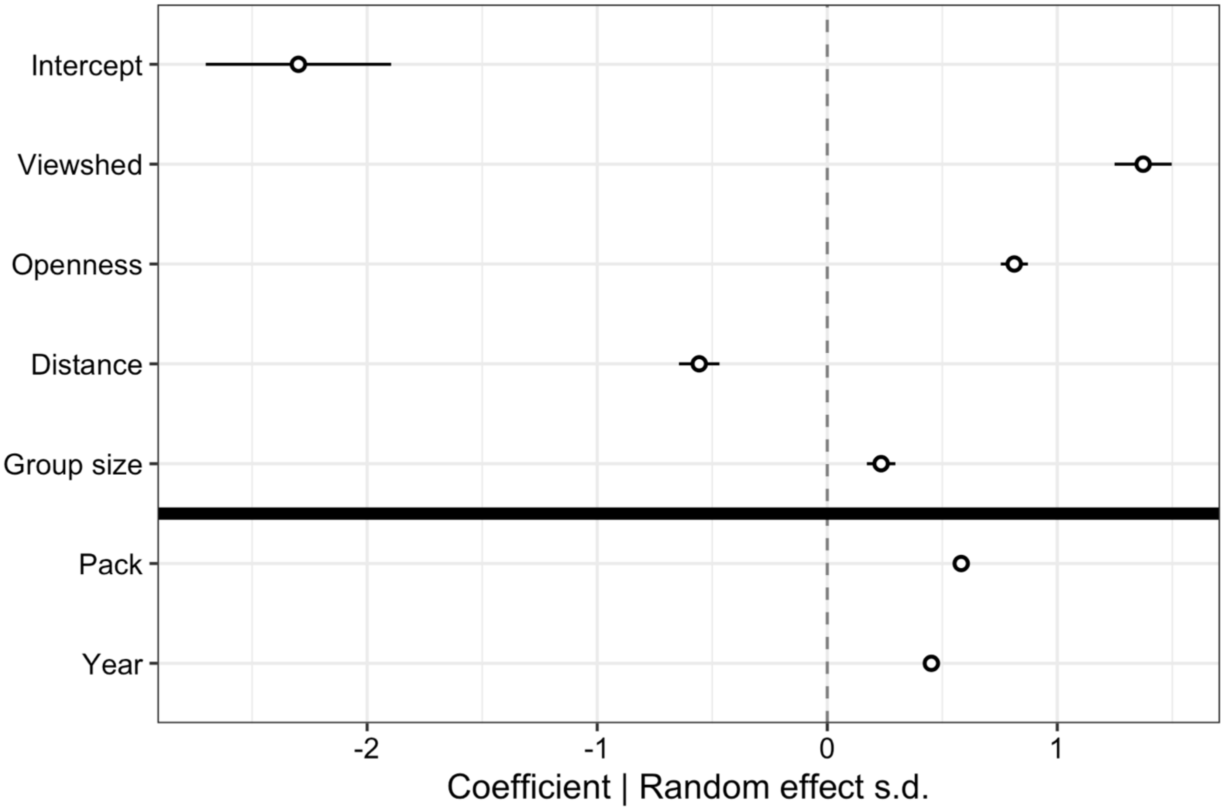

**Figure 3-2. Beta coefficient estimates for top-ranked wolf sightability model.** Error bars represent 95% confidence intervals. Below the solid black line displays the standard deviation for the random effects (pack, year), which is directly comparable to the beta coefficient strength (Harrell Jr 2001).

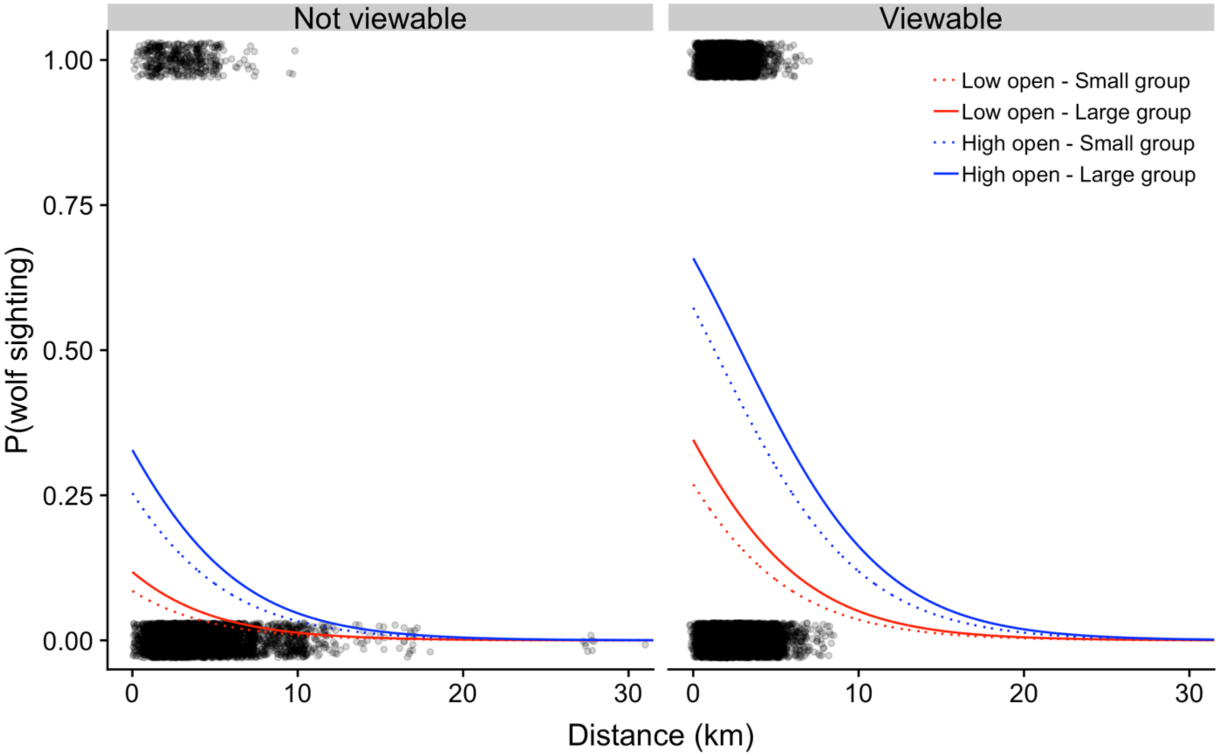

**Figure 3-3. Predicted probability of sighting a wolf group.** Values for low and high represent the lower and upper quartiles (openness: 111.5, 241.8; group size: 6, 12). The displayed low and high openness values describe moderately forested and pretty open areas, respectively.

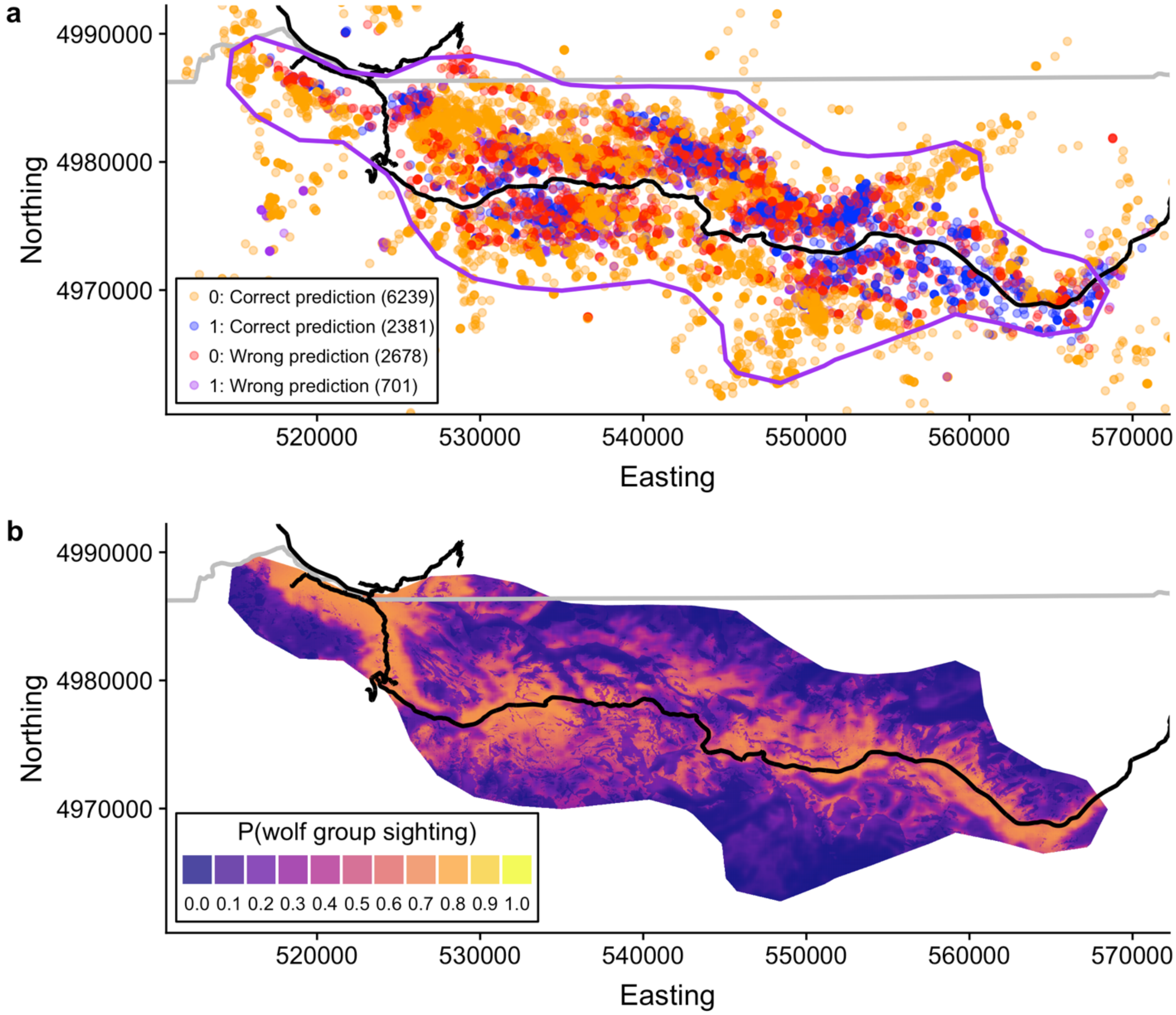

**Figure 3-4. Spatial predictions for wolf sightability model.** Panel (a) displays the classification success for model-based predictions for the actual data set, using the optimal cutpoint (see Table 3-1). The legend reports the confusion matrix for the 11,999 GPS locations. In panel (b), we used the beta coefficients to create spatial predictions (see further details in Appendix S3-C) for a pack that was monitored from the minimum road and common observation points (from before wolf harvest was implemented; see Fig. 3-1a), openness values from 2001 (see Fig. 3-1b), and the 'high' value for group size (12; see Fig. 3-3). Note that the purple line in panel (a) displays the 85% population-level utilization distribution that was used for panel (b), and that the black and gray line in each panel display the minimum road and Yellowstone National Park boundary, respectively.

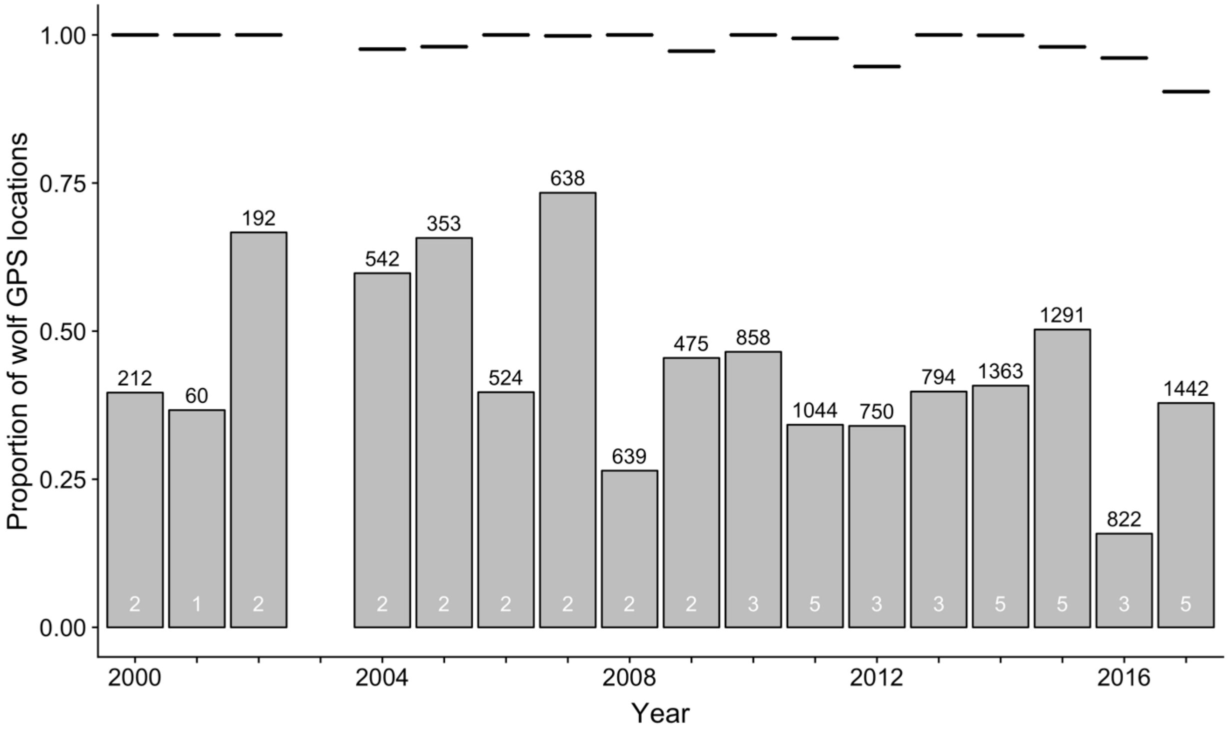

**Figure 3-5. Proportion of wolf GPS locations predicted to be sighted through time.** The white numbers along the x-axis indicate the number of wolf-study periods, and the black numbers on top of each bar indicate the total number of GPS locations acquired, during that winter (see also Fig. S3-A.1). Note that GPS collars generally attempted to record a fix once per hour beginning during the winter of 2004-2005 (year = 2004 on x-axis). Black dashes indicate the proportion of GPS locations inside of Yellowstone National Park.

# Chapter 4: Wolf predation dynamics differ over measures of space and time in the multi-prey system of Yellowstone National Park[3]

## INTRODUCTION

Predation is an ecological and evolutionary force that shapes individuals, populations, and ecosystems (Reznick and Endler 1982, Taylor 1984). Large carnivores often have disproportionately large ecological impacts via predation, despite their rarity and low densities (*cf*. Carbone and Gittleman 2002, Ripple et al. 2014). For example, the effects that large carnivores may exert on prey (and other predator) populations can have cascading effects on ecosystem structure and function (Levi and Wilmers 2012, Ripple et al. 2014). Despite their important ecological role, however, many large carnivores have declined in their range and abundance, largely through direct and indirect conflicts with humans (Ripple et al. 2014). Large carnivore-human conflict may arise because they often kill ungulates that humans raise as livestock or hunt (Treves and Karanth 2003). Such conflict can lead to management that reduces large carnivore populations, but whether these actions lead to the desired increase in ungulate populations is often unclear (Clark and Hebblewhite 2021). Moreover, many ecosystems become ecologically downgraded when predation is functionally absent (Estes et al. 2011). Conserving large carnivores would benefit from further understanding the ecological drivers of their predation metrics (e.g., predator diet, kill rate) to assess predator-prey dynamics (Berryman 1992) and ecosystem impacts of predation. Moreover, knowledge from long-term studies is critical because conclusions from short-term studies often vary widely (Vucetich et al. 2010),

---

[3] Authorship is tentatively proposed as: Matthew C. Metz, Douglas W. Smith, Paul M. Lukacs, Sara H. Williams, Daniel R. Stahler, Daniel R. MacNulty, Mark Hebblewhite. Manuscript is generally prepared for submission as a *Wildlife Monograph* for publication.

because of the stochastic nature of predation. Yet, long-term studies of large carnivore predator-prey dynamics are rare (Gittleman et al. 2001).

Predator-prey dynamics are theoretically driven by how frequently a predator kills their prey in relation to prey abundance (i.e., the predator's functional response) and how many of these predators live in a system (i.e., the predator's numerical response). Describing the first component, the functional response, is challenging for wide-ranging large carnivores for many reasons, including that most large carnivores live in complex systems with multiple prey and multiple predators, despite the tendency to simplify these systems to single predator-single prey dynamics (Montgomery et al. 2019). Estimating how frequently predators kill each prey species is therefore important to evaluate how large carnivore predation influences prey species abundance. Describing the latter component, the numerical response, requires estimating predator abundance, and some fundamental differences in the numerical response are expected in systems with multiple prey species. From the predator's perspective, the total functional response (i.e., including all species) describes how frequently the predator acquires the food that theoretically affects their numerical response (Holling 1959, Messier 1994). Alternative prey in multi-prey environments may therefore increase the number of predators in relation to their primary prey, particularly at lower primary prey abundances (Messier 1995). Together, the functional and numerical responses describe the predator's total predation rate on a prey species (Holling 1959, Messier 1995). Predation rate – the proportion of the prey population killed by predators per unit time – is the predation metric that best describes the effect of predation on prey growth rate (Messier 1994, Vucetich et al. 2011). Ecological theory suggests predation rate is stabilizing to predator-prey dynamics when density dependent, has no stabilizing effect when density independent, and is destabilizing when inversely density dependent (Fig. 4-1; Sinclair and Pech 1996). Whether predation rate is density dependent, density independent, or inversely density dependent – as well as its slope or shape, linear or non-linear – can differ across prey abundance, resulting from precisely how the product of the functional and numerical responses differs across prey abundance (Messier 1995).

In multi-prey environments, estimating kill rate (i.e., the number of prey killed per predator per unit time; the y-axis of the functional response) for specific prey species first requires estimating predator diet. Predator diet describes how various prey (i.e., species, sex-age class) are used (e.g., killed), and essentially describes the predator's dietary niche (Grinnell 1917). Overall, this dietary niche is affected by a wide range of ecological and evolutionary factors that influence how frequently predators kill a particular prey. For example, the appearance of prey species in predator diet may be affected by migration (Fryxell and Sinclair 1988) and/or body size (Sinclair et al. 2003). In fact, prey and predator species body size are central factors that shape predation dynamics, with individual predator species often focusing on an 'ideal' body sized prey (Sinclair et al. 2003, Owen-Smith and Mills 2008). The less frequent killing of larger prey species is driven by the inherent risk(s) associated with hunting dangerous prey that predators sometimes take on, but seek to minimize (MacNulty et al. 2012). Prey body size alone, however, does not dictate predator diet because of the complex nature of the factors that affect prey vulnerability, such as prey age (Murie 1944, Peterson 1977, Pettorelli et al. 2011, Owen-Smith 2015). Juvenile prey are especially vulnerable and often comprise the largest portion of predator diet (Gervasi et al. 2015). Advanced age similarly predisposes prey to being killed by a large carnivore, especially coursing ones (*cf.* Wright et al. 2006, Sergeyev et al. 2021). The resultant diet of large carnivores is ultimately influenced by a complex set of factors, including size and age, that affects the relative vulnerability of prey to predators.

To what extent these factors associated with vulnerability jointly affect predation dynamics is also influenced by seasonality. Seasonal birth pulses of prey that are highly vulnerable to predation leads to seasonal peaks in carnivore diet of such young age classes (Linnell et al. 1995, Barber-Meyer et al. 2008, Sand et al. 2008, Knopff et al. 2010). Prey nutritional condition changes with seasonal changes in resource productivity and life history (Parker et al. 2009), mostly declining during winter in temperate northern ecosystems (Parker et al. 2009, Metz et al. 2012). Seasonality thus has a large effect on the type of prey killed by predators in northern temperate climates (Knopff et al. 2010, Metz et al. 2012, Wilmers et al. 2020), as well as the tropics (Owen-Smith 2008). Disparate use of prey types is expected to have important implications for how predators affect prey populations (e.g., Gervasi et al. 2012). Yet, it often remains largely unknown how predator diet varies over longer longitudinal time periods, and how variation in predator diet affects kill rate of large carnivores, especially in multi-prey communities.

Kill rate measures how frequently predators kill prey, i.e., the number of prey killed per predator per unit time. Kill rate is critical to understanding the impact of predators on prey because it *i*) is an essential component of predator-prey models as a part of the functional response (e.g., Holling 1959) and ii) can be used with predator abundance to empirically estimate predation rate (e.g., Vucetich et al. 2011, Peterson et al. 2014). Kill rate is affected by many factors beyond prey abundance, such as predator characteristics (Thurber and Peterson 1993, Nilsen et al. 2009, Knopff et al. 2010), interactions with competitors (Höner et al. 2002, Tallian et al. 2017a), and, in temperate climates, winter conditions (Huggard 1993) and/or seasonality (Nilsen et al. 2009, Knopff et al. 2010, Metz et al. 2012). Our understanding of ecological drivers of kill rate in multi-prey systems is, however, especially limited by the lack of long-term studies where relative availability of important prey species may display significant changes. For example, Messier's (1994) classic study of wolf kill rate of moose is a synthesis of single predator-single prey systems across snapshots in time from dozens of studies and may not reflect dynamics as densities of prey change within one specific system. Moreover, kill rate itself ignores an often overlooked secondary, but often important (Moleón et al. 2014, Pereira et al. 2014), component of diet for many large carnivores, scavenging.

Despite the importance of predation by large carnivores, interspecific, and even intraspecific, kleptoparasitism may also be a key process by which carnivores acquire food (Pereira et al. 2014, Prugh and Sivy 2020). Many large carnivores also frequently scavenge on carrion that did not originate through predation (Moleón et al. 2014, Pereira et al. 2014). Both of these forms of scavenging (kleptoparasitism, non-predation), can affect the rate that large carnivores kill prey (Höner et al. 2002, Moleón et al. 2014, Tallian et al. 2017a, Mellard et al. 2021). Moreover, if scavenging is important in a predator-prey system, overlooking scavenging could also lead to biases in the estimated effect of a predator on prey. For example, if some prey species are commonly scavenged, rather than killed, the strength of predation would be overestimated if large carnivores were assumed to have killed all prey they fed on. Consumption of scavenged carrion sometimes occurs in seasonal pulses (Moleón et al. 2014), and may be the primary manner some prey species (i.e., especially large prey) are consumed by carnivores because of constraints in their hunting ability (MacNulty et al. 2020a). For example, the largest ungulates rarely die from predation in the Serengeti Ecosystem (Sinclair et al. 2003). But when they do die (often of starvation) and are scavenged, they are a significant source of biomass to predators precisely because of their large size (Schaller 1972, Pereira et al. 2014). The death of large prey may also not directly influence the associated prey population in the sense that many of these losses arise from compensatory mortality (Errington 1946, Boyce et al. 1999). But associated benefits from scavenging to predator abundance could produce important effects on predator-prey dynamics, fostering, for example, apparent competition or apparent mutualism dynamics (Holt 1977, Holt and Bonsall 2017). Indeed, scavenging can alter predator-prey dynamics in a number of ways, including those that promote stability (Focardi et al. 2017, Mellard et al. 2021). Regardless of its origin, a key point remains that the effect of carrion on large carnivore abundance and predator-prey dynamics is often overlooked (Moleón et al. 2014).

Each of these metrics of large carnivore predation (i.e., predator diet, kill rate, scavenging rate) may also differ across longer time scales (e.g., decades) as populations of predators and prey change. For example, over a nearly three decade period wolves (*Canis lupus*) on Isle Royale had higher kill rates when wolves were increasing, compared to a subsequent time period when wolves declined (Post et al. 2002). In another example, following the elimination of rinderpest in the Serengeti Ecosystem, wildebeest (*Connochaetes taurinus*) and buffalo (*Syncerus caffer*) populations rapidly increased, and their prevalence in the diet of African lions (*Panthera leo*) and/or hyenas (*Crocuta crocuta*) also subsequently dramatically increased (Grange et al. 2004). Longitudinal changes such as those observed in the Serengeti Ecosystem could represent cases where a predator's niche breadth expands. Here, we view the dietary niche as an important component of the Grinnellian definition of the niche (Grinnell 1917, Hurlbert 1978). Such niche expansion, or contraction, would result from shifts in diet composition that could be the result of changes in the availability of prey that each vary in their vulnerability to predation and/or limitations in predator hunting ability (Newsome et al. 2009, Knopff et al. 2010, Tallian et al. 2017b). An additional consequence of within-population variation of predator diet is that sampling across a predator population may be necessary to better estimate predator diet for the population. Even this improvement, however, would still overlook whether various prey types (i.e., species, sex-age class) are represented in an unbiased manner among detected carcasses.

Unequal detection of prey in predator diet is a problem that has long plagued research of large carnivore predation. For example, continuous, but labor intensive, observation of large carnivores was sometimes needed to accurately estimate predation metrics such as diet and kill rate in geographic areas without snow (e.g., Schaller 1972, Mills and Shenk 1992). Detecting predation in areas with snow has been historically easier, and a substantial portion of the knowledge of large carnivore kill rate comes from temperate climates during winter (e.g., O'Donoghue et al. 1998). Wolves have been a major focus of predation studies in winter, using methodology that leveraged aerial observation and/or aerial snow back-tracking (Ballard et al. 1987, Hayes et al. 2000, Vucetich et al. 2002) or ground-based snow backtracking (Hebblewhite et al. 2003). Detection of predation events has typically been assumed to be perfect. While researchers often acknowledged that estimated kill rates represented minimum numbers, few attempted to correct this bias. Estimating kill rates have recently been improved through identifying and field-searching Global Positioning System (GPS) location clusters from radiocollared large carnivores (Anderson Jr. and Lindzey 2003, Merrill et al. 2010). But even GPS cluster methods have limitations imposed by smaller prey and the social dynamics of some large carnivores (Webb et al. 2008, Bacon et al. 2011, Metz et al. 2011). Mark-recapture methods, however, provide a generally applicable framework to estimate spatiotemporally variable ecological phenomenon. While often applied to estimate animal abundance, mark-recapture methods have only rarely been developed to estimate the number of large carnivore kills (e.g., Smith et al. 2004) by explicitly incorporating detection probability.

Detection probability is a thorn in the side of ecologists, but failing to account for its influence can result in biased estimates of ecological parameters (MacKenzie et al. 2002, Kellner and Swihart 2014). The primary way imperfect detection could manifest in studies of predation is to underestimate diet of more difficult to find prey species and/or sex-age classes, especially those of smaller body size (e.g., Smith et al. 2004, Webb et al. 2008). Landscape characteristics that render predation events more difficult to detect could similarly bias detection of predator kills (i.e., roads, topography; Buckland et al. 2001, Metz et al. 2020c). Few studies have estimated how detection probability affects the number of prey acquired (Smith et al. 2004, Metz et al. 2011), and none have attempted to estimate the demographic characteristics of undetected carcasses, at least to our knowledge. Because most ecological systems contain multiple prey species that predators use (Montgomery et al. 2019), detection of prey killed by carnivores will be imperfect and variable (Smith et al. 2004, Webb et al. 2008, Bacon et al. 2011, Lodberg-Holm et al. 2021). And because predators kill prey of differing reproductive value (e.g., Wright et al. 2006), just estimating the number of prey missed will result in a biased understanding of predator-prey relationships.

The wolf-prey system of Yellowstone National Park (YNP), USA provides a globally-relevant opportunity to evaluate the influence of time on predator-prey dynamics. Following wolf extirpation in the 1930's, wolves and their prey have been intensively studied since their reintroduction in 1995–1997 (Smith and Bangs 2009), which was conducted in large part to restore interactions with ungulate populations (Varley and Brewster 1992). Since reintroduction, ungulate populations have dramatically changed across time and in different ways in different areas of YNP. For example, the northern Yellowstone elk (*Cervus canadensis*) population has declined, and then stabilized, due to the influence of human hunters and large carnivores (e.g., wolves, mountain lions [*Puma concolor*], grizzly bears [*Ursus arctos*]; Vucetich et al. 2005, Peterson et al. 2014, MacNulty et al. 2020b). In contrast to elk, northern Yellowstone bison (*Bison bison*) abundance has increased (Tallian et al. 2017b). Similarly, some resident interior YNP populations of elk have declined as a result of wolf predation (e.g., Garrott et al. 2020). Per recommendations prior to wolf reintroduction (e.g., Boyce and Gaillard 1992, Messier et al. 1995), post-reintroduction studies have evaluated the effects of wolf predation dynamics on ungulate populations. Fundamental to this work has been studies focused on wolf diet and kill rate, which were essential components to the pre- and post-reintroduction modeling efforts that predicted and evaluated wolf-elk dynamics (e.g., Boyce and Gaillard 1992, Vucetich et al. 2005, Varley and Boyce 2006, Becker et al. 2009b, Vucetich et al. 2011). Now, 25 years later, many of these questions are still of pressing interest (Smith and Peterson 2021), especially for the northern Yellowstone elk population that now winters amongst a much larger bison population than in 1995. How wolf predation dynamics have shifted across time, as ungulate populations have also changed, provides a powerful opportunity for ecologists to address questions regarding wolf-prey dynamics (i.e., wolf numerical response, wolf functional response, wolf predation rate), and help understand the consequences of wolf predation on ungulate population dynamics in YNP and beyond. This in turn can also help understand the role of wolf predation in the broader ecological community (Peterson et al. 2020, Stahler et al. 2020).

Elk have been the dominant species that wolves have killed in YNP, other areas of the Greater Yellowstone Ecosystem (GYE), and more broadly across the western United States following wolf recovery (Husseman et al. 2003, Smith et al. 2004, Becker et al. 2009a, Metz et al. 2012, Nelson et al. 2016, Woodruff and Jimenez 2019, Metz et al. 2020a, Orning et al. 2021). The dominance of elk in the diet of wolves is likely due to their medium-large body size that make them a preferred prey for wolves (Mech et al. 2015). Similarly, in Europe, red deer (*Cervus elaphus*) are often the most important component of wolf diet in multi-prey systems (Jędrzejewski et al. 2000). In YNP, wolf use (and selection) among elk sex-age classes has been affected by changes in availability and seasonality (Smith et al. 2004, Wright et al. 2006, Becker et al. 2009a, Metz et al. 2018, MacNulty et al. 2020b, Metz et al. 2020a, Hoy et al. 2021). For example, calves or male-adults are more frequently killed during winter following poorer forage conditions or when winter is more severe (Wilmers et al. 2020). Wolf diet is also affected by seasonal spatial variation (Nelson et al. 2016, Metz et al. 2020a) as ungulate migrations within the GYE change elk availability to territorial wolves (Craighead et al. 1972, Houston 1982, Geremia et al. 2014, Rickbeil et al. 2019). Nonetheless, how wolves kill elk relative to other species, and how wolves kill sex-age classes within elk, is also likely to change over time (Becker et al. 2009a, Tallian et al. 2017b, Metz et al. 2020a). Given that prey abundances in YNP have dramatically changed across time and space, evaluating how wolf use of prey (e.g., diet) has changed over time, while also accounting for detection probability and space, will help provide a clear picture of the role of wolf predation in these predator-prey dynamics.

The clarity of this picture, however, also requires combining species-specific use of prey (i.e., wolf diet) with total wolf kill rate (i.e., kill rate across species) to estimate species-specific kill and scavenging rates (and their summation, wolf acquisition rate) over time. Wolf kill rate in YNP (and throughout their global range) is similarly affected by seasonality (Smith et al. 2004, Metz et al. 2012), prey age structure (Sand et al. 2012), and competition with other large carnivore species (Tallian et al. 2017a), for example. Yet, questions remain about how kill (and scavenging) rate(s) changes across time as prey populations fluctuate, especially in multi-prey systems. Work from the wolf-elk-bison system in the Madison-Firehole of YNP highlighted that kill rate on elk increased with increasing elk abundance after controlling for pack size (Becker et al. 2009b), as expected under classic predator-prey theory (*sensu* Fig. 4-1; Holling 1959, Messier 1994). Bison abundance did not affect kill rate on elk in this multi-prey system, however. But it is unclear how kill rates on elk may have been affected by the actual acquisition of bison by wolves, as opposed to bison abundance. Evaluating how kill and scavenging rate, while accounting for imperfect detection (e.g., Smith et al. 2004), have changed over time is a key step in evaluating the resultant effects of wolf restoration in YNP. Understanding how the dramatic changes in elk and bison abundance in northern Yellowstone have affected wolf predation metrics will provide insight into the ecological role of predation in both driving and responding to these changes. Yellowstone's Northern Range is often used as a textbook, though controversial, example of wolf restoration causing elk declines and trophic cascades (Kauffman et al. 2010, Beschta and Ripple 2016, Painter et al. 2018, Peterson et al. 2020, Brice et al. 2022), but the future of this work will require explicit consideration for how the complexity of opposing trends in elk and bison population trajectories affects wolf predation dynamics and thus the role of wolves (Peterson et al. 2014).

Here, we ultimately tested ecological hypotheses related to wolf predation across YNP (Fig. 4-2) using estimates of wolf predation metrics (e.g., wolf diet, kill rate; Table 4-1) that accounted for imperfect detection. As such, we first estimated the numerator of the number of feeding events (i.e., each wolf-killed or wolf-scavenged ungulate by a wolf pack) through mark-recapture methodology. We estimated the number of feeding events within two periods that corresponded respectively to when wolf packs were generally roaming (i.e., not tending a homesite; autumn/winter) or denning (i.e., tending a homesite; spring/summer). These two time periods broadly differ in other ecological ways (see below in this section), but distinction between these two time periods critically affected how we collected data and thus developed our mark-recapture estimator. We independently detected wolf feeding events (i.e., killed or scavenged prey) on ungulates through three different field methods; ground observation (since 1997), aerial observation (since 1997), and GPS cluster methods (since 2009) during the roaming period. We expanded the mark-recapture methodology of Smith et al. (2004) to also include data from the GPS cluster searches (e.g., Anderson Jr. and Lindzey 2003), and estimated the number of feeding events (i.e., when a wolf pack acquired an ungulate) in a Bayesian mark-recapture model through data augmentation (Royle et al. 2007b, Royle and Dorazio 2012). We also modified the mark-recapture methodology of Metz et al. (2011) to estimate the number of feeding events during the denning period (since 2008) in a similar mark-recapture Bayesian model. In the denning period we used the independent detection of field-searched feeding events by two GPS-collared wolf pack mates (*sensu* Metz et al. 2011). Within both periods, we estimated the number of feeding events on ungulates for individual wolf pack-sessions, which were defined as a continuous time-period during which we planned (e.g., weather-dependent) daily attempts to detect feeding events for a wolf pack. Our mark-recapture methodology allowed us to estimate the number of feeding events for pack-sessions monitored by multiple or only one detection source.

We expected the detection probability of feeding events to be affected by covariates related to wolf-prey ecology and the landscape where feeding events occurred (Smith et al. 2004, Metz et al. 2020c). We hypothesized, for example, that a feeding event being of larger biomass would positively affect detection probability for all detection sources. Hypothesized effects during the roaming period were especially complex because covariates were expected to influence feeding event detection differently across the three different detection methods. For example, we expected that distance from an observation point (e.g., road) would negatively affect detection probability for ground-based observers (Buckland et al. 2001, Smith et al. 2004), but we had no reason to hypothesize an effect of distance on GPS cluster or air detection. Overall, we expected detection probability during the roaming period to be highest for GPS clusters and lower for the ground and air methods. We expected detection probability to be highest for GPS clusters because this method used information from all times of the day, while ground and air methods were restricted to operating during daylight hours. Moreover, the ground method was generally restricted to attempting to observe wolf packs from the road (Smith et al. 2004, Metz et al. 2020c) and the air method gathered only a 'snapshot' of wolf activity during a single flight (Smith et al. 2004). During the roaming period, we hypothesized feeding event detection would only be affected by ecological covariates such as feeding event biomass (positive) and pack size (negative). Each of these covariates may affect handling time of feeding events and the latter may also have a negative influence because each pack member is less likely to be at every feeding event when pack size is greater (Metz et al. 2011). We expected pack size to be more influential on detection during the denning period, in comparison to the roaming, because of the penchant for wolf packs to forage in multiple groups (Peterson et al. 1984, Benson and Patterson 2015). Across both periods, we simply expected that accounting for detection probability would increase our estimates for the number of feeding events, but that relative changes would be influenced by precisely which and/or how many methods (sources) were employed for a pack-session.

The ecological importance of this abundance model, however, was to overcome the bias associated with lowered detection probabilities before estimating six key 'predation' metrics to test ecological hypotheses related to how wolves have responded to, and influenced, changing prey dynamics in Yellowstone National Park since their reintroduction a quarter-century ago. Specifically, we estimated: *i*) wolf diet (i.e., prey composition [proportion species or sex-age class]), *ii*) niche breadth [0 (highly specialized) – 1 (highly generalized); Hurlbert 1978], *iii*) kill rate (kills/wolf/unit time), *iv*) scavenging rate (scavenges/wolf/unit time), *v*) prey acquisition rate (feeding events/wolf/unit time), which is the summation of the prior two metrics, and *vi)* predation rate (proportion of prey population killed by wolves), on only elk (Table 4-1). The first two predation metrics described the manner in which wolves obtained food from different sources, the next three described the rate at which wolves obtained prey, and the final one captured an element required to assess their potential impact on their primary prey.

We estimated the first five of these predation metrics during five seasonal months: *i*) early winter (mid-November to mid-December), *ii*) late winter (March), *iii*) May, *iv*) June, and *v*) July that differed in ecological characteristics that affect predation dynamics (Table 4-1). For example, kill rate is affected by winter severity increasing from early to late winter (Huggard 1993, Post et al. 1999, Smith et al. 2004). We expressed the first five of these predation metrics with the unit expressed as both the number and biomass (kg) of ungulates because how the metric is expressed, or originates from in the case of wolf diet and niche breadth, can have dramatic effects on inference (e.g., Metz et al. 2012). In many cases, we also estimated these predation metrics for sex-age classes of elk and bison (Table 4-1), because of their associated importance in predator-prey dynamics (Peterson et al. 1998, Gervasi et al. 2012, Hoy et al. 2015). The final predation metric, wolf predation rate on elk, was annually estimated using our estimates for kill rate (number of elk per wolf per day), along with estimates for wolf and elk abundance (Fig. 4-3). We used these six predation metrics to test overarching ecological hypotheses that stemmed from classic predator-prey theory (Fig. 4-1; Holling 1959, Messier

1995, Sinclair and Pech 1996). We tested hypotheses with predation metrics from throughout YNP but set the stage here through the focused backdrop of the past twenty-five years of wolf-prey dynamics in northern Yellowstone. The northern part of Yellowstone thus constitutes the core where *i*) we tested our hypotheses most extensively and *ii*) the wolf population increased, declined, and 'stabilized' (term used for simplicity), the wintering elk population declined and stabilized, and the bison population increased (Fig. 4-3). Classic predator-prey theory predicts that wolf predation metrics would respond to these dramatic changes in populations of their prey, and, that their responses can tell us something about the nature of wolf predation on their prey (Holling 1959, Messier 1995, Sinclair and Pech 1996).

We predicted that the general decline in elk abundance would cause all wolf predation metrics on elk to decline in a density-dependent fashion through time, while those on bison and deer would increase. For example, we predicted that kill rate on elk would decline through time as elk abundance also declined (Messier 1994). Yet, we also expected that wolves would expand their niche breadth through time in response to the concurrent increase in bison (*sensu* Grange et al. 2004). We expected metrics describing acquisition (i.e., kills and scavenges) would most dramatically change, because we expected wolves to primarily acquire bison through facultative scavenging (Pereira et al. 2014). Taken together, we expected that wolves would be increasingly characterized as diet generalists (Levins 1968). But we expected wolves to acquire food (biomass) at similar per-capita rates throughout time because the needs of an individual wolf are essentially fixed (Peterson and Ciucci 2003). Moreover, we predicted the benefits from scavenging bison would be 'supersized' because we expected wolves to mostly scavenge on large biomass adults, as observed and expected in other systems (e.g., Carbyn et al. 1998, Pereira et al. 2014). Nonetheless, similar per-capita rates of food acquisition across time do not necessarily suggest that wolves' numerical response will overcome the effects of fewer 'ideal' prey (i.e., elk) and remain the same. The numerical response of wolves may instead decline, as observed in Northern YNP (Fig. 4-3); yet the numerical response in the region of 'lower' primary prey abundance may be greater than would be predicted for a system with only the primary prey, with important implications on primary prey dynamics. For example, Messier (1995) showed that if the number of wolves is buoyed by alternative prey (a positive Y-intercept of wolf versus prey abundance), then the resultant predation rate response will be at least partially inversely density dependent at lower primary prey abundance, and with thus destabilizing consequences for the primary prey (see also Sinclair and Pech 1996, Hebblewhite 2013). In contrast, if wolf abundance is driven only by elk abundance, predation rate would be a hump-shaped response, with a stabilizing density-dependent region at 'lower' abundances (Messier 1995). Therefore, we predicted that if kill rate on elk did indeed decline as elk abundance declined, that predation rate on elk would be inversely density dependent at 'lower' elk abundances if wolf abundance was positively affected by the multi-prey nature of Northern YNP, and hump-shaped (density dependent at 'lower' elk abundances) if elk were the overwhelming driving force behind wolf abundance (Messier 1995).

Beyond the predictions from this classic predator-prey theory, we also tested other aspects of predator-prey dynamics related to how predation dynamics are driven by prey vulnerability and space (Mech and Peterson 2003, Owen-Smith 2015, Kohl et al. 2018). We expected wolves to minimize their risks while hunting, and to maximize their intake rates, through killing the most vulnerable prey. For example, because elk calves are inherently the most vulnerable sex-age class of elk, we expected wolves to most frequently kill them when elk abundance was highest and the number of available elk calves was likely greatest (Hoy et al.

2020, MacNulty et al. 2020b). We expected similar effects from within year changes in availability. For example, we predicted the per-capita number of prey killed would be greatest during June when neonate availability peaks in Northern YNP (Barber-Meyer et al. 2008). We also predicted that vulnerability would drive some sex-age classes to be infrequently acquired through predation. Specifically, we expected bison adults, especially males, to be primarily scavenged. However, changes in ungulate availability over geographic space may also affect predation dynamics.

We similarly took advantage of variation in prey availability within and between two broad subsystems (Northern, Interior; Smith et al. 2004) of YNP. Within each of these subsystems, differences in elevation (Northern) or thermal feature distribution (Interior) affected ungulate distribution that we predicted would affect wolf predation metrics. Specific hypotheses were related to the predation metric, but we generally expected that migratory timing would affect predation metrics (Fryxell and Sinclair 1988). In Northern YNP, for example, we expected wolves that lived in the upper elevations to have a wider diet in early winter, in comparison to late winter, because elk were more likely to have already migrated from this area. For Interior YNP, we expected dramatic differences in the effect of time on wolf predation metrics depending on if wolf territories overlapped the Madison-Firehole elk population (Garrott et al. 2020). We predicted longitudinal patterns that would be similar to those for Northern YNP for packs who lived amongst the Madison-Firehole elk population that declined in a similar manner to the northern Yellowstone elk population, even if the mechanisms behind these two elk population declines differed (Peterson et al. 2014, Garrott et al. 2020, MacNulty et al. 2020b). In contrast, we did not expect wolf diet to change in other parts of Interior YNP because available prey, i.e., late migrating elk in early winter and some resident bison throughout winter, had changed less. These spatial and seasonal comparisons complimented with dynamics in Northern YNP and provided useful contrasts to help illuminate similarities and differences in predator-prey dynamics throughout Yellowstone.

## STUDY AREA

We conducted our study primarily within ~9,000 km$^2$ YNP, Wyoming, USA (Fig. 4-2). YNP varies in elevation from 1,500–3,300 meters and is primarily forested, but also contains large open grasslands and thermally-influenced areas. The lower elevations of YNP are part of the ~1,530 km$^2$ Northern Range (~1,000 km$^2$ within YNP), a well-known wintering range for many of Yellowstone's ungulates (Houston 1982). The Northern Range, included within our 'Northern subsystem' (hereafter, Northern YNP) where we most intensively studied wolf predation, had reduced winter severity, snow depths, and limited thermal activity in comparison to Interior YNP (Fig. 4-2). The more extensive thermal activity in the higher-elevation Interior YNP reduces snow-cover locally providing local foraging refugia (Garrott et al. 2002, Geremia et al. 2014).

Within each YNP subsystem (Northern, Interior), we also defined spatial zones (hereafter, 'zone'; *sensu* Metz et al. 2020a). Specifically, we defined these zones as Northern-Lower, Northern-Middle, Northern-Upper, Interior-West, and Interior-Central (Fig. 4-2). We defined Northern zones through leveraging previously defined sectors for the Northern Range that were guided by spatial differences in minimum elevation and snowpack (White et al. 2012). We defined the Interior zones to characterize whether packs were likely to have access (Interior-West) or not (Interior-Central) to the areas used by the Madison-Firehole elk population (Messer et al. 2008; see *Elk and bison populations*). For our study, we used these zones when evaluating spatial variation in predation metrics across the broad YNP landscape.

Wolves are among five large carnivores that reside within YNP and the GYE; black bear (*Ursus americanus*), coyote (*Canis latrans*), grizzly bear, and mountain lion are the others. These large carnivores, as well as human hunters outside of YNP, encounter and consume up to eight large ungulate species (bighorn sheep [*Ovis canadensis*], bison, elk, mule deer [*Odocoileus hemionus*], moose [*Alces alces*], mountain goat [*Oreamnos americanus*], pronghorn [*Antilocapra americana*], and white-tailed deer [*O.virgianus*]). In our study, we combined mule deer and white-tailed deer because they were usually indistinguishable from gross morphological characteristics in the field (Metz et al. 2012, Metz et al. 2020a). Elk and bison, and to a lesser extent mule deer, are the most abundant and widespread of these ungulate species. Smaller prey items (e.g., beaver [*Castor canadensis*], rodents, waterfowl) also exist within the study system and are occasionally used by wolves, but we censored all small prey from our study (Appendix S4-A) because small prey comprise a trivial amount of acquired biomass (e.g., Lodberg-Holm et al. 2021) and our focus was on wolf-ungulate dynamics.

### Ungulate populations

Beginning with wolf reintroduction in 1995, Northern Range elk abundance generally declined for about a decade before stabilizing, around 2010, ranging from a high of 19,904 in 1995-1996 to a low of 6,090 in 2014-2015 (Fig. 4-3; Tallian et al. 2017b). With these numerical changes in abundance, the sex-age (class) structure of the population correspondingly changes, affecting the number of various prey types available on the landscape. The spatial distribution of the Northern Range elk population during winter has also changed over time, with the proportion of the elk population wintering within YNP declining since 1995 (White et al. 2012). For example, >60% of the NR elk population has wintered outside of YNP since 2012 and was largely driven by declines in the number of elk inside of YNP (Fig. 4-3). Some elk also remain in Interior YNP during winter, primarily residing in thermally-influenced areas. Most notably, >600 elk over-wintered in the Madison-Firehole of Interior YNP prior to wolf reintroduction (Garrott et al. 2009), although this population has declined to <25, primarily through wolf predation (Garrott et al. 2020). Some additional male-adults are known to be scattered throughout the Interior-West zone within YNP during winter, but very few (or no) elk are typically in Interior-Central following their late fall-early winter migration (Craighead et al. 1972, Rickbeil et al. 2019). Elk numbers within YNP increase during the growing season when more than 20,000 elk from as many as nine populations use YNP. Most of these elk, including many from the Northern Range population, migrate to the higher-elevations of Interior YNP as snow melts and forage quality improves (Craighead et al. 1972, Houston 1982, Rickbeil et al. 2019). Note that many deer, primarily mule deer, similarly return to YNP at the onset of the growing season, with >95% of an estimated 1,700–1,900 mule deer wintering outside of YNP (Mosley and Mundinger 2018). Although deer abundance was annually unknown, we expected their relative availability within Northern YNP was higher during the last decade when total elk and bison abundance was less (Fig. 4-3).

The bison population of YNP consists of the Interior (formally known as the 'Central' subpopulation) and Northern YNP subpopulations that primarily breed within the Interior-Central and Northern-Upper zones, respectively (Geremia et al. 2014). Many individuals within these bison subpopulations also move down in elevation during winter as snow accumulates, although the influence of snow is non-existent (or small) for some Interior bison because of their use of thermally-influenced areas (Geremia et al. 2014). Bison are thus present within all of our spatial zones over winter. Some Interior bison do move to the Northern-Lower zone during winter (Geremia et al. 2014), although this behavior has greatly declined as Northern YNP bison abundance has increased. Movements of both bison subpopulations outside of YNP is restricted by interagency wildlife management policy, and the resultant management removals are also the central factor that regulates bison abundance to a management adopted target (White et al. 2015). YNP bison abundance has ranged from ~2,000 to ~5,000, with the Interior subpopulation being larger than the Northern subpopulation until 2009 (White et al. 2015). However, >60% of the YNP bison population has been characterized as part of the Northern subpopulation for the last decade, representing a major spatiotemporal shift in prey abundance in YNP.

### Wolf population

Reported end-of-December counts (December of 1997–2019) for the number of packs in YNP have ranged from 7 to 16, with YNP wolf population counts between 64 and 172 wolves. The Northern YNP population has numbered between 32 and 98 wolves (Fig. 4-3), outnumbering the Interior YNP population for the first decade of our study despite the Northern Range being 13% of YNP (Smith et al. 2020a). Some wolf packs used both Northern YNP and Interior YNP, most generally through 1) Interior packs using Northern YNP during winter or 2) Northern YNP packs using the Interior during summer. In either case, these wolf movements were likely influenced by seasonal changes in ungulate distribution.

## METHODS

Our overarching goals were first to detect wolf packs feeding at ungulate carcasses (hereafter, feeding events) to then estimate six predation metrics (Table 4-1) during periods of the year when wolf packs were generally roaming or denning or, in the case of predation rate, annually.

We then tested predictions of our overarching hypotheses related to understanding the ecological drivers of wolf predation metrics, expressed in terms of both the number and biomass of prey, across seasons and time. We used a sample of radiocollared wolf packs in YNP that were collared with Very High Frequency (VHF; Telonics, Mesa, AZ, USA) and, starting in 2008, GPS (Lotek, Newmarket, ON, Canada; Telonics; Vectronic Aerospace, Berlin, Germany) radiocollars via helicopter darting or net-gunning. Wolf capture and handling conformed to National Park Service animal capture and handling policies, as well as University of Montana IACUC protocols AUP MH-043-15, AUP MH-056-18 and AUP MH-046-21. We maintained at least one functioning radiocollar, primarily VHF, in most wolf packs in YNP since reintroduction. Hereafter, VHF describes any collar that was radiotracked as all GPS collars were also equipped with VHF signals. GPS collars were programmed to record locations at various fix intervals, but here we only used spatial data for those collars that were *i*) programmed to record a location every 30 (denning period) and 60 (roaming period) minutes and *ii*) were on wolves for which we were searching GPS clusters for (see *Detection method effort* sections below). Hereafter, 'GPS collars' describes only collars for which these two conditions were met.

We estimated predation metrics during annual early (mid-November to mid-December) and late (March) winter sessions during the roaming period (i.e., winter) for wolf packs that spanned much of YNP (Fig. 4-2). We did so for pack-sessions (i.e., a study session for a wolf pack) that generally lasted 30 days ($\bar{x} = 29.5 \pm 0.1$ SE; range: 8 – 30; $n = 349$) and occurred from November 1997 until March 2020, censoring pack-sessions prior to November 1997 because detection of feeding events between methods was non-independent in the initial years post-reintroduction (see Smith et al. 2004, Smith et al. 2020b). We also estimated predation metrics for May, June, and July during summers from 2008 to 2020 in the denning period for wolf packs that lived in Northern YNP, not the Interior (Fig. 4-2). Packs were monitored during the 3-month denning period for an average of 76.8 days (± 4.4 SE; range: 30 – 92; *n* = 20; see Table S4-A.1b). We assigned year for all analyses as the year during the onset of winter for the roaming period and as the calendar year for the denning period.

## Wolf pack characteristics

We considered groups of wolves to be packs when they travelled together during our study sessions. Two key characteristics for each wolf pack-session was where the pack resided (i.e., inside or outside of YNP; YNP subsystem and zone) and pack size. We used a central spatial location of wolf packs to censor packs (e.g., if they occurred outside of YNP) and to test drivers of wolf diet across YNP over space and time (see below in this section). We estimated territory centroids with a 70% Minimum Convex Polygon (MCP) that leveraged as much as 3 months of VHF data to increase sample size (Appendix S4-A). Pack size served two purposes for our study. First, we used pack size as a covariate in our models (i.e., roaming, denning) that estimated feeding event abundance because *i*) larger wolf packs consistently acquire more ungulates (e.g., Post et al. 1999, Hayes et al. 2000) and *ii*) pack size may have also affected feeding event attendance by individual wolves and/or handling time by the pack, and thus, detection probability. Second, we used pack size to estimate prey acquisition rate (or kill rate) on a per-capita basis (i.e., prey per wolf per unit time).

### ROAMING PERIOD

We hierarchically censored packs from our study that *i*) were not radiocollared for most of a study session, *ii*) had ≤60% of their daily VHF locations inside of YNP during a study session, or *iii*) centered their territory in the most southern portion of YNP (Appendix S4-A). We censored these packs because we primarily focused our sampling effort, including radiocollaring, in the core of YNP. Following this censoring, we monitored 61 packs during 385 pack-sessions ($\bar{x}$ = 8.4 ± 0.4 SE packs per session; range: 4 – 14). However, we did not detect any feeding events during 36 pack-sessions, and we therefore also censored these pack-sessions when estimating wolf predation metrics. Consequently, our final dataset used data from 54 packs during 349 pack-sessions ($\bar{x}$ = 7.6 ± 0.4 SE packs per session; range: 3 – 14; Fig. 4-4) to evaluate wolf predation metrics during the roaming period.

We used the centroid of the pack's territory (from *iii*) to assign pack-sessions to a subsystem (Northern, Interior) and zone of YNP (Fig. 4-2; Appendix S4-A). First, we assigned each pack-session as Northern or Interior depending on if the centroid was in the Northern subsystem or not (Fig. 4-2). Among the 349 pack-sessions where we detected at least one feeding event, 227 were Northern and 122 were Interior (Table 4-2; Figs. S4-A.1, S4-A.2). Next, we used the centroid to assign the zone as Northern-Lower (*n* = 51), Northern-Middle (*n* = 84), Northern-Upper (*n* = 92), Interior-West (*n* = 54), or Interior-Central (*n* = 68; Figs. S4-A.2, S4-A.3).

We estimated pack size for most pack-sessions (i.e., 343 of 349) from daily counts of wolf packs. Because wolf packs were not always together (e.g., Metz et al. 2011, Benson and Patterson 2015), we summed unique wolf groups for each day, resulting in a single minimum count for each pack on each day that they were observed (see *Roaming period – Detection method effort* below). We then selected the value that was acquired on at least two days during the study session (*n* = 289; following Smith et al. 2004) or the maximum count acquired during the study session (*n* = 54), depending on the number of days with observations (see Appendix

S4-A). In the rare cases (i.e., 6 of 349) where pack size estimates were clearly a poor representation of known pack size during the (maximum) 30-day study session, we assigned a known pack size (see Appendix S4-A).

### DENNING PERIOD

All packs studied during the denning period resided in Northern YNP (Figs. 4-2, 4-4). As we did for the roaming period, we also assigned a spatial zone for each pack-session (Table 4-2). In this case, we used the GPS locations of the GPS-collared wolves (Appendix S4-A). Pack size during the denning period represented the number of wolves that were at least one year-old (i.e., newborn pups were not included). Because wolf packs forage less cohesively during denning (Peterson et al. 1984, Metz et al. 2011), complete pack counts were difficult to acquire. We therefore estimated pack size from summer observations and/or used pack size estimates from late winter (see above), adjusted for known mortalities or dispersals that affected pack size over the denning period. Rarely, new packs formed after the breeding season that were not in existence during late winter. For such packs, we estimated pack size from summer observations.

Pack size was occasionally (i.e., 2 of 20 pack-sessions) complicated by fundamental changes in it during the (maximum) 3-month duration of denning period sessions, which was three times longer than the maximum duration of roaming period sessions. We therefore used different values for a pack-session during the denning period, dependent on the purpose of using pack size. First, we used the mean daily pack size for the pack-session to represent pack size in our abundance model. We did so because our model (specifically, Eqn. 2) required a single pack size estimate for the pack-session. Second, we used the same daily values to determine the most frequently associated with each month within a pack-session and used that value when we estimated the per-capita rate that wolves acquired or killed prey during a month.

### Estimating feeding event abundance through mark-recapture

We estimated the number of feeding events during a pack-session in a mark-recapture, closed-population framework, where detection histories were recorded as 1 (detected), 0 (not detected), or NA (not looked for) (Borchers et al. 2002). We met the assumption of a closed population through limiting feeding events to those ‘born’ within a pack-session, i.e., the wolf pack first acquired (i.e., killed or scavenged) the ungulate within a study session. We estimated abundance of feeding events using a Bayesian framework and data augmentation (Royle and Dorazio 2012). Data augmentation involves beginning with the rows of data from detected (in our case) feeding events and then adding enough rows that have all 0 detection histories, representing *potential* ‘missed’, or undetected, feeding events. Then, a Bayesian model is used to estimate which of these additional rows represent truly undetected feeding events and which were not actually feeding events. The estimate for feeding event abundance is subsequently determined as the summation of the rows that represent detected and undetected feeding events. Our mark-recapture models built on the pioneering work of Smith et al. (2004) to estimate feeding event abundance for wolf packs in YNP during the roaming period, and the work of Metz et al. (2011) to do the same for the denning period. We relied on the putatively independent detections of feeding events by different detection methods to provide information for capture-recapture. As such, our work was similar to conventional mark-recapture studies with multiple capture occasions, especially those that include multiple observers (Schwarz and Seber 1999). In either the roaming or denning period, method-specific detection was permitted during a feeding event 'lifespan', which we defined as two days during the roaming period and three days during the denning period (Fig. 4-5). Each of these lifespans were determined by the feeding patterns of wolves (Appendix S4-A) and, for the roaming period, the distribution of our time-specific detection data.

During the roaming period, we used the detection methods of aerial observation, ground observation, and/or GPS cluster searches (Fig. 4-6; Smith et al. 2004; *sensu* Knopff et al. 2009). For denning periods, we estimated feeding events through only GPS cluster detections, but leveraged independent detection of wolf pack feeding events by each GPS-collared wolf packmate (hereafter, detection 'source' for denning period; Fig. 4-7; Metz et al. 2011). Different detection methods (or sources) were employed during pack-sessions, however, affecting how each feeding event could be detected. Specifically, all pack-sessions during the roaming period were monitored by the air, but only some pack-sessions were monitored by GPS cluster searches and/or ground observation (Fig. 4-6b). Similarly, only some pack-sessions during the denning period were monitored by two detection sources (i.e., GPS-collared wolves; Fig. 4-7). We therefore recorded method-specific effort throughout each pack-session that we then used to define whether specific detection methods (or sources) were available to detect feeding events during each feeding event lifespan. Here, 'availability' ignored any method-specific detections during a previous occasion – an important difference from the detection histories (see *Roaming period – Mark-recapture feeding event abundance model* below). We leveraged these availability histories of detected feeding events, along with knowledge of which detection methods were employed during a pack-session (Fig. 4-6b), when we estimated availability for 'missed' feeding events during a pack-session.

We first review the methodology that we employed to detect feeding events for the roaming and denning periods before presenting the specific Bayesian model that we used to estimate feeding event abundance within each period. We therefore first describe *i*) the detection method effort that defined availability and *ii*) the detected feeding events themselves, including the associated covariates that we hypothesized may have affected their detection. We then describe the Bayesian model(s) that we used to estimate feeding event abundance in both the roaming and denning periods. Finally, we detail how we turned these abundance estimates into predation metric estimates specific to demographic class (e.g., species) and acquisition type (i.e., wolf killed or scavenge). This final step was necessary to test our hypotheses of drivers of wolf predation dynamics in the multi-prey system of YNP.

### ROAMING PERIOD

We detected feeding events by YNP packs during the roaming period through ground-based observations, aerial-based observations, and/or GPS cluster searches. To ensure independence, a critical assumption of mark-recapture methods, the observers for the ground and aerial methods did not share information about the presence or absence of a feeding event. Because GPS clusters were searched after wolves left a carcass and we sometimes leveraged (mostly) ground and aerial observations to 'search' GPS clusters (see Appendix S4-A), the presence or absence of a feeding event at GPS clusters was often known prior (or in lieu of) field searches. Ungulate carcasses are easily detectable during field searches during winter, which likely eliminates any potential concern about violating independence.

*Detection method effort.* We recorded detection method-specific effort for each day of a pack-session. This allowed us to define whether a feeding event was available (1) or not (0) to be detected by each detection method during a day, which was our 'capture occasion' (but see *Roaming period – Mark-recapture feeding event abundance model* for specifics about GPS cluster capture occasion). Availability equaled 1 for a day for the air or ground method when that method attempted to radiotrack and observe a pack on a day. The air method attempted to locate wolf packs through a daily radiotracking flight. This flight typically occurred shortly after dawn in a Piper Supercub (PA-18), as weather allowed. We conducted a radiotracking flight on 14.1 days (± 0.8 SE; range: 4 – 23) during each (typically) 30-day winter session and attempted to observe as many packs during each flight as weather allowed. For a subset of concurrently monitored wolf packs (Figs. 4-4, 4-6 [blue and *most of* green-filled box plots in Fig. 4-6b]), the assigned ground team attempted to radiolocate that wolf pack at dawn and then attempted to maintain visual observation(s) of that pack and its members through dusk. For each detection method on each day, we recorded whether each method attempted to find, radiolocated, and visually observed each pack. On average, the aerial method attempted to radiolocate and observe packs on 13.0 days (± 0.3 SE; range: 3 – 23; *n* = 349), and the ground method on 29.2 days (± 0.3 SE; range: 14 – 30; *n* = 133), during each roaming period pack-session.

Starting in November 2009, we also detected feeding events through searching wolf GPS clusters, using data from 30 GPS-collared wolves in 11 packs over 44 pack-sessions (green-filled box plots in Fig. 4-6b). We identified GPS clusters at the individual wolf-level, sometimes with multiple wolves, in the same pack-session (Appendix S4-A). Initially, we field-searched GPS clusters identified by the model of Metz et al. (2011). Subsequently, we used GPS clusters reidentified using the R package `GPSeqClus` (Clapp et al. 2021) to standardize cluster characteristics, including times of GPS cluster detections (Appendix S4-A). We defined the minimum cluster size as 2 locations, the centroid as the mean, the search radius as 100-m, and the window to allow new cluster locations as 3 days. We searched 4,505 of 4,765 (94.5%) GPS clusters (Appendix S4-A; Table S4-A.1a). For each day (sunset-adjusted for alignment to aerial and ground methods), we recorded whether any GPS clusters were searched for a pack (Appendix S4-A). Availability equaled 1 for the GPS cluster method for a pack-session day if any GPS cluster location was searched.

How pack-sessions were monitored led to substantial differences in the number of feeding events that were detected (see Fig. 4-8). Therefore, we formally classified how each pack-session (n=349) was monitored (hereafter, ‘pack-type’) as (hierarchically) including the GPS method ($n$ = 44), the ground method ($n$ = 92), or only the air method ($n$ = 213). We explicitly used this hierarchical pack-type in the biological process portion of our abundance model, where we evaluated and accounted for the underlying influence of pack size on the number of feeding events (e.g., Post et al. 1999, Hayes et al. 2000), to overcome bias associated with more feeding events being detected during pack-sessions that employed more (and/or ‘better’) detection methods (Fig. 4-8; see Eqn. 2 in *Roaming period – Mark-recapture feeding event abundance model* below). We also created a more detailed pack-type* that we leveraged to provide informative priors for availability during a pack-session for the data augmentation (see Eqn. 6 in *Mark-recapture feeding event abundance model* below; Table S4-A.1a). Essentially, the assigned pack-type* informed the model how frequently a particular method was available to detect feeding events during a pack-session (Table S4-A.1a).

The temporal patterns in the combined attempts to locate wolf packs by these three detection methods defined the number, and thereby also proportion, of days during a pack-session with any detection effort (hereafter, ‘effort-days’). An effort-day was defined as a day where at least one detection method attempted to find a pack within a 2-day window (associated with feeding event lifespan; see above in this section). Accordingly, an effort-day for a pack-session required an attempt by any detection method on *i*) that day, *ii*) the previous day, or *iii*) the subsequent day. We also explicitly used the number of effort-days in our abundance model to define the duration of a pack-session where there was an attempt to find a feeding event. This allowed us to standardize abundance estimates to represent the number of feeding events expected to have been detected if each day during the study-session had been an 'effort-day' (see Eqns. 2, 7 in *Roaming period – Mark-recapture feeding event abundance model* below).

*Detected feeding events*. We detected 2,343 pack-level feeding events, associated with 2,307 unique ungulate carcasses (i.e., 1.4% of the time multiple packs fed from the same ungulate carcass), during the roaming period (Fig. 4-6b; Appendix S4-A). We assigned each feeding event to a pack through detection method observations (or wolf GPS locations) that placed a wolf pack at, or in the near vicinity of, the ungulate carcass. We detected, on average, 6.7 (± 0.3 SE; range: 1 – 29) feeding events for the 349 pack-sessions that were included in our abundance model. Some detected feeding events were part of multiple carcass events, but we treated the detection of each independently because these carcasses were sometimes spread across space and time. Moreover, 24% (26 of 107) of multi-carcass events contained feeding events within them that were not detected by the same combination of detection methods.

For each detected feeding event, we recorded the date of method-specific detection (Fig. 4-5). Once a feeding event was detected by a method, that method ceased looking for it (i.e., methods could only detect a feeding event once). The initial date of feeding event detection by any method set the foundation for creating a 2-day 'feeding event lifespan' when method-specific detection was permitted (Fig. 4-5). We limited the detection period to 2-days because the vast majority (95.6%) of feeding events that were detected by multiple detection methods were detected by all (relevant) methods within two days. More specifically, 548 feeding events were initially detected by multiple detection methods, and only 24 (4.4%) of those included a detection by one of the methods after the 2-day window. We censored these method-specific detections because these detection probabilities, which also would have needed to account for availability, were not estimable for such small sample sizes (i.e., each of these detections were for a specific method on a specific day). In total, we therefore censored 9 ground, 21 air, and 1 GPS method detections (from 1,176 [2.6%] method-specific detections of the 548 feeding events). After this censoring, 525 feeding events were detected by multiple methods.

We used our observations, and/or carcass necropsies, to determine whether a pack had killed or scavenged an acquired ungulate. For example, wolves were occasionally observed approaching intact carcasses that they did not kill or necropsies revealed no evidence of predation (see Metz et al. 2012 for further details). We characterized scavenging as; 1) feeding on an ungulate that did not die from predation (e.g., malnutrition), 2) feeding on an ungulate killed by other wolves, 3) feeding on a cougar kill, 4) feeding on a gut pile from a human-harvested ungulate, or 5) feeding on an ungulate in a NPS management-related carcass dump. We condensed these categories for analyses so that ‘scavenging’ represented any feeding event where the ungulate was not killed by the associated wolf pack.

In addition to cause of death, we also assessed and/or confirmed species, sex, and age through our observations and/or field necropsies. We necropsied 1,709 of 2,307 (74%) detected carcasses, including 1,670 of 1,950 (86%) in the more accessible Northern subsystem. Note we defined deer *spp.* as a species (see *Study Area* above). We assigned species in 2,247 of 2,307 cases (97%; Appendix S4-A). We also assigned an age (i.e., calf, yearling, known-aged adult) through cementum annuli, tooth eruption, or physical characteristics in 1,652 of 2,307 cases. If we could not determine the age, we were usually able to assign at least some characteristics (e.g., female-adult). Finally, we estimated a spatial location for each of the 2,307 carcasses using either a GPS unit during necropsies and aerial detections or topographic maps (Appendix S4-A). Each of these characteristics (i.e., species, sex, age or age class, spatial location) were informative for our abundance estimator because they allowed the assignment of covariates that may affect feeding event detection, thus allowing us to test our hypotheses related to detection probability.

*Covariates affecting feeding event detection*. We expected that method-specific detection would be affected by a number of factors, including feeding event biomass, wolf pack size, the number of radio collars, openness (a measure of forest cover), distance from observers, and viewshed (most of which have been included in previous work assessing detection probability in this system; Metz et al. 2020c), associated with feeding events. We expected that feeding event biomass, pack size, and the number of collars could affect detection for each method, openness could affect air or ground method detection, and distance and viewshed could affect ground method detection. We ultimately refer to these (potential) effects as covariate-occasions where, for example, biomass-G1 would refer to the effect of feeding event biomass on ground detection on day 1. Each covariate may have differential effects on each detection method (hypothesized directional effects for covariate-occasions displayed in Fig. 4-6c), and the strength of those (potential) effects may also differ between day 1 and 2 of the feeding event lifespan for the ground or air (Fig. 4-5). For example, we expected that biomass would have a greater effect on day 2 for the ground or air because a larger feeding event size may retain a wolf pack for a longer duration, thereby increasing the probability that the feeding event would still be detected on day 2. Here, we provide brief details of how we defined each covariate for each feeding event in our detection model (see Eqn. 5 in *Roaming period – Mark-recapture feeding event abundance model* below).

Feeding event biomass was determined from previously developed seasonal, age and sex-specific growth curves of live biomass for deer and elk (Murphy et al. 1998). For all other species, we used published and unpublished age and sex-specific estimates of live biomass. Following Wilmers et al. (2003) and Miller et al. (2013), we adjusted each estimate of live biomass by 68% or 79% for large or small ungulates to estimate edible biomass available for consumption (Appendix S4-B). Each feeding event was assigned all edible biomass unless the carcass was fed on by multiple packs or the carcass was usurped from a cougar (see Metz et al. 2012). We assigned biomass for 2,283 of 2,343 feeding events; note that values were assigned whenever possible through also using composite values across species sex-age classes (e.g., feeding event known to be adult bison, but of unknown sex; Appendix S4-B).

We also expected that pack size and the number of radiocollars in a pack could affect feeding event detection based on previous work in YNP (Metz et al. 2020c). We assigned pack size as described in *Wolf pack characteristics* above. For the number of radiocollars, we assigned the mean number of collars for the pack-session, derived from daily estimates for the number of collars present in the pack. The number of radiocollars represented the mean number of VHF collars for air and ground method detection, and the mean number of GPS collars for GPS method detection.

Spatial covariates (i.e., openness, distance, viewshed) were assigned through the recorded spatial location of each feeding event. We extracted values for spatially variable covariates using the spatial locations for each carcass and raster layers with a cell size of ~9.7 meters. Openness described how forested a 500 x 500 m window was, using LANDFIRE vegetation data and following the temporal assignment described in Metz et al. (2020c). Distance from an observer represented the minimum distance from a viewing road or ground-based observation point (Metz et al. 2020c). Viewshed described whether a spatial pixel was predicted to be observable (1) or not (0) from the road or ground-based observation points (Metz et al. 2020c). We did not extract the road or viewshed covariates for Interior wolf packs because the ground method only operated in Northern YNP.

*Mark-recapture feeding event abundance model*. The core element of our Bayesian feeding event abundance model was the detection histories that form the basis of mark-recapture models (Schwarz and Seber 1999). We defined the detection history for each feeding event as a five-occasion detection history where the associated detection information for occasions 1 and 2 represented the ground method on days 1 and 2 (hereafter, G1 and G2), occasions 3 and 4 represented the air method on days 1 and 2 (hereafter, A1 and A2), and occasion 5 represented the GPS method during the entire 2-day window (hereafter, GPS1; Figs. 4-5, 4-6c; Appendix S4-C). The GPS method was condensed to a single day for simplicity because 563 of the 567 detections that occurred in the 2-day detection window occurred on day 1. Detection during each occasion was specifically recorded as 1 (feeding event detected), 0 (feeding event not detected, but effort occurred), or NA (no effort by detection method, including when feeding event detected by that method during the previous method-specific detection occasion; Fig. S4-C.1). Additionally, our model included the accompanying availability histories (*sensu* Diefenbach et al. 2007; see below) for each feeding event, which simply specified whether a method attempted (1) or did not attempt (0) to find a pack – not the feeding event itself – on each of the five occasions (Fig. S4-C.1).

We used these detection and availability histories to estimate feeding event abundance for each pack-session while accounting for imperfect detection using data augmentation in a Bayesian mark-recapture framework. In data augmentation, recall that all 0 detection history rows are added to the observed data to simply allow space for the estimation of undetected (in our case) feeding events (Fig. 4-6d; Royle et al. 2007a). The number of all 0 detection history rows (see *Estimating feeding event abundance through mark-recapture* above) added to the data is not important, provided a non-informative prior is used (in our case, for our inclusion parameter $\omega$; see Eqns. 1, 2 below) and the number of rows is indeed sufficient to not bias estimates (Royle et al. 2007a). For each of the 349 roaming pack-sessions, we added 35 rows with a detection history of 00000. Thirty-five rows would represent 35 'missed' feeding events in a (maximum) 30-day period, a value likely never to be observed for any wolf pack. These 35 rows also contained a NA-filled 5-occasion availability history, which were populated through an informative prior based on the availability histories of the detected feeding events for all pack-sessions of the same pack-type* (Table S4-C.1a). Providing these informative priors allowed us to *i*) ignore any influence of method-specific day 1 detection (i.e., availability never equaled 0 on a pack-session day where the detection method was operational) and *ii*) assign the appropriate detection methods that were operational during a specific pack-session. For example, the availability columns for G1, G2, and GPS1 for the augmented rows of a pack-session monitored by only the air would essentially be populated with zeros (see Table S4-C.1a). Posterior checks of estimates for pack-session *N* indicated that 35 rows per pack-session provided sufficient space for these estimates of *N*, as the posterior distribution for estimated *N* never approached 35. The covariate columns for the augmented rows were defined as NA, except that we defined pack size and the number of collars for a pack-session from the observed data.

Priors for these NA-filled covariates that were leveraged by the data augmentation process were described by the mean and precision of the respective covariates.

Our estimate for abundance was ultimately based on summing the *z* parameter in our model, which described the inclusion of a row of data as a feeding event that occurred. The inclusion ($z = 1$) of feeding event *i* for pack-session *g* was dependent on the outcome of a Bernoulli trial with an occurrence probability of $\psi_{i,g}$, which was also influenced by the ecological factor of pack size that is well known to positively affect the number of carcasses fed on by wolf packs (Thurber and Peterson 1993, Schmidt and Mech 1997). Specifically,

$$z_{i,g} \sim Bernoulli(\psi_{i,g}) \tag{1}$$

$$logit(\psi_{i,g}) = \omega_{g_d} \times prop.sess_g \times prop.pack.effort_g + \beta_1 X_g \tag{2}$$

where $\omega_{g_d}$ is the intercept for a pack-session of pack-type *d*. Here, the nested *d* grouped together pack-sessions by pack-type (hierarchically, GPS, Ground, or Air; see *Roaming period – Detection method effort* above) and winter season (early or late) to account for the associated bias in the number of detected feeding events during pack-session *g* (Fig. 4-8). The proportion of a 30-day session that a pack existed and/or was included (i.e., was radiocollared) was described by $prop.sess_g$ and the proportion of pack-session *g* that were effort-days (see *Roaming period – Detection method effort* above) was described by $prop.pack.effort_g$. These two terms were offsets (*sensu* Kery 2010) that simply adjusted the number of detected feeding events during pack-session *g* to the number expected to have been detected over 30 days, again simply accounting for their associated biases (Fig. S4-C.2). $\beta_1 X_g$ described the biological effect of (standardized) pack size on occurrence probability, which we termed ‘pack size psi’.

The detection of a feeding event was affected by our observation process. Specifically, detection of feeding event *i* on occasion *j* was dependent on their being an attempt to observe feeding event *i* on occasion *j* and, for those feedings events that were available for detection on occasion *j*, was the event then detected? The detection (or non-detection) was represented by a Bernoulli trial with a probability defined by *p.eff*, which was the product of inclusion (*z*), detection probability (*p*), and availability (*a*). The *z* parameter forced *p.eff* to 0 when $z = 0$. Accordingly, our observation model was:

$$Y_{i,j,g} \sim Bernoulli(p.eff_{i,j,g}) \tag{3}$$

$$p.eff_{i,j,g} = z_{i,g} \times p_{i,j,g} \times a_{i,j,g} \tag{4}$$

$$logit(p_{i,j,g}) = \alpha_j + [\mathbf{B}\boldsymbol{X}_{\boldsymbol{i,j}}\boldsymbol{I}_{\boldsymbol{i,j}}] \tag{5}$$

$$a_{i,j,g} \sim Bernoulli(mu.a_{j,g_{t^*}}) \tag{6}$$

where $z_{i,g}$ describes the inclusion of feeding event *i* and links the observation model to Eqn. 1, $p_{i,j,g}$ represents the detection of feeding event *i* on detection occasion *j* ($j$ = 1-5) for pack-session *g*, $\alpha_j$ represents the intercept for detection probability for each detection occasion, and [BXI$_{i,j}$] is the matrix of (standardized) covariates (X) and the indicator variable (I) for feeding event *i* during detection occasion *j*. Indicator variables equaled 0 for covariate-occasions where we did not hypothesize an effect (i.e., distance and viewshed for A1, A2, GPS1; openness for GPS1; Fig. 4-6c) or where the effect of a covariate-occasion was ultimately removed (Fig. S4-C.3), and equaled 1 for all others. The parameter $mu.a_{j,g_{t^*}}$ was influenced by the previously highlighted informative prior that described how frequently detection methods had effort (i.e., availability = 1) during detected feeding events. Here, pack-sessions were grouped through $t^*$ (i.e., their pack-type*), which provided increased information about method-specific effort during a pack-session (e.g., the presence of a GPS-collared wolf for only part of a study session; see Table S4-C.1a).

The estimate for feeding event abundance for pack-session *g* was then:

$$\frac{\sum z_{i,g}}{prop.pack.effort_g} \tag{7}$$

where the outcomes for the Bernoulli trials for *z* during a pack-session were summed and then divided by $prop.pack.effort_g$. The numerator of Eqn. 7 was equal to those feeding events represented by the orange and blue-filled portions of the bars in Fig. 4-6d. Dividing by $prop.pack.effort_g$ resulted in an estimate for the number of feeding events that also included study session days when no detection effort occurred. These additional feeding events are represented by the green-filled portions of the bars in Fig. 4-6d.

We used a stepwise Bayesian model selection procedure to reduce the covariates hypothesized to affect detection probability on occasion *j*, desiring to ultimately develop a parsimonious detection model for our abundance estimator (Gelman et al. 2013). We identified where 95% credible intervals for covariate-occasions overlapped zero, and then removed such covariate-occasions by refitting the model with all remaining covariate-occasions as active (i.e., I = 1 in Eqn. 5), and all other covariate-occasions as not active (i.e., I = 0). If any covariate did not affect any detection occasion, we removed the covariate. We followed this procedure until no credible intervals overlapped zero (Gelman et al. 2013). We made one exception to this model building procedure for openness because our initial model included a negative effect for A1, which was biologically unrealistic (i.e., being in a more forested location should not increase detection; Metz et al. 2020c). Therefore, we used an informative but positive prior based on Metz et al. (2020c), specified as dunif(0,5), and then evaluated the posterior distribution of the beta coefficient for openness for each occasion before retaining (i.e., I = 1) or removing (i.e., I = 0) the openness-occasion (see *Results*). We excluded covariates in detection model(s) where we did not augment the data to reduce both processing time and the chance of including spurious covariate-occasions, given the complexity of our detection process. Upon identifying a model where no covariate-occasions overlapped zero (noting the exception for openness), we began the augmentation process, and continued to exclude covariate-occasions until we developed a parsimonious detection model that included only the most important covariate-occasions. No covariates showed evidence of collinearity (maximum |r| = 0.16) or correlation.

We fit our Bayesian models using R version 3.6.3 (R Core Team 2020) with JAGS 4.3.0 (Plummer 2003), through the R package `R2jags` 0.6-1 (Su and Yajima 2020). For all model(s), we used non-informative priors (except for openness and *mu.a*), ran three different chains for 30,000 iterations, with a burn-in period of 10,000 iterations/chain. Upon model convergence, we visually inspected model outputs using the R package `mcmcplots` (Curtis 2018), assessed Rhat values, and then derived posterior distributions, means, and medians for all estimated parameters.

*Estimating the characteristics of undetected feeding events.* We used our mark-recapture model to estimate the number of feeding events for wolf packs, but not the demographic (i.e., species, sex-age class) and acquisition (i.e., wolf-killed or scavenged) characteristics of undetected ('missed') feeding events. We predicted prey demographic characteristics of these undetected feeding events as a multinomial response and predicted prey acquisition as a binomial response using the `rmultinom()` or `rbinom()` functions in base R (see Eqns. 8–10 below). We also made predictions for a small portion of detected feeding events with unknown characteristics, but we omitted the description of these predictions because we followed the same process as for those undetected feeding events predicted through Eqn. 8. We only estimated sex-age class for the two most used prey species, elk and bison (see *Results*), doing so after the initial multinomial prediction for species. Because estimated feeding event abundance for a pack-session represented the mean of the posterior distribution from our Bayesian model, we made required demographic (and acquisition) predictions for feeding events rounded up to the nearest integer. We then used the proportions for each demographic class (and subsequently acquisition type) among these predictions with the mean estimate for relevant feeding events to derive the relevant estimated number of feeding events.

We first estimated demographic characteristics for undetected feeding events that occurred during effort-days (i.e., the numerator in Eqn. 7; blue fill in Fig. 4-6d) through leveraging the detected feeding event data. Specifically, we predicted whether undetected feeding event *i* for pack-session *g* was demographic class *c* (species: bison, deer, elk, bighorn sheep, moose, pronghorn; sex-age class: calf, yearling, female-adult, male-adult) as:

$$c_{i,g} \sim Multinomial\left(\left(1 - p_{c_t}\right) \times \ prop.diet_{c_{s,u}}\right) \tag{8}$$

In the first part of Eqn. 8, $p_{c_t}$ represented the probability of detecting a feeding event of demographic class *c* by the detection methods that operated for the pack-type (*t*) of pack-session *g* (Appendix S4-D). For clarity, what demographic class *c* represented depended on what we were estimating because we used this equation to 1) predict species and then 2) to predict sex-age class when unknown and the species was an elk or bison. Among prey species, we only estimated detection probability for bison, deer, and elk because other species rarely occurred in wolf diet (see *Results*). We therefore assumed detection probability for *i*) bighorn sheep and pronghorn were the same as deer and *ii*) moose was the same as elk. Similarly, we combined calves and yearlings when estimating detection probability for sex-age class of elk or bison, thereby using the same estimate of detection probability for calves and yearlings. We estimated these detection probabilities for species and sex-age class through simple Bayesian detection models where we included only feeding events detected for wolf packs monitored by ≥ 2 detection methods (Appendix S4-D). We condensed all ground and aerial detections to a single occasion and did not include any covariate effects. For pack-sessions whose pack-type was ground or GPS, we used estimates of detection probability while ignoring availability, because some detection effort occurred daily (Figs. 4-6b, S4-C.2). But for pack-sessions monitored through only aerial effort, we used estimates for detection probability that included availability. We did so because detecting feeding events in these cases was only possible when there was aerial effort.

In the latter portion of Eqn. 8, $prop.diet_{c_{s,u}}$ represented the proportion of detected feeding events of demographic class *c* during season *s* (early or late winter) for pack-sessions of zone *u* (Interior-West, Interior-Central, Northern-Upper, Northern-Middle, Northern-Lower). The proportion used was defined through a 3-year moving average that was centered on the year-of-interest, although we sometimes lengthened the window because of small sample size. For example, the moving average for species and elk sex-age class sometimes included data from additional years and, in the case of bison, we *i*) estimated the proportion of each sex-age class across all years and, *ii*) for Northern YNP zones, also across all zones. Similarly, we also occasionally used spatial areas that were less focused than zone *u* (e.g., we grouped all feeding events across the three Northern zones; see Appendix S4-D for full details).

We also made predictions for undetected feeding events (following Eqn. 8) that existed when no detection methods were operating i.e., when availability was 0 (those first added through Eqn. 7; green-fill in Fig. 4-6d). For example, this was common when pack-sessions were monitored through only aerial effort. To do so, we followed the same process as above, but altered Eqn. 8 to,

$$c_{i,g} \sim Multinomial\left(prop.diet_{c_{s,u}}\right) \tag{9}$$

so that proportional diet (for species, and then also for sex-age class of elk and bison) also now included the predictions that originated through Eqn. 8. The effect of $p$ was removed because no effort occurred to detect these feeding events, meaning that their composition was not affected by detection probability. All estimated feeding events contained information about their demography following Eqn. 9. We then assigned a biomass value to undetected feeding events using demographic class-specific values from detected feeding events (Appendix S4-B).

Next, we similarly predicted how feeding events were acquired, i.e., killed or scavenged. Scavenging was simplified to represent the perspective of the wolf pack that was assigned the feeding event, meaning a feeding event was only assigned as a wolf kill if that pack killed the ungulate. We predicted each feeding event as a wolf kill (*k* = 1) or scavenge (*k* = 0) as:

$$k_{i,g} \sim Binomial\big(\, prop.wolf.kill_{c^*{}_{s,a}}\big) \qquad (10)$$

where *prop.wolf.kill* represented the proportion of feeding events that were wolf kills of detailed-demographic class $c^*$ (elk young [i.e., calf or yearling], female-adult, or male-adult; bison young, female-adult, or male-adult; deer; moose; bighorn sheep; pronghorn) during season *s* (early or late winter) for pack-sessions of subsystem *a* (Northern or Interior YNP). We used these detailed-demographic classes because our observed data indicated that the likelihood of scavenging differed among sex-age classes of frequently used elk and bison (Appendix S4-D). We broadly grouped feeding events across space (i.e., Northern or Interior YNP) and time (i.e., across all years) because of sample size limitations and exploratory analyses revealed that the proportion of feeding events that were scavenged did not greatly vary across years.

### DENNING PERIOD

We detected feeding events only through searching wolf GPS clusters during the denning period (*sensu* Metz et al. 2011), and did not use aerial or ground methods. Although we only had one field method for detecting feeding events during the denning period, we were still able to build similar mark-recapture models by leveraging individual GPS-collared wolves as independent detection sources (Fig. 4-7). This obviously required having multiple wolves in some pack-sessions, and then constructing availability histories to account for when only one GPS-collared wolf was in a pack. Having two GPS-collared wolves in a pack-session would be akin to employing two of the three detection methods (ground, air, GPS) for a roaming period pack-session (Fig. 4-6). Conversely, having one GPS-collared wolf would be similar to a pack-session during the roaming period that was monitored by only one of those methods.

*Detection method effort*. We detected feeding events by searching GPS clusters, created with the same rules as during the roaming period but with GPS locations acquired every 30 minutes to improve detection of small-body sized neonate prey (Webb et al. 2008). We searched GPS clusters for 23 wolves in 11 packs during 20 unique pack-sessions (Fig. 4-4, bottom panel). These 20 denning period sessions spanned 52 month-sessions, 18 in May ($\bar{x}$ = 29.6 ± 1.0 SE days per pack-session; range: 17 – 31; n = 18), 20 in June ($\bar{x}$ = 30.0 ± 0.0 SE; n = 20), and 14 in July ($\bar{x}$ = 28.9 ± 1.2 SE; range: 19 – 31; n = 14). We censored data from (at least part of a study session for) two wolves for which we initially searched clusters because of dispersal, radiocollar failure, and/or our methodological framework could not be applied to a pair of wolves where both were GPS-collared (Appendix S4-A). Following censoring, we field-searched 5,871 of 6,394 (91.8%) non-censored GPS clusters by searching each GPS cluster (Appendix S4-A). At GPS clusters where wolf packs were actively raising pups (i.e., homesites), we included only obvious, and very rare, carcass sites to avoid double-counting feeding events because wolves commonly carry prey remains to their homesites (Packard 2003). Given this, we also included 136 additional homesite clusters as searched despite not searching them. We thereby ultimately classified 6,007 of the 6,394 (93.9%) clusters as searched (Table S4-A.1b).

Similar to the roaming period, we defined whether each feeding event was available to be detected by a detection source, i.e., wolf-1 and wolf-2, within a pack-session. We defined availability as 1 if the wolf belonged to the pack during the 3-day period when we considered a feeding event to be active (Appendix S4-A). Defining availability similarly allowed us to account for the unequal distribution in effort that resulted from having a different number of detection sources (here, 1 or 2 GPS-collared wolves in a pack) for feeding events during some pack-sessions.

We accounted for differences in effort among pack-sessions to overcome bias in the number of feeding events detected during a pack-session. First, we characterized pack-type for each pack-session as having one or two GPS collars (Table S4-A.1b) to overcome the bias that results from having a different number of detection sources (i.e., GPS-collared wolves) in the pack, similar to the effect of multiple detection methods in the roaming period model above (Fig. 4-8). Second, we defined the proportion of a 92-day pack-session, which represented the maximum length for a pack-session during the denning period, where at least one GPS location belonging to a GPS cluster was searched. Lastly, we defined the proportion of GPS clusters that were searched during a pack-session. These latter two pieces of data were used as offsets in our denning period abundance model to overcome their associated biases (see *Denning Period – Mark-recapture feeding event abundance model* below). For example, fewer feeding events are obviously detected when the duration of a pack-session is shorter, all else being equal.

*Detected feeding events*. We detected 846 pack-level feeding events, associated with 838 unique ungulate carcasses, through our GPS cluster searches (Appendix S4-A). On average, we detected 42.3 (± 4.0 SE; range: 15 – 99; *n* = 20) feeding events during each pack-session. Feeding events were occasionally part of multi-carcass events, but we again treated each independently because individual feeding events did not always occur within the same GPS cluster. We assigned detection to an individual wolf if the wolf had a GPS cluster with a GPS location within 100-m of the carcass within 3 days of the feeding event 'birth', which was defined here by the first GPS cluster location after the specified date and time of death. Most detections occurred with the first location for the wolf on the first day (Appendix S4-A).

We necropsied all carcasses during the denning period and assigned the demographic (e.g., species) and acquisition (i.e., wolf-killed or scavenged) characteristics of each feeding event following methods described above in *Roaming period – Detected feeding events* and Appendix S4-A. We assigned species for 831 of 838 carcasses (99.2%; Appendix S4-A), and an age in 754 (90.0%) of these cases. We did not assign age class for only 16 (2.0%) carcasses.

*Covariates affecting feeding event detection*. We expected that detection during the denning period would be affected by covariates associated with the feeding event. As during the roaming period, we hypothesized that feeding event biomass (see Appendix S4-B) would positively affect detection and pack size (see *Wolf pack characteristics above* and Appendix S4-A) would negatively affect detection (Fig. 4-7). The other hypothesized covariates (e.g., wolf age class) differed from the roaming period because of differences in our methodology or aspects of wolf life history.

We hypothesized that wolf age class (yearling = 0; adult = 1) or whether a wolf was a denning female (no = 0; yes = 1) affected whether a wolf detected a feeding event because of their potential effect on how frequently a wolf attended a homesite. Previous work suggests that yearlings may attend homesites less frequently (e.g., Ballard et al. 1991) and we therefore hypothesized that being an adult (here, simply not a yearling) may positively affect detection. However, we expected being a denning female would negatively affect detection probability because of the related maternal demands (Packard 2003). We identified whether a female was a breeder who produced and tended to pups through evaluating GPS data (i.e., unsuccessful GPS locations become frequent when females enter a den; Walsh et al. 2016). Females remained a denning female in our data set throughout the denning period unless all the pups died, which we identified through field observations and through a lack of GPS locations at a homesite.

*Mark-recapture feeding event abundance model*. We used data augmentation to estimate feeding event abundance in a mark-recapture framework during the denning period, with the conceptual framework the same as the roaming period. We again leveraged detection and availability data, but here each capture occasion represented the individual wolf during the entire 3-day feeding event 'lifespan' (Fig. 4-5). Accordingly, there were only two capture occasions for each feeding event. Each of these two detection occasions was again represented by a 1 (detected), 0 (not detected), or NA (no effort by detection source), and each of the availability occasions was again represented by a 1 or 0 that indicated whether a GPS-collared individual (i.e., wolf-1 or wolf-2) was present (1) or not (0) for the pack-session during the feeding event lifespan (Fig. S4-C.4).

One other notable change for the roaming period model was how we structured the data, necessitated by differences in the detection sources between the denning and roaming period. Most simply, the covariates hypothesized to affect detection during the denning period were sometimes individual-level covariates. Wolf-1 and wolf-2, for example, were each either a breeding female or not. We therefore structured the data during the roaming period in a long format (Fig. 4-7), allowing for individual-level covariates. This resulted in each feeding event having two rows of data that each identified the detection of the feeding event by an individual wolf.

To estimate undetected feeding events in the denning period model for each of the 20 pack-sessions, we added 160 rows with 00 detection histories and NA-filled availability occasions. Given our long format, these 160 rows represented only 80 potential feeding events (i.e., half of 160) for the pack-session. Posterior checks of *N* for each pack-session again indicated that we provided sufficient augmented rows for the abundance estimation. As during the roaming period, we specified covariates specific to the pack-session (i.e., pack size) and, in this case, individual wolf (i.e., denning female, age class) for the augmented data, and described biomass by its mean and precision.

The inclusion ($z = 1$) of feeding event *i* for pack-session *g* was described in the same way as during the roaming period, and thus also described by Eqns. 1 and 2 (see *Roaming period – Mark-recapture feeding event abundance model* above). In this specification of Eqn. 2 when we accounted for the ecological factor of pack size (Fig. S4-C.5), we specified the intercept as $\omega_{g_t}$ because we only grouped pack-sessions by their pack-type *t* (one or two GPS-collared wolves). During the denning period, the terms $prop.sess_g$ and $prop.pack.effort_g$ in Eqn. 2 represented the proportion of a 92-day period with at least one GPS-collared wolf and the proportion of total GPS clusters for the pack-session that were searched, respectively (see *Denning Period – Detection method effort* above; Fig. S4-C.6).

The observation part of the denning period model was adapted to account for feeding event *i* occurring on *j* rows of data so that Eqns. 3–6 for the Roaming model were now adapted for the Denning model to be

$$Y_{j,g} \sim Bernoulli(p.eff_{j,g}) \tag{11}$$

$$p.eff_{j,g} = z_{i_{j,g},g} \times p_{j,g} \times a_{j,g} \tag{12}$$

$$logit(p_{j,g}) = \alpha + [\mathbf{B}\boldsymbol{X}_{\boldsymbol{j,g}}] \tag{13}$$

$$a_{j,g} \sim Bernoulli(mu.a_{j,g}) \tag{14}$$

where the primary changes from Eqns. 3–6 involved only using $i$ (of feeding event $i$) as a subscript on $z$. Here, the maximum values for $j$ equaled 2, and $j = 1$ and $j = 2$ represented the two capture occasions for wolf-1 and wolf-2, respectively. The indicator variable(s) for covariate-occasions was no longer required as covariates were simply removed during the model-building process, which was not possible during the roaming period when some covariates were retained only for certain capture occasions because of the inherent meaning of each capture occasion (e.g., ground method on day 1). The parameter $mu.a_{j,g}$ was again influenced by an informative prior that similarly described availability during detected feeding events, but in this case did so for the feeding events within only pack-session $g$ (see Table S4-C.1b). The final estimate for feeding event abundance for pack-session $g$ was again then estimated through Eqn. 7. Here, dividing through by $prop.pack.effort_g$ provided an estimated that accounted for not all GPS clusters being searched.

We used the same Bayesian stepwise technique as during the roaming period to reduce the covariates in our detection model (Fig. S4-C.7), and used all uninformative priors on covariates for the denning period. We fit and evaluated models in the same way as during the roaming period, and then extracted the same parameter estimates.

*Estimating the characteristics of undetected feeding events.* Similar to the roaming period, we needed to estimate the characteristics for each estimated, but undetected, feeding event. We again estimated species and then sex-age class for elk and bison, but we also estimated whether the feeding event was a neonate for other ungulate species. The initial prediction for species during the denning period was complicated, however, because of the high degree of species overlap (with respect to the key detection covariate of biomass; see *Results*) that results from the ungulate birthing seasons (Appendix S4-D). We therefore first leveraged a binomial classification of feeding event size when predicting species (see below). Regardless, we followed a similar procedure as during the roaming period to predict demographic (and acquisition) characteristics.

We first, however, simply distributed the undetected feeding events among the months of the (maximum) 92-day study session. We did so because feeding events were not uniformly detected over a (maximum) 3-month pack-session that spanned changes in adult vulnerability (Metz et al. 2012) and neonate availability (e.g., Barber-Meyer et al. 2008). We therefore first estimated the number of feeding events for each pack-session *g* during seasonal month *m*:

$$N_{m,g} = N_g \times prop.n_{adj_{m,g}} \tag{15}$$

where $N_g$ represented the estimate for the entire pack-session and $prop.n_{adj_{m,g}}$ was determined as:

$$prop.n_{adj_{m,g}} = \frac{\dfrac{n_{detected_{m,g}}}{prop.pack.effort_{m,g}}}{\sum_{m=1}^{n} \dfrac{n_{detected_{m,g}}}{prop.pack.effort_{m,g}}} \tag{16}$$

Eqn. 16 simply estimated the proportion of feeding events in month *m* (of *n*, where *n* = 1, 2, or 3) of pack-session *g* as a function of monthly patterns in both the number of detected feeding events and the proportion of GPS clusters searched during the pack-session (Fig. S4-C.6). We then distributed $N_{m,g}$ to those that represented feeding events with or without effort to detect them depending on if they were estimated through the numerator or completion, respectively, of Eqn. 7. Doing so allowed us to either account, or not account, for detection probability when predicting feeding event characteristics, which was similar to the roaming period (i.e., applying either Eqn. 8 or 9 during the roaming period).

The process of predicting demographic characteristics was then similar to the one used for the roaming period, with the most important difference being that feeding event size was the key initial variable of interest for the denning period. That is, we estimated simple detection probabilities for the denning period while accounting for feeding event biomass (Appendix S4-D). Again, we did so because significantly more overlap in among-prey species biomass exists during the denning period because of the ungulate birthing period(s) (Appendix S4-D). We also accounted for pack size during the denning period because of fundamental seasonal differences in wolf foraging ecology (Metz et al. 2011, Benson and Patterson 2015; see Appendix S4-D). Accordingly, we built simple Bayesian detection models where we included only those feeding events detected when two wolves were available for detection. We characterized each feeding event as small (<90 kg) or large (>90 kg), and each pack as the same dependent on if their pack size was below or above the median value of 8.5 wolves (Appendix S4-D).

We used the resultant detection probabilities (Appendix S4-D) to first predict whether undetected feeding events, from periods with effort, were small or large through Eqn. 8. Here, $p$ represented the detection probability for a small or large feeding event for a small or large pack with one or two GPS-collared wolves. The proportion diet in Eqn. 8 represented the proportion of all feeding events that were small or large during the same month for pack-sessions within that spatial zone, across all years (Appendix S4-D). Similar to the roaming period, we then predicted the size of all remaining feeding events through Eqn. 9 (Appendix S4-D).

Upon estimating the size of all undetected feeding events, we then used Eqns. 9 and 10 to predict the demographic and acquisition characteristics, respectively, of feeding events when unknown. We used data that described the proportion of demographic classes for each month and zone during the denning period, across all years to predict demographic class through Eqn. 9

(Appendix S4-D). Demographic class was expanded here to also include whether feeding events were neonates or not, including for species beyond elk and bison. At this point, we again assigned biomass values when needed in the same manner as during the roaming period (Appendix S4-B). Finally, we again used Eqn. 10 to predict whether a feeding event was a wolf kill or not. Data was specific to demographic class for elk and bison in Eqn. 10, while the other, more rarely acquired species were pooled together. We also combined data across all zones and months because of small sample size (Appendix S4-D).

### Wolf predation metrics

We tested our overarching hypotheses for changes in estimated wolf predation metrics over season, time, and geographic space (Table 4-1). We specifically tested for changes in wolf diet, niche breadth, kill rate, scavenging rate, and acquisition rate, often doing so *i*) for metrics expressed as both the number and biomass of prey and *ii*) among only primary prey (i.e., elk, bison, deer in Northern YNP; elk, bison, moose in Interior YNP; see *Results*). Within wolves' two most frequently used prey species (elk, bison), we also estimated most metrics for sex-age classes (e.g., calf, female-adult, male-adult; Table 4-1). We evaluated seasonal (i.e., across all five months that we measured: early winter, late winter, May, June, July) changes in predation metrics, but for only Northern YNP where we collected data during the denning period (Table 4-1). We tested hypotheses related to time for both Northern and Interior YNP (Table 4-1). Additionally, we tested specific factors (e.g., pack size, snow depth) that affected kill and scavenging rates across seasons for only Northern YNP. Finally, we evaluated how wolf predation rate on elk in northern Yellowstone was affected by time and elk abundance.

We generally estimated predation metrics at the population-level (i.e., across all pack-sessions during a seasonal month and relevant geographic space). In some cases, however, we estimated statistics at the pack-level (i.e., only from that pack-session). Regardless, we often also provide estimates at the pack-level in Appendix S4-E to display any potential differences in interpretation (*sensu* Jost et al. 2005).

We present our methods for testing our hypotheses related to wolf predation metrics first for Northern YNP and then for Interior YNP. The methodological approaches were the same for the more limited analyses associated with Interior YNP, and we therefore did not detail each employed analytical step for Interior YNP. Instead, we highlighted only the differences.

### WOLF DIET IN NORTHERN YNP

*Seasonal variation in prey species in Northern YNP wolf diet.* We first report the number and proportions of the various prey species that wolf packs acquired and killed across the seasonal months. Proportions in wolf diet were calculated as the proportion of a prey species among the *i*) total number of acquired feeding events (hereafter, ‘prop-number acquired’), *ii*) total biomass of acquired feeding events (‘prop-biomass acquired’), and *iii*) total number of wolf-killed (for the pack of interest) feeding events (‘prop-number killed’). We also calculated proportion wolf diet among the total number of wolf-scavenged feeding events (‘prop-number scavenged’), but we did not always report this metric. Instead, we usually discuss the influence of scavenging on diet proportions as the difference between acquisition and killing. We compared the median and quantile values for wolf diet across the seasonal months. Overall, we expected elk to dominate wolf diet across seasons. Among alternative prey, we expected bison to be most important in terms of biomass, and deer to be more frequent during the months within the denning period, but to always be rare in terms of biomass.

*Effect of time and space on prey species in Northern YNP wolf diet.* We predicted that wolf diet has changed through time. Most specifically, we expected elk to have declined in wolf diet, while we expected bison and deer to have increased in wolf diet. We expected bison would most prominently increase with time through predation metrics that included scavenged feeding events because bison are difficult for wolves to kill (e.g., MacNulty et al. 2014, Tallian et al. 2017b). We tested whether the diet of the three most frequently used prey species (elk, bison, and deer in Northern YNP, censoring all other prey), were affected by time (i.e., year; defined by the start of winter) within the early and late winter seasons. We only evaluated the explicit influence of year for the roaming period because our time series was complete and encompassed the elk population decline (Fig. 4-3) for only the roaming period (Fig. 4-4). We used Dirichlet regression (Douma and Weedon 2019) in the R package `DirichletReg` (Maier 2021) to test for an influence of year on wolf diet proportions. We modeled the response of proportion diet expressed in three ways to reflect different aspects of predator-prey dynamics (e.g., Vucetich et al. 2011); proportion (hereafter, 'prop.') of the number acquired, prop-biomass acquired, and prop-number killed.

Next, to test how the effect of year varied over space within Northern YNP, we also evaluated the effect of time on wolf diet (prop-number acquired, prop-biomass acquired, prop-number killed) within each spatial zone by developing individual Dirichlet regression models for pack-sessions of each zone. We compared differences in diet over time between Northern-Lower, Northern-Middle, and Northern-Upper zones (Figs. 4-2, S4-A.3; Tables 4-1, 4-2). We developed individual zone models because we expected different effects of year in each zone.

We also hypothesized that the changes in relative ungulate abundances over time would affect predation patterns during the denning period. Our data set during the denning period was more limited than the roaming period; we annually sampled 1-2 wolf packs during the denning period from 2008–2020, except 2019 (Fig. 4-4). Nonetheless, we expected that time similarly affected predation metrics during the seasonal months within the denning period. We therefore tested how predation metrics during the denning period were affected by time-stages (Fig. 4-3b). While doing so, we also revisited seasonal diet variation across all months (see *Seasonal variation in prey species in Northern YNP wolf diet* above), now through the lens of these time-stages to facilitate comparison. Here (and for later analyses), we characterized wolf diet during four time-stages (hereafter, 'quarter') where the relative abundance of elk and bison changed (Fig. 4-3b): 1) 1997–2001 (average elk:bison ratio = 24.9 [YNP], 30.6 [Total]; $n$ = 5 years); 2) 2002–2007 (6.9 [YNP], 10.0 [Total]; $n$ = 6 years); 3) 2008–2013 (1.6 [YNP], 3.2 [Total]; $n$ = 6 years); 4) 2014–2019 (0.5 [YNP], 2.0 [Total]; $n$ = 6 years). We again compared wolf diet proportions across months through their medians and quantile values, but now with an increased focus on patterns in time and space.

*Niche breadth over time in Northern YNP.* We tested our overarching hypothesis that niche breadth of Northern YNP wolf packs increased over time during the roaming period. Here, we were interested in doing so at the pack-level to embrace heterogeneity in food acquisition among wolf packs (but present population-level results in Appendix S4-E). We tested how diet changed through time by calculating Levins' standardized measure of niche breadth ($B$; Levins 1968, Hurlbert 1978), which measures the degree of specialization for a consumer as 0 (highly specialized) to 1 (highly generalized), for each pack-session ($n$ = 227) as:

$$B_i = \frac{\left[\left(\frac{1}{\sum_{i=1}^{n} p_{ig}^2}\right) - 1\right]}{(n-1)} \tag{17}$$

where $p_{ig}$ is the proportion of species $i$ in the diet of pack-session $g$. We similarly determined this statistic among only the three primary prey species in Northern YNP (elk, bison, deer) for our three measures of wolf diet (i.e., prop-number acquired, prop-biomass acquired, prop-number killed). We first evaluated the effect of time (i.e., year) on niche breadth using quasi-binomial model regression (Faraway 2016), expecting from Dirichlet regression models (see *Results*) that time would have a fundamental effect on niche breadth. We then added *i)* pack size and *ii*) spatial zone, and evaluated additive model combinations (e.g., year + pack size + zone as the most complex model) to test effects of group size and spatial variation on niche breadth. We made Northern-Upper the reference category because alternative prey (i.e., not elk) tended to be greatest in this zone earlier in time. We expected differences in space because the spatial zones are related to elevation, which influences the over-winter distribution of both elk and bison in northern Yellowstone over winter (White et al. 2012, Geremia et al. 2014).

*Sex-age class of elk and bison in wolf diet.* We evaluated how each sex-age class for wolves' two most commonly used prey (elk, bison; see *Results*) contributed to wolf diet to evaluate 1) from which of these sources wolves mostly acquired their food from and 2) how sex-age class structured predation patterns may affect ungulate dynamics (specifically by later turning these into rates; see *Effect of time on wolf acquisition-related rates on sex-age class of elk and bison in Northern YNP* below). Following Metz et al. (2012), we grouped sex-age class as neonates (<4 months), calf (5–14 months), yearling (15–26 months), and then female-adult and male-adult for individuals >26 months. Vulnerability of neonate calves is uniquely high during their first few months of life (Linnell et al. 1995, Barber-Meyer et al. 2008), and we also desired to group age classes together throughout the denning period. We similarly evaluated the composition of these sex-age classes expressed as prop-number acquired, prop-biomass acquired, and prop-number killed. We also calculated the coefficient of variation (CV) of proportional diet for elk sex-age classes for roaming period sessions, when sample size was greater, through the R package `cvcqv` (Beigy 2019). We hypothesized that calves, followed by adult-males, would be the most variable sex-age classes in wolf diet. We also hypothesized that metrics of acquisition, which included scavenging, would be the driven by adults, especially for bison.

### WOLF DIET IN INTERIOR YNP

We evaluated how changes (in West zone), or lack thereof (in Central zone), of relative elk and bison abundance over time affected the composition of species and niche breadth for the roaming period for Interior YNP wolf pack-sessions. We similarly used Dirichlet regression (wolf diet) and quasi-binomial regression (niche breadth) to test for the effect of year, and included whether wolf packs were 'West' or 'Central'. We hypothesized that wolves' use of elk would decline with year in the West zone because of similar declines in elk to Northern YNP. We expected that the decline of elk in wolf diet would be most obvious for early winter because previous work showed that wolves killed bison more frequently during late winter, even when Madison-Firehole elk abundance was higher (Becker et al. 2009b). Conversely, in the Central zone, where elk were always historically very rare, we did not expect an effect of year on wolf diet in the Central zone where most elk have always migrated away from. We did expect wolves' use of elk to generally be higher during early winter in both zones, especially for the Central zone because late migrants may still be present during early winter. For these reasons, we hypothesized that niche breadth (*B*) increased with year for West, but not Central, YNP.

## ACQUISITION, KILL, AND SCAVENGING RATES IN NORTHERN YNP

Wolf diet describes how wolves acquire their food but does not by itself provide an expectation for how prey or wolf abundance may be affected (Vucetich and Peterson 2004, Vucetich et al. 2011). Predation metrics that turn diet into rates, such as kill and scavenging rates, are required to understand potential impacts on each prey species. We used the model-based estimates for feeding events, *N*, and the associated biomass estimates, as the numerators (hereafter, 'number-prey' or 'biomass-prey') for testing how per-capita acquisition, kill, and/or scavenging rates changed across seasons, over time, and across space. We used per-capita estimates for rates, and reported the numerator using units that we thought were most digestible, i.e., the per-capita number per 30-days and the per-capita biomass per-day. We estimated acquisition, kill, and scavenging rates for all prey combined and separately for the three primary prey species (elk, bison, and deer in Northern YNP; elk, bison, and moose in interior YNP) and all other species combined. We also estimated these rates among sex-age classes of elk and bison. We primarily evaluated population-level rates, but also used pack-level rates on some occasions to assess the influence of pack size. We censored data for population-level rates from the denning period in 2020 because the only rate estimated was for a wolf pair and was thus greatly affected by pack size (see *Results*).

*Seasonal variation in wolf acquisition-related rates on prey species in Northern YNP.* We first tested for differences in rates across seasonal months to evaluate how general intraannual changes in the ecological conditions associated with temperate climates affected the rate that wolves acquired, killed, and scavenged prey. We hypothesized that acquisition and kill rate would peak during June when expressed as number-prey because elk neonate availability peaks at this time (e.g., Barber-Meyer et al. 2008). Conversely, we expected biomass-prey rates to peak during late winter and May because ungulate nutritional condition is generally poorest during these times of year (Parker et al. 2009, Metz et al. 2012) and elk calf abundance is presumably near its annual low point (or birthing is just beginning during the latter half of May; Barber-Meyer et al. 2008).

We expected scavenging rates to similarly peak during late winter because of weather severity (Parker et al. 2009), but also expected that scavenging rates on female-adult bison that occasionally die from birthing complications may also elevate scavenging rates during the earlier months of the denning period (Jones et al. 2010). We used ANOVA to test for seasonal differences in per-capita rates, and then used Tukey's tests (Day and Quinn 1989) to test for differences between the seasonal months. We did so for 'total' rates across all species combined and then also for elk, bison, and deer. We also tracked kill rates of neonates during the denning period to test for changes in the contribution of this highly vulnerable, abundant prey type as they emerge and then rapidly decline in their availability (Linnell et al. 1995, Barber-Meyer et al. 2008). We used population-level rates to test how rates differed among seasonal months (but present pack-level rates in Appendix S4-E).

*Effect of time and space on wolf acquisition-related rates on prey species in Northern YNP.* We next tested our overarching hypotheses related to how acquisition, kill, and scavenging rate for elk, bison, and deer were affected by the temporal shift in the ungulate populations (Fig. 4-3). We tested for these changes during the four temporal quarters of our study (Fig. 4-3b). We again used ANOVA and Tukey's to test for differences in species-specific acquisition, kill, and scavenging rates between quarters. We hypothesized that kill rate on elk would be lower during the latter quarters, especially during late winter. We expected the most dramatic differences for elk during late winter because not all migrant elk have left YNP by early winter (White et al. 2012). We hypothesized that rates on bison would be higher during the latter quarters, and that the most dramatic differences would be for acquisition and scavenging rates (i.e., those that did not solely rely on the contribution of wolf-kills) because bison are difficult for wolves to kill (MacNulty et al. 2014, Tallian et al. 2017b). We expected that kill rate on deer would be higher during the latter quarters and greatest during late winter following elk migration out of YNP by late December.

We next tested hypotheses related to how the rate of biomass-prey acquired was affected by time and pack size, the latter of which has been previously demonstrated to affect per-capita food acquisition in wolves (e.g., Thurber and Peterson 1993, Schmidt and Mech 1997). Here, we first assessed for whether changes over time in how (e.g., from which species, killed or scavenged; see *Results*) wolves acquired food resulted in changes to the per-capita rate of food acquisition across time during the roaming period. We used population-level rates for this first test. Next, however, we used pack-level rates to test how pack size affected the per-capita rate of biomass-prey acquired within each season. Our goal for this second test was primarily to see whether the known effect of pack size (e.g., Thurber and Peterson 1993) clearly extended to non-winter seasons.

*Factors affecting kill rates on elk in Northern YNP.* Elk in YNP (and elsewhere in the United States Northern Rockies) have been the dominant prey killed by wolves for the last two-plus decades (e.g., Metz et al. 2020a). We therefore evaluated ecological factors affecting kill rate (number-prey) on elk. Elk abundance is the main factor from classic predator-prey theory expected to affect kill rate (Messier 1994). We used linear models to evaluate the effect of relevant factors from our and other systems, including elk abundance, pack size (Thurber and

Peterson 1993, Schmidt and Mech 1997), winter severity (for winter seasons; Huggard 1993, Mech et al. 2001), and the proportion of diet from neonates/calves (denning/roaming; Metz et al. 2012, Sand et al. 2012). We also initially considered forage biomass available to elk during the previous growing season because we expected elk nutritional condition may affect kill rate (Wilmers et al. 2020). However, we ultimately censored forage biomass because final models (see below) did not include this covariate and we did not have data for 4 of 23 years. However, we note we kept forage for the scavenging rate models on elk (see below).

We included total (Northern Range) elk abundance (Fig. 4-3) for denning period seasons, using total elk abundance because all or most of these elk migrate into YNP during the growing season (Houston 1982). We did not, however, include wintering YNP elk abundance during winter seasons because YNP elk abundance and the alternative prey covariate (see below in this section) were too strongly correlated (e.g., r = 0.49 in early winter and r = 0.63 in late winter), and the alternative prey covariate outperformed elk abundance in univariate models for the roaming period. Censoring elk abundance from this analysis highlights the challenge of identifying the density-dependent nature of wolf predation in multi-prey systems, which we solve later in Chapter 5 using dynamic mathematical models (see also *Discussion*). Regardless, we still tested for effects of other (i.e., non-prey abundance) covariates on wolf kill rates on elk during the roaming period seasons.

We hypothesized that increasing alternative prey in the diet would negatively affect kill rate on elk (Metz et al. 2020b), and therefore included the proportion of biomass acquired from all prey that were not wolf-killed elk (e.g., all bison, scavenged elk). This covariate, as well as the proportion calves/neonates, was estimated from our feeding event abundance model. Pack size was characterized as described above (see *Wolf pack characteristics* above), but log-transformed here to account for the non-linear effect of pack size on kill rate (e.g., Thurber and Peterson 1993). Winter severity represented the mean value of daily measurements of snow depth at Tower Falls, WY (www.ncdc.noaa.gov/cdo-web/search) during winter sessions. We tested for an effect of these factors using kill rates on elk estimated at the pack-level during each seasonal month ($n$ = 101 [early winter]; $n$ = 126 [late winter]; $n$ = 18 [May]; $n$ = 20 [June]; $n$ = 14 [July]), primarily to increase sample size for denning period months. We developed models specific to each season because 1) of fundamental differences in predation metrics (see *Results*; Metz et al. 2012) and 2) we considered different covariates during roaming and denning period months.

For linear models of wolves' kill rate on elk, we developed all additive models without random effects using the R package lme4 (Bates et al. 2015) and evaluated models through $\text{AIC}_c$ using the R package `AICcmodavg` (Mazerolle 2020). We also screened against collinearity and, after removing elk abundance (see above), no other covariates were strongly correlated (maximum $|r| = 0.13$ [roaming months], 0.39 [denning months]). We then removed models with uninformative covariates (Arnold 2010) and re-evaluated our reduced model set through $\text{AIC}_c$. We did not consider any interactions amongst covariates. Finally, we added random effects for year and spatial zone to our top model, and then evaluated the relative contribution of fixed and (retained) random effects using the `rsq` package (Zhang 2021). We standardized all continuous covariates to facilitate ease of comparison amongst covariates on different scales.

*Factors affecting scavenging rates on elk and bison in Northern YNP*. Recent work also highlights the theoretical importance of scavenging to large carnivore population abundance and community dynamics (Focardi et al. 2017, Mellard et al. 2021). But the factors that affect scavenging rate by large carnivores, and how those may be affected by characteristics of the ungulate species, are poorly understood. We therefore followed the same model-building process that we used with wolf kill rates on elk. Unlike kill rate, which was normally distributed, scavenging rate was overdispersed (Fig. S4-E.1). Thus, we fit negative binomial general linear models of scavenging rate with the `mass` package (Ripley et al. 2021) to evaluate the factors that affected the rate wolves scavenged elk and bison. For each prey species, we tested the importance of pack size, population abundance, snow depth, and forage productivity. We also considered interactions between *i*) snow and population abundance and *ii*) forage and population abundance. Based on the importance of forage, we retained forage for the elk models, but censored it from the bison models. We could not include elk and bison abundance in the same models because these populations were highly correlated (r = -0.85).

*Effect of time on wolf acquisition-related rates on sex-age class of elk and bison in Northern YNP.* Finally, we also tested for temporal differences in kill and scavenging rates on sex-ages classes within our two primary prey, elk and bison. Previous work highlights the importance of prey demography for inferences about the effects of large carnivore predation on ungulate population dynamics (e.g., Gervasi et al. 2012, Hoy et al. 2021). Similar considerations may also be crucial when considering the importance of various prey to large carnivore population dynamics, given that large-bodied adult ungulates are the most likely to die in ways that are unrelated to predation in many terrestrial systems (e.g., Sinclair et al. 2003). We therefore evaluated how time affected the rate that wolves acquired, killed, or scavenged elk and bison sex-age classes through leveraging the four quarters that we identified (Fig. 4-3b), again using ANOVA and Tukey's tests to specifically test for differences between quarters.

### ACQUISITION, KILL, AND SCAVENGING RATES IN INTERIOR YNP

We also evaluated the effect of time on acquisition and kill rates within the West and Central zones, comparing these two systems for general differences. We did so in the same manner as for Northern YNP.

### PREDATION RATE IN NORTHERN YNP

We used population-level estimates for kill rates on elk from the roaming period, bi-annual counts of resident NR wolf abundance (Table 4-3; Smith et al. 2020a), and estimates for northern Yellowstone elk abundance (Table 4-3; Fig. 4-3) to develop estimates for wolf predation rate on elk for 1997–2019 (Table 4-1). Predation rate describes the proportion of the elk population killed by wolves and is the most informative predation metric for directly assessing the influence of wolf predation on elk population dynamics (Messier 1995, Sinclair and Pech 1996, Vucetich et al. 2011). We estimated predation rate during winter (6 months) and annually (12 months) because we were interested in evaluating whether resident NR wolf predation had different theoretical effects on the NR elk population that wintered inside of YNP versus the total elk population. We assessed these theoretical effects through evaluating the nature of the relationship between predation rate and elk abundance.

We directly estimated predation rate (PR) during year *i* as:

$$PR_i = \frac{\sum_1^n kr_{i,j} \times d_j \times W_{i,j}}{E_i} \tag{18}$$

where *n* represented the number of three-month periods (*n* = 2 for estimates of winter predation rate; *n* = 4 for estimates of annual predation rate), *kr* represented the kill rate (number elk killed per wolf per day) in year *i* during a three-month period *j*, *d* represented the number of days in period *j*, *W* represented resident Northern YNP wolf abundance in year *i* during three-month period *j*, and *E* represented the elk abundance during year *i*. We began each year *i* in November to generally align estimates of wolf predation with the elk counts that occurred during winter (Fig. 4-3). We estimated predation rate for four three-month periods: *i*) November–January ($d$ = 92), where we used early winter kill rate and December wolf abundance (Fig. 4-3), *ii*) February–April ($d$ = 89), late winter kill rate and March wolf abundance (Smith et al. 2020a), *iii*) May–July ($d$ =92) mean winter kill rate x 0.7 (seasonal correction factor; Messier 1994) and March wolf abundance, and *iv*) August–October ($d$ =92), mean winter kill rate x 0.7 and subsequent December wolf abundance (Table 4-3). Here, wolf abundance represented only counts of resident Northern YNP wolves, meaning that we did not include *i*) wolves that primarily lived outside YNP and ii) wolves that primarily lived in Interior YNP. These wolves killed northern Yellowstone elk but we expected excluding these wolves would have minimal influence on our inferences because we expected, for example, wolf density was much lower outside of YNP.

We used Eqn. 18 to estimate wolf predation rate in three ways. First, we estimated predation rate during a 6-month 'winter' season using *i and ii* above and the estimate for the elk population wintering inside of YNP (solid line in Fig. 4-3a) to represent wolf predation rate for 'Winter-YNP'. The relationship between this estimate and elk abundance provides insight into how wolf predation affected abundance of elk wintering within YNP, which is the segment of the elk population that has most dramatically declined (Fig. 4-3; White et al. 2012, MacNulty et al. 2020b). Second, we used the same estimates for kill rate and wolf abundance and the estimate for the total elk population (dashed line in Fig. 4-3a) to represent wolf predation rate for 'Winter-Total'. The relationship between predation rate and elk abundance here provides insight into how spatial refuge outside YNP may change the nature of the relationship between predation rate and elk abundance during winter. Third, we estimated an annual predation rate using *i*–*iv* above and the estimate for the total elk population (dashed line in Fig. 4-3a) to represent wolf predation rate for 'Annual-Total'. This relationship between elk abundance and wolf predation rate is ultimately the one that best describes how resident NR wolf predation rate affects elk abundance, overall.

## RESULTS

### Wolf pack characteristics

#### ROAMING PERIOD

We included 349 pack-sessions where we detected at least one feeding event. Among these, 227 were characterized as Northern YNP and 122 as Interior YNP (Fig. 4-4). The spatial assignment of packs from MCP centroids were well aligned with the percent of time that wolves were detected in the Northern subsystem exclusively during study sessions (Table 4-2). Pack size averaged 9.6 wolves (± 0.3 SE; range: 2 – 27; $n$ = 349). Pack size did not differ between Northern and Interior YNP, with pack size averaging 9.5 and 9.8 wolves, respectively. However, pack size tended to be greater during early winter in both YNP subsystems. Average pack size decreased from 11.1 (± 0.5 SE; range: 2 – 27; $n$ = 101) to 8.1 (± 0.4 SE; range: 2 – 25; $n$ = 126) from early to late winter in Northern YNP ($t$ = 4.53; df = 195.6; $P$ = < 0.001), and from 11.0 (± 0.7 SE; range: 3 – 24; $n$ = 56) to 8.7 (± 0.6 SE; range: 2 – 20; $n$ = 66) in Interior YNP ($t$ = 2.46; df = 112.8; $P$ = 0.02). Year did not affect pack size in either subsystem during either winter season (Fig. S4-E.2). Although year did not affect pack size, the number of packs that were monitored changed over time, reflective of wolf population size (i.e., compare Figs. 4-3, 4-4).

#### DENNING PERIOD

We included 20 pack-sessions, all of which were for Northern YNP. Three of these pack-sessions were for packs who centrally located their territory in Northern-Lower, 9 in Northern-Middle, and 8 in Northern-Upper (Table 4-2). Pack size, from our single pack-session estimates, averaged 8.3 (± 0.8 SE; range: 2 – 15; $n$ = 20) individuals.

## General monitoring effort

### ROAMING PERIOD

We typically monitored packs for 30-day sessions during the roaming period, although some pack-sessions were shorter. We therefore standardized the following numbers as those expected for a pack-session of 30-days, if a pack-session was shorter than 30 days. The omnipresent aerial method, on average, attempted to locate each pack on 13.7 (± 0.3 SE; range: 3 – 27.3) days during each pack-session. During these aerial attempts, we obtained radiolocations on packs on 13.1 (± 0.3 SE; range: 3 – 27.3) days, and visually observed packs on 11.9 (± 0.3 SE; range: 3 – 23) days, during a pack-session (Fig. S4-E.3). For the aerial method, there was a recent seven-year period, however, when the plane tended to fly less frequently (Fig. S4-E.4).

We monitored a subset of pack-sessions using the ground method ($n$ = 133). On average, observers using the ground method attempted to observe these packs on 29.8 (± 0.1 SE; range: 20 – 30) days during a pack-session. For these pack-sessions, ground observers obtained radiolocations on 28.2 (± 0.2 SE; range: 13 – 30) days, and visually observed packs on 21.2 (± 0.4 SE; range: 6 – 29) days during a study session (Fig. S4-E.3). For the ground method, there were no obvious effects of time on effort-related metrics (Fig. S4-E.4).

## Feeding event abundance

### ROAMING PERIOD

Using our roaming period Bayesian mark-recapture model (Eqns. 1–7) we estimated that 3,998.6 feeding events existed on the landscape during effort-days (orange and blue-filled sections of Fig. 4-6d; Fig. S4-C.2), and 4,960.6 during all study session days (now also including green-filled sections of Fig. 4-6d; Fig. S4-C.2), during the 349 pack-sessions where we detected at least one feeding event. This estimate of 4,960.6 across all roaming period pack-sessions represented a 112% increase from the 2,343 feeding events that were just detected (Fig. 4-9a).

Our Bayesian model selection approach led to a roaming period model that retained effects of biomass, distance, openness, pack size, the number of radiocollars, and viewshed on detection for some occasions (i.e., dependent on method and, for the air and ground methods, day of feeding event lifespan; Fig. 4-10a). When using the informative prior during our final model development, we removed openness-A1 because the estimates for this beta coefficient had a median value of <0.01 for the full, initial model ('Non-augmented – model 1' in Fig. S4-C.3). Evaluations of Bayesian Rhat values were all near 1 (Fig. S4-E.5), suggesting that chains for pack-session abundance estimates mixed well.

The biological effect of pack size on feeding event occurrence ($\psi_{i,g}$) was significant ($\beta$ = 0.31; 95% CI: 0.24, 0.38), positively affecting the probability that $\psi_{i,g}$ was indeed a feeding event (Fig. 4-10a). The detection model included effects that were positive for biomass on detection occasions G2, A1, A2, and GPS1 (e.g., for A1, $\beta$ = 0.34; 95% CI: 0.23, 0.45; see Table S4-C.2 for all beta coefficient estimates), negative for distance on G1 and G2, positive for openness on G1, G2, and A2, negative for pack size on A1 and GPS1, positive for the number of collars on GPS1, and positive for viewshed on G1 (Fig. 4-10a). Overall, the effects of covariate-occasions on detection were in the same direction as predicted.

Variation in pack-type, with the associated variation in detection probabilities (Fig. S4-E.6) and effort-days (Fig. S4-C.2), resulted in non-uniform increases amongst methods from naïve to estimated feeding event abundance among pack-sessions (Figs. 4-11a, S4-E.7). Pack-sessions monitored only by air (*n* = 213) had the largest percent increase in estimated feeding event abundance; on average, estimates for these pack-sessions increased by 150% and 292% for only effort-days and the entire study session, respectively. Estimates for pack-sessions monitored by all three detection methods (but excluding 'partial GPS'; *n* = 38) increased relatively little in comparison to the naïve (on average, 10% for both estimates). Pack-sessions monitored by the ground and air methods (two methods) made up 26% of all pack-sessions (Fig. 4-6b). Estimates for these 92 pack-sessions increased by 56% for both effort-days and all days. The lack of any substantial difference in estimates for effort-days and all study session days for packs monitored by ≥2 methods, which therefore must have included either ground or GPS, was the result of these packs having daily attempts to detect feeding events.

We also estimated detection probabilities through simplified Bayesian models (i.e., without the influence of any covariates) for species (elk, bison, deer) and sex-age class (for only elk and bison) to leverage in predictions in Eqn. 8 (see Appendix S4-D for model details). We estimated, for example, that mean detection for an elk by the air was 0.49 (95% CI: 0.46, 0.52; filled red circles in 'Available feeding events' in Fig. 4-12) or 0.35 (95% CI: 0.32, 0.37; open red circles in 'All feeding events' in Fig. 4-12) depending on if a flight occurred during the 2-day feeding event window. Effort (i.e., availability) only meaningfully affected detection for the air because effort was usually constant for the ground and GPS methods, given the ground or GPS method was employed for a pack-session (Fig. S4-C.2). For both the ground and air methods, detection of elk and bison were similar. For example, the probability of detecting a bison for the ground method was 0.64 (95% CI: 0.57, 0.72), while the probability of detecting an elk was 0.72 (95% CI: 0.69, 0.74), ignoring any effect of availability (i.e., open blue circles in 'All feeding events' in Fig. 4-12). The probability of detecting a deer by the ground method was lower in this same scenario ($p$ = 0.31; 95% CI: 0.22, 0.41). Conversely, probability of detection for the GPS method was similarly high (minimum $p$ = 0.88; open green circles in 'All feeding events' in Fig. 4-12) across all species. Overall, differences among the probability of detecting different sex-age class were underwhelming and sometimes counterintuitive based on expectations from biomass alone (Fig. S4-D.1). For example, the average detection probability for the ground method for elk sex-age class was lower for male-adults ($p$ = 0.65; 95% CI = 0.60, 0.69; open blue circles in 'All feeding events' in Fig. S4-D.1) than for female-adults ($p$ = 0.80; 95% CI = 0.76, 0.84) or young ($p$ = 0.72; 95% CI = 0.68, 0.76), although the credible intervals overlapped with the latter.

### DENNING PERIOD

We detected 846 feeding events during the denning period. Our abundance model, however, estimated 1,211.8 and 1,297.5 feeding events depending on if the proportion of GPS clusters that were searched was accounted for or not (i.e., the numerator or result of Eqn. 7). This total estimate of 1,297.5 feeding events represented a 53% increase from the 846 detected feeding events (Fig. 4-9b).

The number of feeding events that we estimated through our denning period Bayesian mark-recapture model (Eqns. 1, 2, 7, 11–14) was influenced by a simpler suite of covariates affecting the detection process, including just biomass and pack size (Fig. 4-10b). Evaluations of Bayesian Rhat values were all near 1, suggesting that chains for pack-session abundance estimates mixed well. The top model showed that the number of feeding events was again affected by the positive influence of pack size in the biological process model (i.e., $\psi_{i,g}$; *ß* = 0.41; 95% CI: 0.25, 0.57; Fig. 4-10b). Detection probability was positively affected by feeding event biomass (*ß* = 0.19; 95% CI: 0.04, 0.34), and pack size negatively affected detection (*ß* = -0.27; 95% CI: -0.46, -0.07). Each of these covariates influenced detection as expected. The other hypothesized covariates of denning female and wolf age class did not affect detection probability during the denning period (Fig. S4-C.7).

The percent increase from naïve to estimated feeding event abundance during a denning pack-session was also affected by the number of detection sources (i.e., GPS-collared wolves) (Figs. 4-11b, S4-E.8). Estimates of feeding events from pack-sessions with one GPS-collared wolf throughout the entire pack-session (*n* = 13) increased by 60% and 70% over raw detections depending on if the proportion of GPS clusters searched was adjusted for (i.e., the numerator or result of Eqn. 7). This distinction (i.e., the just-reported 60% or 70% over detected feeding events) is important only because the first number (i.e., gray boxes in Fig. 4-11b) is representative of the increase that resulted from our model *per se*, while the latter number (i.e., black boxes in Fig. 4-11b) accounted for additional undetected feeding events that were missed simply because not all GPS clusters were searched. The number of feeding events obviously increased less for the six pack-sessions that had two GPS-collared wolves (*n* = 6), specifically by 23% and 34% (Fig. 4-11b).

Feeding event characteristics during the denning period were also estimated following the initial abundance estimates through leveraging data on wolf diet across spatial zone (Appendix S4-D) and a simplified Bayesian model that accounted for differences in detection among feeding events of different sizes (i.e., above or below 90 kg) and wolf pack size (i.e., above or below 8.5 wolves). This model predicted, for example, that a large-sized feeding event in a large pack had a detection probability of 0.74 (95% CI: 0.68, 0.79) for a pack with one GPS collar and 0.93 (95% CI: 0.90, 0.96) for a pack with two GPS collars (Fig. S4-D.7).

## Wolf predation metrics

### WOLF DIET IN NORTHERN YNP

*General summary of species in Northern YNP wolf diet.* We estimated that there were 3,382.3 feeding events during 227 roaming period pack-sessions (average duration = 29.4 days) and 1,297.5 feeding events during 20 denning period pack-sessions (average duration = 76.8 days) for Northern YNP wolf packs. Using our multinomial approach, we estimated that 2,844.2 (84.1%) were elk, 308.6 (9.1%) were bison, and 197.1 (5.8%) were deer (including both *O. hemionus* and *O. virgianus*) during the roaming period, and 978.4 were elk (75.4%), 172.1 were bison (13.3%), and 122.9 were deer (9.5%) during the denning period. Collectively, these three species made up 99.0% and 98.1% of all feeding events during the roaming and denning periods (see Figs. S4-E.9, S4-E.10). The remaining 1 or 1.9% included moose, bighorn sheep, and pronghorn.

Among the dominant species, elk and deer were usually wolf kills in our data set, while bison were often scavenged. Wolves killed 2,602.4 of 2,844.2 (91.5%) elk and 186.6 of 197.1 (94.7%) deer during the roaming period, and 962.8 of 978.4 (98.4%) elk and 121.9 of 122.9 (99.2%) deer during the denning period. Conversely, wolves scavenged 204.7 of 308.6 (66.3%) bison during the roaming period, and 70.4 of 172.1 (40.9%) bison during the denning period.

The relative contribution of each species, however, also tended to vary between the months that we studied wolf diet (Fig. 4-13). And our perspective of diet also depended on the estimate of diet, recalling that we examined prop-number acquired, prop-biomass acquired, and prop-number at the 'population-level'. Focusing first on diet simply as prop-number acquired (the most natural extension from our abundance model), elk were always the most common species that wolf packs acquired, but the median value was greatest during early winter (median = 0.90; interquartile range [IQR] = 0.78, 0.94; *n* = 23) and lowest during May (median = 0.73; IQR = 0.66, 0.79; *n* = 12) and July (median = 0.74; IQR = 0.65, 0.76; *n* = 9). Among deer, the median value for prop-number acquired was ≤0.06 for all months except July (median = 0.20; IQR = 0.16, 0.22; *n* = 9; Fig. 4-13), while, for bison, the median value peaked at 0.18 (IQR: 0.13, 0.32; *n* = 12) during May, when some wolf packs killed neonate bison. Outside of May the median value for prop-number acquired bison never exceeded 0.10 (Fig. 4-13).

Seasonal differences in the contribution of species were accentuated when we considered prop-biomass acquired, not merely prop-number acquired (Fig. 4-13). Biomass is more important from a wolf numeric response perspective, for example. Prop-biomass acquired estimates for bison were approximately double those of prop-number acquired during June and winter seasons (e.g., late winter prop-number acquired = 0.10 [IQR: 0.03, 0.21; *n* = 23] and prop-biomass acquired = 0.17 [IQR: 0.09, 0.41; *n* = 23]; Fig. 4-13). Those in May increased less dramatically from 0.18 (median; IQR: 0.13, 0.32) to 0.25 (median; IQR: 0.17, 0.29). When expressed as prop-biomass acquired, the increase in bison was usually reflected in corresponding changes in elk, since the small size of deer resulted in their rarely being important for prop-biomass acquired (Fig. 4-13). Accordingly, prop-biomass acquired from elk varied greatly during some months (e.g., during late winter; median = 0.82; IQR = 0.56, 0.91; *n* = 23; Fig. 4-13).

The prop-number killed among elk showed less variation than either the number or biomass of acquired prey (Fig. 4-13). For example, the coefficient of variation during late winter for prop-number killed (12.6; 95% CI: 9.4, 16.9) was approximately half that of prop-biomass acquired (19.1; 95% CI: 16.2, 24.0). Wolves tended to kill bison more during May (median = 0.10; IQR: 0.08, 0.22) when they killed bison neonates. The seasonal patterns for deer were same as those for the prop-number acquired. These evaluations of wolf diet changed, however, when we considered how they varied over time and space within YNP.

*Effect of time and space on species in Northern YNP wolf diet.* Overall, the results from our Dirichlet regression models generally matched our hypothesized effects of a longitudinal decline in wolves' use of elk concurrent to an increase in their use of bison and deer. Here, we first present the results of these models in prop-biomass acquired at the population-level, which is likely the most important metric from wolves' perspective. Year had a significant, positive effect on prop-biomass acquired from bison during both early ($p$ = 0.02) and late winter ($p$ = 0.01; top row of Fig. 4-14; Fig. S4-E.11). For elk and deer, however, the effect of year on prop-biomass acquired was not statistically significant. Yet during early winter, prop-biomass acquired of elk was predicted to have declined from 0.93 in 1997 to 0.60 in 2019 (though not statistically significant), increased from 0.04 to 0.31 for bison (significant), and increased from 0.03 to 0.09 for deer (also not significant). During later winter, prop-biomass acquired decreased from 0.94 to 0.41 for elk (not significant), increased from 0.04 to 0.53 for bison (significant), and increased from 0.02 to 0.06 for deer (not significant). If we had instead modeled the response at the pack-level (i.e., $n$ = 101 for early winter and $n$ = 126 for late winter), temporal patterns (but not always significance for the effect of year on species), and thus also inferences, were quite similar (also for prop-number acquired and prop-number killed; see Fig. S4-E.11). Occasional, subtle differences at the pack-level did hint, however, at the importance of certain prey species for certain pack-sessions (see Fig. S4-E.11).

The longitudinal trends in Dirichlet regression models for prop-number acquired and prop-number killed of elk and bison were similar, with some differences related to magnitude and significance. For example, for elk during late winter, year had a significant, negative effect on the prop-number acquired (middle row of Fig. 4-14) and prop-number killed (bottom row of Fig. 4-14). In contrast, for bison, year only had a significant effect on bison for prop-biomass acquired. Prop-number metrics for deer did increase through time during early (e.g., 0.02 in 1997 to 0.20 in 2019 for prop-number killed) and late winter (e.g., 0.02 to 0.23 for prop-number killed), although year was only significant for early winter (Fig. 4-14).

We expected the effect of time on wolf diet to vary across space (i.e., zone) because Northern YNP prey species abundance and distribution has varied in space and across time (e.g., White et al. 2012, Geremia et al. 2014), and therefore also tested for longitudinal differences in diet within spatial zones (Fig. 4-15; Lower, Middle, and Upper zones of Northern YNP; see Fig. S4-A.3) also using Dirichlet regression models. Across winter season and spatial zone, year generally had a significant negative effect on prop-biomass acquired from elk, with notable differences in the magnitude of that effect across the three zones of Northern YNP (Fig. 4-15; see Fig. S4-E.11 for pack-level results). For example, prop-biomass acquired from elk during early winter was predicted to be 0.96 in 1997 and 0.76 in 2019 for Northern-Lower packs, but 0.91 in 1997 and 0.47 in 2019 for Northern-Upper packs (Fig. 4-15). The across-zone variation in the effect of year on prop-biomass acquired among species differed during late winter in that prop-biomass has trended most upwards for Northern-Lower (Fig. 4-15). Our longitudinal models predicted that wolves increased their prop-biomass acquired through bison by 7, 9, and 8 times for Northern-Lower, Northern-Middle, and Northern-Upper, respectively, during early winter and 66, 19, and 7 times during late winter.

The results from our models about the effect of time on wolf diet also highlight how coarser annual evaluations of seasonal variation (Fig. 4-13) could be considered incomplete. In our case, the initial picture of denning period wolf diet suggests that wolves' use of bison, and possibly deer, were higher (and elk lower) than they were over the entire 23-year duration of our study. This is because our denning period diet estimates only occurred during the latter two quarters (2008–present), when prop-biomass acquired from bison had also increased during winter seasons (Fig. 4-16). Considering that increased bison use by wolves seems to extend across seasons since 2008, it is likely that wolves' use of bison was often low during the first decade when we did not measure wolf diet during the denning period. Spatial variation across Northern YNP also affected diet during the denning period (Figs. 4-17, S4-E.12, S4-E.13). For example, the use of bison during the denning period was consistently high in the Northern-Upper zone (Fig. 4-17), where bison primarily resided during most of our denning period. Conversely, wolves' use of bison was almost non-existent in Northern-Lower, although we only measured diet for three packs in this zone during the denning period. The extent to which these spatial patterns affect population-level diet during the summer denning period is unknown.

*Niche breadth over time in Northern YNP.* Building on our analyses of wolf diet, we tested our hypothesis of increasing niche breadth over time during the roaming period. Our estimates for niche breadth (*B*) clearly suggested Northern YNP wolf packs have acquired and killed prey increasingly as generalists over time. For example, *B*, calculated through the number-acquired averaged 0.04 (median = 0; range: 0 – 0.29; $n = 21$) and 0.02 (median = 0; range: 0 – 0.11; $n = 25$) during early and late winter, respectively, during the first five years of our study (1997–2001), but 0.39 (median = 0.34; range: 0.03 – 0.87; $n = 17$) and 0.52 (median = 0.53 range: 0.05 – 0.98; $n = 20$) for the most recent five years (2015–2019). The top quasibinomial regression models (black lines in each panel of Fig. 4-18) confirmed a positive influence of year on niche breadth across all metrics (i.e., biomass-acquired, number-acquired, number-killed) and seasons. Expanding our models to also evaluate the influence of pack size and/or spatial zone suggested that pack size was not an important factor (Fig. S4-E.14), and we therefore censored this covariate from all models. We did, however, observe a significant, negative effect of zone on niche breadth during early winter suggesting that niche-breadth declined in lower elevation zones (Fig. 4-18), a pattern that was also consistent at the population-level (Fig. S4-E.15). The effect of zone was only significant in late winter for number-killed (Figs. 4-18, S4-E.14) indicating that niche breadth increased generally in lower elevation zones of Northern YNP. The pattern in which niche breadth tended to be higher during early winter at higher elevations but lower at these higher elevations during late winter was consistent with predictions based on the winter movements of bison.

*Elk sex-age class in wolf diet in Northern YNP.* Important longitudinal changes have occurred in wolf diet at the species-level, but Northern YNP wolves have predominantly killed elk across all seasonal months (Figs. 4-13, 4-16). Across these months, the youngest age class was most common amongst wolf-killed elk during June, July, and early winter (Fig. 4-19). Six-month-old calves represented 0.41 (median; IQR: 0.30, 0.51; *n* = 23) of prop-killed elk during early winter, while neonates represented 0.68 (median) of wolf-killed elk in both June (IQR: 0.64, 0.74; *n* = 12) and July (IQR: 0.61, 0.75; *n* = 9). Neonates also represented one in four wolf-killed elk during May (median = 0.24; IQR: 0.14, 0.30; *n* = 12), despite wolves killing neonates almost exclusively during only the latter half of May. Regardless of the numerical contribution of neonates, the biomass-acquired from neonate elk was usually swamped by other elk sex-age classes (Fig. 4-19). Female-adults were the most frequently killed sex-age class in May (median

= 0.40; IQR: 0.29, 0.54; *n* = 12), and male-adults were the most frequently killed in late winter (median = 0.39; IQR: 0.30, 0.47; *n* = 23).

There was, however, variation in wolf diet among elk sex-age classes, which we highlight for the roaming period months. During early winter, the coefficient of variation in the prop-calves killed was 35.2 (95% CI: 26.5, 45.2), like that of female-adults (30.6; 95% CI: 21.9, 40.9; Fig. S4-E.16). Conversely, male-adults were more variable amongst wolf-killed elk in early winter (49.9; 95% CI: 36.5, 65.0), but the least variable in late winter (29.9; 95% CI: 22.5, 38.7; Figs. 4-19, S4-E.16). There was no obvious influence of spatial zone on wolf diet among elk sex-age classes during the roaming period (Fig. S4-E.17). But wolf diet among elk sex-age classes did display some trends through time (Fig. 4-20). For example, prop-calves tended to be greater earlier and more recently in time, during both early and late winter (Figs. 4-20, S4-E.18). Male-adults tended to increase during early winter throughout the initial years of our study, before leveling off. Female-adults initially made up a greater portion of wolf-diet during early winter (Figs. 4-20, S4-E.18), and their proportional contribution has tended to be lower during more recent years during late winter.

The overwhelming majority of elk in wolf pack diet resulted from the pack killing the elk, as can be inferred by the lack of difference between the panels for number-acquired, which included scavenging, and number-killed elk in Fig. 4-13. Prop-biomass scavenged was 0.08 (median; IQR: 0.03, 0.09) during early winter and 0.08 (median; IQR: 0.06, 0.16) during late winter (i.e., note the consistency between number-acquired and number-killed in Fig. 4-19). Wolves mostly scavenged male-adult elk (i.e., 64% and 67% of scavenged elk biomass during early and late winter, respectively), who are more likely to die of malnutrition, when they did scavenge elk. Among 149 detected adult elk that were not killed by the wolf pack assigned the feeding event, ~70% were wolves feeding on ungulates that did not die through predation, nearly 8% were usurped from cougars, and the remainder (*n* = 30; 20%) were themselves wolf kills initially belonging to other packs (Fig. S4-E.19). Regardless, very few of the elk that wolves acquired were through scavenging, in comparison to wolf kills.

*Bison sex-age class in wolf diet in Northern YNP.* Unlike elk, scavenging strongly shaped bison sex-age class composition because nearly 70% of all bison biomass, and 57% of the number, in wolf diet came from scavenged bison. For example, compare the differences in bison in the number-acquired and number-killed in Fig. 4-13. Male-adult bison led proportional biomass contribution across all month-sessions, providing, on average, at least 41% (minimum median = 0.45 [proportion]) of bison biomass per month (Fig. 4-21). Scavenged male-adults were, on average, 84% of the acquired adult-male biomass during late winter sessions (median = 1.0 [proportion]; IQR: 0.81, 1.0; *n* = 19; see also Fig. S4-E.20). The primary exception to male-adults dominating biomass was during May when male-adults (median = 0.45; IQR: 0.21, 0.61; *n* = 12) and female-adults (median = 0.40; IQR: 0.34, 0.51; *n* = 12) provided a nearly equivalent share (Fig. 4-21). Most biomass from female-adults came from scavenging year-round except early winter (e.g., May mean scavenging = 0.96; median = 1.0; IQR: 1.0, 1.0; *n* = 11). In early-winter, female-adult bison were often killed (proportion of kills = 0.80; IQR: 0.51, 1.0; *n* = 12), but this was highly variable (see Fig. 4-21). Younger individuals were generally killed more often, in comparison to other sex-age classes, when they appeared among the feeding events during a pack-session. That is, bison calves were killed, on average, 67% of the time during early winter (median = 1.0 [proportion]; IQR: 0.25, 1.0; detected or estimated in 6 of 18 sessions) and 49% of the time during late winter (median = 0.46 [proportion]; IQR: 0.00, 1.0; 15 of 20 sessions) sessions. When acquired, neonate bison during the denning period were also typically killed instead of being scavenged. For example, 94% (median = 1.0 [proportion]; IQR: 1.0, 1.0; *n* = 11) of neonates during May, and 98% (median = 1.0 [proportion]; IQR: 1.0, 1.0; *n* = 7) during June were killed by wolves. However, the contribution of smaller-sized neonates to overall biomass acquired through bison was small as acquired neonates made up 0.07 (median; IQR: 0.05, 0.08; *n* = 12) and 0.13 (median; IQR: 0.06, 0.35; *n* = 9) of biomass acquired during May and June, respectively. Among the 169 scavenged feeding events, 16 (9%) were in a management carcass dump (located in Northern-Lower), 147 (87%) were wolf scavenging bison that did not die from predation (and were not in the management carcass dump), and 6 were wolf packs scavenging on bison killed by other wolf packs (4%; Fig. S4-E.19).

### WOLF DIET IN INTERIOR YNP

We estimated 1,578.2 feeding events from the 376 detected feeding events during 122 roaming period pack-sessions. We estimated 875.9 (55.5%) were elk, 655.6 (41.5%) were bison, and 36.8 (2.3%) were moose, which accounted for 99.4% of all feeding events. The remainder were deer, and these largely originated from Interior YNP packs visiting Northern YNP (see Fig. S4-E.9).

For wolf packs in the West zone (which included the Madison-Firehole elk population) during early winter, 0.78 (median; IQR = 0.70, 1.00; *n* = 16) of prop-biomass acquired was from elk, with the rest coming from bison (median = 0.13; IQR = 0.00, 0.30; *n* = 16; Fig. 4-22). Prop-biomass acquired from elk (median = 0.46; IQR = 0.37, 0.61; *n* = 22) and bison (median = 0.54; IQR = 0.39, 0.63; *n* = 22) tended to be nearly equal for Central zone wolf packs during early winter. Wolves tended to acquire more bison biomass in both zones during late winter (Fig. 4-22), with 0.59 (median; IQR = 0.48, 0.70; *n* = 20) and 0.86 (median; IQR = 0.72, 0.94; *n* = 21) of prop-biomass acquired coming from bison for West and Central wolves, respectively. The conversion to prop-number acquired or killed resulted in similar patterns as for Northern YNP, but the changes were less dramatic for Interior YNP wolf packs (Fig. 4-22). For example, prop-biomass during late winter that was acquired from bison for Central wolves declined from 0.86 (see above) to 0.72 (median; IQR = 0.53, 0.90; $n = 21$) for prop-number acquired and to 0.59 (median; IQR = 0.38, 0.84) for prop-killed bison.

As expected, we found the clearest evidence for an effect of year on metrics of diet mostly in the West zone (Fig. 4-23), but no significant trend in the Central zone. In the West zone, the general pattern was a decline in prop-biomass acquired from elk from ~0.9 to ~0.5 in early winter, though not statistically significant (Fig. 4-23). During late winter, prop-biomass acquired from bison significantly increased from ~0.25 to ~0.75, concurrent with a decline in elk in the diet that was not itself significant, however (Fig. 4-23). The patterns in the Central zone were different than the West Zone. We found marginal evidence for increasing prop-biomass acquired during early winter (Fig. 4-23), but there was no support of an effect of year during late winter for any metric (Fig. S4-E.21).

Niche breadth increased with time in the West zone for Interior wolf packs in 5 of 6 models. Niche breadth in the West Zone increased during early winter from $\beta \cong 0.25$ to $\beta \cong 0.50$ (biomass-acquired) in the last decade because wolf diet was often comprised of just elk in the first decade. Conversely, the effect of time on niche breadth in the Central zone was unclear, variable, and often not significant (Figs. 4-24, S4-E.22). The cases where niche breadth was significantly affected by time in the Central zone were themselves variable and underwhelming (Fig. 4-24). If there was any trend, it was toward narrowing niche breadth as the diet of Central YNP wolves became even more concentrated on bison.

## ACQUISITION, KILL, AND SCAVENGING RATES IN NORTHERN YNP

*Seasonal variation in wolf acquisition-related rates on prey species in Northern YNP.* The rates that wolf packs acquired and killed prey also generally varied across the seasonal months of the year (Fig. 4-25), recalling that we estimated these rates at the population-level (see Fig. S4-E.23 through Fig. S4-E.26 for figures related to pack-level rates). Total (i.e., including all species) biomass-acquired rates differed across seasonal months ($F_{4,72} = 9.73$, $P < 0.0001$), and peaked during late winter (median = 10.0 kg/wolf/day; IQR = 9.0, 10.9; $n = 23$) and May (median = 9.6 kg; IQR: 9.0, 12.9; $n = 11$). These rates from late winter and May significantly differed from all other months besides June (median = 7.8 kg/wolf/day; IQR = 7.5, 10.0; $n = 11$). Early winter had the lowest biomass-acquired rate (median = 5.7 kg/wolf/day; IQR = 5.5, 7.3; $n = 23$), similarly low as in July (median = 6.6 kg/wolf/day; IQR = 6.0, 8.1; $n = 9$). Biomass-acquired rates only from elk ($F_{4,72} = 9.66$, $P < 0.0001$) also significantly differed seasonally, while biomass-acquired rates from bison were much less variable (Fig. 4-25; $F_{4,72} = 2.46$, $P = 0.05$). The subsequent tests for differences between months for only elk were similar as for total biomass, except that late winter and May were now different than all other months including June when only considering biomass from elk.

There were also seasonal differences in the rate that wolves killed elk ($F_{4,72} = 26.2$, $P < 0.0001$), bison ($F_{4,72} = 7.54$, $P < 0.0001$), and deer ($F_{4,72} = 10.41$, $P < 0.0001$). Subsequent pairwise comparisons for kill rate on elk indicated that only late winter (median = 1.4 elk/wolf/day; IQR: 1.1, 1.8; $n = 23$), May (median = 1.8 elk/wolf/day; IQR: 1.5, 2.2; $n = 11$), and July (median = 1.4 elk/wolf/day; IQR: 1.3, 2.1; $n = 9$) did not differ from one another. June (median = 2.7 elk/wolf/day; IQR: 2.2, 3.1; $n = 11$), driven by the consistent high kill rates on neonates (Fig. 4-25), and early winter (median = 1.0 elk/wolf/day; IQR: 0.9, 1.1; $n = 23$), which had the lowest kill rates, differed from these other months. Kill rates on bison were higher in May (median = 0.4 bison/wolf/day; IQR: 0.2, 0.5; $n = 11$) than in comparison to both winter seasons (median was <0.1 bison/wolf/day during each), while those in June (median = 0.2 bison/wolf/day) also differed from those in early winter. Finally, seasonal differences in kill rates on deer were driven by those from July (median = 0.4 deer/wolf/day; IQR: 0.3, 0.5; $n = 9$) always being different than other months.

*Effect of time and space on wolf acquisition-related rates on prey species in Northern YNP.* The coarse lens of these seasonal tests, however, ignored the changes in prey abundance that occurred over time (Fig. 4-3). We tested for the effect of time on the rates wolves acquired, killed, and scavenged their three primary prey by evaluating whether rates differed among the four quarters of our study. Through this lens, important changes over time were apparent, at least for the roaming period months (Figs. 4-26, 4-27; see also Figs. S4-E.27, S4-E.28, S4-E.29). Kill rate on wolves' primary prey of elk did not decline through time during early winter (e.g., $F_{3,19} = 1.65$, $P = 0.21$ for number-elk killed/wolf/30 days; Figs. 4-26, 4-27, S4-E.27). Nonetheless, kill rates on elk declined from median values that were ~1.1 elk/wolf/30 days during quarter-1 and quarter-2 to ~0.9 elk/wolf/30 days during each of the latter two quarters. In turn, kill rates on number-bison ($F_{3,19} = 5.43$, $P = 0.007$) and deer ($F_{3,19} = 9.07$, $P = < 0.001$) did differ among the four quarters (Fig. 4-27), because each increased during the most recent quarter when YNP elk abundance was lowest (Fig. 4-3b). Moreover, differences in scavenging biomass-rates on bison were marginally significant during early winter ($F_{3,19} = 2.52$, $P = 0.09$; Figs. 4-26, 4-27). Despite scavenging biomass-rates on bison not being significantly different across time while those from killing were, their median rates were comparable (i.e., killing = 0.95 kg bison/wolf/day, scavenging = 0.80 kg bison/wolf/day; Figs. 4-26, 4-27).

Late winter kill rates on elk did, however, decline in a manner consistent with predictions from classic predator-prey theory ($F_{3,19} = 9.39$, $P < 0.0001$; Figs. 4-26, 4-27). Kill rates on elk, for example, were half during quarter-4 (0.9 elk/wolf/30 days; IQR: 0.9, 1.0) what they were during quarter-1 (median = 2.1 elk/wolf/30 days; IQR: 1.7, 2.3). These longitudinal differences in kill rates on elk during late winter were inversely paralleled by differences in scavenging and kill rates on bison that differed across all units (Fig. 4-27). For example, wolves rarely scavenged biomass from bison during quarter-1 (i.e., median = 0 kg bison/wolf/day), but median biomass-scavenged rates from bison increased to 3.2 kg bison/wolf/day (IQR: 3.0, 3.7) during quarter-4. Also adding in wolf-killed bison resulted in wolf biomass-acquired rates of 3.8 kg bison/wolf/day (IQR: 3.5, 4.2) during quarter-4. In comparison, wolf biomass-acquired rates from elk during quarter-4 were 5.3 kg elk/wolf/day (IQR: 4.8, 5.8; Figs. 4-26, 4-27). Deer also increased across quarters, but these changes were of much less magnitude from the perspective of the wolf population. For example, the maximum observed biomass-acquired rate from deer was 0.7 kg deer/wolf/day (Fig. 4-27).

Longitudinal changes in rates concurrent with the stabilizing elk population (i.e., during quarter-3 and quarter-4) during the denning period were less obvious. For elk, only June differed between periods, with quarter-4 (median = 2.1 elk killed/wolf/30 days) having number-kill rates that were less than those of quarter-3 (median = 3.1 elk killed/wolf/30 days; Figs. S4-E.28, S4-E.29). Besides this month for elk, only the number of bison ever showed any evidence of differing between quarter-3 and quarter-4 (Figs. S4-E.28, S4-E.29). It is unclear whether the general lack of differences among rates during the denning period was the result of a relatively small sample size that spanned only the latter two quarters or because spatial variation in prey availability may have also affected our results.

Despite all the changes in prey abundance over 23 years (Fig. 4-3b), the end-result for individual wolves during the roaming period was that they acquired total food at similar per-capita rates (black lines in Fig. 4-28a; see also Fig. S4-E.30). The mechanisms of food acquisition, however, obviously changed, with bison and scavenging becoming emergent defining features of Northern YNP wolf diet (Fig. 4-28). Biomass-acquired rates have remained less variable in early winter in comparison to late winter (Fig. 4-29). Finally, biomass-acquired rates were clearly influenced by pack size during early and late winter (Fig. 4-30). May, June, and July biomass-acquired rates also appeared to be, despite small sample size (Fig. 4-30).

*Factors affecting kill rates on elk in Northern YNP.* Our roaming period models did not include elk abundance because we removed this covariate from consideration because it was highly correlated with prop-alternative biomass, which strongly outperformed elk abundance in univariate models. Pack size strongly affected kill rate on elk across all seasonal months, while other covariate effects differed among months (see Table S4-E.1 through Table S4-E.5 for AIC results). Also consistent was that random effects did not generally improve model fit during roaming period months but did in two of three denning period months.

During early winter, pack size and prop-alternative biomass were the only covariates to affect kill rate, and they both did so negatively (Fig. 4-31), as expected. In the top early season model the strengths of pack size and prop-alternative biomass were similar (pack size: $\beta$ = -0.31 [95% CI: -0.37, -0.24]; prop-alternative biomass: $\beta$ = -0.24 [95% CI: -0.30, -0.17]). The addition of year and zone as random effects only improved the $R^2$ from 0.56 to 0.58.

The best model for late winter kill rate on elk included the same random and fixed effects, and also snow depth and prop-calves (Fig. 4-31). Here, the directional effects for pack size ($\beta$ = -0.58 [95% CI: -0.66, -0.49]) and prop-alternative biomass ($\beta$ = -0.41 [95% CI: -0.50, -0.32]) were the same as during early winter, but each were considerably stronger during late winter. The effects of snow depth ($\beta$ = 0.11 [95% CI: 0.01, 0.20]) and prop-calves ($\beta$ = 0.11 [95% CI: 0.02, 0.20]) on late winter kill rate were comparatively weak, and similar in their strength to those of the random effects (Fig. 4-31). The amount of variation in kill rate explained in this late winter model was high (i.e., $R^2$ = 0.73, with the fixed-effects explaining 0.68 of the 0.73).

The denning period models also indicated that pack size was an important factor negatively affecting kill rate on elk in all three months (Fig. 4-31). Pack size was the only fixed effect in the top model for May (Table S4-E.3), and it had a strong negative effect on kill rate during May ($\beta$ = -1.35 [95% CI: -1.81, -0.90]). The top model for May did not retain any random effects, but still explained 71% of the variation in kill rate with pack size as the only covariate. Like in May, pack size was the sole fixed effect in the top model during June (Table S4-E.4), and it had a strong negative effect on kill rate ($\beta$ = -1.75 [95% CI: -2.38, -1.03]). The random effects for year and zone did improve model fit for June, increasing the $R^2$ value from 0.50 to 0.75. Finally, pack size had a weaker effect during July ($\beta$ = -0.23 [95% CI: -0.41, -0.07]) when prop-neonate also positively affected kill rate ($\beta$ = 0.57 [95% CI: 0.42, 0.74]). Here, the fixed-effect model for July already explained 86% of the variation in kill rate on elk, with a random effect for zone increasing the $R^2$ value to 0.88.

*Factors affecting scavenging rates on elk and bison in Northern YNP.* The factors that affected scavenging rates on elk and bison differed between species and seasons (see Table S4-

E.6 through Table S4-E.9 for AIC results). During early winter for elk, the top model included only pack size, but explained only 13% of the variation in scavenging rate on elk. However, pack size was not significant in this top model ($P = 0.11$ for the 19-year data set including the forage covariate, which we used here for elk because of the importance of forage during late winter for elk; see below), nor were any other covariates (including pack size) significant in any of the other top models. In essence, our evaluation of scavenging rates on elk during early winter revealed a highly stochastic process without explanatory covariates. Similarly, we detected no covariates that significantly affected scavenging rate on bison during early winter. The top supported model for early winter was the model including only bison abundance, but bison abundance was not significant ($P = 0.16$) and the model only explained 7% of the variation in scavenging rates on bison.

Scavenging models from late winter, however, both helped explain variation in scavenging rates on elk and bison. For elk, forage biomass during the previous summer was an important predictor of scavenging rate during late winter; we thus used the data set from the 19 years that we had data on forage. The top model, which explained 30% of the variation in scavenging rates on elk during late winter, included a negative effect for both forage biomass ($\beta = -0.43$ [95% CI: -0.84, -0.01]) and pack size ($\beta = -0.46$ [95% CI: -0.87, -0.03]), but not elk abundance. Our interpretation was that scavenging declined following higher forage biomass on summer ranges in the preceding growing season. A model that included a random effect for zone did not further explain variation in scavenging rates on elk.

For scavenging rate on bison during late winter, the top-ranked model included only a positive effect for bison abundance ($\beta = 0.78$ [95% CI: 0.33, 1.26]). This top-ranked model explained 33% of the variation in wolf scavenging rates on bison during late winter. A model with a random effect for zone was also not retained for bison during late winter. All significant covariates within these late winter scavenging models affected scavenging rates in the hypothesized direction.

*Effect of time on wolf acquisition-related rates on sex-age class of elk and bison in Northern YNP.* We expected kill rate on sex-age classes of elk would also be affected by density-dependent predation processes. In accordance with these predictions, we did find that kill rate on sex-age classes differed throughout time (Fig. 4-32), including among quarters during the roaming period for five of six possible season and sex-age class combinations (Fig. 4-33). Each of the two most reproductively valuable demographic classes of the elk population (calves, female-adults) experienced declines in the rate that wolves killed them. In the case of calves, early winter differences ($F_{3,19} = 6.85$, $P < 0.01$) were driven by quarter-3 being lower than quarter-1 and quarter-2, while late winter rates differed because of the higher kill rates on calves during quarter-1 ($F_{3,19} = 10.76$, $P < 0.001$) differing from all other quarters (Figs. 4-32, 4-33). Longitudinal differences in kill rates on female-adults displayed basic similarities to those on elk calves, at least in the sense that they also differed during early ($F_{3,19} = 3.3$, $P = 0.04$) and late ($F_{3,19} = 4.20$, $P = 0.02$) winter because kill rates were lower during the latter half of our study. In this case, quarter-4 was different than quarter-1 during early winter and quarter-3 during late winter. Kill-rates on male-adults during early winter displayed opposite longitudinal patterns, significantly differing ($F_{3,19} = 4.24$, $P = 0.02$) due to lower kill rates in quarter-1 in comparison to quarter-2 and quarter-3. Late winter kill rates on male-adults were marginally different ( $F_{3,19} = 2.65$, $P = 0.08$; Figs. 4-32, 4-33). Lower kill rates on neonates and female-adult elk in quarter-4, in comparison to quarter-3, also occurred during some denning period months (Figs. S4-E.31, S4-E.32).

Per-capita scavenging rates on elk only differed among quarters for adult-males during early winter (e.g., $F_{3,19} = 5.27$, $P < 0.01$ for biomass-scavenged; Fig. S4-E.32), doing so as a result of quarter-3 differing from quarter-1 (see also S4-E.33). Scavenging rates on bison, however, did show some important differences through time. Significant differences existed between biomass-scavenged rates during late winter for both male-adults ($F_{3,19} = 3.79$, $P = 0.03$) and female-adults ($F_{3,19} = 6.76$, $P < 0.01$). These differences were driven by quarter-3 and quarter-4 marginally differing from quarter-1 for male-adults, and by quarter-4 differing from quarter-1 and quarter-2 for female-adults (Fig. 4-34; see also Figs. S4-E.34, S4-E.35, S4-E.36). In early winter, scavenging rate itself did not significantly differ for any sex-age class, but the contribution of scavenging was important in the sense that biomass-acquired rates differed for male-adults during early winter ($F_{3,19} = 4.82$, $P = 0.01$). Additionally, biomass-acquired rates for female-adults were marginally significantly different ($F_{3,19} = 2.58$, $P = 0.08$), as were calves during late winter ($F_{3,19} = 2.48$, $P = 0.09$). Finally, kill rates on bison neonates were higher in quarter-4, in comparison to quarter-3, during June (Figs. S4-E.35, S4-E.36), although this observation may have been primarily driven by where we sampled in space (Fig. S4-A.3).

### ACQUISITION, KILL, AND SCAVENGING RATES IN INTERIOR YNP

Overall, the most striking pattern in longitudinal trends in the rates that wolves acquired biomass from elk or bison in the Interior was for the West zone during late winter, where there was clear evidence in a decline in per capita biomass-acquired from elk, and a corresponding increase in biomass-acquired from bison (Fig. 4-35). Per-capita rates during early winter in the West-zone were dominated by elk throughout most of the study (Fig. 4-35). Biomass-acquired rates were dominated by bison during late winter for Central wolves (Fig. 4-35). Rates during late winter in Interior-Central displayed a large amount of variation, largely because there was often only one pack of wolves living in this zone (Fig. S4-A.3). Wolf biomass-acquired rates were similar on elk and bison during early winter in the Central zone (Fig. 4-35).

### PREDATION RATE IN NORTHERN YNP

Estimates for resident Northern YNP wolf predation rate on elk were affected by elk abundance, with the nature of each relationship determined by which elk abundance defined the denominator in predation rate (Eqn. 18; Figs. 4-36, 4-37). For predation rates estimated only during winter (i.e., for 6 months), wolf predation rate was clearly inversely density dependent when elk abundance represented those elk wintering inside YNP (Winter-YNP in Fig. 4-36a), but appeared to be hump-shaped when elk abundance represented the total northern Yellowstone population (Winter-Total in Fig. 4-36a). Annual estimates for predation rate, which described the overall effect of resident Northern YNP wolf predation, were similarly hump-shaped on the total northern Yellowstone population (Annual-Total in Fig. 4-36a).

Estimates for winter predation rate on elk wintering in YNP peaked during quarter-4 (Winter-YNP in Fig. 4-36b), averaging 0.12 (range: 0.08 – 0.18), much greater than quarter-1 ($\bar{x} = 0.03$; range: 0.02 – 0.04). Winter-YNP rates differed across quarters ($F_{3,19} = 9.28$, $P < 0.001$), with differences observed between quarter-1 and all other quarters. Estimates for predation rates also differed across periods for Winter-Total ($F_{3,19} = 11.7$, $P < 0.001$) and Annual-Total ($F_{3,19} = 13.3$, $P < 0.0001$). Subsequent tests revealed that predation rates differed, in both cases, between quarter-1 and both quarter-2 and quarter-3, and then also between quarter-2 and quarter-4. As such, quarter-2 differed from all other quarters besides quarter-3. Quarter-2 represented the period when predation rate was highest (e.g., $\bar{x} = 0.09$; range: 0.06 – 0.12 [Annual-Total]; $\bar{x} =$

10,601 [elk abundance]), greater than that of quarter-1 ($\bar{x}$ = 0.04; range: 0.03 – 0.06 [Annual-Total]; $\bar{x}$ = 16,694 [elk abundance]) and of quarter-4 ($\bar{x}$ = 0.05; range: 0.04 – 0.06 [Annual-Total]; $\bar{x}$ = 7,485 [elk abundance]).

## DISCUSSION

How predators respond to and affect ungulate abundance are key questions for wildlife ecologists and managers in ecosystems worldwide where large carnivores reside. The landscape where wolves reside in YNP today is much different in comparison to the one where they were reintroduced beginning in 1995. The ungulates available to wolves dramatically changed through time, leading to a landscape that became defined by less vulnerable prey species. Our work took advantage of the decline and stabilization of the elk population, and the increase in the bison population (Fig. 4-3), to evaluate how wolf predation metrics responded to and influenced elk (and bison) abundance. Our first central finding was that most wolf predation metrics demonstrated dynamically changing predator-prey relationships over time. For example, wolf diet changed dramatically from one dominated by elk, to a much broader diet that increasingly included bison. Indeed, the increasing importance of bison, often through scavenging, to the predator-prey dynamic represents our second major finding, and challenges simple predictions of the role of wolves from single-predator-prey models. The challenge of multiple prey is demonstrated by the strong inverse correlation between bison and elk abundances, complicating simple interpretations of wolf-prey dynamics in the Yellowstone system. Despite this challenge our third major finding is support for density-dependent predation rate across ‘lower’ elk abundances that is at least partially consistent with the role of wolves in shaping the tail end of the decline and recent stabilization of elk. Overall, our results show a shift from dynamics driven largely by just wolves and elk to one instead driven by the dynamic between wolves, elk, and bison especially in northern Yellowstone. In this discussion, we first briefly highlight these three major findings. But since our results all depend on the Bayesian feeding event model, we then discuss results and performance of this model. We then discuss in detail these three major findings from the perspective of our predation metrics, and conclude with implications for the Yellowstone system and beyond.

Our first central finding was that every wolf predation metric was generally affected by time as predicted by classic predator-prey theory. Such theory (Holling 1959, Sinclair 1989, Messier 1995) predicts that for predation to be a stabilizing, regulatory factor, kill rate (for example) on the primary prey (elk in our system) must be density dependent, at least over some ranges of elk abundance. Our results support this prediction from density-dependent declines in wolf diet (Figs. 4-14, 4-23) leading to increasing niche breadth (Figs. 4-18, 4-24) across most of Yellowstone. These changes in diet have resulted in wolf diet in northern Yellowstone, for example, shifting over time from almost exclusively consisting of elk to now being defined by nearly equivalent contributions of biomass from elk and bison (Fig. 4-14). These changes in diet were reflected to a degree in density-dependent declines in kill rate. We found elk killed per wolf per unit time (i.e., kill rate) by Northern YNP wolves declined, but only during late winter (and not early winter), over time (Figs. 4-26, 4-27). However, kill rate did decline on female-adults and calves, most important to ungulate dynamics (Errington 1946, Gaillard et al. 2000), over time during both early and late winter (Figs. 4-32, 4-33). Declining kill rate with declining elk abundance would tend to stabilize elk population dynamics under classic predator-prey theory (Boyce and Gaillard 1992, Messier 1994). However, density-dependent kill rates may not be the only mechanism stabilizing elk population dynamics because of *i*) the effect of bison and spatial variation in the increasingly multi-prey system of YNP and *ii*) any density-dependent changes in the numerical response, critical to the effect of predation on prey abundance (Messier 1994), are not yet included.

The longitudinal declines in wolf kill rate on elk reveals the importance of our second central finding related to how wolves in Northern YNP acquired food. Wolves shifted over time to increasingly become generalist consumers as defined by their niche (diet) breadth (Fig. 4-18), driven by the changes in the prey community (Fig. 4-3). Undoubtedly, wolves are still mostly defined by the prey they kill, but wolves increasingly functioned as facultative scavengers of bison throughout YNP (e.g., Fig. 4-28b). In the Northern YNP subsystem, facultative scavenging was driven by bison abundance, and the importance of prey sex-age class was also evident here since most bison that were scavenged were adults, especially males (Fig. 4-21; see also Fig. 4-34). Most importantly, per-capita acquisition rate, though variable, did not necessarily change. Scavenging allowed wolves to acquire food during winter months at the same per-capita rate throughout the last twenty-three years (Figs. 4-28, 4-29). Nonetheless, the wolf population in Northern YNP also declined (Figs. 4-3, 4-29), suggesting that density-dependent processes related to wolves' primary prey affected their numerical response.

Our third major finding was the density-dependent nature of wolf predation rate on elk. Here, we observed two relationships between predation rate and elk abundance (Fig. 4-36). First, we considered wolf predation rate during winter only on the Northern Range elk population that resided within YNP (Winter-YNP in Fig. 4-36). Here, wolf predation rate during winter on elk was inversely density dependent (e.g., negative slope in Fig. 4-1), increasing at lower elk abundance, and thus suggested to be destabilizing (Messier 1995, Sinclair and Pech 1996). However, when we considered the total northern Yellowstone elk population including the portion wintering outside YNP, wolf predation rate was hump-shaped, both for just winter (Winter-Total in Fig. 4-36) and annually (Annual-Total in Fig. 4-36). This hump-shaped pattern that is density dependent at ‘lower’ abundances instead suggests that predation by Northern YNP wolves was a stabilizing force. Increased facultative scavenging is itself also capable of invoking stability and the hump-shaped pattern in predation rate (Wilson and Wolkovich 2011, Focardi et al. 2017). Thus, in combination, our results suggest wolf predation may be at least partially stabilizing in northern Yellowstone and consistent with the role of wolf regulation of elk to a lower stable equilibrium (see Chapter 5).

Next, we discuss specific findings related to our Bayesian abundance models first, and second, results of our analyses of changes in predation metrics over time.

### Estimating feeding event abundance through mark-recapture methods

The intense field work of detecting wolf predation events over nearly 25 years was the foundation of our study (Smith et al. 2020b), and represents amongst the longest predator-prey field studies of large carnivores in the world. Our study updated a previously developed mark-recapture estimator of wolf kill rate (Smith et al. 2004) using only two methods (air, ground) in a Bayesian framework. Our Bayesian model accounted for new methodological complexities and added new detection methods (i.e., GPS-collared detections during the roaming period) not required in Smith et al. (2004). Our work highlights the critical importance of accounting for detection probability and sampling effort (e.g., Figs. 4-9, 4-11, 4-12), and provides a framework that can be adapted for other complex detection problems, even if our specific modeling approach was tailored to Yellowstone. To illustrate the critical role of detection, consider the 26% (*n* = 92; Fig. 4-6b) of all roaming period pack-sessions that were monitored by the combined efforts of the air and ground. Our model increased feeding events for these pack-sessions 56% despite the ground method attempting to observe these wolf packs from sunup to sundown. Across all pack-sessions, we detected 2,343 feeding events by wolves in the roaming period during days with sampling effort (i.e., effort-days; see Fig. S4-C.2), but predicted 3,999 feeding events during these same days (4,961 during all study session days) – thereby detecting 59% of estimated feeding events during effort-days (47% during all study session days) – through also accounting for method-specific effort (i.e., availability). Though tailored to our system, adaptations to other species and predator-prey systems can be easily made. In fact, we did so when adapting our complex roaming period abundance model to the simpler model of the denning period (Fig. 4-7). But the main finding of our modeling approach is that large mammal predator-prey ecologists working across similar systems need to directly address whether detection of predation events is imperfect. Even in Yellowstone, amongst the world's best studied systems with as many as 3 detection methods and massive field effort, detection was quite imperfect.

Detecting killsites using aerial methods has been prominent among wolf predation studies, where previous studies estimated kill rate by counting the number of kills during a period of continuous daily monitoring (sampling period). For example, Dale et al. (1995) defined the sampling period beginning on the day after the first detected kill and ended the sampling period on the day of the last kill. However, this overestimates kill rate especially for short sampling periods (Hebblewhite et al. 2003). In our study, we minimized bias from sampling period duration through study design, i.e., 30-day pack-sessions (Fig. S4-C.2) and by not truncating pack-sessions (Hebblewhite et al. 2003). But previous studies have rarely, if ever, accounted for detection probability. Our work underscores Smith et al. (2004) and demonstrates the importance of detection probability for studies of large mammal predator-prey systems. Of course, we recognize that differences in Yellowstone may lead to higher detection probabilities by the airplane in other systems. For example, our study area contains areas that often have minimal snow cover, making aerial (or ground) backtracking to killsites infeasible. With sufficient snow cover, aerial or ground backtracking can provide a reliable method to improve detection rates and estimate kill rate in other systems (Hebblewhite et al. 2003) and species (e.g., Amur tiger, *Panthera tigris*, Yudakov and Nikolaev 2012). Yet aerial monitoring was long considered the standard in wolf-prey ecology. While our aerial detection probabilities (Figs. 4-12, S4-E.6) may have been relatively low compared to other studies, our results clearly show that detection probability is likely to be <1. And though many previous studies implicitly acknowledged their kill rates were likely minimum estimates, not until Smith et al. (2004) and our work has the magnitude of this potential bias been revealed. In future studies, it will be critical to account for imperfect detection when estimating predation metrics.

The results of our Bayesian feeding event models are estimates and subject to the effects of our own assumptions. Our assumptions would have primarily affected packs monitored by only the air method that did not operate daily (Figs. S4-E.3, S4-E.4), and would have done so in two ways. First, we assumed our first detection of any feeding event was on day-1 because we did not record the state of consumption upon detection. Future work would minimize any bias associated with this assumption by evaluating aerial day-1 detection, which would be seemingly most influential for larger feeding events where wolves may spend longer periods of time feeding. Second, some feeding events detected by only one method were occasionally included when they likely should not have been. For example, wolves remaining at a feeding event on day-3 or returning to a carcass. However, these events were exceedingly rare in our data, where

~1% of all feeding events detections for pack-sessions with multiple detection methods operating occurred after day-2. The result of this violation would likely have been minimal as we only included feeding events where it looked as if the carcass was 'fresh' and wolves had been actively feeding. In these cases, their inclusion would have represented a Type II error and increased kill rates. Despite any of these caveats, our estimates for packs monitored by the ground and air were well correlated with an index method used by Martin et al. (2018) that reduced the influence of days without observations of wolf packs, although our estimates were slightly higher as a result of accounting for detection probability. Our methodology was also an improvement from Smith et al. (2004) and Martin et al. (2018) in that it results in estimates from a greater number of pack-sessions and/or a larger spatial extent. Our model specifically advances Smith et al. (2004) by also including *i*) a biological process model that incorporates the underlying effect of pack size on the number of feeding events (i.e., Eqn. 2) and *ii*) the method that has quickly become the workhorse of large carnivore predation studies, GPS collars.

The advancement of GPS technology has fundamentally changed how species interactions, including large carnivore predation, are investigated (Merrill et al. 2010, Kays et al. 2015, Wilmers et al. 2015). Since the early 2000's, dozens of studies worldwide have employed GPS collars to find feeding events and estimate kill rate. Most, however, still implicitly assumed that detection of feeding events was perfect (but see Blecha and Alldredge 2015), or, neglected to adjust resultant field estimates for the proportion of potential cluster sites searched (Elbroch et al. 2018). Thus, many GPS cluster search-based methods may similarly suffer from the imperfect detection we report, and could benefit from adapting our Bayesian models that account for search effort and capitalize on multiple radiocollared individuals in a mark-recapture framework (e.g., in other social species such as African lions or African wild dogs, *Lycaon albipictus*). Like other studies, we first integrated GPS data into our field methods as the technology reliably emerged by 2008 in YNP. GPS clusters did in fact detect feeding events the best during the roaming period (Figs. 4-12, S4-E.6), with detection enhanced by multiple GPS collars in the pack (Fig. 4-10a). While some studies have had success predicting species and/or body size from predicted feeding sites, like many studies, we relied on field searches of GPS clusters. This will likely continue to be necessary in multi-prey systems, and, especially to discriminate scavenging (Elbroch et al. 2018). For example, in preliminary classification models, we experienced underwhelming predictive accuracy for kill sites (let alone prey species) at wolf GPS clusters (Metz, M., *unpublished data*). Our approach is also novel because, at least for wolves, there are still few studies of wolf predation during the summer. We also used GPS-collared wolves to estimate kill rates during the denning period, updating the work of Metz et al. (2011) to estimate feeding events in a Bayesian model that took advantage of multiple GPS-collared wolves in the same pack. Here, we also used a framework that accounted for availability, which provides an accessible model that could be used for wolves and other large carnivore species. Across seasons, our Bayesian feeding abundance models emphasize the importance of accounting for imperfect detection that forms the basis for the rest of our results.

## Wolf diet

Our wolf diet (i.e., prey composition) results differed depending on if wolf scavenging was included. Wolf-killed prey in Northern YNP were dominated by elk for most seasons (Fig. 4-13), and deer were often the second-ranked prey among prop-killed (Fig. 4-13). Yet, deer are small and provide little biomass. Bison were less well represented among prop-killed in Northern YNP, with two caveats. First, bison were often second-ranked during May and June when wolves killed neonates (Figs. 4-13, 4-16), but this observation was affected by space (Fig. S4-E.12). For example, bison were more likely to be a part of diet for wolf packs overlapping the summering range of bison in the Northern-Upper zone. Second, bison were better represented among prop-killed in roaming period months during the last quarter time period (Figs. 4-14, 4-16), suggesting these predation dynamics could continue to shift to more bison in the future. Wolves in Northern YNP could be learning to more successfully hunt bison, although evidence for such learning in large carnivores does not exist to our knowledge and suggests an important area for future research. Conversely, these most recent observations of increased bison in the diet could be the result of consistently low elk:bison ratios (Fig. 4-3b) and some pack compositions fulfilling the narrow requirements needed to kill bison (Tallian et al. 2017b). For example, Tallian et al. (2017b) showed how successfully killing a bison required having large wolf packs encountering smaller groups of bison with calves present. Longitudinal results from the roaming period in the Interior-West zone were similar to those from Northern YNP, although bison became featured in wolf diet earlier (Fig. 4-23). Bison were more prominent among prop-killed, especially during late winter (Fig. 4-22), in the West in comparison to Northern YNP. But as we predicted, bison were always most prominent among prop-killed for Central wolves (Fig. 4-23), largely because these wolves did not usually have resident elk available to them during roaming period months because almost all elk migrated to lower elevations with reduced snow cover. Taken together, our results suggest that the composition of wolf-killed prey is driven by the classic individual-level factors related to prey vulnerability and seasonal drivers of prey availability such as migration (Fryxell and Sinclair 1988, Mech and Peterson 2003, Pereira et al. 2014). Regardless, characterizing wolf diet is only important from the perspective of the prey when leveraged with kill-rate data to turn the number of prey into kill rates (and ultimately, predation rates; see *Kill, Scavenging, and Acquisition Rates* below). Wolf diet is important, however, for describing predator diet composition and breadth (i.e., niche). However, our view of wolf diet is incomplete if we omit scavenging, which increasingly became important in YNP.

Scavenging increased through time and was dominated by bison. The median prop-biomass acquired during late winter through scavenging on bison increased from 0 to 0.36 during quarter-1 and quarter-4, respectively (Fig. 4-28b; see also Fig. 4-16). This scavenging on bison contributed to a niche breadth for Northern YNP wolves that increased through time during both early and late winter (Fig. 4-18). Niche breadth also clearly differed across space during only early winter when niche breadth was generally lower in the Northern-Lower and Northern-Middle zones, in comparison to Northern-Upper (Fig. 4-18). This result was likely driven by bison migration from upper elevations of Northern YNP in mid-winter after our early winter study session (Geremia et al. 2014). Changing prey distribution of the Madison-Firehole elk population, which also declined over time (Garrott et al. 2009, Garrott et al. 2020), drove the same pattern of increasing niche breadth for Interior-West wolves (Fig. 4-24). Conversely, the inconsistent, often flat, and often insignificant effect of year suggests that the Interior-Central landscape changed relatively little through time from wolves' perspective (Fig. 4-24). But these simple measures of niche breadth mask the changes in the sex-age classes of prey acquired over time by wolves.

The sex- and age- structure, i.e., demography, of prey killed by predators ultimately affects the strength of predation on the prey population, i.e., how compensatory or additive predation impacts on prey are (Errington 1946). This data on predator diet must ultimately be combined with kill rate data to assess the strength of predation (see *Kill, Scavenging, and Acquisition Rates* below), but an important first step to this end is to determine predator diet. Our study showed wolves killed young elk in Northern YNP when these elk were expected to be most prominent on the landscape across seasons (i.e., during June, July, early winter; Fig. 4-19) and over time (Fig. 4-20). The proportion of calves killed over time initially declined during the roaming period, especially in early winter (Figs. 4-20, S4-E.18), driven by changes in elk abundance (Wilmers et al. 2020). Prop-calves among wolf kills tended to be the most variable sex-age class during late winter (Fig. S4-E.16), which aligns well with the relationship between variation in calf survival and variation in ungulate growth rate (Gaillard et al. 2000). However, female adult survival is the parameter that ungulate population dynamics tend to be most sensitive to changes in (Gaillard et al. 2000). Perhaps unsurprisingly then, females tended to contribute similarly to wolf diet during early and late winter (Fig. 4-19) and throughout much of our study. A critical period, however, when adult females made up a higher proportion of wolf kills was during late winter from 2005-2012 (Figs. 4-20, S4-E.18), a key period of decline for the elk population (Fig. 4-3; see further discussion below). But the tendency of wolves to kill senescent-aged adult females suggest weaker predation impacts than their frequency within diet alone (Wright et al. 2006, MacNulty et al. 2020b, Hoy et al. 2021). Surprisingly, despite the changes we report, the tendency for wolves to kill senescent adult females has remained constant over time (MacNulty et al. 2020b). Finally, the proportion of male elk killed by wolves tended to be higher following quarter-1. The initial, dramatic increase in male adults over time was largely driven by changes in elk abundance (Wilmers et al. 2020), and began to be higher around when the elk population began a critical period of decline (see below). Previous work suggests that the prop-wolf kills of males during this mid-point of our study, as well as generally during late winter, were the results of their nutritional condition (Metz et al. 2012, Wilmers et al. 2020).

Males are likely most sensitive to changes in their nutritional condition during winter following the energetic demands of the rut immediately prior (Metz et al. 2018, Chapter 2).

In general, our results complimented previous work from our and other systems. For example, our work highlighting that young prey are numerically dominant in diet mirrors other work for mountain lions (Knopff et al. 2010, Ruth et al. 2019), wolves (Jędrzejewski et al. 2000, Sand et al. 2008), and numerous other carnivores (Pereira et al. 2014). Moreover, the increased proportion of males in particular when they are nutritionally compromised is also similar to other work (Pole et al. 2004, Owen-Smith 2008). These results support the contention that wolf predation on elk tends to focus on the weak and vulnerable, rendering much of their predation impacts more compensatory in nature. The biggest strength of our within-elk diet work, however, was that we combined it with our estimates of kill rate to estimate kill rate specific to elk sex-age class through time (see *Kill, Scavenging, and Acquisition Rates* below). This was critical to characterize how large carnivores affect the elk population (e.g., Gervasi et al. 2012). However, considering diet of only wolf-killed elk ignores an important part of wolf diet, scavenging.

The composition of scavenged prey might seem inconsequential, but that perspective would ignore how relative contributions to overall diet may also affect predator abundance. Proportion-scavenging in our system was dominated by bison (Fig. 4-28b), which was driven by scavenging on adult females and especially large-biomass adult males (see Fig. S4-E.20 for prop-biomass acquired). Wolves scavenged on bison that originated in a number of ways, commonly including bison that fell through ice during winter and female-adults that likely died from birthing complications during the spring. We did not measure predation metrics during late summer, when male-adults also die from rut-inflicted injuries, providing another possible seasonal boom in scavenging opportunities. While death from such 'natural' non-predation mortality and accidents is a trivial component of bison population dynamics (White et al. 2015), with ~4,000 bison in northern Yellowstone, even a small percentage of these kind events provides ample resources for facultative scavenging. Scavenging on bison also occurred in other periods (e.g., early winter in Fig. 4-28b) and these known seasonal booms already cover a good portion of the year, suggesting that scavenging on bison is now an important and enduring feature of wolf-prey dynamics in Northern YNP. Male-adults were also the most likely sex-age class to be scavenged within elk (e.g., Fig. S4-E.33), often dying from malnutrition. These events were most frequent during late winter, but have also increased during early winter (see *Kill, Scavenging, and Acquisition Rates* below). Nonetheless, female-adult and especially male-adult bison represented the largest prey available to wolves in YNP, with males upwards of 500 kg of edible mass (Mattson 1997), and they had a huge impact on prey acquisition rates. In this manner, our findings echo results of previous studies in the Serengeti Ecosystem, where Sinclair et al. (2003) showed that the decreasing vulnerability of larger body sized prey, such as buffalo, giraffes, and elephants in that system meant predators tended to regulate prey abundance only of medium to smaller body sized prey. In contrast, in the Serengeti Ecosystem, food tended to regulate the abundance of larger body sized prey (Sinclair et al. 2003). In YNP, bison are regulated through interagency management at approximately 4,000–5,000 bison (Plumb et al. 2009, White et al. 2015), which ultimately also regulates the amount of bison biomass available for scavenging.

### Kill, scavenging, and acquisition rates

Our results about prop-killed at the species-level suggest that wolf kill rate on elk is the most meaningful measure of wolf kill rate, and thus we focus on the per-capita number of elk killed. Wolf kill rate on elk was clearly influenced by density-dependent processes during late winter, as predicted by classic predator-prey theory (e.g., Messier 1994). During this season, the number of elk killed per wolf declined from >2 to <1 elk killed per wolf per 30 days (Figs. 4-26, 4-27). Early winter kill rates on elk did not significantly differ through time, but nonetheless tended to be lower. Additionally, early winter kill rates on adult-females and calves, the most important segments for future population growth (Gaillard et al. 2000, Wright et al. 2006, Raithel et al. 2007), have declined in early winter (Fig. 4-33). These sex and age-specific kill rates support predictions of density-dependent predation and may be the mechanism leading to apparent stability of the elk population in the last decade at around 2,500 elk inside of YNP (Fig. 4-3). This observation also supports our earlier interpretation that wolf predation on elk may have become more compensatory in its nature (Errington 1946, Boyce et al. 1999), as highlighted by how the number of prey is not always a sufficient metric to fully evaluate the effect of predation (Gervasi et al. 2012, Hoy et al. 2015). Nonetheless, the number of prey is often the best metric available, and its simplistic nature is useful considering the complexity already present within multiple prey systems.

We did not attempt to use kill rates to estimate the shape of the wolf-elk functional response, despite that we have previously with an index of kill rate for a subset of these packs and years (Metz et al. 2020). Although that was amongst our initial goals of this study, there are several important reasons – both statistical and ecological – that lead to our conclusion that a different approach was necessary. First, sample sizes from empirically estimated kill rates will almost always render attempts to distinguish the shape of the functional response futile (Marshal and Boutin 1999). For example, Metz et al. (2020b) had similar difficulty distinguishing between a Type II and Type III wolf functional response on elk in YNP. In fact, we think it unlikely given environmental stochasticity and the important role of bison scavenging especially at ‘low’ elk abundance that the distinction between Type II and III models actually matters to predator-prey dynamics. Ecologically, in both our previous efforts and in this study (Fig. 4-31) we showed that kill rates were negatively affected by other food besides wolf-killed elk, which is driven by the contribution of bison (Metz et al. 2020b). Indeed, the extremely strong inverse correlation between elk and bison abundances means simple single species functional response models are unlikely to provide a reliable avenue for disentangling how wolf predation affects elk dynamics. As an example, our simple linear models of factors affecting kill rate on elk were better explained by the proportion of alternative prey in the diet than by elk abundance (see *Methods - Factors affecting kill rates on elk in Northern YNP*), given both could not be included in the same model because of their high collinearity. Instead, recent dynamic predator-prey models in the wolf-moose-caribou systems of the Boreal forests and mountains of Alberta emphasize that multi-prey dynamics can lead to non-intuitive results such as apparent competition, extinction, and very different equilibria (Serrouya et al. 2015). The general structure of such mathematical models can help disentangle confounded mechanisms such as our elk and bison correlations – and the confounding contribution of scavenging. Therefore, we leave addressing the predator-prey dynamics of wolves, elk, and bison, and the consequences of scavenging, to Chapter 5.

A key area of complexity that our work advanced was providing rigorous estimates of scavenging rates for wolf-prey systems. Key within our system were the scavenging rates on bison, like the diet and number of bison killed we discussed earlier, also increased through time (Figs. 4-26, 4-27). Our general linear models suggested that kill rate on elk during winter was most negatively affected by alternative prey use (Fig. 4-31), outside of the nuisance covariate of pack size (see Fig. 4-30). This effect extended over both winter seasons, although it was stronger during late winter (Fig. 4-31) when scavenging was also more prominent (Fig. 4-28b). In contrast to factors affecting wolf kill rates on elk, however, wolf scavenging rate on bison was an increasing linear function of available bison abundance in our system. Taken together, our work suggests that scavenging has become a critical component of the Northern YNP system, affecting both the ability of wolves to maintain a relatively constant per capita acquisition rate of biomass (Figs. 4-28a, 4-29) and kill rate on elk. As such, scavenging, particularly on dangerous bison that are infrequently killed in Northern YNP (see also Tallian et al. 2017b), may play a critical in shaping predator-prey dynamics.

For example, novel work on the role of scavenging in large mammal predator-prey dynamics shows that even the presence of scavenging can alter food web dynamics and stability. Though usually considered only as a prey species of wolves through Eurasia, recent field studies show wild boar (*Sus scrofa*) often scavenge wolf-killed prey. Focardi et al. (2017) built a series of dynamical mathematical models of predator-prey dynamics in this system and showed that scavenging can stabilize predator-prey dynamics and lead to higher equilibria densities of the primary prey, deer, and wild boar. Building on this work, and our empirical results, in Chapter 5 we developed a similar set of dynamical models parameterized with our data to test for the effect of scavenging on wolf-elk dynamics in Northern YNP. We found that like Focardi et al. (2017), the mere presence of scavenging of bison by wolves lead to similarly more stable and higher equilibria densities of elk and wolves. Taken together, our empirical results and dynamical modeling in Chapter 5 emphasize the crucial importance of scavenging to the present and future of YNP wolf-prey dynamics.

### Predation rate on elk

Classic predator-prey theory highlights that understanding the impacts of predation on prey depends on how predation rate changes with prey density. For example, in his classic study on moose, Messier (1994, 1995) demonstrated that if predation rate is a density-dependent function of prey abundance (e.g., positive slope in Fig. 4-1), it will tend to regulate prey to a lower, but stable, prey density equilibrium. Alternatively, if predation rate is inversely density dependent, it can act as a ratchet, increasing predation rate as the prey population declines in an accelerating fashion, destabilizing population dynamics. And hump-shaped patterns in predation rate are a mix of both, but also lead to stable equilibria. Here, with our focus on field estimates of kill rate, we adopted a similar approach as Peterson et al. (2014) to calculate three measures of resident Northern YNP wolf predation rate on elk in northern Yellowstone as a function of two measures of elk abundance. These three measures of predation rate were specifically winter predation rate on elk that winter inside of YNP, winter predation rate on the total northern Yellowstone elk population, and annual predation rate on the total northern Yellowstone elk population.

The effects of space on how the denominator of elk abundance is represented leads to contrasting conclusions about the role of wolf predation rate on elk population dynamics. Considering just the effects of wolf predation from winter on elk wintering inside YNP, we observed a strong inversely density-dependent predation rate (Winter-YNP in Fig. 4-36). Early in the study, wolf predation rate was low, ~0.03, but increased to ~0.12 as the elk population wintering inside YNP declined. Paradoxically, increasing predation rates occurred despite lower kill rates on elk, overall (Figs. 4-26, 4-27; see also Vucetich et al. 2011 for the disconnect between kill and predation rate). Such inversely density-dependent predation is consistent with continued elk declines and would result in no clear stability point for elk wintering inside YNP.

Similarly, Hebblewhite (2013) also reported inversely density-dependent predation rates by wolves on elk in the Bow Valley of Banff National Park where elk declined from approximately 1,000 to <100 in 25 years following wolf recovery. Another example was the West zone (Madison-Firehole) of Interior Yellowstone where inversely density-dependent wolf predation contributed to the rapid elk population decline (Garrott et al. 2009). Though earlier studies have suggested that increasing wolf predation rate on elk in YNP did not lead to declining elk population growth rate (Vucetich et al. 2011), our longer study suggests this is increasingly likely in the last two quarters at least for elk wintering within YNP.

However, once we considered the effects of space by considering the entire elk population inside and out of YNP, we observed a hump-shaped pattern in predation rate both for just estimates of winter (Winter-Total) and annual predation rate (Annual-Total; Fig. 4-36). Such a hump-shaped predation rate would tend to lead to a stable equilibrium density of about 10,000 elk. Over time, we observed wolf predation rates that peaked in the second quarter, with winter predation rates reaching ~0.05, and annual predation rates ~0.09, of the total elk population. These levels of predation rates by wolves, in of themselves, would be unlikely to cause elk populations to decline. But the hump shape and resultant equilibria strongly suggest that the effects of wolf predation on elk in YNP, combined with spatial structure and bison scavenging, is regulating total Northern Range elk abundance at an intermediate equilibria abundance of ~10,000 elk.

Our findings about wolf predation rate apply to only resident Northern YNP wolves (see *Methods – Predation Rate in Northern YNP*), although we do not suspect that including additional wolves would change our inferences. We suspect that inferences would be unaffected because the wolf numerical response on the Northern Range is known to be dominated by resident Northern YNP wolves. Given the importance of the numerical response in driving predation rate, especially at lower prey abundances (Messier 1994), our inferences would likely remain unchanged if comparatively few wolves were added to wolf abundance. That being said, future work should *i*) explicitly include additional relevant wolves, both from outside YNP and Interior YNP, in estimates of the wolf numerical response and *ii*) estimate kill rates outside of YNP, where wildlife management policy (White et al. 2015) may limit the influence of bison scavenging and elk abundance has remained similar (see Fig. 4-3).

## Conclusions

Of course, our focus on just the wolf-elk-bison portion of the YNP system, in particular the Northern YNP subsystem, overlooks other mortality sources and whether these other mortality sources are similarly density dependent. Given that the maximum reproductive rate of elk is ~28% per year (Eberhardt et al. 1996), our highest estimated predation rates by Northern YNP wolves alone would be insufficient by themselves to cause elk populations to decline. Previous studies emphasized that human harvest of elk was also explicitly managed in a density-dependent fashion, a legacy from the period before wolf reintroduction when the NPS and state of Montana cooperated to harvest female elk outside YNP specifically to reduce elk abundance (Varley and Boyce 2006, Boyce 2018). Our study, like previous work (Peterson et al. 2014), emphasizes that wolf predation rates in the first-time quarter on elk in YNP were quite low, incapable of driving the northern Yellowstone elk population decline. Time-series analyses by Vucetich et al. (2005) instead suggest that human harvest was super-additive during the early period following wolf recovery, likely because human harvest removed prime-aged reproductive females (Wright et al. 2006). This harvest, when combined with climatic factors, helped explain initial elk population declines, not wolf predation (Vucetich et al. 2005). Recent studies have also emphasized the broad suite of large carnivores and their effects on elk including mountain lions and especially grizzly bears in YNP (Peterson et al. 2014, MacNulty et al. 2020b). Both of these large carnivores have recovered to some degree, though not from extirpation like wolves, and certainly comprise significant mortality sources for elk affecting their dynamics (Barber-Meyer et al. 2008, Ruth et al. 2019). However, whether predation by these other species is just a limiting factor, or a regulating factor capable of contributing to a stable equilibrium elk population size is uncertain. Cougar predation in YNP was demonstrated to be inversely density dependent from 1988–2004 (Ruth et al. 2019), overlapping the time when wolf predation rate was also inversely density dependent (i.e., the right side of the hump-shape in Fig. 4-36). Yet, the complete relationship for cougar predation rate to elk abundance is unknown. Recent declines in the proportion of elk in cougar diet, to deer as opposed to the shift to bison by wolves (Stahler et al. 2020), suggests that cougar predation rate could have changed in a similar density-dependent manner as wolf predation rate did (i.e., the left side of the hump-shape in Fig. 4-36), but this remains unknown. Whether bear predation rate is density dependent in YNP is unknown, although previous studies have suggested bear predation tends to be density independent (e.g., Hebblewhite et al. 2018). Nonetheless, our study demonstrates evidence that density-dependent wolf predation rates over time, combined with wolf scavenging on bison, can provide perhaps one of several stabilizing forces contributing to an emerging equilibrium of about 10,000 elk on Yellowstone's Northern Range.

In conclusion, the predator-prey system in YNP and the Greater Yellowstone Ecosystem is complicated in both fundamental components of their ecology (multiple predator and prey species) and the effects of humans. This complexity challenges simple conclusions, for example, of the effects of wolves on their prey. Like other long-term studies of wolves and their prey on Isle Royale, conclusions of our study would have changed if we focused on any one five-year period (Vucetich et al. 2010). And the search for general conclusions across three comparative wolf-prey systems of Banff, YNP, and Isle Royale similarly struggled to do more than highlight the lack of generality regarding the question of the impact of wolves on prey (Vucetich et al. 2011). Ultimately, we reduced this complexity to evaluate the influence of wolves on their primary prey through the most essential metric of classic predator-prey theory, predation rate. Doing so resulted in a take-home message that predation by wolves is consistent with regulation of elk to a stable lower density equilibrium, but even this generalization is nuanced. Wolf-prey dynamics were strongly affected by both bison scavenging and spatial structure that were perhaps underappreciated before our study. This highlights the challenge of seeking generality from complexity. That classic predator-prey theory, based on single-predator, single-prey species might not best represent complex food webs such as YNP (see also Chapter 5) suggests the need for new multispecies predator-prey models that can expand to include predation by mountain lions, grizzly bears, and even humans (e.g., Clark 2021). Nonetheless, our work demonstrates that understanding the effects of large carnivores will require new and innovative approaches that advance theory and complexity to understand ecological systems, including ours.

## LITERATURE CITED

Anderson Jr., C. R., and F. G. Lindzey. 2003. Estimating cougar predation rates from GPS location clusters. The Journal of Wildlife Management **67**:307-316.

Arnold, T. W. 2010. Uninformative parameters and model selection using Akaike's Information Criterion. Journal of Wildlife Management **74**:1175-1178.

Bacon, M. M., G. M. Becic, M. T. Epp, and M. S. Boyce. 2011. Do GPS clusters really work? Carnivore diet from scat analysis and GPS telemetry methods. Wildlife Society Bulletin **35**:409-415.

Ballard, W. B., L. A. Ayres, C. L. Gardner, and J. W. Foster. 1991. Den site activity patterns of gray wolves, Canis lupus, in southcentral Alaska. Canadian Field-Naturalist **105**:497-504.

Ballard, W. B., J. S. Whitman, and C. L. Gardner. 1987. Ecology of an exploited wolf population in south-central Alaska. Wildlife Monographs **98**:1-54.

Barber-Meyer, S. M., L. D. Mech, and P. J. White. 2008. Elk calf survival and mortality following wolf restoration to Yellowstone National Park. Wildlife Monographs **169**:1-30.

Bates, D., M. Machler, B. Bolker, and S. Walker. 2015. Fitting linear mixed-effects models using lme4. Journal of Statistical Software **67**:1-48.

Becker, M. S., R. A. Garrott, P. J. White, C. N. Gower, E. J. Bergman, and R. Jaffe. 2009a. Wolf prey selection in an elk-bison system: choice or circumstance? Pages 305-335 *in* R. A. Garrott, P. J. White, and F. G. R. Watson, editors. The Ecology of Large Mammals in Central Yellowstone: Sixteen Years of Integrated Field Studies. Elsevier, San Diego.

Becker, M. S., R. A. Garrott, P. J. White, R. Jaffe, J. J. Borkowski, C. N. Gower, and E. J. Bergman. 2009b. Wolf kill rates: predictably variable? Pages 339-365 *in* R. A. Garrott, P. J. White, and F. G. R. Watson, editors. The Ecology of Large Mammals in Central Yellowstone: Sixteen Years of Integrated Field Studies. Elsevier, San Diego.

Beigy, M. 2019. cvcqv: Coefficient of variation (cv) with confidence intervals. R Package version 1.0.0.

Benson, J. F., and B. R. Patterson. 2015. Spatial overlap, proximity, and habitat use of individual wolves within the same packs. Wildlife Society Bulletin **39**:31-40.

Berryman, A. A. 1992. The orgins and evolution of predator-prey theory. Ecology **73**:1530-1535.

Beschta, R. L., and W. J. Ripple. 2016. Riparian vegetation recovery in Yellowstone: The first two decades after wolf reintroduction. Biological Conservation **198**:93-103.

Blecha, K. A., and M. W. Alldredge. 2015. Improvements on GPS location cluster analysis for the prediction of large carnivore feeding activities: ground-truth detection probability and inclusion of activity sensor measures. Plos One **10**:e0138915.

Borchers, D. L., S. T. Buckland, and W. Zucchini. 2002. Estimating animal abundance: closed populations. Springer, London.

Boyce, M. S. 2018. Wolves for Yellowstone: dynamics in time and space. Journal of Mammalogy **99**:1021-1031.

Boyce, M. S., and J.-M. Gaillard. 1992. Wolves in Yellowstone, Jackson Hole, and the North Fork of the Shoshone River: simulating ungulate consequences of wolf recovery. Pages 4:71-4:115 *in* J. D. Varley and W. G. Brewster, editors. Wolves for Yellowstone? A report to the United States Congress. Volume IV Research and Analysis. National Park Service, Yellowstone National Park, WY.

Boyce, M. S., A. R. E. Sinclair, and G. C. White. 1999. Seasonal compensation of predation and harvesting. Oikos **87**:419-426.

Brice, E. M., E. J. Larsen, and D. R. MacNulty. 2022. Sampling bias exaggerates a textbook example of a trophic cascade. Ecology Letters **25**:177-188.

Buckland, S. T., D. R. Anderson, K. P. Burnham, J. L. Laake, D. L. Borchers, and L. Thomas. 2001. Introduction to distance sampling: estimating abundance of biological populations. Oxford University Press, New York.

Carbone, C., and J. L. Gittleman. 2002. A common rule for the scaling of carnivore density. Science **295**:2273-2276.

Carbyn, L. N., N. J. Lunn, and K. Timoney. 1998. Trends in the distribution and abundance of bison in Wood Buffalo National Park. Wildlife Society Bulletin **26**:463-470.

Clapp, J. G., J. D. Holbrook, and D. J. Thompson. 2021. GPSeqClus: An R package for sequential clustering of animal location data for model building, model application and field site investigations. Methods in Ecology and Evolution **12**:787-793.

Clark, T. J. 2021. Large carnivore recolonization reshapes population and community dynamics: implications for harvest management. University of Montana, Missoula, MT.

Clark, T. J., and M. Hebblewhite. 2021. Predator control may not increase ungulate populations in the future: a formal meta-analysis. Journal of Applied Ecology **58**:812-824.

Craighead, J. J., G. Atwell, and B. W. O'Gara. 1972. Elk migrations in and near Yellowstone National Park. Wildlife Monographs **29**:3-48.

Curtis, S. M. 2018. mcmcplots: Create Plots from MCMC Output. R package version 0.4.3.

Dale, B. W., L. G. Adams, and R. T. Bowyer. 1995. Winter wolf predation in a multiple ungulate prey system, Gates of the Arctic National Park, Alaska. Pages 223-230 *in* L. N. Carbyn, S. H. Fritts, and D. R. Seip, editors. Ecology and conservation of wolves in a changing world. Canadian Circumpolar Institute, Edmonton, Alberta.

Day, R. W., and G. P. Quinn. 1989. Comparisons of treatments after an analysis of variance in ecology. Ecological Monographs **59**:433-463.

Diefenbach, D. R., M. R. Marshall, J. A. Mattice, and D. W. Brauning. 2007. Incorporating availability for detection in estimates of bird abundance. The Auk **124**:96-106.

Douma, J. C., and J. T. Weedon. 2019. Analysing continuous proportions in ecology and evolution: A practical introduction to beta and Dirichlet regression. Methods in Ecology and Evolution **10**:1412-1430.

Eberhardt, L. E., L. L. Eberhardt, B. L. Tiller, and L. L. Cadwell. 1996. Growth of an isolated elk population. The Journal of Wildlife Management **60**:369-373.

Elbroch, L. M., B. Lowrey, and H. U. Wittmer. 2018. The importance of fieldwork over predictive modeling in quantifying predation events of carnivores marked with GPS technology. Journal of Mammalogy **99**:223-232.

Errington, P. L. 1946. Predation and vertebrate populations. The Quarterly Review of Biology **21**:144-177.

Estes, J. A., J. Terborgh, J. S. Brashares, M. E. Power, J. Berger, W. J. Bond, S. R. Carpenter, T. E. Essington, R. D. Holt, J. B. C. Jackson, R. J. Marquis, L. Oksanen, T. Oksanen, R. T. Paine, E. K. Pikitch, W. J. Ripple, S. A. Sandin, M. Scheffer, T. W. Schoener, J. B. Shurin, A. R. E. Sinclair, M. E. Soule, R. Virtanen, and D. A. Wardle. 2011. Trophic downgrading of planet Earth. Science **333**:301-306.

Faraway, J. J. 2016. Extending the linear model with R: generalized linear, mixed effects and nonparametric regression models. Chapman and Hall/CRC, New York, NY.

Focardi, S., M. Materassi, G. Innocenti, and D. Berzi. 2017. Kleptoparasitism and scavenging can stabilize ecosystem dynamics. The American Naturalist **190**:398-409.

Fryxell, J. M., and A. R. E. Sinclair. 1988. Causes and consequences of migration by large herbivores. Trends in Ecology & Evolution **3**:237-241.

Gaillard, J.-M., M. Festa-Bianchet, N. G. Yoccoz, A. Loison, and C. Toigo. 2000. Temporal variation in fitness components and population dynamics of large herbivores. Annual Review of Ecology and Systematics **31**:367-393.

Garrott, R. A., L. L. Eberhardt, J. K. Otton, P. J. White, and M. A. Chaffee. 2002. A geochemical trophic cascade in Yellowstone's geothermal environments. Ecosystems **5**:659-666.

Garrott, R. A., P. J. White, C. Gower, M. S. Becker, S. Drimal, K. L. Hamlin, and F. G. R. Watson. 2020. Wolves and Elk in the Madison Headwaters. Pages 189-190 *in* D. W.

Smith, D. R. Stahler, and D. R. MacNulty, editors. Yellowstone wolves: Science and discovery in the world's first national park. University of Chicago Press, Chicago, IL.

Garrott, R. A., P. J. White, and J. J. Rotella. 2009. The Madison headwaters elk herd: transitioning from bottom–up regulation to top–down limitation. Pages 489-517 *in* R. A. Garrott, P. J. White, and F. G. R. Watson, editors. The Ecology of Large Mammals in Central Yellowstone: Sixteen Years of Integrated Field Studies. Elsevier, San Diego.

Gelman, A., J. B. Carlin, H. S. Stern, D. B. Dunson, A. Vehtari, and D. B. Rubin. 2013. Bayesian data analysis. 3rd edition. Chapman & Hall/CRC Press, Boca Raton, FL.

Geremia, C., P. J. White, J. A. Hoeting, R. L. Wallen, F. G. R. Watson, D. Blanton, and N. T. Hobbs. 2014. Integrating population-and individual-level information in a movement model of Yellowstone bison. Ecological Applications **24**:346-362.

Gervasi, V., E. B. Nilsen, and J. D. C. Linnell. 2015. Body mass relationships affect the age structure of predation across carnivore–ungulate systems: a review and synthesis. Mammal Review **45**:253-266.

Gervasi, V., E. B. Nilsen, H. Sand, M. Panzacchi, G. R. Rauset, H. C. Pedersen, J. Kindberg, P. Wabakken, B. Zimmermann, J. Odden, O. Liberg, J. E. Swenson, and J. D. C. Linnell. 2012. Predicting the potential demographic impact of predators on their prey: a comparative analysis of two carnivore–ungulate systems in Scandinavia. Journal of Animal Ecology **81**:443-454.

Gittleman, J. L., S. M. Funk, D. W. Macdonald, and R. K. Wayne. 2001. Carnivore Conservation. Cambridge University Press, Cambridge, UK.

Grange, S., P. Duncan, J.-M. Gaillard, A. R. E. Sinclair, P. J. P. Gogan, C. Packer, H. Hofer, and M. East. 2004. What limits the Serengeti zebra population? Oecologia **140**:523-532.

Grinnell, J. 1917. The niche-relationships of the California Thrasher. The Auk **34**:427-433.

Hayes, R. D., A. M. Baer, U. Wotschikowsky, and A. S. Harestad. 2000. Kill rate by wolves on moose in the Yukon. Canadian Journal of Zoology **78**:49-59.

Hebblewhite, M. 2013. Consequences of ratio-dependent predation by wolves for elk population dynamics. Population Ecology **55**:511-522.

Hebblewhite, M., D. R. Eacker, S. Eggeman, H. Bohm, and E. H. Merrill. 2018. Density-independent predation affects migrants and residents equally in a declining partially migratory elk population. Oikos **127**:1304-1318.

Hebblewhite, M., P. C. Paquet, D. H. Pletscher, R. B. Lessard, and C. J. Callaghan. 2003. Development and application of a ratio estimator to estimate wolf kill rates and variance in a multiple-prey system. Wildlife Society Bulletin **31**:933-946.

Holling, C. S. 1959. The components of predation as revealed by a study of small-mammal predation of the European pine sawfly. The Canadian Entomologist **91**:293-320.

Holt, R. D. 1977. Predation, apparent competition, and the structure of prey communities. Theoretical Population Biology **12**:197-229.

Holt, R. D., and M. B. Bonsall. 2017. Apparent competition. Annual Review of Ecology, Evolution, and Systematics **48**:447-471.

Höner, O. P., B. Wachter, M. L. East, and H. Hofer. 2002. The response of spotted hyaenas to long-term changes in prey populations: functional response and interspecific kleptoparasitism. Journal of Animal Ecology **71**:236-246.

Houston, D. B. 1982. The Northern Yellowstone Elk: Ecology and Management. Macmillan Publishing, New York.

Hoy, S. R., D. R. MacNulty, M. C. Metz, D. W. Smith, D. R. Stahler, R. O. Peterson, and J. A. Vucetich. 2021. Negative frequency-dependent prey selection by wolves and its implications for predator-prey dynamics. Animal Behaviour **179**:247-265.

Hoy, S. R., D. R. MacNulty, D. W. Smith, D. R. Stahler, X. Lambin, R. O. Peterson, J. S. Ruprecht, and J. A. Vucetich. 2020. Fluctuations in age structure and their variable influence on population growth. Functional Ecology **34**:203-216.

Hoy, S. R., S. J. Petty, A. Millon, D. P. Whitfield, M. Marquiss, M. Davison, and X. Lambin. 2015. Age and sex-selective predation moderate the overall impact of predators. Journal of Animal Ecology **84**:692-701.

Huggard, D. J. 1993. Effect of snow depth on predation and scavenging by gray wolves. The Journal of Wildlife Management **57**:382-388.

Hurlbert, S. H. 1978. The measurement of niche overlap and some relatives. Ecology **59**:67-77.

Husseman, J. S., D. L. Murray, G. Power, C. Mack, C. R. Wenger, and H. Quigley. 2003. Assessing differential prey selection patterns between two sympatric large carnivores. Oikos **101**:591-601.

Jędrzejewski, W., B. Jędrzejewska, H. Okarma, K. Schmidt, K. Zub, and M. Musiani. 2000. Prey selection and predation by wolves in Białowieża Primeval Forest, Poland. Journal of Mammalogy **81**:197-212.

Jones, J. D., J. J. Treanor, R. L. Wallen, and P. J. White. 2010. Timing of parturition events in Yellowstone bison *Bison bison*: implications for bison conservation and brucellosis transmission risk to cattle. Wildlife Biology **16**:333-339.

Jost, C., G. Devulder, J. A. Vucetich, R. O. Peterson, and R. Arditi. 2005. The wolves of Isle Royale display scale-invariant satiation and ratio-dependent predation on moose. Journal of Animal Ecology **74**:809-816.

Kauffman, M. J., J. F. Brodie, and E. S. Jules. 2010. Are wolves saving Yellowstone's aspen? A landscape-level test of a behaviorally mediated trophic cascade. Ecology **91**:2742-2755.

Kays, R., M. C. Crofoot, W. Jetz, and M. Wikelski. 2015. Terrestrial animal tracking as an eye on life and planet. Science **348**:aaa2478.

Kellner, K. F., and R. K. Swihart. 2014. Accounting for imperfect detection in ecology: a quantitative review. Plos One **9**:e111436.

Knopff, K. H., A. A. Knopff, A. Kortello, and M. S. Boyce. 2010. Cougar kill rate and prey composition in a multiprey system. Journal of Wildlife Management **74**:1435-1447.

Knopff, K. H., A. A. Knopff, M. B. Warren, and M. S. Boyce. 2009. Evaluating global positioning system telemetry techniques for estimating cougar predation parameters. Journal of Wildlife Management **73**:586-597.

Kohl, M. T., D. R. Stahler, M. C. Metz, J. D. Forester, M. J. Kauffman, N. Varley, P. J. White, D. W. Smith, and D. R. MacNulty. 2018. Diel predator activity drives a dynamic landscape of fear. Ecological Monographs **88**:638-652.

Levi, T., and C. C. Wilmers. 2012. Wolves–coyotes–foxes: a cascade among carnivores. Ecology **93**:921-929.

Levins, R. 1968. Evolution in changing environments: some theoretical explorations. Princeton University Press, Princeton, NJ.

Linnell, J. D. C., R. Aanes, and R. Andersen. 1995. Who killed Bambi? The role of predation in the neonatal mortality of temperate ungulates. Wildlife Biology **1**:209-223.

Lodberg-Holm, H. K., B. S. Teglas, D. B. Tyers, M. D. Jimenez, and D. W. Smith. 2021. Spatial and temporal variability in summer diet of gray wolves (*Canis lupus*) in the Greater Yellowstone Ecosystem. Journal of Mammalogy **102**:1030-1041.

MacKenzie, D. I., J. D. Nichols, G. B. Lachman, S. Droege, A. J. Royle, and C. A. Langtimm. 2002. Estimating site occupancy rates when detection probabilities are less than one. Ecology **83**:2248-2255.

MacNulty, D. R., D. W. Smith, L. D. Mech, J. A. Vucetich, and C. Packer. 2012. Nonlinear effects of group size on the success of wolves hunting elk. Behavioral Ecology **23**:75-82.

MacNulty, D. R., D. R. Stahler, and D. W. Smith. 2020a. Limits to Wolf Predatory Performance. Pages 149-155 *in* D. W. Smith, D. R. Stahler, and D. R. MacNulty, editors. Yellowstone wolves: Science and discovery in the world's first national park. University of Chicago Press, Chicago, IL.

MacNulty, D. R., D. R. Stahler, T. Wyman, J. Ruprecht, L. M. Smith, M. T. Kohl, and D. W. Smith. 2020b. Population dynamics of northern Yellowstone elk after wolf reintroduction. Pages 184-199 *in* D. W. Smith, D. R. Stahler, and D. R. MacNulty, editors. Yellowstone wolves: Science and discovery in the world's first national park. University of Chicago Press, Chicago, IL.

MacNulty, D. R., A. Tallian, D. R. Stahler, and D. W. Smith. 2014. Influence of group size on the success of wolves hunting bison. Plos One **9**:e112884.

Maier, M. J. 2021. DirichletReg: Dirichlet regression for compositional data in R. R package version 0.7-1.

Marshal, J. P., and S. Boutin. 1999. Power analysis of wolf-moose functional responses. The Journal of Wildlife Management **63**:396-402.

Martin, H. W., L. D. Mech, J. Fieberg, M. C. Metz, D. R. MacNulty, D. R. Stahler, and D. W. Smith. 2018. Factors affecting gray wolf (*Canis lupus*) encounter rate with elk (*Cervus elaphus*) in Yellowstone National Park. Canadian Journal of Zoology **96**:1032-1042.

Mattson, D. J. 1997. Use of ungulates by Yellowstone grizzly bears *Ursus arctos*. Biological Conservation **81**:161-177.

Mazerolle, M. J. 2020. AICcmodavg: model selection and multimodel inference based on (Q) AIC (c). R package version 2.3-1.

Mech, L. D., and R. O. Peterson. 2003. Wolf-prey relations. Pages 131-157 *in* L. D. Mech and L. Boitani, editors. Wolves: Behavior, ecology, and conservation. University of Chicago Press, Chicago, IL.

Mech, L. D., D. W. Smith, and D. R. MacNulty. 2015. Wolves on the hunt: the behavior of wolves hunting wild prey. University of Chicago Press, Chicago, IL.

Mech, L. D., D. W. Smith, K. M. Murphy, and D. R. MacNulty. 2001. Winter severity and wolf predation on a formerly wolf-free elk herd. The Journal of Wildlife Management **65**:998-1003.

Mellard, J. P., S. Hamel, J.-A. Henden, R. A. Ims, A. Stien, and N. Yoccoz. 2021. Effect of scavenging on predation in a food web. Ecology and Evolution **11**:6742-6765.

Merrill, E., H. Sand, B. Zimmermann, H. McPhee, N. Webb, M. Hebblewhite, P. Wabakken, and J. L. Frair. 2010. Building a mechanistic understanding of predation with GPS-based movement data. Philosophical Transactions of the Royal Society of London B: Biological Sciences **365**:2279-2288.

Messer, M. A., R. A. Garrott, S. Cherry, P. J. White, F. G. R. Watson, and E. Meredith. 2008. Elk winter resource selection in a severe snow pack environment. Pages 137-156 *in* R. A.

Garrott, P. J. White, and F. G. R. Watson, editors. The Ecology of Large Mammals in Central Yellowstone: Sixteen Years of Integrated Field Studies. Elsevier, San Diego.

Messier, F. 1994. Ungulate population models with predation: a case study with the North American moose. Ecology **75**:478-488.

Messier, F. 1995. On the functional and numerical responses of wolves to changing prey density. Pages 187-198 *in* L. N. Carbyn, S. H. Fritts, and D. R. Seip, editors. Ecology and conservation of wolves in a changing world. Canadian Circumpolar Institute, Edmonton, Alberta.

Messier, F., W. C. Gasaway, and R. O. Peterson. 1995. Wolf-ungulate interactions in the Northern Range of Yellowstone: Hypotheses, research priorities, and methodologies. Fort Collins, CO.

Metz, M. C., D. J. Emlen, D. R. Stahler, D. R. MacNulty, D. W. Smith, and M. Hebblewhite. 2018. Predation shapes the evolutionary traits of cervid weapons. Nature Ecology & Evolution **2**:1619-1625.

Metz, M. C., M. Hebblewhite, D. W. Smith, D. R. Stahler, D. R. MacNulty, A. Tallian, and J. A. Vucetich. 2020a. What wolves eat and why. Pages 157-168 *in* D. W. Smith, D. R. Stahler, and D. R. MacNulty, editors. Yellowstone wolves: Science and discovery in the world's first national park. University of Chicago Press, Chicago, IL.

Metz, M. C., D. W. Smith, D. R. Stahler, D. R. MacNulty, and M. Hebblewhite. 2020b. Wolf Predation on Elk in a Multi-Prey Environment. Pages 169-183 *in* D. W. Smith, D. R. Stahler, and D. R. MacNulty, editors. Yellowstone wolves: Science and discovery in the world's first national park. University of Chicago Press, Chicago, IL.

Metz, M. C., D. W. Smith, J. A. Vucetich, D. R. Stahler, and R. O. Peterson. 2012. Seasonal patterns of predation for gray wolves in the multi-prey system of Yellowstone National Park. Journal of Animal Ecology **81**:553-563.

Metz, M. C., J. SunderRaj, D. W. Smith, D. R. Stahler, M. T. Kohl, K. A. Cassidy, and M. Hebblewhite. 2020c. Accounting for imperfect detection in observational studies: modeling wolf sightability in Yellowstone National Park. Ecosphere **11**:e03152.

Metz, M. C., J. A. Vucetich, D. W. Smith, D. R. Stahler, and R. O. Peterson. 2011. Effect of sociality and season on gray wolf (*Canis lupus*) foraging behavior: implications for estimating summer kill rate. Plos One **6**:e17332.

Miller, C. S., M. Hebblewhite, Y. K. Petrunenko, I. V. Seryodkin, N. J. DeCesare, J. M. Goodrich, and D. G. Miquelle. 2013. Estimating Amur tiger (*Panthera tigris altaica*) kill rates and potential consumption rates using global positioning system collars. Journal of Mammalogy **94**:845-855.

Mills, M. G. L., and T. M. Shenk. 1992. Predator--prey relationships: The impact of lion predation on wildebeest and zebra populations. Journal of Animal Ecology **61**:693-702.

Moleón, M., J. A. Sánchez-Zapata, N. Selva, J. A. Donázar, and N. Owen-Smith. 2014. Inter-specific interactions linking predation and scavenging in terrestrial vertebrate assemblages. Biological Reviews **89**:1042-1054.

Montgomery, R. A., R. J. Moll, E. Say-Sallaz, M. Valeix, and L. R. Prugh. 2019. A tendency to simplify complex systems. Biological Conservation **233**:1-11.

Mosley, J. C., and J. G. Mundinger. 2018. History and status of wild ungulate populations on the Northern Yellowstone Range. Rangelands **40**:189-201.

Murie, A. 1944. The wolves of Mount McKinley. US Government Printing Office, Washington, DC.

Murphy, K. M., G. S. Felzien, M. G. Hornocker, and T. K. Ruth. 1998. Encounter competition between bears and cougars: some ecological implications. Ursus **10**:55-60.

Nelson, A. A., M. J. Kauffman, A. D. Middleton, M. D. Jimenez, D. E. McWhirter, and K. Gerow. 2016. Native prey distribution and migration mediates wolf (*Canis lupus*) predation on domestic livestock in the Greater Yellowstone Ecosystem. Canadian Journal of Zoology **94**:291-299.

Newsome, S. D., M. T. Tinker, D. H. Monson, O. T. Oftedal, K. Ralls, M. M. Staedler, M. L. Fogel, and J. A. Estes. 2009. Using stable isotopes to investigate individual diet specialization in California sea otters (*Enhydra lutris nereis*). Ecology **90**:961-974.

Nilsen, E. B., J. D. C. Linnell, J. Odden, and R. Andersen. 2009. Climate, season, and social status modulate the functional response of an efficient stalking predator: the Eurasian lynx. Journal of Animal Ecology **78**:741-751.

O'Donoghue, M., S. Boutin, C. J. Krebs, G. Zuleta, D. L. Murray, and E. J. Hofer. 1998. Functional responses of coyotes and lynx to the snowshoe hare cycle. Ecology **79**:1193-1208.

Orning, E. K., K. M. Dugger, and D. A. Clark. 2021. Gray wolf (*Canis lupus*) predation patterns following recent recolonization in a multi-predator, multi-prey system. Canadian Journal of Zoology **99**:902-911.

Owen-Smith, N. 2008. Changing vulnerability to predation related to season and sex in an African ungulate assemblage. Oikos **117**:602-610.

Owen-Smith, N. 2015. Mechanisms of coexistence in diverse herbivore–carnivore assemblages: demographic, temporal and spatial heterogeneities affecting prey vulnerability. Oikos **124**:1417-1426.

Owen-Smith, N., and M. G. L. Mills. 2008. Predator–prey size relationships in an African large-mammal food web. Journal of Animal Ecology **77**:173-183.

Packard, J. M. 2003. Wolf Behavior: Reproductive, Social, and Intelligent. Pages 35-65 *in* L. D. Mech and L. Boitani, editors. Wolves: Behavior, ecology, and conservation. University of Chicago Press, Chicago.

Painter, L. E., R. L. Beschta, E. J. Larsen, and W. J. Ripple. 2018. Aspen recruitment in the Yellowstone region linked to reduced herbivory after large carnivore restoration. Ecosphere **9**:e02376.

Parker, K. L., P. S. Barboza, and M. P. Gillingham. 2009. Nutrition integrates environmental responses of ungulates. Functional Ecology **23**:57-69.

Pereira, L. M., N. Owen-Smith, and M. Moleon. 2014. Facultative predation and scavenging by mammalian carnivores: seasonal, regional and intra-guild comparisons. Mammal Review **44**:44-55.

Peterson, R. O. 1977. Wolf ecology and prey relationships on Isle Royale. US Government Printing Office, Washington, DC.

Peterson, R. O., R. L. Beschta, D. J. Cooper, N. T. Hobbs, D. B. Johnston, E. J. Larsen, K. N. Marshall, L. E. Painter, W. J. Ripple, and J. R. Rose. 2020. Indirect Effects of Carnivore Restoration on Vegetation. Pages 205-222 *in* D. W. Smith, D. R. Stahler, and D. R. MacNulty, editors. Yellowstone wolves: Science and discovery in the world's first national park. University of Chicago Press, Chicago, IL.

Peterson, R. O., and P. Ciucci. 2003. The wolf as a carnivore. Pages 104-130 *in* L. D. Mech and L. Boitani, editors. Wolves: Behavior, ecology, and conservation. University of Chicago Press, Chicago.

Peterson, R. O., N. J. Thomas, J. M. Thurber, J. A. Vucetich, and T. A. Waite. 1998. Population limitation and the wolves of Isle Royale. Journal of Mammalogy **79**:828-841.

Peterson, R. O., J. A. Vucetich, J. M. Bump, and D. W. Smith. 2014. Trophic cascades in a multicausal world: Isle Royale and Yellowstone. Annual Review of Ecology, Evolution, and Systematics **45**:325-345.

Peterson, R. O., J. D. Woolington, and T. N. Bailey. 1984. Wolves of the Kenai peninsula, Alaska. Wildlife Monographs **88**:3-52.

Pettorelli, N., T. Coulson, S. M. Durant, and J.-M. Gaillard. 2011. Predation, individual variability and vertebrate population dynamics. Oecologia **167**:305-314.

Plumb, G. E., P. J. White, M. B. Coughenour, and R. L. Wallen. 2009. Carrying capacity, migration, and dispersal in Yellowstone bison. Biological Conservation **142**:2377-2387.

Plummer, M. 2003. JAGS: a program for analysis of Bayesian graphical models using Gibbs sampling. Pages 1-10 *in* Proceedings of the 3rd International Workshop on Distributed Statistical Computing, Vienna, Austria.

Pole, A., I. J. Gordon, M. L. Gorman, and M. MacAskill. 2004. Prey selection by African wild dogs (*Lycaon pictus*) in southern Zimbabwe. Journal of Zoology **262**:207-215.

Post, E., R. O. Peterson, N. C. Stenseth, and B. E. McLaren. 1999. Ecosystem consequences of wolf behavioural response to climate. Nature **401**:905-907.

Post, E., N. C. Stenseth, R. O. Peterson, J. A. Vucetich, and A. M. Ellis. 2002. Phase dependence and population cycles in a large-mammal predator-prey system. Ecology **83**:2997-3002.

Prugh, L. R., and K. J. Sivy. 2020. Enemies with benefits: integrating positive and negative interactions among terrestrial carnivores. Ecology Letters **23**:902-918.

Raithel, J. D., M. J. Kauffman, and D. H. Pletscher. 2007. Impact of spatial and temporal variation in calf survival on the growth of elk populations. Journal of Wildlife Management **71**:795-803.

Reznick, D., and J. A. Endler. 1982. The impact of predation on life history evolution in Trinidadian guppies (*Poecilia reticulata*). Evolution **36**:160-177.

Rickbeil, G. J. M., J. A. Merkle, G. Anderson, M. P. Atwood, J. P. Beckmann, E. K. Cole, A. B. Courtemanch, S. Dewey, D. D. Gustine, M. J. Kauffman, D. E. McWhirter, T. Mong, K. Proffitt, P. J. White, and A. D. Middleton. 2019. Plasticity in elk migration timing is a response to changing environmental conditions. Global Change Biology **25**:2368-2381.

Ripley, B., B. Venables, D. M. Bates, K. Hornik, A. Gebhardt, D. Firth, and M. B. Ripley. 2021. mass. R Package version 7.3-55.

Ripple, W. J., J. A. Estes, R. L. Beschta, C. C. Wilmers, E. G. Ritchie, M. Hebblewhite, J. Berger, B. Elmhagen, M. Letnic, M. P. Nelson, O. J. Schmitz, D. W. Smith, A. D. Wallach, and A. J. Wirsing. 2014. Status and ecological effects of the world's largest carnivores. Science **343**:1241484.

Royle, J. A., and R. M. Dorazio. 2012. Parameter-expanded data augmentation for Bayesian analysis of capture–recapture models. Journal of Ornithology **152**:S521-S537.

Royle, J. A., R. M. Dorazio, and W. A. Link. 2007a. Analysis of multinomial models with unknown index using data augmentation. Journal of Computational and Graphical Statistics **16**:67-85.

Royle, J. A., M. Kéry, R. Gautier, and H. Schmid. 2007b. Hierarchical spatial models of abundance and occurrence from imperfect survey data. Ecological Monographs **77**:465-481.

Ruth, T. K., P. C. Buotte, and M. G. Hornocker. 2019. Yellowstone cougars: ecology before and during wolf restoration. University Press of Colorado, Louisville, CO.

Sand, H., J. A. Vucetich, B. Zimmermann, P. Wabakken, C. Wikenros, H. C. Pedersen, R. O. Peterson, and O. Liberg. 2012. Assessing the influence of prey–predator ratio, prey age structure and packs size on wolf kill rates. Oikos **121**:1454-1463.

Sand, H., P. Wabakken, B. Zimmermann, Ö. Johansson, H. C. Pedersen, and O. Liberg. 2008. Summer kill rates and predation pattern in a wolf–moose system: can we rely on winter estimates? Oecologia **156**:53-64.

Schaller, G. B. 1972. The Serengetti lion: a study of predator-prey relations. University of Chicago, Chicago.

Schmidt, P. A., and L. D. Mech. 1997. Wolf pack size and food acquisition. The American Naturalist **150**:513-517.

Schwarz, C. J., and G. A. F. Seber. 1999. Estimating animal abundance: review III. Statistical Science **14**:427-456.

Sergeyev, M., B. R. McMillan, K. R. Hersey, and R. T. Larsen. 2021. How Size and Condition Influence Survival and Cause-Specific Mortality of Female Elk. The Journal of Wildlife Management **85**:474-483.

Serrouya, R., B. N. McLellan, and S. Boutin. 2015. Testing predator–prey theory using broad-scale manipulations and independent validation. Journal of Animal Ecology **84**:1600-1609.

Sinclair, A. R. E. 1989. Population regulation in animals. Pages 197–241 *in* J. Cherrett, editor. Ecological Concepts: The Contribution of Ecology to an Understanding of the Natural World. Blackwell, Melbourne.

Sinclair, A. R. E., S. Mduma, and J. S. Brashares. 2003. Patterns of predation in a diverse predator–prey system. Nature **425**:288-290.

Sinclair, A. R. E., and R. P. Pech. 1996. Density dependence, stochasticity, compensation and predator regulation. Oikos **75**:164-173.

Smith, D. W., and E. E. Bangs. 2009. Reintroduction of wolves to Yellowstone National Park: history, values, and ecosystem restoration. Pages 92-125 *in* M. W. Hayward and M. Somers, editors. Reintroduction of top-order predators. Wiley-Blackwell, Oxford.

Smith, D. W., K. A. Cassidy, D. R. Stahler, D. R. MacNulty, Q. Harrison, B. Balmford, E. E. Stahler, E. E. Brandell, and T. Coulson. 2020a. Population Dynamics and Demography. Pages 77-92 *in* D. W. Smith, D. R. Stahler, and D. R. MacNulty, editors. Yellowstone wolves: Science and discovery in the world's first national park. University of Chicago Press, Chicago, IL.

Smith, D. W., T. D. Drummer, K. M. Murphy, D. S. Guernsey, and S. B. Evans. 2004. Winter prey selection and estimation of wolf kill rates in Yellowstone National Park, 1995–2000. Journal of Wildlife Management **68**:153-166.

Smith, D. W., M. C. Metz, D. R. Stahler, and D. R. MacNulty. 2020b. How We Study Wolf-Prey Relationships. Pages 139-139 *in* D. W. Smith, D. R. Stahler, and D. R. MacNulty, editors. Yellowstone wolves: Science and discovery in the world's first national park. University of Chicago Press, Chicago, IL.

Smith, D. W., and R. O. Peterson. 2021. Intended and unintended consequences of wolf restoration to Yellowstone and Isle Royale National Parks. Conservation Science and Practice:e413.

Stahler, D. R., C. C. Wilmers, A. Tallian, C. B. Anton, M. C. Metz, T. K. Ruth, D. W. Smith, K. A. Gunther, and D. R. MacNulty. 2020. Competition and Coexistence among Yellowstone's Meat Eaters. Pages 223-241 *in* D. W. Smith, D. R. Stahler, and D. R. MacNulty, editors. Yellowstone wolves: Science and discovery in the world's first national park. University of Chicago Press, Chicago, IL.

Su, Y.-S., and M. Yajima. 2020. R2jags: Using R to run 'JAGS'. R Package Version 0.6-1.

Tallian, A., A. Ordiz, M. C. Metz, C. Milleret, C. Wikenros, D. W. Smith, D. R. Stahler, J. Kindberg, D. R. MacNulty, P. Wabakken, J. E. Swenson, and H. Sand. 2017a. Competition between apex predators? Brown bears decrease wolf kill rate on two continents. Proc. R. Soc. B **284**:20162368.

Tallian, A., D. W. Smith, D. R. Stahler, M. C. Metz, R. L. Wallen, C. Geremia, J. Ruprecht, C. T. Wyman, and D. R. MacNulty. 2017b. Predator foraging response to a resurgent dangerous prey. Functional Ecology **31**:1418-1429.

Taylor, R. J. 1984. Predation. Springer, New York.

Thurber, J. M., and R. O. Peterson. 1993. Effects of population density and pack size on the foraging ecology of gray wolves. Journal of Mammalogy **74**:879-889.

Treves, A., and K. U. Karanth. 2003. Human-carnivore conflict and perspectives on carnivore management worldwide. Conservation Biology **17**:1491-1499.

Varley, J. D., and W. G. Brewster. 1992. Wolves for Yellowstone? A report to the United States Congress. Volume IV Research and Analysis. National Park Service, Yellowstone National Park, WY.

Varley, N., and M. S. Boyce. 2006. Adaptive management for reintroductions: updating a wolf recovery model for Yellowstone National Park. Ecological Modelling **193**:315-339.

Vucetich, J. A., M. Hebblewhite, D. W. Smith, and R. O. Peterson. 2011. Predicting prey population dynamics from kill rate, predation rate and predator–prey ratios in three wolf-ungulate systems. Journal of Animal Ecology **80**:1236-1245.

Vucetich, J. A., and R. O. Peterson. 2004. The influence of prey consumption and demographic stochasticity on population growth rate of Isle Royale wolves Canis lupus. Oikos **107**:309-320.

Vucetich, J. A., R. O. Peterson, and M. P. Nelson. 2010. Will the future of wolves and moose always differ from a sense of their past?*in* M. Musiani, L. Boitani, and P. C. Paquet, editors. The World of Wolves: New Perspectives on Ecology, Behaviour, and Management. University of Calgary Press, Calgary, AB.

Vucetich, J. A., R. O. Peterson, and C. L. Schaefer. 2002. The effect of prey and predator densities on wolf predation. Ecology **83**:3003-3013.

Vucetich, J. A., D. W. Smith, and D. R. Stahler. 2005. Influence of harvest, climate and wolf predation on Yellowstone elk, 1961-2004. Oikos **111**:259-270.

Walsh, P. B., S. A. Sethi, B. C. Lake, B. A. Mangipane, R. Nielson, and S. Lowe. 2016. Estimating denning date of wolves with daily movement and GPS location fix failure. Wildlife Society Bulletin **40**:663-668.

Webb, N. F., M. Hebblewhite, and E. H. Merrill. 2008. Statistical methods for identifying wolf kill sites using global positioning system locations. Journal of Wildlife Management **72**:798-807.

White, P. J., K. M. Proffitt, and T. O. Lemke. 2012. Changes in elk distribution and group sizes after wolf restoration. The American Midland Naturalist **167**:174-187.

White, P. J., R. L. Wallen, and D. E. Hallac. 2015. Yellowstone Bison: Conserving an American Icon in Modern Society. The Yellowstone Association, Yellowstone National Park.

Wilmers, C. C., R. L. Crabtree, D. W. Smith, K. M. Murphy, and W. M. Getz. 2003. Trophic facilitation by introduced top predators: grey wolf subsidies to scavengers in Yellowstone National Park. Journal of Animal Ecology **72**:909-916.

Wilmers, C. C., M. C. Metz, D. R. Stahler, M. T. Kohl, C. Geremia, and D. W. Smith. 2020. How climate impacts the composition of wolf killed-elk in northern Yellowstone National Park. Journal of Animal Ecology **89**:1511-1519.

Wilmers, C. C., B. Nickel, C. M. Bryce, J. A. Smith, R. E. Wheat, and V. Yovovich. 2015. The golden age of bio-logging: how animal-borne sensors are advancing the frontiers of ecology. Ecology **96**:1741-1753.

Wilson, E. E., and E. M. Wolkovich. 2011. Scavenging: how carnivores and carrion structure communities. Trends in Ecology & Evolution **26**:129-135.

Woodruff, S. P., and M. D. Jimenez. 2019. Winter predation patterns of wolves in northwestern Wyoming. The Journal of Wildlife Management **83**:1352-1367.

Wright, G. J., R. O. Peterson, D. W. Smith, and T. O. Lemke. 2006. Selection of northern Yellowstone elk by gray wolves and hunters. Journal of Wildlife Management **70**:1070-1078.

Yudakov, A., and I. Nikolaev. 2012. Winter ecology of the Amur tiger, Dalnauka, Vladivostok.

Zhang, D. 2021. rsq: r-squared and related measures. R package version 2.2.

# TABLES.

**Table 4-1. Tracking the estimation of predation metrics across space and time.** We estimated predation metrics in two YNP subsystems (Northern YNP, Interior YNP) during five seasonal months that spanned two periods (roaming, denning). The five seasonal months (and associated period) were May (denning), June (denning), July (denning), early winter (roaming), and late winter (roaming). We estimated the first five (of six) predation metrics for seasonal months during the roaming period from 1997–2019 and during the denning period from 2008–2020. We estimated each of these five predation metrics at the prey species-level, and also estimated some metrics by sex-age class for elk and bison in Northern YNP. 'Season' indicates that we compared the metric across seasons (with the footnote indicating which seasons were compared). 'Quarter' and 'Year' respectively indicate that we evaluated the effect of time across ~6-year blocks (quarter; see Fig. 4-3b) and/or as a continuous variable (year), primarily to test whether predation dynamics differed over time in a manner that was consistent with predictions from classic predator-prey theory. We only evaluated the final predation metric, predation rate, for wolf predation on elk in Northern YNP. We did so by evaluating how predation rate changed in relation to elk abundance and year.

| Predation metric | Northern YNP | Interior YNP |
|---|---|---|
| 1. Wolf diet | | |
| Species | Season[2], Quarter[2], Year[3] | Season[3], Year[3] |
| Elk | Season[2], Quarter[2], Year[3] | - |
| Bison | Season[2], Quarter[2], Year[3] | - |
| 2. Niche breadth | | |
| Species | Year[3] | Year[3] |
| 3-5. Rates[1] | | |
| Species | Season[2], Quarter[2], Year[3] | Season[3], Year[3] |
| Elk | Season[2], Quarter[2], Year[3] | Season[3], Year[3] |
| Bison | Season[2], Quarter[2], Year[3] | Season[3], Year[3] |
| 6. Predation rate | | |
| Elk | Abundance[4], Year[4] | - |

[1] Rates measured were (3) kill rate, (4) scavenging rate, and (5) acquisition rate.

[2] Data originated from the roaming and denning period and spanned all five seasonal-months.

[3] Data originated from the roaming period and included early winter and late winter.

[4] Data originated from the roaming period and a seasonal correction factor was applied.

**Table 4-2.** Summary of spatial affiliation for monitored wolf pack-sessions. 'Data set' indicates whether any feeding events were detected or not during a pack-session and is only applicable during the roaming period. The pack-sessions that only appear in the italicized data for the 'All' data set were censored from the manuscript. 'YNP Subsystem' and 'Spatial zone' were determined through seasonal 70% MCP centroids (Appendix S4-A). For the roaming period, the right-most three columns indicate the pack's use of Northern YNP during the session (Appendix S4-A; Fig. 4-2). For the denning period, these numbers simply indicate which zone was assigned for a pack-session.

| Season | Data set | YNP Subsystem | Spatial zone | Yes | Partial | No |
|---|---|---|---|---|---|---|
| Roaming | Detected | Northern | Northern-Lower | 49 | 1 | 1 |
| Roaming | Detected | Northern | Northern-Middle | 81 | 1 | 2 |
| Roaming | Detected | Northern | Northern-Upper | 90 | 2 | 0 |
| Roaming | Detected | Interior | West | 2 | 4 | 62 |
| Roaming | Detected | Interior | Central | 3 | 9 | 42 |
| *Roaming* | *All* | *Northern* | *Northern-Lower* | *57* | *1* | *1* |
| *Roaming* | *All* | *Northern* | *Northern-Middle* | *85* | *1* | *2* |
| *Roaming* | *All* | *Northern* | *Northern-Upper* | *98* | *2* | *1* |
| *Roaming* | *All* | *Interior* | *West* | *2* | *5* | *73* |
| *Roaming* | *All* | *Interior* | *Central* | *4* | *9* | *44* |
| Denning | - | Northern | Northern-Lower | 3 | - | - |
| Denning | - | Northern | Northern-Middle | 9 | - | - |
| Denning | - | Northern | Northern-Upper | 8 | - | - |

**Table 4-3. Numbers used to calculate predation rate for resident Northern YNP wolves on the northern Yellowstone elk population.** Year begins in November. Elk abundances from Fig. 4-3. Kill rate estimates (number of elk killed per wolf per day) are for the population-level for all wolf packs characterized as 'Northern YNP' (see Table 4-2). Wolf abundances are from annual counts of the resident Northern Range YNP wolf population (Smith et al. 2020a). 'EW' represents early winter (same numbers as Fig. 4-3); 'LW' represents late winter; 'EW+1' indicates the count is for early winter in year *t*+1.

| Year | Elk (Total) | Elk (YNP) | Kill rate (EW) | Kill rate (LW) | Wolves (EW) | Wolves (LW) | Wolves (EW+1) |
|---|---|---|---|---|---|---|---|
| 1997 | 15,509 | 12,376 | 0.0356 | 0.0693 | 32 | 30 | 42 |
| 1998 | 15,517 | 11,928 | 0.0327 | 0.0765 | 42 | 33 | 35 |
| 1999 | 19,106 | 16,372 | 0.0396 | 0.0753 | 35 | 30 | 65 |
| 2000 | 17,609 | 15,089 | 0.0382 | 0.0568 | 65 | 52 | 70 |
| 2001 | 15,729 | 12,278 | 0.0339 | 0.0547 | 70 | 57 | 78 |
| 2002 | 12,662 | 9,846 | 0.0365 | 0.0575 | 78 | 70 | 98 |
| 2003 | 10,724 | 8,275 | 0.0382 | 0.0468 | 98 | 69 | 84 |
| 2004 | 12,808 | 8,831 | 0.0307 | 0.0433 | 84 | 69 | 54 |
| 2005 | 10,192 | 5,045 | 0.0418 | 0.0616 | 54 | 42 | 75 |
| 2006 | 8,913 | 5,997 | 0.0390 | 0.0464 | 75 | 56 | 94 |
| 2007 | 8,309 | 3,701 | 0.0294 | 0.0508 | 94 | 84 | 57 |
| 2008 | 9,771 | 5,643 | 0.0350 | 0.0710 | 57 | 51 | 40 |
| 2009 | 7,601 | 3,959 | 0.0460 | 0.0597 | 40 | 39 | 38 |
| 2010 | 6,398 | 3,609 | 0.0343 | 0.0692 | 38 | 33 | 38 |
| 2011 | 5,248 | 2,029 | 0.0261 | 0.0278 | 38 | 34 | 34 |
| 2012 | 5,268 | 1,585 | 0.0241 | 0.0394 | 34 | 23 | 34 |
| 2013 | 5,749 | 1,561 | 0.0238 | 0.0464 | 34 | 31 | 42 |
| 2014 | 6,090 | 1,853 | 0.0296 | 0.0312 | 42 | 36 | 50 |
| 2015 | 6,872 | 2,100 | 0.0253 | 0.0301 | 50 | 38 | 41 |
| 2016 | 7,616 | 1,156 | 0.0305 | 0.0304 | 41 | 36 | 33 |
| 2017 | 9,502 | 2,617 | 0.0381 | 0.0351 | 33 | 31 | 39 |
| 2018 | 7,636 | 1,984 | 0.0331 | 0.0362 | 39 | 32 | 55 |
| 2019 | 7,196 | 1,827 | 0.0183 | 0.0317 | 55 | 42 | 79 |

**FIGURES.**

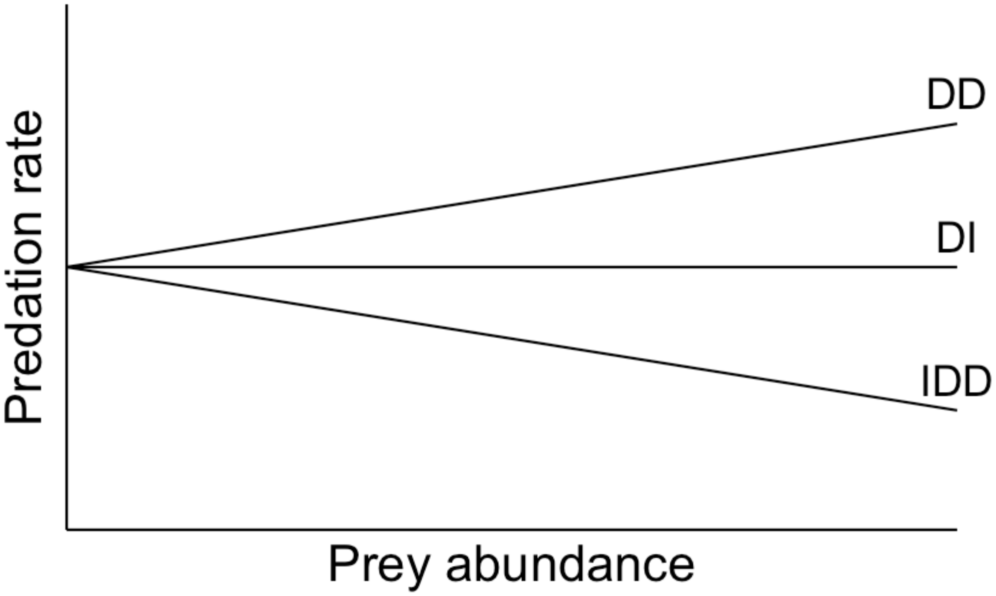

**Figure 4-1. Simplified relationships between predation rate and prey abundance predicted from classic predator-prey theory.** ‘DD’ represents density dependent, ‘DI’ represents density independent, and ‘IDD’ represents inversely density dependent. Here, DD and IDD predation rates are represented as linear, but they can also adopt non-linear functions. Adapted from Sinclair and Pech (1996).

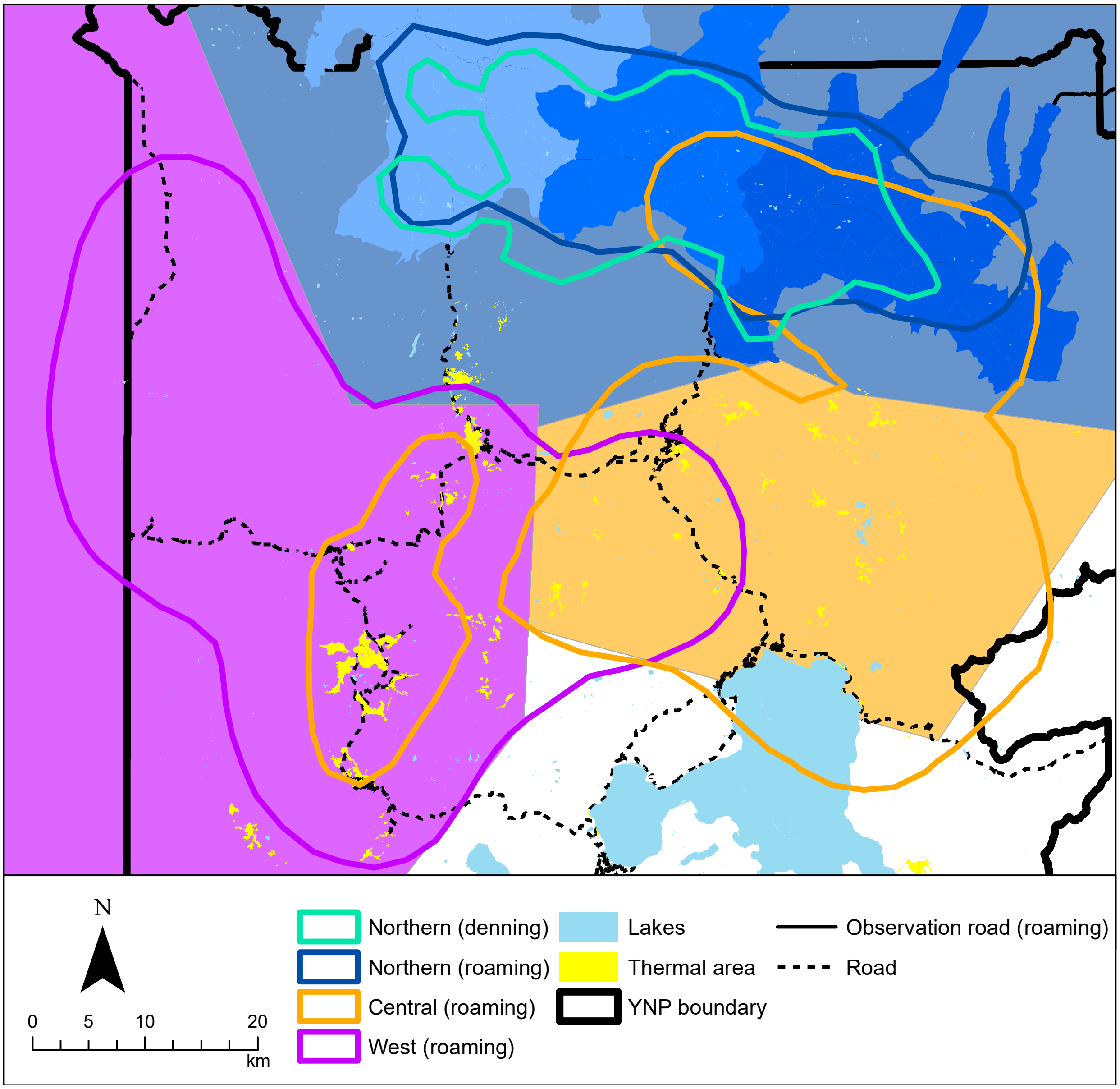

**Figure 4-2. Study area and long-term, seasonal distribution of wolf packs.** The largest blue-filled area displays the Northern YNP subsystem, while the Interior YNP subsystem was all area outside of Northern YNP. The purple- and orange-filled polygons indicate the Interior-West and Interior-Central zones, respectively. The historic Northern Range is at the core of the Northern YNP subsystem, and sectors within this historic boundary guided zone assignment ('Northern-Lower' = light blue; 'Northern-Middle' = medium blue; 'Northern-Upper' = dark blue) within Northern YNP (see Appendix S4-A). Outlined (but not filled) polygons represent estimates for 85% population-level utilization distributions for pack-sessions with a detected feeding event (*n* = 369 across both periods), characterized as the corresponding period (i.e., roaming or denning) and spatial affiliation.

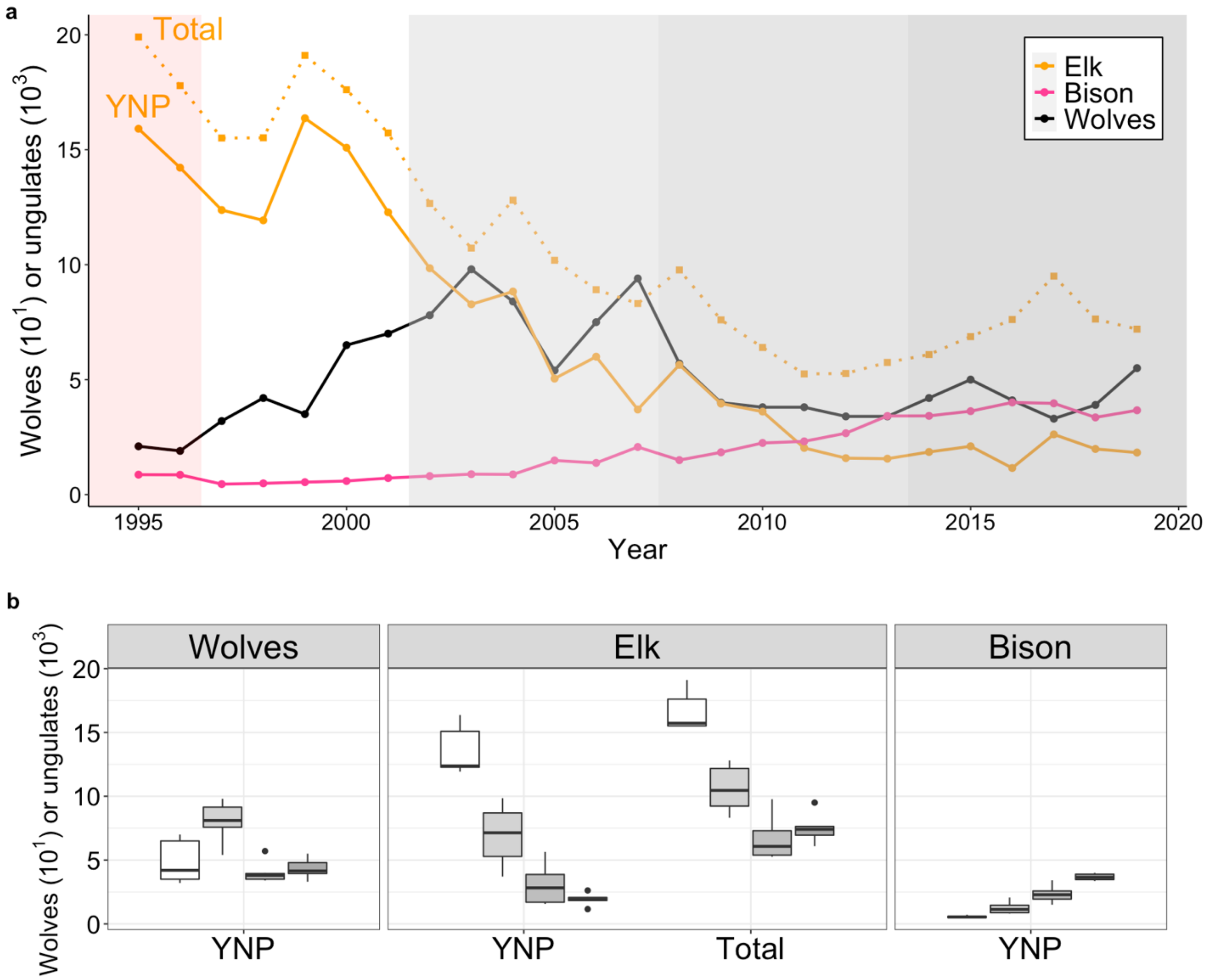

**Figure 4-3. Northern Yellowstone wolf, elk, and bison abundance.** Panel (a) displays abundance estimates from end-of-calendar year counts for resident Northern YNP wolves (Smith et al. 2020a), maximum summer counts for Northern YNP bison (White et al. 2015), and sightability-corrected winter estimates for Northern Range elk (Tallian et al. 2017b). The estimates for elk are displayed for the entire Northern Range population ('Total') and for the portion of the population that winters inside of YNP ('YNP'). 'YNP' is a subset of 'Total'. The red shaded area highlights censored years, while the white-to-dark gray shading is related to the 'quarters' in panel (b). Panel (b) displays box plots for wolf, elk, and bison abundance for four quarters (left to right plotting): 1) 1997–2001 (*n* = 5), 2) 2002–2007 (*n* = 6), 3) 2008–2013 (*n* = 6), and 4) 2014–2019 (*n* = 6). Box plots display the median and quartiles, with whiskers extending to the last data point within 1.5-times interquartile range). All subsequent box plots display the same.

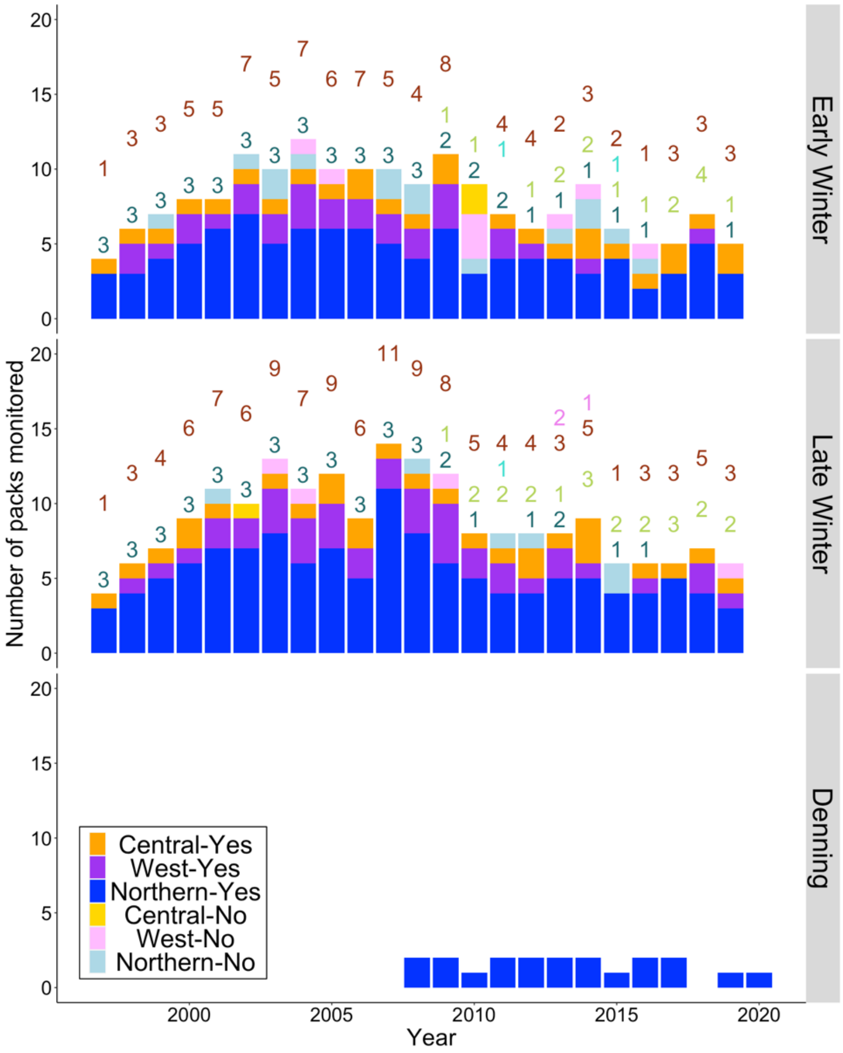

**Figure 4-4. Number of YNP packs monitored during study sessions.** The color of the bar (see legend) indicates the spatial affiliation (i.e., Northern, Central, West) for the pack during the study session. The darker shade of each color indicates that we detected ≥1 feeding event during a pack-session ('Yes'), while the lighter shade indicates that no feeding events were detected ('No'). Pack-sessions with no detected feeding events ('No') were censored from our analyses. The numbers above the bar display the number of packs, following censoring, monitored through the various detection methods during the study session. Each combination of detection methods (contributing to the pack-type*; see text and Table S4-C.1a) is represented by numbers of a different color. Specifically (and from bottom to top in appearance above bars), dark teal indicates the pack was monitored by Ground and Air; lime green by Ground, Air, and GPS; turquoise by Ground, Air, and partial-GPS; brick red by Air; violet by Air and GPS. Numbers are not displayed for the denning period because all packs were monitored through only GPS cluster searches. Note that a pack is displayed here if it was monitored and included for the study session, even if it did not exist for the entire study session. See Fig. S4-A.3 for additional information about the spatial zone of Northern YNP pack-sessions.

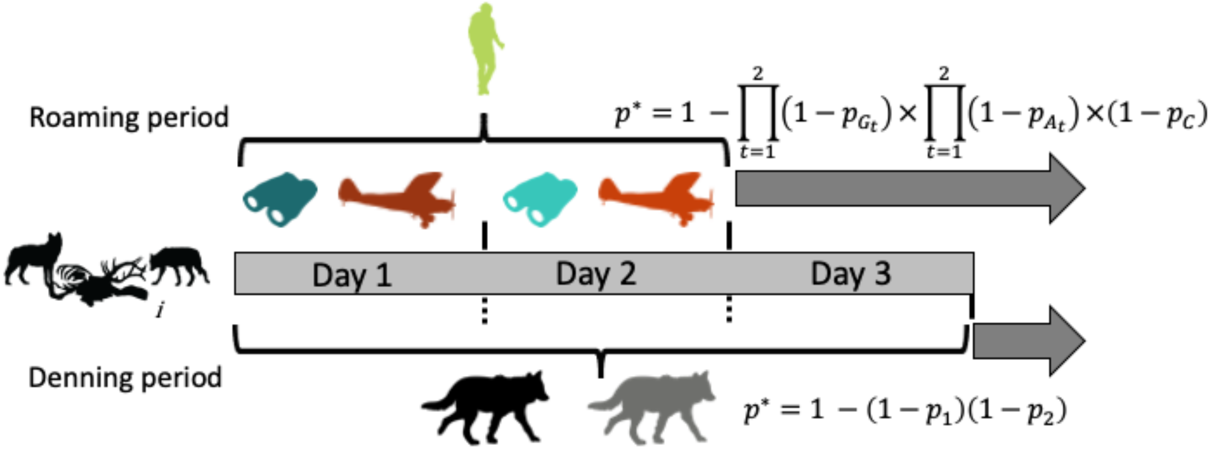

**Figure 4-5. Simplified detection process for feeding events.** Feeding events on ungulate carcasses were detected by up to three detection methods (ground [binoculars icon], air [plane icon], GPS cluster [hiker icon]) during the roaming period. Detection of a feeding event was permitted during a 2-day 'feeding event lifespan' during the roaming period. Immediately following sunset (see Appendix S4-A for full details) ended each day within this lifespan during the roaming period, with the precise day being of consequence for only the air and ground methods. For these detection methods, time-dependent detection was recorded on day *t* (note different color ground and air icons on days 1 and 2). GPS cluster detection was recorded over the duration of the feeding event lifespan. During the roaming period, GPS cluster detection was at the pack-level, meaning that a feeding event was detected (1) or not (0) by any GPS-collared wolf in the pack. During the denning period, up to two GPS-collared wolves (black and gray wolf icons) within a pack were the detection sources, and their detection of a feeding event was independently determined through whether they created a GPS cluster at a feeding event at any point during a 3-day lifespan (see Appendix S4-A for full details). For both periods, rare detections that occurred following the lifespan, represented by the dark gray arrows, were censored. The equation for whether a feeding event was detected at least once ($p^*$), assuming all detection methods (or sources) were available, is displayed for the roaming and denning periods.

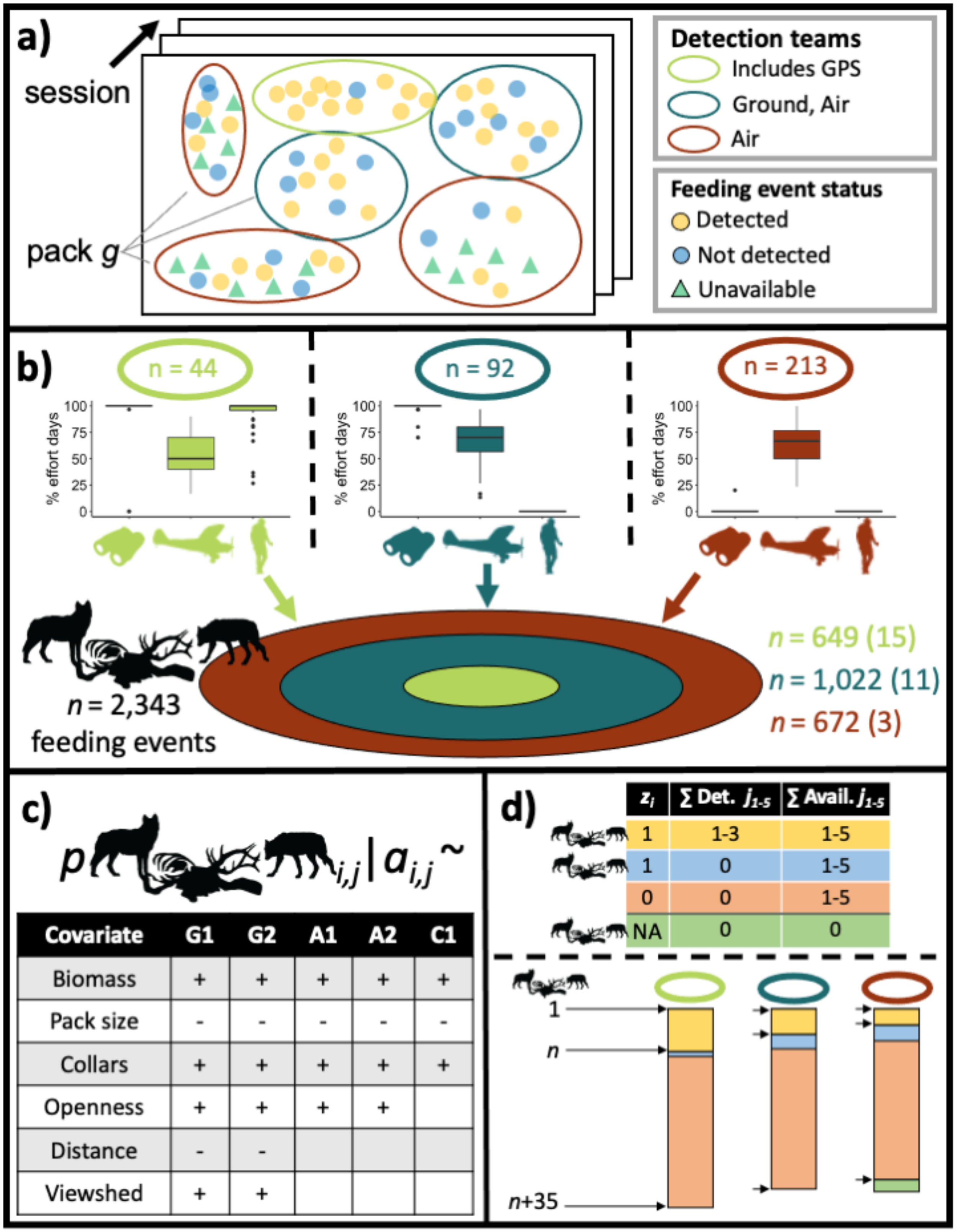

**Figure 4-6. Winter feeding event detection process and abundance estimator. (a)** The feeding event detection process in hypothetical space for all wolf packs. Packs with lime green

outline were monitored by GPS cluster, air, and (usually) ground methods, dark teal by only ground and air methods, and brick red by only air method. Circles represent available feeding events where a detection method(s) worked ≥1 day of the 2-day detection window, with the color indicating whether a feeding event was detected. Green triangles represent unavailable feeding events that "lived" during 2-day windows without detection effort. **(b)** Across all winter sessions and for the 349 pack-sessions where we detected at least one feeding event, 44 packs included GPS cluster method effort, 92 packs were monitored by ground and air methods effort, and 213 by only air method effort. The box plots display the proportion of a pack-session where that detection effort contributed to total effort-days (i.e., included an attempt by that detection method during a potential 2-day detection window). The summation of this effort resulted in 2,343 detected feeding events. The oval displays the proportion of total feeding events detected across the three pack-types, with the corresponding sample size (and mean for a pack-session) also reported. **(c)** Probability of detecting (*p)* feeding event *i* during occasion *j*, provided it was available to be detected (i.e., $a_{ij} = 1$), was hypothesized to be influenced by various covariates. Hypothesized directional effects are shown; we did not expect all covariates to affect each detection method. **(d)** The total number of feeding events was estimated in a data augmentation framework where each row was estimated to be a detected feeding event (orange), an undetected feeding event that was available (blue), or a not predicted feeding event that was subsequently ignored (red). Following this initial estimation using data augmentation (i.e., Eqns. 1–6), unavailable feeding events (green) were then estimated through a ratio-estimator that accounted for the proportion of a study session with effort-days (i.e., Eqn. 7), thereby estimating the hypothetical green triangles in panel (a). The top portion of panel (d) displays the characteristics of a feeding event, again noting that the feeding events represented by the green row were secondarily estimated (i.e., $z_i$ = NA). The bottom portion of panel (d) displays hypothetical estimates for different pack-types (see panel b). The estimated number of feeding events is represented by the summation of the orange, blue, and green fill. Here, we detected *n* feeding events for a pack (orange fill), and then estimated what portion of 35 additional 'missed' feeding events (blue fill + red fill) were estimated to exist (blue fill). The green-filled portion typically existed only for packs monitored by only the air method, although it would be theoretically possible for these feeding events to exist for the other pack-types if there was no effort for a pack-session on consecutive days.

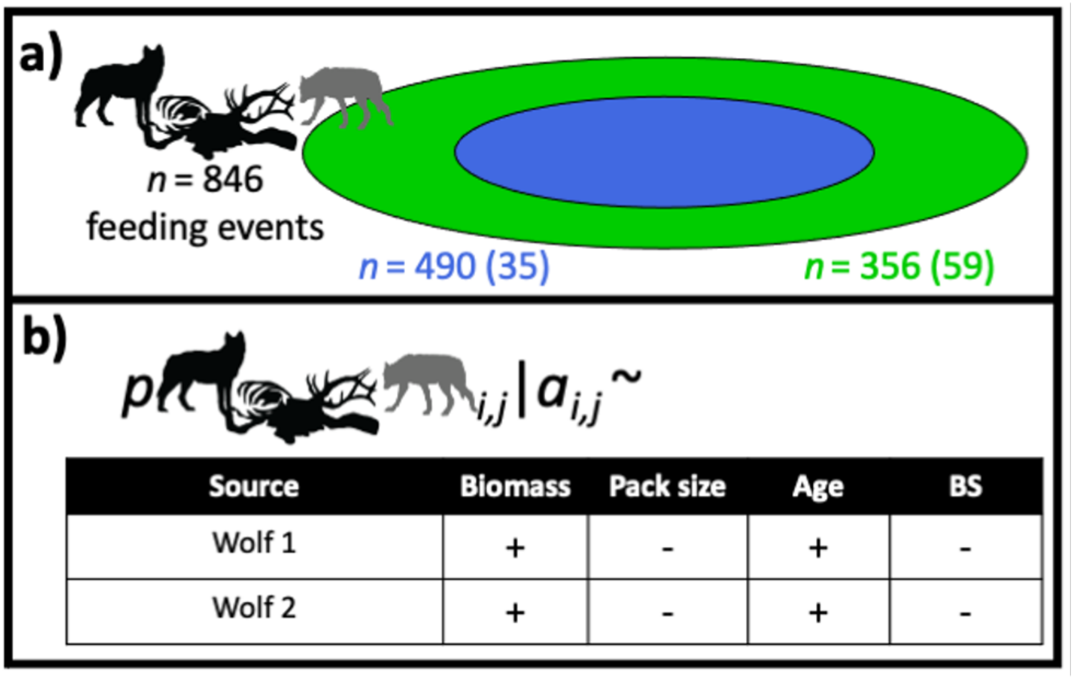

| Source | Biomass | Pack size | Age | BS |
|---|---|---|---|---|
| Wolf 1 | + | - | + | - |
| Wolf 2 | + | - | + | - |

**Figure 4-7. Estimating feeding event abundance during the denning period.** (a) Feeding events during the denning period were detected during pack-sessions where 1 or 2 GPS-collared wolves were the detection sources. In total, we detected 846 feeding events, 490 from 14 pack-sessions ($\bar{x}$ = 35) studied through one GPS-collared wolf in the pack (blue fill) and 356 from 6 pack-sessions ($\bar{x}$ = 53.3) with two GPS-collared wolves present in the pack (green fill). (b) We used these feeding events with information about detection and availability by two detection sources (i.e., wolf-1 [black wolf icon] and wolf-2 [gray wolf icon]) to estimate feeding event abundance in a data augmented model (see Fig. 4-6d). Hypothesized effects of covariates on detection did not differ between wolf-1 and wolf-2.

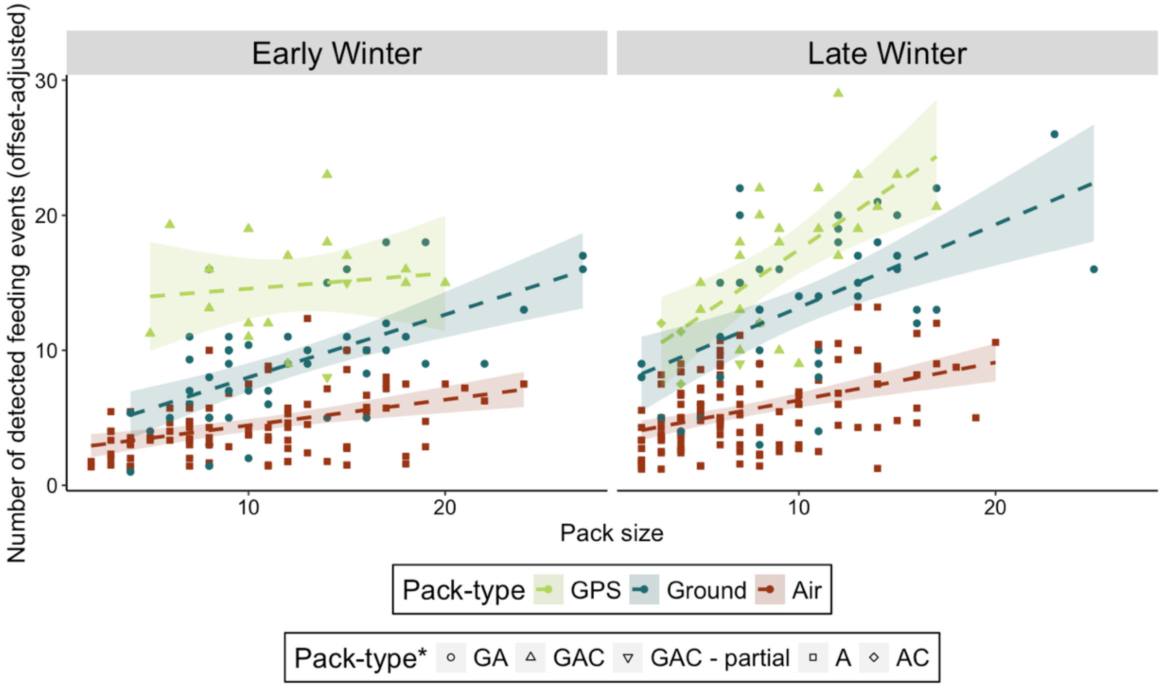

**Figure 4-8. Effect of pack size on the number of detected feeding events during roaming period pack-sessions.** Pack-sessions are faceted and grouped as they were in the linear model on occurrence (Eqn. 2). The color indicates the pack-type, i.e., whether pack monitoring hierarchically included GPS cluster searches (lime green), ground method attempts (dark teal), or only aerial method attempts (brick red). The shape provides increased detail of how the pack was monitored during the study session (i.e., pack-type*; GA = Ground & Air, GAC = Ground, Air, & GPS, GAC – partial = Ground, Air, & partial GPS, A = Air, AC = Air & GPS; see text for additional details). Here, the number of detected feeding events was determined using the correction factors in Eqn. 2 (i.e., *prop.sess, prop.pack.effort*; see also Fig. S4-C.2).

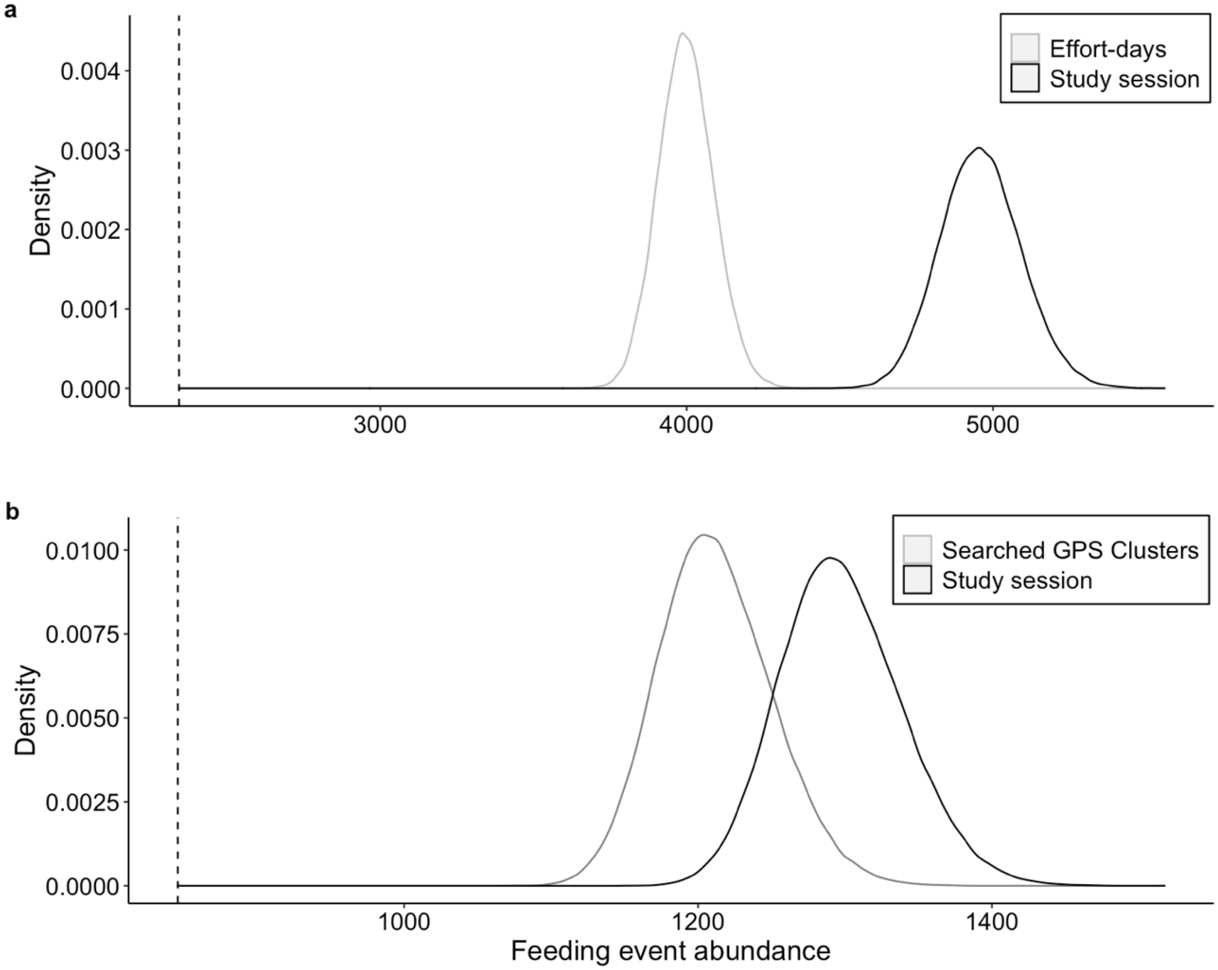

**Figure 4-9. Posterior predictions for the total number of feeding events during the (a) roaming and (b) denning periods.** The dashed, vertical lines indicate the number of feeding events detected. 'Effort-days' in panel (a) represents the resultant model-based estimates for feeding event abundance for 2-day periods with effort (i.e., total availability ≥1), while 'Searched GPS Clusters' in panel (b) represents these estimates prior to accounting for unsearched GPS clusters during a denning period pack-session. 'Study session' represents the estimate while also including additional feeding events from *i*) 2-day periods during the roaming period when no detection methods operated and *ii*) during the denning period for unsearched GPS clusters. The distributions here represent the summed predictions for each of the 60,000 post-burn-in iterations (i.e., 3 chains, each with 20,000 post-burn-in iterations). Predictions originate from 349 pack-sessions for the roaming period and from 20-pack sessions for the denning period. Note that the scales differ between panels for both the x- and y-axis.

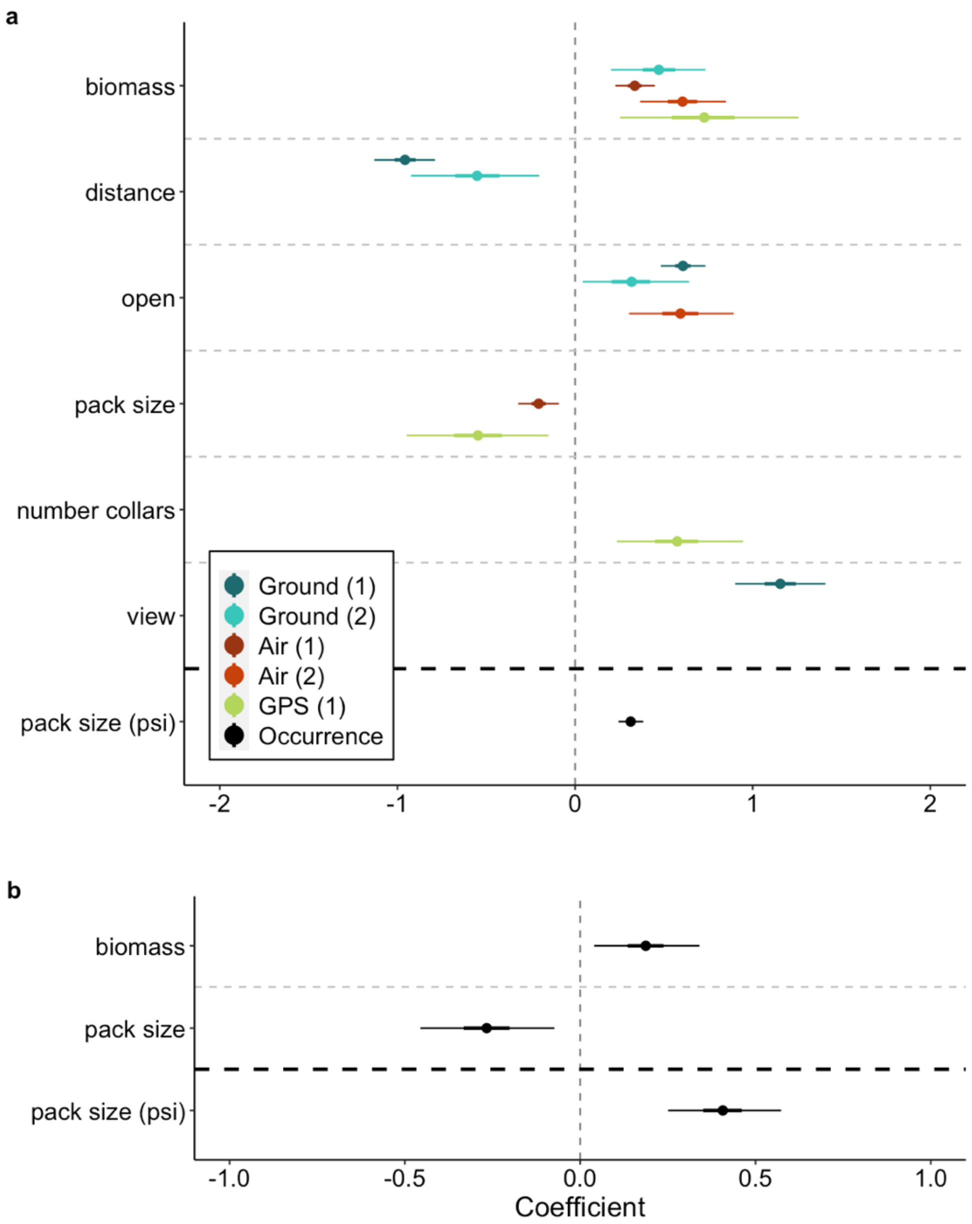

**Figure 4-10. Scaled beta coefficient estimates for feeding event abundance models for wolves in Yellowstone National Park.** For the roaming period model displayed in panel (a), blue, red, and green-shaded circles are the coefficient estimates (with 95% credible intervals represented by thin error bars, and 50% credible intervals by the thick errors bars) for the legend-specified detection occasion, while the black circle is the coefficient for pack size in the biological process model. For the denning period model displayed in panel (b), only one estimate existed for each covariate. The meaning of pack size (psi) is the same as in panel (a).

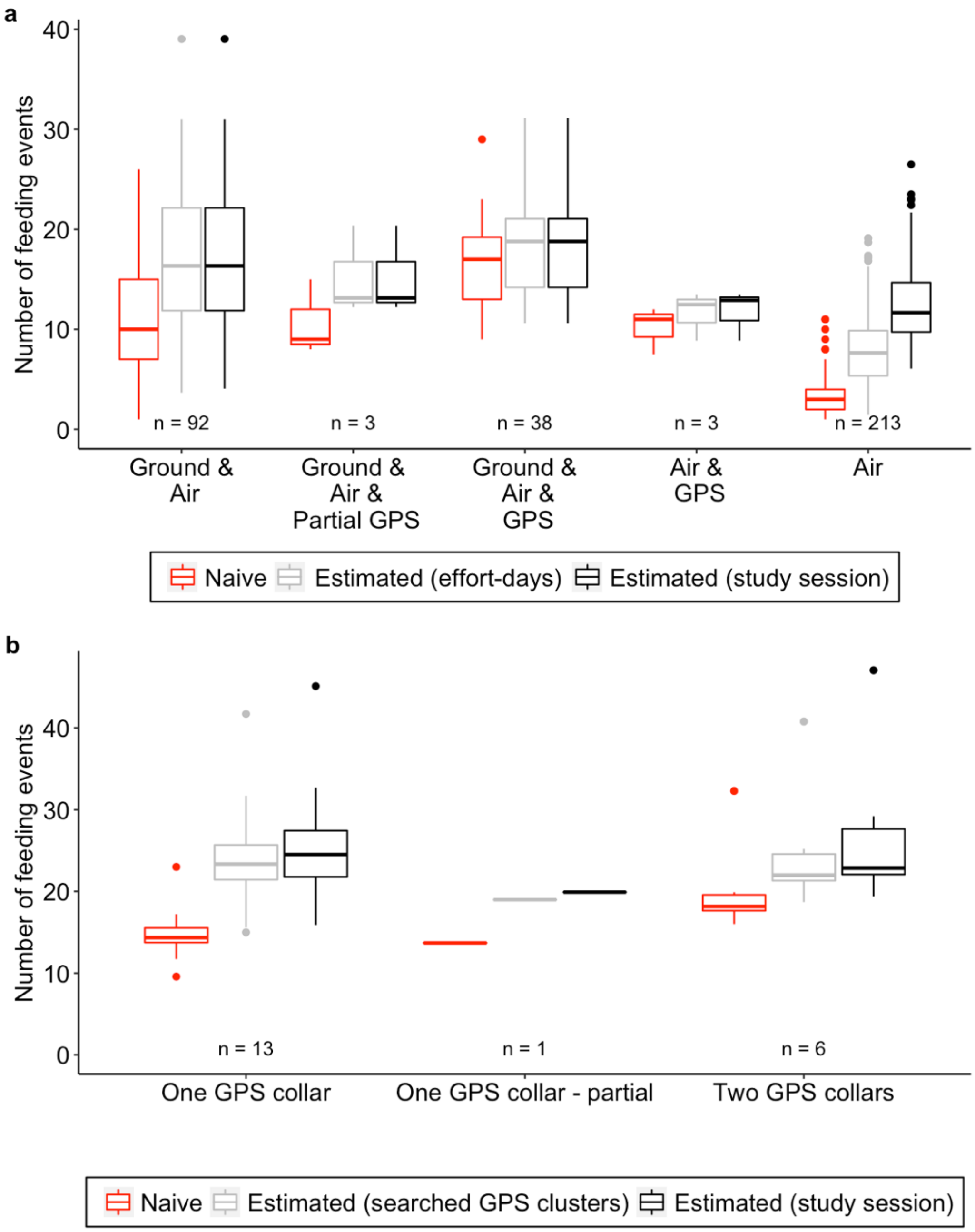

**Figure 4-11. Naïve and estimated feeding events for Yellowstone National Park wolf pack-sessions during (a) roaming (*n* = 349) and (b) denning (*n* = 20) period sessions.** Estimates here were adjusted, for display purposes, to each represent the estimated number of feeding events for a 30-day session. Box plots are grouped by how the pack was monitored, with the color indicating whether the estimate was naïve (red), for just the days with effort occurring within a 2-day window during the roaming period (gray) or for searched GPS clusters during the denning period (gray), or adjusted to estimate the number of feeding events over the duration of that pack's session (black).

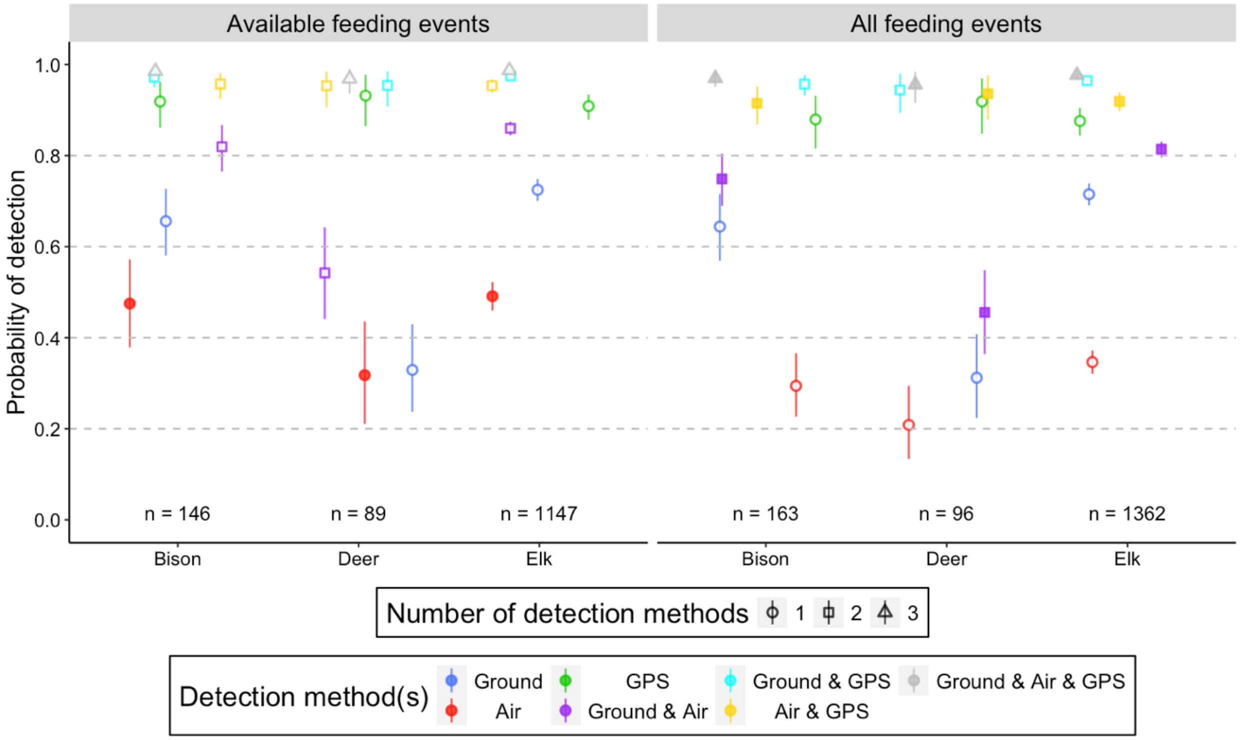

**Figure 4-12. Combined-method detection probabilities for prey species for available feeding events and all feeding events.** Detection probabilities were developed using only feeding events detected during pack-sessions where multiple detection methods attempted to detect feeding events. The left panel ('Available feeding events') describes detection probabilities when method-specific availability was defined as a 1 or 0 depending on if any effort by a method occurred during the two-day feeding event lifespan (Fig. 4-5). The right panel ('All feeding events') defined availability according to the methods that were intended to monitor the pack-session, thereby assuming the applicable methods were always operational within a feeding event lifespan. Each point reports the mean estimate (± 95% credible interval) for detection probability for these detection method(s). We estimated detection probability for all possible method combinations (symbol shape indicates the number of methods in a combination), although our employed method combinations dictated that we only used the detection probabilities for four combinations (Air; Ground & Air; Air & GPS; Ground, Air, & GPS) in Eqn. 8. The detection probabilities that were used in Eqn. 8 are indicated by the filled symbols. Specifically, we used $p_{air}$ from 'Available feeding events' (left panel) for air-only pack sessions and $p_{methods}$ from 'All feeding events' (right panel) for all other pack-sessions. Numbers indicate sample size. See also Appendix S4-D and specifically Fig. S4-D.1.

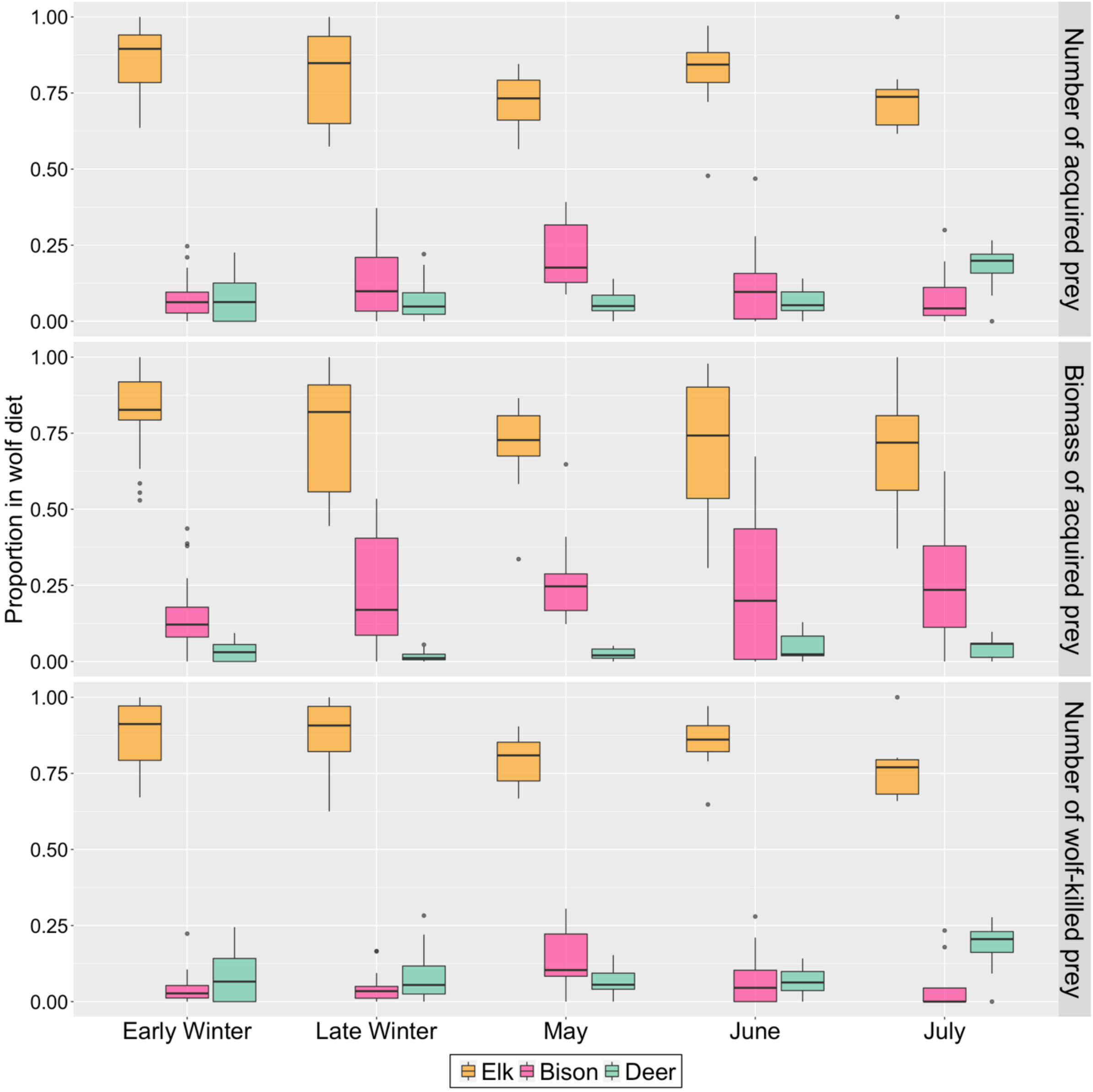

**Figure 4-13. Proportional diet composition for Northern YNP wolves during seasonal months (November 1997–June 2020).** Facets display box plots for month-specific annual estimates of proportional diet calculated for the metric of interest at the 'population-level'.

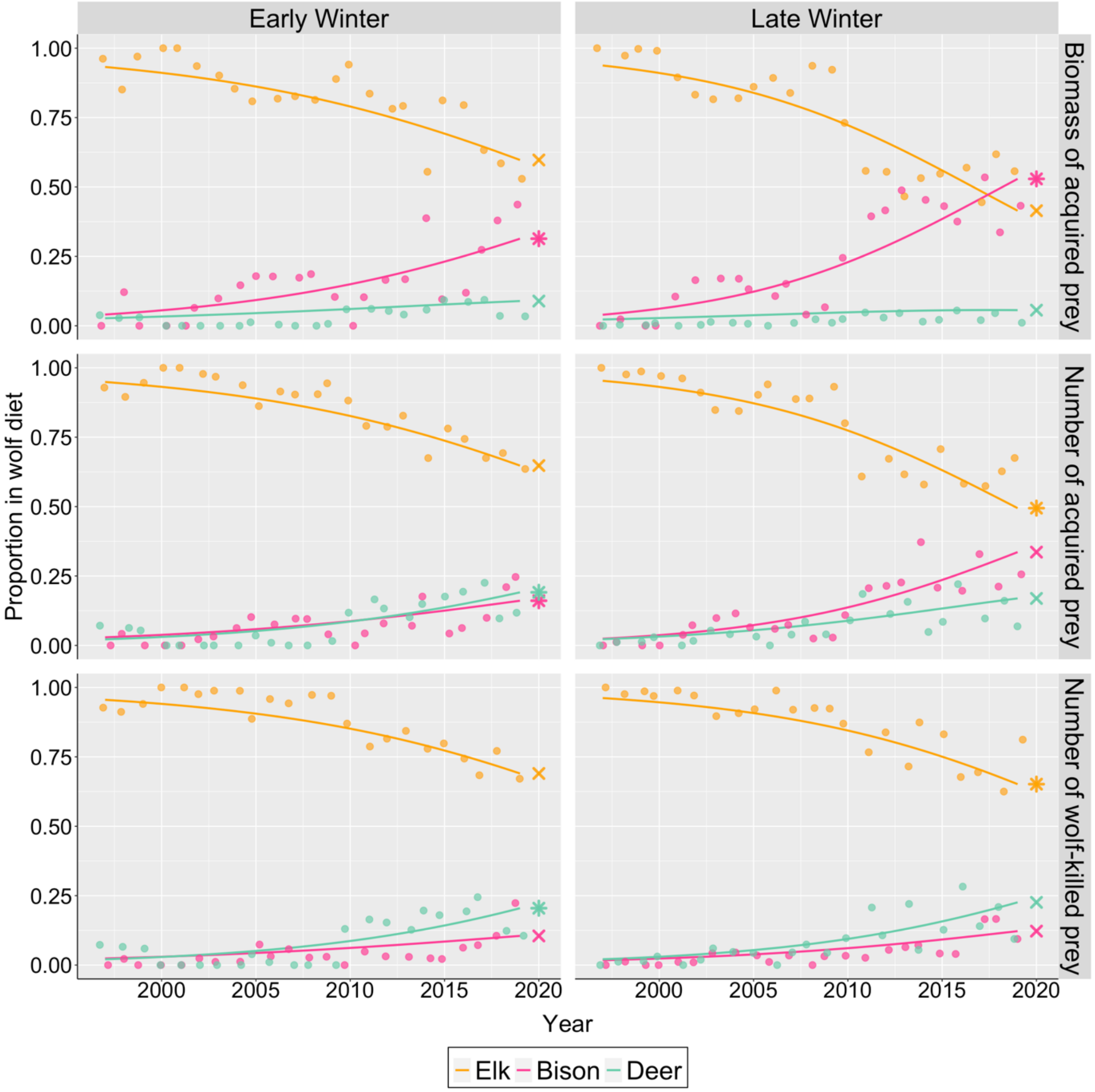

**Figure 4-14. Dirichlet regression model predictions for the effect of time on proportional diet composition of Northern YNP wolves.** Predictions are for single estimate (i.e., population-level) for Northern YNP wolf packs for each season (early or late winter) from 1997–2019 ($n$ = 23 seasonal estimates for each panel). Symbol on far right of each panel indicates whether year was significant in the model for the corresponding species (* indicates $p \leq 0.05$; + indicates $p \leq 0.10$; X indicates $p > 0.10$).

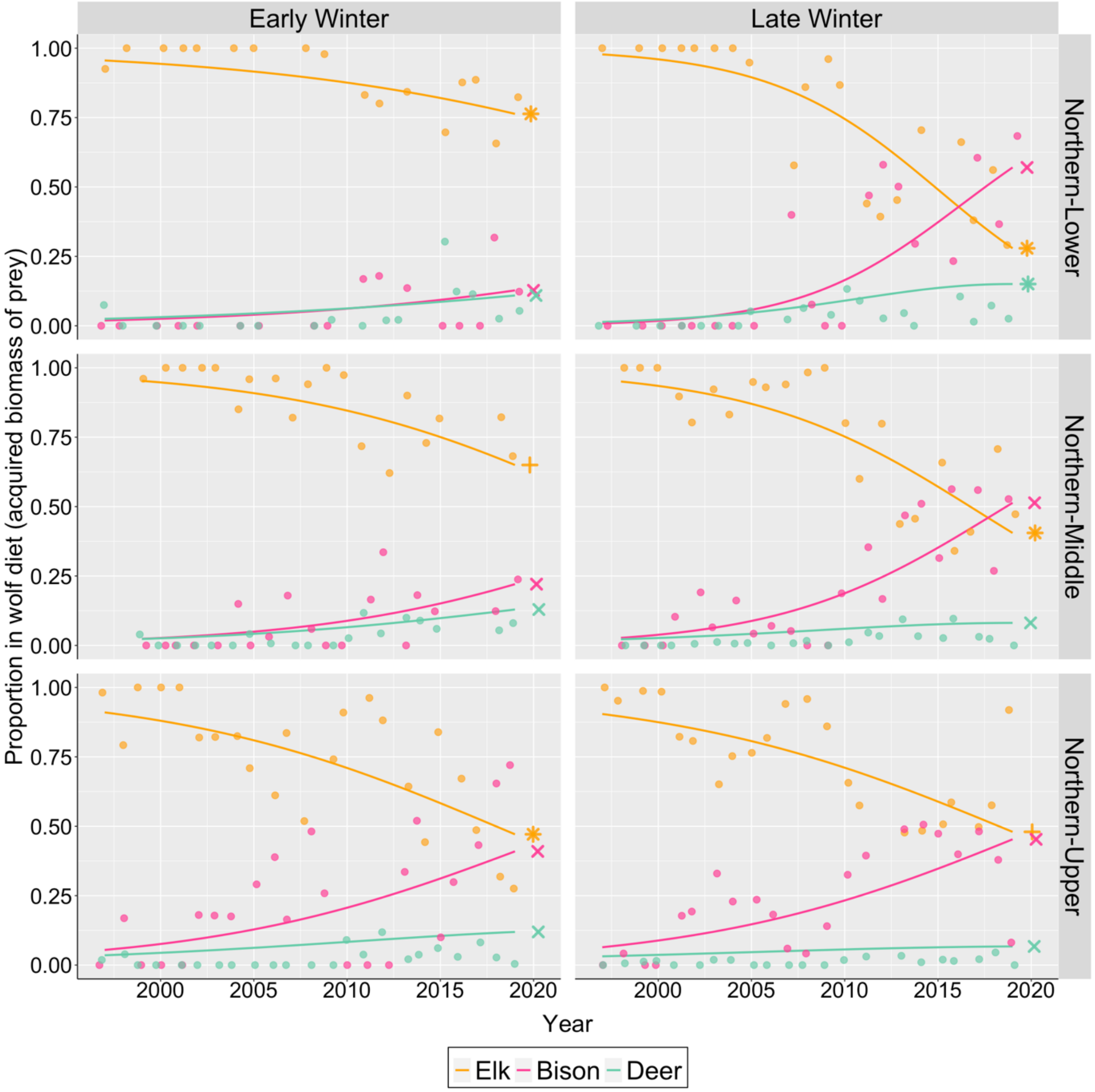

**Figure 4-15. Dirichlet regression model predictions for the effect of time on proportional biomass acquired by Northern YNP wolves across spatial zones.** Remainder of information is the same as Fig. 4-14. See also Fig. S4-E.11.

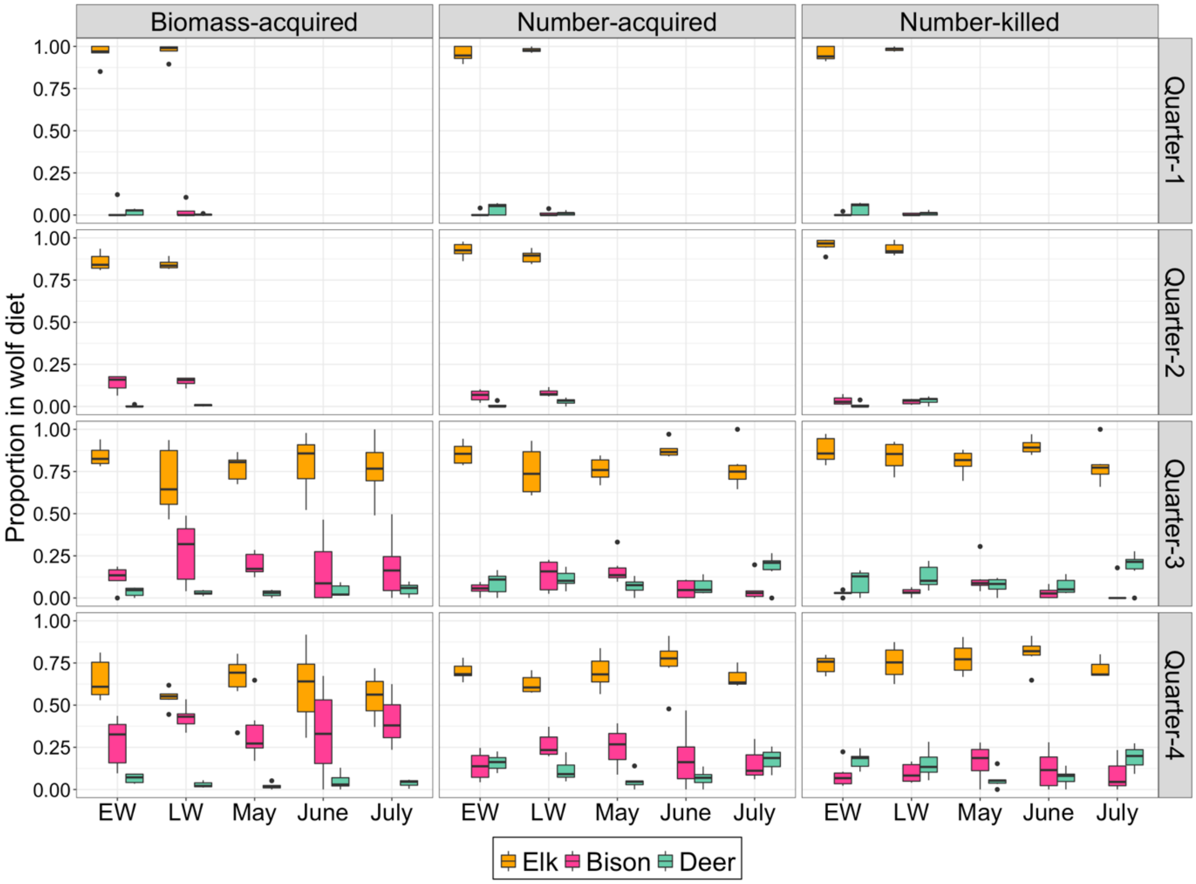

**Figure 4-16. Proportional diet composition for Northern YNP wolves across seasonal months during each quarter.** No data is displayed during denning period months for quarter-1 (1997–2001) and quarter-2 (2002–2007) because no data was collected.

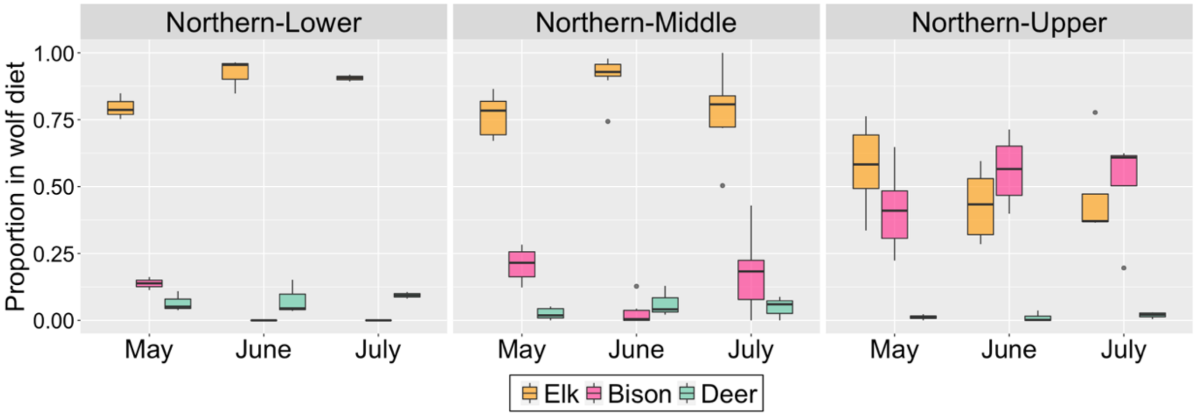

**Figure 4-17. Proportion of biomass acquired for denning period months for Northern YNP wolves, across spatial zones (May 2008–June 2020).** Proportions were calculated at the population-level within each zone. Sample sizes were 3 (May), 3 (June), and 2 (July) for Northern-Lower, 8, 8, and 7 for Northern-Middle, and 5, 7, and 4 for Northern-Upper. See Figs. S4-E.12, S4-E.13 for other metrics during the denning period and all metrics during the roaming period.

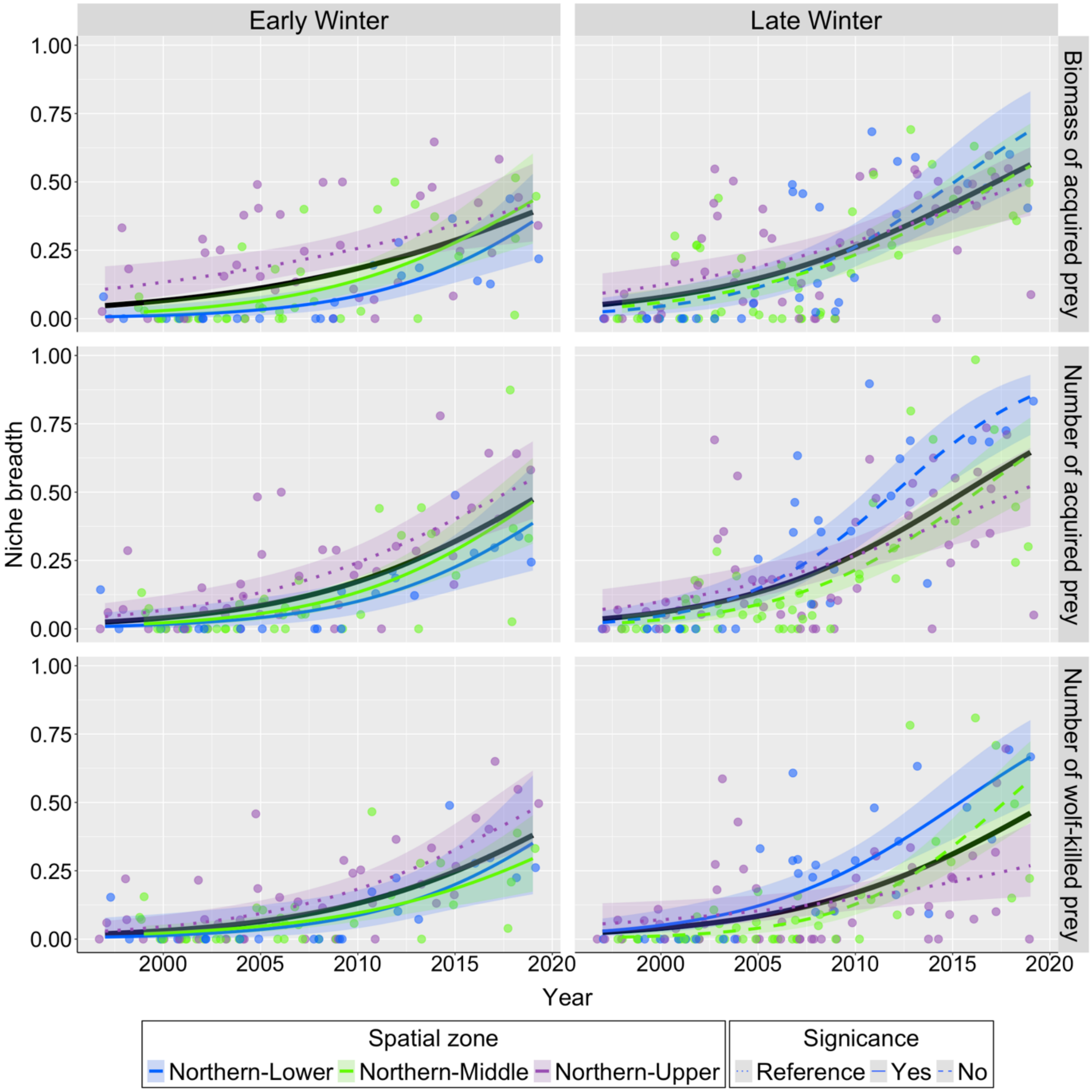

**Figure 4-18. Niche breadth (*B*) through time for Northern YNP wolf packs.** The black line displays the predicted effect of year, which was significant in all panels, on niche breadth for a quasibinomial generalized linear model that only included year. The colored lines display predictions, with 95% confidence intervals, for quasibinomial generalized linear models that also included an effect for spatial zone. The purple line for the reference zone (Northern-Upper) is dotted, while the lines for Northern-Lower (blue) and Northern-Middle (green) are solid if they significantly differed from Northern-Upper and dashed if they did not. See Fig. S4-E.14 for coefficient estimates and Fig. S4-E.15 for population-level estimates.

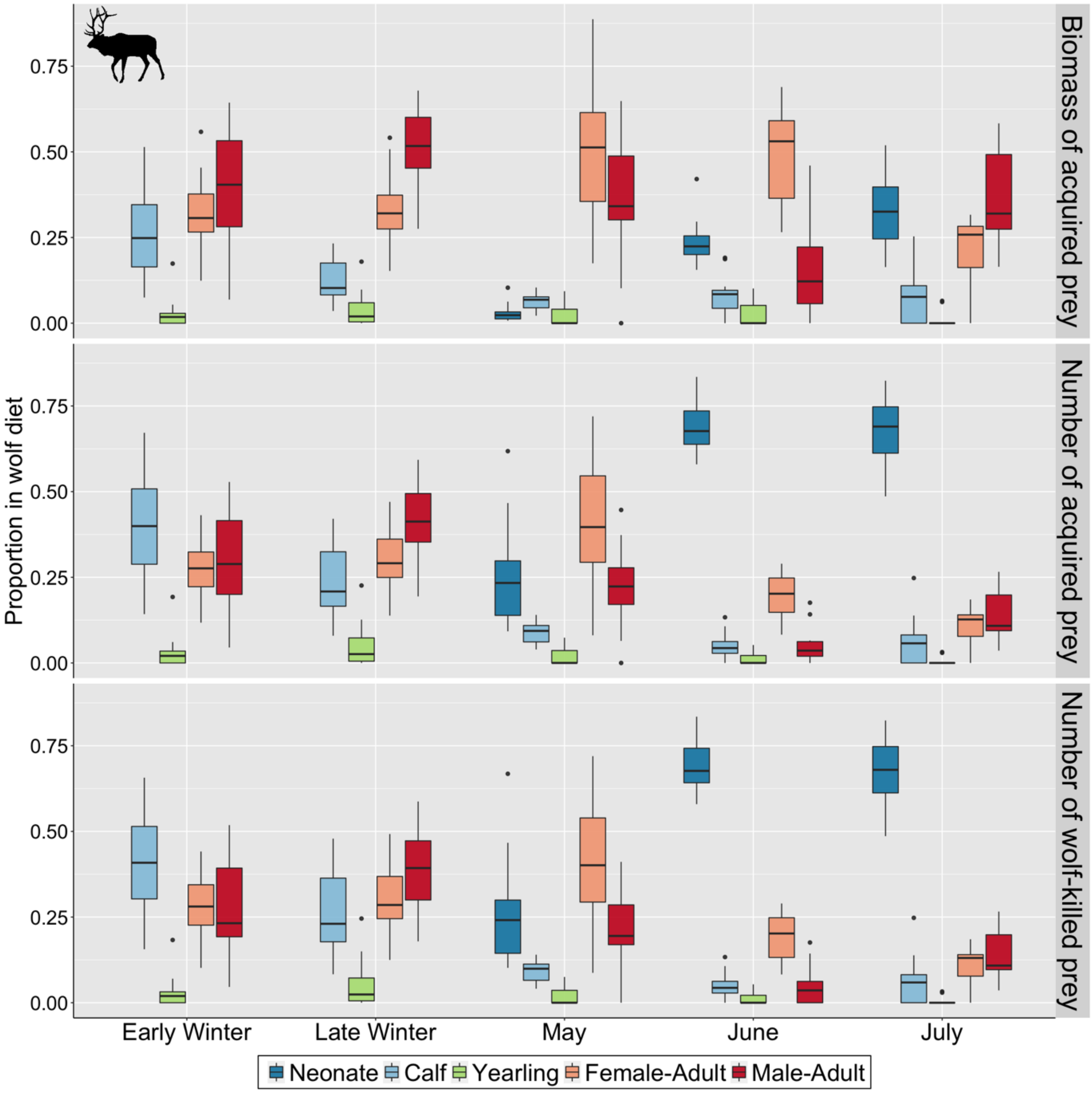

**Figure 4-19. Proportion sex-age class among feeding events on elk for Northern YNP wolves.** Box plots within each panel display variation in estimates where proportions were estimated at the population-level among all acquired elk biomass (top row), all acquired elk number (middle row), or only wolf-killed elk number (bottom row). Month-session sample size for proportional data were 23 for early and later winter, 12 for May and June, and 9 for July.

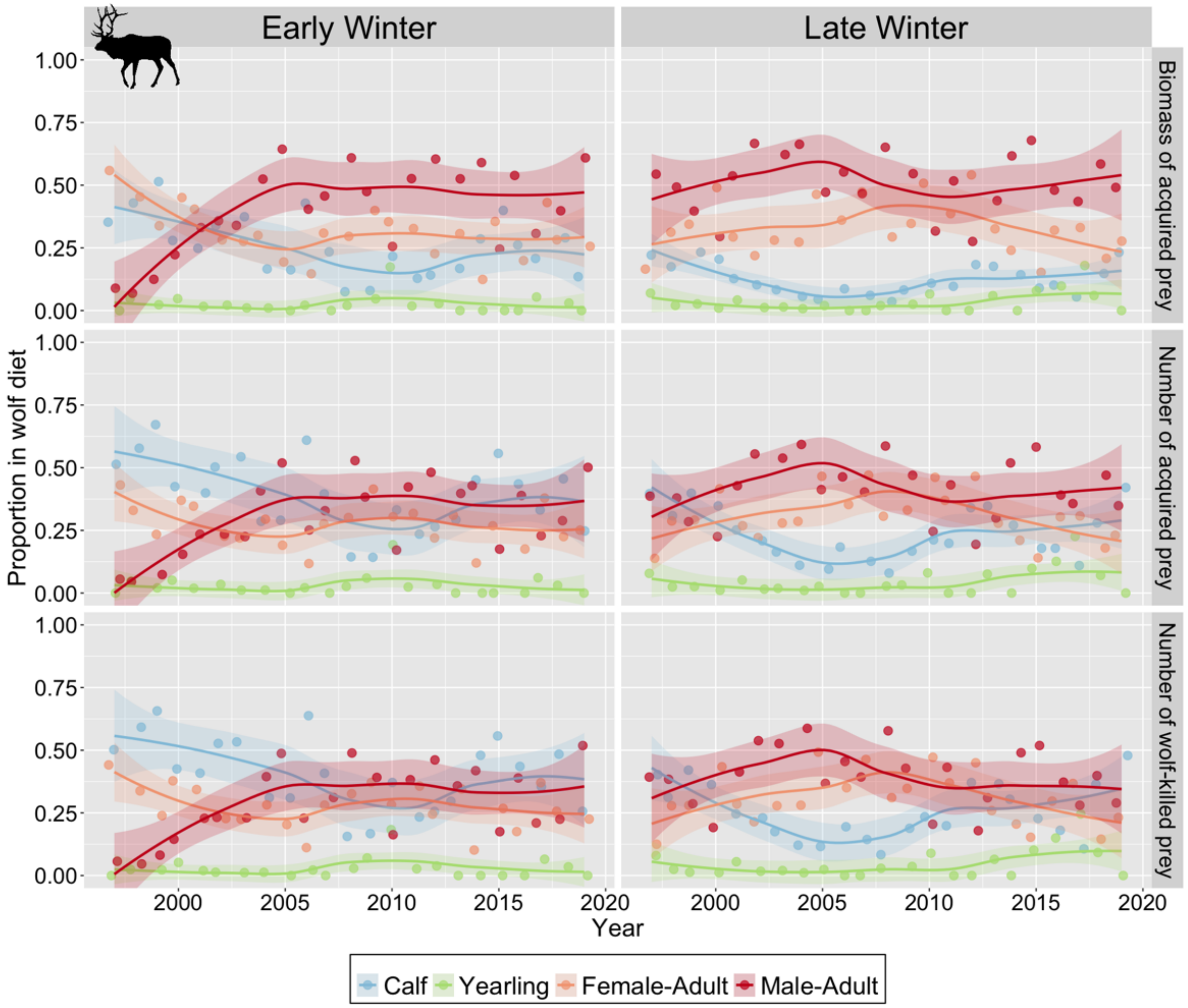

**Figure 4-20. Proportion sex-age class among feeding events on elk for Northern YNP wolves across time.** Lines display 'loess' fit to highlight longitudinal trends.

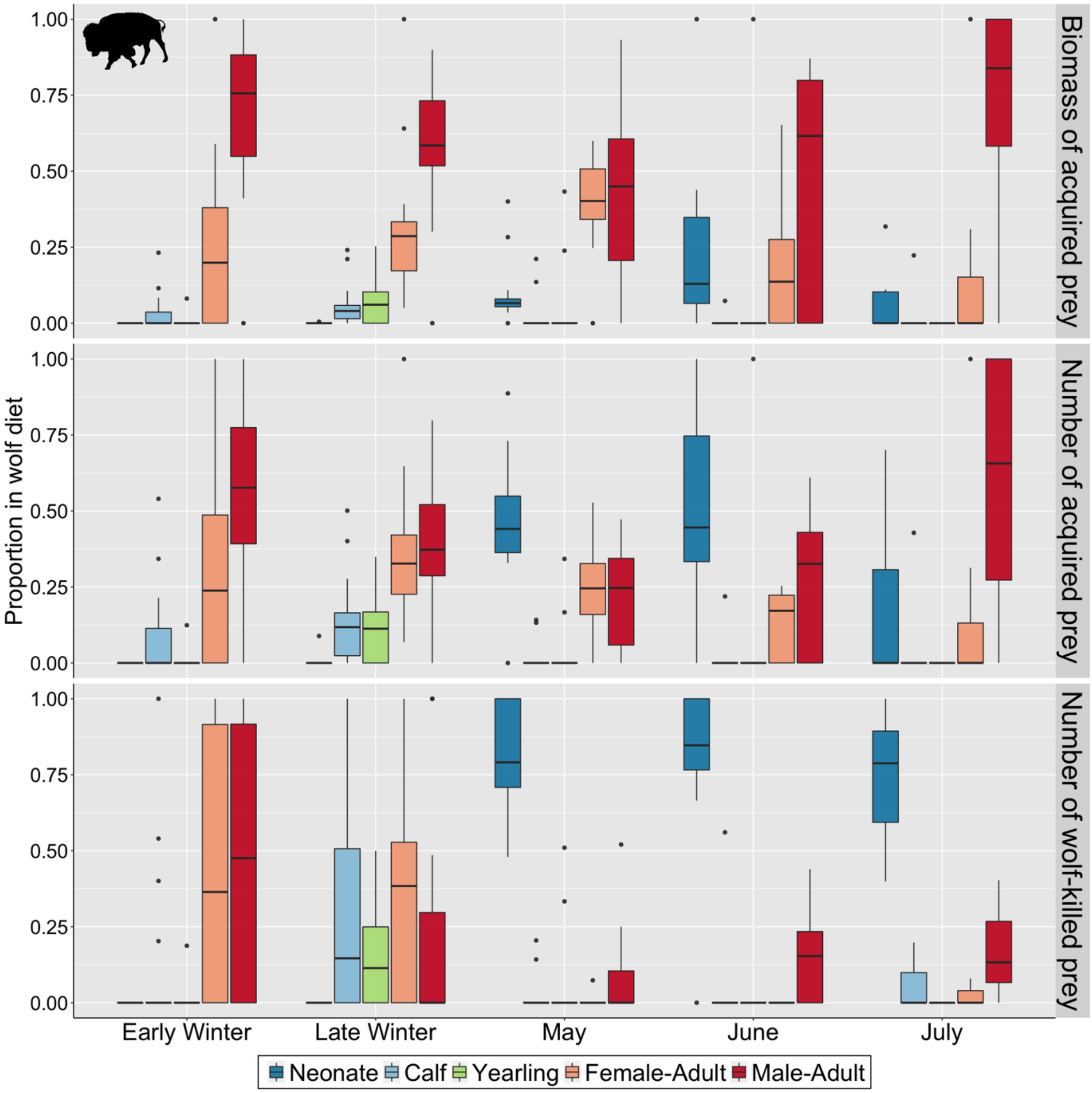

**Figure 4-21. Proportion sex-age class among feeding events on bison for Northern YNP wolves.** Data presented is the same as that in Fig. 4-19. Sample sizes here, however, differ because we did not detect or estimate any bison feeding events during some month-sessions. As such, sample sizes were 18 (early winter), 20 (late winter), 12 (May), 9 (June), and 8 (July).

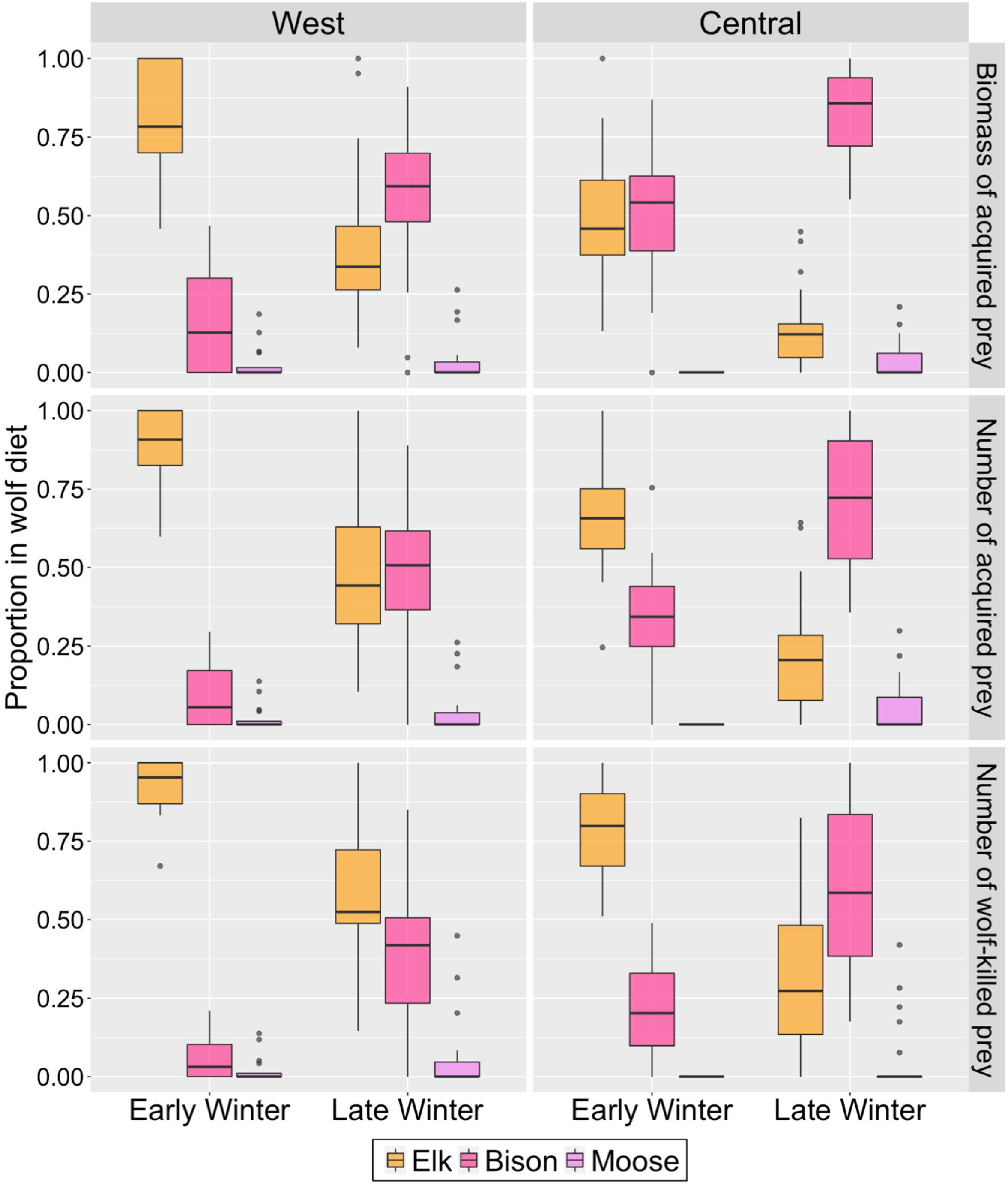

**Figure 4-22. Proportional diet composition for Interior YNP wolves during roaming period sessions (1997–2019).** The types of data are the same as Fig. 4-13, except here the plots are also faceted by zone because of the fundamental difference in Interior YNP zones related to the wintering distribution of the Madison-Firehole elk population.

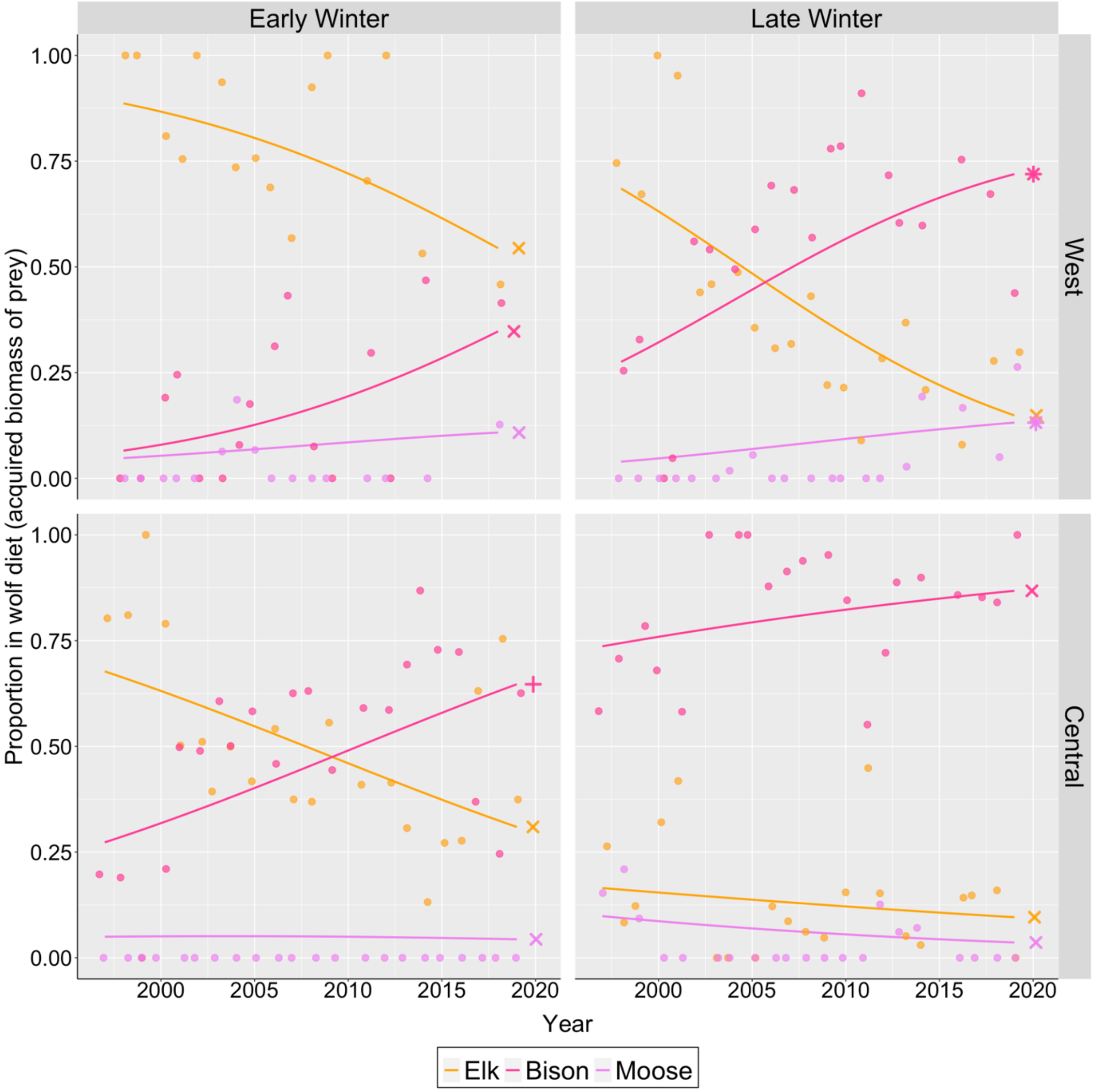

**Figure 4-23. Population-level predictions of prop-biomass acquired for Interior YNP wolves across spatial zones.** Information presented is the same as Fig. 4-15. See also Fig. S4-E.21.

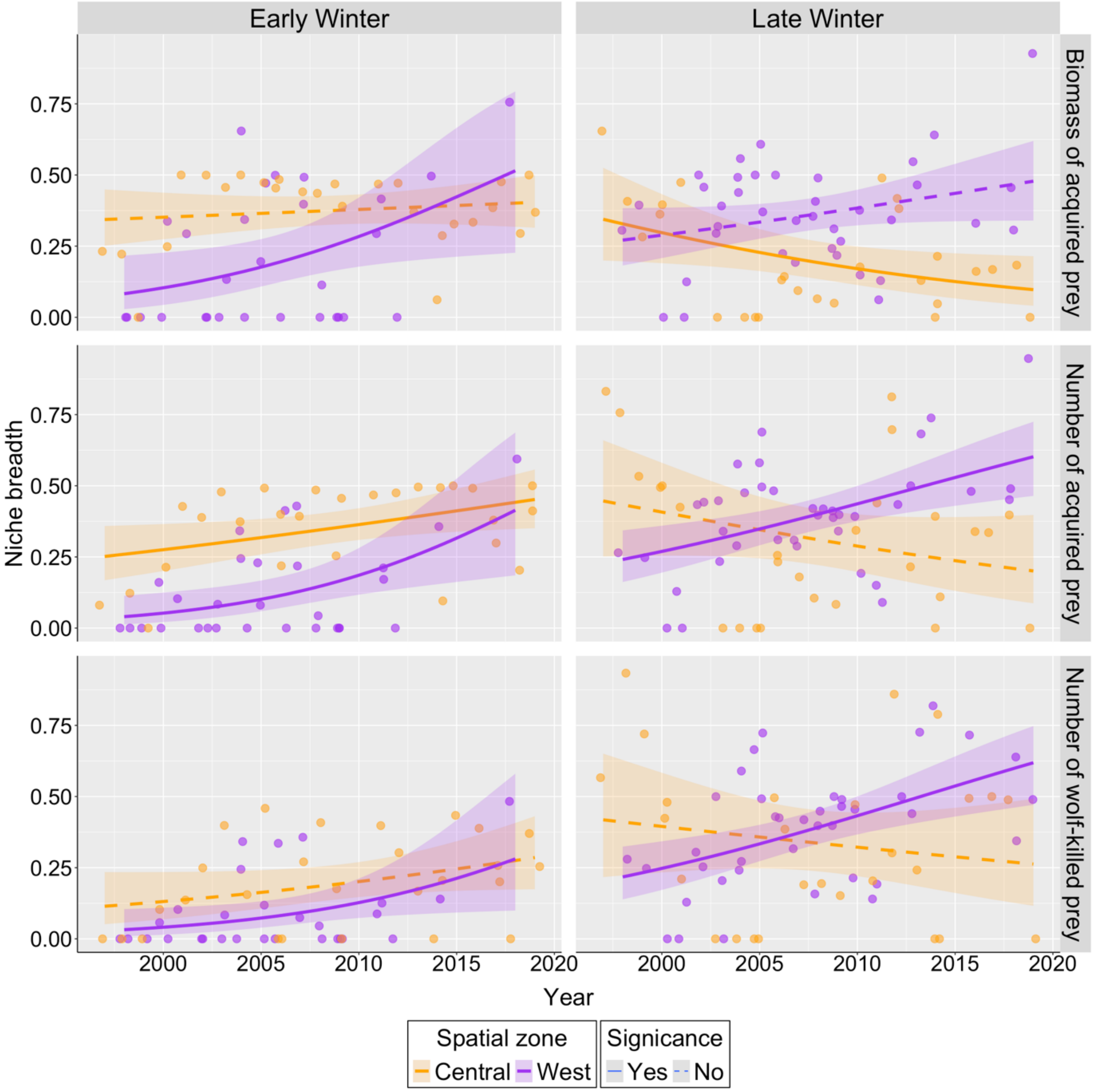

**Figure 4-24. Niche breadth (*B*) through time for Interior YNP wolf packs.** The colored lines show predictions for a quasibinomial generalized linear model developed for the identified spatial zone. Solid lines indicate year was significant in the model for that spatial zone, while dashed lines indicate an insignificant effect of year. See Fig. S4-E.22 for coefficient estimates.

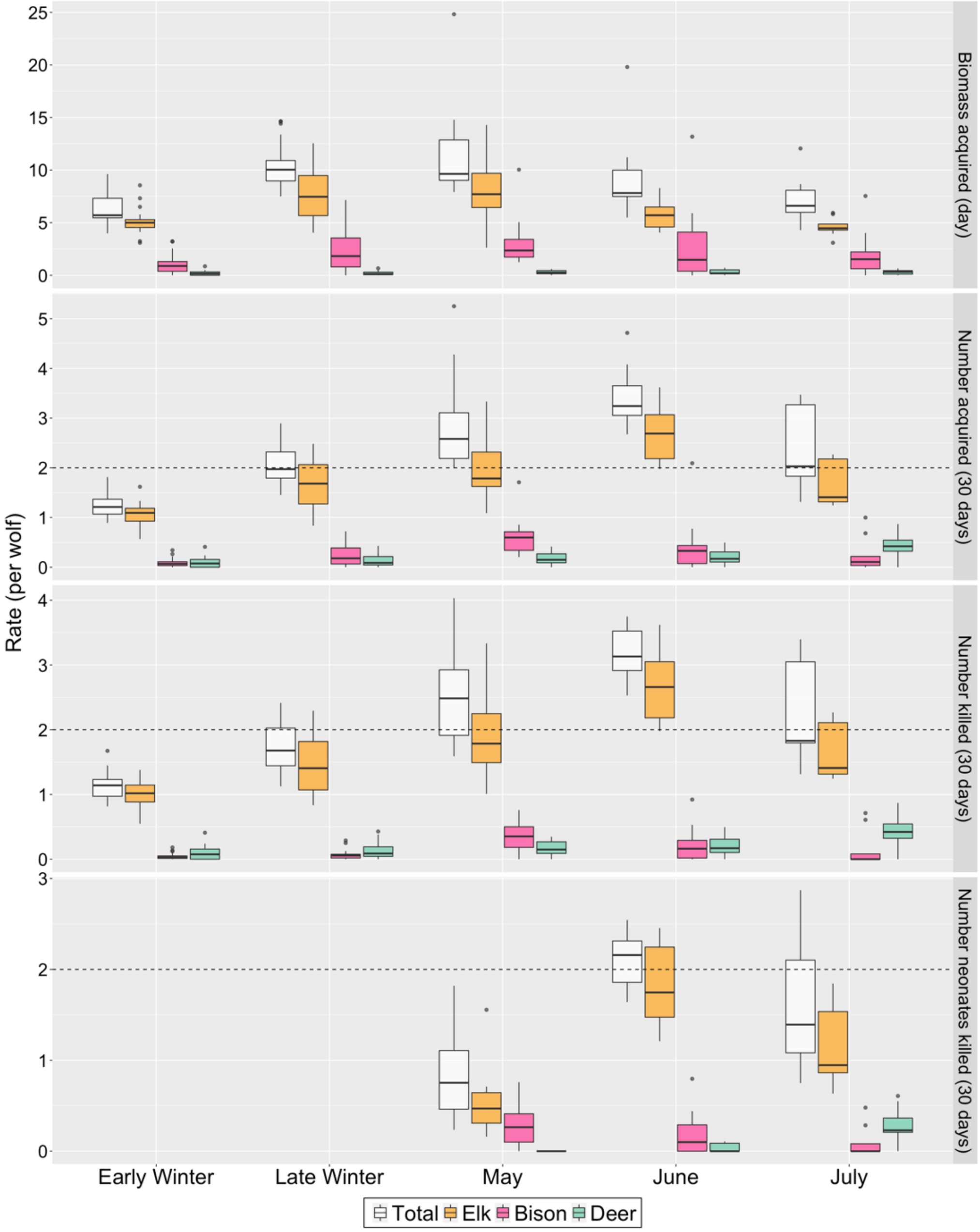

**Figure 4-25. Seasonal per-capita acquisition and kill rates for Northern YNP wolves.** Estimates for rates in terms of biomass acquired, number of prey acquired, number of prey killed, and number of neonate prey killed. Dashed line at 2 in the bottom three plots is to facilitate comparison between these number of prey panels. Estimates are from the population-level with sample sizes of 23 (early winter), 23 (late winter), 11 (May), 11 (June), and 9 (July). See also Fig. S4-E.23 through Fig. S4-E.26 for plots related to the pack-level.

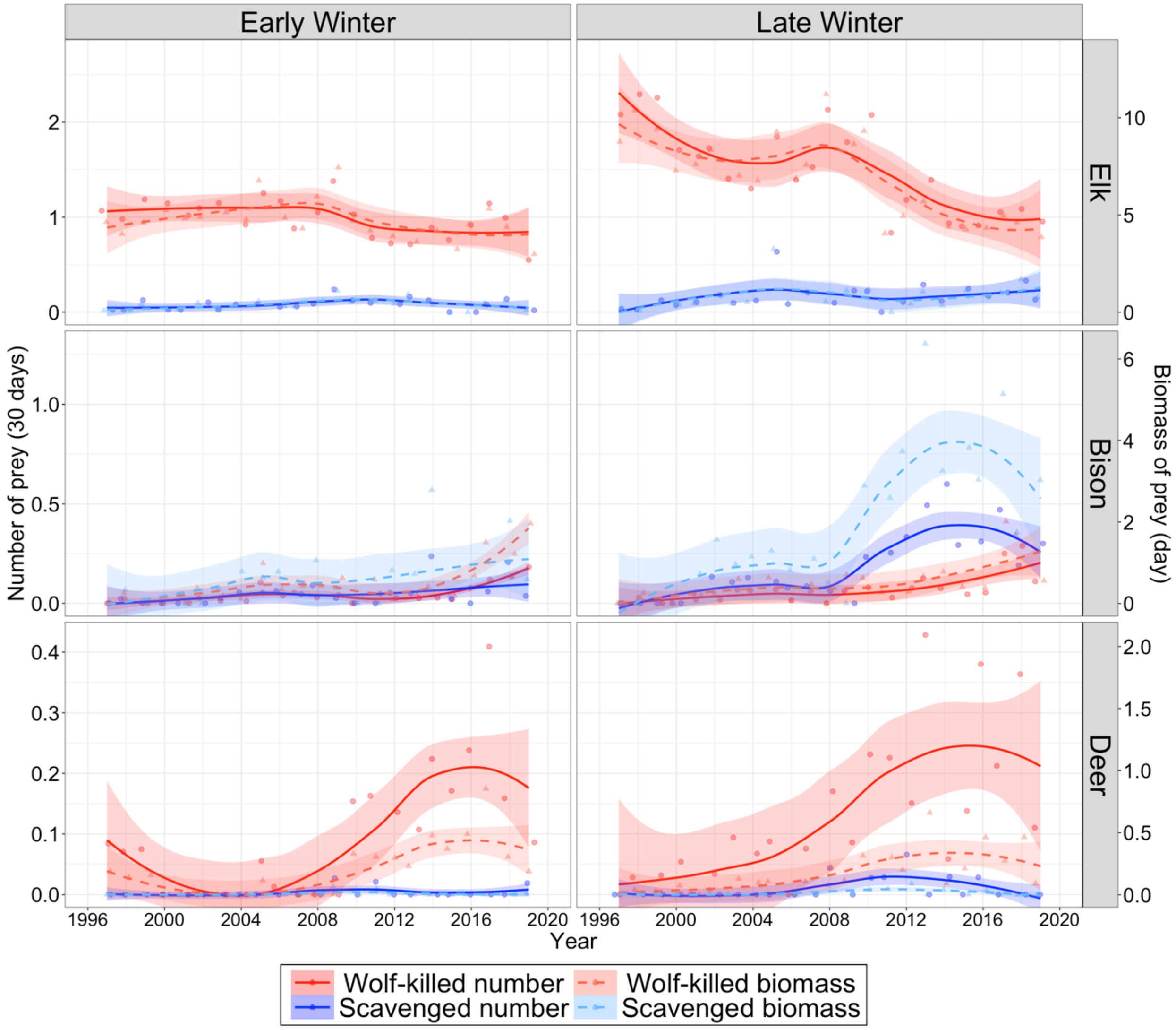

**Figure 4-26. Longitudinal patterns in the rates wolves killed and scavenged primary ungulate prey in Northern YNP, 1997–2019.** Solid lines (and circles) display per-capita rates as the number of prey per 30-days (in relation to left y-axis), while dashed lines (and triangles) display per-capita rates as biomass per day (right y-axis). Kill rates are displayed in red and scavenging rates in blue. Lines display 'loess' fit to highlight longitudinal trends.

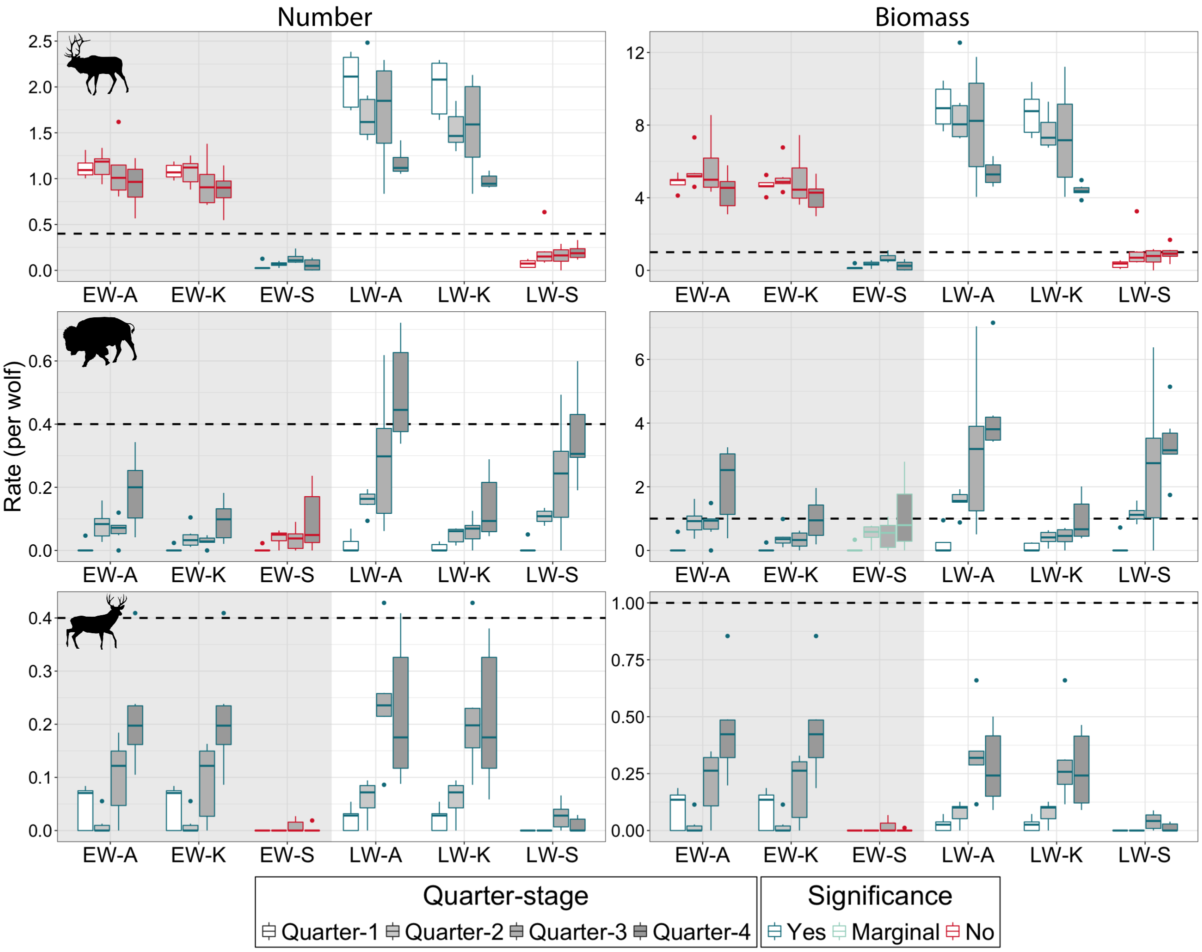

**Figure 4-27. Comparison of per-capita acquisition, kill, and scavenging rates for wolves on elk (top row), bison (middle row), and deer (bottom row) for early and late winter seasons across quarters in Northern YNP.** Elk:bison ratios declined during subsequent quarters (quarter-1 = 1997–2001; quarter-2 = 2002–2007; quarter-3 = 2008–2013; quarter-4 = 2014–2019; Fig. 4-3b**).** The labels on the x-axis indicate whether rate was for early (EW) or late (LW) late winter, and then acquisition (A), kill (K), or scavenging (S). Gray and white shading separates early and late winter rates. Fill of each box indicates quarter and the color of the box (and whiskers) shows the significance level of an ANOVA test for each set of four rates (darker blue indicates $p \leq 0.05$, lighter blue indicates $p \leq 0.10$, and red indicates $p > 0.10$. Note that the y-axis differs among panels. The dashed line at 0.4 (number) and 1 (biomass) in the panels of each column is provided to facilitate comparisons within each column. See also Figs. S4-E.28, S4-E.29 for figures that also include denning period months.

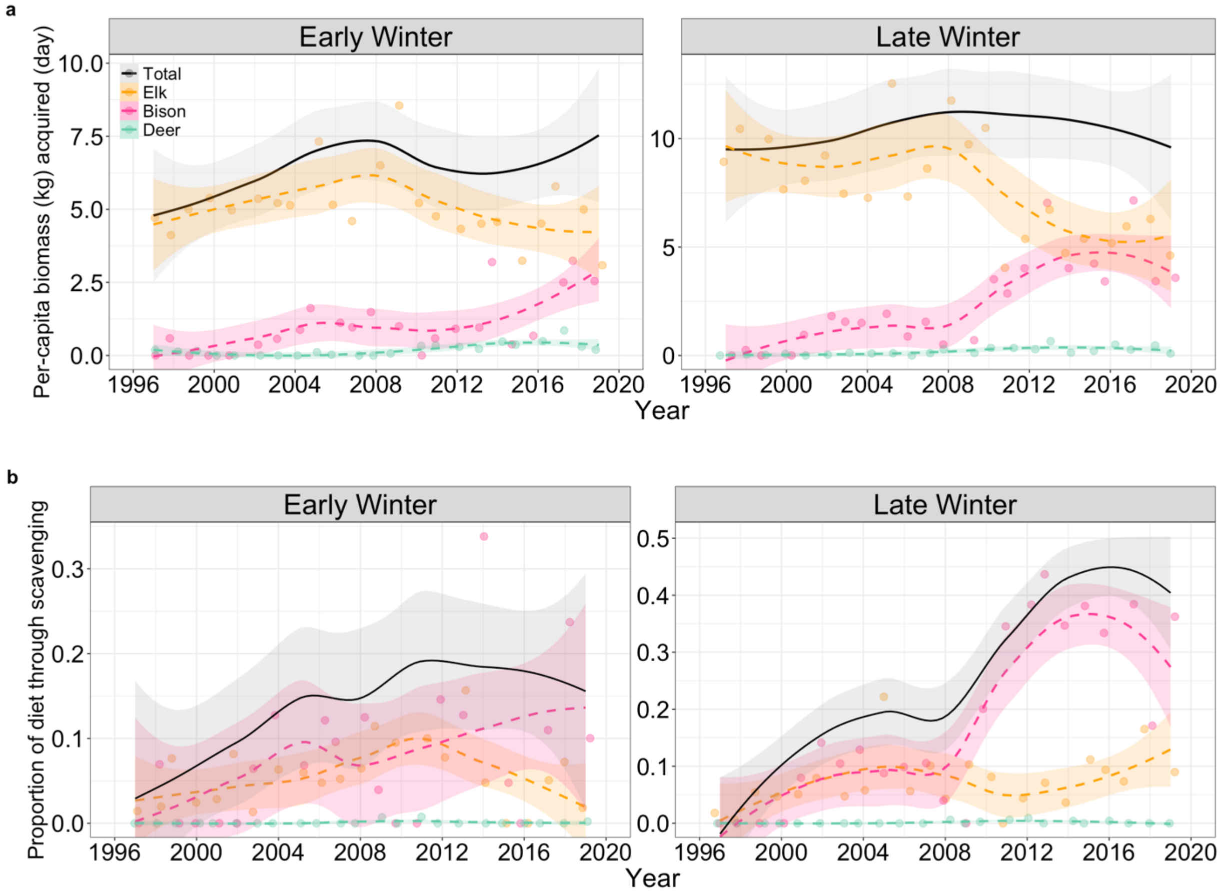

**Figure 4-28. Rates of biomass acquisition and proportion diet through scavenging across time for Northern YNP wolves.** Colored lines in panel (a) display 'loess' predictions for per-capita rates of biomass (kg) acquired from wolves' three primary prey species. The black line displays the 'loess' prediction for all prey combined (i.e., including these three plus any other not shown among colored lines), and thus displays wolves' total biomass acquisition rate. Panel (b) displays the proportion of total biomass that was acquired through scavenging, with the meaning of each colored line paralleling the meanings in panel (a). See also Fig. S4-E.30 for panel (a) expressed in the number of prey-acquired and -killed.

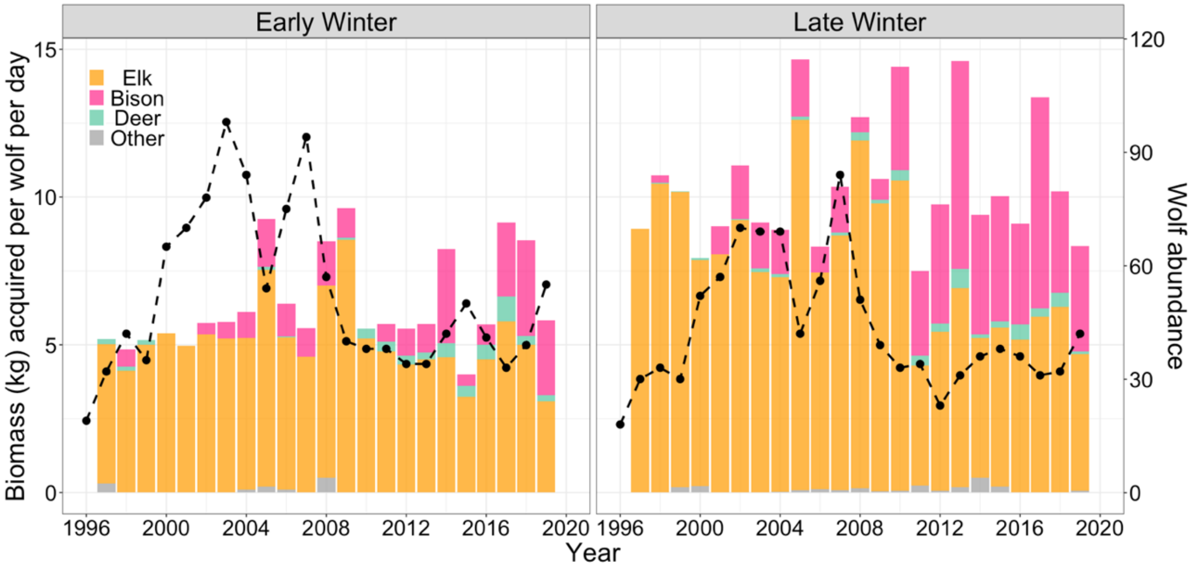

**Figure 4-29. Per-capita rates of biomass acquisition for Northern YNP wolf packs and wolf abundance through time.** Population-level acquisition rates are displayed, along with resident Northern YNP wolf abundance during early and late winter (Smith et al. 2020a).

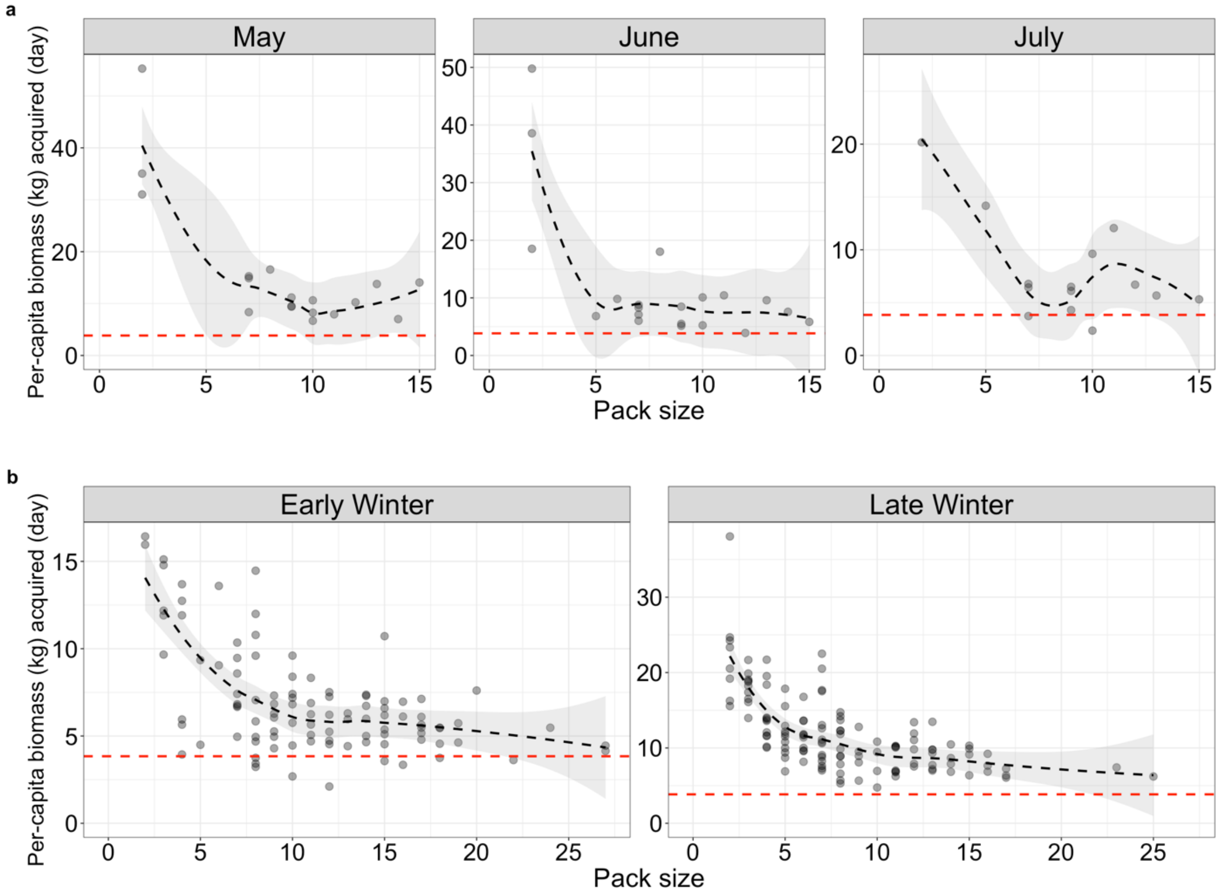

**Figure 4-30. Effect of pack size on per-capita biomass acquisition rate for Northern YNP wolf packs within each seasonal month.** Lines display 'loess' fit. The red dashed line indicates an estimate for the minimum energetic requirements for wolves (3.84 kg/wolf/day; Peterson and Ciucci 2003, Metz et al. 2011).

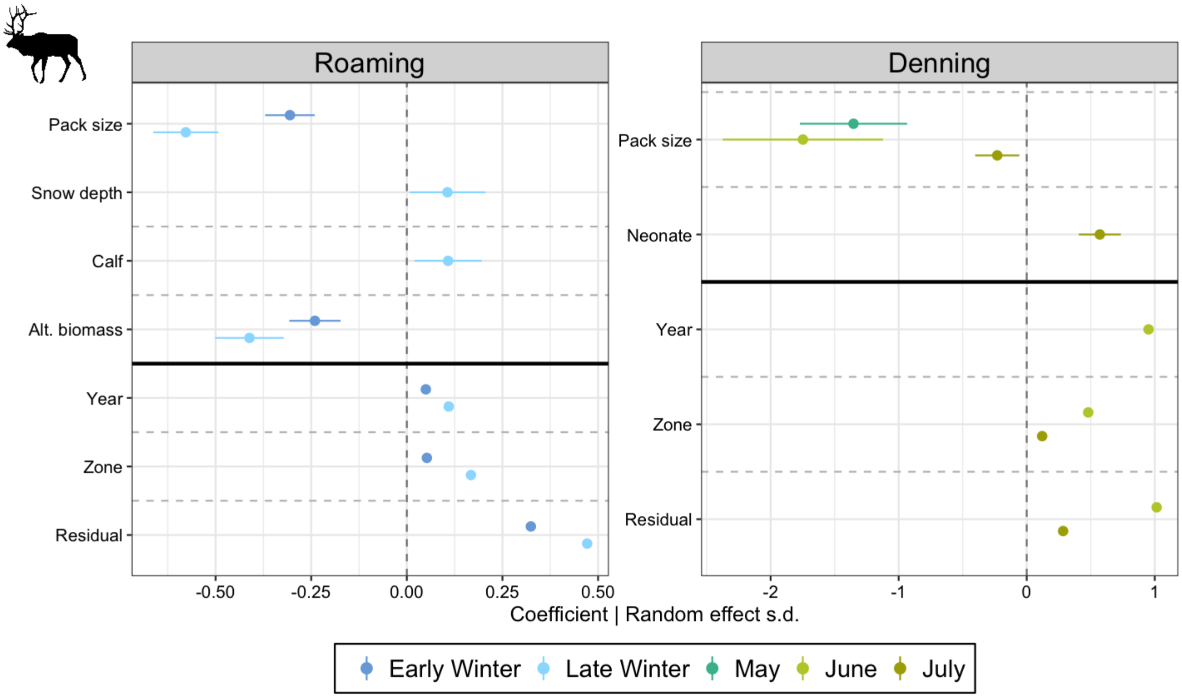

**Figure 4-31. Beta coefficient estimates for models evaluating factors affecting per-capita wolf kill rate on elk in Northern YNP during seasonal months of the roaming and denning periods.** Beta coefficient estimates are displayed with 95% confidence intervals. Below the solid line displays the standard deviation for the random effects and the residual.

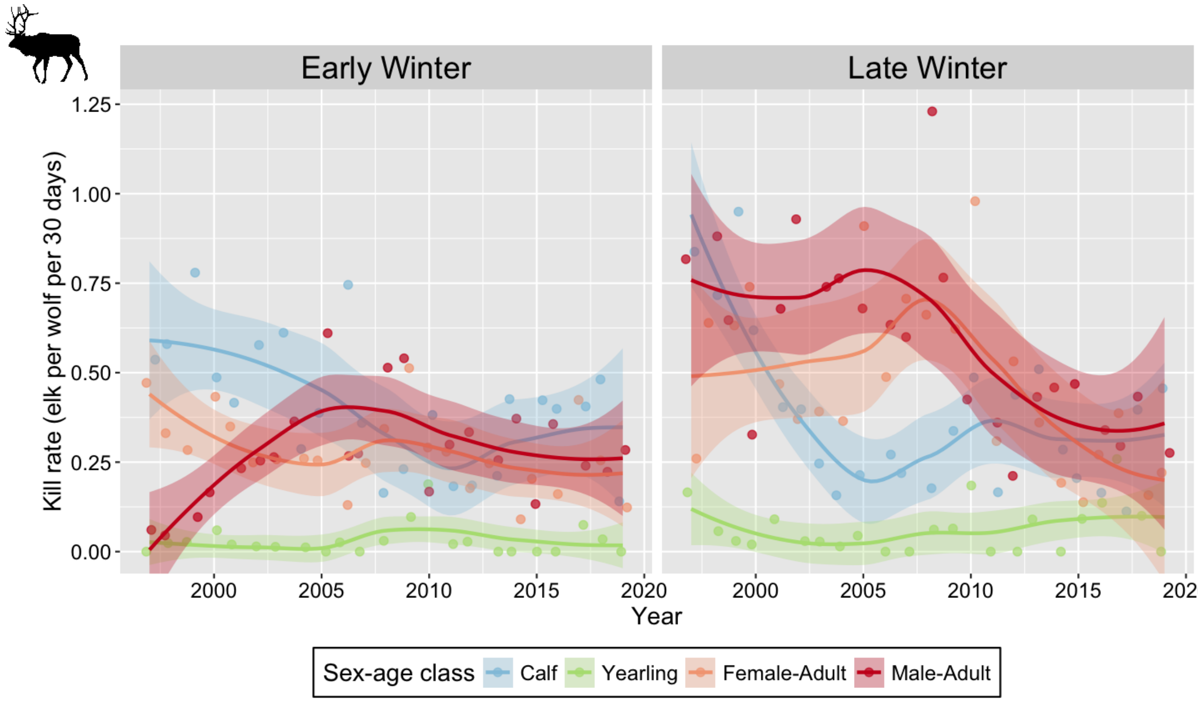

**Figure 4-32. Per-capita kill rates on elk sex-age class for Northern YNP wolves during the roaming period across time.** Lines display 'loess' fit to highlight longitudinal trends.

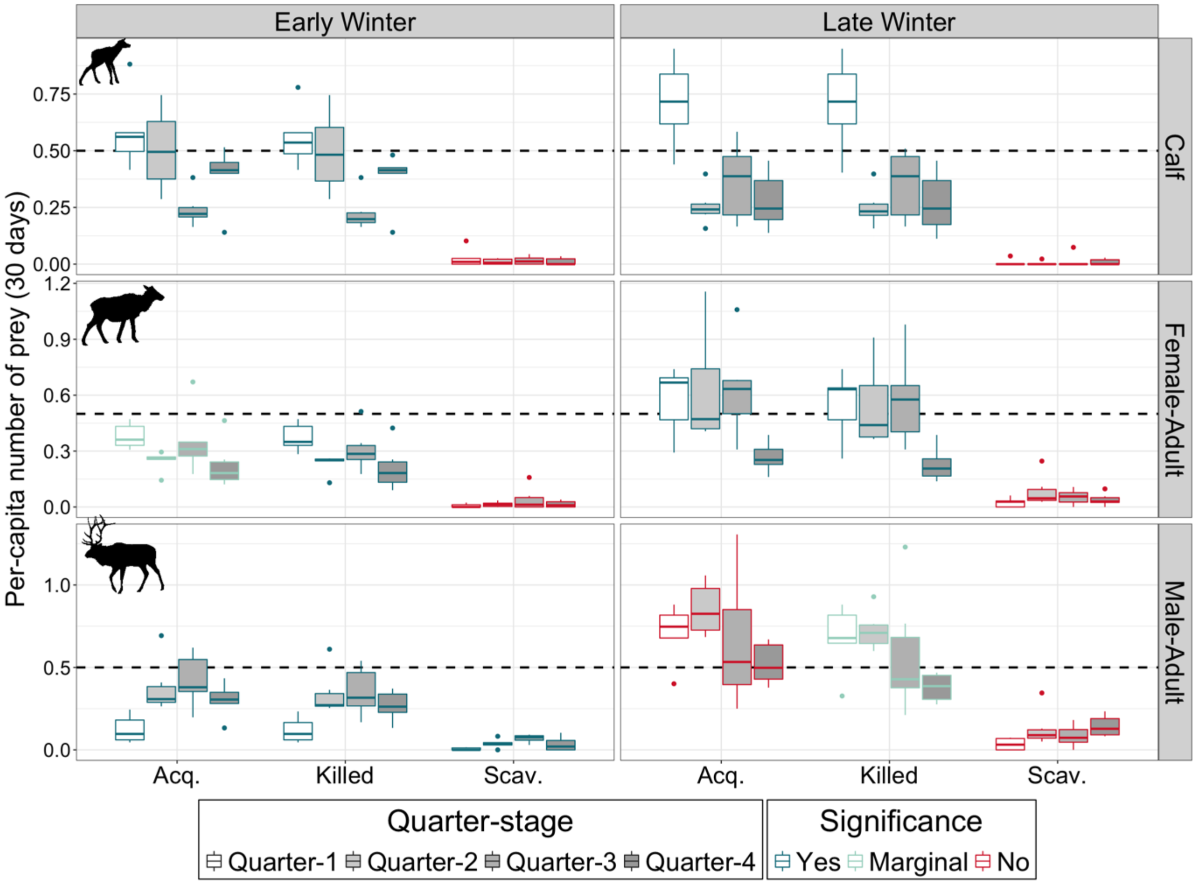

**Figure 4-33. Comparison of per-capita acquisition, kill, and scavenging rates (number-prey) for wolves on elk calves (top row), female-adults (middle row), and male-adults (bottom row) for early and late winter seasons across quarters in Northern YNP.** Dashed line is inserted at 0.5 in each panel to facilitate comparison. The meaning of fill and coloring is the same as in Fig. 4-27.

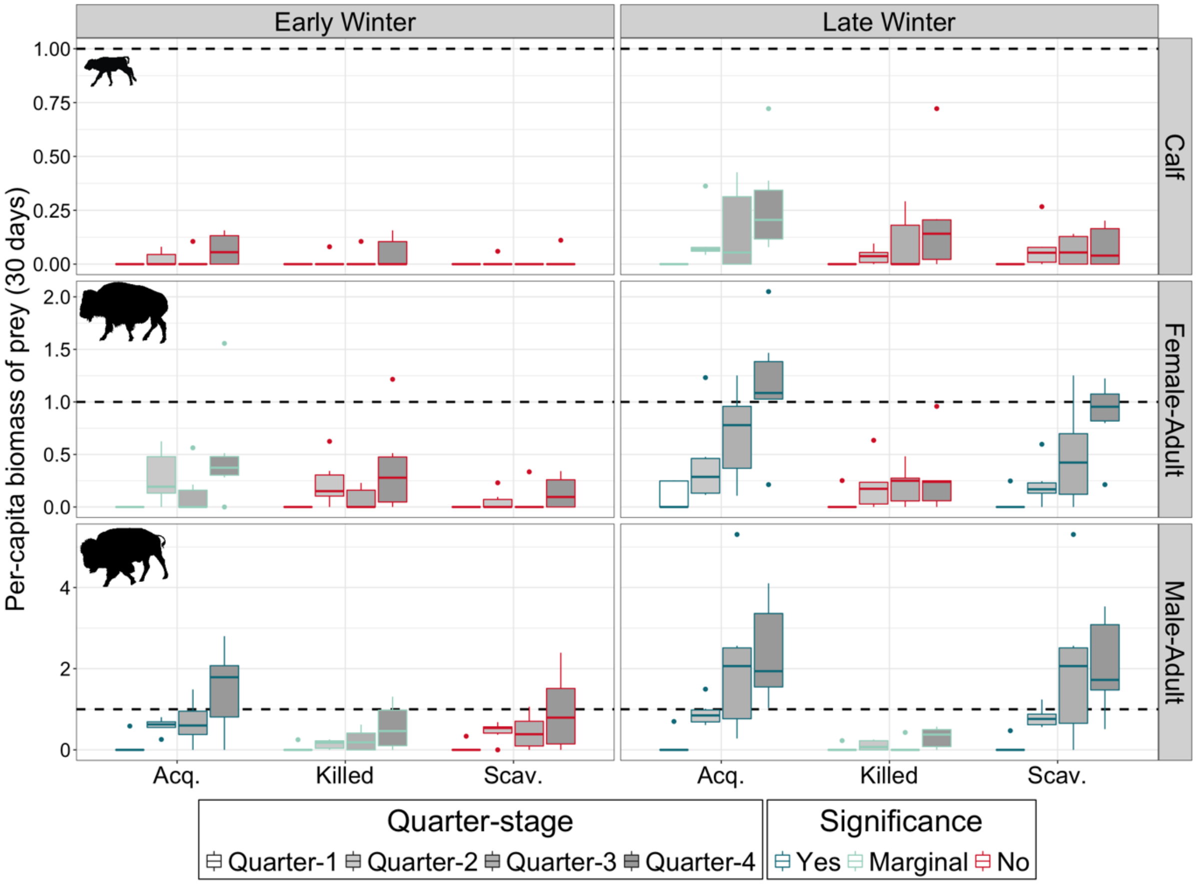

**Figure 4-34. Comparison of per-capita acquisition, kill, and scavenging rates (biomass-prey) for wolves on bison calves (top row), female-adults (middle row), and male-adults (bottom row) for early and late winter seasons across quarters in Northern YNP.** Dashed line is inserted at 1.0 in each panel to facilitate comparison. The meaning of fill and coloring is the same as in Fig. 4-27.

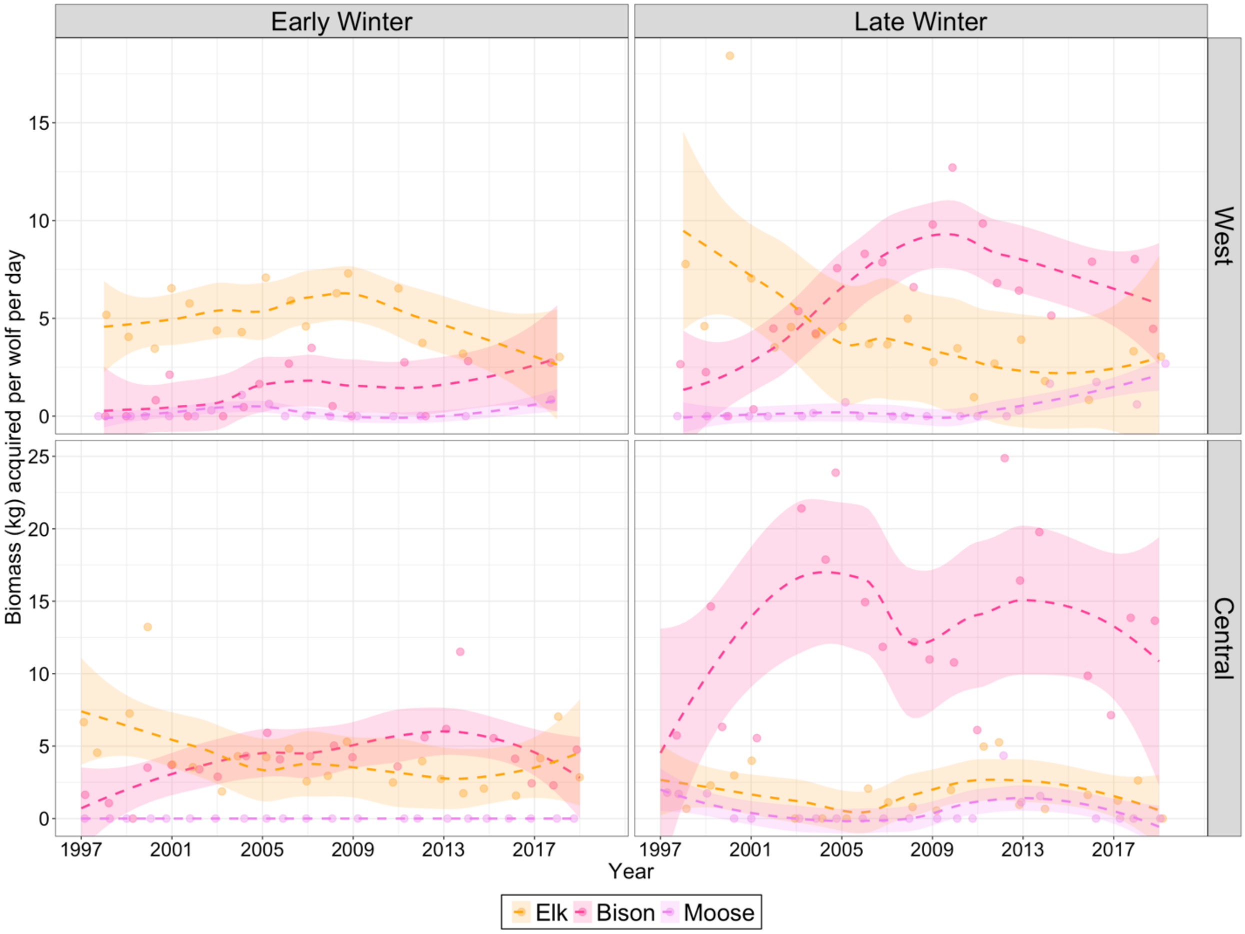

**Figure 4-35. Per-capita rates of biomass acquisition across time in Interior YNP zones.** Data displayed is the same as Fig. 4-28a, except the prey species are elk, bison, and moose. Lines display ‘loess’ fit to highlight longitudinal trends.

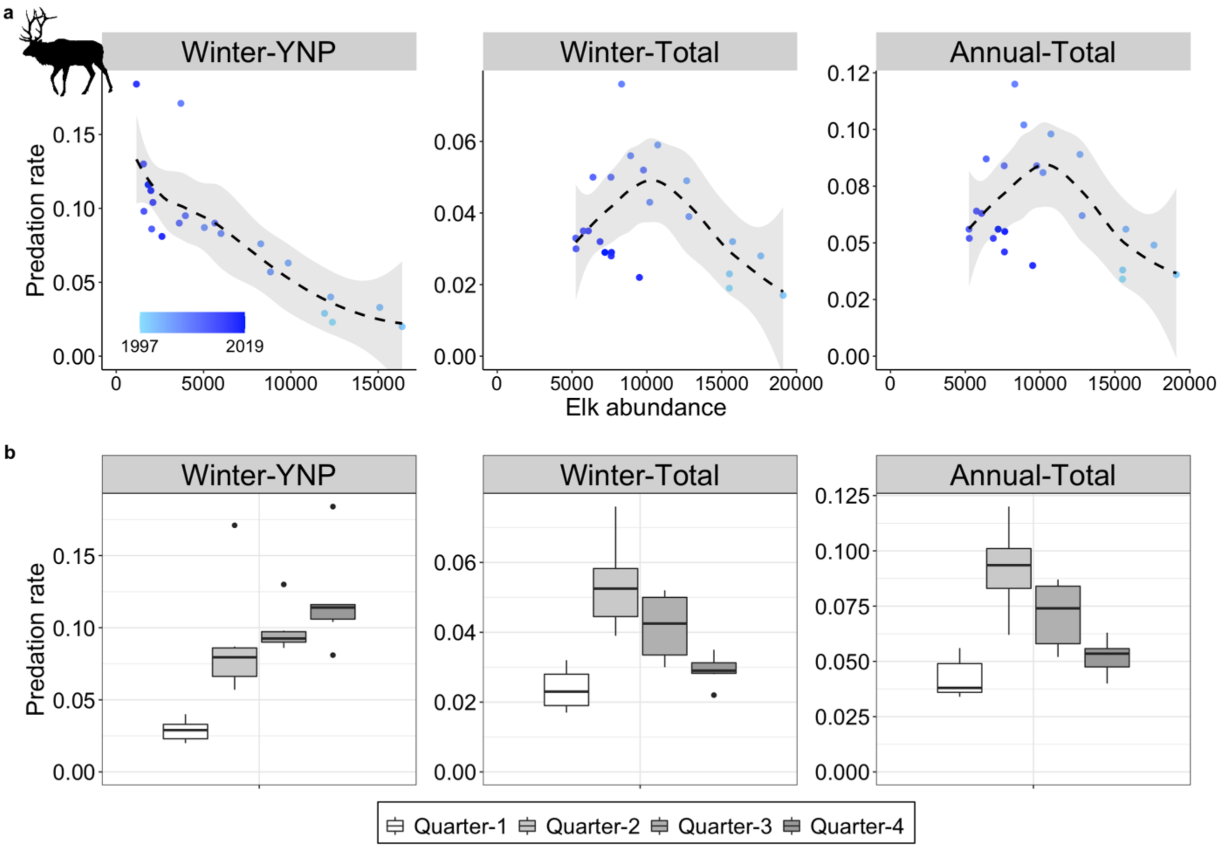

**Figure 4-36. Wolf predation rate for resident Northern YNP wolves across (a) elk abundance and (b) quarters, 1997–2019.** Panel (a) displays changes in resident Northern YNP wolf predation rate for: *i*) 'Winter – YNP': during winter against abundance estimates for elk wintering within YNP (solid line in Fig. 4-3a), *ii*) 'Winter – Total': during winter against abundance estimates for the total northern Yellowstone elk population (dashed line in Fig. 4-3a), and *iii*) the same elk abundance as *ii*, but estimates of predation rate are for the entire year (i.e., not just winter). Lines in panel (a) display 'loess' fit. Panel (b) displays box plots for predation rate across the four quarters (Fig. 4-3b), with facets having the same meaning as in panel (a).

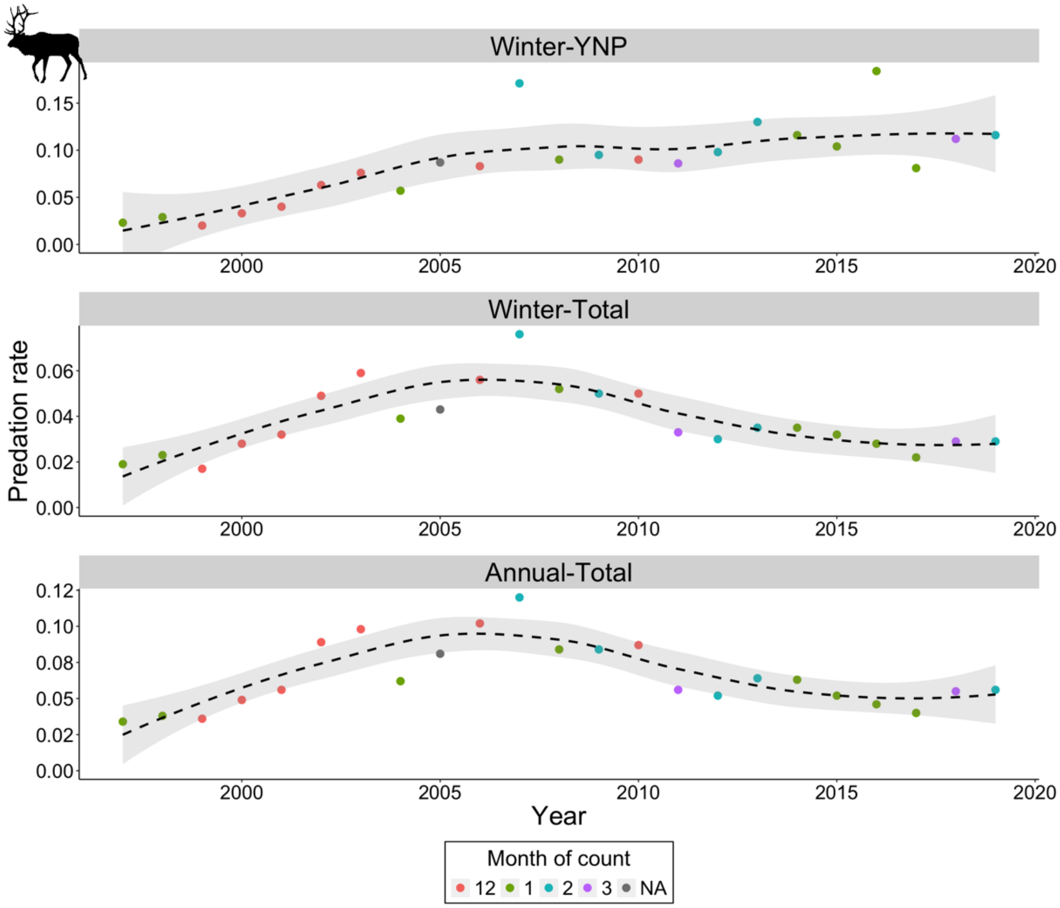

**Figure 4-37. Wolf predation rate for resident Northern YNP wolves through time.** Each panel displays estimates of predation rate, with the meaning of panels the same as in Fig. 4-36, for each year. Year was defined to begin on Nov. 1. The color of each point displays the month of the aerial survey for elk, although estimates for elk abundance were then sightability adjusted (Tallian et al. 2017b). Lines display 'loess' fit to highlight longitudinal trends.

# Chapter 5: Scavenging reshapes large mammal predator-prey dynamics: an example from a wolf-elk-bison system[4]

## INTRODUCTION

Dynamical mathematical models that link predator and prey populations provide a mechanistic framework to disentangle the driving forces behind predator-prey population dynamics (Rosenzweig and MacArthur 1963, Turchin 2013). Populations of predators and prey are linked in dynamical models through the functional response(s) that describes how frequently prey are removed by predators as prey abundance changes (Solomon 1949, Holling 1959, Messier 1994), and then in turn how predators turn this food into their own population growth (i.e., via the predator numerical response). The nature of how predators remove prey and convert them into their numerical response determines predictions for the abundance of each species and key properties of predator-prey dynamics. Dynamical models can help reveal population dynamics, and properties of the system such as stability within the regions where predation is a regulating force reducing prey populations to a lower density equilibria (Rosenzweig and MacArthur 1963, Sinclair 1989, Messier 1995).

Stability for predator and prey populations at lower density equilibria can result from several factors, often due to mechanisms affecting the predator functional response. Spatial refugia (Sih 1987), predator diet choice (Fryxell and Lundberg 1994), prey switching (Murdoch and Oaten 1975), and environmental stochasticity (Clark et al. 2021) all provide mechanisms that can promote stable dynamics under certain conditions. In another example, increasing social complexity from a system with no grouping, to grouping in only prey, and then finally grouping

---

[4] Authorship is tentatively proposed as Metz, M., T.J. Clark, A.D. Luis, D.R MacNulty, D.R. Stahler, C. Geremia, D.W. Smith, & M. Hebblewhite and is generally prepared for submission to Proceedings of the National Academy of Sciences.

in also predators revealed that each increase in social complexity damped the functional response, thus stabilizing lion (*Panthera leo*)-wildebeest (*Connochaetes taurinus*) dynamics (Fryxell et al. 2007). Historically, the field of predator-prey modeling often focused on single predator-single prey models, exploring the impact of these mechanisms on stability and population dynamics.

Ecologists are increasingly recognizing the importance of including multiple prey and/or predators in dynamical predator-prey models, however, because most predators in nature exist in complex ecological communities (Montgomery et al. 2019), and this complexity can result in different properties in predator-prey dynamics. For example, more vulnerable prey species can be reduced, even to extinction, through apparent competition (Sinclair et al. 1998). Here, sharing a common predator results in (often disproportionately) negative effects on prey populations, thus altering predator-prey dynamics (Holt 1977, Serrouya et al. 2015, Holt and Bonsall 2017). But other types of competition can potentially lead to higher equilibrial densities of primary prey, as scavenging on predator kills by competitor predators can increase both stability and prey abundance (Focardi et al. 2017; *cf*. Mellard et al. 2021). Scavenging by predators on resource subsidies may also affect predation dynamics in ways that increase equilibrial prey abundance. For example, songbird nest survival was negatively affected by predators in rural landscapes, but predation did not influence survival in more urban areas where anthropogenic food subsidies were prominent in predator diet (Rodewald et al. 2011). Resource subsidies, *per* se, are not limited, however, to the most anthropogenically-modified landscapes, and may also affect more 'pristine' ecosystems.

Many ecosystems are influenced by scavenging on carrion subsidies that can promote increased stability (Wilson and Wolkovich 2011). Species that also often kill their prey, including apex predators from both marine and terrestrial ecosystems (Kruuk 1972, DeVault et al. 2003, Pereira et al. 2014, Moleón et al. 2015, Hammerschlag et al. 2016), are among the many species that use carrion subsidies. For example, tiger shark (*Galeocerdo cuvier*) scavenging on green turtles (*Chelonia mydas*) has been suggested as a significant part of their food acquisition over the nearly 6-month turtle nesting season (Hammerschlag et al. 2016). In terrestrial systems, data suggest that large prey are difficult to kill (Scheel 1993, MacNulty et al. 2007, Owen-Smith and Mills 2008, Tallian et al. 2017) and therefore the largest prey rarely die through predation (e.g., Sinclair et al. 2003). Instead, mortality for such large prey can often be dominated by starvation-related deaths, and these individuals may often be scavenged by large carnivores after dying (Pereira et al. 2014, see also Moleón et al. 2015). The facultative use of carrion subsidies by widespread, generalist predators may therefore be an important force affecting predator numerical and functional responses and, thus, predator-prey dynamics (Rose and Polis 1998, Moleón et al. 2014). The consequences of this behavior to predator-prey dynamics, however, are poorly understood for many ecosystems (Moleón et al. 2014). The increased trophic linkages should theoretically promote stability as predators expand their niche breadth through additional food web links (Wilson and Wolkovich 2011). Yet, the requisite data make such evaluations of stability, and to general changes to predator and prey abundance, rare.

The well-studied wolf (*Canis lupus*)-prey system of northern Yellowstone National Park (hereafter, 'Northern YNP') provides a compelling empirical and theoretical opportunity to evaluate the consequences of scavenging to predator-prey dynamics (Fig. 5-1). For twenty-plus years, wolves have strongly selected elk (*Cervus canadensis*) as their primary prey through their direct killing, even increasingly so as elk abundance has declined (Metz et al. 2020). Despite the potential for prey switching by wolves as their primary prey abundance has declined, prey switching to bison (*Bison bison*) in northern Yellowstone has not been observed (Tallian et al. 2017). The lack of prey switching is the result of bison being more dangerous than elk (Garrott et al. 2007, Tallian et al. 2017), and leads to an expectation of lower equilibrium abundances for elk than if prey switching had occurred (Messier 1995, Sinclair and Pech 1996, Garrott et al. 2007). However, the use of bison by wolves, primarily through facultative scavenging, has steadily increased in Northern YNP (Tallian et al. 2017, Metz et al. 2020). The consequences of feeding dynamics that include facultative scavenging are poorly understood, both in our study system and, more broadly, across the many ecosystems that contain large, dangerous prey (Ripple et al. 2015).

We leveraged data from the Northern YNP wolf-elk-bison system to both conceptualize how kill and scavenging rates varied over prey species abundance and to parameterize elements of a series of dynamical predator-prey models (e.g., Rosenzweig and MacArthur 1963, Fryxell et al. 2007, Focardi et al. 2017, Serrouya et al. 2020). We then used these dynamical models to evaluate whether and how scavenging a large, infrequently killed prey species can affect stability and equilibrial properties of the population dynamics of wolves and their primary prey. We hypothesized that scavenging would affect stability properties and equilibrial primary prey (e.g., elk) abundance, with its relative influence dependent on its prominence in predator diet. To test this hypothesis, we developed a series of dynamical models where we increased the complexity of the ecological system. We first developed a single predator (wolf)-single prey (elk) model, then added a secondary prey (bison) that was only killed, and then finally also added scavenging on this secondary prey (bison). We predicted long-term population abundances in each of these models where we varied parameters that influenced the functional response, for both killing and scavenging on prey. We then assessed *i)* the relative abundance of each species, primarily focused on the predator (wolf) and primary prey (elk) and *ii*) characteristics related to the stability of these populations. Drawing from recent syntheses (Wilson and Wolkovich 2011) and recent modeling in similar food webs (Focardi et al. 2017), we hypothesized that predator-prey models including scavenging would be more likely to promote stable dynamics at abundances that were greater than scenarios devoid of scavenging.

## METHODS

We first used estimates for kill rate, scavenging rate, elk abundance, and bison abundance from Northern YNP to estimate single predator-single prey functional response models (Chapter 4) prior to developing our dynamical predator-prey models. Here, we were simply interested in identifying the general shape of key functional responses across relevant prey abundances to guide how we developed the structure of our dynamical models. For simplicity, we did not identify, nor include in our dynamical models (see *Dynamical model(s) structure* below), a functional response for wolf scavenging on elk because wolves mostly killed elk (see Fig. 5-1). We were specifically interested in testing the influence of predator scavenging on large, infrequently killed prey on predator-prey dynamics. Accordingly, we used per-capita annual kill rates on elk and bison and scavenging rates on bison that were estimated through a mark-recapture framework (Chapter 4). These annual rates were based on daily rates estimated at the population-level (*sensu* Jost et al. 2005) and across the winter for wolf packs that lived in Northern YNP (Chapter 4; see also Table S5-A.1). We used sightability-corrected estimates for northern Yellowstone elk abundance within YNP (Tallian et al. 2017), and numbers for northern YNP bison abundance that were obtained during late summer counts (White et al. 2015). To this rate and abundance data, we fit a series of single predator-single prey Hollings disc equations using the R package `minpack.lm` (Elzhov et al. 2016). The resultant estimates for the functional response suggested that Type II functional response models for wolf-killed elk, wolf-killed bison, and wolf-scavenged bison would be appropriate for the range of prey species abundances that we developed our dynamical models over (Fig. 5-2; Fig. S5-A.1; Table S5-A.1).

### Dynamical model(s) structure

Next, we used Type II functional responses that affected prey and predator abundance, formulated through the multispecies disc equation (Charnov 1976, Fryxell and Lundberg 1994), to develop a series of three discrete-time predator-prey models, thereby allowing us to isolate the effect of scavenging on wolf-elk-bison dynamics. Discrete-time models were appropriate because they matched the timing of reproduction of this predator and these prey species. We specifically created three models of the ecological system where: 1a) wolves only killed elk (i.e., single predator-single prey), 1b) wolves killed elk and bison, and 2) wolves killed elk and bison and scavenged bison as,

1) Predation only models:
    a. Wolf-elk

$$E_{t+1} = E_t + r_E E_t \left(1 - \frac{E_t}{K_E}\right) - W_t \left(\frac{\alpha_E E_t}{1 + \alpha_E h_E E_t}\right) \tag{1}$$

$$W_{t+1} = W_t \left(\frac{b\alpha_E E_t}{1 + \alpha_E h_E E_t} - dW_t\right) \tag{2}$$

where $E$ represented elk abundance, $K_E$ represented nutritional carrying capacity for elk, $\alpha_E$ represented the attack rate (or searching efficiency; Arditi and Ginzburg 2012) on elk, $h_E$ represented the handling time on wolf-killed elk, $W$ represented wolf abundance, $b$

represented the conversion efficiency with which wolves turned prey into their own reproduction, and *d* represented a wolf death rate that was density-dependent (Serrouya et al. 2020), consistent with previous studies that identified wolf numerical responses as being characterized as Type II (Messier 1994, Hebblewhite 2013). Note that the $\alpha$ parameter in the functional response (here and in the following models) is determined by the product of four parameters that describe the spatial overlap between predators and prey, predator travel distance, the effective search distance of the predator, and predator encounter success (see equation in Table 5-1 and *Parameter estimates* below; Serrouya et al. 2020).

b. Wolf-elk-bison

$$E_{t+1} = E_t + r_E E_t\left(1 - \frac{E_t}{K_E}\right) - W_t\left(\frac{\alpha_E E_t}{1 + \alpha_E h_E E_t + \alpha_B h_B s B_t}\right) \tag{3}$$

$$B_{t+1} = B_t + r_B B_t\left(1 - \frac{B_t}{M_B}\right) - W_t\left(\frac{\alpha_B B_t}{1 + \alpha_B h_B s B_t + \alpha_E h_E E_t}\right) \tag{4}$$

$$W_{t+1} = W_t\left(\frac{b(\alpha_E E_t + \alpha_B s B_t)}{1 + \alpha_E h_E E_t + \alpha_B h_B s B_t} - dW_t\right) \tag{5}$$

where the new parameters of *B* represented bison abundance, $M_B$ represented the management capacity for bison, and *s* represented the size conversion for bison (see Table 5-1 and *Parameter estimates* below). The remaining new parameters ($B$, $r_B$, $\alpha_B$, $h_B$) had the same meaning, but now for bison.

2) Predation and scavenging model:

a. Wolf-elk-bison-scavenging

$$E_{t+1} = E_t + r_E E_t\left(1 - \frac{E_t}{K_E}\right) - W_t\left(\frac{\alpha_E E_t}{1 + \alpha_E h_E E_t + \alpha_B h_B s B_t + \alpha_{B^*} h_B s B_t}\right) \tag{6}$$

$$B_{t+1} = B_t + r_B B_t\left(1 - \frac{B_t}{M_B}\right) - W_t\left(\frac{\alpha_B B_t}{1 + \alpha_B h_B s B_t + \alpha_E h_E E_t + \alpha_{B^*} h_B s B_t}\right) \tag{7}$$

$$W_{t+1} = W_t\left(\frac{b(\alpha_E E_t + \alpha_B s B_t + \alpha_{B^*} s B_t)}{1 + \alpha_E h_E E_t + \alpha_B h_B s B_t + \alpha_{B^*} h_B s B_t} - dW_t\right) \tag{8}$$

where the new parameter of $\alpha_{B*}$ represented the search efficiency (or attack rate) by wolves on scavenged bison.

**Parameter estimates**

We generally parameterized our three models (i.e., Models 1a, 1b, 2a above) using data we collected from Northern YNP (e.g., Appendix S5-A) or previous studies (Table 5-1). Prey models were characterized by maximum prey growth rates ($r_i$) of 0.28 for elk (Eberhardt et al. 1996) and 0.27 for bison (Gates and Larter 1990). The elk population in each model was affected by wolf predation and density-dependent population growth rate. We used a carrying capacity ($K_E$) of 16,000 for elk, assuming a carrying capacity that was 5,000 less than a previous estimate of 21,000 for the entire Northern Range (i.e., also including area outside of YNP; Coughenour and Singer 1996). We modeled the bison population for the two models including bison with density-dependent growth rate where maximum abundance was influenced by wildlife management policy (Plumb et al. 2009, White et al. 2015), as opposed to nutritional carrying capacity. We used 4,000 bison to represent the management capacity ($M_B$) for the Northern Range (White et al. 2015).

We ensured our functional response estimates provided reasonable approximation(s) of the rate that wolves may have killed or scavenged prey (Fig. 5-2), yet note that our parameter-derived estimates generally had slightly higher asymptotes because we expected summer kill rates to increase the overall asymptote (Chapter 4; Metz et al. 2012). We leveraged empirical data from YNP (Appendix S5-A) on functional response mechanisms to parameterize the Hollings disc equations in our dynamical models. Functional responses were affected by the $\alpha$ and $h$ parameters, which each differed across species and/or acquisition type (i.e., kill or scavenged), and then also the $s$ parameter that adjusted the average size of bison to be 2.12 times that of elk (e.g., Garrott et al. 2007; but specific number derived from data in Chapter 4). We defined handling time as the proportion of a year that a wolf maximally spent handling a particular type of prey item, which is typically estimated as the inverse of the functional response asymptote (Arditi and Ginzburg 2012, Serrouya et al. 2020). However, we made two modifications. First, we specified $h_E$ as the inverse of the number of elk killed (maxKR) at $K_E$ multiplied by 0.7 [$h_E$ = (1 / maxKR)*0.7] to account for higher wolf kill rates during summer (Metz et al. 2012, Chapter 4). This also ensured wolf predation was strong enough to affect elk abundance in at least some of our modeling scenarios. Second, we divided $h_E$ by 2.12 (i.e., the body size conversion of bison) to represent maximum handling time on wolf-acquired bison. We made this second assumption because our empirical functional response models for wolf-acquired bison did not reach an asymptote.

The $\alpha_i$ parameter was determined from empirical data as the product of spatial overlap ($o_i$), travel distance ($t$), effective search distance ($l_i$), and encounter success ($c_i$) (Table 5-1; Serrouya et al. 2020). Based on the YNP system, we used a spatial overlap for wolves and both ungulate populations as 1, thereby using the same formulation as Fryxell et al. (2007). We used data from GPS-collared wolves to estimate the daily travel distance as 12.6 km (Fig. S5-A.2). We used 0.25 km, 0.50 km, and 0.75 km for effective search distance ($l$) for wolf-killed elk, varying this parameter to test how predator-prey dynamics differed when we varied how efficiently wolves located their primary prey (see *Data analysis* below). Each of these values was below a threshold search distance of 1 km that previous work suggests (Middleton et al. 2013). However, Middleton et al. (2013) excluded adult-males that are less likely to be encountered (as defined by MacNulty et al. 2007) by wolves (Winnie and Creel 2007), undoubtedly reducing this encounter distance threshold for a population of elk. We used a value of 0.025 km for effective search distance for wolf-killed bison, as wolves frequently traveled in the immediate vicinity of bison that did not represent an encounter per our definition (MacNulty et al. 2007). This reasoning was less meaningful for wolf-scavenged bison where we used a similar value of 0.03 km. Regardless, our primary interest for the scavenging functional response was simply to create a general shape that resembled the observed empirical relationship (Fig. 5-2).

The final step in determining the shape of the functional response was how we defined encounter success (*c*). We varied this parameter when it represented the 'scavenging encounter success' on bison to ultimately represent scavenging levels that were low ($c = 0.001$), medium ($c = 0.002$), and high ($c = \sim 0.003$; see *Data Analysis* below). Here, the medium value for *c* led to a reasonable approximation of the observed functional response for wolf-scavenged bison (i.e., compare Figs. 5-2 and 5-3). Finally, we used estimates for the proportion of encounters that an individual elk or bison died during a wolf-prey encounter to estimate *c* as 0.00525 for elk and 0.00129 for bison for the functional responses describing the rates of wolf-killed prey (Fig. S5-A.3). Thus, we had three estimates of the functional response for wolf-killed elk and wolf-scavenged bison, and one for wolf-killed bison, that we combined in various ways to test how wolf-prey dynamics were predicted to differ (see *Data analysis* below).

The final parameters for Eqns. 1– 8 were those related to wolf births and deaths, i.e., the numerical response. We estimated $b$, which represented the efficiency with which wolves turned prey into their own reproduction as 0.052. We specifically estimated this value as:

$$b = \frac{pups_{wolf} \times 1.2}{prey\ acquired} \tag{9}$$

where $pups_{wolf}$ represented an estimate for the number of pups born per individual wolf (calculated from observations of the number of pups born and end-of-biological-year counts of the Northern YNP wolf population), 1.2 was a correction factor that acknowledged that not all pups that were born were observed, and *prey acquired* equaled 18.5, which was the maximum number of elk killed by wolves in a year from our observed functional response models (Fig. 5-2). We used this value for *prey acquired* instead of the one that we further modified when calculating $h_E$ because the value produced by Eqn. 9 (0.052) produced reasonable dynamics when also combined with our estimate for *d*. We estimated this last parameter (*d*) through first estimating an annual proportional decline in the wolf population (0.41 [including the loss of all newborn pups]; Fig. S5-A.4), and then dividing by 80 (a representation for a maximum wolf population) to scale this number to a per-capita risk of dying. Perhaps most importantly, the resultant value of 0.005 similarly contributed to reasonable predictions for wolf abundance.

## Model analysis

We used our equations (i.e., Eqns. 1–8) describing the three different models to predict wolf and ungulate abundance for 500 years, using starting values of 60 wolves, 10,000 elk, and 300 bison. Importantly, estimates for key parameters (e.g., stability, mean abundance after reaching stability) were insensitive to starting values (M. Metz, *unpubl. data*). We predicted these populations for our three defined models – wolf-elk, wolf-elk-bison, and wolf-elk-bison-scavenging. For all three models, we varied the efficiency with which wolves located elk by varying search efficiency (*l*) to equal 0.25 km (hereafter, low-efficiency), 0.5 km (medium-efficiency), and 0.75 km (high-efficiency), thereby changing the shape of the functional response for wolf-killed elk (Fig. 5-3a). For the model that included scavenging on bison, we similarly used three values for the encounter success parameter (*c*) for wolf-scavenged bison to also change this functional response (Fig. 5-3b). This allowed us to test our primary hypothesis with three levels of scavenging (low-scavenge, medium-scavenge, high-scavenge) in addition to the models devoid of scavenging. In total, we tracked fifteen sets of dynamics (hereafter, 'scenarios'), three wolf-elk, three wolf-elk-bison, and nine wolf-elk-bison-scavenging scenarios.

For each scenario, we first tracked the annual abundance and growth rate of each population. We recorded, if applicable, the duration until when a population reached a stable equilibrium, defining the stable equilibrium point as the time when the population no longer subsequently grew at a rate that exceeded $r = 0.001$. If a population did not reach a stable equilibrium, we identified whether a population displayed other characteristics of stability (e.g., stable limit cycles) or displayed chaotic dynamics that were unstable. We summarized characteristics of population abundance (e.g., mean, coefficient of variation [CV], range, limit cycle length) for the final 300 years, after any population that reached a stable equilibrium did so (see *Results*). We compared predator and prey population dynamics across these fifteen theoretical scenarios.

## RESULTS AND DISCUSSION

The dynamics of elk and wolf abundance varied across modeled scenarios, but bison abundance always quickly grew to $M_B$ (Fig. 5-4), which was expected given our specification of $M_B$ and the functional response for wolf-killed bison (Fig. 5-3b). Elk were regulated by wolves below $K_E$ in all scenarios, with elk abundance generally higher when *i*) wolves were less efficient predators (i.e., effective search distance [$l_i$] was lower) and *ii*) models included scavenging (Fig. 5-5). The precise conclusions, however, depended on the model type (e.g., wolf-elk), wolf efficiency (e.g., low [$l$ = 0.25 km]), and, to a lesser extent, scavenging level (e.g., low). A general conclusion, however, was that higher wolf efficiency led to lower and, ultimately, less stable primary prey abundance. This latter result is predicted by theory (Rip and McCann 2011), and mirrors results from previous wolf-prey modeling exercises showing increased predatory efficiency can destabilize predator-prey dynamics (Serrouya et al. 2015, Focardi et al. 2017, Clark 2021).

First considering a model with only wolves and elk, the low search-efficiency scenario resulted in predictions for an elk population that quickly reached a stable equilibrium after 23 years at 11,283 individuals, as indicated by the mean population over the final 300 years (Figs. 5-5a, 5-6, S5-A.5). This abundance represented the highest stable equilibrium abundance for elk across all fifteen scenarios. Conversely, elk abundance was predicted to display stable limit cycles (length = 50 years) and average 3,778 individuals (46.1% [CV]; range: 1,366 – 6,329) in the high-efficiency scenario for the wolf-elk model. Wolf abundance was predicted to be greatest during the medium-efficiency scenario, where the average stable equilibrium population of 46.7 wolves regulated elk abundance at 7,160 individuals. Wolf abundance was lowest ($\bar{x}$ = 32.8; 42.0%[CV]; range: 12.4 – 50.6; Figs. 5-5c, 5-6, S5-A.5), and again displayed stable limit cycles of 50 years, during the high-efficiency scenario. The wolf-elk only model structure is reflective of how many systems have been treated in the literature, as single predator-single prey. Our results across the three scenarios in a wolf-elk model were generally as expected based on previous wolf-prey dynamical models (e.g., Serrouya et al. 2015, Clark et al. 2021). For example, it was unsurprising that the medium and high-efficiency scenarios with functional responses that reached their asymptote quicker led to lower, and less stable in the high-efficiency scenario, elk abundance. Based on the correspondence between the medium-predation efficiency scenario and empirical data from our system (e.g., see Chapter 4), we believe this middle scenario reflects YNP dynamics the most closely.

Adding a second prey (bison) led to decreases in stable equilibrium abundance of primary prey to 10,998 (-2.5% change) and 6,449 (-9.9% change) for the low- and medium-efficiency scenarios (Fig. 5-5). Wolf populations stabilized at 42 (+4.5% change) and 46 (-1.1% change). Both populations reached their stable equilibria about two decades later for the medium-efficiency scenario, in comparison to the single predator-prey wolf-elk model. Population cycles for elk were similar (i.e., cycle length for elk, and wolves, increased from 50 to 54 years) and had slightly higher amplitudes for the high-efficiency scenario in the two-prey model, but this was accompanied by a higher mean abundance (4,523; 56.8%[CV]; range: 855 – 8,291; Fig. 5-5c) than in the wolf-elk, high-efficiency scenario (recall a mean of 3,778). The resultant minimum predicted population of 855 elk in the high-efficiency wolf-elk-bison model was the lowest of any observed prediction for elk. The wolf population in this high-efficiency scenario responded with abundances and growth rates that also ranged widely ($\bar{x}$ = 33.8; 54.7% [CV]; range: 6.7 – 56.3; Figs. 5-5c, 5-6, S5-A.5). Overall, adding difficult to kill bison decreased elk (and wolf) abundance when dynamics reached a stable equilibrium, and decreased properties of stability when they did not reach a stable equilibria.

Adding scavenging fundamentally changed patterns of species abundance among scenarios of the same wolf efficiency. The least affected by adding scavenging were the low-efficiency scenarios where stable equilibrium elk abundance for all three scavenging scenarios was in between the predicted stable equilibrium abundances for the wolf-elk and wolf-elk-bison models (Fig. 5-5a). Moreover, the time to the stable equilibria was also similar (Figs. 5-4a, 5-5a, S5-A.5a). Wolf abundance was predicted to be higher, however, in all three scavenging scenarios for low-efficiency, with the most wolves predicted for high-scavenging levels ($\bar{x}$ = 49.1; Figs. 5-5a, 5-6). This prediction for higher wolf abundance in models including scavenging was also true across models of medium- and high-efficiency. However, the medium- and high-efficiency scenarios differed from the low-efficiency scenario in that the elk population was also predicted to be the higher than wolf-elk or wolf-elk-bison systems for the medium- and high-efficiency scenarios.

The model with scavenging for medium-efficiency wolves was predicted to reach a stable equilibrium, with that stable equilibria arising more slowly than in medium-efficiency models devoid of scavenging. Elk abundance in these medium-efficiency scenarios was predicted to be 8,840 (low-scavenge), 8,959 (medium-scavenge), and 9,051 (high-scavenge), which represented percent increases of +23.5%, +25.1%, and +26.4% from the medium-efficiency, wolf-elk model (Fig. 5-5b). Again, these elk abundances were predicted to be higher while wolf populations were also predicted to be higher (Fig. 5-5b). For example, a stable equilibrium abundance of 57.6 wolves was predicted for the medium-efficiency, high-scavenge scenario. The influence of scavenging seemed to slow the time to reach a stable equilibrium, with the fastest time to a stable equilibrium point for a wolf or elk population being 80 years (high-scavenge; Figs. 5-5b, S5-A.5b).

Similar general increases in elk and wolf abundance for models including scavenging were observed for the high-efficiency scenarios, in comparison to the high-efficiency wolf-elk and wolf-elk-bison models without scavenging. The inclusion of scavenging did not cause wolf or elk populations to reach a stable equilibrium, however, for the high-efficiency scenario (Figs. 5-6, S5-A.5). In fact, elk populations had larger amplitude population cycles (but with the same cycle lengths), albeit at a higher abundance where the low-point was, at worst, near the high-point of other high-efficiency models (Fig. 5-5c). But interestingly, amplitude in wolf population cycles did decrease (Fig. 5-5c). For example, the difference between minimum and maximum wolf population equaled 6.4 for the high-efficiency, high-scavenge scenario, but the difference between min and max wolf abundance was 38.2 and 49.6 for the high-efficiency wolf-elk and wolf-elk-bison systems without scavenging, respectively (Fig. 5-5c). Thus, scavenging also tended to increase stability properties of wolf population abundance in our scenarios.

Our work here was motivated by the wolf-prey dynamics in the northern Yellowstone system, but we did not seek to predict the dynamics of these specific populations because we did not consider transient dynamics or include additional factors known to affect elk abundance, such as other predators (Barber-Meyer et al. 2008, Peterson et al. 2014, MacNulty et al. 2020) or human harvest (Vucetich et al. 2005, Wright et al. 2006, Peterson et al. 2014, MacNulty et al. 2020). Nonetheless, we adopted some properties of the northern Yellowstone system, such as wildlife management policy regulating bison, that structured parts of our results. As such, the scavenging subsidies received by our predator population were also regulated by the Interagency management goals for bison (Plumb et al. 2009). The degree to which this scavenging affects primary prey population dynamics is influenced by the overall nature of how the predator acquires its food, from predation to scavenging (see Fig. 1 in Wilson and Wolkovich 2011). In their review, Wilson and Wolkovich (2011) proposed that as a prey population moves from being regulated by top-down predation to bottom-up food regulation, the degree to which predation impacts prey shifts as more prey (e.g., in our multi-prey system, bison) enter the food web via scavenging. These results mirror Sinclair et al. (2003) that showed increased body size of ungulates in the Serengeti rendered their dynamics increasingly food regulated, with declining predation rates for increasing prey body size. Yet large prey would present a large source of scavenged biomass (e.g., Pereira et al. 2014). Similarly, our dynamical models suggest that systems with dangerous large prey will be driven by scavenging dynamics.

Overall, scavenging dramatically reshaped dynamics except in the low-efficiency scenarios, scenarios where prey abundance was always near its highest. We argue the low-efficiency scenarios are the least likely to reflect empirical dynamics of wolves, elk and bison well in YNP. For example, the search radius of the low-efficiency scenarios, 0.25 km for wolves and elk, seems unlikely to be the threshold for wolf-elk encounters based on empirical systems, and thus these dynamics seem the least plausible. Each of the other two efficiency scenarios (medium and high) combined with scavenging yielded increases in both the predator and prey populations, as well as generally more stable dynamics, in comparison to models without scavenging. The mere presence of scavenging, regardless of the level, reshaped these dynamics in ways predicted by theory. For example, these observations are well aligned with previous research that indicates that weak ecological links are important to consumer-resource dynamics in that they both promote greater abundances (Fig. 5-5b, 5-5c) and reduce oscillations (wolves in Fig. 5-5c; McCann et al. 1998). Recent syntheses suggest that the importance of scavenging may be underestimated by up to 16 times in food webs, and that up to 25% of terrestrial food-web links may be scavenging in terrestrial systems (Wilson and Wolkovich 2011). Our results also echo recent results of similar modeling on wolf-red deer-wild boar dynamics in Italy. Previous studies had revealed the surprising finding that omnivorous wild boar are both prey of wolves and kleptoparasites of wolf-killed prey such as red deer. Building a similar dynamical model as ours for this wolf-boar-deer system, Focardi et al. (2017) showed that increased scavenging tended to stabilize wolf and deer dynamics, and often lead to higher abundances as well. Thus, our results combined with previous theoretical models (McCann et al. 1998, Focardi et al. 2017) and empirical studies (Wilson and Wolkovich 2011) all emphasize the growing appreciation of the critical role scavenging can play in shaping the dynamics of predator-prey systems.

## LITERATURE CITED

Arditi, R., and L. R. Ginzburg. 2012. How species interact: altering the standard view on trophic ecology. Oxford University Press, New York, NY.

Barber-Meyer, S. M., L. D. Mech, and P. J. White. 2008. Elk calf survival and mortality following wolf restoration to Yellowstone National Park. Wildlife Monographs **169**:1-30.

Charnov, E. L. 1976. Optimal foraging: attack strategy of a mantid. The American Naturalist **110**:141-151.

Clark, T. J. 2021. Large carnivore recolonization reshapes population and community dynamics: implications for harvest management. University of Montana, Missoula, MT.

Clark, T. J., J. S. Horne, M. Hebblewhite, and A. D. Luis. 2021. Stochastic predation exposes prey to predator pits and local extinction. Oikos **130**:300-309.

Coughenour, M. B., and F. J. Singer. 1996. Elk population processes in Yellowstone National Park under the policy of natural regulation. Ecological Applications **6**:573-593.

DeVault, T. L., O. E. Rhodes Jr., and J. A. Shivik. 2003. Scavenging by vertebrates: behavioral, ecological, and evolutionary perspectives on an important energy transfer pathway in terrestrial ecosystems. Oikos **102**:225-234.

Eberhardt, L. E., L. L. Eberhardt, B. L. Tiller, and L. L. Cadwell. 1996. Growth of an isolated elk population. The Journal of Wildlife Management **60**:369-373.

Elzhov, T. V., K. M. Mullen, A.-N. Spiess, and B. Bolker. 2016. 'minpack. lm'. R package **1.2-1**.

Focardi, S., M. Materassi, G. Innocenti, and D. Berzi. 2017. Kleptoparasitism and scavenging can stabilize ecosystem dynamics. The American Naturalist **190**:398-409.

Fryxell, J. M., and P. Lundberg. 1994. Diet choice and predator—prey dynamics. Evolutionary Ecology **8**:407-421.

Fryxell, J. M., A. Mosser, A. R. E. Sinclair, and C. Packer. 2007. Group formation stabilizes predator–prey dynamics. Nature **449**:1041-1043.

Garrott, R. A., J. E. Bruggeman, M. S. Becker, S. T. Kalinowski, and P. J. White. 2007. Evaluating prey switching in wolf–ungulate systems. Ecological Applications **17**:1588-1597.

Gates, C. C., and N. C. Larter. 1990. Growth and dispersal of an erupting large herbivore population in northern Canada: the Mackenzie wood bison (*Bison bison athabascae*). Arctic **43**:231-238.

Hammerschlag, N., I. Bell, R. Fitzpatrick, A. J. Gallagher, L. A. Hawkes, M. G. Meekan, J. D. Stevens, M. Thums, M. J. Witt, and A. Barnett. 2016. Behavioral evidence suggests facultative scavenging by a marine apex predator during a food pulse. Behavioral Ecology and Sociobiology **70**:1777-1788.

Hebblewhite, M. 2013. Consequences of ratio-dependent predation by wolves for elk population dynamics. Population Ecology **55**:511-522.

Holling, C. S. 1959. The components of predation as revealed by a study of small-mammal predation of the European pine sawfly. The Canadian Entomologist **91**:293-320.

Holt, R. D. 1977. Predation, apparent competition, and the structure of prey communities. Theoretical Population Biology **12**:197-229.

Holt, R. D., and M. B. Bonsall. 2017. Apparent competition. Annual Review of Ecology, Evolution, and Systematics **48**:447-471.

Jost, C., G. Devulder, J. A. Vucetich, R. O. Peterson, and R. Arditi. 2005. The wolves of Isle Royale display scale-invariant satiation and ratio-dependent predation on moose. Journal of Animal Ecology **74**:809-816.

Kruuk, H. 1972. The spotted hyena: a study of predation and social behavior. University of Chicago Press, Chicago, IL.

MacNulty, D. R., L. D. Mech, and D. W. Smith. 2007. A proposed ethogram of large-carnivore predatory behavior, exemplified by the wolf. Journal of Mammalogy **88**:595-605.

MacNulty, D. R., D. R. Stahler, T. Wyman, J. Ruprecht, L. M. Smith, M. T. Kohl, and D. W. Smith. 2020. Population dynamics of northern Yellowstone elk after wolf reintroduction. Pages 184-199 *in* D. W. Smith, D. R. Stahler, and D. R. MacNulty, editors. Yellowstone wolves: Science and discovery in the world's first national park. University of Chicago Press, Chicago, IL.

McCann, K., A. Hastings, and G. R. Huxel. 1998. Weak trophic interactions and the balance of nature. Nature **395**:794-798.

Mellard, J. P., S. Hamel, J.-A. Henden, R. A. Ims, A. Stien, and N. Yoccoz. 2021. Effect of scavenging on predation in a food web. Ecology and Evolution **11**:6742-6765.

Messier, F. 1994. Ungulate population models with predation: a case study with the North American moose. Ecology **75**:478-488.

Messier, F. 1995. On the functional and numerical responses of wolves to changing prey density. Pages 187-198 *in* L. N. Carbyn, S. H. Fritts, and D. R. Seip, editors. Ecology and conservation of wolves in a changing world. Canadian Circumpolar Institute, Edmonton, Alberta.

Metz, M. C., M. Hebblewhite, D. W. Smith, D. R. Stahler, D. R. MacNulty, A. Tallian, and J. A. Vucetich. 2020. What wolves eat and why. Pages 157-168 *in* D. W. Smith, D. R. Stahler, and D. R. MacNulty, editors. Yellowstone wolves: Science and discovery in the world's first national park. University of Chicago Press, Chicago, IL.

Metz, M. C., D. W. Smith, J. A. Vucetich, D. R. Stahler, and R. O. Peterson. 2012. Seasonal patterns of predation for gray wolves in the multi-prey system of Yellowstone National Park. Journal of Animal Ecology **81**:553-563.

Middleton, A. D., M. J. Kauffman, D. E. McWhirter, M. D. Jimenez, R. C. Cook, J. G. Cook, S. E. Albeke, H. Sawyer, and P. J. White. 2013. Linking anti-predator behaviour to prey demography reveals limited risk effects of an actively hunting large carnivore. Ecology Letters **16**:1023-1030.

Moleón, M., J. A. Sánchez-Zapata, E. Sebastián-González, and N. Owen-Smith. 2015. Carcass size shapes the structure and functioning of an African scavenging assemblage. Oikos **124**:1391-1403.

Moleón, M., J. A. Sánchez-Zapata, N. Selva, J. A. Donázar, and N. Owen-Smith. 2014. Inter-specific interactions linking predation and scavenging in terrestrial vertebrate assemblages. Biological Reviews **89**:1042-1054.

Montgomery, R. A., R. J. Moll, E. Say-Sallaz, M. Valeix, and L. R. Prugh. 2019. A tendency to simplify complex systems. Biological Conservation **233**:1-11.

Murdoch, W. W., and A. Oaten. 1975. Predation and population stability. Advances in Ecological Research **9**:1-131.

Owen-Smith, N., and M. G. L. Mills. 2008. Predator–prey size relationships in an African large-mammal food web. Journal of Animal Ecology **77**:173-183.

Pereira, L. M., N. Owen-Smith, and M. Moleon. 2014. Facultative predation and scavenging by mammalian carnivores: seasonal, regional and intra-guild comparisons. Mammal Review **44**:44-55.

Peterson, R. O., J. A. Vucetich, J. M. Bump, and D. W. Smith. 2014. Trophic cascades in a multicausal world: Isle Royale and Yellowstone. Annual Review of Ecology, Evolution, and Systematics **45**:325-345.

Plumb, G. E., P. J. White, M. B. Coughenour, and R. L. Wallen. 2009. Carrying capacity, migration, and dispersal in Yellowstone bison. Biological Conservation **142**:2377-2387.

Rip, J., and K. McCann. 2011. Cross-ecosystem differences in stability and the principle of energy flux. Ecology Letters **14**:733-740.

Ripple, W. J., T. M. Newsome, C. Wolf, R. Dirzo, K. T. Everatt, M. Galetti, M. W. Hayward, G. I. Kerley, T. Levi, and P. A. Lindsey. 2015. Collapse of the world's largest herbivores. Science Advances **1**:e1400103.

Rodewald, A. D., L. J. Kearns, and D. P. Shustack. 2011. Anthropogenic resource subsidies decouple predator–prey relationships. Ecological Applications **21**:936-943.

Rose, M. D., and G. A. Polis. 1998. The distribution and abundance of coyotes: the effects of allochthonous food subsidies from the sea. Ecology **79**:998-1007.

Rosenzweig, M. L., and R. H. MacArthur. 1963. Graphical representation and stability conditions of predator-prey interactions. The American Naturalist **97**:209-223.

Scheel, D. 1993. Profitability, encounter rates, and prey choice of African lions. Behavioral Ecology **4**:90-97.

Serrouya, R., M. Dickie, C. DeMars, M. Wittmann, and S. Boutin. 2020. Predicting the effects of restoring linear features on woodland caribou populations. Ecological Modelling **416**:108891.

Serrouya, R., M. J. Wittmann, B. N. McLellan, H. U. Wittmer, and S. Boutin. 2015. Using predator-prey theory to predict outcomes of broadscale experiments to reduce apparent competition. The American Naturalist **185**:665-679.

Sih, A. 1987. Prey refuges and predator-prey stability. Theoretical Population Biology **31**:1-12.

Sinclair, A. R. E. 1989. Population regulation in animals. Pages 197–241 *in* J. Cherrett, editor. Ecological Concepts: The Contribution of Ecology to an Understanding of the Natural World. Blackwell, Melbourne.

Sinclair, A. R. E., S. Mduma, and J. S. Brashares. 2003. Patterns of predation in a diverse predator–prey system. Nature **425**:288-290.

Sinclair, A. R. E., and R. P. Pech. 1996. Density dependence, stochasticity, compensation and predator regulation. Oikos **75**:164-173.

Sinclair, A. R. E., R. P. Pech, C. R. Dickman, D. Hik, P. Mahon, and A. E. Newsome. 1998. Predicting effects of predation on conservation of endangered prey. Conservation Biology **12**:564-575.

Solomon, M. 1949. The natural control of animal populations. The Journal of Animal Ecology **18**:1-35.

Tallian, A., D. W. Smith, D. R. Stahler, M. C. Metz, R. L. Wallen, C. Geremia, J. Ruprecht, C. T. Wyman, and D. R. MacNulty. 2017. Predator foraging response to a resurgent dangerous prey. Functional Ecology **31**:1418-1429.

Turchin, P. 2013. Complex population dynamics. Princeton University Press, Princeton, NJ.

Vucetich, J. A., D. W. Smith, and D. R. Stahler. 2005. Influence of harvest, climate and wolf predation on Yellowstone elk, 1961-2004. Oikos **111**:259-270.

White, P. J., R. L. Wallen, and D. E. Hallac. 2015. Yellowstone Bison: Conserving an American Icon in Modern Society. The Yellowstone Association, Yellowstone National Park.

Wilson, E. E., and E. M. Wolkovich. 2011. Scavenging: how carnivores and carrion structure communities. Trends in Ecology & Evolution **26**:129-135.

Winnie, J., and S. Creel. 2007. Sex-specific behavioural responses of elk to spatial and temporal variation in the threat of wolf predation. Animal Behaviour **73**:215-225.

Wright, G. J., R. O. Peterson, D. W. Smith, and T. O. Lemke. 2006. Selection of northern Yellowstone elk by gray wolves and hunters. Journal of Wildlife Management **70**:1070-1078.

# TABLES.

**Table 5-1. Parameter meanings and values for dynamical predator-prey models in Northern Yellowstone National Park.** Source of values provided when applicable.

| Parameter | Meaning | Value(s) | Source |
|---|---|---|---|
| $E$ | Elk abundance | 10,000 (starting) | |
| $B$ | Bison abundance | 300 (starting) | |
| $W$ | Wolf abundance | 60 (starting) | |
| $r_{(i)}$ | Intrinsic growth rate | 0.28 (E); 0.27 (B) | Eberhardt et al. 1996; Gates and Larter 1990 |
| $K_E$ | Elk carrying capacity | 16,000 | Coughenour and Singer 1996 (modified) |
| $M_B$ | Bison management capacity | 4,000 | |
| $\alpha_i$ | Alpha parameter | $o_i$ x $t$ x $l_i$ x $c_i$ | |
| $o_i$ | Wolf-prey overlap | 1 | |
| $t$ | Travel (km) | 12.6 | Fig. S5-A.2 |
| $l_{(E)}$ | Effective search (killed elk) | 0.25, 0.5, 0.75 | |
| $l_{(B)}$ | Effective search (killed bison) | 0.025 | |
| $l_{(B^*)}$ | Effective search (scavenged bison) | 0.003 | |
| $c_E$ | Encounter success (killed elk) | 0.00053 | Fig. S5-A.3 |
| $c_B$ | Encounter success (killed bison) | 0.00129 | Fig. S5-A.3 |
| $c_{B^*}$ | Encounter success (scavenged bison) | 0.001, 0.002, 0.0029 | |
| $h_E$ | Handling time (elk) | 0.0379 | Fig. 5-2 (adapted) |
| $h_B$, $h_{B^*}$ | Handling time (bison) | 0.0179 | Fig. 5-2 (adapted) |
| $d$ | Death rate | 0.0051 | Fig. S5-A.4 |
| $s$ | Bison:elk (size ratio) | 2.13 | Chapter 4 |
| $b$ | Wolf conversion efficiency | 0.0522 | Yellowstone Wolf Project (*unpub.*); Fig. 5-2 |

**FIGURES.**

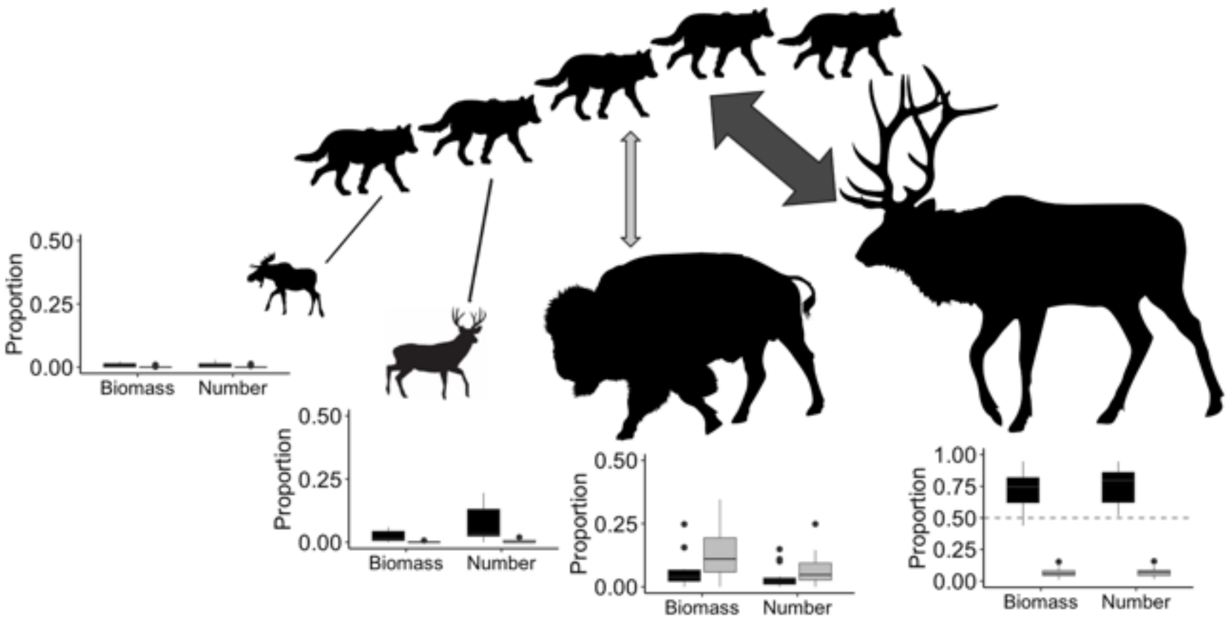

**Figure 5-1. Dynamics of the Northern Yellowstone National Park wolf-prey system.** The relative sizes of prey species are representative of their long-term relative abundances (deer represents mule deer [*Odocoileus hemionus*] and white-tailed deer [*O.virgianus*]; moose [*Alces alces*] represents all 'other' prey – i.e., moose, bighorn sheep [*Ovis canadensis*], pronghorn [*Antilocapra americana*]). The width of the prey-wolf links represents the proportional biomass acquired by wolves during winter from that species over the entire study, with the color indicating the proportion acquired through scavenging or predation (light to dark, respectively). The box plots display annual variation in the proportion of total prey acquired in terms of biomass or number of prey from wolf predation (black fill) or scavenging (gray fill). The y-axis for elk is the only that ranges from 0–1, with the dashed line at 0.5 indicating the maximum value for the y-axis for the other prey. Theoretical models censored contributions from species such as deer *spp*. and moose, as well as scavenging on elk.

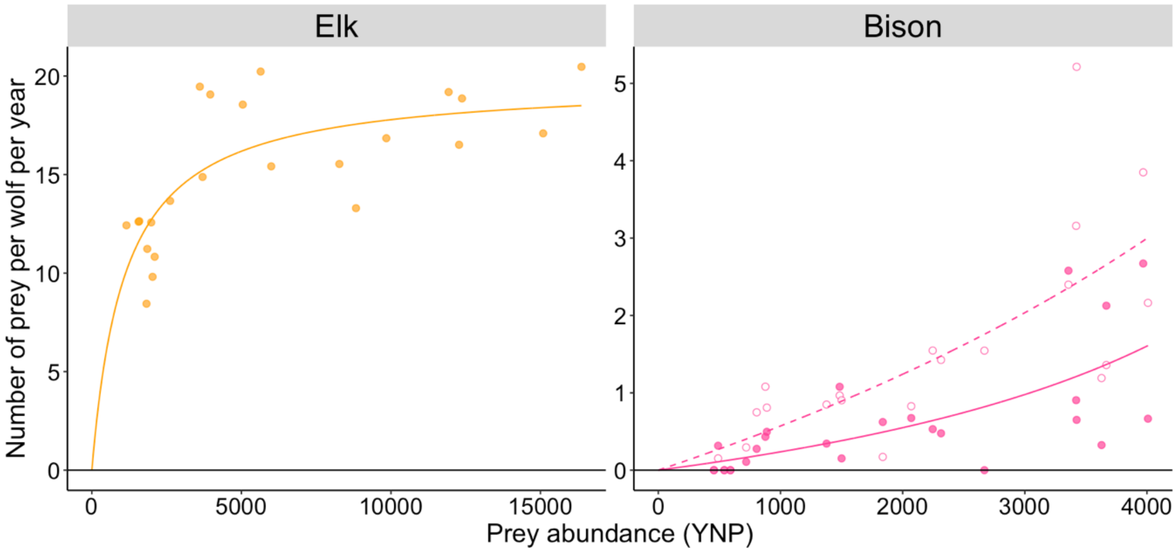

**Figure 5-2. Functional response estimates directly from winter estimates of wolf kill and scavenging rates on elk and bison in Northern YNP.** The estimates represent best-fitting approximations of the Type II Hollings disc equation. See Fig. S5-A.1 for estimates of Type I and Type III functional responses. Note that kill and scavenging rates for wolves on bison did not begin to reach an asymptote within the range of observed bison abundances.

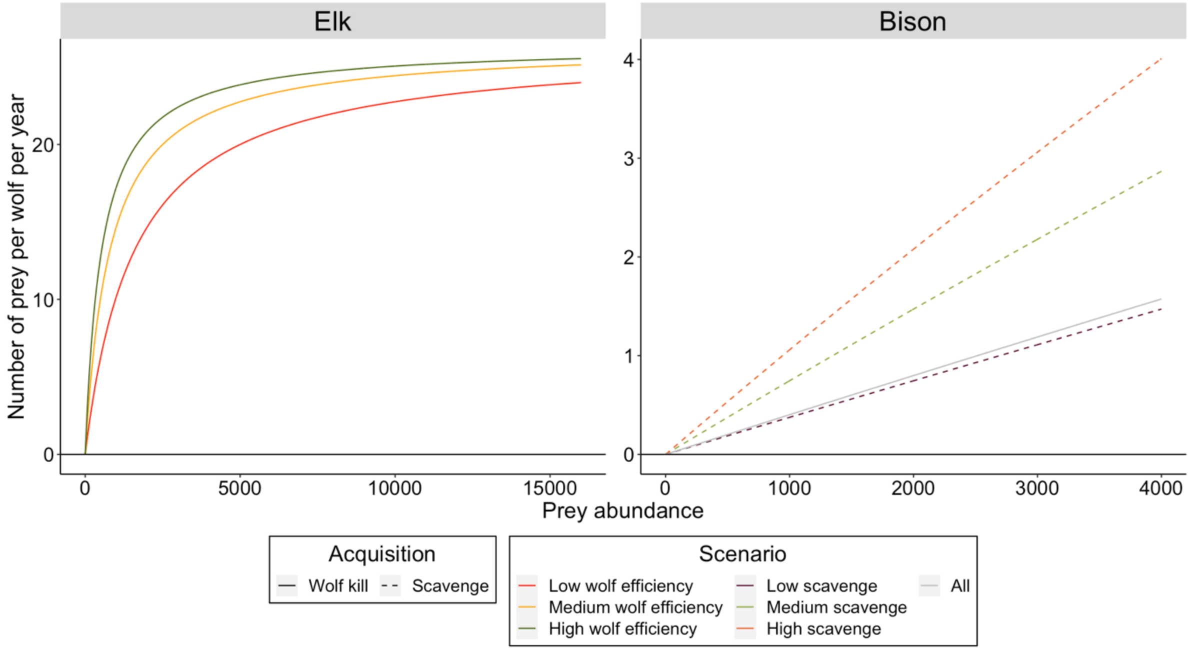

**Figure 5-3. Functional response estimates from parameter values.** Three lines are presented for wolf-killed elk and wolf-scavenged bison, representing the different scenarios that were modeled.

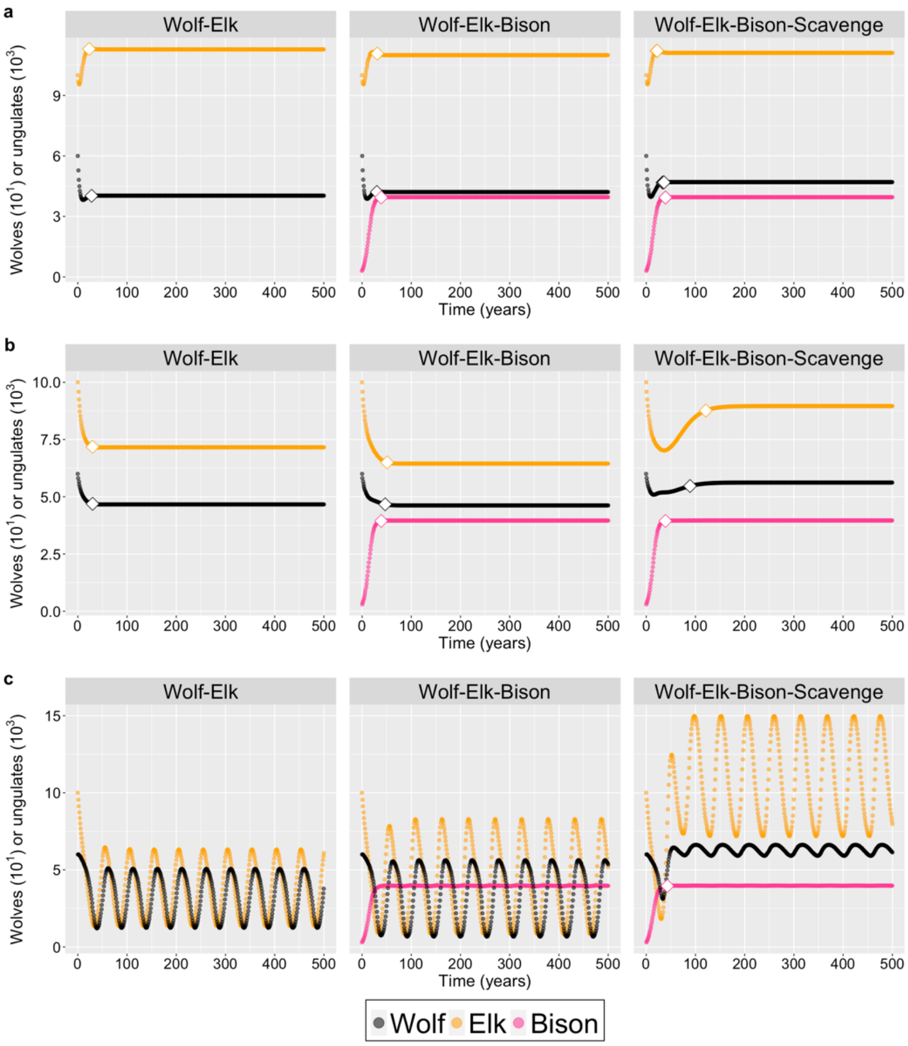

**Figure 5-4. Predicted population dynamics for wolf, elk, and bison populations where the search efficiency for wolves was (a) low (0.25 km), (b) medium (0.5 km), and (c) high (0.75 km).** In all scenarios for populations that included scavenging (right-most column), the dynamics are displayed for only the medium scavenging scenario. Diamonds display predicted stable equilibria where population growth rate (*r*) never again exceeded 0.001. Note the y-axis differs between panels a-c.

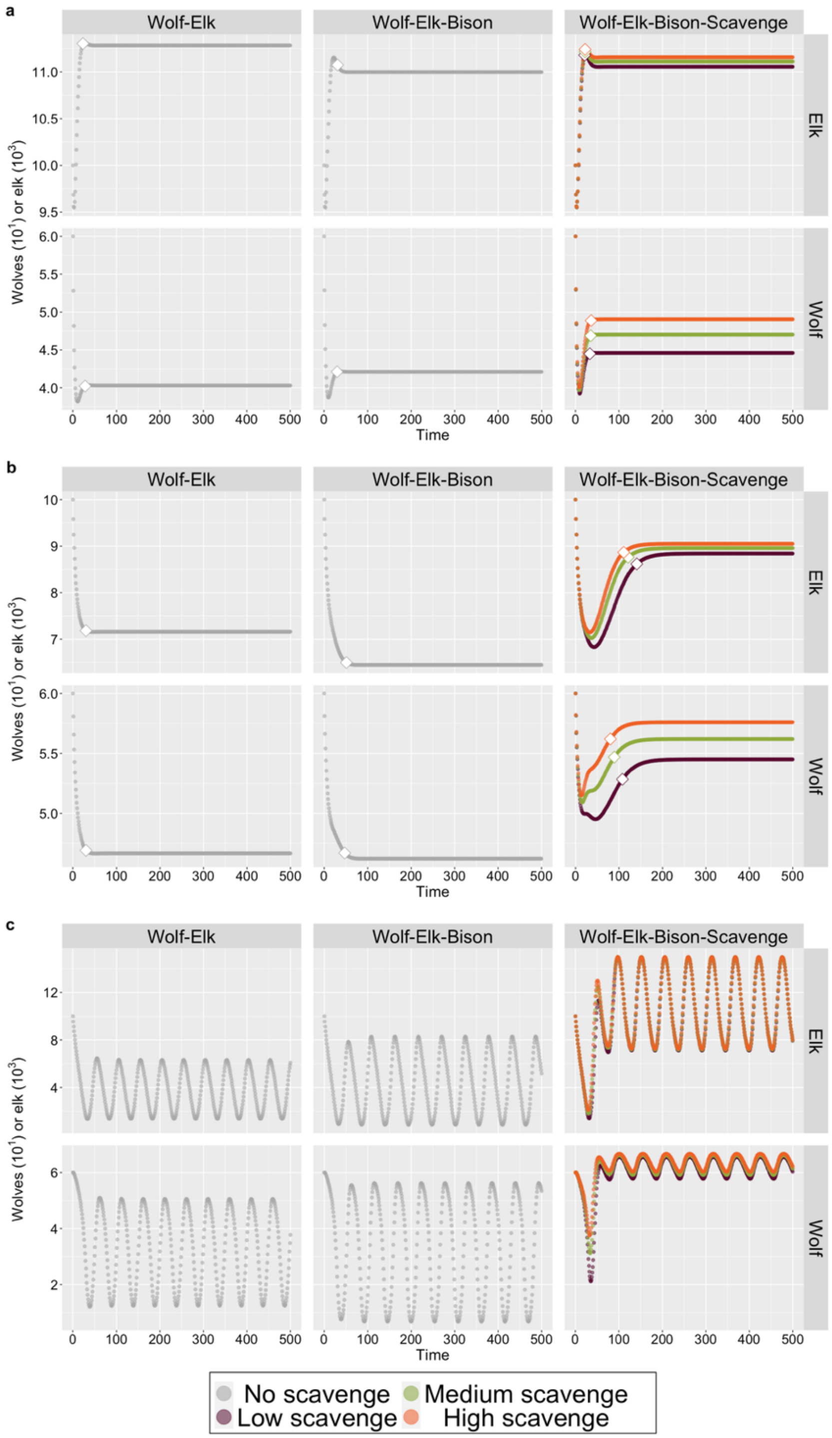

**Figure 5-5. Predicted population dynamics for elk and wolf populations where the search efficiency for wolves was (a) low (0.25 km), (b) medium (0.5 km), and (c) high (0.75 km).** In all scenarios that included scavenging (right-most column), the different colors display the associated dynamics. Diamonds display predicted stable equilibria where population growth rate (*r*) never again exceeded 0.001. Note the y-axis differs between panels a-c and that the left two columns and the green-filled circles in the right-most column are displayed in Fig. 5-4.

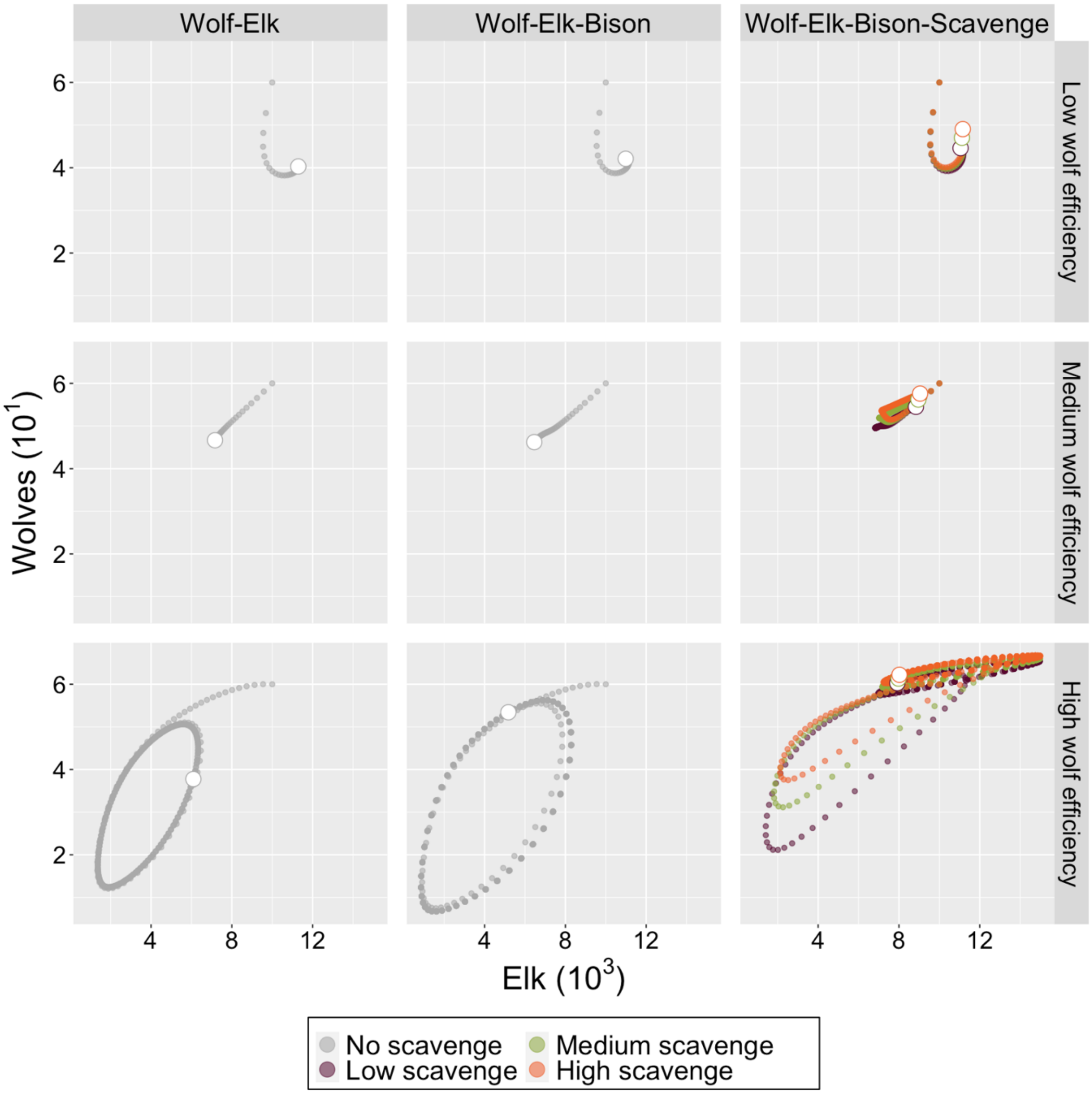

**Figure 5-6. Phase plane plots for predicted population dynamics for elk and wolf populations where the search efficiency for wolves was low (0.25 km), medium (0.5 km), and high (0.75 km).** The white-filled circle displays the respective population at year 500. Displayed dynamics are those also depicted in Fig. 5-5.

# SUPPLEMENTARY MATERIALS

## Chapter 2: Appendix S2.

**Table S2-1. Model selection results of factors affecting the probability of attack given an encounter with male elk.** We evaluated the effects of log-transformed wolf group size (wolves), the number of elk (elk), and whether elk groups contained pedicled individual(s) (pedicled). Panels identify the top models describing the probability that **a,** an encounter would include an attack for encounters with solitary or ≥ 2 adult male elk, and **b,** an encounter would include an attack for only encounters with ≥ 2 male elk. Models with a $\Delta AIC_c < 6$ are displayed. Our ability to differentiate among the top models was limited by our relatively small sample size. Nonetheless, the number of wolves (wolves) and whether or not a pedicled individual was present (pedicled) were in the top model for **a** and **b**. See Fig. S2-3 for non-standardized and standardized beta coefficient estimates for models within 4 $\Delta AIC_c$ units of the top model.

**a,** Probability of attack given an encounter with male elk (groups or solitary animals)

| Model | K | LL | AICc | ΔAICc | $w_i$ |
|---|---|---|---|---|---|
| (1) pedicled + wolves | 3 | -21.63 | 49.72 | 0.00 | 0.42 |
| (2) wolves | 2 | -22.97 | 50.17 | 0.45 | 0.33 |
| (3) pedicled + wolves + elk | 4 | -21.61 | 52.03 | 2.30 | 0.13 |
| (4) wolves + elk | 3 | -22.91 | 52.29 | 2.57 | 0.12 |

**b,** Probability of attack given an encounter with groups of ≥ 2 male elk

| Model | K | LL | AICc | ΔAICc | $w_i$ |
|---|---|---|---|---|---|
| (1) pedicled + wolves | 3 | -14.41 | 35.54 | 0.00 | 0.52 |
| (2) pedicled + wolves + elk | 4 | -13.89 | 37.03 | 1.49 | 0.25 |
| (3) wolves | 2 | -16.92 | 38.18 | 2.65 | 0.14 |
| (4) wolves + elk | 3 | -16.44 | 39.61 | 4.07 | 0.07 |

**Table S2-2. Antler condition for 223 wolf-killed adult male elk (2004 – 2016).**

| Year | Unknown | Pedicled | One Antler | Antlered |
|---|---|---|---|---|
| 2004 | 3 | 4 | 0 | 18 |
| 2005 | 1 | 18 | 0 | 10 |
| 2006 | 0 | 1 | 0 | 12 |
| 2007 | 0 | 7 | 1 | 17 |
| 2008 | 1 | 12 | 1 | 20 |
| 2009 | 1 | 10 | 0 | 14 |
| 2010 | 0 | 2 | 0 | 10 |
| 2011 | 0 | 3 | 0 | 6 |
| 2012 | 0 | 4 | 1 | 8 |
| 2013 | 0 | 0 | 0 | 5 |
| 2014 | 1 | 2 | 0 | 4 |
| 2015 | 0 | 5 | 0 | 11 |
| 2016 | 0 | 4 | 0 | 6 |

**Table S2-3. Model selection results of factors affecting the probability of a wolf-killed adult male elk (≥ 5 years old) being a pedicled individual.** We evaluated the effects of day in March (day), elk age (age), elk femur marrow percent fat (marrow), elk abundance (elk), and winter severity (winter). Models were developed using 139 wolf-killed male elk detected from 2004 – 2016. Models with a $\Delta AIC_c < 6$ are displayed. See Fig. S2-8 for non-standardized and standardized beta coefficient estimates for models within 4 $\Delta AIC_c$ units of the top model.

| **Model** | **K** | **LL** | **AICc** | **ΔAICc** | ***w*$_i$** |
|---|---|---|---|---|---|
| day + marrow + elk | 4 | -65.04 | 138.38 | 0.00 | 0.25 |
| day + marrow + elk + winter | 5 | -64.96 | 140.36 | 1.98 | 0.09 |
| elk * marrow + day | 5 | -65.00 | 140.45 | 2.07 | 0.09 |
| day + marrow + elk + age | 5 | -65.04 | 140.53 | 2.15 | 0.09 |
| day + marrow | 3 | -67.22 | 140.61 | 2.23 | 0.08 |
| age * marrow + day + elk | 6 | -64.33 | 141.29 | 2.91 | 0.06 |
| elk * age + day + marrow | 6 | -64.80 | 142.23 | 3.85 | 0.04 |
| winter * marrow + day + elk | 6 | -64.90 | 142.44 | 4.06 | 0.03 |
| elk * marrow + day + winter | 6 | -64.93 | 142.50 | 4.11 | 0.03 |
| day + marrow + age | 4 | -67.10 | 142.51 | 4.12 | 0.03 |
| day + marrow + elk + winter + age | 6 | -64.95 | 142.54 | 4.16 | 0.03 |
| day + marrow + winter | 4 | -67.13 | 142.57 | 4.19 | 0.03 |
| elk * marrow + day + age | 6 | -64.99 | 142.62 | 4.24 | 0.03 |
| age * marrow + day + elk + winter | 7 | -64.17 | 143.20 | 4.82 | 0.02 |
| age * marrow + day | 5 | -66.91 | 144.28 | 5.89 | 0.01 |
| elk * age + day + marrow + winter | 7 | -64.71 | 144.28 | 5.90 | 0.01 |

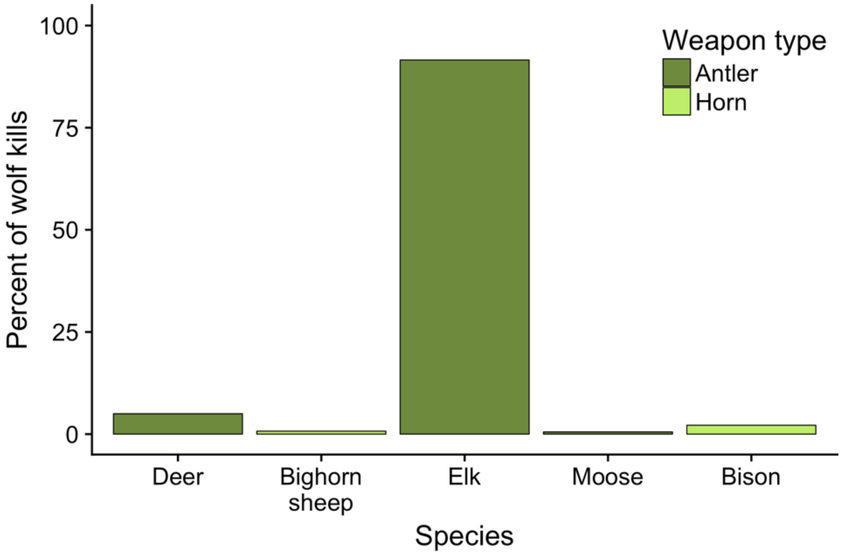

**Figure S2-1. Percent of wolf-killed ungulates in northern Yellowstone during winter.** Percent of each species calculated from 1,104 wolf-killed ungulates detected during 30-day early (mid-November to mid-December) and late (March) winter monitoring periods from November 2003 – March 2016.

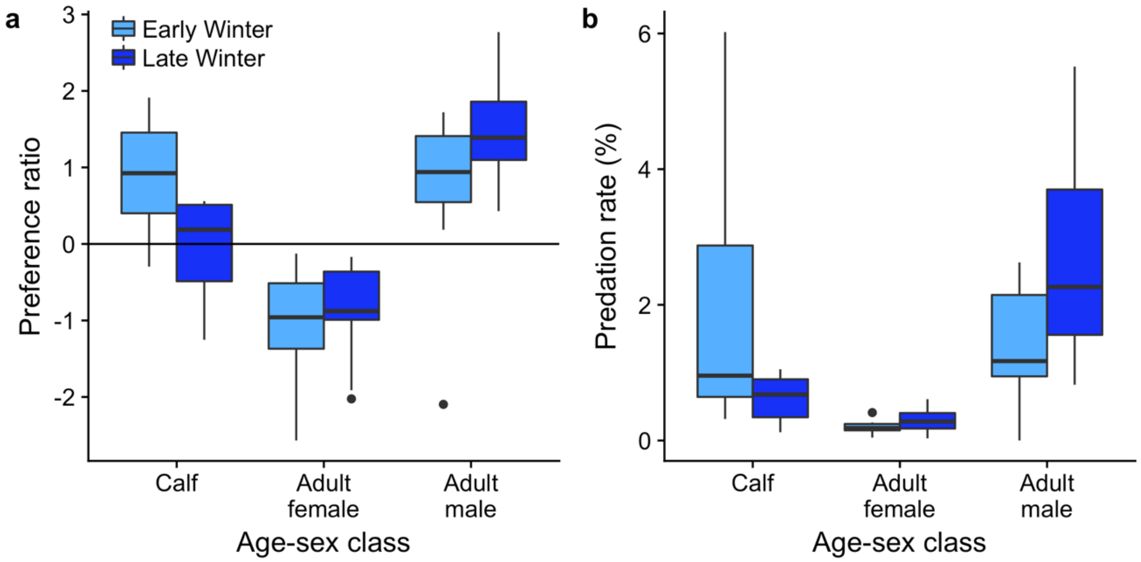

**Figure S2-2. Wolf preference ratio and predation rate in northern Yellowstone. a,** Wolf preference ratio (Eqn 1) for elk calves, adult females, and adult males. **b,** Wolf predation rate on elk calves, adult females, and adult males (number of age-sex specific kills divided by age-sex specific elk abundance). Each panel displays a box plot of annual estimates from 30-day study periods[44], November 2003 – March 2016 (no estimates for four years because elk age-sex surveys did not occur). Wolf predation statistics use data about wolf kill composition and kill rate from three wolf packs that were intensively monitored by aerial and ground-based observations during each study period (*n* = 14 total packs)[74]. These wolf predation statistics include only wolf kills detected by aerial and ground-based observations and do not correct for variation in detection probability among wolf kills of differing size[74,75]. Wolf abundance estimates are for resident northern Yellowstone National Park wolves during early and late winter. Total elk abundance was estimated as described in *Methods*[43], while the age-sex composition of the elk population was determined during a late winter population-wide survey conducted by the Northern Yellowstone Cooperative Wildlife Working Group[44]. The specific equation used in panel **b** was *total northern YNP wolf abundance* x *wolf kill rate on elk* x *proportion age-sex class among detected wolf-killed elk*, divided by *abundance of age-sex class elk for northern Yellowstone*. The box plots display the median, as well as the first and third quartiles. Whiskers extend from the inter-quartile range to the largest value that is no further than 1.5 * inter-quartile range, in each direction. Filled circles represent outliers.

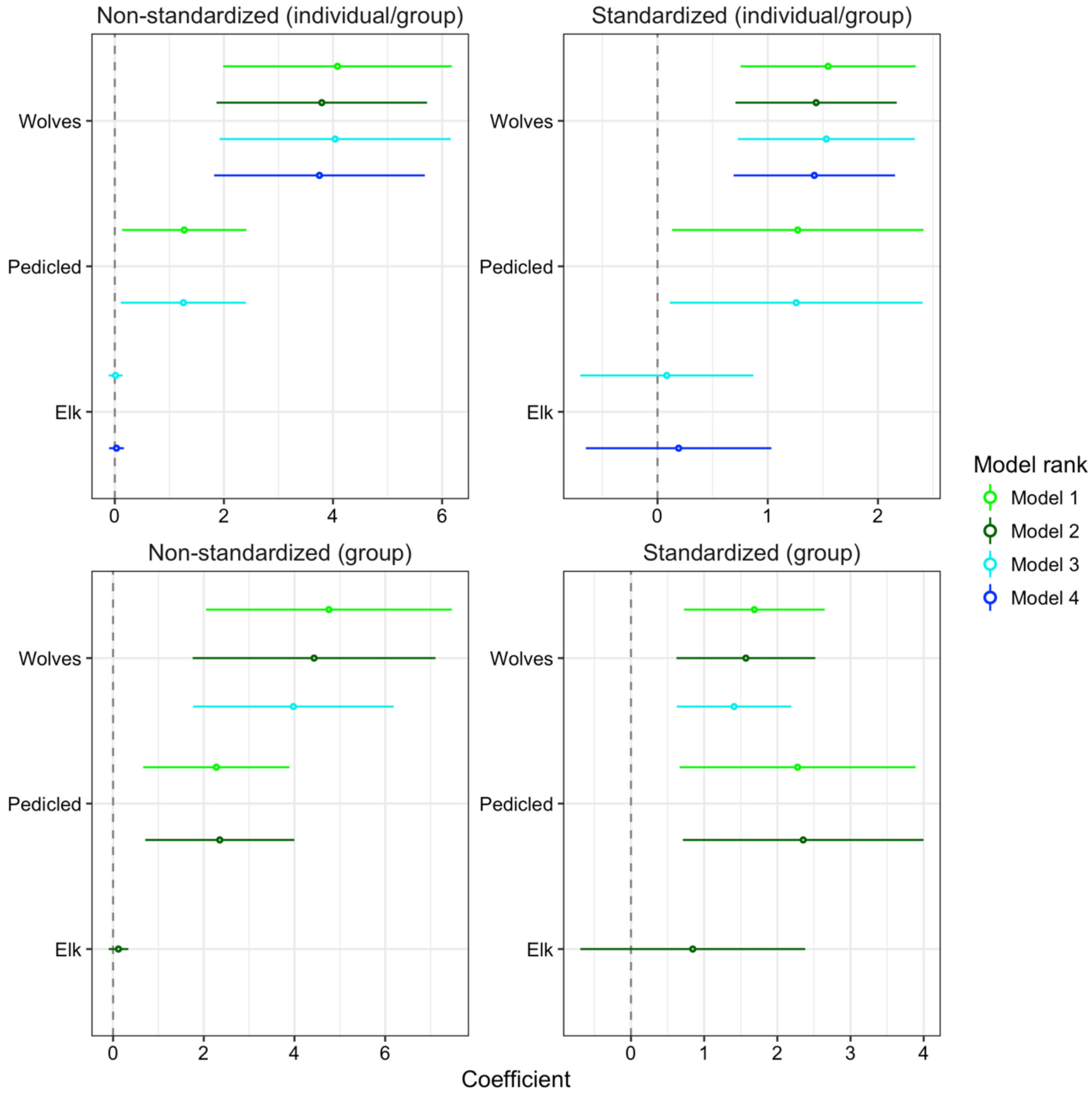

**Figure S2-3. Beta coefficients for top models describing factors affecting the probability of attack given an encounter with male elk**. 'Wolves' represents wolf group size (log transformed), 'Pedicled' represents whether a pedicled individual(s) was present, and 'Elk' represents the number of elk. Panels display either non-standardized or standardized beta coefficients for models describing the likelihood that an encounter with solitary or ≥ 2 adult male elk included an attack (top row) and an encounter with ≥ 2 adult male elk included an attack (bottom row). Coefficients are displayed for models within 4 $\Delta AIC_c$ units of the top model (Table S2-1). Error bars represent 85% confidence intervals. Model numbers identifying each model represent the model rank from Table S2-1.

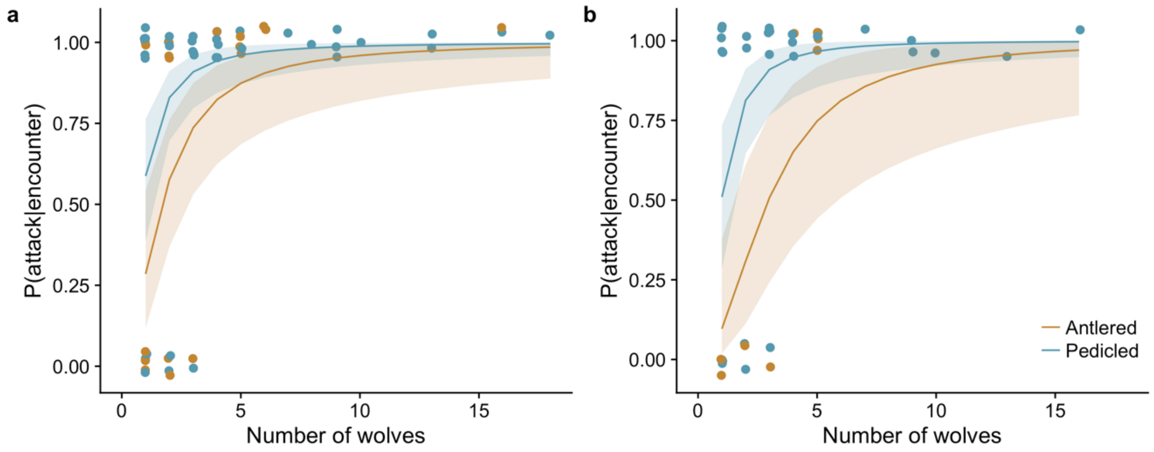

**Figure S2-4. Predictions for top models describing factors affecting the probability of attack given an encounter with male elk**. Panels display predictions for the top model (Table S2-1) describing the probability that wolves **a,** attacked solitary or groups of ≥ 2 adult male elk, and **b,** attacked groups of ≥ 2 adult male elk only. Shaded areas represent 85% confidence intervals.

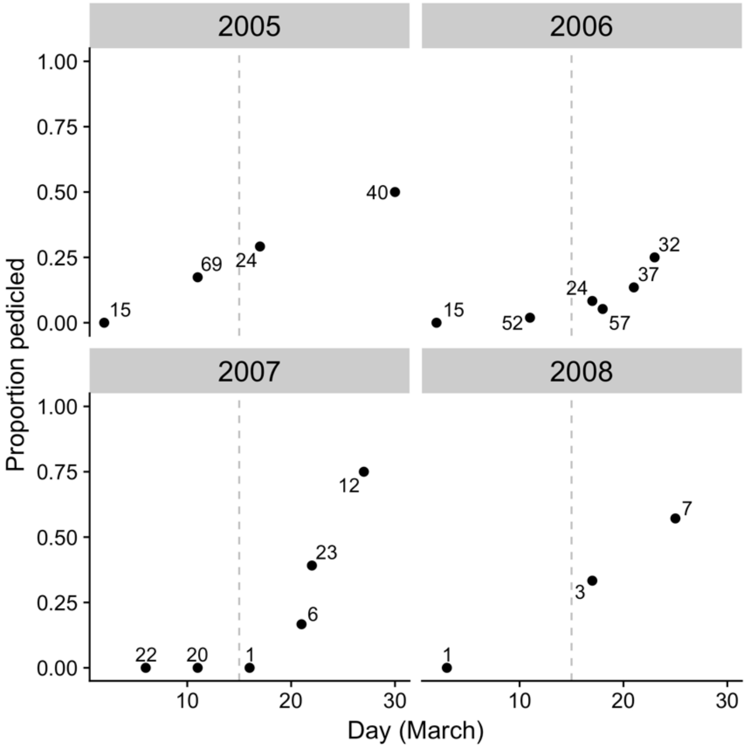

**Figure S2-5. Proportion of male elk that had cast their antlers during each male elk antler classification survey (2005 – 2008).** Numbers indicate the number of individual male elk classified as pedicled or antlered during each survey. Dashed gray lines indicate the mid-point of the month that distinguishes ‘Early March’ from ‘Late March’.

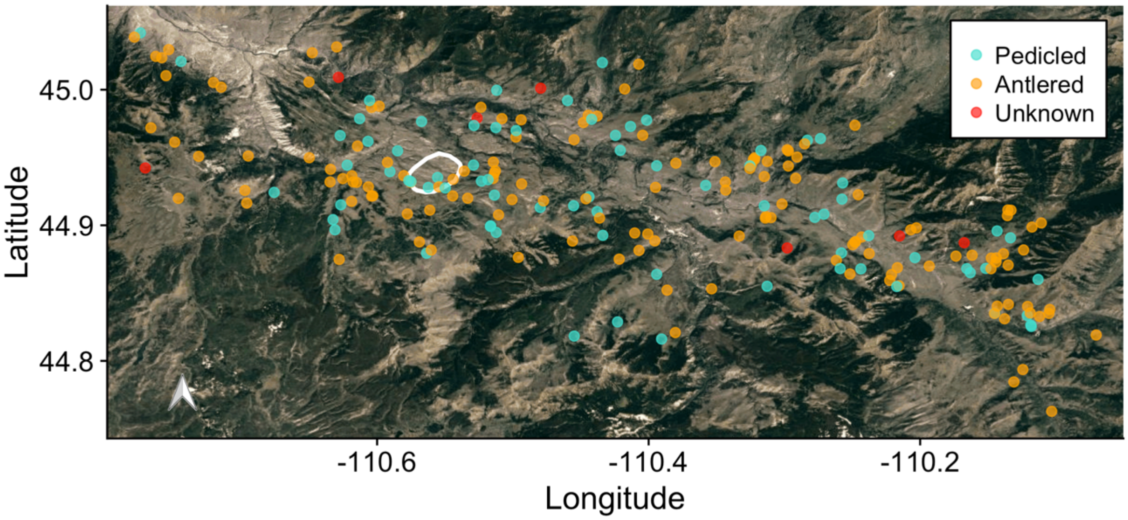

**Figure S2-6. Geographic distribution of 223 wolf-killed adult male elk detected during March (2004 – 2016).** The white-lined polygon represents the 6.7 km$^2$ male elk classification survey unit (Fig. S2-5).

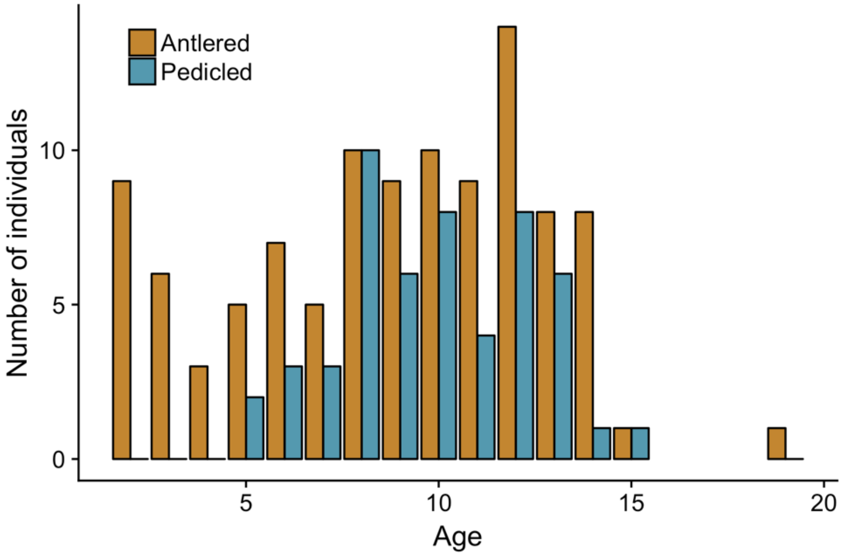

**Figure S2-7. Age of wolf-killed adult male elk during March (2004 – 2016)**. Ages are displayed for the 157 individuals where we determined both the individual's age and nutritional condition.

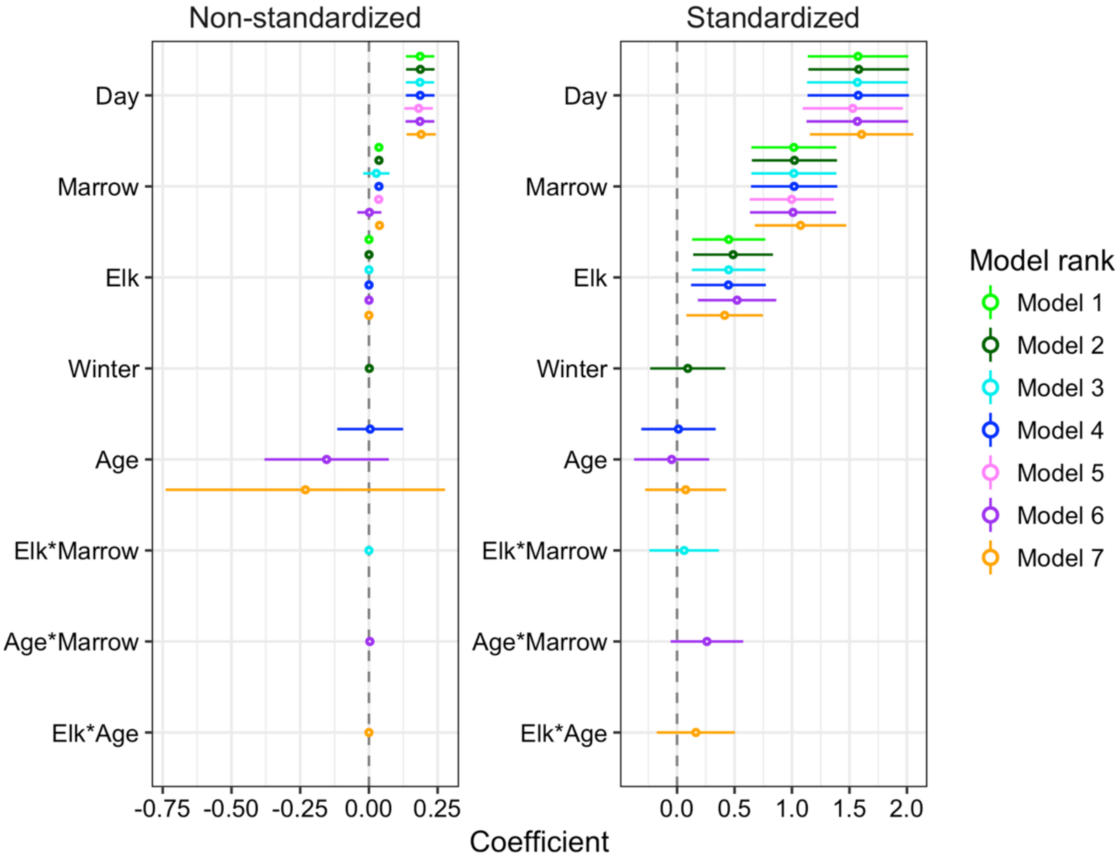

**Figure S2-8. Beta coefficients for top models describing factors affecting the probability of a wolf-killed adult male elk (≥ 5 years old) being a pedicled individual.** 'Day' represents the day in March, 'Marrow' represents elk femur marrow percent fat, 'Elk' represents elk abundance, 'Winter' represents winter severity, and 'Age' represents the elk's age. Non-standardized and standardized beta coefficients are displayed for models within 4 $\Delta AIC_c$ units of the top model (Table S2-3). Error bars represent 85% confidence intervals. Model numbers identifying each model represent the model rank from Table S2-3.

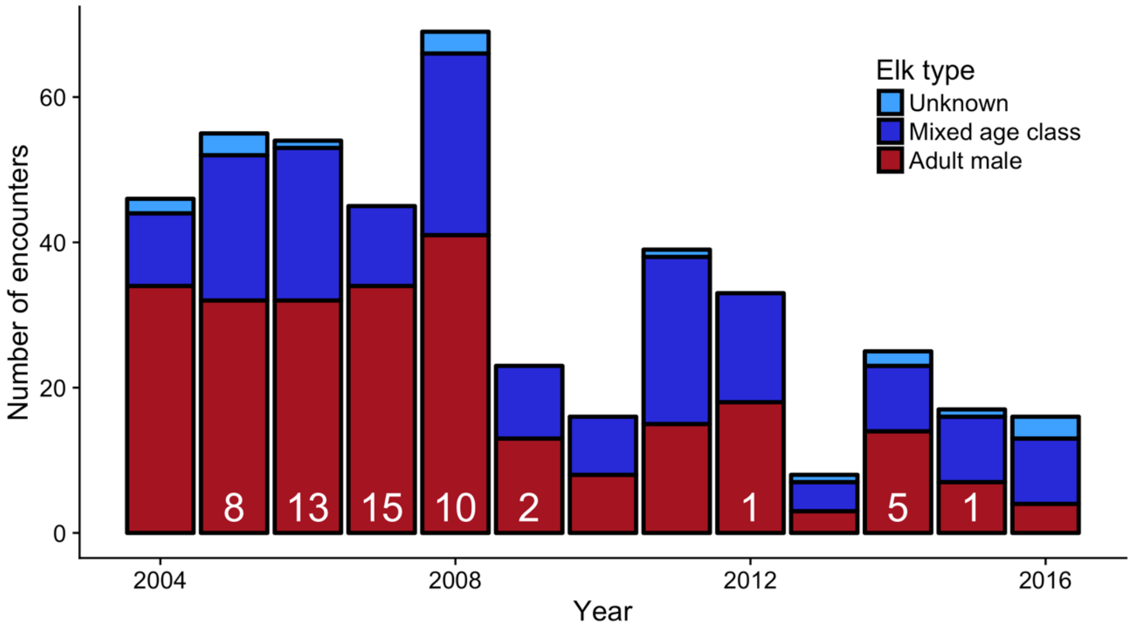

**Figure S2-9. Number of observations of wolf-elk encounters during March (2004 – 2016).** White numbers indicate the number of encounters included in our analysis of how the presence of pedicled individual(s) affected the probability of wolves attacking male elk.

# Chapter 3: Appendix S3-A. Supporting tables and figures for observed-unobserved wolf sightability model.

**Table S3-A.1. Model selection results for factors affecting the probability of sighting a wolf group.** Models with a ΔBIC < 10 are displayed. Models also included a random effect for pack and year.

| Model | K | LL | BIC | ΔBIC | $w_i$ |
|---|---|---|---|---|---|
| (1) VS + Dist + Open + Group | 7 | -5467.76 | 11001.27 | 0.00 | 0.97 |
| (2) VS + Dist + Open + Group + Harvest | 8 | -5466.39 | 11007.92 | 6.65 | 0.03 |

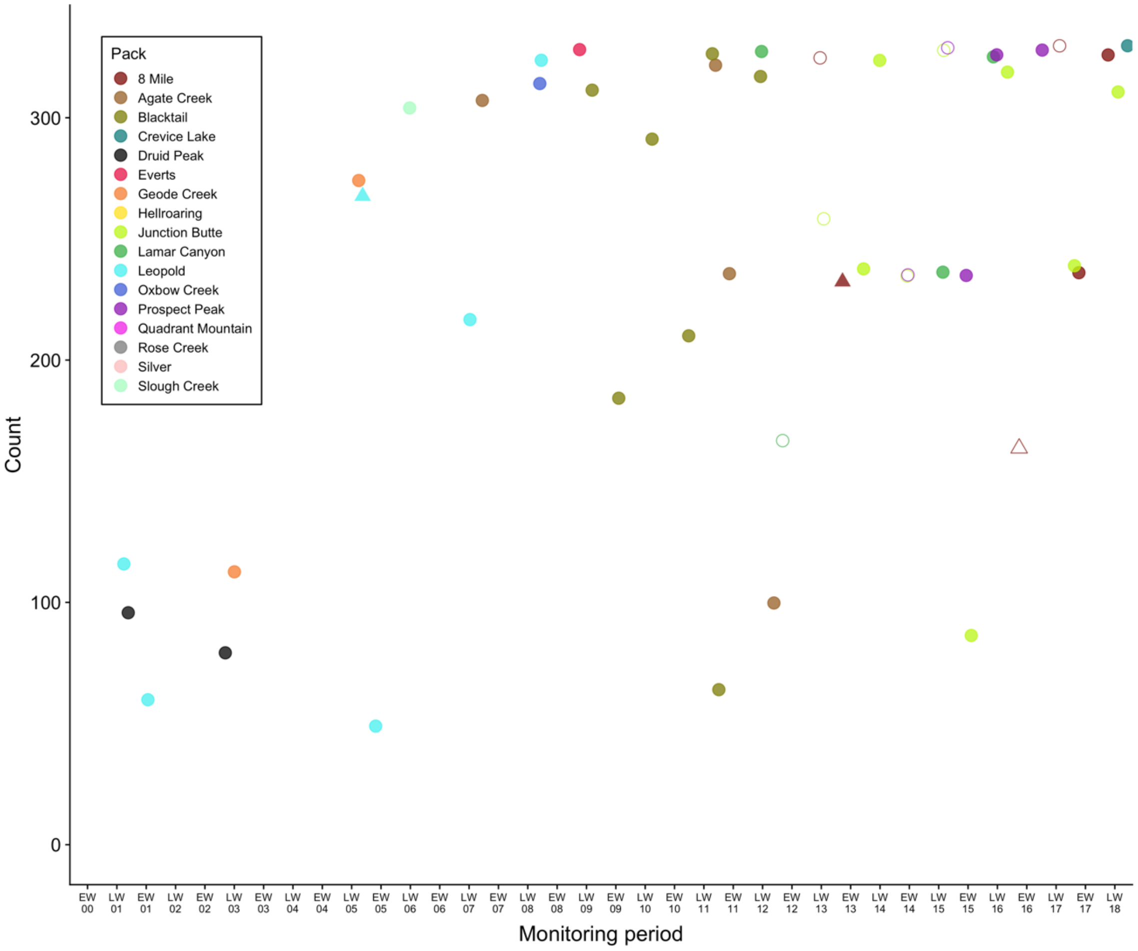

**Fig. S3-A.1. Number of GPS locations, by pack and study period, for observed-unobserved sightability model.** Both observed and unobserved locations are displayed because the unobserved locations were also acquired wolf GPS locations. Symbol color indicates the pack, symbol fill indicates harvest (open = harvest, filled = no harvest), and symbol shape indicates which road was used by the observation crew (circle = minimum, triangle = maximum; see Fig. 3-1).

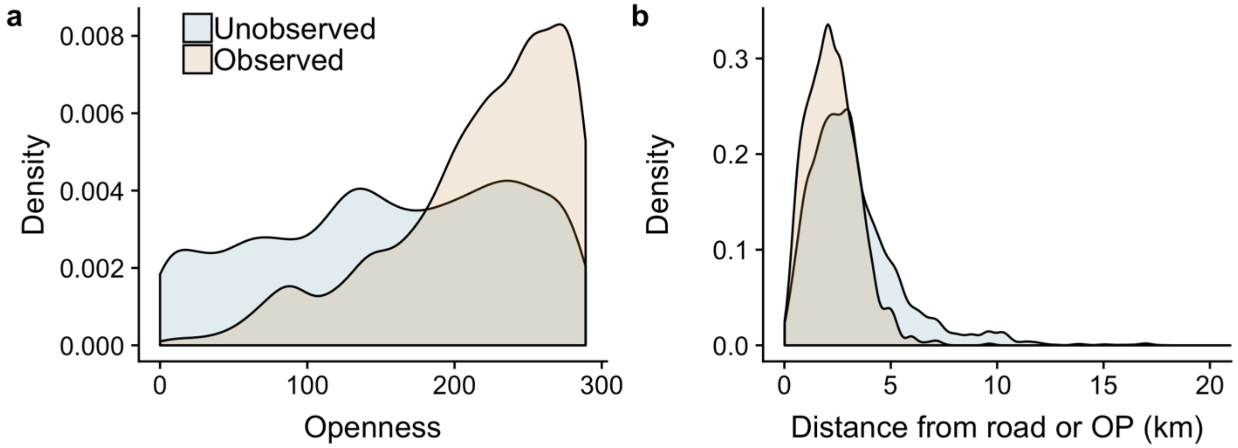

**Fig. S3-A.2. Distribution of openness and distance covariates.** Density of the observed - unobserved data for (a) openness and (b) distance. The distance covariate shown here in panel (b) is for the pack-road and common observation points. The maximum distance value displayed is 20 km, but the density was calculated using all locations (24 values were greater than 20 km).

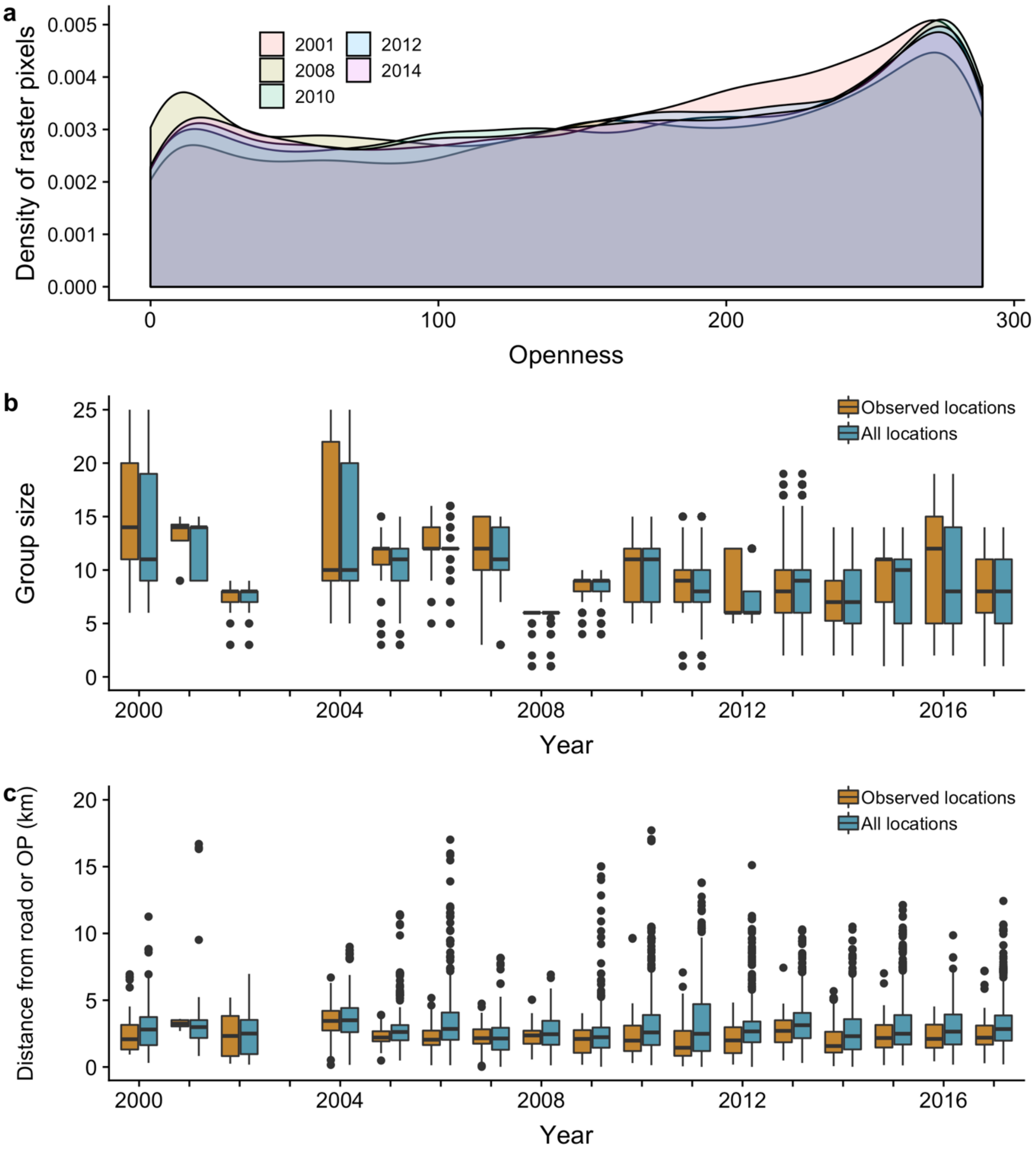

**Fig. S3-A.3. Temporal variation in covariates.** Panel (a) displays densities of raster pixels for the five years of openness data (see Methods). To create these densities, we randomly sampled (without replacement) 12,000 values from each year's openness raster, clipped to the overall 85% wolf utilization distribution (Figs. 3-1c, 3-4). Panels (b) and (c) display box-and-whisker plots describing group size and distance from observer locations (for the pack-road and common observation points), respectively, with each shown for observed and all (i.e., including unobserved) locations. The maximum distance value displayed in panel (c) is 20 km (as in Fig. S3-A.2), and some outlying data points are therefore not shown.

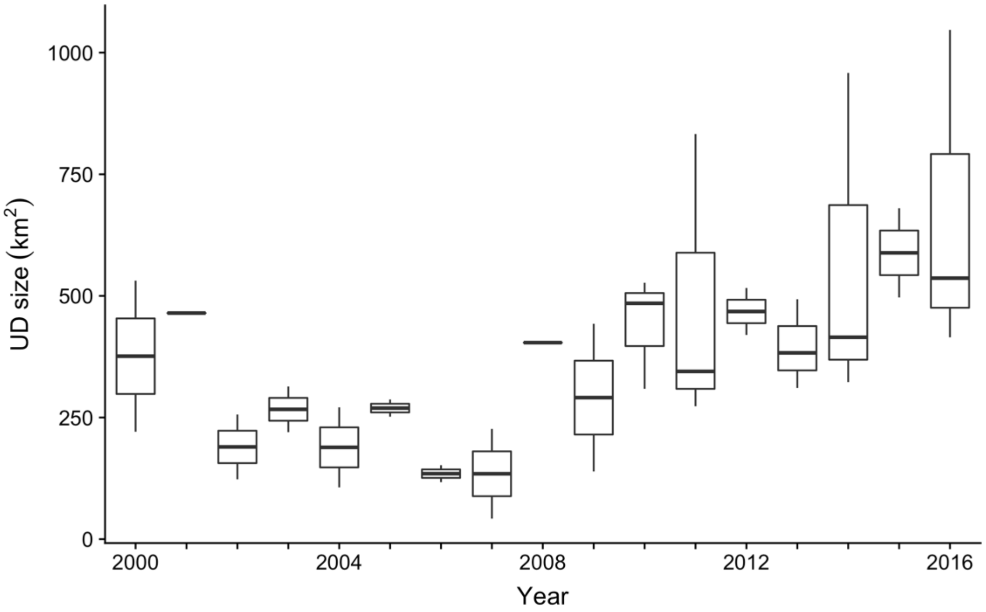

**Fig. S3-A.4. Utilization distribution size (km$^2$) for GPS-collared wolf packs.** For each pack during each winter, the utilization distribution was defined by the 95% contour. If applicable, early and late winter locations for a pack were combined in order to create a single winter estimate of range size. Here, we chose to display 95% UDs, but the temporal pattern was the same for other values that we explored (i.e., 80%, 85%, 90%).

# Chapter 3: Appendix S3-B. Additional p(wolf group sighting) models.

## METHODS

### Observed-unobserved models.

We developed an additional formulation of our observed-unobserved wolf sightability model that differed from the one presented in the main text because we also included hard-to-reach observation points (Fig. S3-B.1). The inclusion of these additional observation points (potentially) affected the values of two covariates, *distance* and *viewshed.* Here, the covariate values for the 'All OP' model were created in the same way as for the 'Common OP' model presented in the main text, except here the values were created using the additional observation points as well (Fig. S3-B.1). We developed and evaluated this 'All OP' model in the exact same way as we did the 'Common OP' model.

### Observed-available models.

#### STUDY AREA

Our study area for the observed-available sightability model was defined by the movements of 18 wolf packs that resided primarily within northern Yellowstone National Park during 23 winters (1995 – 2018; Figs. S3-B.1, S3-B.2; note that many figures from the main text and supporting information figures have been recreated for the observed-available data at the end of Appendix S3-B; in most cases, we also included the results from the observed-unobserved models to facilitate comparison). Because all of the wolf packs included in the observed-unobserved model (see Main text) were also included here, the general description of the study area is the same.

#### WINTER STUDY WOLF SIGHTINGS AND DATA PREPARATION

The data for the observed-unobserved model, which relied on the presence of GPS-collared wolves, was for a subset of packs that we collected ground-based observational data for since November 1995. Here, our complimentary observed-available sightability model – akin to a used-available Resource Selection Framework (RSF) framework – included ground observations of radio-collared wolf groups from all winter studies that have occurred since the 1995 reintroduction of wolves (Fig. S3-B.2).

For each day that a wolf pack was observed, we leveraged data that described the first location where each wolf group was observed. Because members of wolf packs are not always together (Peterson et al. 1984, Metz et al. 2011), multiple observations for a wolf pack were possible. We included each observation for a pack when the wolves were observed in multiple, distinct groups on a given day. Ground crews recorded the spatial location of each sighting on a topographic map, and these locations were compared to random locations (see details below) in our observed-available model.

After excluding two locations for which we did not record group size, we used 2,789 observations. On average, we acquired 20.7 observations (± 0.6 SE; range: 2–33) for each pack during each 30-day period (Fig. S3-B.2). To generate the random locations to compare these observations to, we first created a 100% minimum convex polygon (MCP) for each pack during each study period using wolf locations collected through either aerial or ground-based observations. We used a MCP because we acquired only a small number of spatial locations for some packs during some 30-day periods. Note that in one case (i.e., for Junction Butte during Early Winter 2016) we acquired only four locations and we therefore used one location for the pack that was acquired immediately prior to the beginning of the 30-day period to create their MCP. We retained one set (i.e., ground or air) of unique observations for each pack on each day, randomly selecting whether to keep ground or air observations on days where wolves were observed by both ground and air crews. If a pack was in multiple 'groups' and we had observations for more than one group, we developed the MCP using the locations for each group. We created random points, within each pack's territory, using the sp package (Pebesma et al. 2012) in a 3:1 ratio with wolf sightings. Variation in available:observed ratios did not affect which model was identified as the best, and also had minimal effect on beta coefficient strength (*unpublished data*).

### OBSERVED-AVAILABLE WOLF SIGHTABILITY MODEL

Our observed-available sightability model was also developed in a logistic regression framework (Hosmer and Lemeshow 2000). We used the same covariates, mostly generated in the same ways, as were used in the observed-unobserved model (see Main text for details). The exception was wolf group size. Here, we simply randomly sampled with replacement from the observed group sizes for a pack for the 30-day period. As we did for our observed-unobserved model, we estimated wolf sightability using mixed-effect logistic regression models (binomial; observed = 1, available = 0; random effect for 'pack' and 'year'). However, we initially developed our observed-available models without the random effects because some mixed-effect models did not converge.

For the observed-available model, the full logistic regression model is described by the equation:

P(wolf group sighting) = $\mathrm{logit}(\beta_1\, \textit{viewshed} + \beta_2\, \textit{distance} + \beta_3\, \textit{openness} + \beta_4\, \textit{group size} + \beta_5\, \textit{harvest} + \varepsilon_i)$ Appendix S3-B: Eq. 1

where $\beta_x$ is the effect of that covariate's coefficient on the probability of sighting the wolf group. Of note, because of the arbitrary sampling of availability, the true probability of observing wolves is unknown in a used-available design, so there is no intercept value (i.e., no β0, see Manly et al. 2007).

We screened for association and collinearity among covariates, of which we found none (e.g., maximum $r = |0.28|$), and then employed the same process for model building and evaluation that we used for developing and evaluating the observed-unobserved models (see Main text). We initially developed the observed-available models as generalized linear models (i.e., not including the random effects) because some models had convergence issues, including resulting in singular fits. But upon identifying the top observed-available models, we attempted to add the random effects for pack and year – each of the top observed-available models converged with the addition of the random effect for pack.

## RESULTS

### Observed-unobserved all observation point model.

The top-ranked all observation point model included the same covariates as the common observation point model – viewshed, distance, openness, and group size, as well as the random effects for pack and biological year (i.e., winter). Harvest was not included in our top model. The support for our top model was clear ($w_i = 0.96$; Table S3-B.1), and the directionality and strength of each of the covariates were the same as in the common observation point model (Fig. S3-B.3).

As was the case with the common observation point model, the top all observation point model also showed near excellent discriminatory power (AUC = 0.79) and correctly predicted 70% of the GPS locations. Sensitivity (i.e., the correct prediction of 1s) was 0.79, while specificity (i.e., the correct prediction of 0s) was 0.67 (Table S3-B.2). In comparison to the common observation point model, the all observation point model more often predicted sightings to indeed be sightings but the overall classification success was poorer (Table S3-B.2). The slightly better predictions of observed locations as observed, and the slightly poorer predictive success overall, was likely driven by the variable use of harder-to-reach observation points by field crews.

### **Observed-available models.**

#### COVARIATES AFFECTING SIGHTABILITY

The 2,789 observed locations were, on average, 1.9 km (± 0.03 SE) from the closest road or common observation point, while the 8,367 available locations were 3.1 km (± 0.03 SE) away (Fig. S3-B.4). Mean openness values were 211 (± 1.2 SE) and 162 (± 1.0 SE) for the observed and available locations, respectively. Of the 2,789 observed locations, 2,327 (83.4%) were in "viewable" (i.e., *viewshed* = 1) locations, while 5,381 of 8,367 (54.9%) available locations were in "viewable" locations. Finally, of the 135 wolf pack-study periods in our observed-available data set, 12 experienced a harvest event (Fig. S3-B.2).

#### OBSERVED-AVAILABLE SIGHTABILITY MODELS

Regardless of whether using common or all observation points, the top wolf sightability model included only viewshed, distance, and openness. In both cases (i.e., for common or all observation points), this model contained 97% of the BIC weight (Table S3-B.1). Also in both cases, the top model converged with the addition of the random effect for pack (but not year), and we report the predictions for these mixed-effect models hereafter.

The beta coefficients for the top common observation point observed-available model, all of which were significant, indicated that the probability of detecting a wolf group was higher when the location was visible ($\beta = 0.55$; Odds Ratio [OR] = 1.74 [95% CI: 1.54, 1.96]), in a more open area ($\beta = 0.55$; OR = 1.73 [1.64, 1.83]), and closer to the road or observation point ($\beta = -0.46$; OR = 0.63 [0.58, 0.68]; Fig. S3-B.3). The directionality and strength of each covariate was similar for the all observation point model. The directional effect of each of these covariates was as expected, and resulted in predictions for p(sighting) that were similar in their nature to those from the observed-unobserved sightability model (Fig. S3-B.5).

### PREDICTIONS: THE CONFUSION MATRIX, SPACE, AND TIME

Our observed-available common observation point model showed acceptable discriminatory power (AUC = 0.70 for both common and all observation point models; Table S3-B.2). As we did for the observed-unobserved model, we used the optimal cutpoint to predict whether each observation in our data sets was observed or available (Fig. S3-B.6a). Doing so resulted in 59% of locations being correctly predicted from both common and all observation points (Table S3-B.2). Here, for the observed-available model, sensitivity (i.e., the correct prediction of 1s) was 0.82 for both observation point models – noticeably more than specificity (i.e., the correct prediction of 0s), which was 0.51 for both common and all observation points (Table S3-B.2).

## LITERATURE CITED

Harrell Jr, F. E. 2001. Regression modeling strategies: with applications to linear models, logistic regression and survival analysis. Springer, New York.

Hosmer, D. W., and S. Lemeshow. 2000. Applied Logistic Regression. Wiley, New York.

Manly, B. F. L., L. McDonald, D. Thomas, T. L. McDonald, and W. P. Erickson. 2007. Resource selection by animals: statistical design and analysis for field studies. Springer Science & Business Media.

Metz, M. C., J. A. Vucetich, D. W. Smith, D. R. Stahler, and R. O. Peterson. 2011. Effect of sociality and season on gray wolf (*Canis lupus*) foraging behavior: implications for estimating summer kill rate. Plos One **6**:e17332.

Pebesma, E., R. Bivand, M. E. Pebesma, S. RColorBrewer, and A. Collate. 2012. Package ‘sp’. The Comprehensive R Archive Network.

Peterson, R. O., J. D. Woolington, and T. N. Bailey. 1984. Wolves of the Kenai peninsula, Alaska. Wildlife Monographs:3-52.

**Table S3-B.1. Model selection results for factors affecting the probability of sighting a wolf group for the observed-unobserved and observed-available analyses.** Within each dataset (O-U = Observed-unobserved, O-A = Observed-available; separated by the dashed lines), models with a ΔBIC < 10 are displayed. 'OP' identifies which set of observation points were used in the analysis. Model selection results for the observed-unobserved analysis report models that included a random effect for pack and year. Conversely, the model selection results for the observed-available analysis report the results for models without the random effect for pack that was ultimately included (see Appendix S3-B text).

| Dataset | OP | Model | K | LL | BIC | ΔBIC | $w_i$ |
|---|---|---|---|---|---|---|---|
| O-U | Common | (1) VS + Dist + Open + Group | 7 | -5467.76 | 11001.27 | 0.00 | 0.97 |
| O-U | Common | (2) VS + Dist + Open + Group + Harvest | 8 | -5466.39 | 11007.92 | 6.65 | 0.03 |
| O-U | All | (1) VS + Dist + Open + Group | 7 | -5561.71 | 11189.17 | 0.00 | 0.96 |
| O-U | All | (2) VS + Dist + Open + Group + Harvest | 8 | -5560.28 | 11195.71 | 6.54 | 0.04 |
| O-A | Common | (1) VS + Dist + Open | 4 | -5740.48 | 11518.23 | 0.00 | 0.97 |
| O-A | Common | (2) VS + Dist + Open + Group | 5 | -5739.70 | 11526.00 | 7.77 | 0.02 |
| O-A | Common | 3) VS + Dist + Open + Harvest | 5 | -5740.08 | 11526.77 | 8.53 | 0.01 |
| O-A | All | (1) VS + Dist + Open | 4 | -5738.11 | 11513.49 | 0.00 | 0.97 |
| O-A | All | (2) VS + Dist + Open + Group | 5 | -5737.63 | 11521.86 | 8.36 | 0.01 |
| O-A | All | 3) VS + Dist + Open + Harvest | 5 | -5737.69 | 11521.98 | 8.49 | 0.01 |

**Table S3-B.2. Classification success for wolf sightability models.** ‘OP’ identifies which set of observation points were used in the analysis, ‘Locations’ indicates the total number of locations in the dataset, ‘Predict’ indicates the number of locations correctly predicted as a 1 (i.e., above the cutpoint), and ‘Prop. correct’ is the proportion of total locations correctly predicted. Specificity indicates the proportion of 0 (i.e., available or unobserved) locations correctly predicted, and, sensitivity, the same for 1 (i.e., observed) locations. In the Dataset column, ‘O-U’ represents Observed-unobserved, ‘O-A’ represents Observed-available, and a ‘V’ in parentheses indicates this was the validation dataset.

| Dataset | OP | Locations | Predict | Prop. correct | AUC | Cutpoint | Specificity | Sensitivity |
|---|---|---|---|---|---|---|---|---|
| O-U | Common | 11999 | 8620 | 0.72 | 0.80 | 0.26 | 0.70 | 0.77 |
| O-U (V) | Common | 1258 | 955 | 0.76 | - | - | 0.74 | 0.79 |
| O-U | All | 11999 | 8413 | 0.70 | 0.79 | 0.25 | 0.67 | 0.79 |
| O-U (V) | All | 1258 | 918 | 0.73 | - | - | 0.70 | 0.80 |
| O-A | Common | 11156 | 6543 | 0.59 | 0.70 | 0.21 | 0.51 | 0.82 |
| O-A | All | 11156 | 6563 | 0.59 | 0.70 | 0.21 | 0.51 | 0.82 |

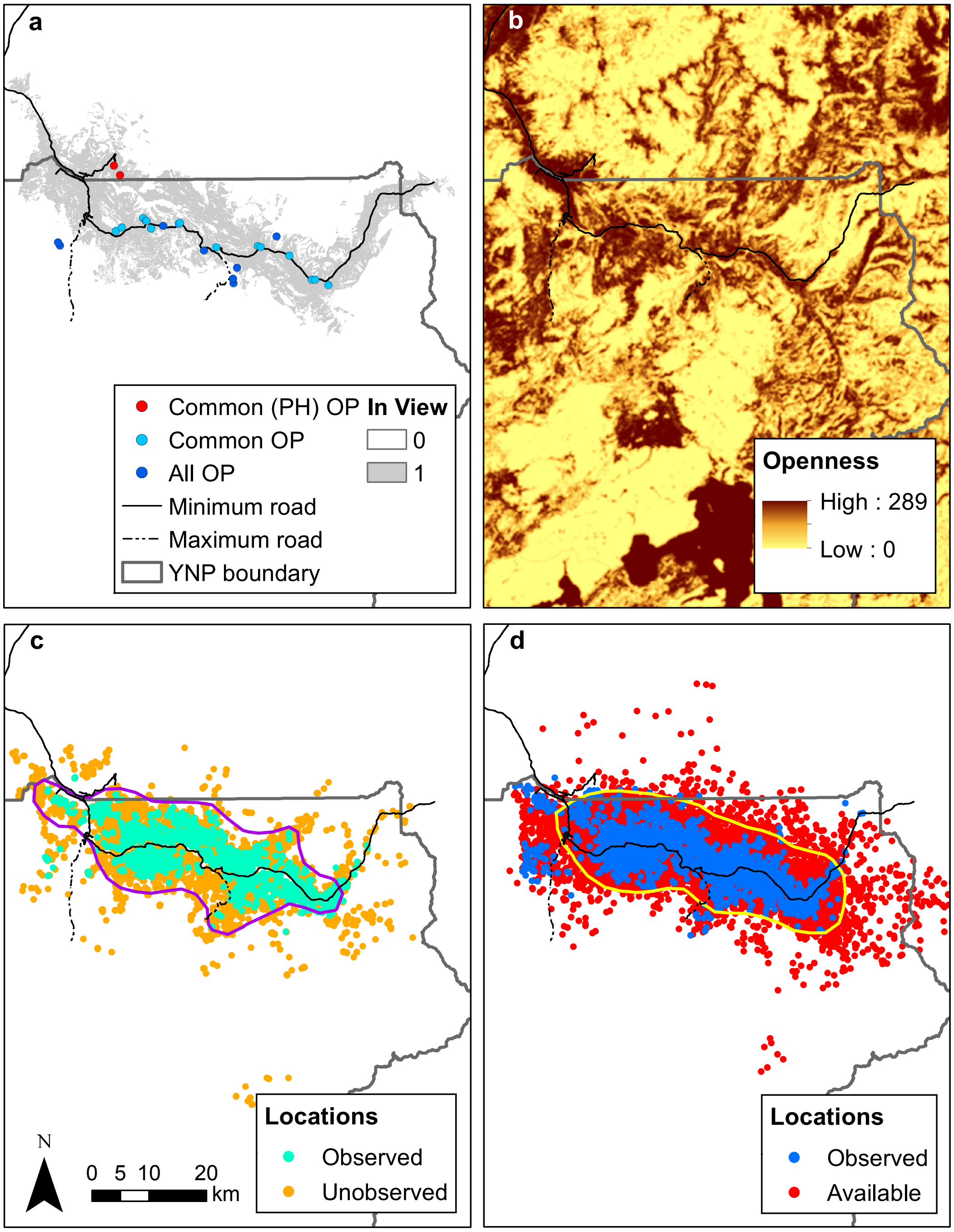

**Figure S3-B.1. Spatial distribution of observation points, covariates, and wolf sightability data.** Panels display (a) observation points (OP; red circles indicate OPs used only before Montana wolf harvest season was implemented; dark blue circles indicate harder-to-reach OPs), the minimum and maximum road, viewshed (from the minimum road and all common OPs; 1 = viewshed-predicted viewable; 0 = viewshed-predicted not viewable), and the Yellowstone National Park boundary (roads and boundary shown in all panels), (b) openness (2001), (c) wolf GPS locations, and (d) observed-available wolf locations. Note that the purple line in panel (c) and the yellow line in panel (d) display 85% population-level utilization distributions that were used in Fig. 3-4 and Fig. S3-B.6, respectively.

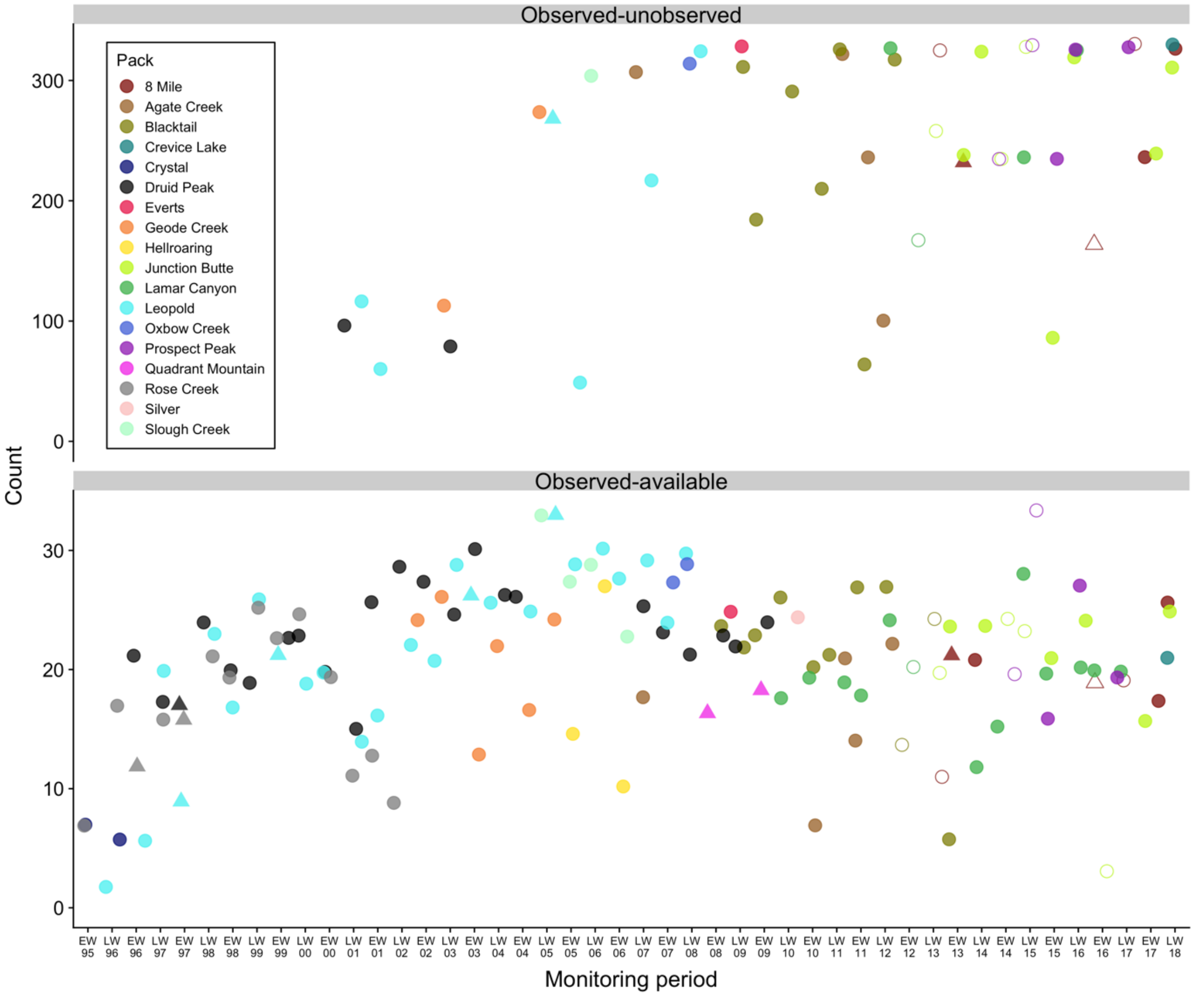

**Figure S3-B.2. Number of locations, by pack and study period, for observed-unobserved (GPS) and observed-available (VHF) sightability models.** Both observed and unobserved locations are displayed for observed-unobserved data because the unobserved locations were also acquired wolf GPS locations. However, only used observations are displayed for the observed-available data. Symbol color indicates the pack, symbol fill indicates harvest (open = harvest, filled = no harvest), and symbol shape indicates which road was used by the observation crew (circle = minimum, triangle = maximum; see Fig. S3-B.1).

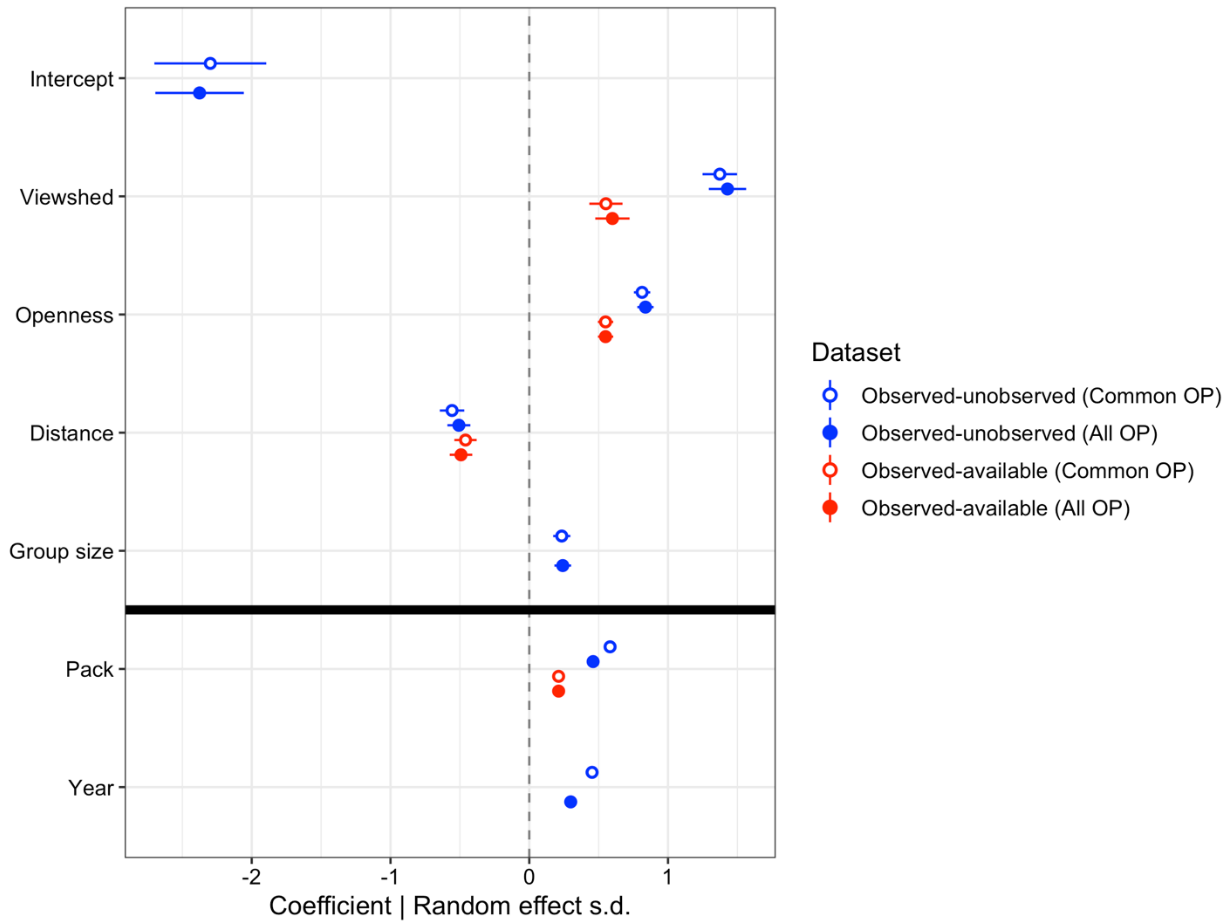

**Figure S3-B.3. Beta coefficient estimates for top-ranked wolf sightability models.** Error bars represent 95% confidence intervals. Below the solid black line displays the standard deviation for the random effects (pack, year), which is directly comparable to the beta coefficient strength (Harrell Jr 2001). In legend text, 'OP' identifies which set of observation points were used in the analysis.

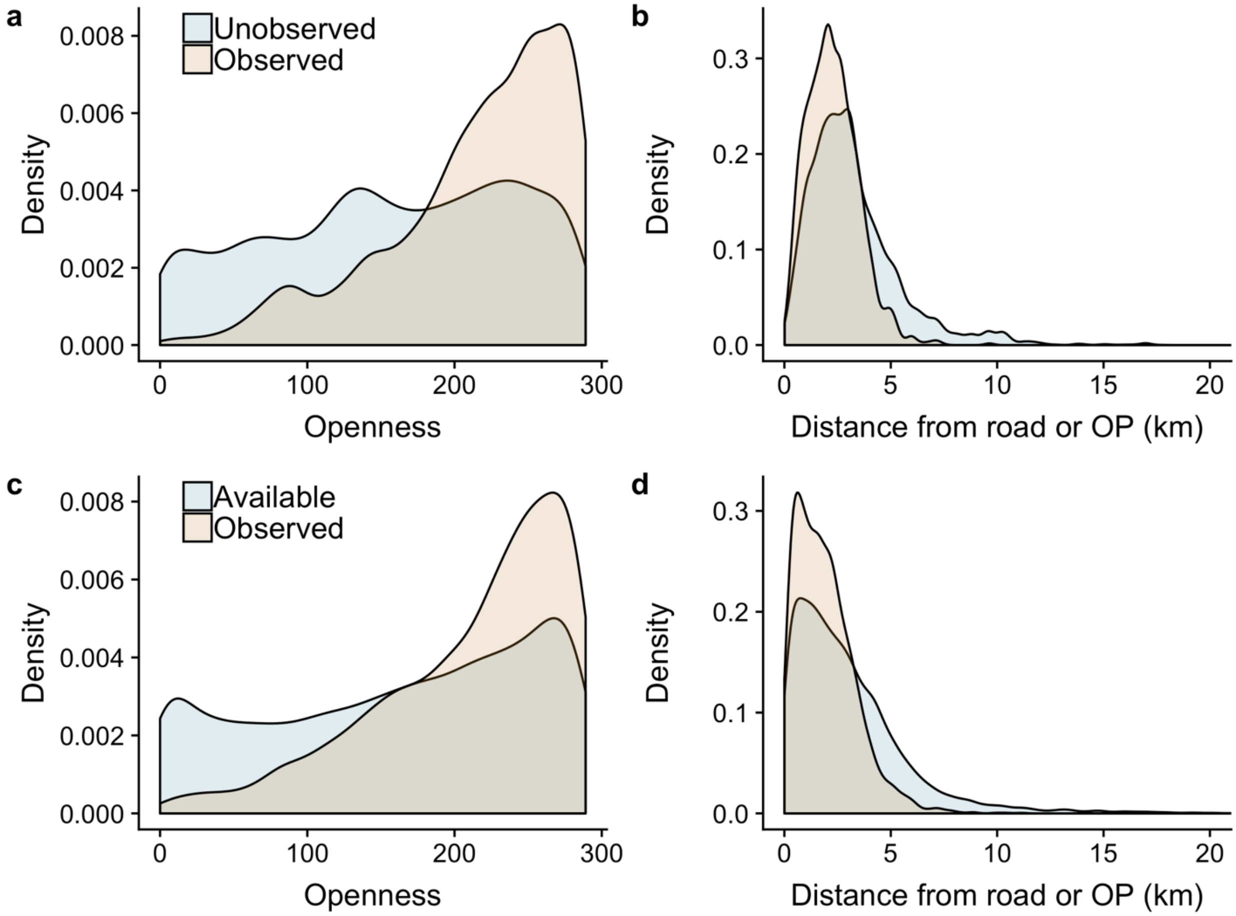

**Figure S3-B.4. Distribution of openness and distance covariates.** Density of the observed-unobserved data for (a) openness and (b) distance. Panels (c) and (d) show the same for the observed-available data. The distance covariate shown here in panels (b) and (d) is for the pack-road and common observation points. The maximum distance value displayed is 20 km, but the densities were calculated using all locations (24 and 39 values were greater than 20 km for the observed-unobserved and observed-available data, respectively).

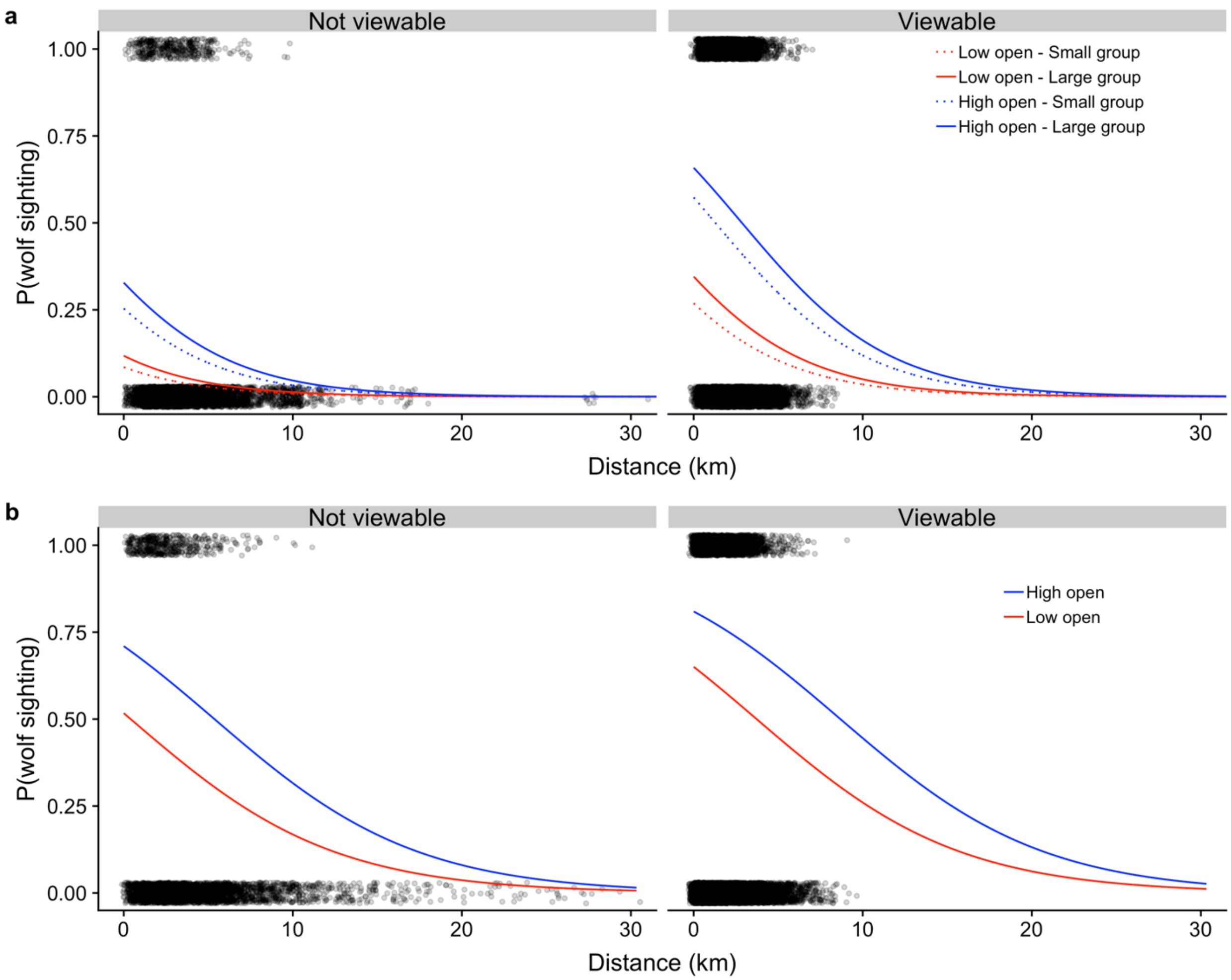

**Figure S3-B.5. Predicted probability of sighting a wolf group for a) observed-unobserved and b) observed-available common observation point model.** Panel (a) is the predictions for the observed-unobserved model (*viewshed* + *distance* + *openness* + *group size*; also presented in the main text). Panel (b) displays the predictions for the observed-available model (*viewshed* + *distance* + *openness*; predictions for the observed-available model do not include the intercept – see Appendix S3-B text). For both panels, values used to display openness are 111.5 (low) and 241.8 (high), and 6 (low) and 12 (high) for group size. These values were the lower and upper quartiles for the observed-unobserved data. For context, the upper and lower quartiles for the observed-available data were 109.4 and 250.0 for openness and 5 and 11 for group size.

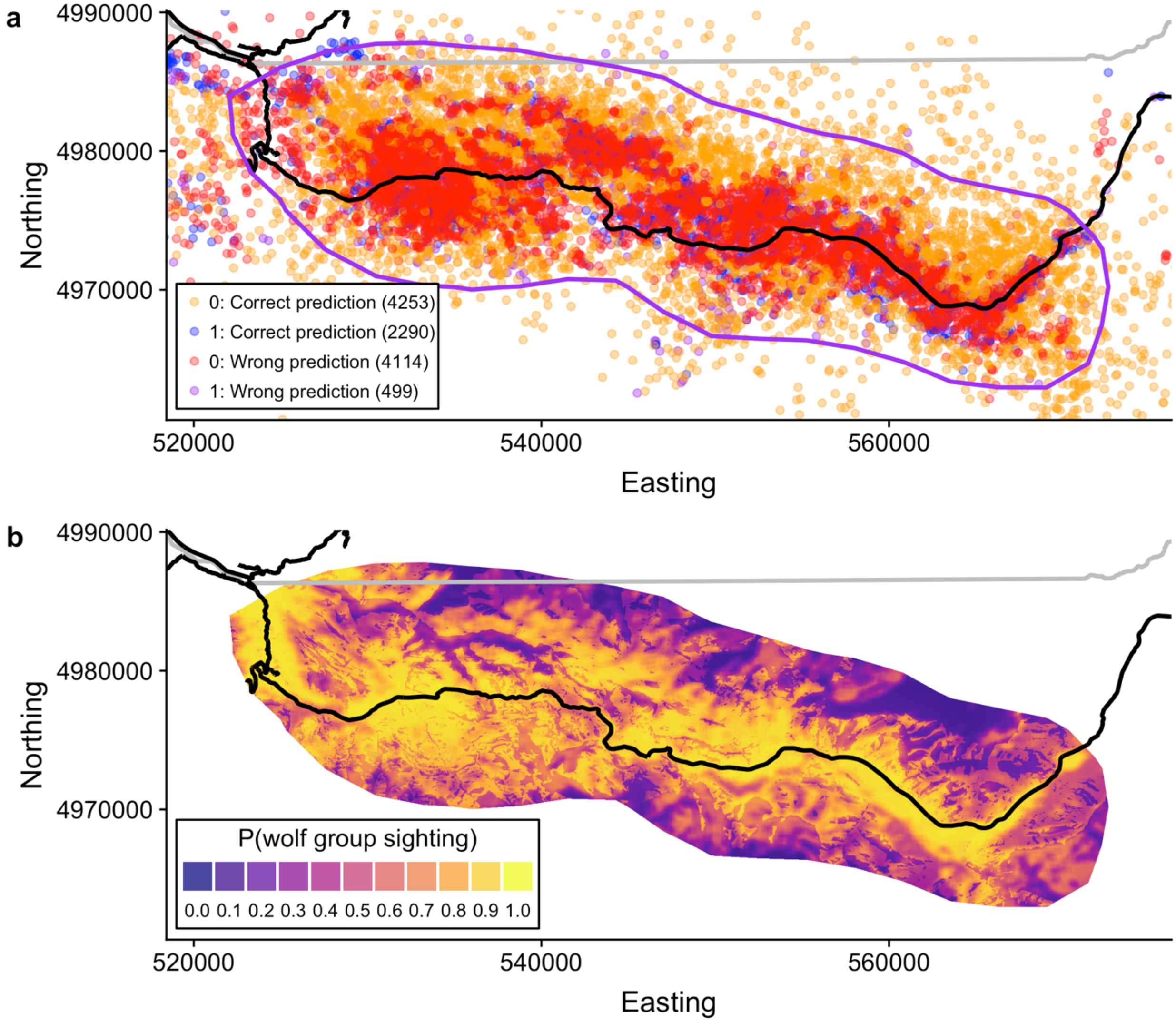

**Figure S3-B.6. Spatial predictions for observed-available wolf sightability model.** Panel (a) displays the classification success for model-based predictions for the actual data set, using the optimal cutpoint (see Table S3-B.2). The legend reports the confusion matrix for the 11,156 observed-available locations. In panel (b), we used the beta coefficients to create spatial predictions (see further details in Appendix S3-C) for a pack that was monitored from the minimum road and common observation points (from before wolf harvest was implemented; see Fig. S3-B.1a) and openness values from 2001 (see Fig. S3-B.1b). Note that the purple line in panel (a) displays the 85% population-level utilization distribution that was used for panel (b), and that the black and gray line in each panel display the minimum road and Yellowstone National Park boundary, respectively.

## Chapter 3: Appendix S3-C. Developing maps for p(wolf group sighting).

For the top observed-unobserved and observed-available sightability model, our mixed-effect models did not converge with non-scaled covariates. To build spatial predictions for our study area (Fig. 3-4b, Fig. S3-B.6b), we therefore standardized the underlying raster values for the continuous covariates (i.e., distance, openness) included in our top models (Table S3-A.1, Table S3-B.1).

We standardized a single raster dataset for each covariate. That is, both distance and openness were time-varying in a sense – there were five years for which openness data was available and distance to an actual wolf location is dependent on the road (minimum or maximum) and observation points being used by observation crews. But given that the 'best' temporal representation of a covariate was used during our analysis, the effect of each covariate should not differ across time. For example, a wolf being in a heavily forested area should always negatively affect p(sighting). Therefore, we built our p(sighting) maps with the coefficients from our top observed-unobserved and observed-available moderate observation point models, but applied them to single rasters for distance (minimum road and moderate observation points) and openness (2001). As such, our raster predictions represent what predicted wolf group sightability looks like for the underlying rasters.

The initial underlying rasters that we extracted our covariates from had a much larger spatial extent than the spatial extent of most wolf locations in our data sets. We therefore clipped our rasters to 85% utilization distributions for the observed-unobserved and observed-available data (Fig. 3-4, Fig. S3-B.6). We used 85% utilization distributions in an attempt to most closely match the statistical nature of the covariates for the rasters and wolf data (Table S3-C.1, Fig. S3-C.1). Ultimately, we standardized these rasters using the scale function in program R, centering and scaling the rasters using the means and standard deviations for the wolf data (Table S3-C.1). To build our p(sighting) maps, we applied equation 1 (observed-unobserved) or Appendix S3-B: equation 1 (observed-available), using the beta coefficients from our top models and these standardized raster values. In both cases, the maps represent the spatial predictions for an "average pack".

**Table S3-C.1. Summary statistics for raster and wolf data for observed-unobserved and observed-available data.**

| Dataset | Data | Covariate | Mean | SD | Minimum | Maximum |
|---|---|---|---|---|---|---|
| O-U | Wolf | Distance | 3.07 | 2.42 | 0.01 | 37.24 |
| O-U | Raster | Distance | 3.01 | 2.17 | 0.00 | 10.41 |
| O-U | Wolf | Openness | 171.42 | 81.79 | 0.00 | 289.00 |
| O-U | Raster | Openness | 166.56 | 88.72 | 0.00 | 289.00 |
| O-A | Wolf | Distance | 2.81 | 2.76 | 0.00 | 30.33 |
| O-A | Raster | Distance | 3.05 | 2.06 | 0.00 | 9.28 |
| O-A | Wolf | Openness | 174.54 | 86.74 | 0.00 | 289.00 |
| O-A | Raster | Openness | 155.99 | 90.12 | 0.00 | 289.00 |

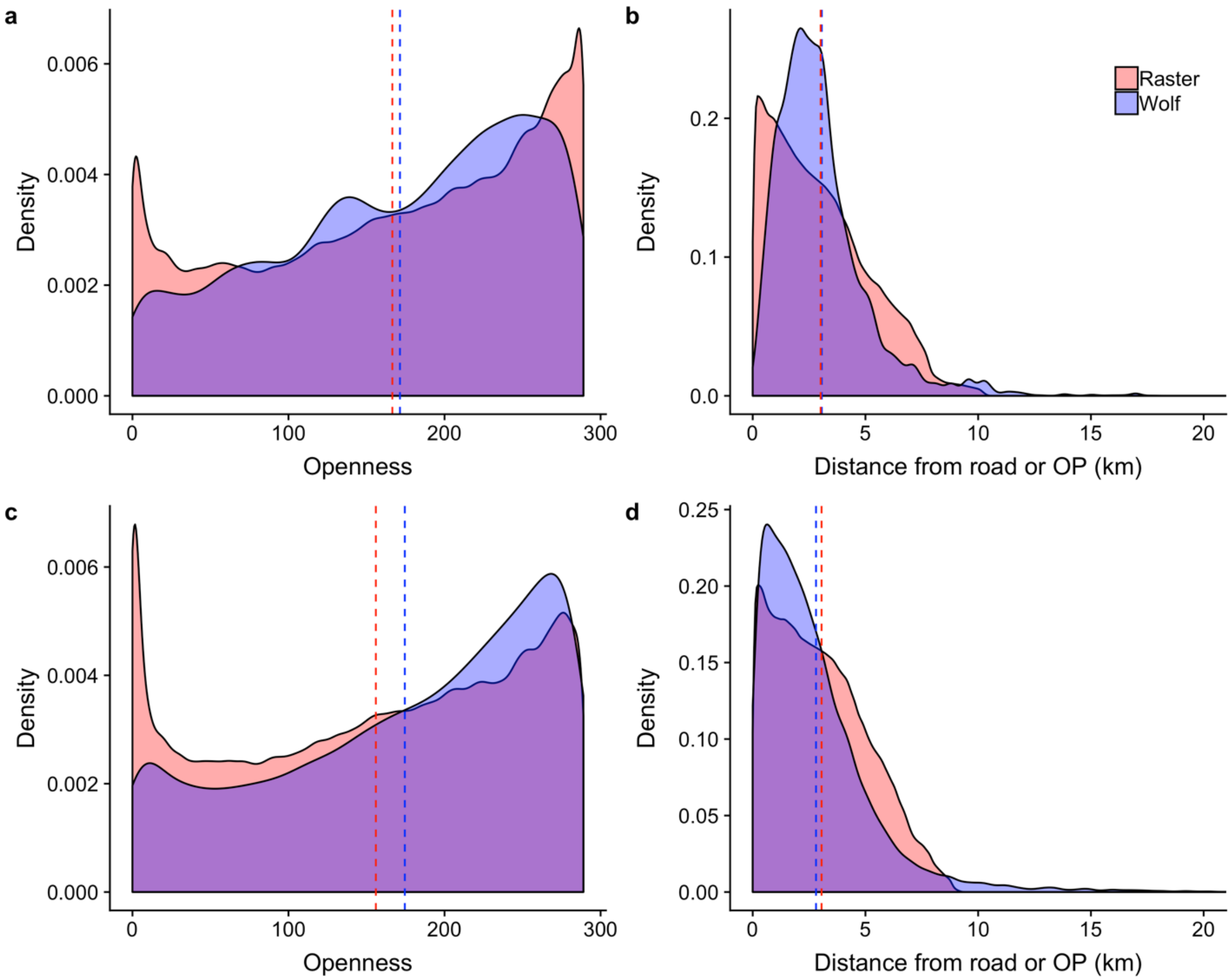

**Figure S3-C.1. Distribution of openness and distance covariates for wolf data and rasters used for spatial predictions.** Panels (a) and (b) display observed-unobserved data, while panels (c) and (d) display observed-available data. Dashed lines represent the mean value (Table S3-C.1).

# Chapter 4: Appendix S4-A. Supporting methodological text and figures.

## SUPPORTING METHODS

### Very High Frequency (VHF) data

Radio-tracking location data from VHF-collared wolves was a foundational data type collected throughout our study. We used this core data to 1) characterize the spatial affiliation(s) for a pack and, consequently, also censor data, 2) score whether we observed a pack for a day (binomial: 1, 0) during a roaming period session, and 3) estimate pack size for both the roaming and denning periods. Here, we provide details related to how we collected data through radio-tracking wolf packs.

During the roaming period and as weather permitted, we attempted to locate wolf packs on each day of each study session. The air method generally radio-tracked each pack once per flight through attempting to locate each VHF-collared wolf within a pack, including when wolves from the pack were in multiple groups. Occasionally, wolf groups without radio-collars were observed; these observations were retained if the pack-session was not ultimately censored from our data. For each location of a wolf group, we recorded the number of wolves present. The number of radio-collared wolves provided a minimum number of wolves for groups that were not (completely) visually observed.

On each day of the study session, ground observers also attempted to locate a focal subset of packs (see Chapter 4). If one of these packs was in multiple groups, the ground observers often attempted to locate secondary groups of wolves. Whether ground observers attempted to locate secondary wolf groups was influenced by staff availability and the conditions surrounding the already observed wolf group(s) (e.g., which and how many wolves were present, had a carcass been detected with them, were radio-signals audible for secondary wolves). With varying frequency, ground observers also opportunistically monitored pack-sessions that were only intended to be monitored by the air method (see Chapter 4).

Air and ground method-acquired locations of pack-groups were then each filtered to a single, distinct set of pack-level locations for each day. To do so, we first censored ‘lone’ wolves who were rarely with the pack (possibly only known from outside the study session), unless a lone wolf was with a group of wolves from the pack on a particular day. Next, we reduced our locations for each monitoring method to a set of unique locations where an individual wolf was only present in one group for the pack on a day and the number of wolves summed across groups in the pack for a day was greatest. These distinct sets of daily pack-group locations were ultimately used to *i*) censor packs, *ii*) characterize how frequently a pack used the Northern subsystem, and *iii*) minimally count the number of wolves for a pack on each day (see *Spatial affiliation* and *Pack size* below).

During the denning period, aerial radio-tracking of wolf packs was done approximately weekly. Opportunistic ground-based radio-tracking occurred with varying intensity, and depended on the movements of a wolf pack and logistical constraints. Because of the infrequent nature of radio-tracking during the denning period, we often used data from late winter sessions, to estimate wolf pack size during the denning period (see *Pack size* below*).*

### SPATIAL AFFILIATION

We used our aforementioned VHF observations during the roaming period to *i*) begin censoring packs and *ii*) characterize how frequently a pack used the Northern subsystem. To do so, we first extracted whether each location was *i*) inside YNP (1 = inside, 0 = outside) and *ii*) within the Northern subsystem (Fig. S4-A.1). We extracted this information for all pack locations that had x,y coordinates assigned. Next, we reduced our data set to a single pack observation for the day. We did so through preferentially selecting the pack's location where the greatest number of wolves were observed, randomly selecting a single location on days where the maximum group size occurred more than once (i.e., because the pack was in multiple groups and/or the air and ground methods each observed a group of wolves with the same maximal count). For context, 8,245 of 9,015 (91.5%) unique group-level observations had x, y coordinates assigned for our 349 pack-sessions that we ultimately included (ground observers: 3,143 of 3,785 [83.0%]; aerial observers: 5,102 of 5,230 [97.6%]). After reducing this data to a single location for each pack-day, 5,996 locations (3,545 aerial and 2,451 ground) remained, with 17.2 locations, on average, for a pack-session (± 0.4 SE; range: 3 – 30). We then used these unique daily observations to first censor all wolf packs with <0.6 locations within YNP (Fig. S4-A.1). For the pack-sessions that remained, we next characterized how frequently a pack used the Northern subsystem ('No' = ≤0.2, 'Partial' = 0.2–0.6, 'Yes' = ≥0.6) because *i*) evaluating wolf predation dynamics in Northern YNP is a primary focus of our research and *ii*) we used a 'stricter' definition of Northern pack-sessions in Chapter 5, where we censored 'Partial' packs.

For those pack-sessions that remained, we also characterized where the pack more precisely resided within YNP. To do so, we created 70% Minimum Convex Polygons for each early or late winter session, using VHF data from 3-month periods (October–December; January–March) to increase sample size for territory estimation. We ultimately used the centroid location to characterize a pack as centering their territory in the 'Northern-Lower', 'Northern-Middle', 'Northern-Upper', 'Interior-Central', or 'Interior-West' zone (Figs. S4-A.2, S4-A.3). To do so, we first characterized a pack as Northern (i.e., centroid in Northern subsystem) or Interior. For Northern pack-sessions, we then extracted which zone the centroid was located within. For those Northern pack-sessions where the centroid was outside of the historic Northern

Range boundary where Northern zones were defined (see Fig. 4-2), we determined their zone through the Euclidean distance between the centroid and the within-Northern Range zone boundaries. For Interior pack-sessions, we characterized each pack session zone as 'Interior-Central' or 'Interior-West', again depending on the centroid location. Initially, we also characterized some pack-sessions as 'Southern' (white space in Fig. 4-2), but we subsequently censored these packs (see Chapter 4). Note that we did retain one pack (Nez Perce, Late Winter 2002) initially classified as Southern, but recharacterized this pack as West, because their territory polygon was fully contained within our West region (the centroid fell outside of West because of an extraterritorial foray). Ten pack-sessions did not have enough VHF locations to estimate a territory. We censored eight of these pack-sessions that were from Southern or fringe-YNP packs, retaining two that were clearly Northern YNP packs. We used the mean easting and northing values from wolf locations to characterize these two pack-sessions, characterizing each as 'Northern-Upper'.

Following censoring, 385 pack-sessions remained for the roaming period. We then censored an additional 36 pack-sessions for which we did not detect any feeding events (Chapter 4; Figs. S4-A.1, S4-A.2). The remaining 349 pack-sessions provided the basis for all analyses during the roaming period.

During the denning season, we only estimated predation metrics for packs that lived in the Northern subsystem of YNP. We similarly created 70% Minimum Convex Polygons to determine the spatial zone for these pack-sessions (Figs. S4-A.2, S4-A.3). To do so, we used the GPS data for the GPS-collared wolves (i.e., those wolves where we were attempting to search GPS clusters for; see Chapter 4) belonging to that pack during the dates of that pack-session (Table S4-A.1b).

## BINOMIAL SCORING OF DAYS FOR AERIAL AND GROUND METHODS

At the conclusion of each day, we scored (binomial: 1, 0) whether we thought the aerial and ground methods each radio-located or visually observed most of the pack for the day. We scored each day in this manner because observations were sometimes affected by wolves being in areas where accurate counts were harder to obtain (*sensu* Metz et al. 2020). Our binomial classification was well supported by the raw data about pack size that described our observations (Fig. S4-A.4).

## PACK SIZE

During the roaming period, we estimated pack size through summing our unique daily observations for each pack or through using previously reported estimates for Yellowstone wolf packs. These previously reported estimates were considered the most representative count at the end of the calendar (end of December) or biological (end of March) wolf year, but were not always representative of pack size during our study sessions. We therefore assigned pack size by 1) using the count that occurred at least twice during a study session (following Smith et al. 2004) when *i)* we located a pack at least 10 times during the study session and *ii)* the pack size was within 3 wolves of those previously reported ($n$ = 289); 2) using the maximum count for the month when *i)* we located a pack less than 10 times during the study session and *ii)* the pack size was within 2 wolves of those previously reported ($n$ = 54). For the remaining 6 (1.7%) occasions when our thresholds were exceeded, we evaluated whether our within study session estimate or known estimates were most representative of the pack's size. We used the high count acquired at least twice for five of the six occasions, and the known estimate for the final occasion.

During the denning period, we usually had little information about pack size because wolves often travel less cohesively (Benson and Patterson 2015) and observing wolves to acquire complete group counts is difficult without snow cover. Moreover, logistical constraints prevented daily tracking (see above). We therefore used our estimates for pack size from late winter, enhanced with data from denning period observations. Specifically, we modified pack size estimates to account for known death or dispersals during the denning period, and also used observations strictly from the denning period when a pack did not exist during the previous late winter session. We used the cumulative knowledge from these observations to characterize pack size for each day of a pack-session. Then, we used these daily estimates to estimate pack size *i*) across the entire denning period pack-session as the mean value for that pack-session and *ii*) within each calendar month of a pack-session as the most frequent value for the month (see Chapter 4).

**Global Positioning System (GPS) data**

We created GPS clusters for wolf-study sessions that included field search effort of GPS locations (Table S4-A.1). For each GPS cluster, we assigned whether we intended to search it, which simply specified whether field efforts to search that wolf's GPS clusters were ongoing. We characterized a cluster as intend-to-search when it contained at least one GPS location from when we were actively attempting to field-search clustered GPS locations for the wolf.

We used the data associated with GPS cluster feeding event detections to develop our model to estimate feeding event abundance for both the roaming and denning periods. In rare cases, we censored information about GPS cluster searches when developing our abundance estimators. Specifically, we censored data not clearly associated with wolf pack-sessions through removing data when wolves were not a member of a pack and when a wolf was only loosely associated with a pack. Additionally, we censored data from one wolf during a denning period because both pack members were GPS-collared, and the censored wolf's collar quit functioning during the pack-session. We also censored 23 clusters from the roaming period, and 12 clusters from the denning period, when a wolf was known to be dispersing from a pack.

### GPS CLUSTER SEARCHES FOR ABUNDANCE ESTIMATORS

*Roaming period.* We searched 4,505 of the 4,765 (94.5%) intend-to-search GPS clusters that were identified for wolves belonging to packs during the roaming period (Table S4-A.1a). Logistical constraints (e.g., field technician safety, private land) sometimes precluded searching GPS clusters. We used multiple field methods to search GPS clusters to maximize the number of clusters searched and eliminate unnecessary field effort. Specifically, we searched GPS clusters in the following ways:

1) <u>Observational feeding event detection</u>: a feeding event(s) was detected through ground or aerial method observations during the time period associated with the GPS cluster. Note that nearly all GPS clusters searched through this method were also searched through boots on the ground (see below) and/or searching the cluster area during the carcass necropsy; thereby also investigating the area for additional carcasses that may have been present.

2) <u>Ground method observation</u>: the ground method observed the wolves at the GPS cluster and did not detect a feeding event. To essentially eliminate the possibility of the ground method not detecting a feeding event(s) that was actually present, we searched GPS clusters through boots on the ground (see below) when wolves were not observed during the period of GPS cluster initiation. If we did not search GPS clusters where feeding events may have been present, we classified the cluster as not being searched.

3) Boots on the ground: Field crews visited the cluster and investigated a ≥ $400m^2$ area around each individual wolf GPS location (Metz et al. 2011).

4) Aerial method observation: Rarely, we classified a GPS cluster as searched by the aerial method if *i*) the aerial method observed the wolves at the GPS cluster, *ii*) the GPS locations that created the cluster were tightly concentrated, *iii*) the wolves were in an area of open cover, and *iv*) logistics prevented searching the GPS locations through boots on the ground.

5) Aerial search: Rarely, we searched a GPS cluster through flying to the GPS cluster and visually observing the site after the wolves had left the area. We did so on only two occasions when the clusters were in the open and logistical constraints prevented us from being able to search the sites through boots on the ground.

6) Wolf homesite: During late winter sessions that immediately precede the wolf denning season, wolves would sometimes investigate historic denning sites. In some of these cases (n = 13), we did not search the associated GPS clusters through boots on the ground because we did not want to interfere with wolf densite selection. Nonetheless, we were confident that no feeding events existed at these GPS clusters, and therefore assigned no carcass as being present.

7) Previous search: Rarely, we classified a cluster as searched through a previous search when logistics prevented us from again searching the cluster. In these cases, the cluster was in the same precise location as a previously searched cluster that contained a feeding event.

8) Carcass dump: Rarely, grizzly bear safety precautions prevented us from searching clusters located at a “carcass dump”, where National Park Service staff occasionally placed animals that died in the immediate vicinity of a road. In these cases, we knew the characteristics of any carcass(es) present at the site.

Because we re-identified our GPS clusters using the R package `GPSeqClus` (Clapp et al. 2021), we did not always search every GPS location of a cluster. We considered these re-identified GPS clusters to be searched when we detected a feeding event or searched ≥60% of the locations (Fig. S4-A.5). We characterized how a cluster was searched by the search type that was most frequent among locations, with the above list displaying the hierarchical order used for the rare cases where the most frequent number was shared by multiple search types.

Boots on the ground, observational feeding event detection, and ground observation combined to be the dominant manner in which a cluster was searched for 4,472 of the 4,505 (99.3%) searched clusters (Table S4-A.2). On average, we searched GPS clusters 6.1 days (± 0.1 SE; range: 0 – 136) after wolves initiated (when we visually observed wolves to search the cluster) or ended the cluster (Fig. S4-A.6).

We used these GPS cluster searches to score (binomial) whether the GPS method attempted to detect any feeding events for a pack on a day by characterizing a day as having GPS method effort if any GPS cluster location on the day was searched. We adjusted dates so that those locations at ≥18 LMT hour during early winter (maximum sunset at Mammoth Hot Springs was 16:56; United States Naval Observatory; http://aa.usno.navy.mil/data) and ≥20 LMT hour (maximum sunset was 18:48) during late winter were assigned to the next date. We also used these adjustments to align GPS cluster feeding event detections with when the aerial or ground method could have first found any feeding events at a cluster (see *Assigning Feeding Events to GPS Clusters* below).

*Denning period.* We searched 6,007 of the 6,394 (93.9%) intend-to-search GPS clusters that were identified for wolves during the denning period (Table S4-A.1b) in the following ways:

1) Boots on the ground: Same as during the roaming season.
2) Wolf homesite: We field-searched most homesite clusters. Often, we did not search every GPS location because of the large number of GPS locations associated with tending pups. In many cases, we therefore searched the homesite clusters by extensively walking throughout the homesite. Additionally, note that we considered homesite clusters that we could not field search as searched when modeling feeding event abundance (see Chapter 4).
3) Wolf homesite (other pack): On one occasion, a wolf created a GPS cluster at another pack's homesite. We assumed there was no feeding event at this GPS cluster.

We determined whether, and how, a cluster was searched during the denning period in the same manner in which we did for the roaming period (Table S4-A.2). We field-searched GPS clusters 19.4 days (± 0.3 SE; range: 0 – 140) after wolves ended a GPS cluster (Fig. S4-A.6). Many clusters that were not quickly searched were either a homesite, or in close proximity to a homesite, and were not quickly searched in order to avoid disturbing the wolf pack.

### ASSIGNING FEEDING EVENTS TO GPS CLUSTERS

We detected feeding events at GPS clusters through our aforementioned search types. For each wolf, we assigned a feeding event as being associated with a cluster when any cluster location was within 100-m of the carcass. In rare cases, we needed to adjust or add carcass "source" locations. Specifically, we adjusted x,y source locations when the precision of the carcass spatial location resulted in no GPS locations for a wolf within 100-m of the actual carcass site (n = 2 [roaming], n = 0 [denning]). We also added a second x,y source location when 1) wolf feeding activity associated with the carcass resulted in field evidence of a carcass only at nearby bedding sites (n = 5 [roaming], n = 1 [denning]) or 2) National Park Service management activities moved carcasses away from roads and/or trails (n = 8 [roaming], n = 2 [denning]). We allowed feeding event assignment to any GPS cluster that had a location within 100-m of any of these source x,y locations. Note that any spatially-varying covariates associated with a feeding event were assigned from the actual carcass location.

Feeding events could be associated with multiple GPS clusters for a wolf, and, therefore, we characterized how a cluster was associated with a feeding event. First, we preferentially identified the cluster containing the actual feeding event as the first cluster *i*) within a 3-day detection window and *ii*) with a location within 50-m of the carcass, when applicable. We used a 3-day detection window because GPS locations often accumulated for 3 days (Fig. S4-A.7; note, however, that GPS detection in our multiple-detection method, mark-recapture estimator during the roaming period was ultimately limited to 2-days; see Chapter 4 and below). The 3-day detection window began when a feeding event was first detected for a pack. During the roaming period, the 3-day detection window could have been initiated by aerial or, in the case of packs monitored by the ground method, ground method detection, if the aerial or ground method detection was from a date before the first GPS location. Second, we assigned carcass association as secondary for all remaining associated clusters within the 3-day detection window. Finally, we characterized any remaining clusters (i.e., those from outside the 3-day detection window) as feeding event revisits, which were not used in our abundance estimation.

From any of the feeding event-associated clusters that began within three days of GPS cluster creation, we assigned the (adjusted) date-time of GPS cluster detection for the wolf as the minimum date-time of a cluster location after the prey animal died (rarely, cluster locations occurred prior to when the prey animal died; 30 of 11,093 intended-to-search cluster locations during the roaming period; 287 of 16,700 intended-to-search cluster locations during the denning period). In cases with multiple wolves in a pack, the minimum (adjusted) date-time of a wolf-level GPS cluster detection represented the pack-level date-time of GPS cluster detection. For a wolf to contribute to a pack-level detection, the wolf had to 1) have clusters searched during the study session and 2) been characterized as a member of the pack at some point during the study session.

GPS clusters were created using 3-day location windows, but feeding event detection was limited to two days for our multi-observer (i.e., detection method), mark-recapture abundance estimator during the roaming period. Therefore, we censored any GPS detections without any GPS locations within two days of the minimum (i.e., across detection methods) date-time of feeding event detection (see Chapter 4). Doing so removed 1 of 568 GPS detections of feeding events by a wolf during the roaming period (Fig. S4-A.7a).

## Carcass data

### ROAMING PERIOD

We ultimately included 2,307 ungulates, and 2,343 feeding events, in our data set for the roaming period following data censoring. We first censored all ungulate carcasses that were not fed on by the 349 pack-sessions included in our analysis. Next, we censored 1) species (e.g., wolves, coyotes, eagles) that wolves killed but did not usually feed on, 2) ungulates that we opportunistically detected while hiking for other purposes (e.g., to necropsy known kills or search GPS clusters) because we often could not definitively assign a pack and these carcasses were precisely what our abundance model was designed to estimate, 3) three secondary ungulates found only while necropsying carcasses detected by the aerial method, 4) ten small prey (4 badgers, 2 leporids, 1 goose, 1 grouse, 1 otter, 1 short-eared owl) and one grizzly bear, and 5) eight ungulates that were detected but from which wolves were unable to feed on (typically because frozen under ice).

We also censored two ungulates that were detected through GPS data after the defined dusk hour on the final day of a study session (see Chapter 4). Finally, we censored feeding events for included pack-sessions that were detected through opportunistic effort (i.e., only the ground method detected feeding events for packs designed to be monitored only by the air method). We did, however, include this ground method knowledge when assigning the biomass covariate values for 21 carcasses that were also acquired by pack-sessions monitored by the ground or GPS methods (see Appendix S4-B).

*Carcass characteristics*. We identified species, sex, and age class of wolf-acquired ungulates through hair and skull characteristics, as well as body size. We did not include whether deer were mule deer or white-tailed deer because deer were usually too consumed to identify beyond ‘deer’. When possible, we identified these demographic characteristics during ground and aerial team observations. But we also necropsied as many carcasses as possible (1,709 of 2,307; 74%), including all that were detected through field GPS cluster searches. During necropsies, we confirmed and/or identified the species, sex, and age (class) through evaluating the same characteristics and/or tooth eruption patterns. When possible and when we could not definitively age the ungulate through tooth eruption patterns, we also extracted a tooth for cementum aging. The demographic characteristics assigned to carcasses were important for assigning our biomass covariate (see Appendix S4-B) and for our analyses that involved this demographic information.

We evaluated how well the aerial team identified demographic characteristics through a subset of data where the aerial team recorded information about the demographic characteristics of carcasses that were later necropsied. The aerial team correctly identified the species on 497 of 506 (98.2%) occasions. Elk and bison represented 479 of the 497 (96.4%) cases of correct species identification, and the aerial team also adequately described the demographic characteristics within these species. For example, the air team correctly identified an adult elk as an adult in 276 of 298 cases (92.6%) and a calf elk as being a calf in 69 of 77 cases (89.6%). Among bison, the air team correctly identified an adult as being an adult in 25 of 27 (92.6%) cases, and correctly identified a calf as such in all 6 cases. This high level of correct identification of demographic characteristics likely resulted in misidentification in non-necropsied carcasses having minimal effect on our results.

Each carcass was assigned a spatial location through the best available measurement. As such, we used 1,492 (64.7%) carcass spatial locations recorded with a GPS unit during necropsies or estimated from wolf GPS locations, 653 (28.3%) recorded from the airplane, and 162 (7.0%) estimated on a topographic map. During many necropsies (*n* = 1,489), we also recorded the spatial location of each carcass using a handheld GPS unit. We used these spatial locations when extracting our spatial covariates (see Chapter 4). From a subset of carcasses where we recorded a spatial location with a handheld GPS unit and at least one other method, aerial carcass locations were 75.9 m (± 2.8 SE; range: 1 – 890; *n* = 541), and topographic map-based estimates were 237.3 m (± 12.5 SE; range: 7 – 2182; *n* = 401), from the handheld GPS unit carcass location. Overall, these errors tended to be relatively small (Fig. S4-A.8) and likely had little effect on our estimates for the number of feeding events.

Rarely, carcasses existed at multiple spatial locations because management concerns caused NPS staff to move carcasses. Specifically, carcasses were moved locally to increase the distance between the carcass and the road or moved a significant distance and then placed in a 'carcass dump' where wolves could potentially feed on them. In these cases, we assigned the first spatial location where the carcass was detected and/or could have been used by the wolves that we ultimately detected at it.

### DENNING PERIOD

We ultimately included 838 ungulates, and 846 feeding events, in our data set for the denning period following the censoring of our data. We specifically censored species (e.g., wolves, coyotes, foxes) that wolves killed but did not usually feed on, 21 small prey (6 badgers, 5 leporids, 2 goose, 2 grouse, 2 unknown waterfowl, 1 ground squirrel, 1 long-tailed weasel, 1 porcupine, 1 unknown bird) and three bears (2 grizzly, 1 black).

## LITERATURE CITED

Benson, J. F., and B. R. Patterson. 2015. Spatial overlap, proximity, and habitat use of individual wolves within the same packs. Wildlife Society Bulletin **39**:31-40.

Clapp, J. G., J. D. Holbrook, and D. J. Thompson. 2021. GPSeqClus: An R package for sequential clustering of animal location data for model building, model application and field site investigations. Methods in Ecology and Evolution **12**:787-793.

Metz, M. C., J. SunderRaj, D. W. Smith, D. R. Stahler, M. T. Kohl, K. A. Cassidy, and M. Hebblewhite. 2020. Accounting for imperfect detection in observational studies: modeling wolf sightability in Yellowstone National Park. Ecosphere **11**:e03152.

Metz, M. C., J. A. Vucetich, D. W. Smith, D. R. Stahler, and R. O. Peterson. 2011. Effect of sociality and season on gray wolf (*Canis lupus*) foraging behavior: implications for estimating summer kill rate. Plos One **6**:e17332.

Smith, D. W., T. D. Drummer, K. M. Murphy, D. S. Guernsey, and S. B. Evans. 2004. Winter prey selection and estimation of wolf kill rates in Yellowstone National Park, 1995–2000. Journal of Wildlife Management **68**:153-166.

**Table S4-A.1a.** GPS-collared wolves included in the roaming period feeding event abundance estimator. All numbers are for clusters including locations for that pack, with searched, total, and proportion referring to unique GPS clusters. In the rare cases where wolves had an identified cluster that spanned their affiliation with two packs, we assigned the pack affiliation with the most locations.

| Session | Wolf | Pack | Searched | Total | Proportion | Start | End^ |
|---|---|---|---|---|---|---|---|
| EW 2009 | 0692F | Blacktail^^ | 67 | 74 | 0.91 | 11/15/09 | 12/14/09 |
| EW 2009 | 0693F | Blacktail^^ | 70 | 79 | 0.89 | 11/15/09 | 12/14/09 |
| LW 2010 | 0642F | Blacktail^^ | 89 | 95 | 0.94 | 3/1/10 | 3/30/10 |
| LW 2010 | 0752F | Blacktail^^ | 79 | 83 | 0.95 | 3/1/10 | 3/30/10 |
| EW 2010 | 0642F | Blacktail | 61 | 89 | 0.69 | 11/15/10 | 12/14/10 |
| LW 2011 | 0775M | Agate Creek | 95 | 98 | 0.97 | 3/1/11 | 3/30/11 |
| LW 2011 | 0777M | Blacktail | 93 | 95 | 0.98 | 3/1/11 | 3/30/11 |
| EW 2011 | 0777M[1] | Blacktail | 23 | 24 | 0.96 | 11/15/11 | 11/22/11 |
| LW 2012 | 0777M[2] | Agate Creek | 28 | 28 | 1 | 3/21/12 | 3/30/12 |
| LW 2012 | 0777M[2] | Blacktail^^ | 44 | 45 | 0.98 | 3/6/12 | 3/21/12 |
| LW 2012 | 0829F | Blacktail^^ | 80 | 83 | 0.96 | 3/1/12 | 3/30/12 |
| LW 2012 | 0832F | Lamar Canyon | 64 | 70 | 0.91 | 3/1/12 | 3/30/12 |
| EW 2012 | 0832F | Lamar Canyon | 54 | 63 | 0.86 | 11/15/12 | 12/6/12 |
| LW 2013 | SW763M | 8 Mile | 101 | 112 | 0.9 | 3/1/13 | 3/30/13 |
| LW 2013 | 0889F | Junction Butte^^ | 63 | 64 | 0.98 | 3/7/13 | 3/30/13 |
| LW 2013 | 0890M[3] | Junction Butte^^ | 44 | 44 | 1 | 3/7/13 | 3/27/13 |
| EW 2013 | SW763M | 8 Mile | 87 | 89 | 0.98 | 11/15/13 | 12/14/13 |
| EW 2013 | 0890M | Junction Butte | 77 | 79 | 0.97 | 11/15/13 | 12/14/13 |
| LW 2014 | 0889F | 755M/889F Group^^ | 53 | 81 | 0.65 | 3/1/14 | 3/30/14 |
| LW 2014 | 0911M | 755M/889F Group^^ | 54 | 75 | 0.72 | 3/1/14 | 3/30/14 |
| LW 2014 | 0890M | Junction Butte^^ | 74 | 76 | 0.97 | 3/1/14 | 3/30/14 |
| LW 2014 | 0907F | Junction Butte^^ | 73 | 74 | 0.99 | 3/1/14 | 3/30/14 |
| LW 2014 | SW763M | Prospect Peak | 77 | 80 | 0.96 | 3/1/14 | 3/30/14 |
| EW 2014 | 0907F | Junction Butte | 82 | 83 | 0.99 | 11/15/14 | 12/14/14 |
| EW 2014 | SW763M | Prospect Peak | 88 | 89 | 0.99 | 11/15/14 | 12/14/14 |
| LW 2015 | 0967M[4] | 967M Group | 19 | 21 | 0.9 | 3/22/15 | 3/30/15 |
| LW 2015 | 0907F | Junction Butte^^ | 80 | 82 | 0.98 | 3/1/15 | 3/30/15 |
| LW 2015 | 0911M | Junction Butte^^ | 75 | 77 | 0.97 | 3/1/15 | 3/30/15 |
| LW 2015 | 0967M[4] | Lamar Canyon | 49 | 59 | 0.83 | 3/1/15 | 3/22/15 |
| LW 2015 | 0964M | Prospect Peak | 79 | 80 | 0.99 | 3/1/15 | 3/30/15 |
| EW 2015 | 0911M | Junction Butte | 27 | 28 | 0.96 | 11/15/15 | 11/24/15 |
| EW 2015 | 0964M | Prospect Peak | 92 | 92 | 1 | 11/15/15 | 12/14/15 |
| LW 2016 | 0993M | Lamar Canyon | 83 | 86 | 0.97 | 3/1/16 | 3/30/16 |

| | | | | | | | |
|---|---|---|---|---|---|---|---|
| LW 2016 | 0996M | Prospect Peak[^^] | 85 | 85 | 1 | 3/1/16 | 3/30/16 |
| LW 2016 | 1012M | Prospect Peak[^^] | 40 | 40 | 1 | 3/1/16 | 3/14/16 |
| EW 2016 | 1005F | 8 Mile | 69 | 74 | 0.93 | 11/15/16 | 12/6/16 |
| LW 2017 | 0962M | 8 Mile[^^] | 82 | 88 | 0.93 | 3/1/17 | 3/30/17 |
| LW 2017 | 0963F[5] | 8 Mile[^^] | 66 | 80 | 0.83 | 3/1/17 | 3/30/17 |
| LW 2017 | 0821F | Prospect Peak[^^] | 74 | 81 | 0.91 | 3/1/17 | 3/30/17 |
| LW 2017 | 0964M | Prospect Peak[^^] | 56 | 61 | 0.92 | 3/1/17 | 3/21/17 |
| EW 2017 | 0962M | 8 Mile | 93 | 94 | 0.99 | 11/15/17 | 12/14/17 |
| EW 2017 | 1047M | Junction Butte | 77 | 77 | 1 | 11/15/17 | 12/14/17 |
| LW 2018 | 0962M | 8 Mile[^^] | 79 | 82 | 0.96 | 3/1/18 | 3/30/18 |
| LW 2018 | 1005F | 8 Mile[^^] | 96 | 98 | 0.98 | 3/1/18 | 3/30/18 |
| LW 2018 | 1107M | Crevice Lake | 89 | 89 | 1 | 3/1/18 | 3/30/18 |
| LW 2018 | 0907F | Junction Butte[^^] | 82 | 84 | 0.98 | 3/1/18 | 3/30/18 |
| LW 2018 | 1047M | Junction Butte[^^] | 75 | 77 | 0.97 | 3/3/18 | 3/30/18 |
| LW 2018 | 1109F | Junction Butte[^^] | 83 | 88 | 0.94 | 3/1/18 | 3/30/18 |
| EW 2018 | 1005F[6] | 1005F Group | 48 | 51 | 0.94 | 11/15/18 | 12/8/18 |
| EW 2018 | 1005F[6] | 1005F/1107M Group[^^] | 30 | 33 | 0.91 | 11/15/18 | 12/8/18 |
| EW 2018 | 1107M[6] | 1005F/1107M Group[^^] | 59 | 62 | 0.95 | 11/15/18 | 12/14/18 |
| EW 2018 | 1107M[6] | Crevice Lake | 43 | 44 | 0.98 | 11/15/18 | 12/14/18 |
| EW 2018 | 0907F | Junction Butte[^^] | 71 | 72 | 0.99 | 11/15/18 | 12/14/18 |
| EW 2018 | 1047M | Junction Butte[^^] | 69 | 69 | 1 | 11/15/18 | 12/14/18 |
| EW 2018 | 1109F | Junction Butte[^^] | 52 | 52 | 1 | 11/15/18 | 12/8/18 |
| LW 2019 | 1105M | 8 Mile[^^] | 96 | 100 | 0.96 | 3/1/19 | 3/30/19 |
| LW 2019 | 1155M | 8 Mile[^^] | 99 | 104 | 0.95 | 3/1/19 | 3/30/19 |
| LW 2019 | 0907F | Junction Butte[^^] | 76 | 79 | 0.96 | 3/1/19 | 3/30/19 |
| LW 2019 | 1047M | Junction Butte[^^] | 74 | 77 | 0.96 | 3/1/19 | 3/30/19 |
| LW 2019 | 1109F | Junction Butte[^^] | 71 | 75 | 0.95 | 3/1/19 | 3/30/19 |
| EW 2019 | 0907F | Junction Butte[^^] | 71 | 71 | 1 | 11/15/19 | 12/14/19 |
| EW 2019 | 1047M | Junction Butte[^^] | 70 | 70 | 1 | 11/15/19 | 12/14/19 |
| LW 2020 | 1232M[7] | 8 Mile[^^] | 43 | 44 | 0.98 | 3/1/20 | 3/14/20 |
| LW 2020 | 1233M[7] | 8 Mile[^^] | 45 | 45 | 1 | 3/1/20 | 3/14/20 |
| LW 2020 | 0907F[7] | Junction Butte[^^] | 42 | 43 | 0.98 | 3/1/20 | 3/13/20 |
| LW 2020 | 1047M[7] | Junction Butte[^^] | 39 | 41 | 0.95 | 3/1/20 | 3/13/20 |
| LW 2020 | 1229F[7] | Junction Butte[^^] | 37 | 38 | 0.97 | 3/1/20 | 3/13/20 |

[^] End date does not include midnight location at conclusion of last day of study session

[^^] Pack included multiple GPS-collared wolves for at least a portion of study session

[1] 0777M dispersed from Blacktail to 777M (Blacktail Satellite). 777M was characterized as Blacktail through 11/22/2011.

[2] 0777M returned to Blacktail on 3/6/12 and dispersed from Blacktail to Agate Creek on 3/21/12. 777M was characterized as Blacktail from 3/6/12 until 3/21/12, and as Agate Creek from 3/21/12 until 3/30/12.

[3] 0890M dispersed from Junction Butte. 890M was characterized as Junction Butte through 3/27/13.

[4] 0967M dispersed from Lamar Canyon to 967M Group. 967M was characterized as Lamar Canyon until 3/22/15, and as 967M Group from 3/22/15 until 3/30/15.

[5] 0963F dispersed from 8 Mile (note one cluster primarily consisted of locations from when 0963F was classified as Unknown). 963F was characterized as 8 Mile until 3/26/17.

[6] Crevice Lake and 1005F Group merged to form 1005F/1107M Group. 1005F was characterized as 1005F Group, and 1107M as Crevice Lake, until 11/30/18. Beginning on 11/30/18, each were then characterized as 1005F/1107M Group.

[7] Study session ended early in response to COVID-19.

**Table S4-A.1b.** GPS-collared wolves included in the denning period feeding event abundance estimator. All numbers are for clusters including locations for that pack, with searched, total, and proportion referring to unique GPS clusters. The 'searched' numbers represent those that were adjusted to include 'homesite clusters' as searched (see Chapter 4 and Appendix S4-A text). In the rare cases where wolves had an identified cluster that spanned their affiliation with two packs, we assigned the pack affiliation with the most locations.

| Session | Wolf | Pack | Searched | Total | Proportion | Start | End^ |
|---|---|---|---|---|---|---|---|
| SS 2008 | 0624F | Leopold^^ | 224 | 263 | 0.85 | 5/1/08 | 7/31/08 |
| SS 2008 | 0625F | Leopold^^ | 161 | 183 | 0.88 | 5/1/08 | 7/31/08 |
| SS 2008 | 0626F | Oxbow Creek^^ | 283 | 332 | 0.85 | 5/1/08 | 7/31/08 |
| SS 2008 | 0627M | Oxbow Creek^^ | 275 | 312 | 0.88 | 5/1/08 | 7/31/08 |
| SS 2009 | 0692F | Blacktail^^ | 249 | 254 | 0.98 | 5/1/09 | 7/31/09 |
| SS 2009 | 0693F | Blacktail^^ | 195 | 197 | 0.99 | 5/1/09 | 7/31/09 |
| SS 2009 | 0684M | Everts^^ | 311 | 323 | 0.96 | 5/1/09 | 7/31/09 |
| SS 2009 | 0685M | Everts^^ | 280 | 289 | 0.97 | 5/1/09 | 7/31/09 |
| SS 2010 | 0642F | Blacktail^^ | 220 | 224 | 0.98 | 5/1/10 | 7/31/10 |
| SS 2010 | 0752F | Blacktail^^ | 235 | 241 | 0.98 | 5/1/10 | 7/31/10 |
| SS 2011 | 0775M | Agate Creek | 86 | 93 | 0.92 | 6/1/11 | 6/30/11 |
| SS 2011 | 0777M | Blacktail | 311 | 317 | 0.98 | 5/1/11 | 7/31/11 |
| SS 2012 | 0777M[1] | Blacktail^^ | 116 | 118 | 0.98 | 5/1/12 | 5/28/12 |
| SS 2012 | 0829F | Blacktail^^ | 342 | 362 | 0.94 | 5/1/12 | 7/31/12 |
| SS 2012 | 0777M[1] | Junction Butte | 245 | 250 | 0.98 | 6/1/12 | 7/31/12 |
| SS 2013 | SW763M | 8 Mile | 247 | 283 | 0.87 | 5/1/13 | 7/31/13 |
| SS 2013 | 0890M | 889F/890M Group^^^ | 344 | 364 | 0.95 | 5/1/13 | 7/31/13 |
| SS 2014 | 0911M[2] | 911M Group | 171 | 191 | 0.9 | 5/13/14 | 6/30/14 |
| SS 2014 | 0890M | Junction Butte^^ | 170 | 178 | 0.96 | 5/1/14 | 6/30/14 |
| SS 2014 | 0907F | Junction Butte^^ | 138 | 151 | 0.91 | 5/1/14 | 6/30/14 |
| SS 2015 | 0964M | Prospect Peak | 254 | 258 | 0.98 | 5/1/15 | 7/31/15 |
| SS 2016 | 0994M | Junction Butte | 229 | 236 | 0.97 | 5/1/16 | 7/22/16 |
| SS 2016 | 0996M | Prospect Peak | 237 | 241 | 0.98 | 5/1/16 | 7/22/16 |
| SS 2017 | 0962M | 8 Mile | 224 | 231 | 0.97 | 5/1/17 | 6/30/17 |
| SS 2017 | 1047M | Junction Butte | 248 | 262 | 0.95 | 5/1/17 | 6/30/17 |
| SS 2019 | 0907F | Junction Butte | 136 | 152 | 0.89 | 5/1/19 | 7/19/19 |
| SS 2020 | 1200M | Carnelian Creek | 76 | 89 | 0.85 | 5/15/20 | 6/30/20 |

^End date does not include midnight location at conclusion of last day of study session

^^Pack included multiple GPS-collared wolves for at least a portion of study session. All were characterized as 'Two GPS collars' for abundance model except Blacktail–SS 2012.

^^^GPS-collared wolf censored from this wolf pair

[1] 0777M dispersed from Blacktail to Junction Butte. He was last characterized as Blacktail on 5/28/12, and first characterized as Junction Butte on 6/1/12.

[2] 0911M dispersed from Junction Butte to 911M Group. 0911M dispersed from Junction Butte to form 911M Group on 5/13/14. 0911M data from Junction Butte was censored.

**Table S4-A.2. Dominant search type of intend-to-search GPS clusters.**

| Search type | Roaming - count (%) | Denning - count (%) |
|---|---|---|
| Observational feeding event detection | 404 (8.5) | |
| Ground method observation | 354 (7.4) | |
| Boots on the ground | 3,714 (77.9) | 5,484 (85.8) |
| Aerial method observation | 11 (0.2) | |
| Aerial search | 2 (<0.1) | |
| Wolf homesite | 13 (0.3) | 522 (8.2) |
| Wolf homesite (other pack) | | 1 (<0.1) |
| Previous search | 3 (0.1) | |
| Carcass dump | 4 (0.1) | |
| Not searched | 260 (5.5) | 387 (6.1) |
| **Total GPS clusters** | **4,765** | **6,394** |

Technical notes:

- Cluster searches were classified as the most frequent classification among searched cluster locations (see Appendix S4-A text).
- Clusters ($n_{roaming} = 23$, $n_{denning} = 12$) were excluded when the pack was not an abundance estimator pack (see Appendix S4-A text).
- During November 2010, significant snow affected our ability to confidently search some GPS locations through boots on the ground. Therefore, 12 clusters that we attempted to search during that period are among those considered to be “not searched”.
- Note that 135 of 522 (26%) ‘Wolf homesite’ clusters were not field-searched (see Chapter 4 and Appendix S4-A text).

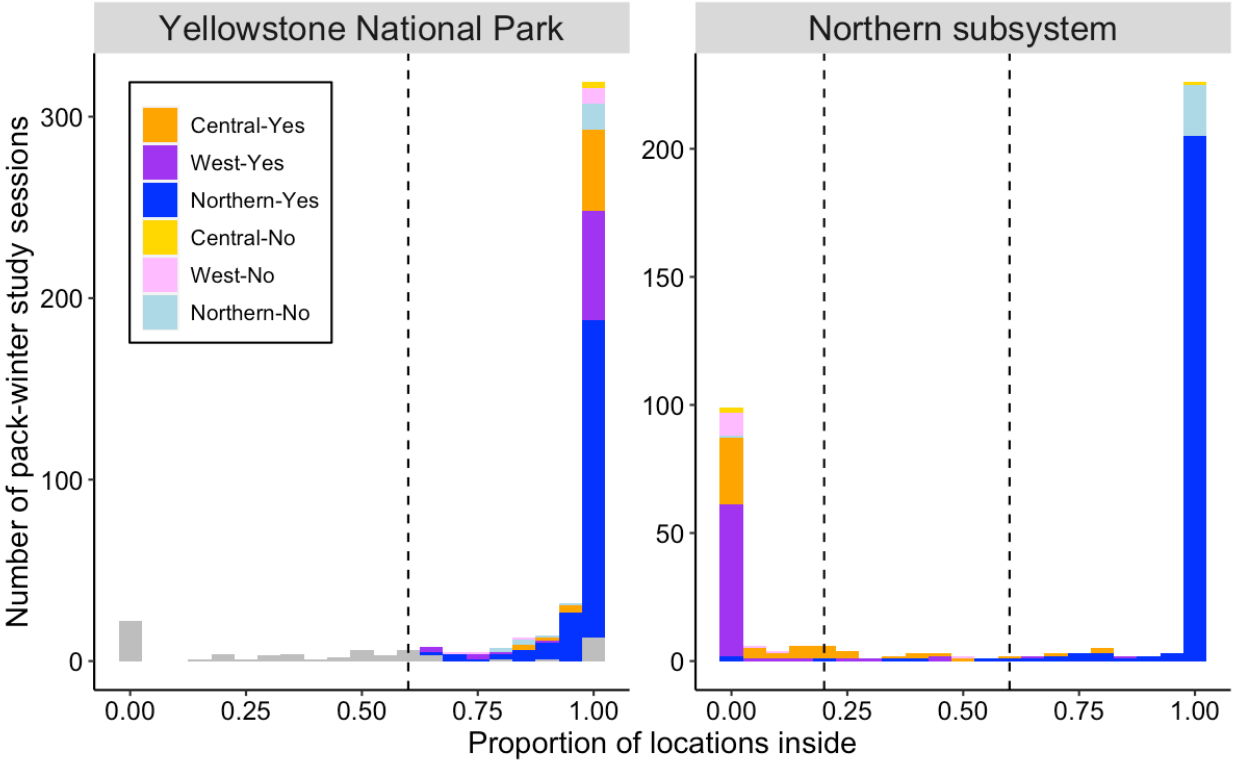

**Figure S4-A.1. Proportion of location days within Yellowstone National Park (YNP) and Northern subsystem boundaries for pack-sessions during the roaming period.** Proportion of location days, as determined from locations that had x,y locations assigned, within each boundary (see Fig. 4-2 and Appendix S4-A text). For the YNP panel, 456 radio-collared pack sessions with locations are displayed, while the Northern subsystem panel displays the proportion of locations for the 385 sessions following spatial censoring related to YNP (i.e., those pack-sessions ≥0.6 on YNP panel and not located in Southern YNP). The dashed lines on the Northern subsystem panel indicate where packs were characterized as non-Northern YNP packs (≤ 0.2), partial Northern YNP packs (0.2–0.6), and Northern YNP packs (≥ 0.6). The fill color for these 385 pack-sessions displays the spatial affiliations from territories. The lighter shade for each spatial affiliation was ultimately censored because no feeding events were detected (see also Table 4-2). The gray fill in the YNP panel indicates the pack-session was not among the 385 pack-sessions displayed in the Northern subsystem panel.

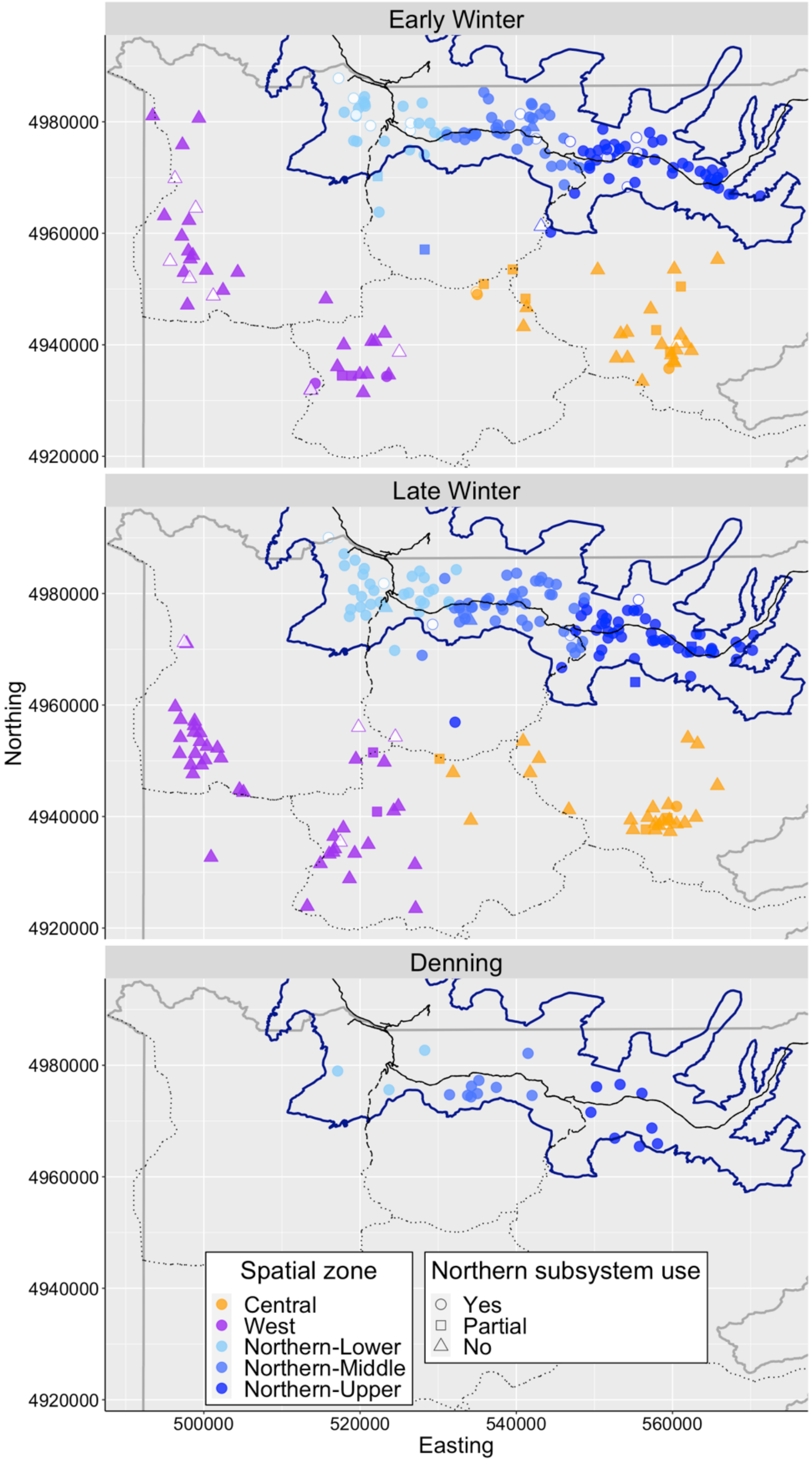

**Figure S4-A.2. Centroid locations for pack-session territories.** Color indicates spatial zone, while fill indicates whether feeding events were detected (fill = color) or not (fill = white). Centroid locations are shown for 403 pack-sessions, excluding the two roaming period pack-sessions with <5 VHF locations (see Appendix S4-A text), that remained prior to the final censoring related to whether feeding events were detected.

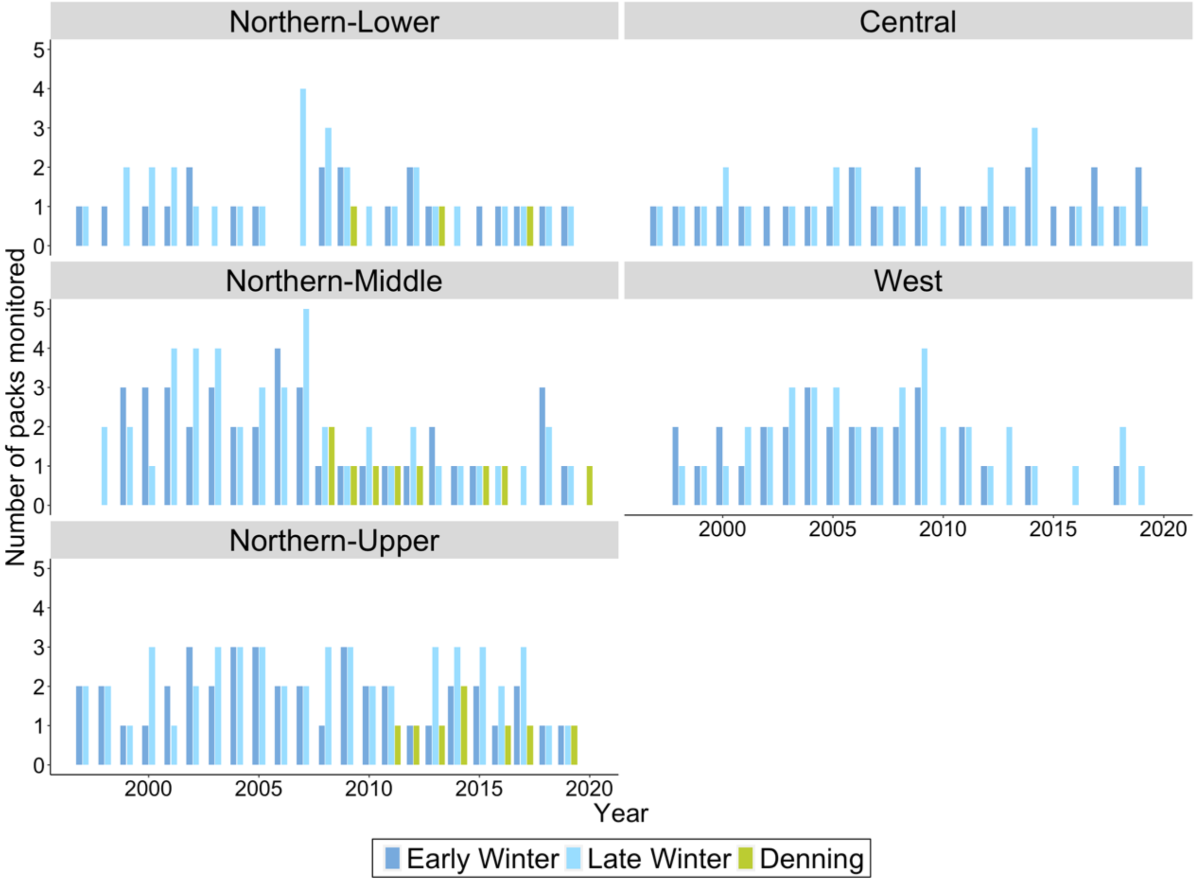

**Figure S4-A.3. Number of pack-sessions with predation metrics estimated within each spatial zone of Yellowstone National Park (November 1997–June 2020).** Population-level values for predation metrics were based on summed values for pack-sessions within a season (e.g., early winter; month-sessions during the denning period not displayed here) and spatial zone. When required, values also summed across panels. For example, 'Northern YNP' population-level values were based on values that summed across pack-sessions from Northern-Lower, Northern-Middle, and Northern-Upper.

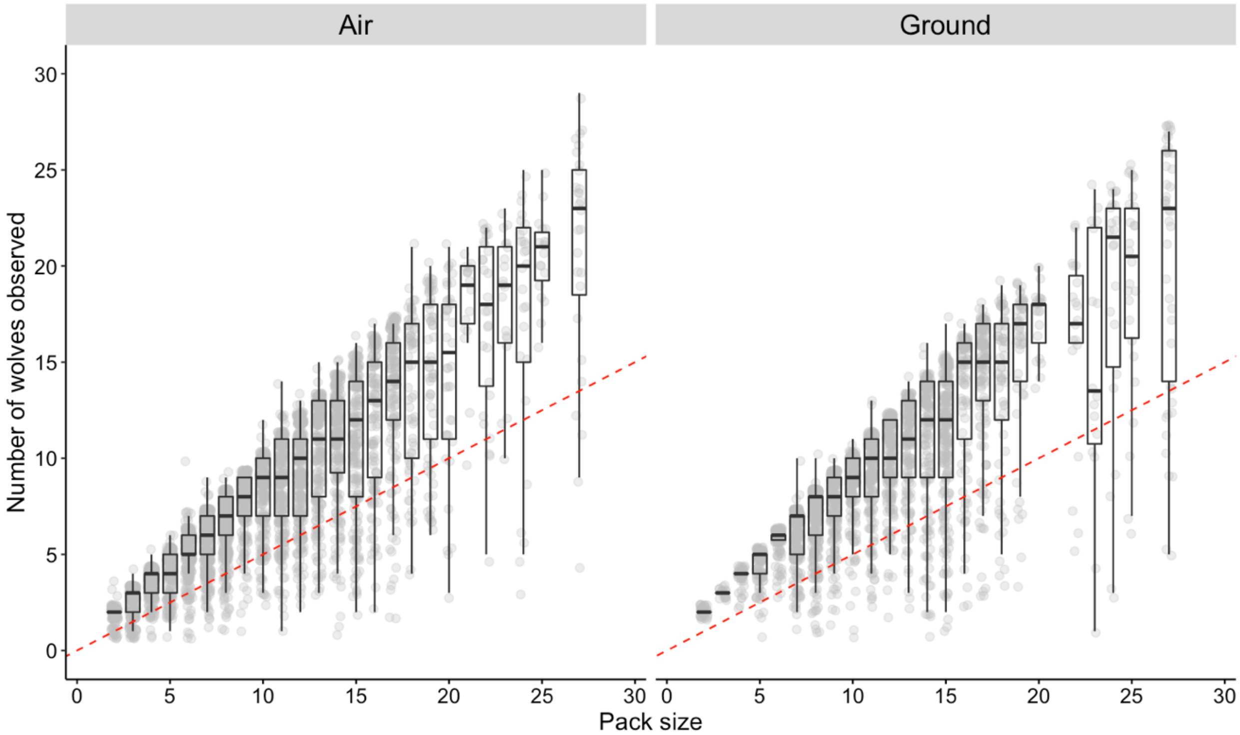

**Figure S4-A.4. Number of wolves observed on a day and pack size for days classified as visual = 1.** We scored days, for each detection method, as a 1 when we observed a 'significant' portion of the pack. Values above the red, dashed line represent days where at least half of the pack was visually observed. Not all days classified as visual = 1 have more than half of the wolves observed, partially because we included days when we believed most of the pack was present (counts are sometimes affected by landscape characteristics such as forest cover; Metz et al. 2020). Data is displayed for the 349 roaming period pack-sessions included in our final data set.

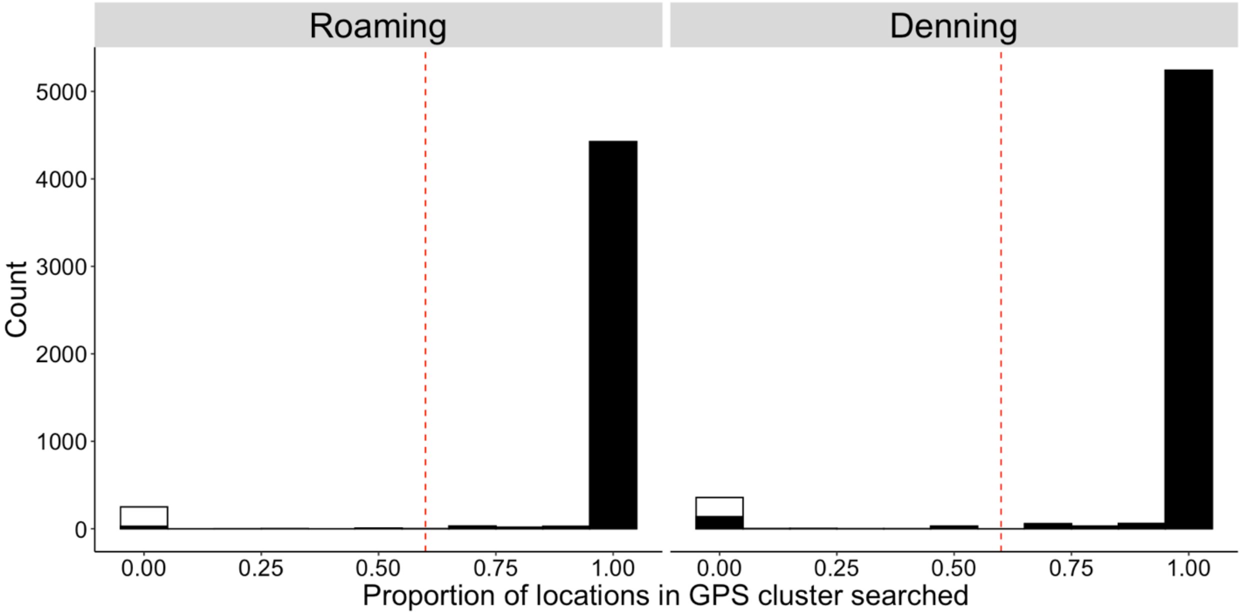

**Figure S4-A.5. Proportion of GPS locations within a GPS cluster that were searched.** The red line at 0.6 represents the minimum proportion of locations needed to be considered 'searched' except for the rare cases when a carcass was detected at the cluster. The white-filled portions of bars represent cases where clusters were not searched strictly due to logistical constraints (e.g., staff availability, GPS locations on private land). All 4,765 GPS clusters are displayed for the roaming period, while 5,786 non-homesite GPS clusters are displayed for the denning period.

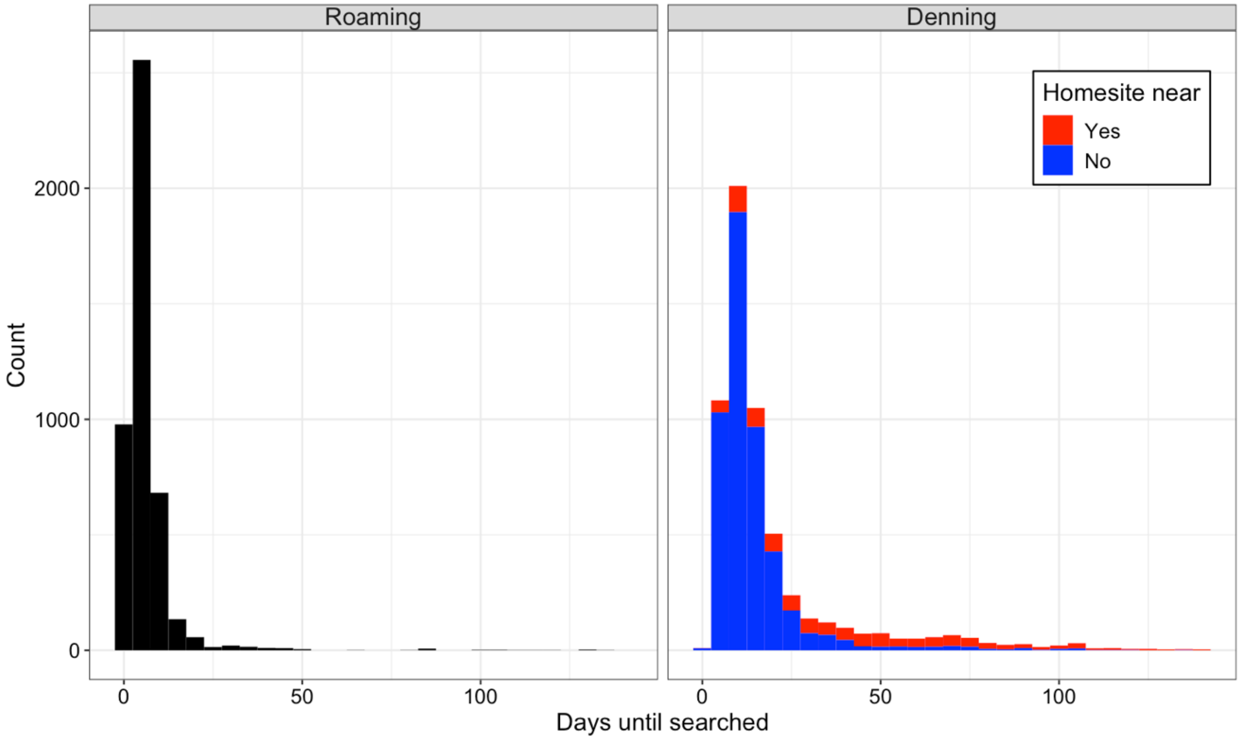

**Figure S4-A.6. Number of days until GPS clusters were searched for 10,377 searched GPS clusters ($n_{roaming}$ = 4,505, $n_{denning}$ = 5,872).** Note that the number searched does not include the additional 135 homesite clusters that were ultimately considered to be searched. 'Homesite near' indicates that a homesite was within 1 km and is displayed to highlight how the long duration until many clusters were searched during the denning period was driven by their proximity to an active wolf homesite.

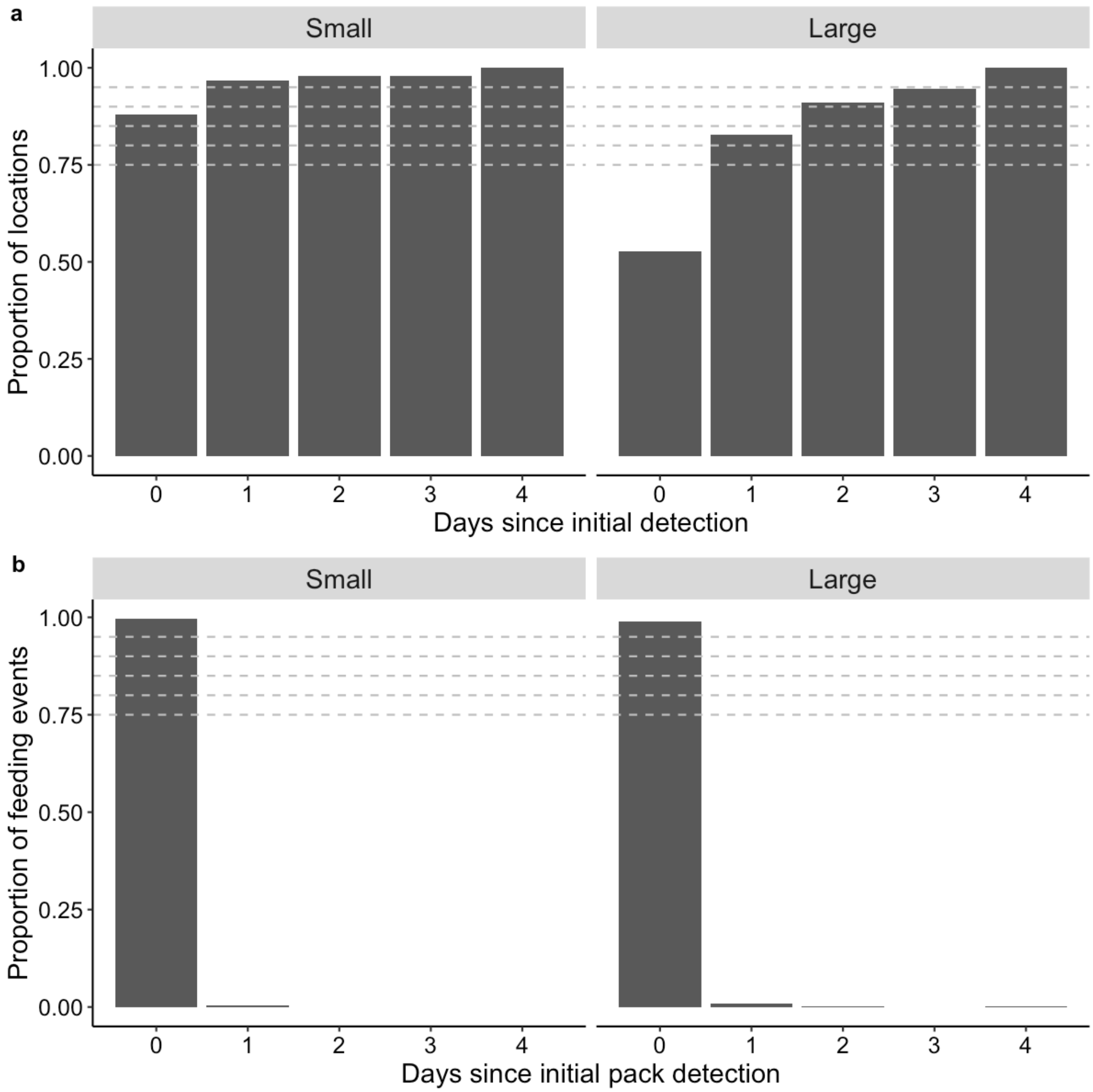

**Figure S4-A.7a. Patterns of feeding event attendance during the roaming season.** The dashed lines highlight when various thresholds (0.75, 0.80, 0.85, 0.90, 0.95) are reached. Panel (a) displays how clustered GPS locations continue to accumulate within 100-m of a feeding event, while panel (b) displays when the first clustered GPS location within 100-m of a feeding event appears for a wolf. In each of these cases, only feeding events where the GPS wolf appeared within 5 days were included. The data for each row is faceted for small (≤ 90 kg) and large (> 90 kg) feeding events.

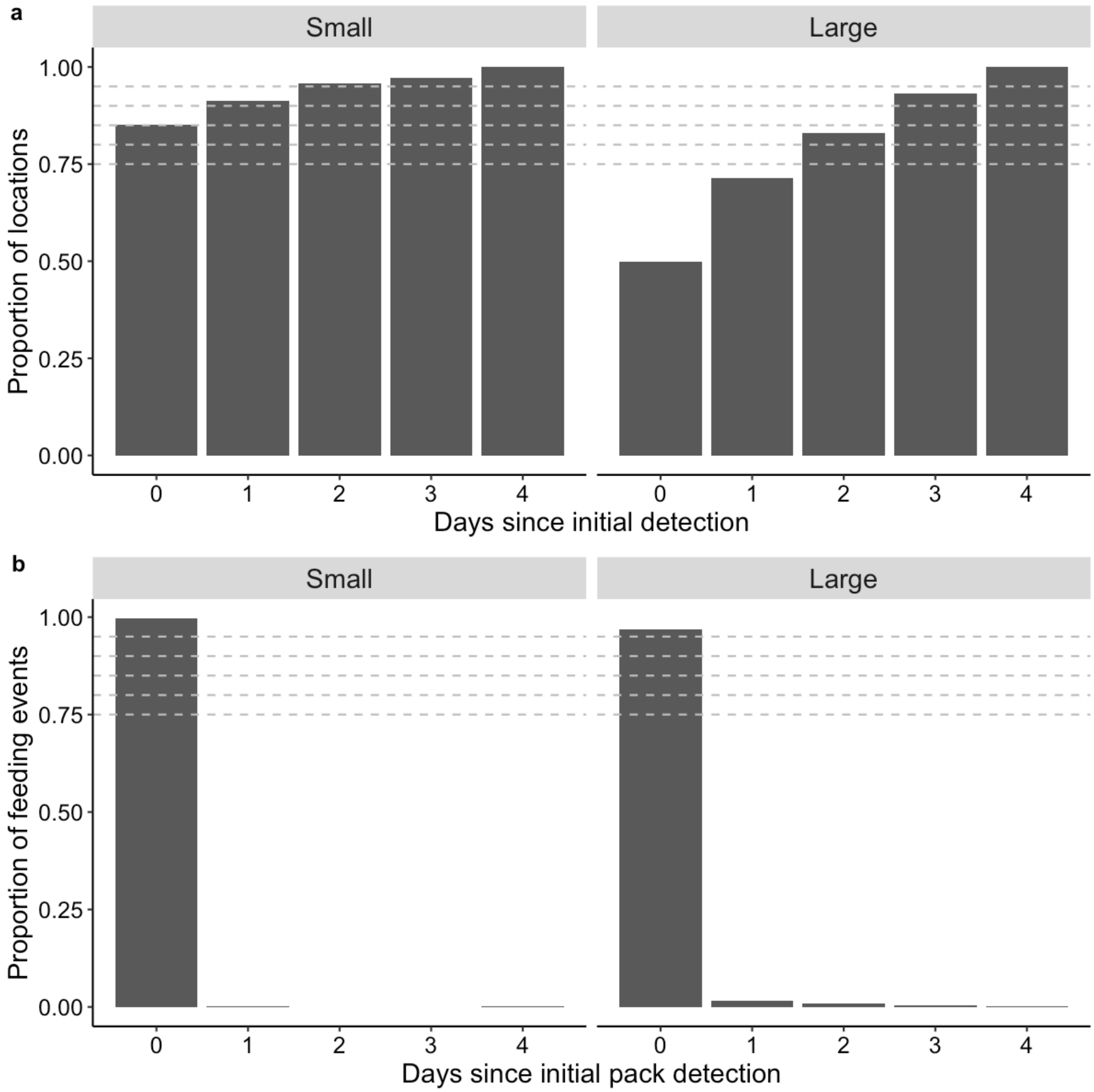

**Figure S4-A.7b. Patterns of carcass attendance during the denning season.** Panels (a) and (b) of Fig. S4-A.7b display the same information as Fig. S4-A.7a.

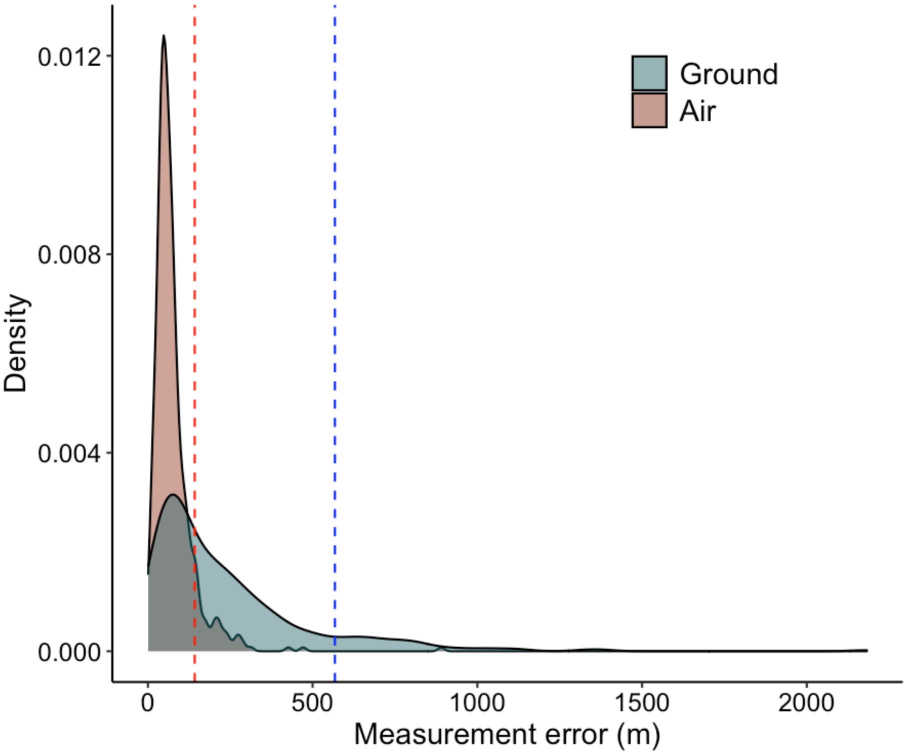

**Figure S4-A.8. Measurement error for carcass locations estimated by the aerial and ground methods.** Measurement error represents the Euclidean distance between a carcass location recorded with a handheld GPS unit and that recorded through 1) aerial teams flying over the carcass and marking a GPS location (note that some of the larger differences are likely be due to instead recording the nearby location of wolves) and 2) ground teams estimating the carcass location using a topographic map. The dashed lines represent the 90th percentile for the respective detection team.

# Chapter 4: Appendix S4-B. Biomass covariate.

## Biomass covariate used in abundance models

Seasonal growth curves developed by Murphy et al. (1998) or estimates from the literature formed the foundation for estimating the biomass covariate for our abundance models (Fig. S4-B.1). We used the growth curves developed by Murphy et al. (1998) to estimate biomass for elk and deer individuals acquired by wolf packs. Together, these species made up 2,612 of the 3,145 (83.0%) unique ungulate carcasses that we detected. Following previous work, we used a single mid-study session estimate for individual elk biomass for a given sex-age during roaming periods (e.g., MacNulty et al. 2009, Metz et al. 2012) and daily estimates for denning periods (Metz et al. 2012). We used the daily predictions for live biomass during the denning period that were developed by Metz et al. (2012) through fitting gompertz equations to the data of Murphy et al. (1998).

Among all elk carcasses, 904 of 2,430 (37.2%) were neonates (<4 months), calves (5–14 months), or yearlings (15–26 months). Because we could very rarely determine the sex for elk neonates and calves, we used the mean of the predicted male and female biomass for all elk neonates and calves. Among elk classified as 'Adult' (i.e., ≥2.5 years old), we cementum-aged 1,131 of 1,470 (76.9%) individuals. Most of these elk were located in northern YNP, where we aged 1,114 of 1,344 (82.9%) adult elk carcasses. We used composite values for a given sex-age class when we did not have a precise age. We used an edible biomass of 79% for elk neonates, and 68% for all other age classes (Wilmers et al. 2003, Miller et al. 2013)

We also used the growth curves of Murphy et al. (1998) to derive biomass estimates for deer ($n$ = 182). However, we could rarely age deer because wolf packs usually fully consumed and disarticulated all deer (i.e., including adults). We therefore often used compositive values for deer and assumed 79% of biomass was edible for all deer.

We used biomass estimates for bison (*n* = 426) from either management-related capture events during winter (Metz et al. 2012) or the literature (Mattson 1997). We used the same biomass estimates throughout the year, except for neonates during the denning period. Bison neonates became an increasingly important part of wolves' diet during the denning period as time since wolf reintroduction increased (Metz et al. 2020). We therefore developed estimates for bison neonates during the roaming period that assumed the same growth pattern as elk. As for elk, we assumed that 68% and 79% of biomass was edible for non-neonates and neonates, respectively.

Estimates for other ungulates came from the literature. Specifically, estimates for moose (*n* = 20) biomass were from Mattson (1997), while those for other species were from Feldhamer et al. (2003). We assumed horse (*n* = 2) and non-neonate moose had 68% edible biomass, and the remainder of species had 79% edible biomass for all sex-age classes.

We used these values to provide biomass estimates for 3,085 of 3,145 feeding events (Fig. S4-B.1). Note that seven of the 3,085 feeding events were neonates of unknown species, all from the denning period. We assumed a biomass value equal to that of an elk neonate for these seven individuals, which made up <1% of all feeding events during the denning period.

**Biomass values for undetected feeding events**

We assigned biomass values for feeding events without values (i.e., the 60 detected feeding events that equaled NA and all undetected feeding events that were estimated through our abundance models) as the mean value among the detected feeding events for each demographic class during each month (Fig. S4-B.1). We determined the mean values following the demographic predictions that we made through Eqns. 8 and 9 in Chapter 4.

## LITERATURE CITED

Feldhamer, G. A., B. C. Thompson, and J. A. Chapman. 2003. Wild mammals of North America: biology, management, and conservation. John Hopkins University Press, Baltimore, MD.

MacNulty, D. R., D. W. Smith, J. A. Vucetich, L. D. Mech, D. R. Stahler, and C. Packer. 2009. Predatory senescence in ageing wolves. Ecology Letters **12**:1347-1356.

Mattson, D. J. 1997. Use of ungulates by Yellowstone grizzly bears *Ursus arctos*. Biological Conservation **81**:161-177.

Metz, M. C., M. Hebblewhite, D. W. Smith, D. R. Stahler, D. R. MacNulty, A. Tallian, and J. A. Vucetich. 2020. What wolves eat and why. Pages 157-168 *in* D. W. Smith, D. R. Stahler, and D. R. MacNulty, editors. Yellowstone wolves: Science and discovery in the world's first national park. University of Chicago Press, Chicago, IL.

Metz, M. C., D. W. Smith, J. A. Vucetich, D. R. Stahler, and R. O. Peterson. 2012. Seasonal patterns of predation for gray wolves in the multi-prey system of Yellowstone National Park. Journal of Animal Ecology **81**:553-563.

Miller, C. S., M. Hebblewhite, Y. K. Petrunenko, I. V. Seryodkin, N. J. DeCesare, J. M. Goodrich, and D. G. Miquelle. 2013. Estimating Amur tiger (*Panthera tigris altaica*) kill rates and potential consumption rates using global positioning system collars. Journal of Mammalogy **94**:845-855.

Murphy, K. M., G. S. Felzien, M. G. Hornocker, and T. K. Ruth. 1998. Encounter competition between bears and cougars: some ecological implications. Ursus **10**:55-60.

Wilmers, C. C., R. L. Crabtree, D. W. Smith, K. M. Murphy, and W. M. Getz. 2003. Trophic facilitation by introduced top predators: grey wolf subsidies to scavengers in Yellowstone National Park. Journal of Animal Ecology **72**:909-916.

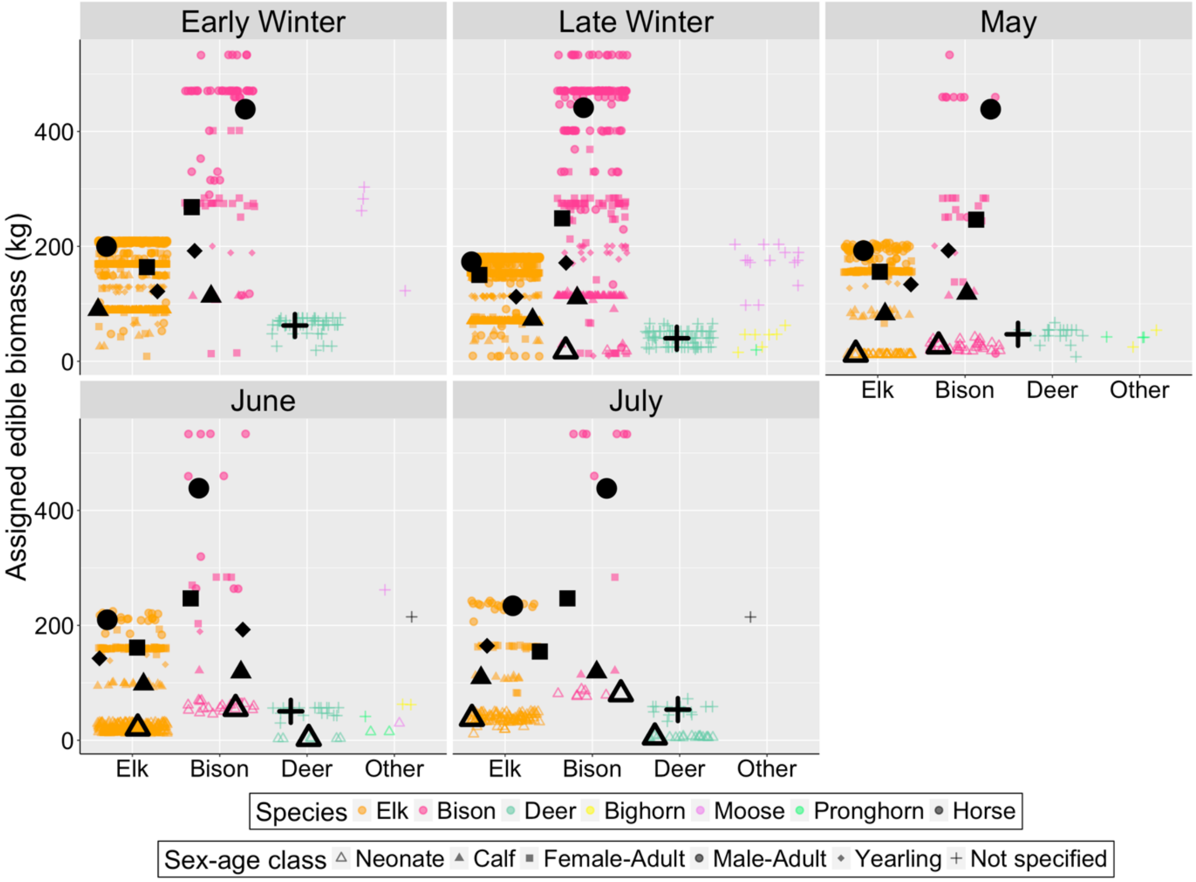

**Figure S4-B.1. Biomass values assigned for demographic classes during the month-sessions that predation metrics were estimated for wolves in Yellowstone National Park.** The colored symbols (*n* = 3,079) represent the values used as inputs for the biomass covariate in our abundance models (see Chapter 4). Here, we only display the sex-age class for elk and bison because these were the only species where this information was predicted for undetected feeding events. The black symbols within each monthly panel represent the mean value used for all estimated feeding events within these month-sessions following the predictions for demographic characteristics (Eqns. 8 and 9 in Chapter 4). These mean values are not displayed for 'Other' species.

## Chapter 4: Appendix S4-C. Supporting information for feeding event mark-recapture abundance models.

### Likelihood for the roaming period

The likelihood for our roaming period model that estimated the probability that a feeding event existed, given that there was sampling effort to look for it, can be described as:

$$\Pr[\psi, p|\text{data}] \propto \prod_{g=1}^{pack-sessions} \prod_{j=1}^{detection\,method} \psi_g \left[ \prod_{\alpha=1}^{occ} p_{detection\,method}(1 - p_{detection\,method}) \right]$$

**Table S4-C.1a. Specified priors for *mu.a* during the roaming period.** Prior values were assigned based on the frequency of flights during a pack-session, pack-type*, and the availability data of the 2,343 detected feeding events. While grouping observations to account for how detection teams intended to monitor pack-sessions, we determined prior values from the proportion of feeding events where availability equaled 1 for that occasion. For example, when calculating the informative prior for G1, feeding events were grouped by *i*) all pack-sessions that were monitored by the ground and *ii*) the remaining pack-sessions. Accordingly, the prior for G1 was then assigned as one of those two values. We specified high precision (100) for ground and GPS detection occasions, and low precision (0.0001) for air occasions.

| **Pack-type*** | **Aerial quartile**[1] | ***n* packs** | **G1** | **G2** | **A1** | **A2** | **GPS** |
|---|---|---|---|---|---|---|---|
| Ground & Air-1 | First | 15 | 0.999 | 0.970 | 0.428 | 0.273 | 0.000 |
| Ground & Air-2 | Second | 23 | 0.999 | 0.970 | 0.618 | 0.428 | 0.000 |
| Ground & Air-3 | Third | 19 | 0.999 | 0.970 | 0.756 | 0.541 | 0.000 |
| Ground & Air-4 | Fourth | 35 | 0.999 | 0.970 | 0.797 | 0.682 | 0.000 |
| Ground & Air-1 & GPS | First | 18 | 0.999 | 0.970 | 0.428 | 0.273 | 0.984 |
| Ground & Air-2 & GPS | Second | 5 | 0.999 | 0.970 | 0.618 | 0.428 | 0.984 |
| Ground & Air-3 & GPS | Third | 9 | 0.999 | 0.970 | 0.756 | 0.541 | 0.984 |
| Ground & Air-4 & GPS | Fourth | 6 | 0.999 | 0.970 | 0.797 | 0.682 | 0.984 |
| Air-1 | First | 55 | 0.001 | 0.001 | 0.428 | 0.273 | 0.000 |
| Air-2 | Second | 46 | 0.001 | 0.001 | 0.618 | 0.428 | 0.000 |
| Air-3 | Third | 59 | 0.001 | 0.001 | 0.756 | 0.541 | 0.000 |
| Air-4 | Fourth | 53 | 0.001 | 0.001 | 0.797 | 0.682 | 0.000 |
| Air-1 & GPS | First | 2 | 0.001 | 0.001 | 0.428 | 0.273 | 0.984 |
| Air-2 & GPS | Second | 1 | 0.001 | 0.001 | 0.618 | 0.428 | 0.984 |
| Air-3 & GPS | Third | 0 | - | - | - | - | - |
| Air-4 & GPS | Fourth | 0 | - | - | - | - | - |
| Ground & Air-1 & Partial GPS | First | 2 | 0.999 | 0.970 | 0.428 | 0.273 | 0.594 |
| Ground & Air-2 & Partial GPS | Second | 1 | 0.999 | 0.970 | 0.618 | 0.428 | 0.594 |
| Ground & Air-3 & Partial GPS | Third | 0 | - | - | - | - | - |
| Ground & Air-4 & Partial GPS | Fourth | 0 | - | - | - | - | - |

[1] Note that the aerial quantile is included in pack-type*. For example, Air-1 indicates that the number of flights that occurred during a pack-session was within the first quantile.

**Table S4-C.1b. Specified priors for *mu.a* during the denning period.** Prior values were assigned according to the proportion of detected feeding events during a pack-session that were available to be detected by wolf-1 or wolf-2.

| Year | Pack | Pack-type* | Wolf-1 | Wolf-2 |
|---|---|---|---|---|
| 2008 | Leopold | Two | 1.00 | 1.00 |
| 2008 | Oxbow Creek | Two | 1.00 | 1.00 |
| 2009 | Blacktail | Two | 1.00 | 1.00 |
| 2009 | Everts | Two | 1.00 | 1.00 |
| 2010 | Blacktail | Two | 1.00 | 1.00 |
| 2011 | Agate Creek | One | 1.00 | 0.00 |
| 2011 | Blacktail | One | 1.00 | 0.00 |
| 2012 | Blacktail | One – partial | 0.43 | 1.00 |
| 2012 | Junction Butte | One | 1.00 | 0.00 |
| 2013 | 8 Mile | One | 1.00 | 0.00 |
| 2013 | 889F/890M Group | One | 0.00 | 1.00 |
| 2014 | 911M Group | One | 1.00 | 0.00 |
| 2014 | Junction Butte | Two | 1.00 | 0.00 |
| 2015 | Prospect Peak | One | 1.00 | 0.00 |
| 2016 | Junction Butte | One | 1.00 | 0.00 |
| 2016 | Prospect Peak | One | 1.00 | 0.00 |
| 2017 | 8 Mile | One | 1.00 | 0.00 |
| 2017 | Junction Butte | One | 1.00 | 0.00 |
| 2019 | Junction Butte | One | 1.00 | 0.00 |
| 2020 | Carnelian Creek | One | 1.00 | 0.00 |

**Table S4-C.2. Beta coefficient estimates for final mark-recapture feeding event abundance model.**

| **Occasion** | **Covariate** | ***ß*** | **sd** | **2.5** | **25** | **75** | **97.5** |
|---|---|---|---|---|---|---|---|
| Occurrence | pack size (psi) | 0.31 | 0.04 | 0.24 | 0.29 | 0.34 | 0.38 |
| Ground (1) | distance | -0.96 | 0.09 | -1.13 | -1.02 | -0.90 | -0.79 |
| Ground (1) | open | 0.61 | 0.06 | 0.48 | 0.56 | 0.65 | 0.73 |
| Ground (1) | view | 1.16 | 0.13 | 0.90 | 1.07 | 1.24 | 1.41 |
| Ground (2) | biomass | 0.47 | 0.14 | 0.20 | 0.38 | 0.56 | 0.73 |
| Ground (2) | distance | -0.55 | 0.18 | -0.92 | -0.68 | -0.42 | -0.20 |
| Ground (2) | open | 0.32 | 0.16 | 0.04 | 0.21 | 0.42 | 0.64 |
| Air (1) | biomass | 0.34 | 0.06 | 0.23 | 0.30 | 0.37 | 0.45 |
| Air (1) | pack size | -0.21 | 0.06 | -0.32 | -0.24 | -0.17 | -0.09 |
| Air (2) | biomass | 0.61 | 0.12 | 0.37 | 0.52 | 0.69 | 0.85 |
| Air (2) | open | 0.59 | 0.15 | 0.30 | 0.49 | 0.69 | 0.89 |
| GPS | biomass | 0.73 | 0.26 | 0.25 | 0.54 | 0.90 | 1.26 |
| GPS | pack size | -0.55 | 0.20 | -0.95 | -0.68 | -0.41 | -0.15 |
| GPS | number collars | 0.57 | 0.18 | 0.24 | 0.45 | 0.69 | 0.94 |

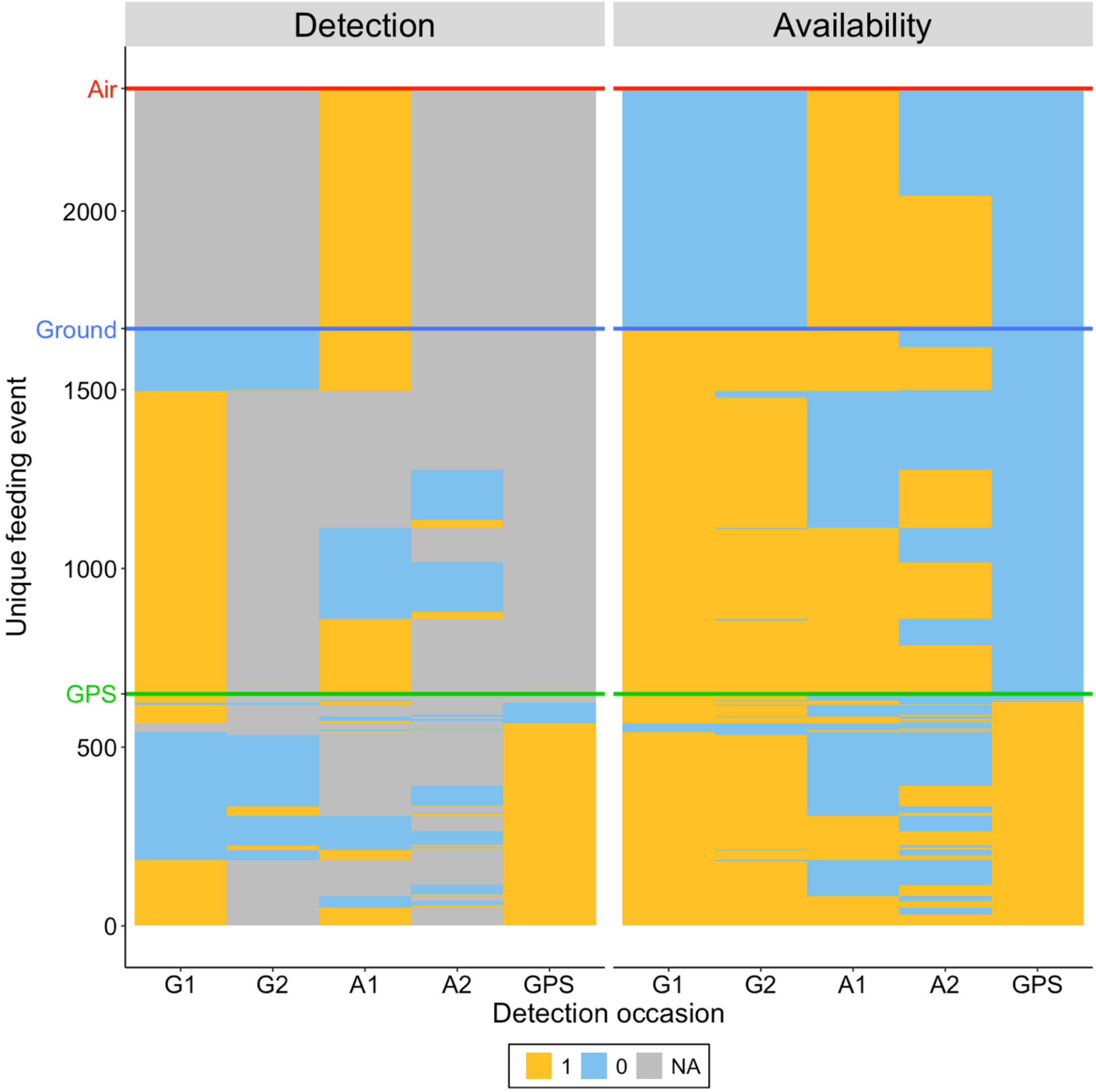

**Figure S4-C.1. Detection and availability histories for detected feeding events during the roaming period.** Detection values equaled 1, 0, or NA, while availability values equaled only 1 or 0. The associated data frame was arranged by pack-type, GPS detection, G1 detection, A1 detection, G2 detection, A2 detection, and then also the availability data in the same order. The colored lines indicate the breakpoints between pack-types.

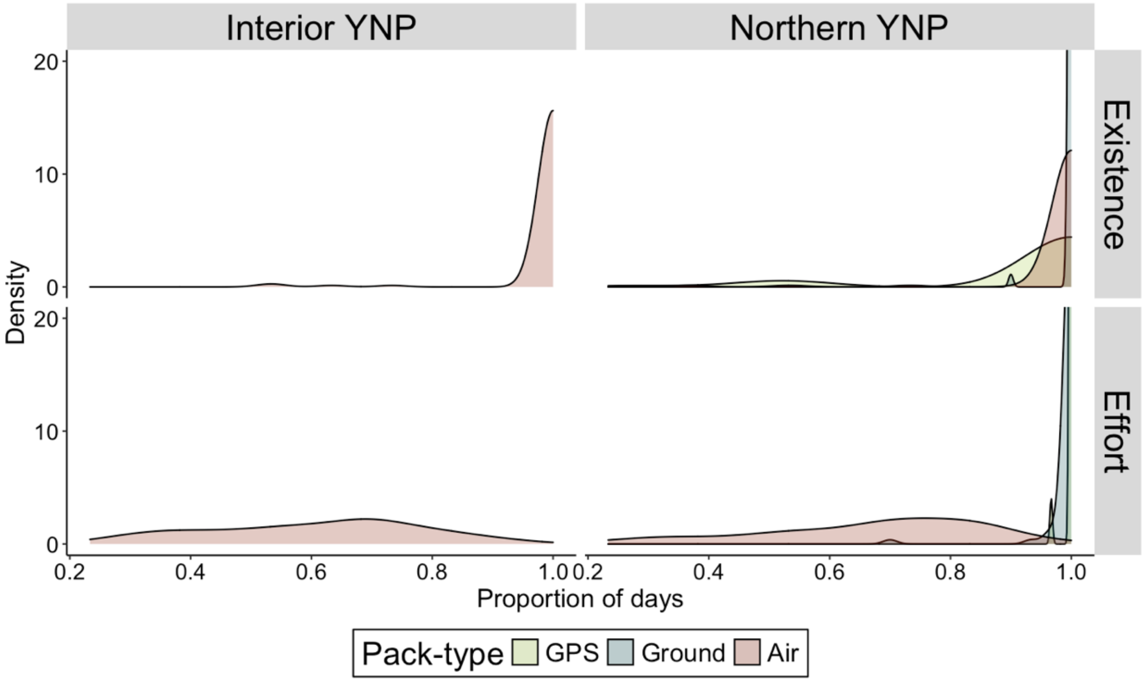

**Figure S4-C.2. Density plots describing 349 roaming period pack-sessions: proportion of days with pack existence and 2-day effort.** The left column displays the data for 122 pack-sessions in Interior YNP and the right column for 227 in Northern YNP. The top row describes the proportion of a 30-day study session that a pack existed and was radio-collared, i.e., *prop.session* in Eqn. 2 of Chapter 4. The bottom row describes the proportion of these pack-session days that included any attempt within a 2-day window, i.e., *prop.pack.effort* in Eqn. 2 of Chapter 4. Fill colors indicate pack-type (green = GPS collar during the pack-session; blue = monitored by the ground and air teams; red = monitored by only the air team). For display purposes, the maximum value displayed for the y-axis was 20, but the maximum value was ~110 for 'Existence' and ~170 for 'Effort'.

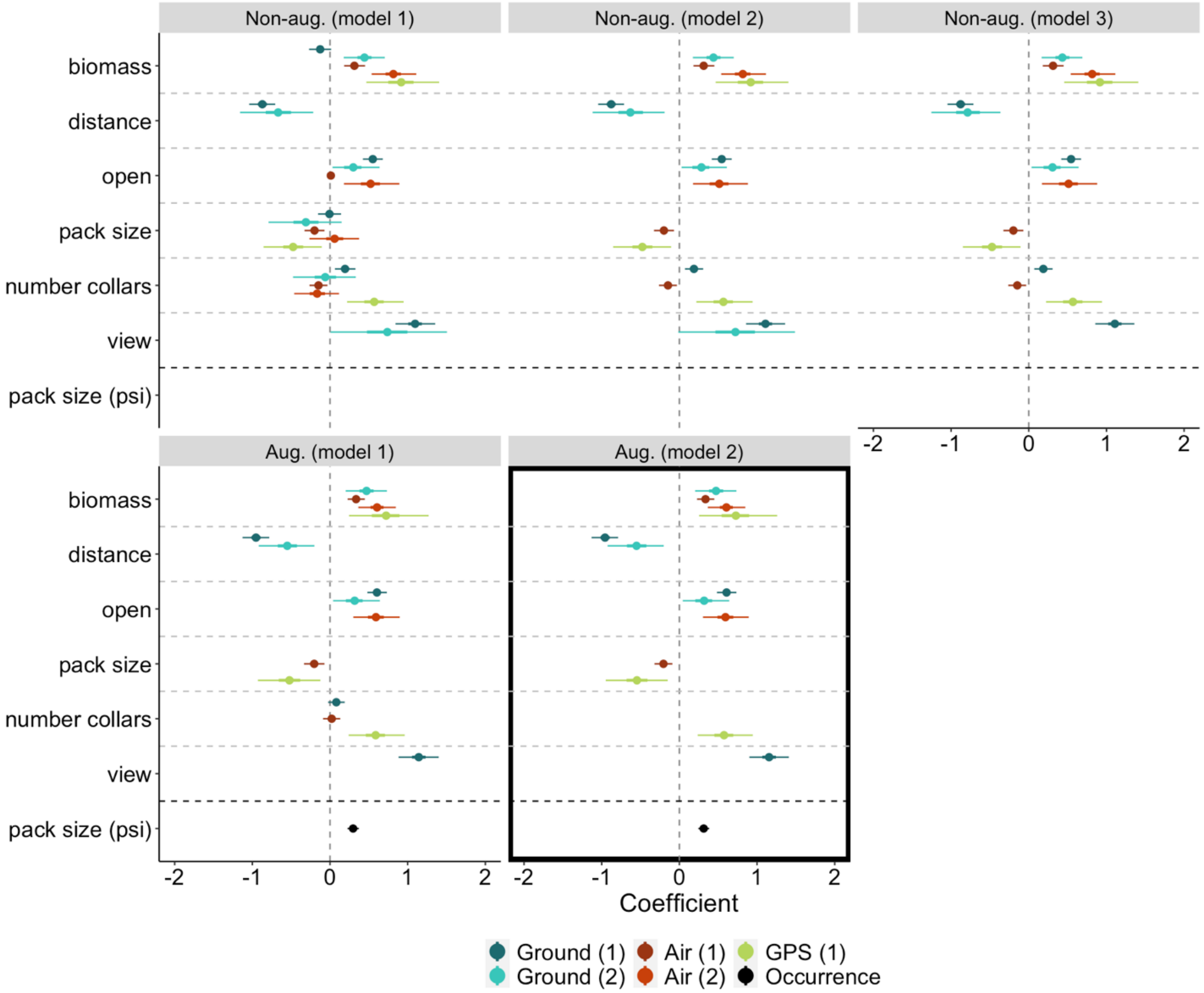

**Figure S4-C.3. Beta coefficient estimates for roaming period abundance model during stepwise removal of covariate-occasions.** Blue, red, and green circles are related to detection occasions (Eqn. 5 in Chapter 4), while the black circle represents the pack size covariate in the biological process model (Eqn. 2 in Chapter 4). Panel titles including 'Non-aug.' indicate the model was not yet augmented with additional rows of all 0 detection histories. The final model, where no 95% credible intervals for covariate-occasions overlapped 0, is identified with a black box around the panel. This highlighted panel is also Fig. 4-10a.

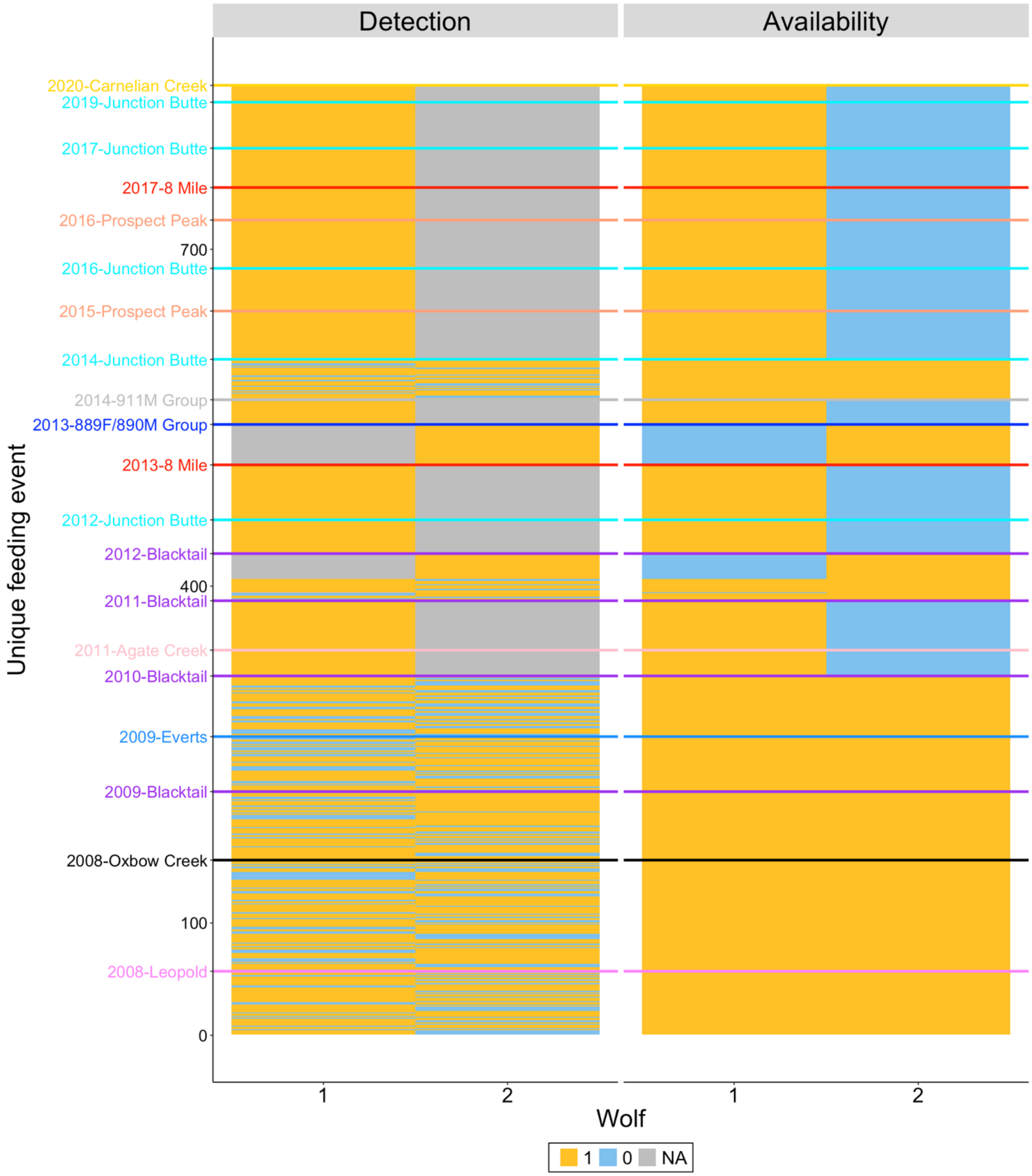

**Figure S4-C.4. Detection and availability histories for detected feeding events during the denning period.** This figure displays the same information as Fig. S4-C.1 did for the roaming period.

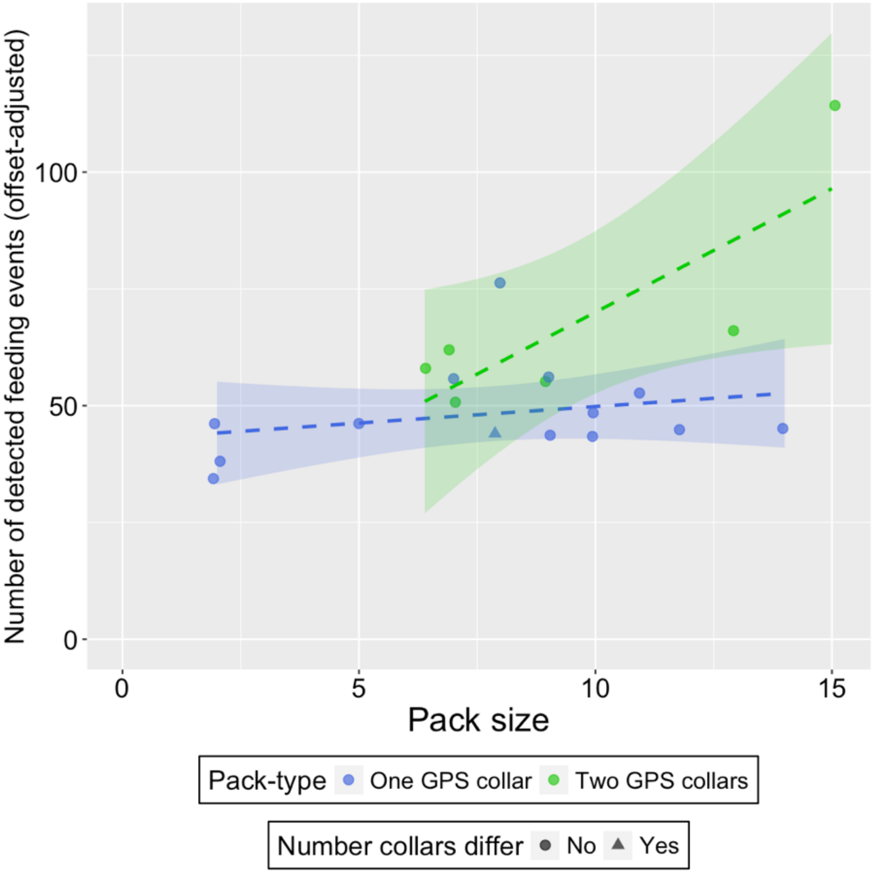

**Figure S4-C.5. Effect of pack size on the number of detected feeding events during denning period pack-sessions.** Pack-sessions are grouped as they were in the linear model on occurrence, with the color indicating how many GPS collars were present for the majority of the pack-session. The shape indicates whether the number of GPS collars changed over the course of that pack-session (Table S4-A.1b). Here, the number of detected feeding events was determined using the correction factors in Eqn. 2 (i.e., *prop.sess, prop.pack.effort*; see also Fig. S4-C.6).

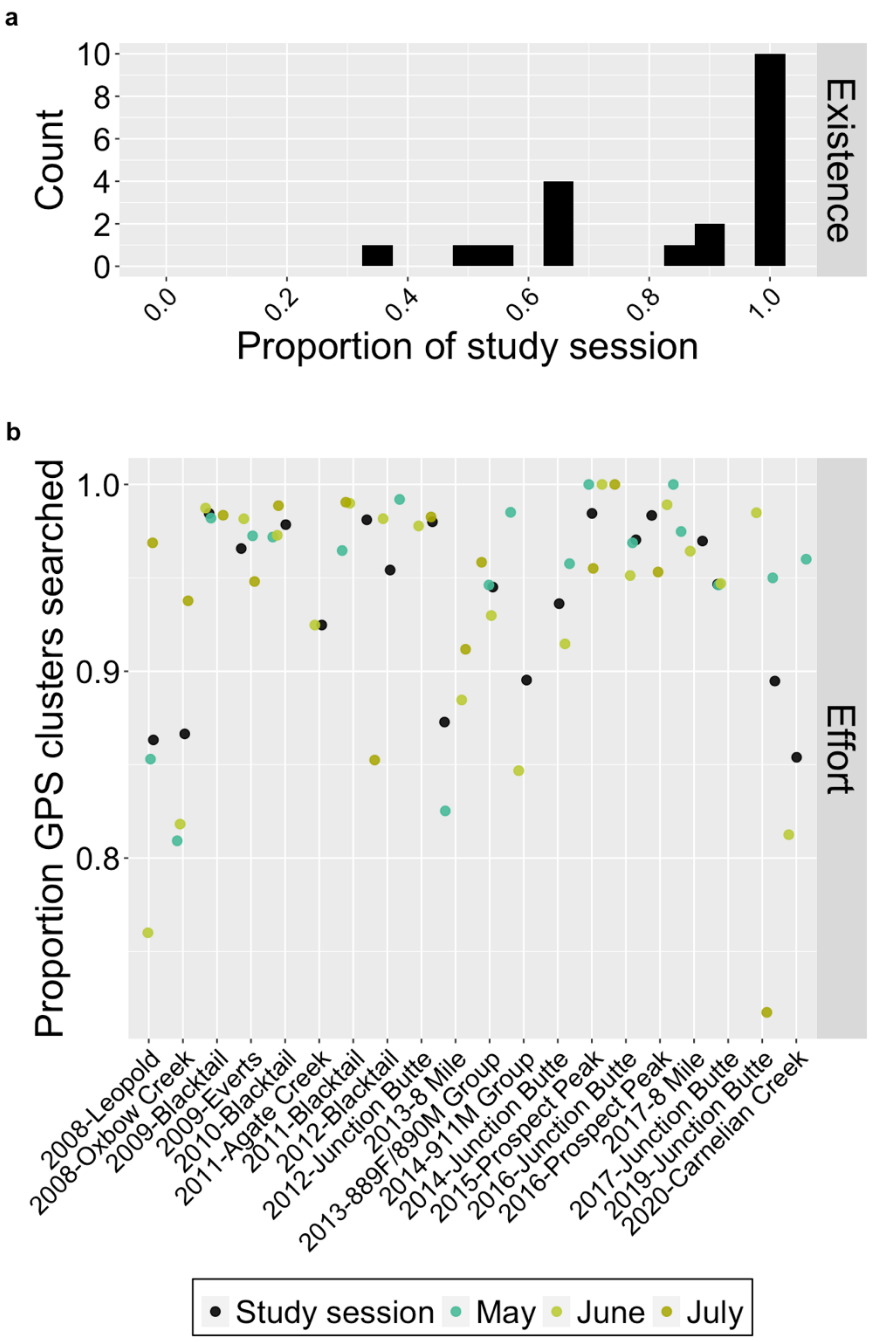

**Figure S4-C.6. Proportion of pack-session with existence and effort during the denning period.** Panel (a) displays the proportion of a denning period study session where a pack existed and GPS clusters were intended to be searched (histogram binwidth = 0.05; see Table S4-A.1b), which defined *prop.session* in Eqn. 2 of Chapter 4. Panel (b) displays the proportion of GPS clusters searched for the entire denning period session (black fill) and individual months (colored fill). The black circles defined *prop.pack.effort* in Eqn. 2, while the colored circles were leveraged for predicting demographic and acquisition characteristics (see Chapter 4 and Appendix S4-D) and for estimating kill rates. Note that the length of monthly sessions could differ among packs (Table S4-A.1b).

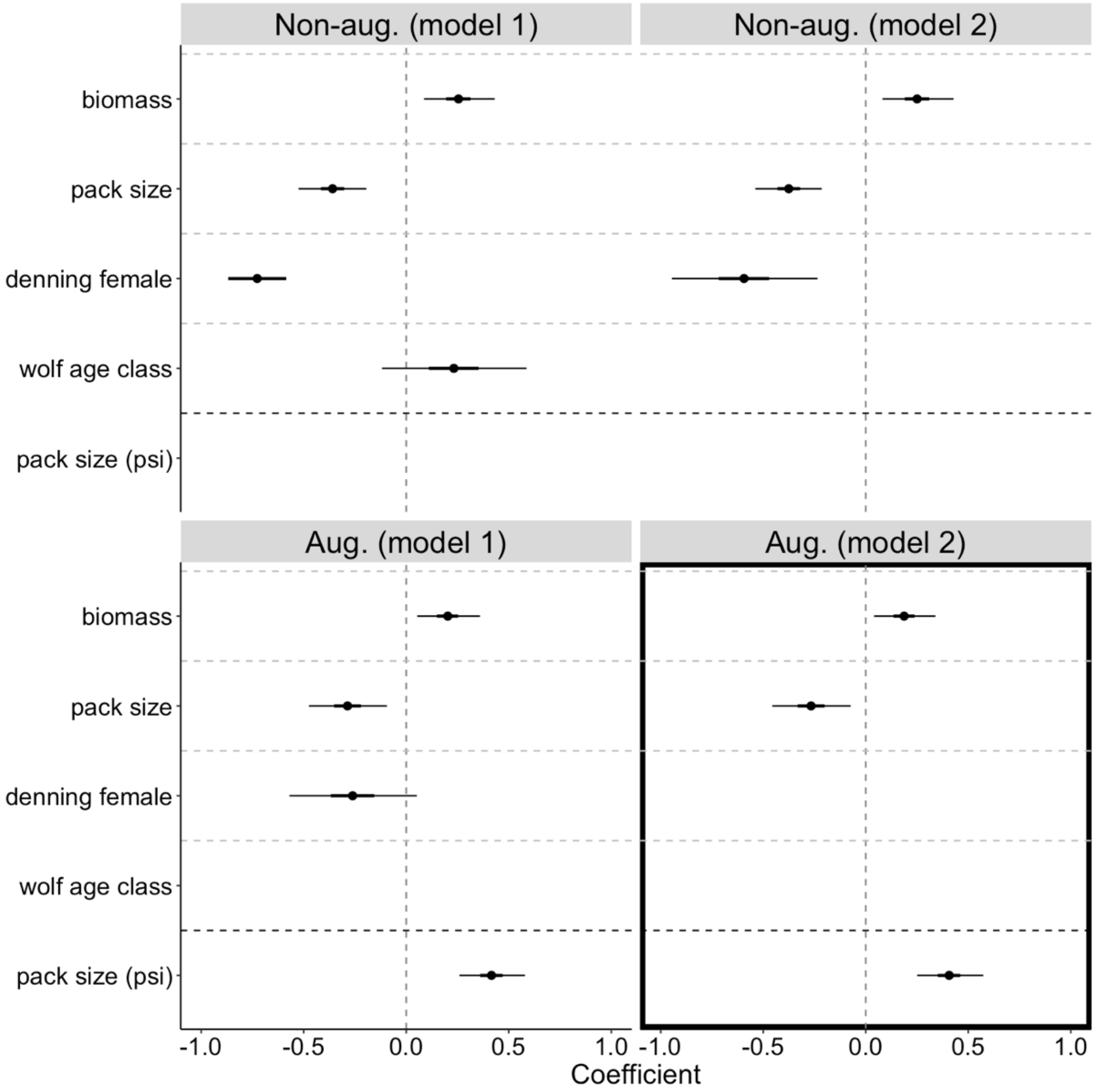

**Figure S4-C.7. Beta coefficient estimates for denning period abundance model during stepwise removal of covariates.** ‘Pack size (psi)’ represents the pack size covariate in the biological process model (Eqn. 2 in Chapter 4), while the remainder of the covariates are related to the detection model. Panel titles including ‘Non-aug.’ indicate the model was not yet augmented with additional rows of all 0 detection histories. The final model, where no 95% credible intervals for covariate overlapped 0, is identified with a black box around the panel. This highlighted panel is also Fig. 4-10b.

## Chapter 4: Appendix S4-D. Predictions for demographic characteristics of feeding events.

The following text details how we defined probability of detection (*p*) and proportion diet (*prop.diet*) in Eqns. 8 and 9 in Chapter 4 when making predictions of demographic characteristics during the roaming and denning periods. Additionally, the following text describes how we defined the proportion of feeding events that were wolf kills (*prop.wolf.kill*) in Eqn. 10 in Chapter 4 for predictions related to acquisition type during the roaming and denning periods.

### ROAMING PERIOD

We expected the demographic characteristics of undetected feeding events to be affected by *i*) the probability of detecting a feeding event of a demographic class, provided it existed on the landscape, and *ii*) the proportion of feeding events on the landscape that were of a particular demographic class. Detection probability was only expected to affect the demographic characteristics of undetected feeding events predicted through Eqns. 1–6 in Chapter 4 (i.e., the numerator in Eqn. 7 in Chapter 4), while those estimated through the execution of Eqn. 7 in Chapter 4 were only expected to be affected by proportional diet. We estimated detection probabilities for each demographic class through simple Bayesian detection models where we did not include time-variation associated with the ground or air methods or any covariates because of the complex nature of the methodology used to detect feeding events during the roaming period (see Fig. 4-6). We estimated proportional diet through the demographic characteristics of feeding events for wolf packs during the roaming period (see details below). We expected proportional diet to differ among the spatial zones of Yellowstone National Park because of general spatial variation in prey availability. Moreover, within-zone differences were expected over time because prey availability changed over our 23-year study duration. The acquisition characteristics of feeding events were not expected to be affected by detection probability and were thus only defined through the characteristics of detected feeding events.

*Probability of detecting a demographic class.* Our goal was to estimate a detection probability for a given demographic class (i.e., species or sex-age class) given the potential cumulative detection methodology (i.e., ground, air, and/or GPS cluster) employed for a pack-session. To do so, we used as many as 1,621 feeding events (69.2% of the total 2,343 feeding events) that we detected during pack-sessions when at least two detection methods were attempting to find feeding events.

We developed detection models for three different demographic data sets: 1) species (elk, bison, deer), 2) elk sex-age class (young [calf or yearling], female-adult, male-adult), and 3) bison sex-age class (young [calf or yearling], female-adult, male-adult). We specified the various classes within each of these three data sets as a result of general differences in sex-age class biomass (Fig. S4-B.1), along with considerations of sample size. For each of these three data sets, we developed two models that either accounted or did not account for availability. We developed these two model structures because we needed to mimic the effort-related conditions for different pack-sessions when estimating detection probability. Accordingly, we first defined availability where each feeding event was assumed available to be detected (i.e., availability = 1) for any method that ever looked for a feeding event during that pack-session. This specification of availability was used when estimating detection probability for pack-sessions monitored by at least two detection methods ('All feeding events' in Fig. S4-D.1). We used this first specification because all of these pack-sessions included either ground or GPS cluster effort (i.e., pack-type* = GPS or Ground [see Chapter 4]), which each generally attempted to detect feeding events during any potential 2-day detection window when employed during a pack-session (see Fig. S4-C.2). Second, we defined availability according to the associated availability data during the 2-day window for each specific feeding event. This latter definition of availability was used while estimating detection probability for pack-sessions monitored by only the airplane (‘Available feeding events’ in Fig. S4-D.1). In total, we developed six detection models for demographic class during the roaming period.

We estimated detection probability for each demographic class *c* within each of these six models through a general Bayesian detection model, where the sample size of feeding events was dependent on the data set (e.g., species or within-species sex age-class that did or did not account for availability), as,

$$p.eff_{i,j} = p_{i,j} \times avail_{i,j} \tag{1}$$

$$logit(p_{i,j}) = \alpha_{dem-class[c],j} \tag{2}$$

where $p_{i,j}$ represents the detection of feeding event *i* of demographic class *c* on detection occasion *j* (*j* = 1–3). Here, *j* = 1 represented the ground method during the 2-day detection window, *j* = 2 represented the air method during the 2-day detection window, and *j* = 3 represented the GPS cluster method during the 2-day detection window. Detection probability (*p*) of demographic class *c* for method (i.e., detection occasion) *j* was equal to the inverse logit of the intercept for demographic class *c*.

The employed detection probabilities for demographic class *c* that were used for each pack-session were dependent on the maximum detection effort during the pack-session, and were determined as,

$$p_{c_t} = 1 - (1 - p_{c_1})(1 - p_{c_2})(1 - p_{c_3}) \tag{3}$$

where the values for $p$ on the right-side of the equation indicate the detection probability for the relevant demographic class *c* for a specific detection method (i.e., ground [1], air [2], or GPS cluster [3]). The resultant $p_{c_t}$, which is a fundamental component of Eqn. 8 in Chapter 4, is the probability of detection for demographic class *c*, dependent upon which combination of detection methods were used during the pack-session (Fig. S4-D.1).

*Proportion diet.* We used two types of data sets to describe proportion diet for each season and zone ($prop.diet_{c_{s,u}}$) in Eqns. 8 and 9 in Chapter 4. Specifically, we first used the proportion diet from only detected feeding events to estimate the characteristics of undetected feeding events when detection effort occurred (i.e., the numerator of Eqn. 7 in Chapter 4) through Eqn. 8 in Chapter 4 (Figs. S4-D.2, S4-D.3, S4-D.4). Second, we updated the proportion diet to also include those feeding events predicted through Eqn. 8 in Chapter 4, and then defined *prop.diet* in Eqn. 9 in Chapter 4 using this data. In either case, we usually used multiple years of data to define this proportion for each season *s* (early or late winter) and spatial zone *u* because sample size was often limiting (see Figs. S4-D.2, S4-D.3). In some cases, we defined less focused spatial zones $u*$ (e.g., Northern, West, Central), also because of sample size limitations (see Fig. S4-D.4). We therefore used a moving average from as many as three, five, seven, nine, or eleven years, with the year of interest centered among these years when possible (i.e., dependent on left or right-truncation). We used the smallest number of years when ≥10 feeding events were detected for packs of the spatial zone. When <10 feeding events were detected, we used proportions defined from all data from that season *s* and zone *u* (or $u*$).

*Proportion wolf-kill.* We expected whether a feeding event was a wolf kill or not to be affected by prey demographic characteristics and weather-induced variation in nutritional condition. However, analyses suggested that the proportion of feeding events that were scavenged did not predictably vary across years (Metz, M., *unpublished data*). We therefore defined $prop.wolf.kill_{c^*_{s,a}}$ in Eqn. 10 in Chapter 4 using data from across all years. Specifically, we defined *prop.wolf.kill* as the proportion of detected feeding events of demographic class $c*$ that were killed by the pack assigned the feeding event. We did so while grouping data by season $s$ (early or late winter) and YNP subsystem $a$ (Northern or Interior YNP; see Fig. S4-D.5).

### DENNING PERIOD

We followed a similar process as during the roaming period to estimate the characteristics of undetected feeding events during the denning period. We again estimated detection probabilities in simple Bayesian detection models, but did so for small (<90 kg) or large (>90 kg) feeding events because of the significant overlap among prey species biomass during the ungulate birthing season(s) (Fig. S4-D.6). We ultimately used these detection probabilities, along with the proportion diet of various demographic classes from detected feeding events, to predict the demographic characteristics of undetected feeding events. These characterizations of proportion diet again included time (in this case, month of the denning period) and spatial zone.

*Probability of detecting a small or large feeding event.* Our goal during the denning period was to estimate detection probability for a small or large feeding event for a pack depending on if one or two detection sources (i.e., GPS-collared wolves) were available for detection. When developing these models for the denning period, we also included whether pack size was less than or greater than the median pack size of 8.5 wolves. We did so because pack size affected detection probability during the denning period (Fig. 4-10b), and the detection process being more straight-forward during the denning period made it easy to accommodate the inclusion of this influential covariate. We used 374 feeding events from the denning period that were detected when two wolves were present during a pack-session to estimate detection probability. We estimated detection probability through similar equations as Eqns. 1 and 2, just adjusting the structure to account for the long format of our data. We then used a variation of Eqn. 3 to estimate detection probabilities for the various combinations of feeding event size and pack size (Fig. S4-D.7). These estimates for detection probability were then used in Eqn. 8 in Chapter 4 when estimating the first portion (i.e., those feeding events estimated through the numerator of Eqn. 7 in Chapter 4) of the monthly composition (small or large) of undetected feeding events.

*Proportion diet.* We estimated measures of proportion diet in three ways that affected the final estimates for demographic characteristics. First, we estimated the proportion of feeding events among detected feeding events that were small or large across month and zone (Fig. S4-D.8). We used this characterization of proportion diet in combination with the detection probabilities for feeding event size (Fig. S4-D.7) to predict feeding event size for the first set of undetected feeding events (i.e., those feeding events estimated through the numerator of Eqn. 7 in Chapter 4) through Eqn. 8 in Chapter 4. Second, and as we did during the roaming period, we subsequently used updated estimates for proportion diet (in this case, for feeding event size) for each month-zone to predict feeding event size for the remaining undetected feeding events (i.e., those first estimated through Eqn. 7 in Chapter 4), which were not affected by detection probability. Lastly, we used the demographic composition of small and large detected feeding events for each month-zone (Fig. S4-D.9) and the now complete estimates for small and large feeding event composition (from the previous two steps), to predict the demographic characteristics of all undetected feeding events. We did so through Eqn. 9, where we just predicted the demographic class once for small feeding events, and then again for large feeding events.

*Proportion wolf-kill.* We estimated the proportion of feeding events that were wolf kills for elk and bison neonates, young (calves or yearlings), female-adults, and male-adults (Fig. S4-D.10). Because of sample size, we estimated acquisition type across all feeding events and did not account for any potential monthly variation. We also necessarily grouped all other prey species together, and assumed that the estimated scavenging proportion of 1.1% was the same across all other ungulate species.

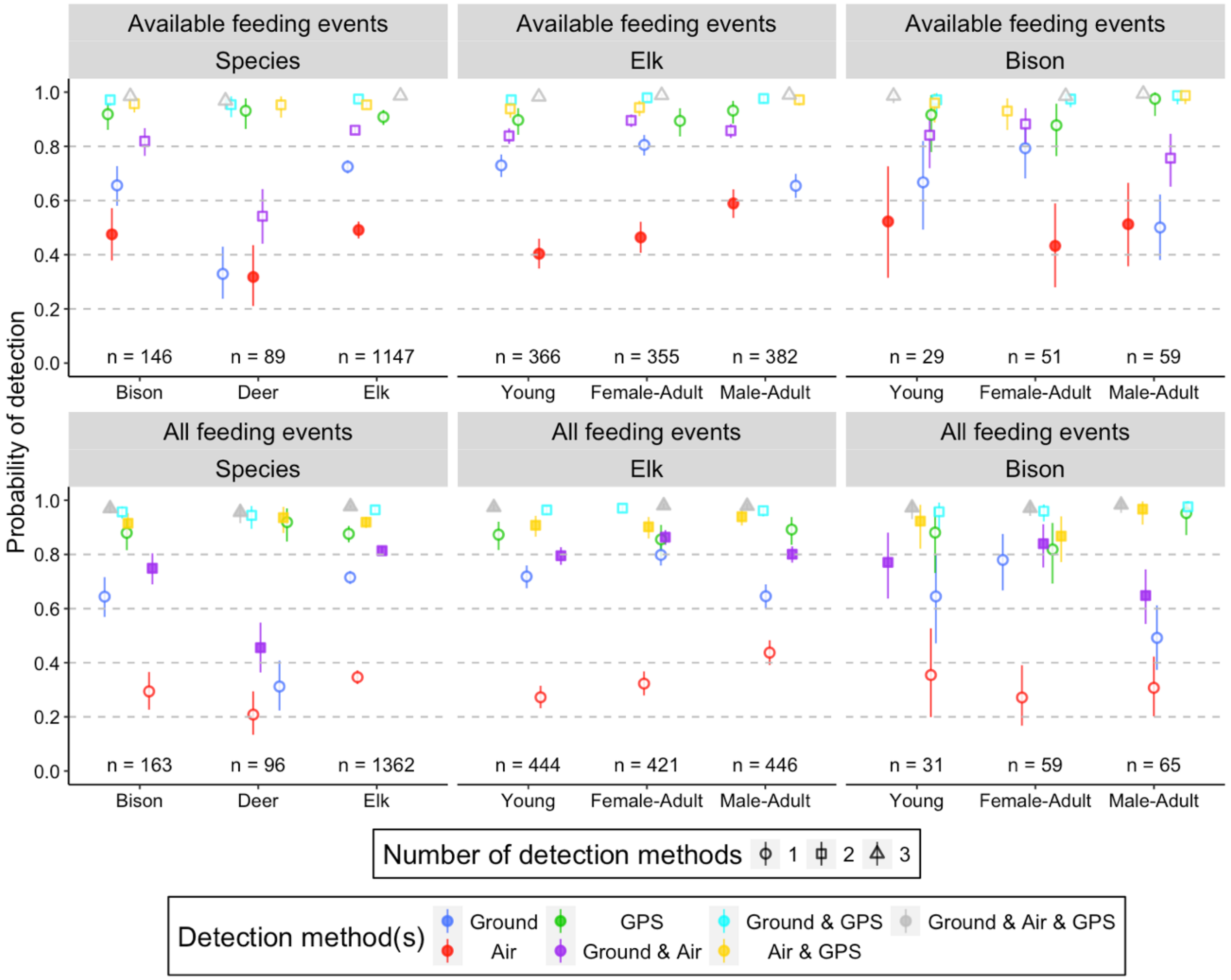

**Figure S4-D.1. Combined-method detection probabilities for prey species, elk sex-age class, and bison sex-age class for available feeding events and all feeding events.** Detection probabilities were developed using only feeding events detected during pack-sessions where multiple detection methods attempted to detect feeding events. Top row describes detection probabilities when method-specific availability was defined as a 1 or 0 depending on if any effort by a method occurred during the two-day feeding event lifespan (Fig. 4-5). The bottom row defined availability according to the methods that were intended to monitor the pack-session, thereby assuming the applicable methods were always operational within a feeding event lifespan. Each point reports the estimate (± 95% credible interval) for detection probability for these detection method(s). We estimated detection probability for all possible method combinations (symbol shape indicates the number of methods in a combination), although our employed method combinations dictated that we only used the detection probabilities for four combinations (Air; Ground & Air; Air & GPS; Ground, Air, & GPS) in Eqn. 8. The detection probabilities that were used in Eqn. 8 are indicated by the filled symbols. Specifically, we used $p_{air}$ from 'Available feeding events' (top row) for air-only pack sessions and $p_{methods}$ from 'All feeding events' (bottom row) for all other pack-sessions. Numbers indicate sample size. Left-most column is also displayed as Fig. 4-12.

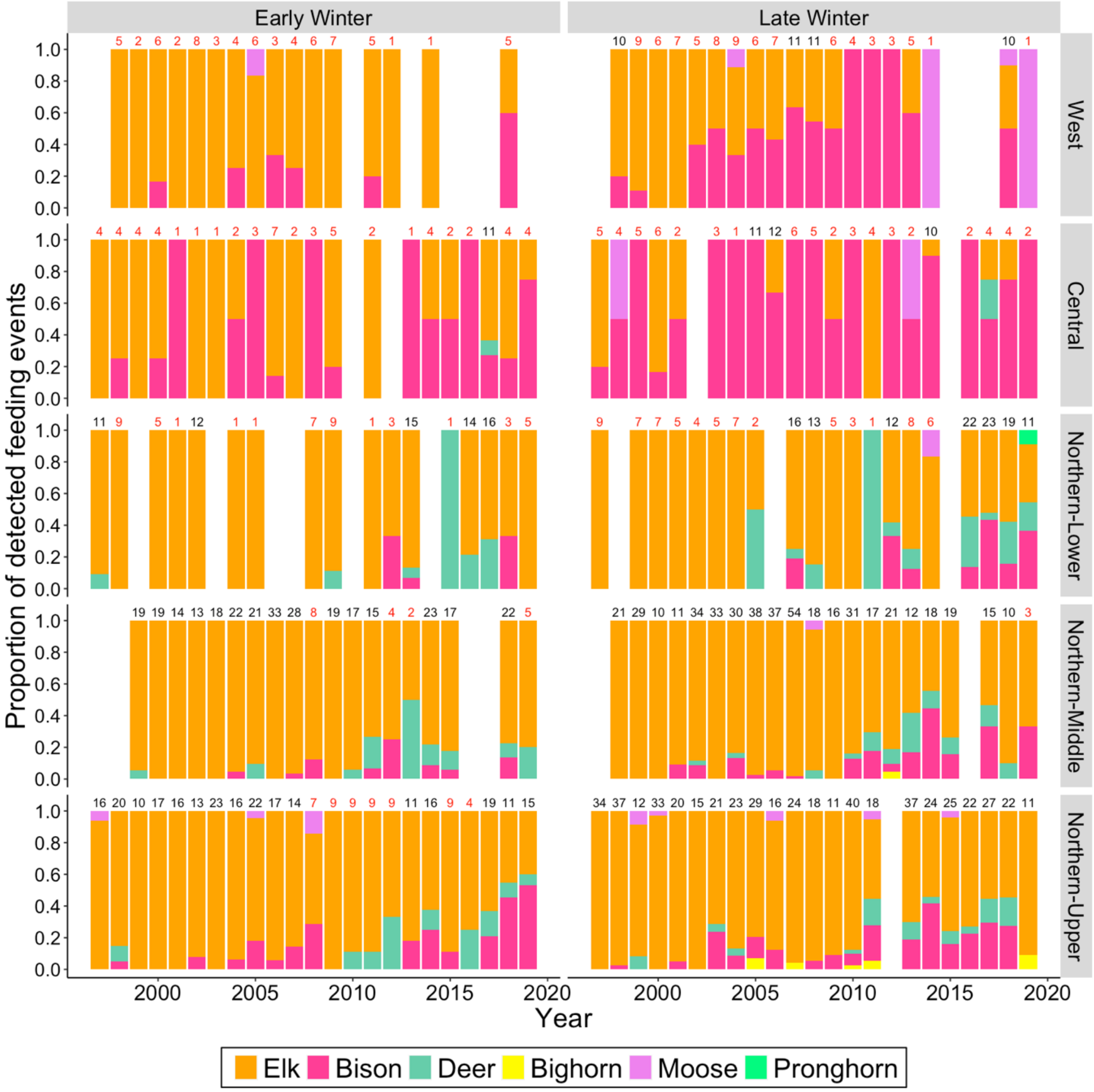

**Figure S4-D.2a. Annual proportion of species among detected feeding events during season and within spatial zone.** Here, the spatial zone represents the zone for the pack (i.e., not necessarily where the carcass lied in space). The number above each bar represents the total number of feeding events detected and is red when <10. Feeding events of unknown species were not included.

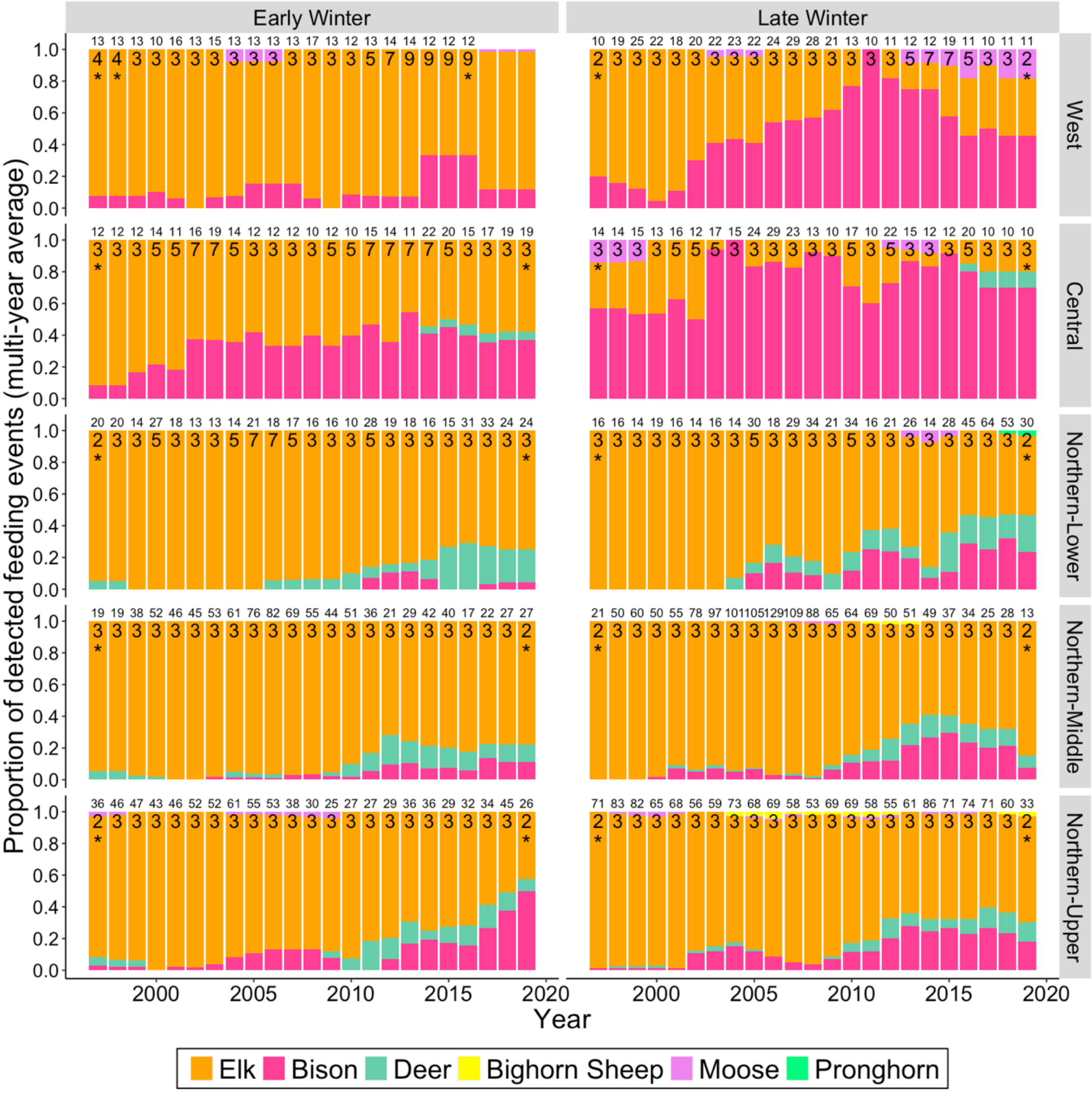

**Figure S4-D.2b. Multi-year proportion of species among detected feeding events during season and within spatial zone.** Each bar is a multi-year average of the data presented in Fig. S4-D.2a. The bar represents a 3-year moving average when ≥10 feeding events were detected. If <10 feeding events were detected, the moving average was expanded (one additional year prior and subsequent) until either ≥10 feeding events were in the sample or 5 years had been added to both sides of the year of interest, if possible. If 10 feeding events were still not available, we then used the proportions from all data for that season-zone. The numbers above each bear represent the sample size, while the number below the top of each bar represents the number of years of data that were used to determine the proportions. An asterisk indicates that less than the maximum number of years were available for this calculation (but the reported number of years is still correct here). No labels on a bar indicate that all data for that season-zone were used.

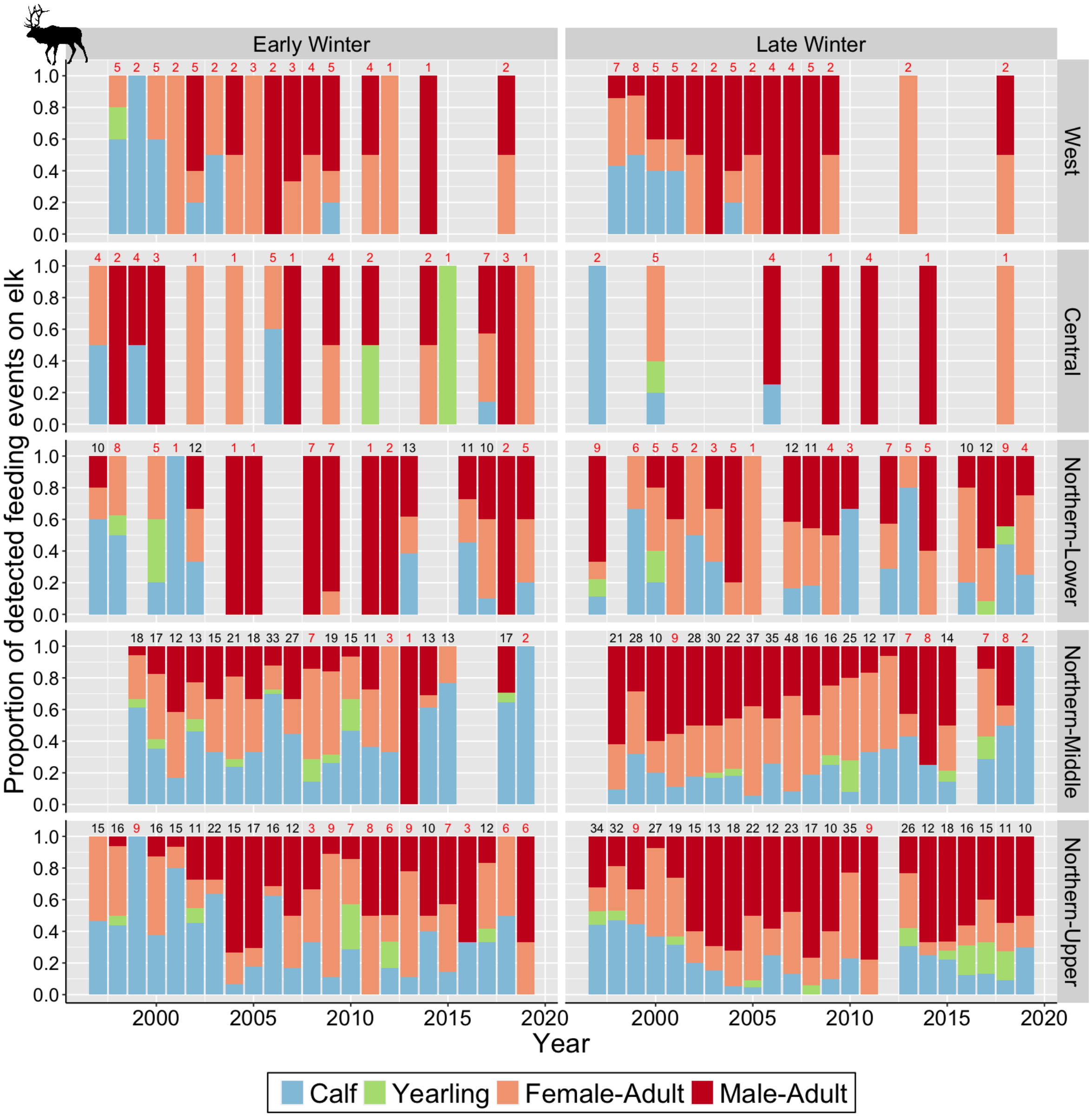

**Figure S4-D.3a. Annual proportion of sex-age classes among detected feeding events on elk during season and within spatial zone.** All other details are the same as Fig. S4-D.2a.

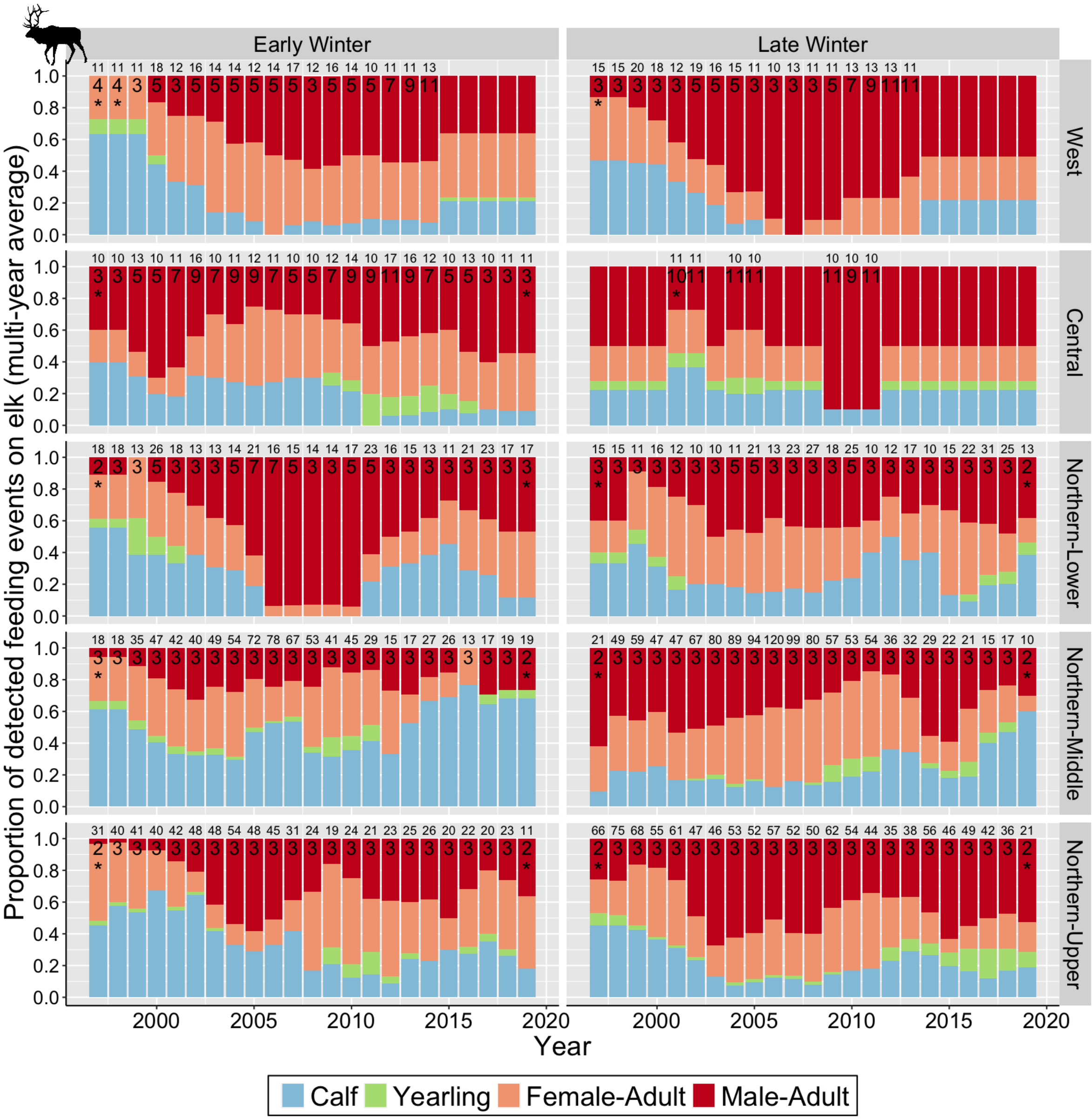

**Figure S4-D.3b. Multi-year proportion of sex-age class among detected feeding events on elk during season and within spatial zone.** All other details are the same as Fig. S4-D.2b.

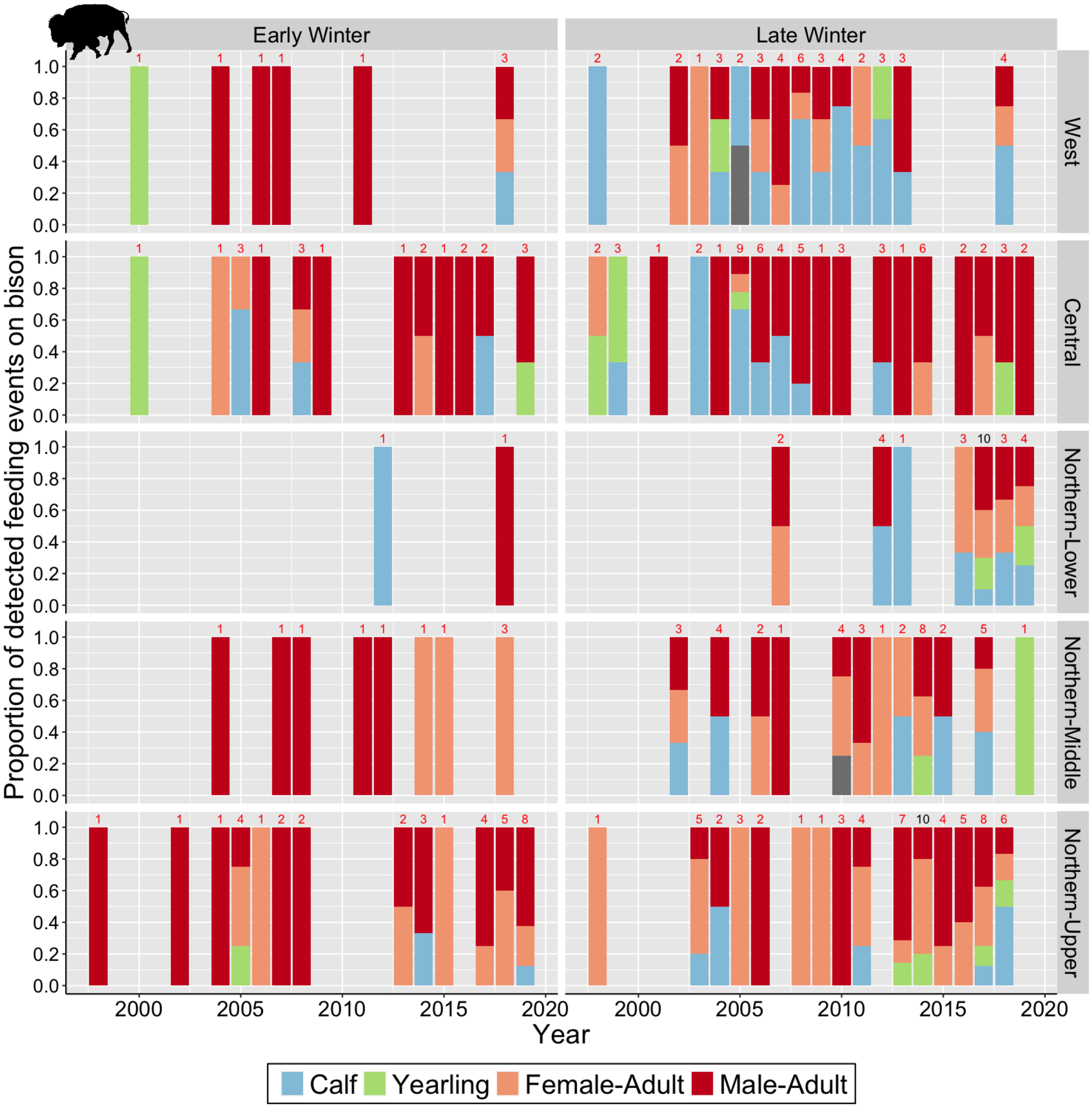

**Figure S4-D.4a. Annual proportion of sex-age classes among detected feeding events on bison during season and within spatial zone.** All other details are the same as Fig. S4-D.2a.

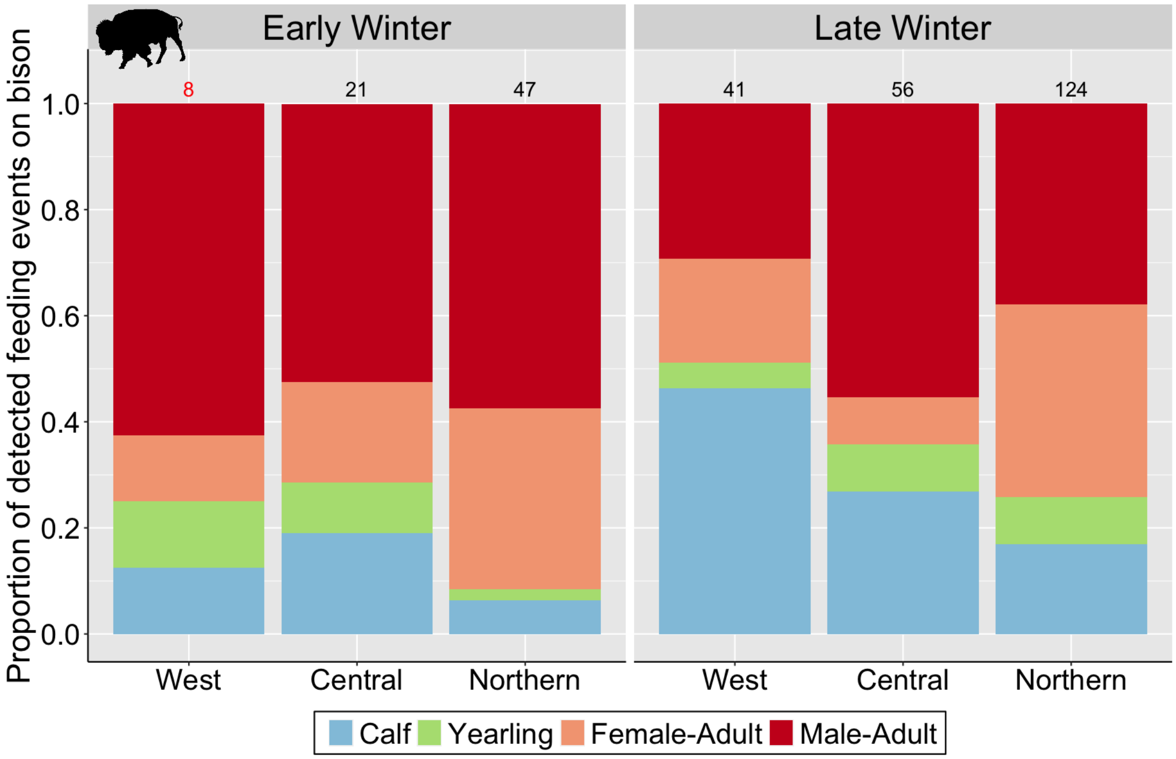

**Figure S4-D.4b. Proportion of sex-age class among detected feeding events on bison during season and within spatial zone *u**.** All years of data are combined, and the number on top of each bar therefore represents the total number of feeding events combined across all years, noting that we censored two neonate bison. Here, all data from Northern zones in Fig. S4-D.4a was combined.

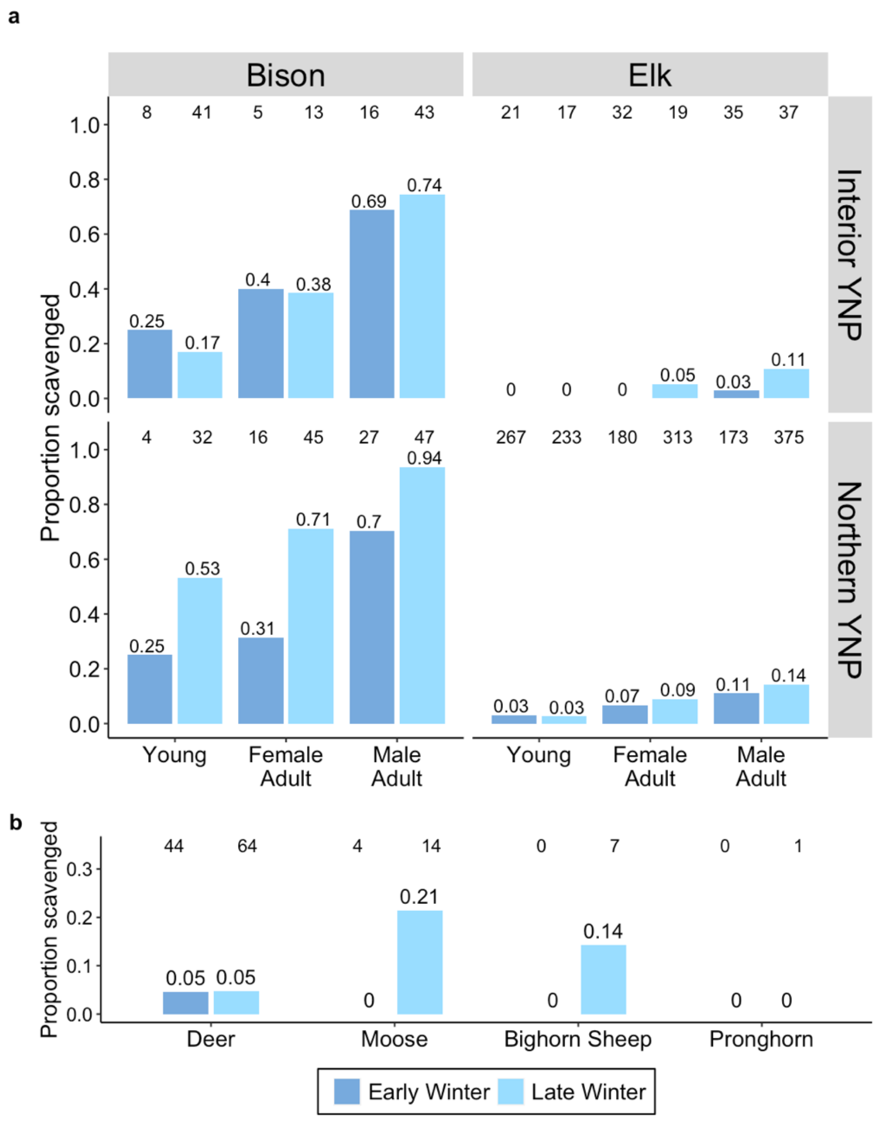

**Figure S4-D.5. Proportion of demographic class, among detected feeding events, that were scavenged across all years.** The number above each bar displays the proportion scavenged (*prop.scav*), noting that 1 – *prop.scav* was the input for Eqn. 10 in Chapter 4. The number on top of each bar displays *prop.scav* and the numbers at the top of each plot display the sample size for the corresponding bar. Total sample size and/or the spatial distribution of feeding events prevented us from considering YNP subsystem for the species displayed in panel (b).

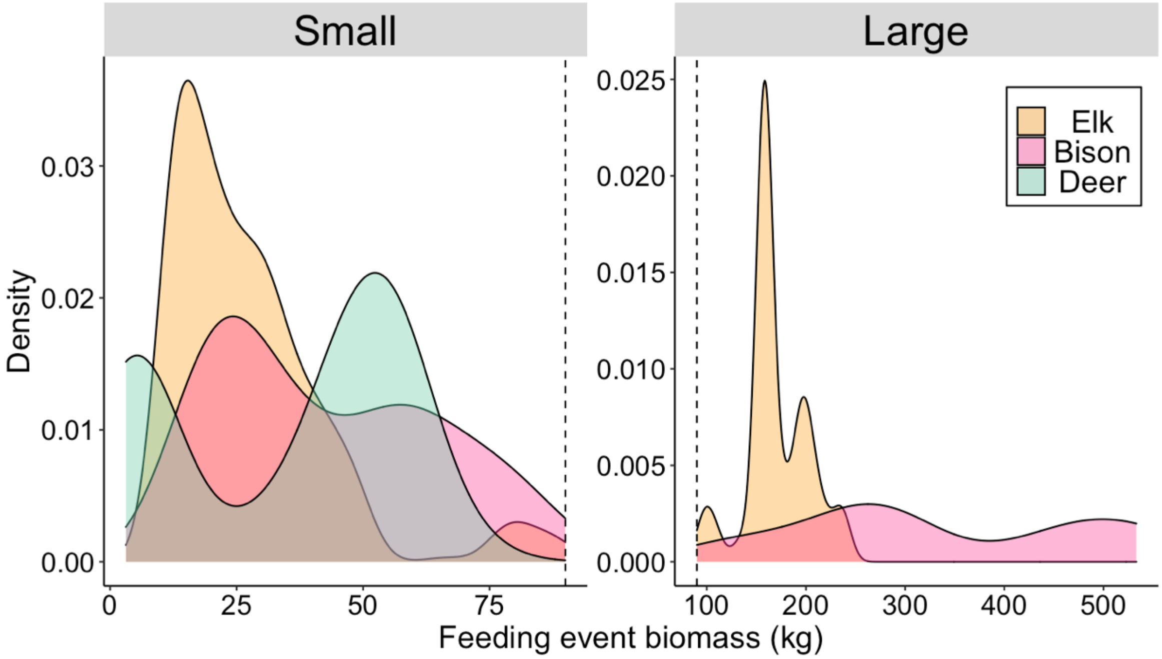

**Figure S4-D.6. Density of primary species across biomass for small and large feeding events during the denning period.**

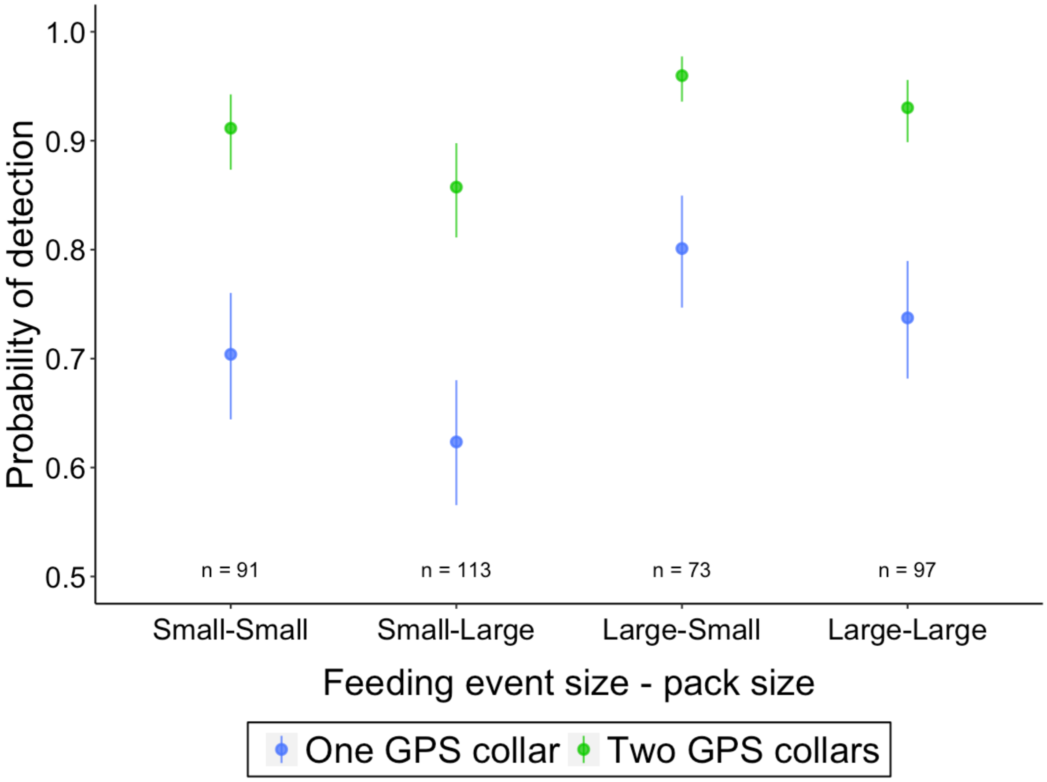

**Figure S4-D.7. Probability of detection for small and large feeding events during the denning period for small or large wolf packs.** Each point displays the estimate for detection probability (± 95% credible interval) that was applied for a pack that had one or two GPS-collared wolves, dependent on their pack size.

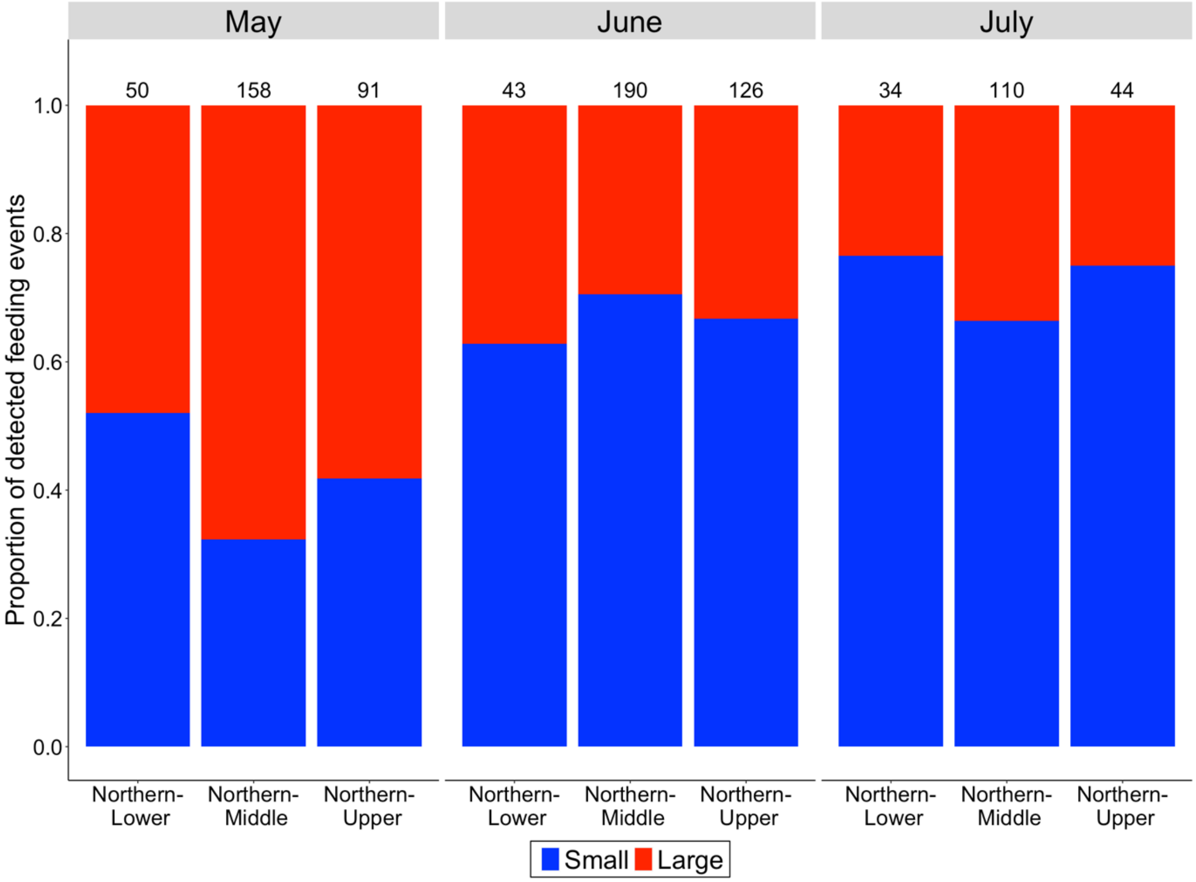

**Figure S4-D.8. Proportion of feeding events during the denning period that were small or large across zone and month.**

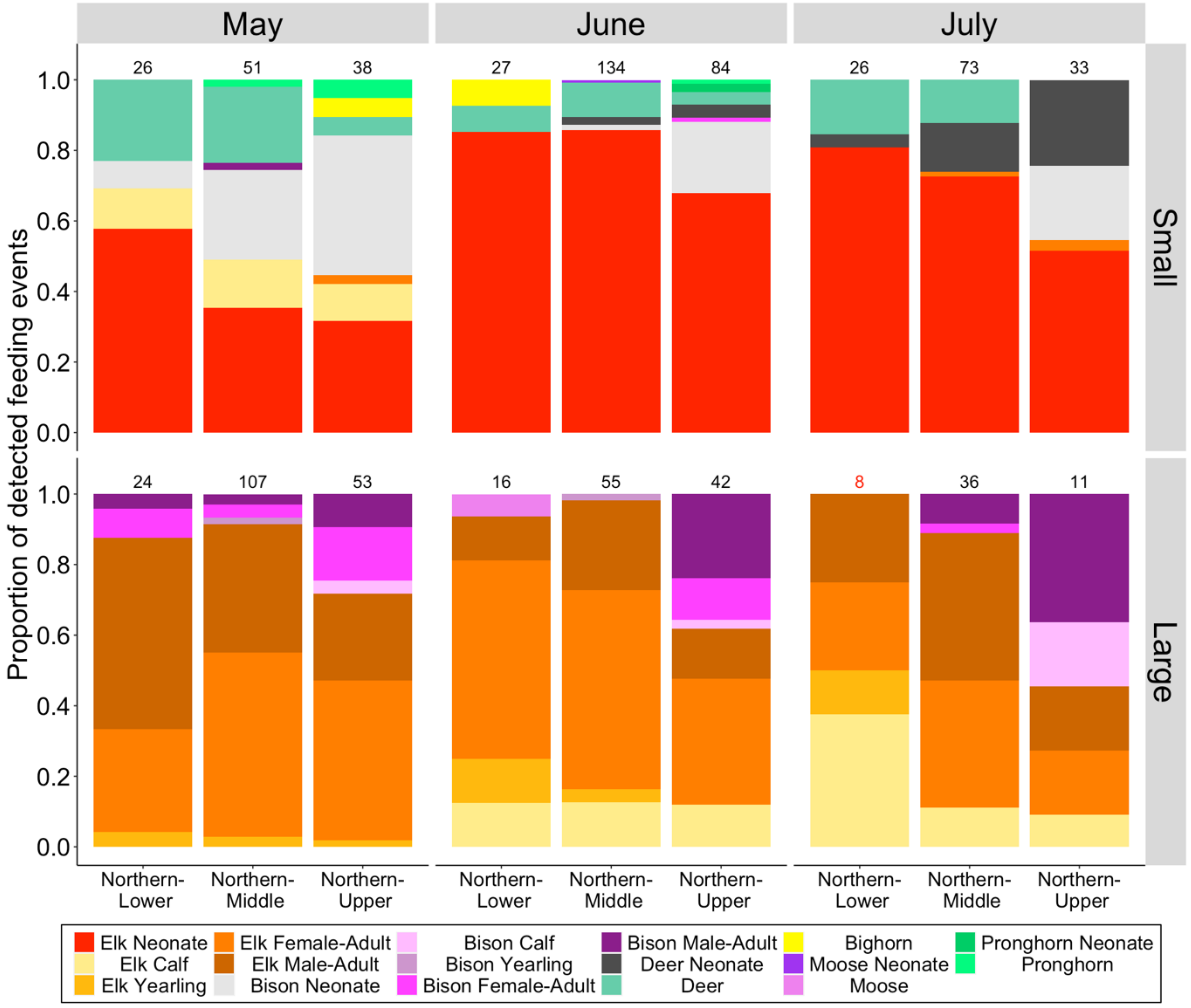

**Figure S4-D.9. Proportion of feeding events of each demographic class during the months of the denning period that were small or large across zone and month.** These proportions defined the proportion diet for our predictions of demographic class through Eqn. 9 of Chapter 4. Note that we censored two horse and predictions for seven neonates that were originally of unknown species.

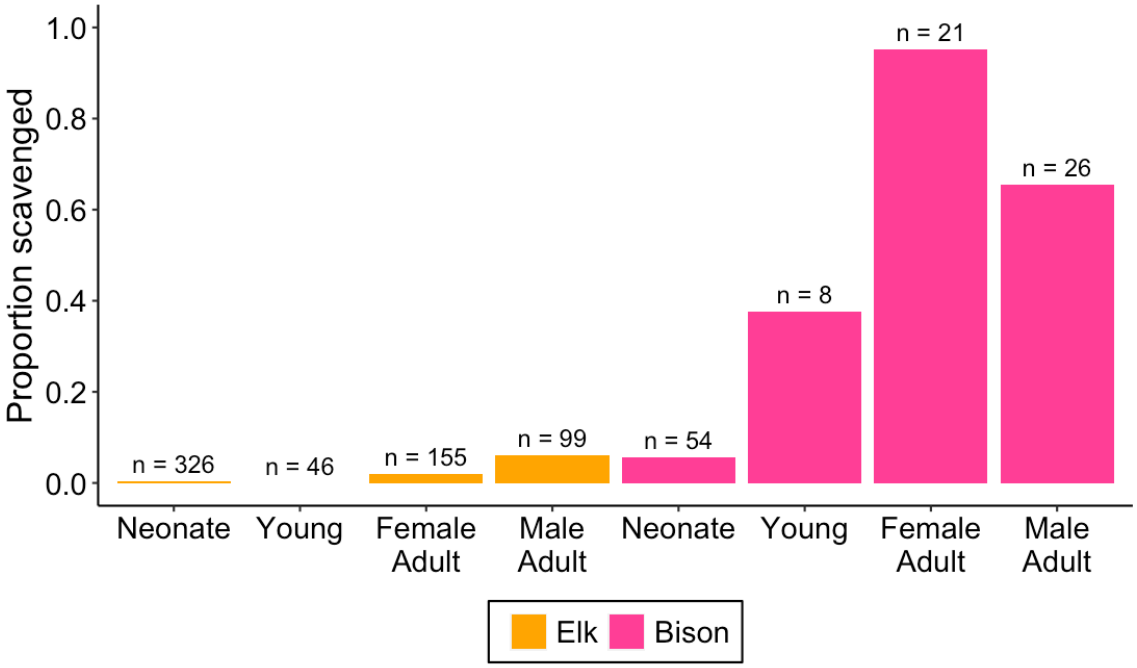

**Figure S4-D.10. Proportion of elk and bison demographic class, among detected feeding events, that were scavenged across all years.** The number above each bar displays the sample size. The input for Eqn. 10 was 1 – *prop.scav*.

# Chapter 4: Appendix S4-E. Supporting tables and figures for Results.

**Table S4-E.1. AIC$_c$ model results for wolf kill rates on elk (early winter).** AIC results for models evaluating factors affecting per-capita kill rate on elk during early winter. Kill rates were collected for 101 packs in Northern YNP during 23 early winter sessions. Here, and also for Table S4-E.2–Table S4-E.9, columns with 'inform' in the title display results for subsequent AIC comparison that included models with only significant covariates. Columns with 'all' display results for initial, full model set. We attempted to add random effects to the top-ranked model 'inform' model.

| Model | K | AIC$_c$ | ΔAIC$_c$ (inform) | $w_i$ (inform) | ΔAIC$_c$ (all) | $w_i$ (all) |
|---|---|---|---|---|---|---|
| pack.size + altern.prey | 4 | 68.24 | 0.00 | 1.00 | 1.94 | 0.14 |
| pack.size + elk.calf | 4 | 103.45 | 35.21 | 0.00 | 37.15 | 0.00 |
| pack.size | 3 | 106.63 | 38.40 | 0.00 | 40.34 | 0.00 |
| snow + altern.prey | 4 | 127.34 | 59.11 | 0.00 | 61.04 | 0.00 |
| altern.prey | 3 | 129.42 | 61.18 | 0.00 | 63.12 | 0.00 |
| snow | 3 | 144.89 | 76.65 | 0.00 | 78.59 | 0.00 |
| snow + pack.size + elk.calf + altern.prey | 6 | 66.30 | NA | NA | 0.00 | 0.37 |
| pack.size + elk.calf + altern.prey | 5 | 66.70 | NA | NA | 0.40 | 0.31 |
| snow + pack.size + altern.prey | 5 | 67.77 | NA | NA | 1.48 | 0.18 |
| snow + pack.size + elk.calf | 5 | 102.70 | NA | NA | 36.40 | 0.00 |
| snow + pack.size | 4 | 105.78 | NA | NA | 39.49 | 0.00 |
| snow + elk.calf + altern.prey | 5 | 128.47 | NA | NA | 62.17 | 0.00 |
| elk.calf + altern.prey | 4 | 130.50 | NA | NA | 64.20 | 0.00 |
| snow + elk.calf | 4 | 144.85 | NA | NA | 78.55 | 0.00 |
| elk.calf | 3 | 147.16 | NA | NA | 80.86 | 0.00 |

**Table S4-E.2. AIC$_c$ model results for wolf kill rates on elk (late winter).** AIC results for models evaluating factors affecting per-capita kill rate on elk during late winter. Kill rates were collected for 126 packs in Northern YNP during 23 late winter sessions. See Table S4-E.1 text for column meanings and additional information.

| Model | K | AIC$_c$ | ΔAIC$_c$ (inform) | $w_i$ (inform) | ΔAIC$_c$ (all) | $w_i$ (all) |
|---|---|---|---|---|---|---|
| snow + pack.size + elk.calf + altern.prey | 6 | 190.26 | 0.00 | 0.69 | 0.00 | 0.69 |
| pack.size + elk.calf + altern.prey | 5 | 192.94 | 2.68 | 0.18 | 2.68 | 0.18 |
| snow + pack.size + altern.prey | 5 | 194.00 | 3.74 | 0.11 | 3.74 | 0.11 |
| pack.size + altern.prey | 4 | 197.27 | 7.02 | 0.02 | 7.02 | 0.02 |
| pack.size | 3 | 257.39 | 67.14 | 0.00 | 67.14 | 0.00 |
| snow + altern.prey | 4 | 295.29 | 105.03 | 0.00 | 105.03 | 0.00 |
| altern.prey | 3 | 298.21 | 107.95 | 0.00 | 107.95 | 0.00 |
| pack.size + elk.calf | 4 | 256.49 | NA | NA | 66.23 | 0.00 |
| snow + pack.size + elk.calf | 5 | 256.82 | NA | NA | 66.56 | 0.00 |
| snow + pack.size | 4 | 257.39 | NA | NA | 67.13 | 0.00 |
| snow + elk.calf + altern.prey | 5 | 294.44 | NA | NA | 104.18 | 0.00 |
| elk.calf + altern.prey | 4 | 296.87 | NA | NA | 106.61 | 0.00 |
| snow | 3 | 325.50 | NA | NA | 135.24 | 0.00 |
| snow + elk.calf | 4 | 325.77 | NA | NA | 135.52 | 0.00 |
| elk.calf | 3 | 326.29 | NA | NA | 136.04 | 0.00 |

**Table S4-E.3. AIC$_c$ model results for wolf kill rates on elk (May).** AIC results for models evaluating factors affecting per-capita kill rate on elk during May. Kill rates were collected for 18 packs in Northern YNP during 12 May sessions. See Table S4-E.1 text for column meanings and additional information.

| Model | K | AIC$_c$ | ΔAIC$_c$ (inform) | $w_i$ (inform) | ΔAIC$_c$ (all) | $w_i$ (all) |
|---|---|---|---|---|---|---|
| pack.size | 3 | 52.12 | 0.00 | 1.00 | 0.00 | 0.37 |
| pack.size + altern.prey | 4 | 52.13 | NA | NA | 0.01 | 0.37 |
| pack.size + elk.neonate | 4 | 55.39 | NA | NA | 3.27 | 0.07 |
| elk + pack.size | 4 | 55.45 | NA | NA | 3.33 | 0.07 |
| pack.size + elk.neonate + altern.prey | 5 | 55.85 | NA | NA | 3.72 | 0.06 |
| elk + pack.size + altern.prey | 5 | 56.04 | NA | NA | 3.92 | 0.05 |
| elk + pack.size + elk.neonate | 5 | 59.29 | NA | NA | 7.16 | 0.01 |
| elk + pack.size + elk.neonate + altern.prey | 6 | 60.46 | NA | NA | 8.34 | 0.01 |
| elk | 3 | 73.91 | NA | NA | 21.79 | 0.00 |
| elk.neonate | 3 | 74.17 | NA | NA | 22.05 | 0.00 |
| altern.prey | 3 | 74.68 | NA | NA | 22.56 | 0.00 |
| elk + elk.neonate | 4 | 76.72 | NA | NA | 24.60 | 0.00 |
| elk + altern.prey | 4 | 77.27 | NA | NA | 25.14 | 0.00 |
| elk.neonate + altern.prey | 4 | 77.40 | NA | NA | 25.28 | 0.00 |
| elk + elk.neonate + altern.prey | 5 | 80.62 | NA | NA | 28.50 | 0.00 |

**Table S4-E.4. AIC$_c$ model results for wolf kill rates on elk (June).** AIC results for models evaluating factors affecting per-capita kill rate on elk during June. Kill rates were collected for 20 packs in Northern YNP during 12 June sessions. See Table S4-E.1 text for column meanings and additional information.

| Model | K | AIC$_c$ | ΔAIC$_c$ (inform) | $w_i$ (inform) | ΔAIC$_c$ (all) | $w_i$ (all) |
|---|---|---|---|---|---|---|
| pack.size | 3 | 77.17 | 0.00 | 1.00 | 0.60 | 0.20 |
| pack.size + altern.prey | 4 | 76.57 | NA | NA | 0.00 | 0.27 |
| pack.size + elk.neonate + altern.prey | 5 | 76.91 | NA | NA | 0.34 | 0.23 |
| pack.size + elk.neonate | 4 | 78.42 | NA | NA | 1.85 | 0.11 |
| elk + pack.size | 4 | 79.54 | NA | NA | 2.97 | 0.06 |
| elk + pack.size + altern.prey | 5 | 79.80 | NA | NA | 3.23 | 0.05 |
| elk + pack.size + elk.neonate + altern.prey | 6 | 80.28 | NA | NA | 3.71 | 0.04 |
| elk + pack.size + elk.neonate | 5 | 80.74 | NA | NA | 4.18 | 0.03 |
| elk.neonate | 3 | 91.17 | NA | NA | 14.60 | 0.00 |
| elk | 3 | 91.54 | NA | NA | 14.97 | 0.00 |
| altern.prey | 3 | 91.87 | NA | NA | 15.30 | 0.00 |
| elk + elk.neonate | 4 | 94.09 | NA | NA | 17.52 | 0.00 |
| elk.neonate + altern.prey | 4 | 94.33 | NA | NA | 17.76 | 0.00 |
| elk + altern.prey | 4 | 94.68 | NA | NA | 18.11 | 0.00 |
| elk + elk.neonate + altern.prey | 5 | 97.66 | NA | NA | 21.10 | 0.00 |

**Table S4-E.5. $AIC_c$ model results for wolf kill rates on elk (July).** AIC results for models evaluating factors affecting per-capita kill rate on elk during July. Kill rates were collected for 14 packs in Northern YNP during 9 July sessions. See Table S4-E.1 text for column meanings and additional information.

| Model | K | $AIC_c$ | $\Delta AIC_c$ (inform) | $w_i$ (inform) | $\Delta AIC_c$ (all) | $w_i$ (all) |
|---|---|---|---|---|---|---|
| pack.size + elk.neonate | 4 | 14.99 | 0.00 | 0.86 | 0.00 | 0.67 |
| elk.neonate | 3 | 18.60 | 3.61 | 0.14 | 3.61 | 0.11 |
| pack.size | 3 | 33.48 | 18.49 | 0.00 | 18.49 | 0.00 |
| elk + pack.size + elk.neonate | 5 | 18.53 | NA | NA | 3.54 | 0.11 |
| pack.size + elk.neonate + altern.prey | 5 | 19.90 | NA | NA | 4.91 | 0.06 |
| elk.neonate + altern.prey | 4 | 21.33 | NA | NA | 6.34 | 0.03 |
| elk + elk.neonate | 4 | 22.64 | NA | NA | 7.65 | 0.01 |
| elk + pack.size + elk.neonate + altern.prey | 6 | 24.46 | NA | NA | 9.47 | 0.01 |
| elk + elk.neonate + altern.prey | 5 | 26.13 | NA | NA | 11.14 | 0.00 |
| altern.prey | 3 | 35.49 | NA | NA | 20.50 | 0.00 |
| pack.size + altern.prey | 4 | 36.13 | NA | NA | 21.13 | 0.00 |
| elk + pack.size | 4 | 37.51 | NA | NA | 22.52 | 0.00 |
| elk | 3 | 38.50 | NA | NA | 23.51 | 0.00 |
| elk + altern.prey | 4 | 39.53 | NA | NA | 24.54 | 0.00 |
| elk + pack.size + altern.prey | 5 | 40.97 | NA | NA | 25.98 | 0.00 |

**Table S4-E.6. AIC$_c$ model results for scavenging rates on elk (early winter).** AIC results for models evaluating factors affecting per-capita scavenging rate on elk during early winter. Scavenging rates were collected for 86 packs in Northern YNP during 19 early winter sessions. See Table S4-E.1 text for column meanings and additional information.

| Model | K | AIC$_c$ | ΔAIC$_c$ (inform) | $w_i$ (inform) | ΔAIC$_c$ (all) | $w_i$ (all) |
|---|---|---|---|---|---|---|
| pack.size | 3 | 49.58 | NA | NA | 0.00 | 0.25 |
| forage + pack.size | 4 | 51.66 | NA | NA | 2.09 | 0.09 |
| forage | 3 | 51.73 | NA | NA | 2.16 | 0.09 |
| pack.size + elk | 4 | 51.74 | NA | NA | 2.16 | 0.08 |
| elk | 3 | 51.76 | NA | NA | 2.18 | 0.08 |
| snow + pack.size | 4 | 51.77 | NA | NA | 2.20 | 0.08 |
| snow | 3 | 51.78 | NA | NA | 2.21 | 0.08 |
| forage + pack.size + elk | 5 | 53.88 | NA | NA | 4.30 | 0.03 |
| forage + elk | 4 | 53.89 | NA | NA | 4.31 | 0.03 |
| forage + snow + pack.size | 5 | 53.90 | NA | NA | 4.32 | 0.03 |
| snow + elk | 4 | 53.93 | NA | NA | 4.35 | 0.03 |
| forage + snow | 4 | 53.93 | NA | NA | 4.35 | 0.03 |
| snow + pack.size + elk | 5 | 53.99 | NA | NA | 4.42 | 0.03 |
| forage * elk | 5 | 55.99 | NA | NA | 6.42 | 0.01 |
| forage + snow + elk | 5 | 56.12 | NA | NA | 6.54 | 0.01 |
| forage * elk + pack.size | 6 | 56.15 | NA | NA | 6.58 | 0.01 |
| snow * elk | 5 | 56.18 | NA | NA | 6.60 | 0.01 |
| forage + snow + pack.size + elk | 6 | 56.18 | NA | NA | 6.61 | 0.01 |
| snow * elk + pack.size | 6 | 56.25 | NA | NA | 6.67 | 0.01 |
| forage * elk + snow | 6 | 58.25 | NA | NA | 8.68 | 0.00 |
| snow * elk + forage | 6 | 58.43 | NA | NA | 8.86 | 0.00 |
| forage * elk + pack.size + snow | 7 | 58.52 | NA | NA | 8.95 | 0.00 |
| snow * elk + pack.size + forage | 7 | 58.54 | NA | NA | 8.96 | 0.00 |

**Table S4-E.7. AIC$_c$ model results for scavenging rates on elk (late winter).** AIC results for models evaluating factors affecting per-capita scavenging rate on elk during late winter. Scavenging rates were collected for 109 packs in Northern YNP during 19 early winter sessions. See Table S4-E.1 text for column meanings and additional information.

| Model | K | AIC$_c$ | ΔAIC$_c$ (inform) | $w_i$ (inform) | ΔAIC$_c$ (all) | $w_i$ (all) |
|---|---|---|---|---|---|---|
| forage + pack.size | 4 | 101.75 | 0.00 | 0.71 | 0.00 | 0.24 |
| pack.size | 3 | 103.55 | 1.79 | 0.29 | 1.79 | 0.10 |
| forage + pack.size + elk | 5 | 103.32 | NA | NA | 1.57 | 0.11 |
| forage + snow + pack.size | 5 | 103.54 | NA | NA | 1.79 | 0.10 |
| forage | 3 | 104.09 | NA | NA | 2.33 | 0.07 |
| pack.size + elk | 4 | 104.52 | NA | NA | 2.77 | 0.06 |
| forage + snow + pack.size + elk | 6 | 105.05 | NA | NA | 3.29 | 0.05 |
| forage + snow | 4 | 105.27 | NA | NA | 3.52 | 0.04 |
| forage * elk + pack.size | 6 | 105.49 | NA | NA | 3.74 | 0.04 |
| snow + pack.size | 4 | 105.70 | NA | NA | 3.95 | 0.03 |
| forage + elk | 4 | 105.72 | NA | NA | 3.97 | 0.03 |
| elk | 3 | 106.47 | NA | NA | 4.71 | 0.02 |
| snow + pack.size + elk | 5 | 106.72 | NA | NA | 4.96 | 0.02 |
| forage + snow + elk | 5 | 106.86 | NA | NA | 5.11 | 0.02 |
| forage * elk + pack.size + snow | 7 | 107.17 | NA | NA | 5.42 | 0.02 |
| snow * elk + pack.size + forage | 7 | 107.33 | NA | NA | 5.58 | 0.01 |
| snow | 3 | 107.49 | NA | NA | 5.74 | 0.01 |
| forage * elk | 5 | 107.87 | NA | NA | 6.12 | 0.01 |
| snow + elk | 4 | 108.56 | NA | NA | 6.80 | 0.01 |
| forage * elk + snow | 6 | 108.90 | NA | NA | 7.15 | 0.01 |
| snow * elk + pack.size | 6 | 108.95 | NA | NA | 7.19 | 0.01 |
| snow * elk + forage | 6 | 109.05 | NA | NA | 7.29 | 0.01 |
| snow * elk | 5 | 110.59 | NA | NA | 8.84 | 0.00 |

**Table S4-E.8. AIC$_c$ model results for scavenging rates on bison (early winter).** AIC results for models evaluating factors affecting per-capita scavenging rate on bison during early winter. Scavenging rates were collected for 101 packs in Northern YNP during 23 early winter sessions. See Table S4-E.1 text for column meanings and additional information.

| Model | K | AIC$_c$ | ΔAIC$_c$ (inform) | $w_i$ (inform) | ΔAIC$_c$ (all) | $w_i$ (all) |
|---|---|---|---|---|---|---|
| bison | 3 | 37.58 | NA | NA | 0.00 | 0.35 |
| snow | 3 | 39.63 | NA | NA | 2.05 | 0.13 |
| pack.size | 3 | 39.64 | NA | NA | 2.06 | 0.13 |
| snow + bison | 4 | 39.64 | NA | NA | 2.07 | 0.13 |
| pack.size + bison | 4 | 39.74 | NA | NA | 2.16 | 0.12 |
| snow * bison | 5 | 41.53 | NA | NA | 3.95 | 0.05 |
| snow + pack.size | 4 | 41.79 | NA | NA | 4.21 | 0.04 |
| snow + pack.size + bison | 5 | 41.86 | NA | NA | 4.28 | 0.04 |
| snow * bison + pack.size | 6 | 43.78 | NA | NA | 6.21 | 0.02 |

**Table S4-E.9. AIC$_c$ model results for scavenging rates on bison (late winter).** AIC results for models evaluating factors affecting per-capita scavenging rate on bison during late winter. Scavenging rates were collected for 126 packs in Northern YNP during 23 late winter sessions. See Table S4-E.1 text for column meanings and additional information.

| Model | K | AIC$_c$ | ΔAIC$_c$ (inform) | $w_i$ (inform) | ΔAIC$_c$ (all) | $w_i$ (all) |
|---|---|---|---|---|---|---|
| bison | 3 | 104.70 | 0.00 | 1.00 | 0.00 | 0.44 |
| pack.size + bison | 4 | 105.92 | NA | NA | 1.22 | 0.24 |
| snow + bison | 4 | 106.84 | NA | NA | 2.13 | 0.15 |
| snow + pack.size + bison | 5 | 108.09 | NA | NA | 3.39 | 0.08 |
| snow * bison | 5 | 108.91 | NA | NA | 4.21 | 0.05 |
| snow * bison + pack.size | 6 | 110.20 | NA | NA | 5.50 | 0.03 |
| pack.size | 3 | 115.89 | NA | NA | 11.18 | 0.00 |
| snow | 3 | 116.59 | NA | NA | 11.89 | 0.00 |
| snow + pack.size | 4 | 118.02 | NA | NA | 13.31 | 0.00 |

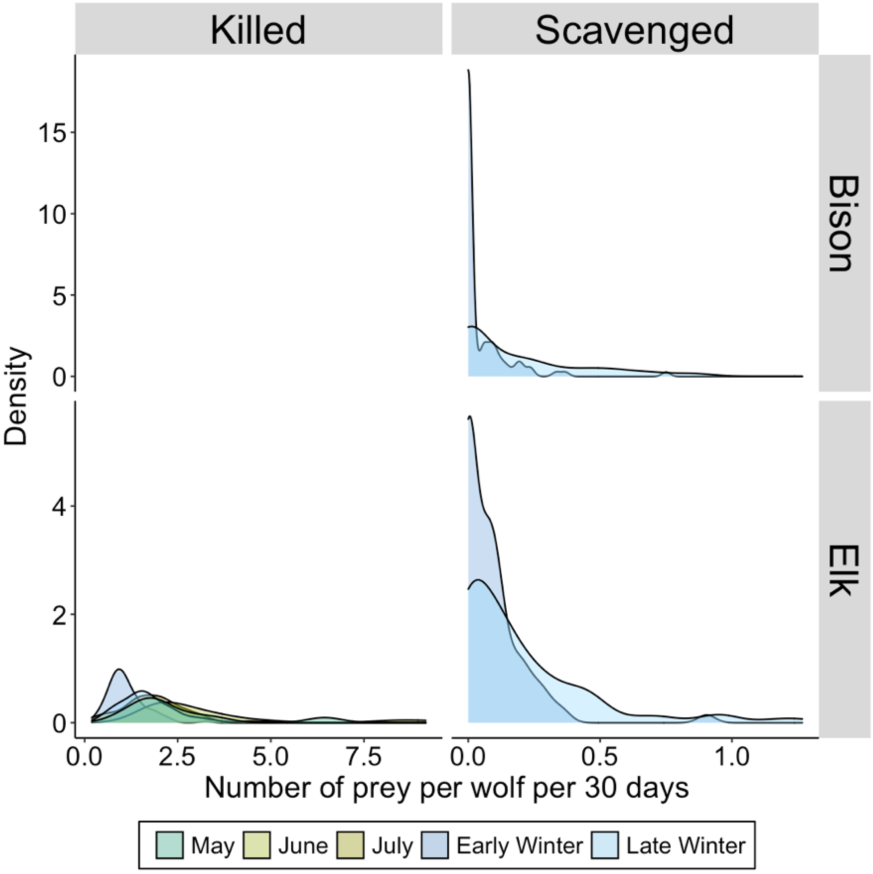

**Figure S4-E.1. Distribution of kill and scavenging rates used in general linear models.** See Table S4-E.1–Table S.4-E.9 for information about sample size.

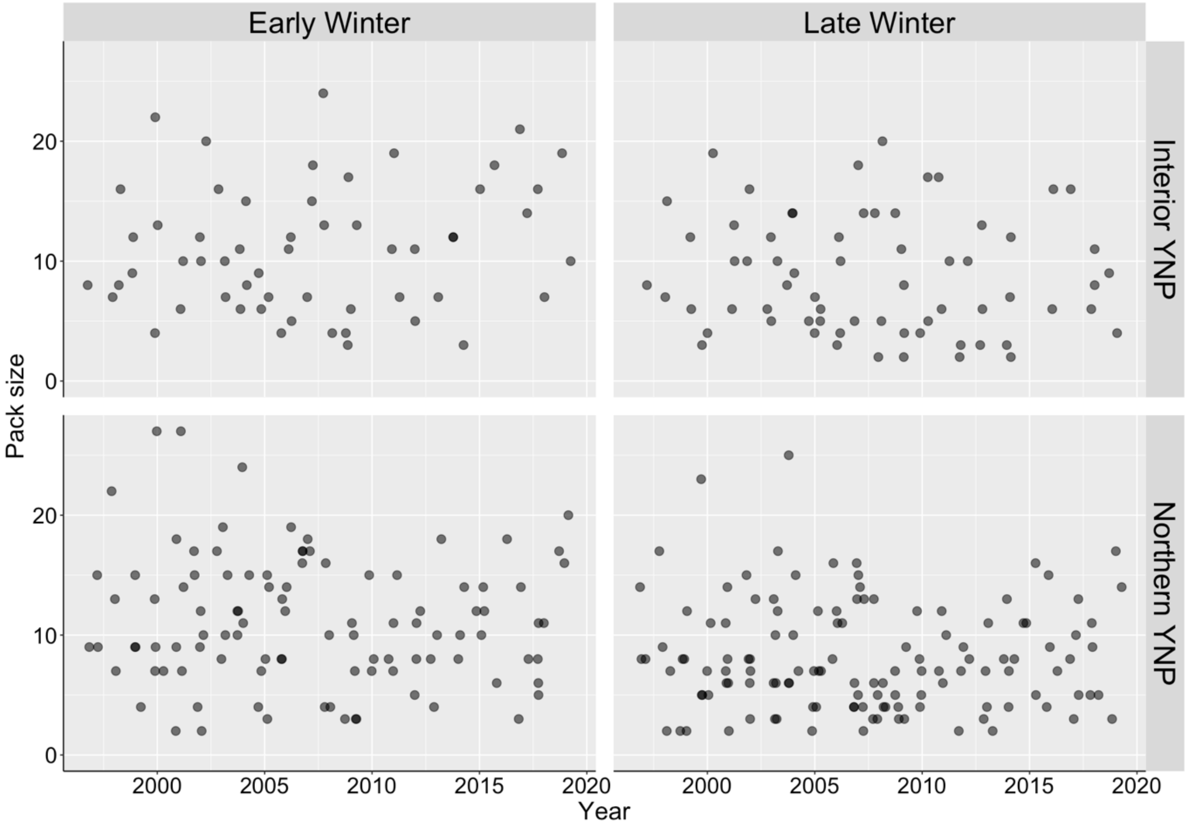

**Figure S4-E.2. Pack size estimates during the roaming period across time (*n* = 349).**

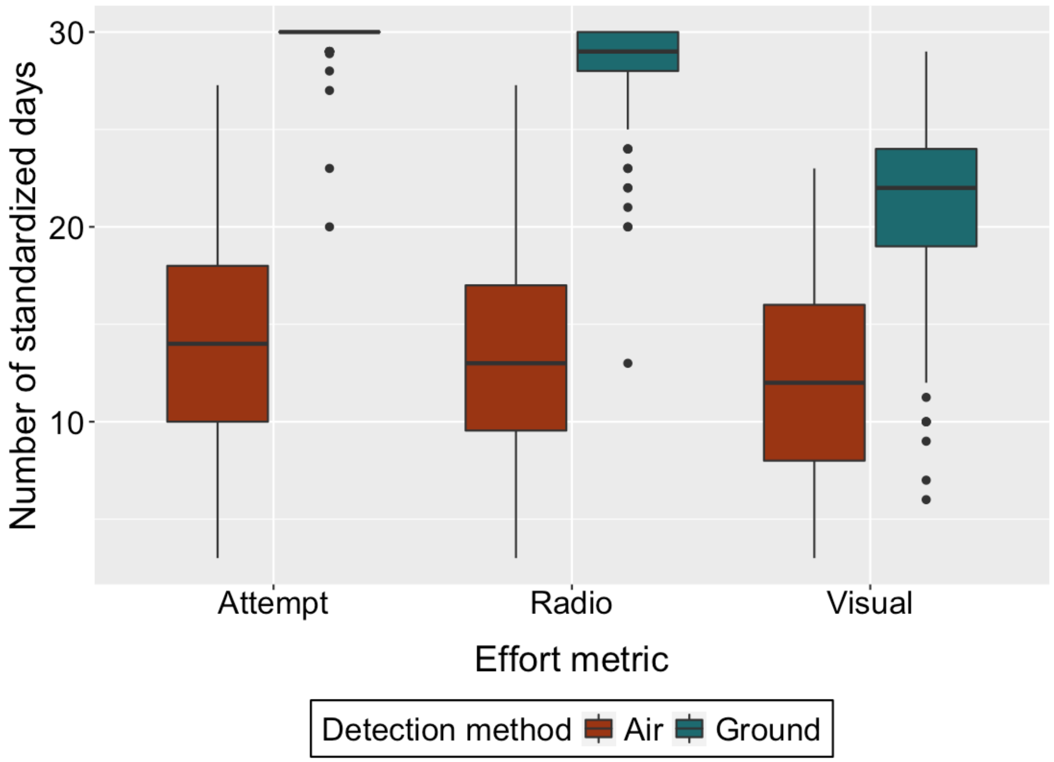

**Figure S4-E.3. Effort-related metrics for aerial and ground methods.** Number of days during a pack-session (standardized for a 30-day pack-session) with an attempt, radiolocation, or visual observation. See Appendix S4-A for additional methodological details.

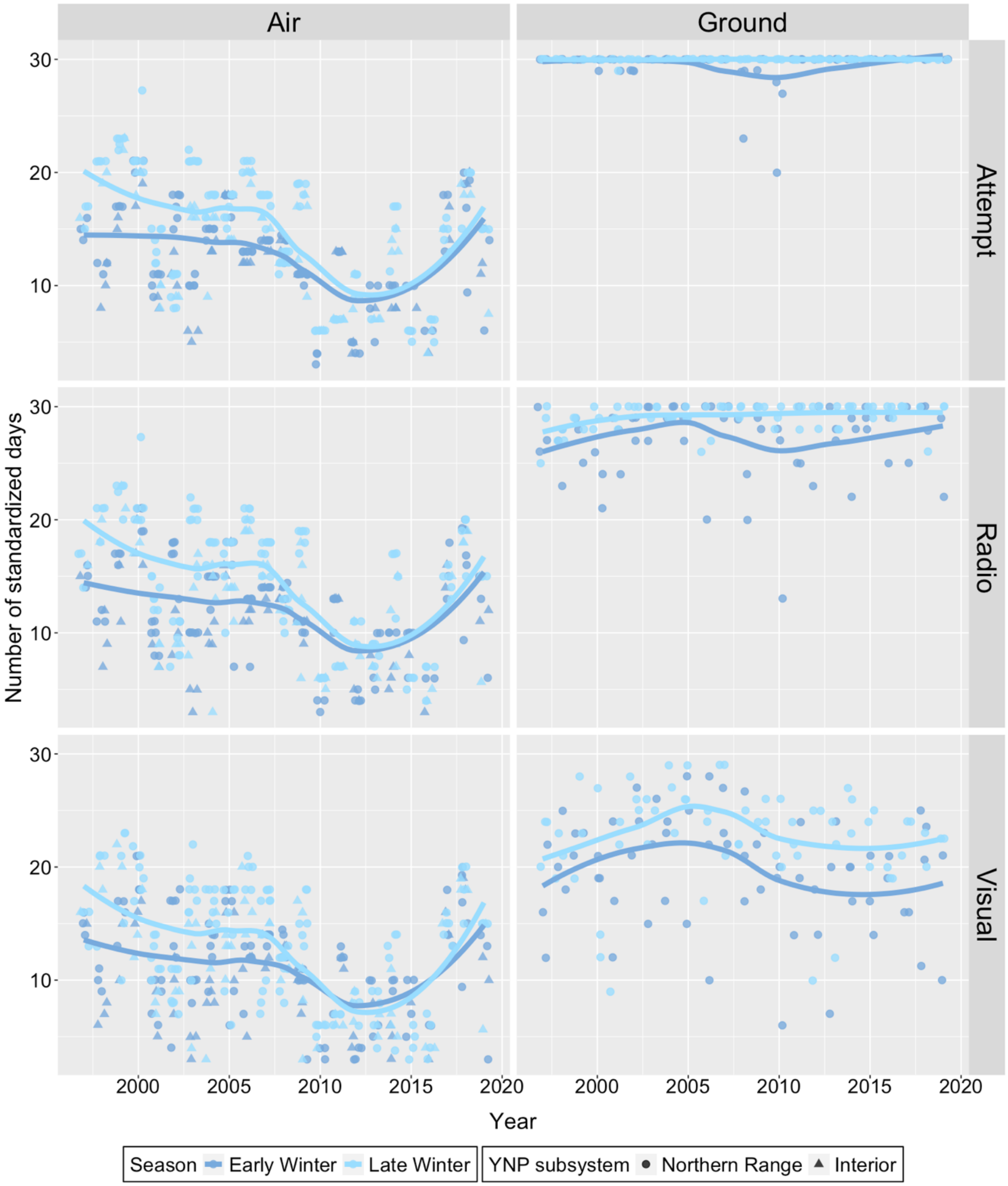

**Figure S4-E.4. Longitudinal patterns in effort-related metrics for ground and aerial methods.** The dashed lines display a 'loess' fit for the season (color), but ignore YNP subsystem (shape; only applicable for Air).

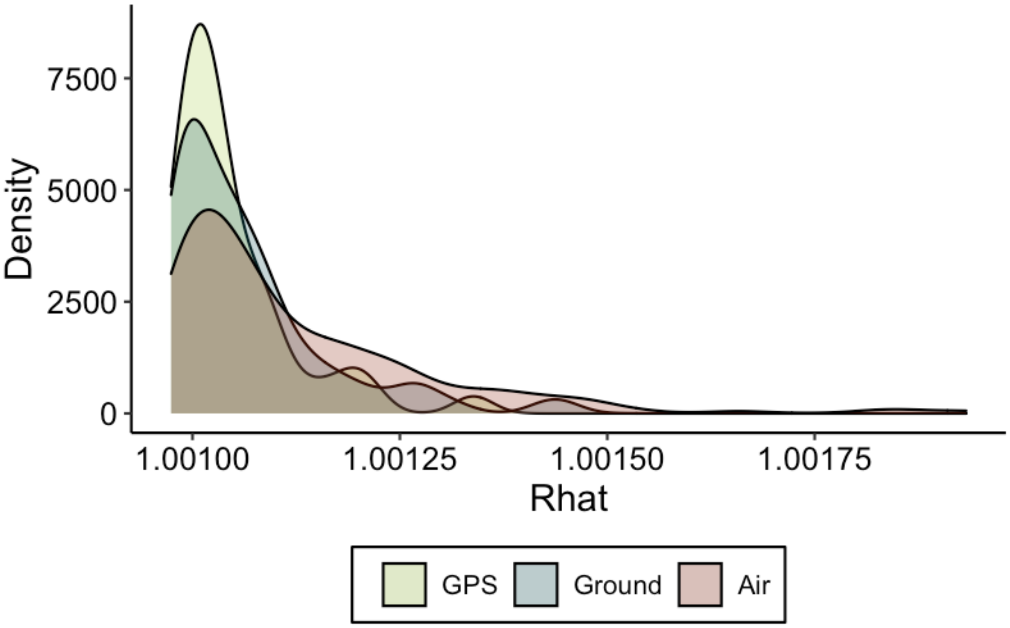

**Figure S4-E.5. R-hat values for 349 pack-session feeding event abundance estimates during the roaming period.**

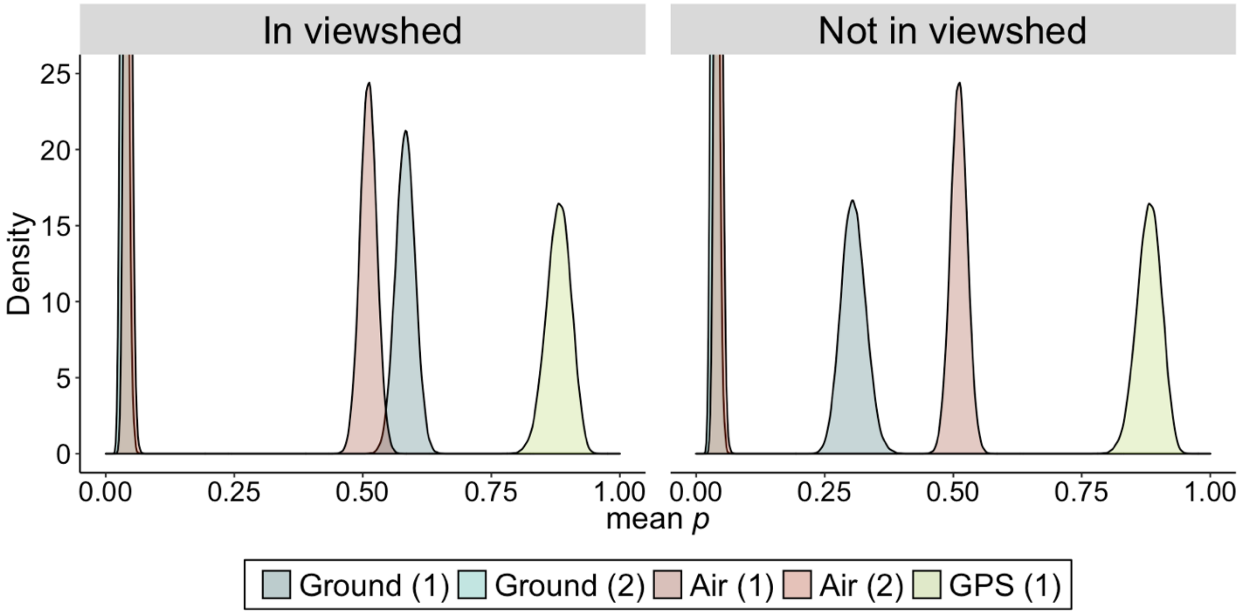

**Figure S4-E.6. Posterior distributions for the mean probability of detection for each detection occasion during the roaming period.** Distributions of mean *p* are displayed for the mean value of all covariates. The distribution for air and GPS method detection occasions are the same in both panels because viewshed did not affect *p* for these detection occasions.

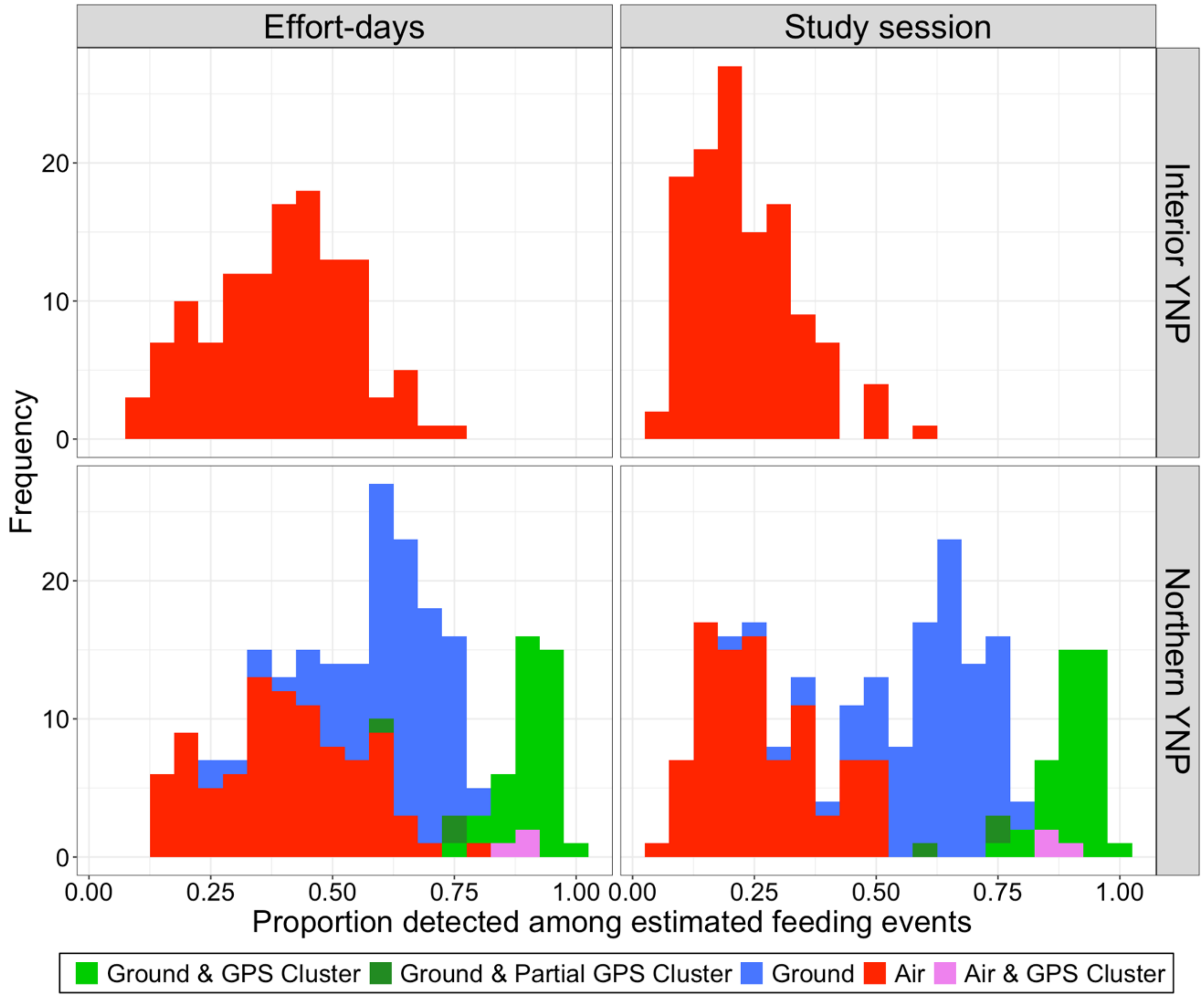

**Figure S4-E.7. Proportion of estimated feeding events that were detected during each pack-session during the roaming period.** Histogram binwidth = 0.05.

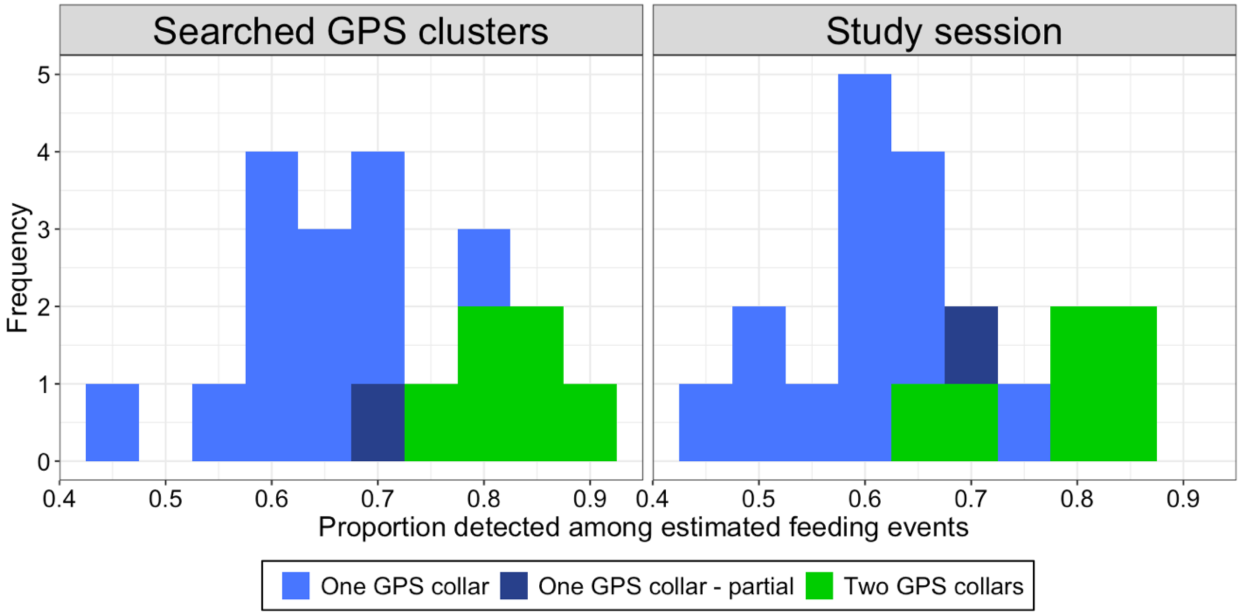

**Figure S4-E.8. Proportion of estimated feeding events that were detected during each pack-session during the denning period.** Histogram binwidth = 0.05.

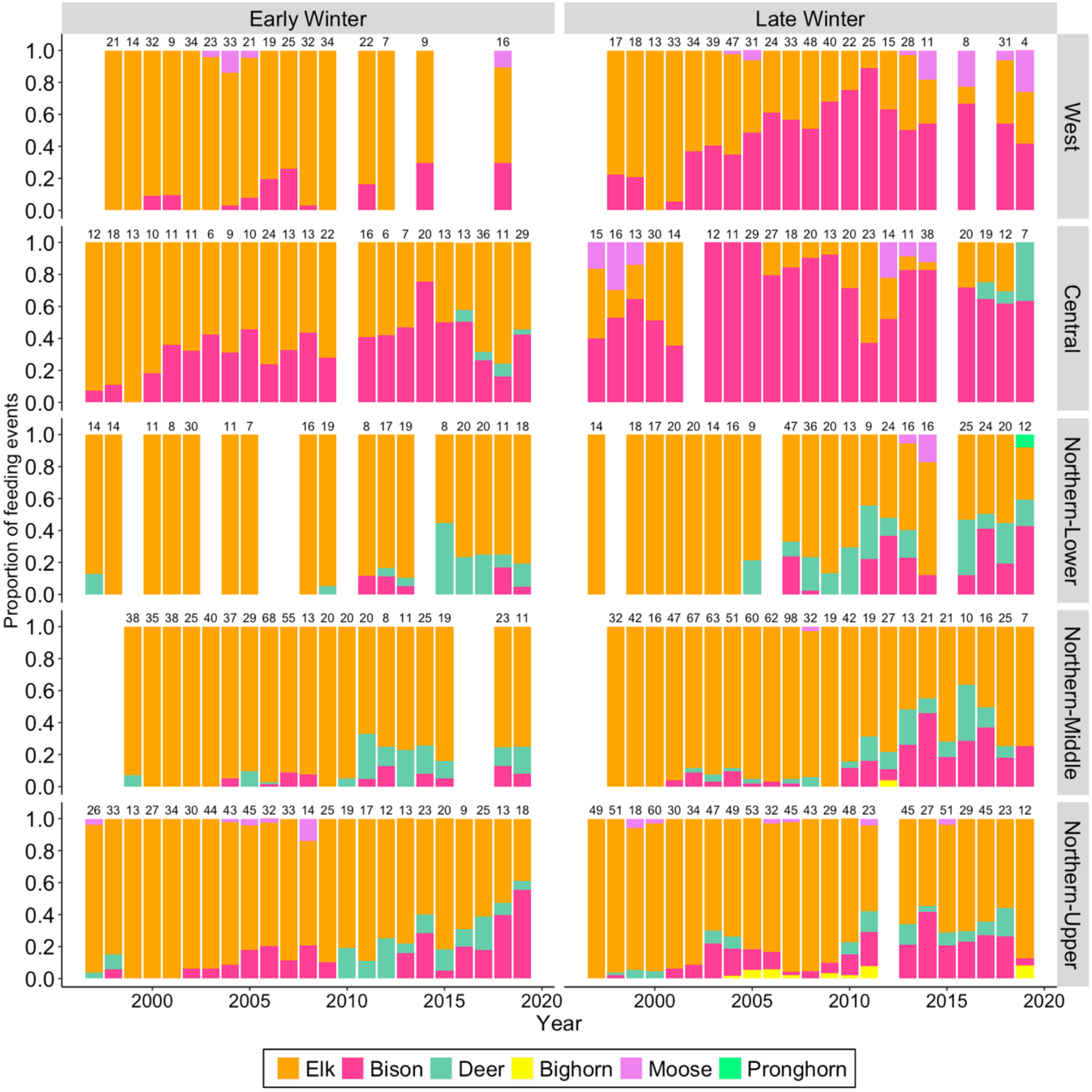

**Figure S4-E.9. Annual proportion of species among estimated feeding events during roaming period seasons and within spatial zones.** Numbers at the top of each bar represent the total number of estimated feeding events, rounded to the nearest integer for display purposes.

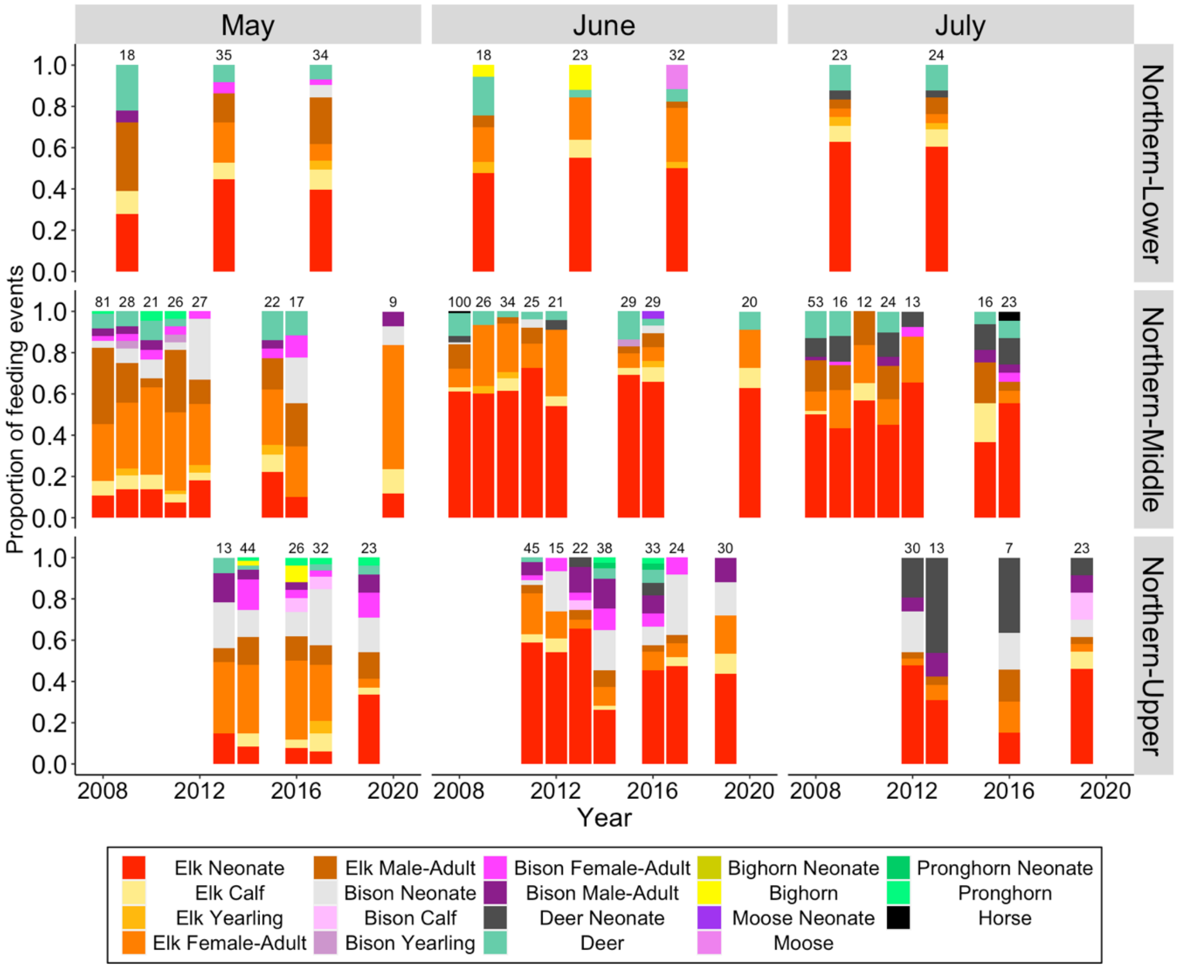

**Figure S4-E.10. Annual proportion of species among estimated feeding events during denning period months and within spatial zones.** Numbers at the top of each bar represent the total number of estimated feeding events, rounded to the nearest integer for display purposes.

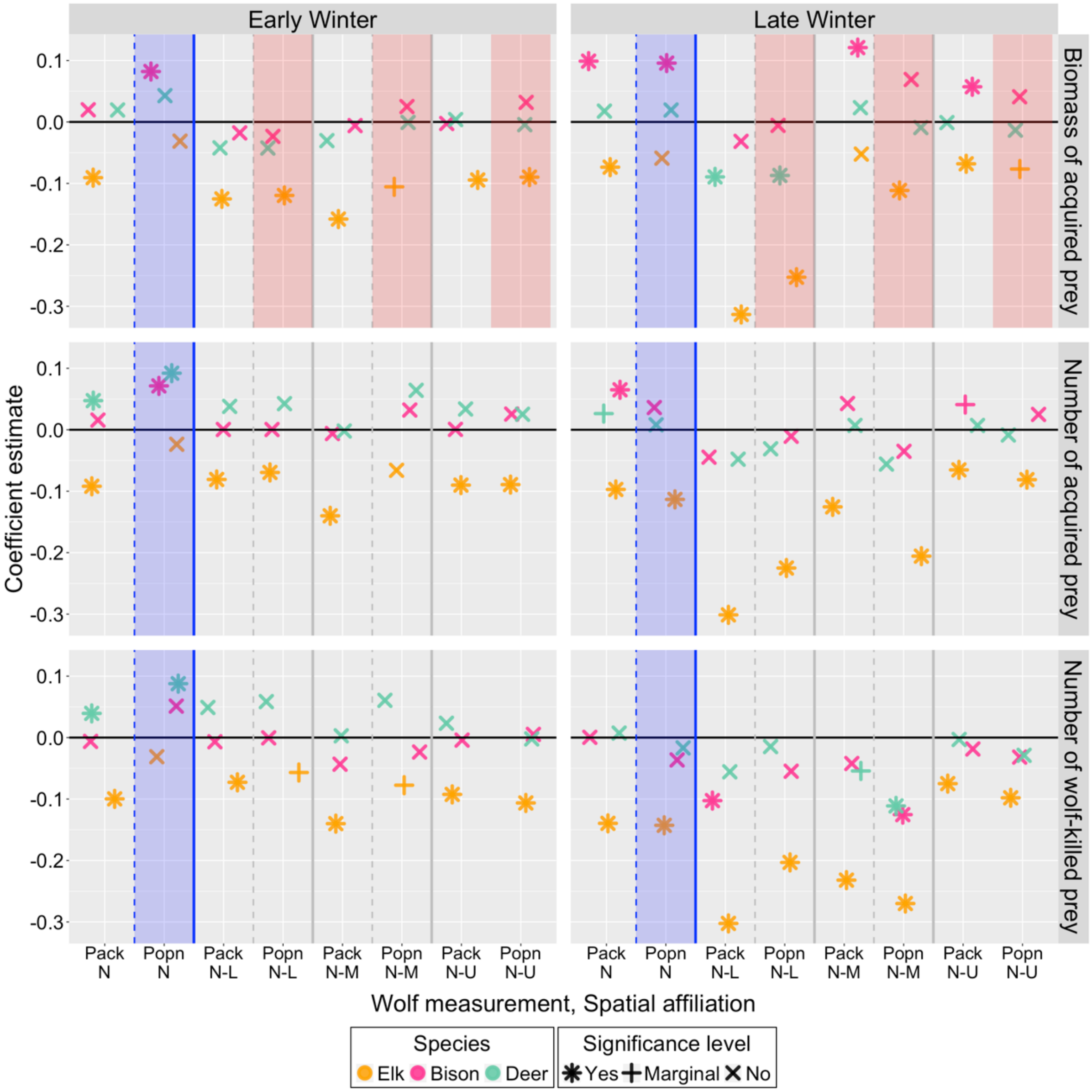

**Figure S4-E.11. Coefficient estimates for the effect of year on wolves' proportional diet composition in Dirichlet regression models for Northern YNP wolf pack-sessions.** Facet labels are the same as in Fig. 4-14. The data displayed in Fig. 4-14 is highlighted with blue shading, and the data displayed in Fig. 4-15 is highlighted in red. Black horizontal line is at 0, and above or below this line indicates a positive or negative effect of year. For some context about the effect of time, see the patterns displayed in Figs. 4-14 and 4-15 while considering the coefficient estimates presented here.

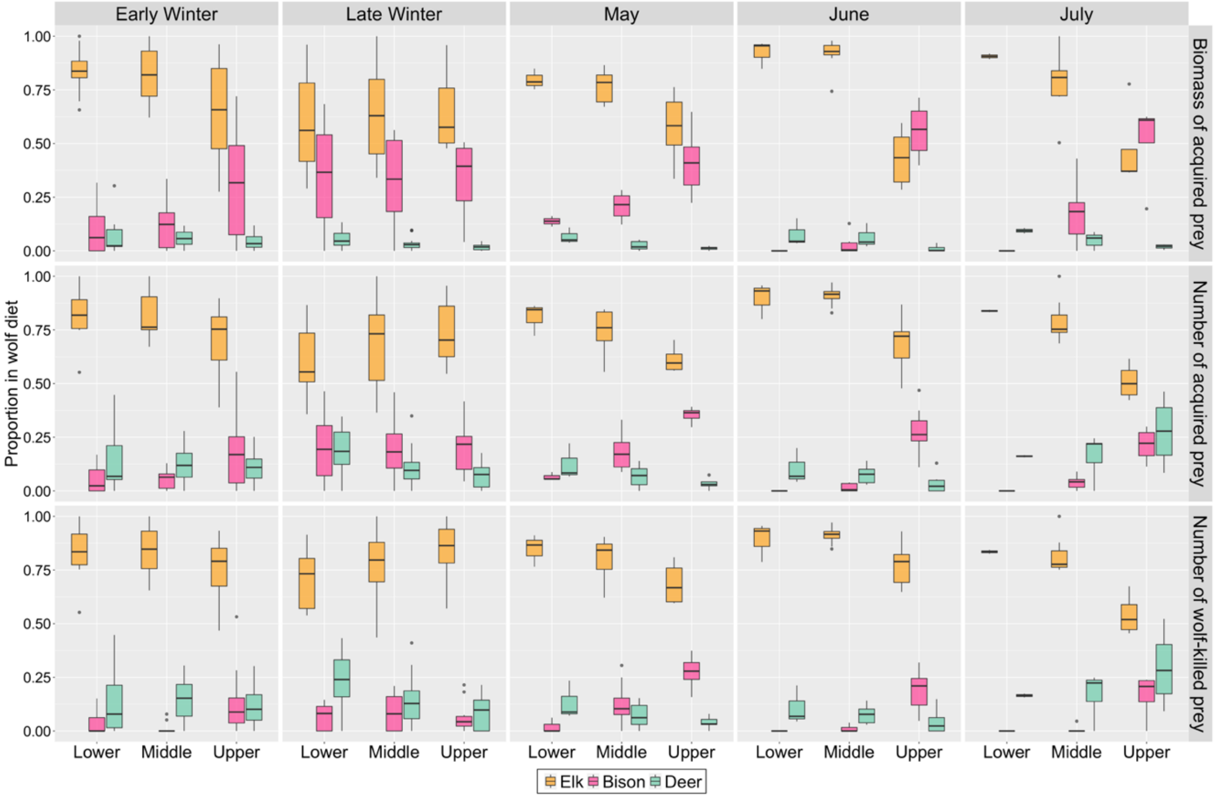

**Figure S4-E.12. Proportional diet composition for Northern YNP wolves during month-sessions (May 2008–June 2020) across spatial zones.** Data for biomass during the denning period is the same data presented as in Fig. 4-17. Roaming period sessions from 2008–2019 are displayed here as well. Sample sizes for these sessions were 10 (early winter) and 11 (late winter) for Northern-Lower, 10 and 12 for Northern-Middle, and 12 and 11 for Northern-Upper. See Fig. S4-E.13 for entire longitudinal data set for roaming period sessions.

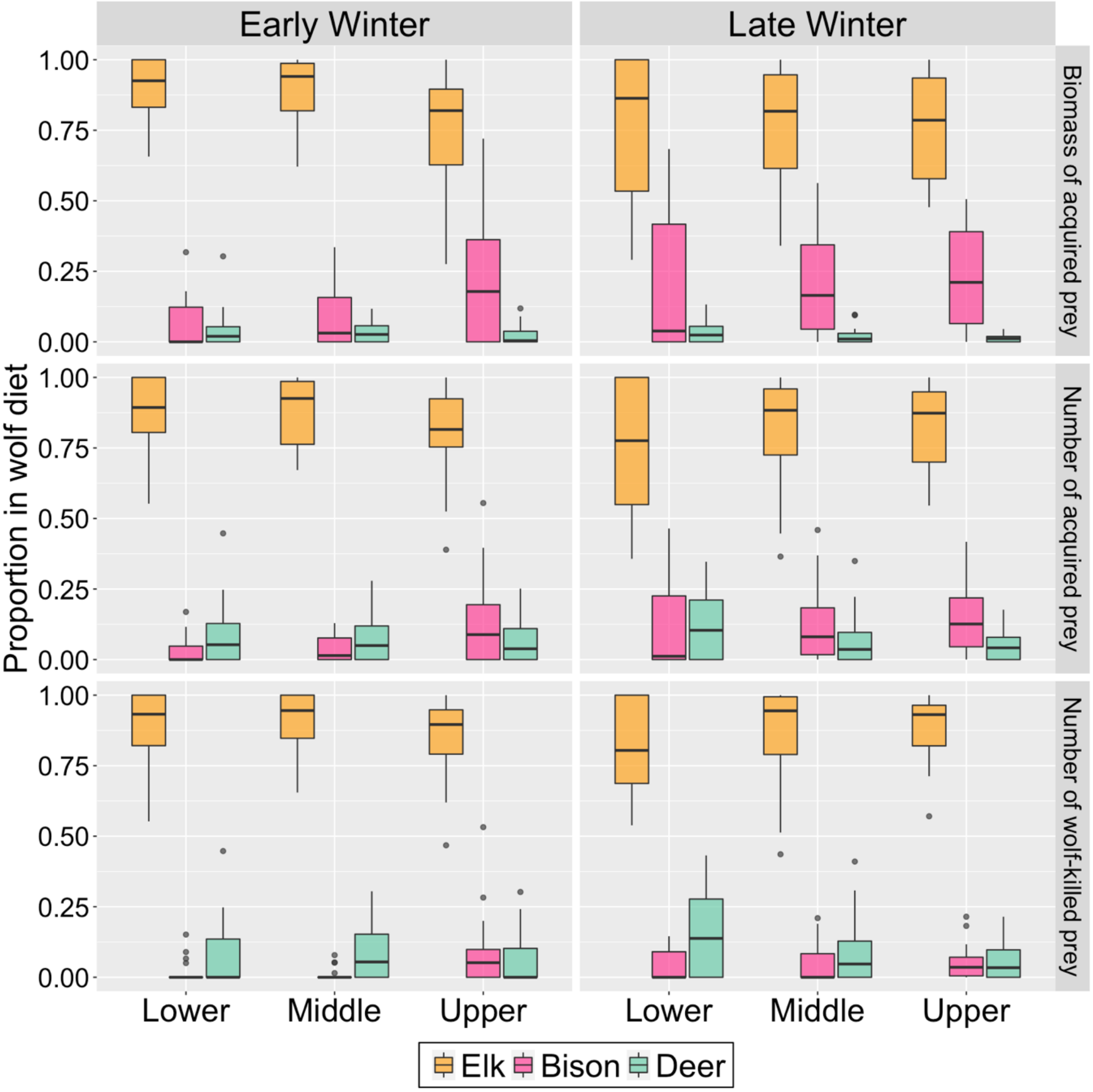

**Figure S4-E.13. Proportional diet composition for Northern YNP wolves during roaming period month-sessions (1997–2019) across spatial zones.** Plot displays entire longitudinal data set for the roaming periods. Sample sizes for these sessions were 17 (early winter) and 20 (late winter) for Northern-Lower, 19 and 22 for Northern-Middle, and 23 and 22 for Northern-Upper. The rest of the information is the same as Fig. S4-E.12.

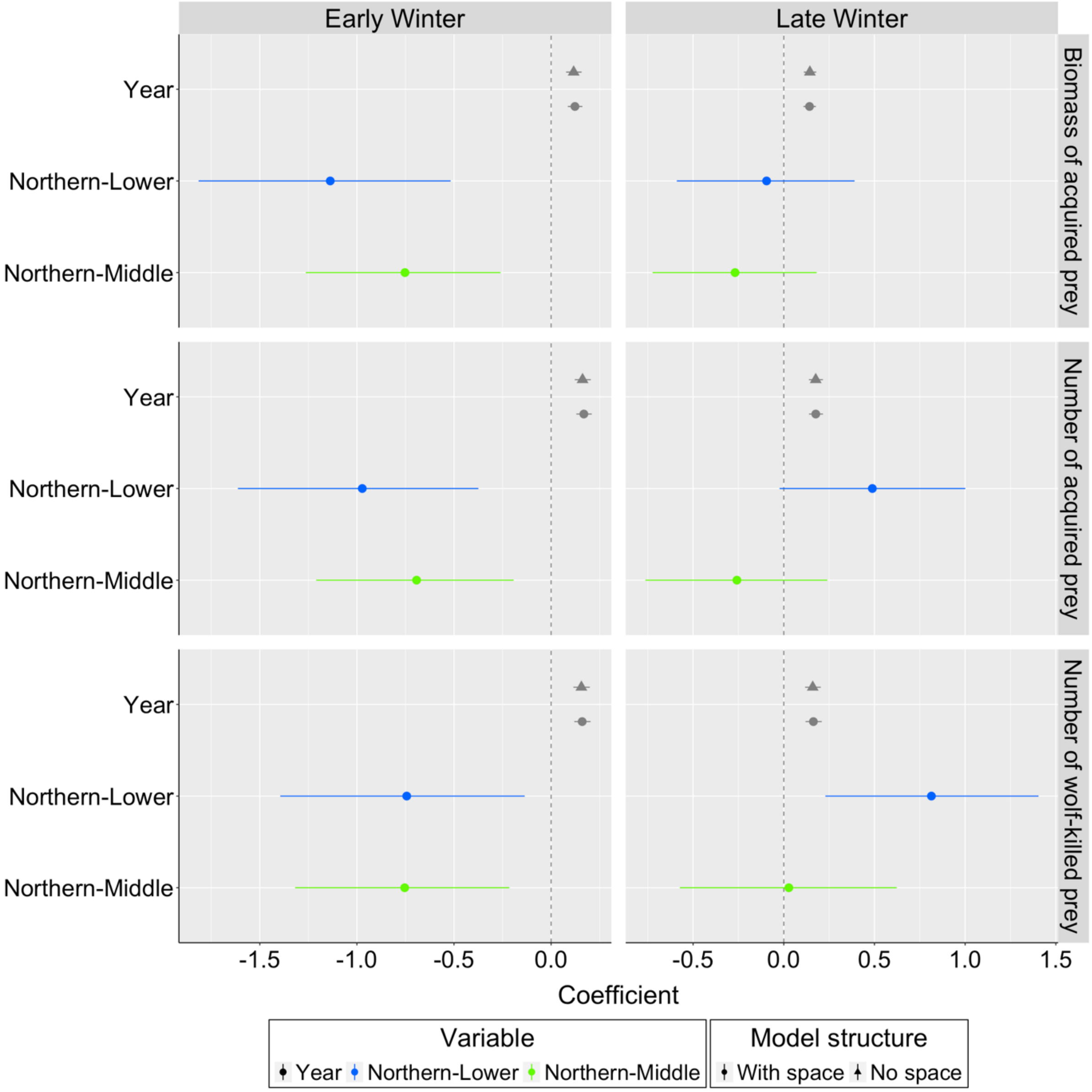

**Figure S4-E.14. Coefficient estimates for the effect of year and spatial zone on niche breadth for Northern YNP wolf packs.** Spatial zones of 'Northern-Lower' and 'Northern-Middle' are in relation to the 'Northern-Upper' reference category. Error bars represent 95% confidence intervals. Note different x-axis scales for 'Early Winter' and 'Late Winter' panels. See also Fig. 4-18 for the longitudinal predictions of niche breadth.

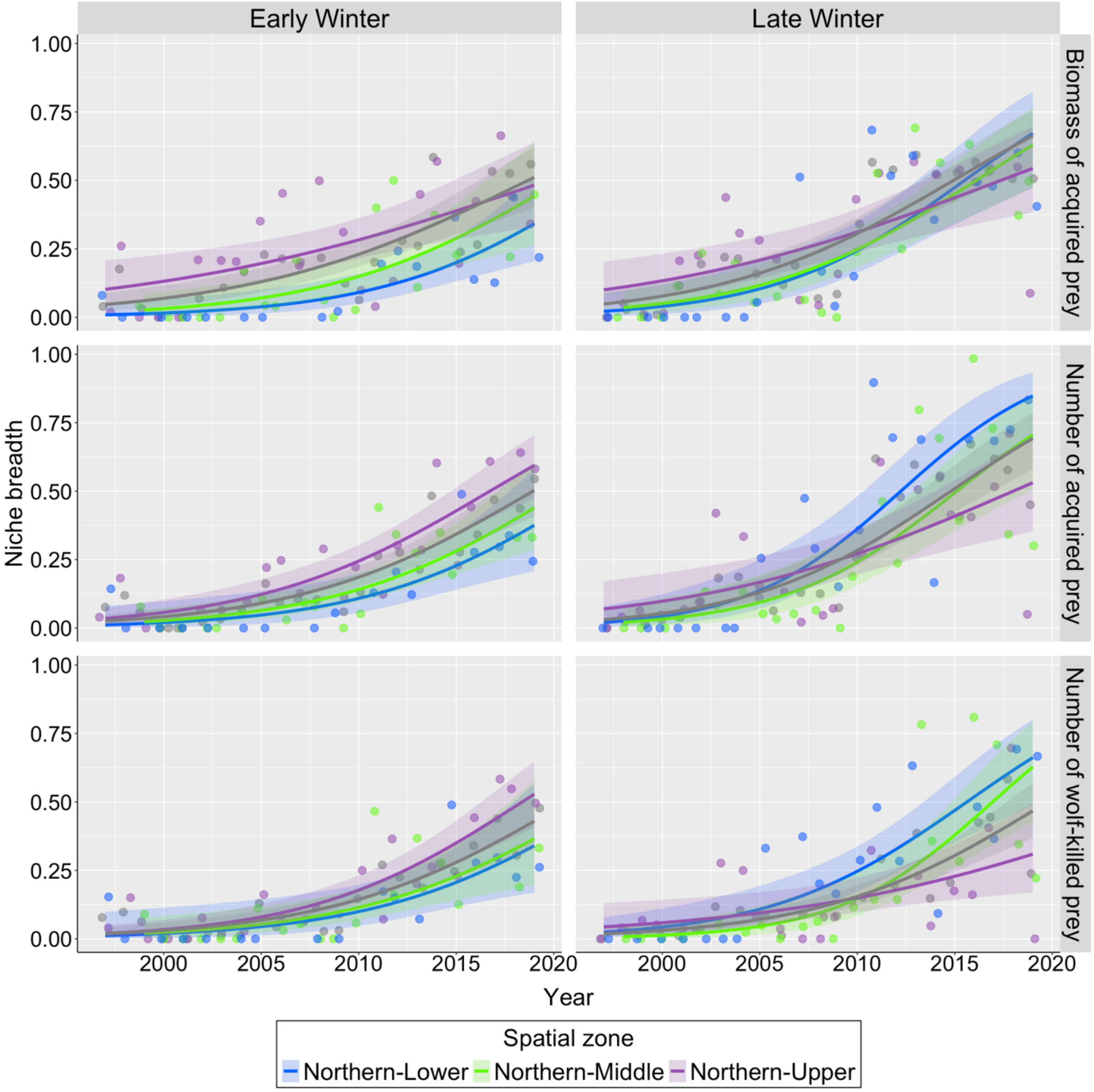

**Figure S4-E.15. Niche breadth (*B*) through time for Northern YNP wolf population.** Here, estimates for *B* were calculated at the population-level. The predicted lines represent four individual models, noting that the gray line ignored spatial zone. The effect of year was significant in all cases. See Fig. 4-18 for additional details.

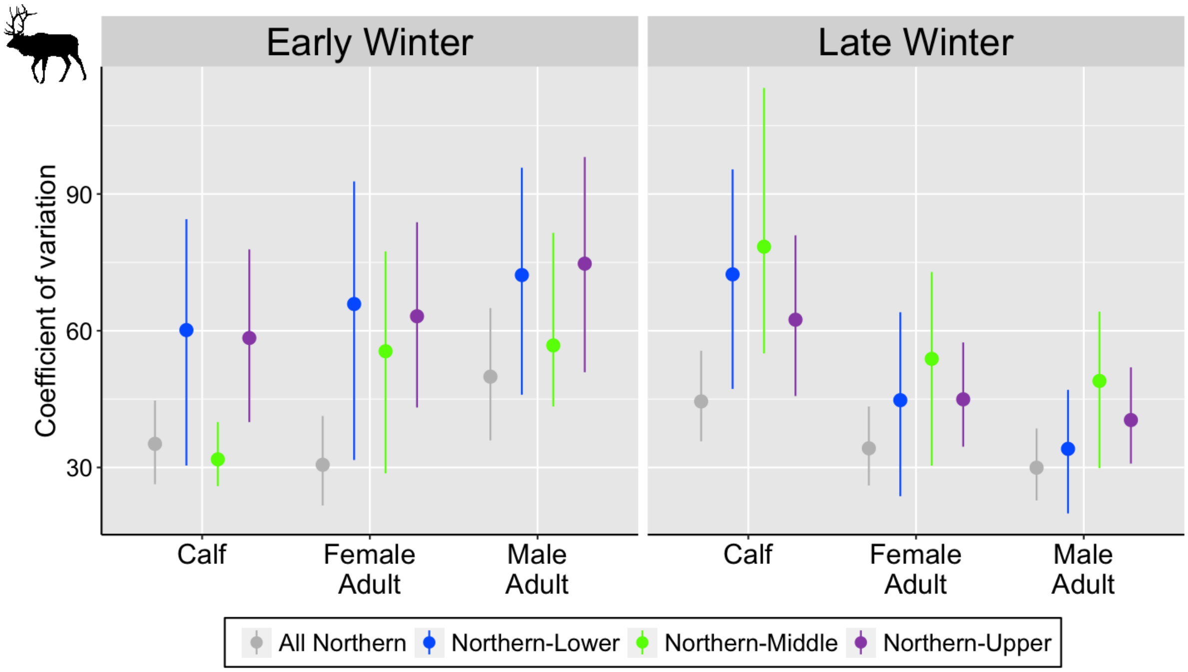

**Figure S4-E.16. Coefficient of variation for proportion of sex-age class among Northern YNP wolf-killed elk.** Coefficient of variation estimates are displayed ± 95% confidence intervals, estimated with the "basic" method through the R package cvcqv (Beigy 2019).

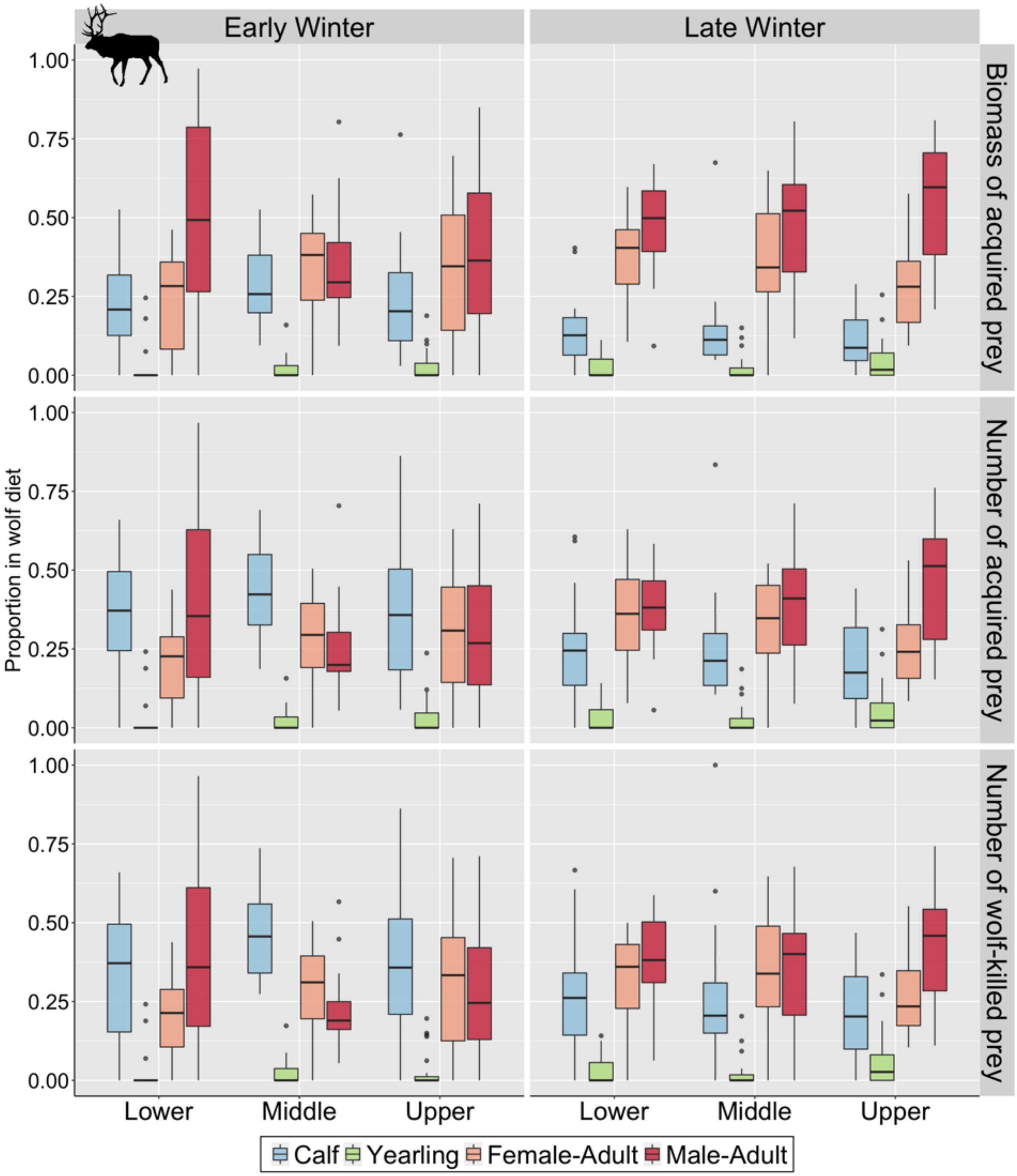

**Figure S4-E.17. Proportion sex-age class among feeding events on elk across spatial zones for Northern YNP wolf pack-sessions.**

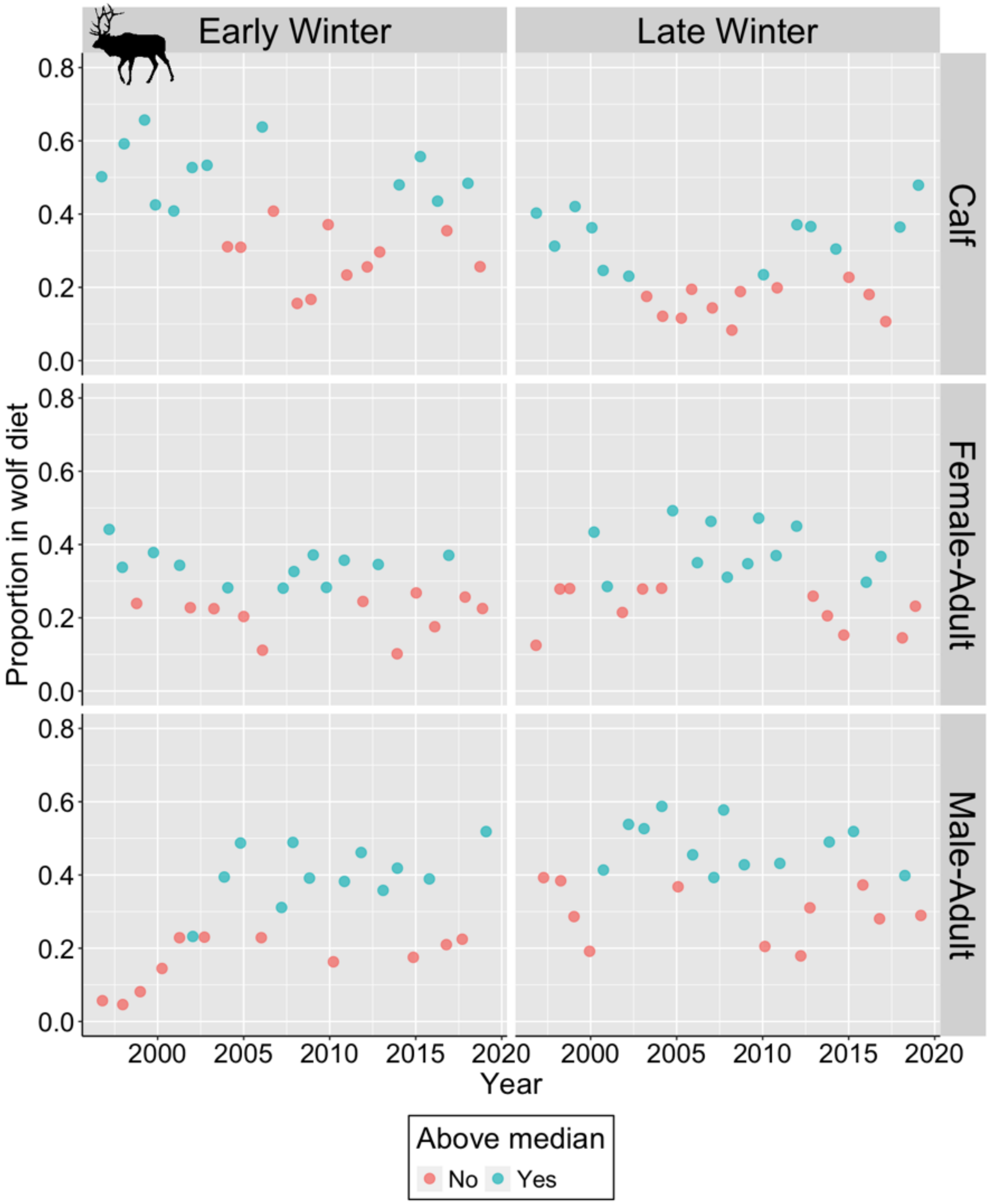

**Figure S4-E.18. Proportion of elk sex-age class among Northern YNP wolf-killed elk across time.** Above or below the median refers to whether the proportion in a season-year was above or below the median for that sex-age class during that season.

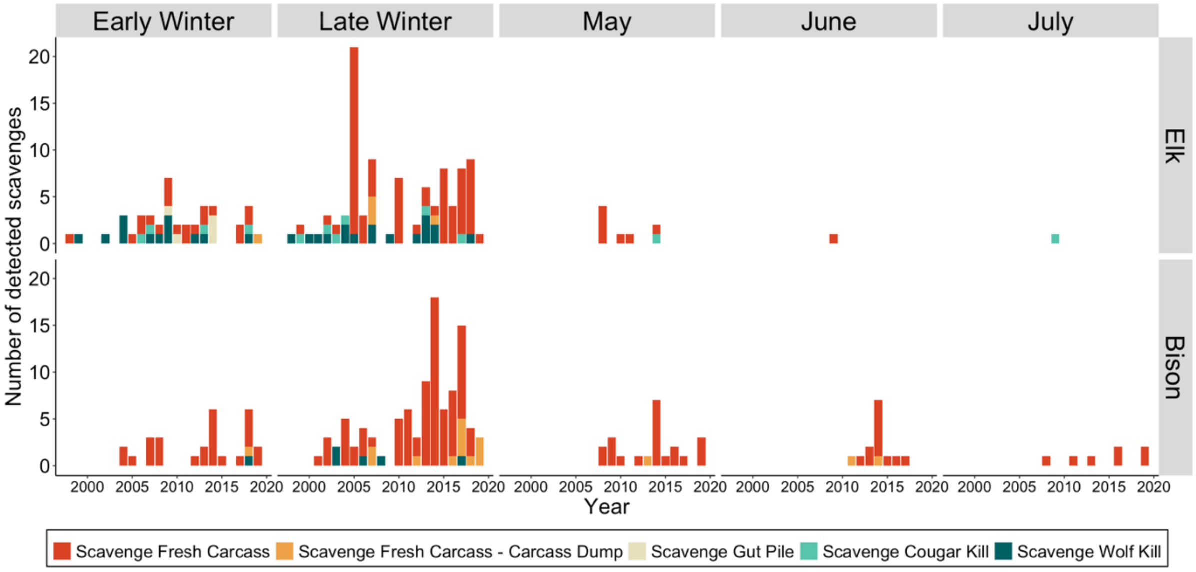

**Figure S4-E.19. Source of scavenging events among detected feeding events.**

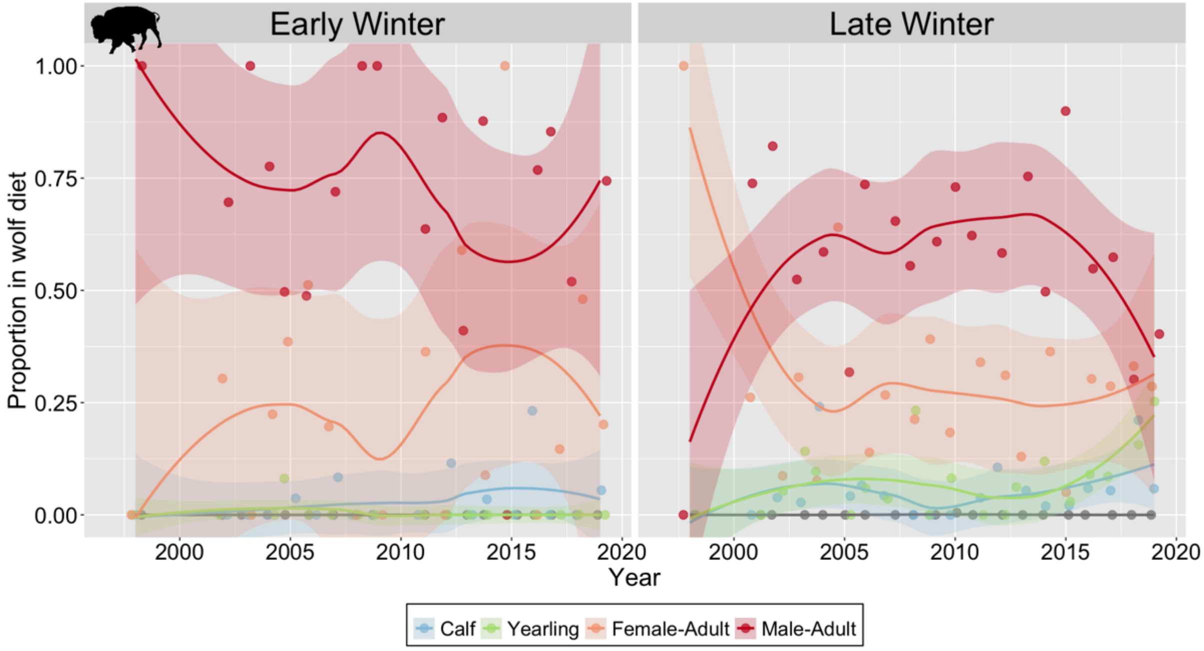

**Figure S4-E.20. Proportion of biomass acquired from bison sex-age classes in Northern YNP wolf pack diet across time.** Lines display 'loess' fit to highlight longitudinal trends.

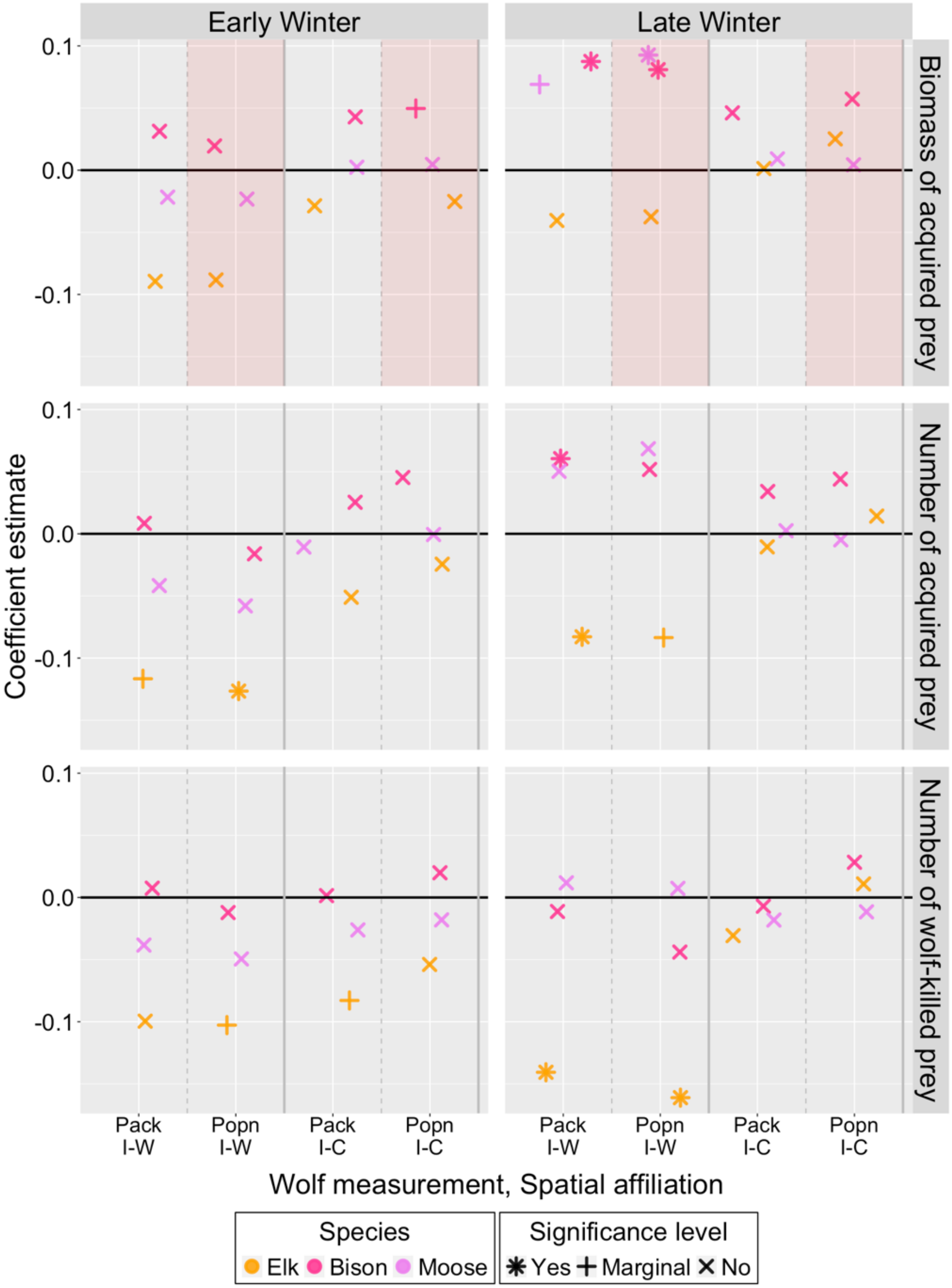

**Figure S4-E.21. Coefficient estimates for the effect of year on wolves' proportional diet composition in Dirichlet regression models for Interior YNP wolf pack-sessions.** Information is the same as Fig. S4-E.11 except red shaded area here references data displayed in Fig. 4-23.

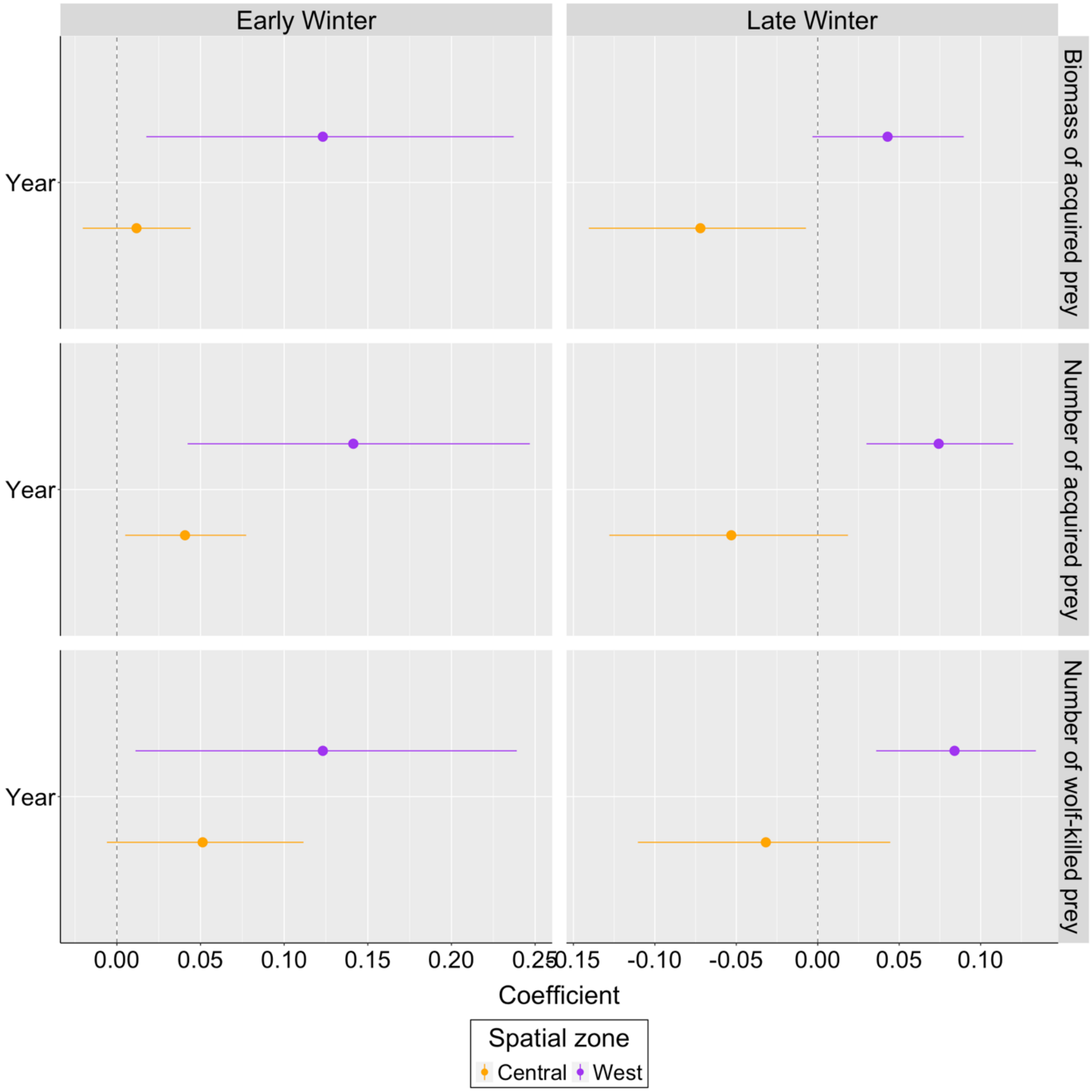

**Figure S4-E.22. Coefficient estimates for the effect of year on niche breadth for Interior YNP wolf pack-sessions.** Spatial zone indicates the data set used to develop the model. Error bars represent 95% confidence intervals. Note different x-axis scales for ‘Early Winter’ and ‘Late Winter’ panels. See also Fig. 4-24 for the longitudinal predictions of niche breadth.

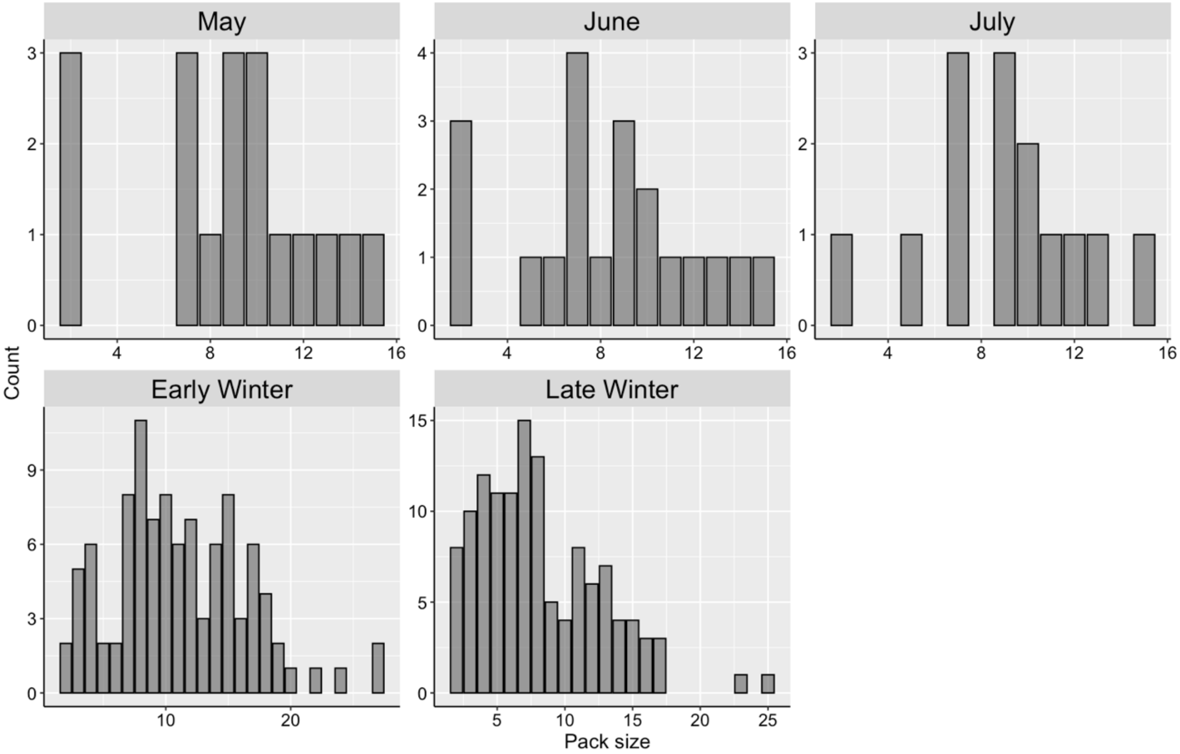

**Figure S4-E.23. Distribution of pack sizes during seasonal months with rate (e.g., kill rate) estimates.**

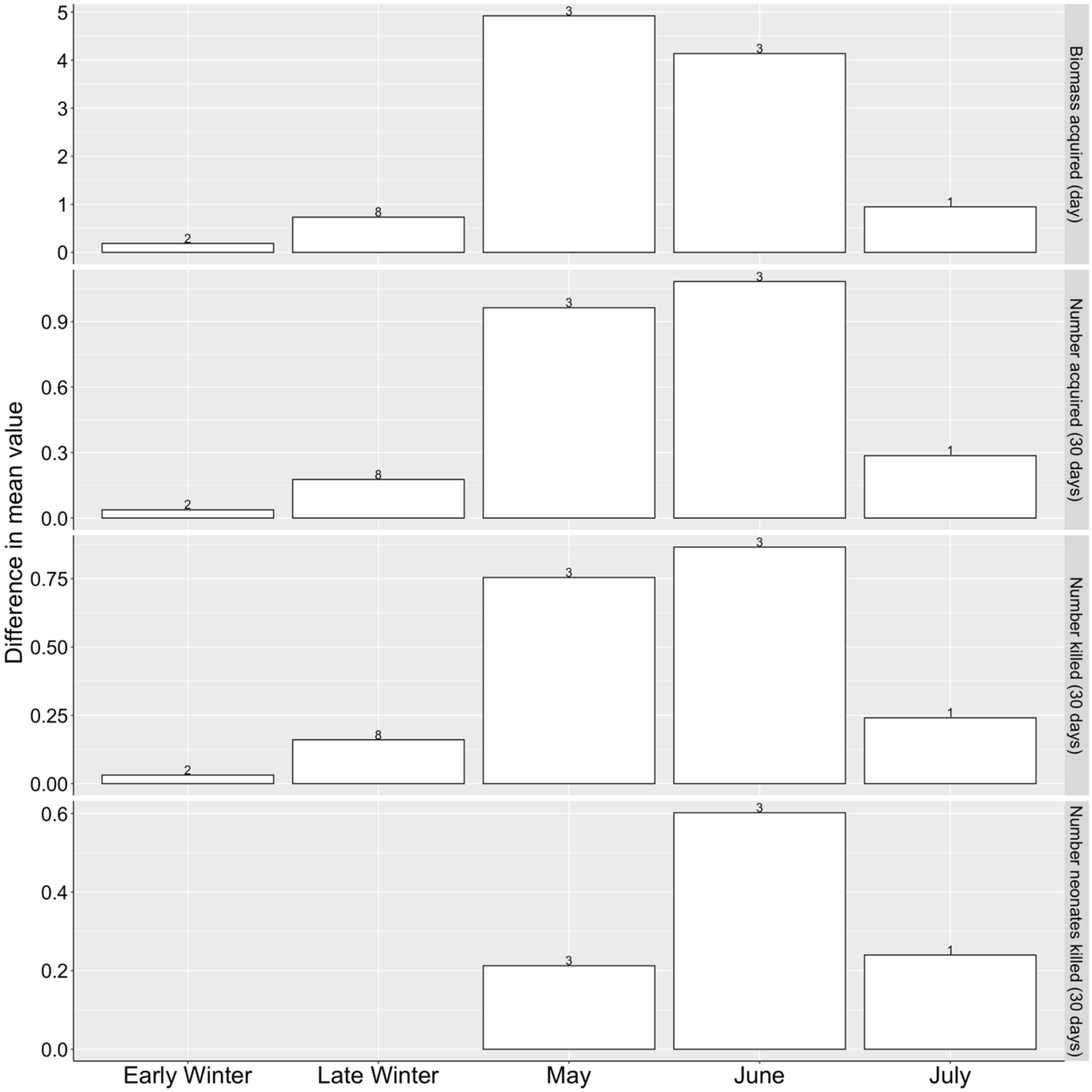

**Figure S4-E.24. Effect of removing wolf pairs on rate metrics related to wolf predation.** Rates from wolf pairs were removed for seasonal comparisons due to the tendency for wolf pairs to have a large effect on estimated rates. Despite their prevalence in our data set from the denning period, these packs are relatively infrequent in the Northern YNP wolf population. For example, see the distribution of pack size for the roaming period sessions in Fig. S4-E.23, which is more representative of the distribution of pack sizes in the wolf population. Note the different scales for the y-axis for each panel. Number above each bar indicates how many pack-sessions were removed.

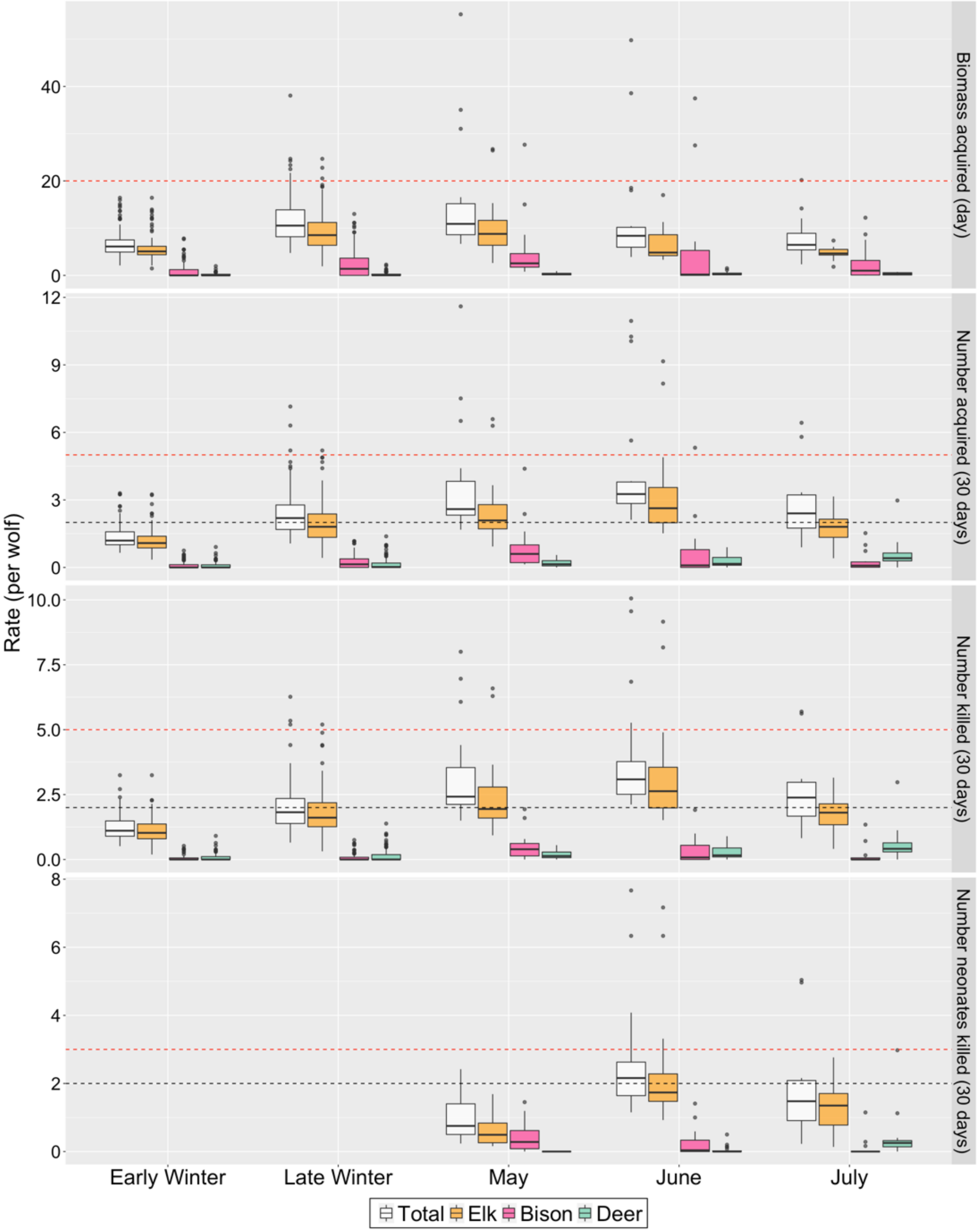

**Figure S4-E.25. Seasonal acquisition and kill rates at the pack-level for Northern YNP pack-sessions.** Same as Fig. 4-25, except this plot shows all data (1997–2020) for rates calculated at the pack-level. Red lines are related to the maximum values shown in Fig. S4-E.26 and are displayed to assist comparison. Inferences from this plot are limited by the large influence of wolf pairs during the denning period, because of small sample size.

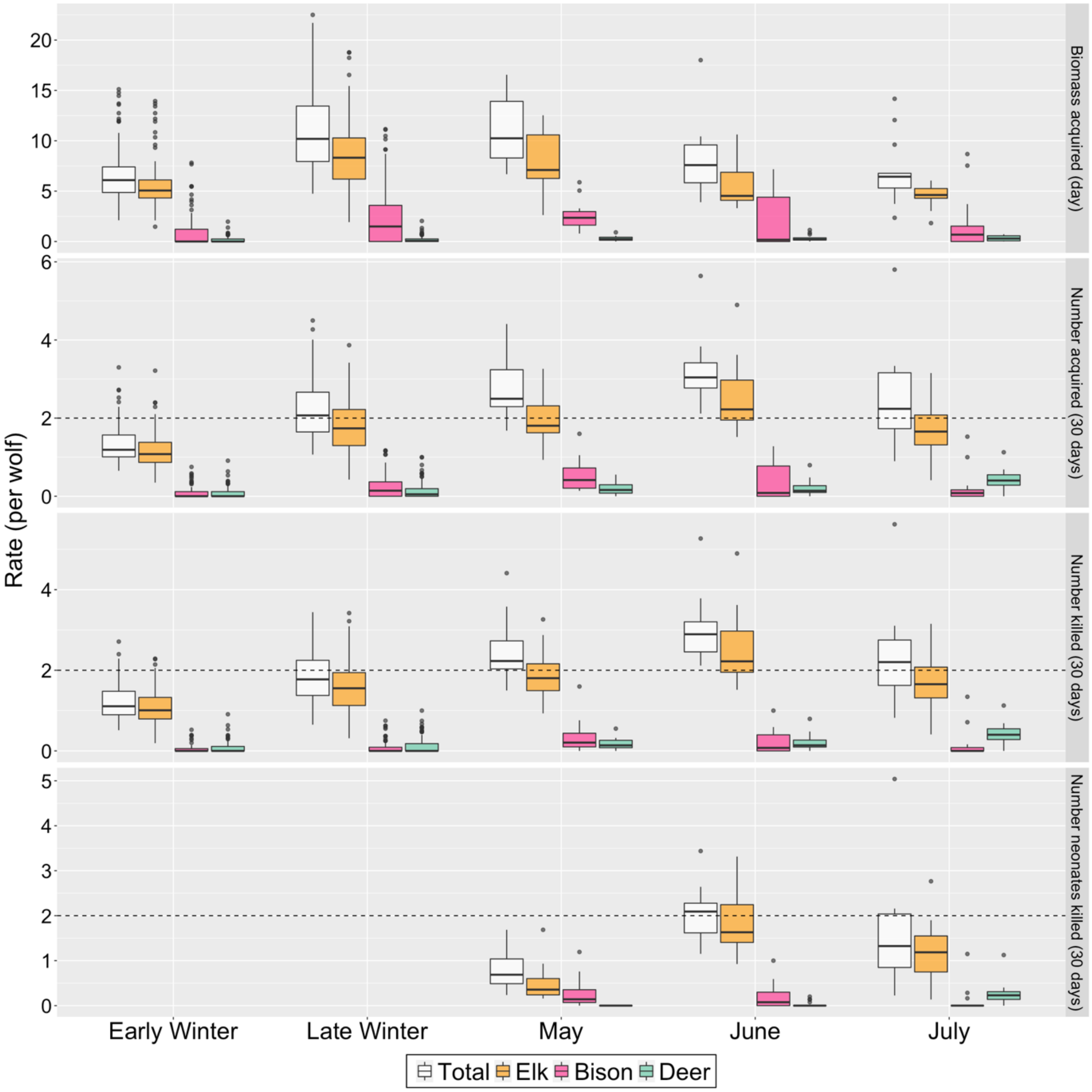

**Figure S4-E.26. Seasonal acquisition and kill rates at the pack-level for Northern YNP pack-sessions (wolf pairs censored).** Same as Fig. S4-E.25, except data from wolf pairs was censored from data displayed in this plot.

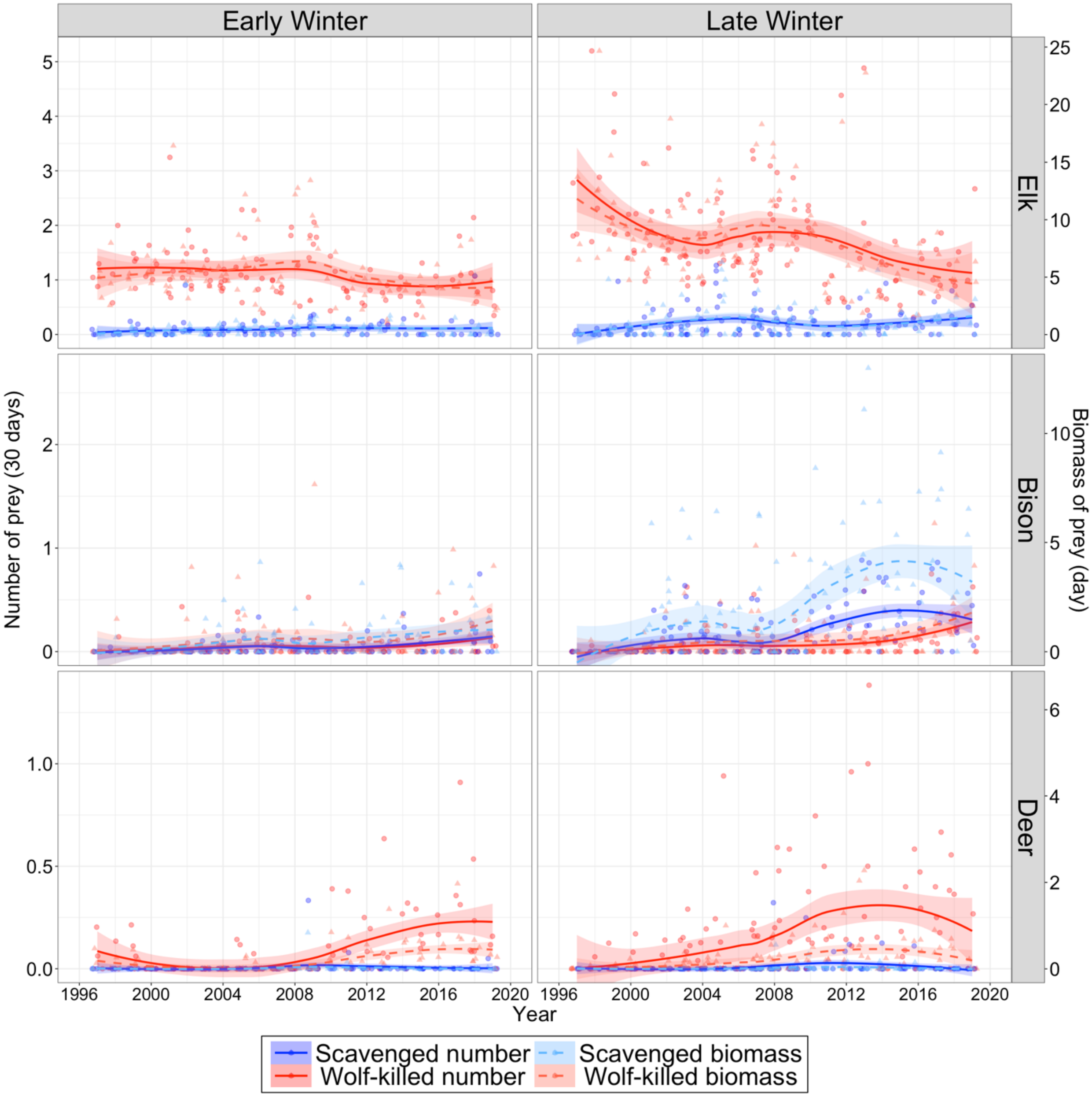

**Figure S4-E.27. Longitudinal patterns in the rates wolves killed and scavenged primary ungulate prey in Northern YNP, 1997–2019 (pack-level rates).** Same as Fig. 4-26, except rates are at the pack-level.

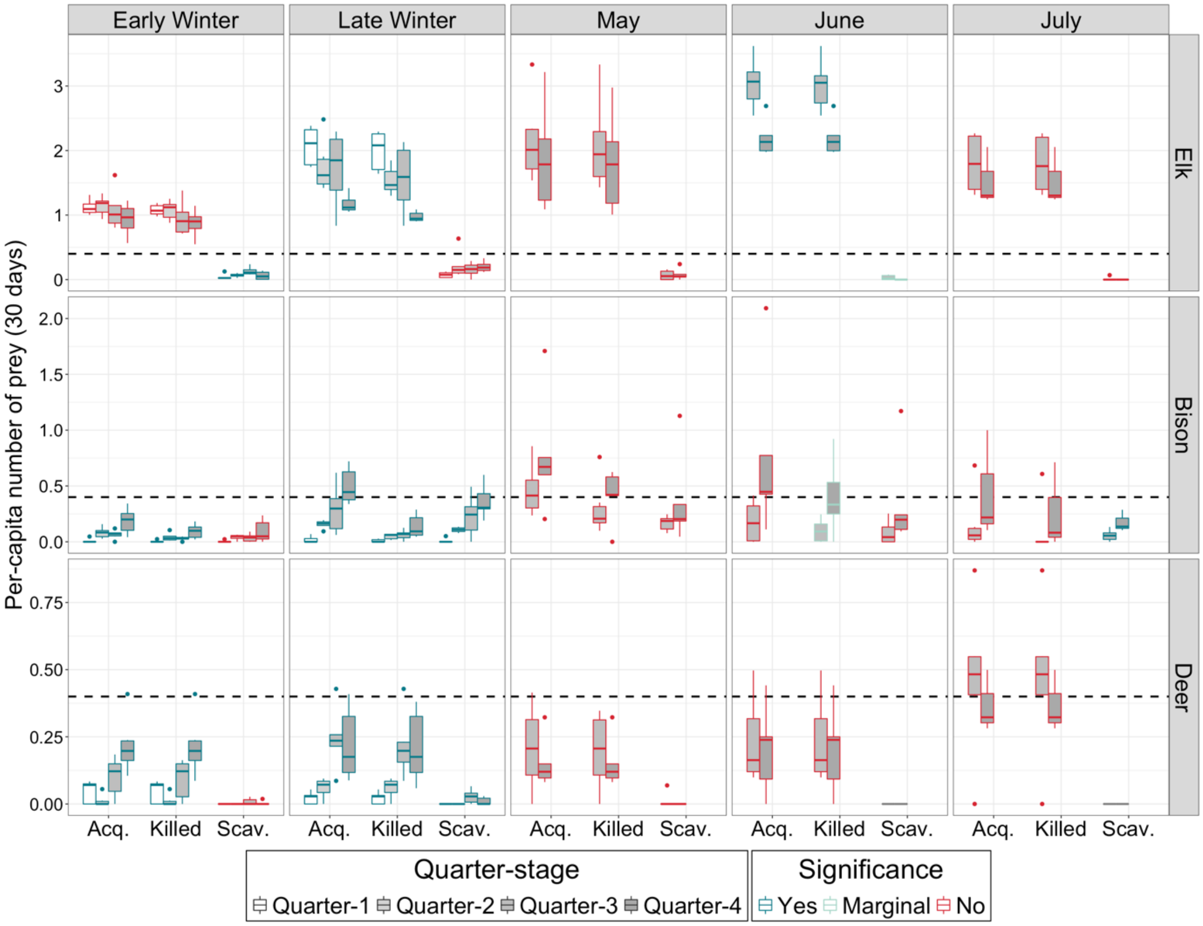

**Figure S4-E.28. Comparison of per-capita acquisition, kill, and scavenging rates (number-prey) for wolves on elk (top row), bison (middle row), and deer (bottom row) for all seasonal months across quarters in Northern YNP.** Dashed line is inserted at 0.4 in each panel to facilitate comparison. The winter season columns are the same as displayed in the left column of Fig. 4-27, and the meaning of all coloring is the same as Fig. 4-27.

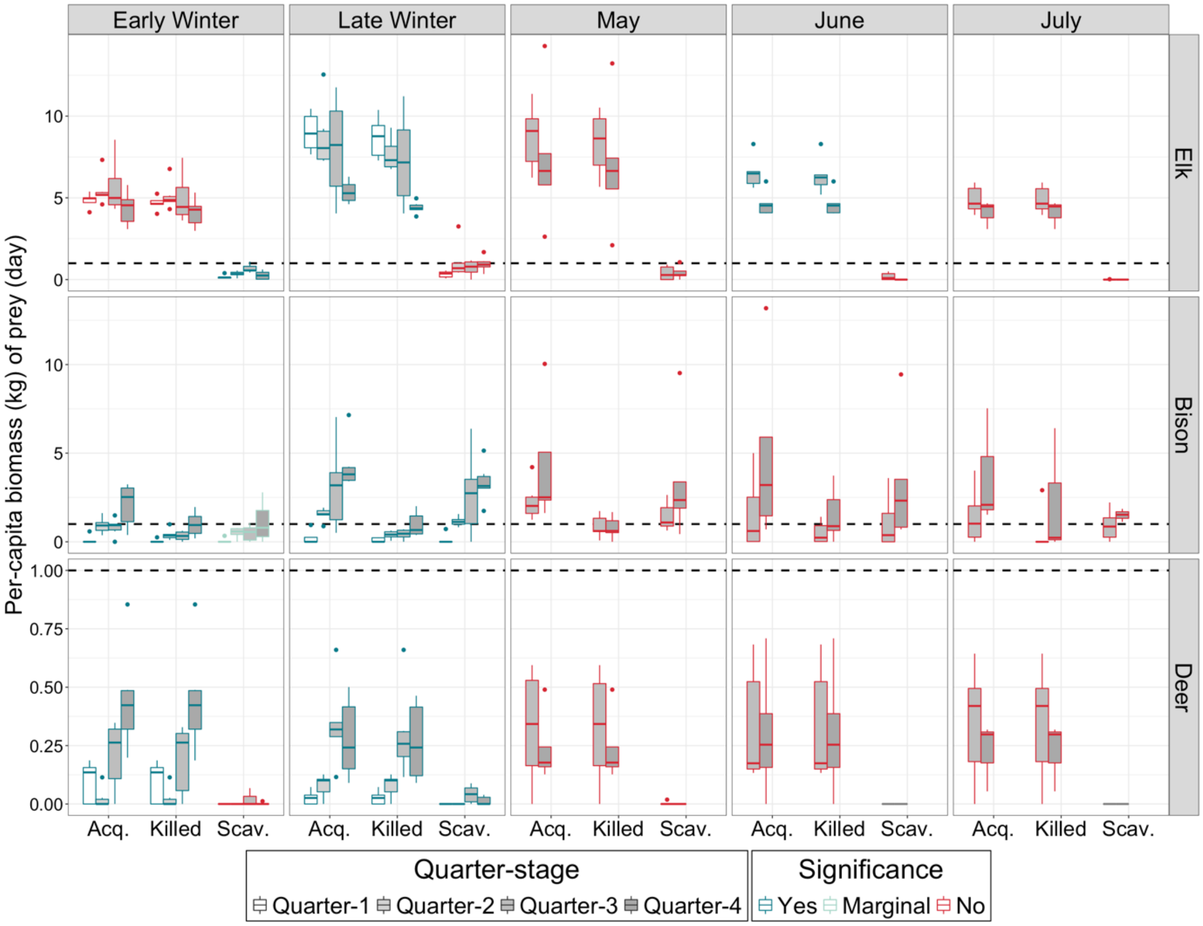

**Figure S4-E.29. Comparison of per-capita acquisition, kill, and scavenging rates (biomass-prey) for wolves on elk (top row), bison (middle row), and deer (bottom row) for all seasonal months across quarters in Northern YNP.** Dashed line is inserted at 1.0 in each panel to facilitate comparison. The winter season columns are the same as displayed in the right column of Fig. 4-27, and the meaning of all coloring is the same as Fig. 4-27.

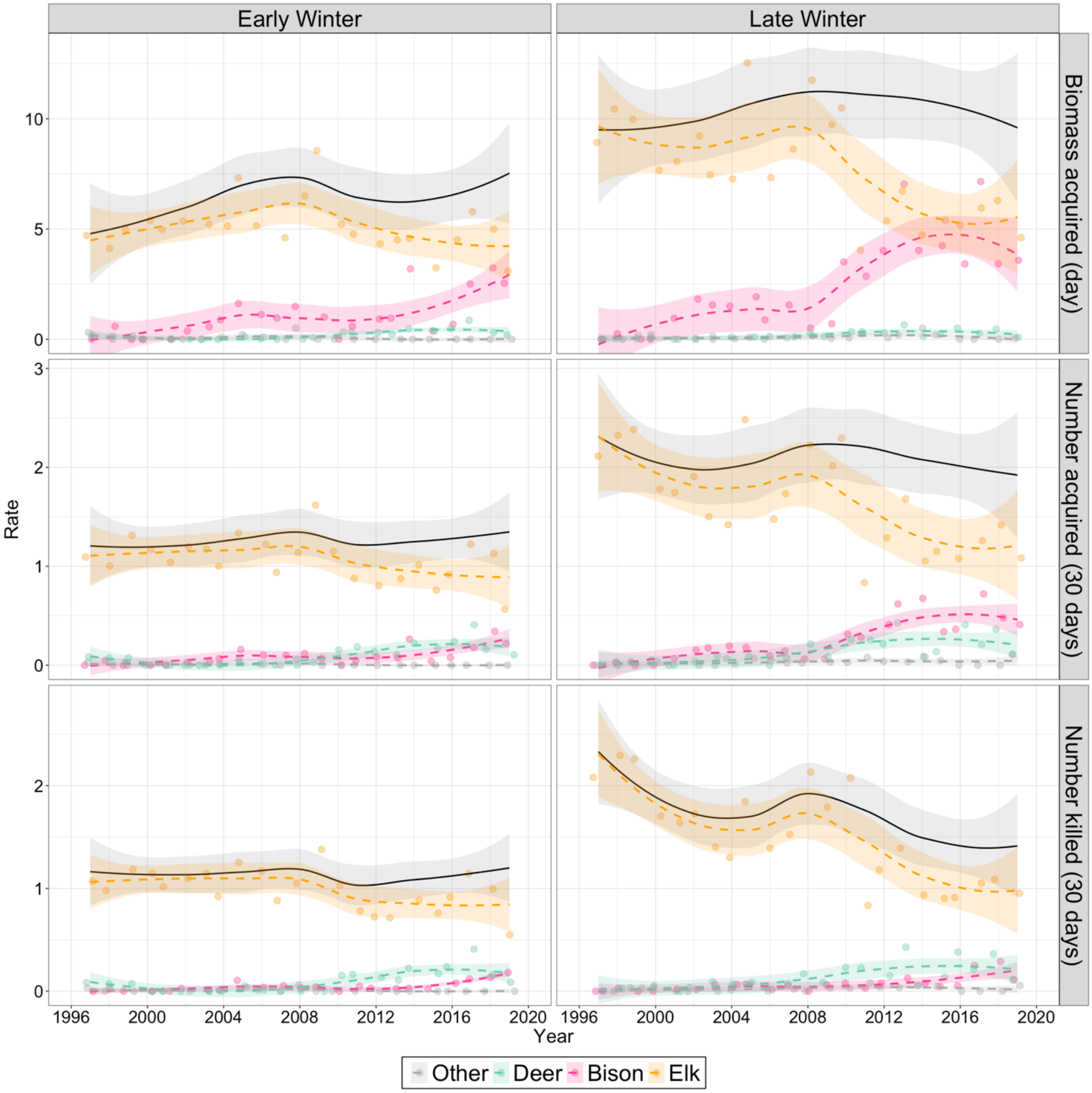

**Figure S4-E.30. Acquisition-related rates across time in Northern YNP.** Top row (biomass acquired) is the same as Fig. 4-28a. Bottom two rows display longitudinal trends in the number of prey. Data is for the 'population-level' and lines display 'loess' fit to highlight longitudinal trends.

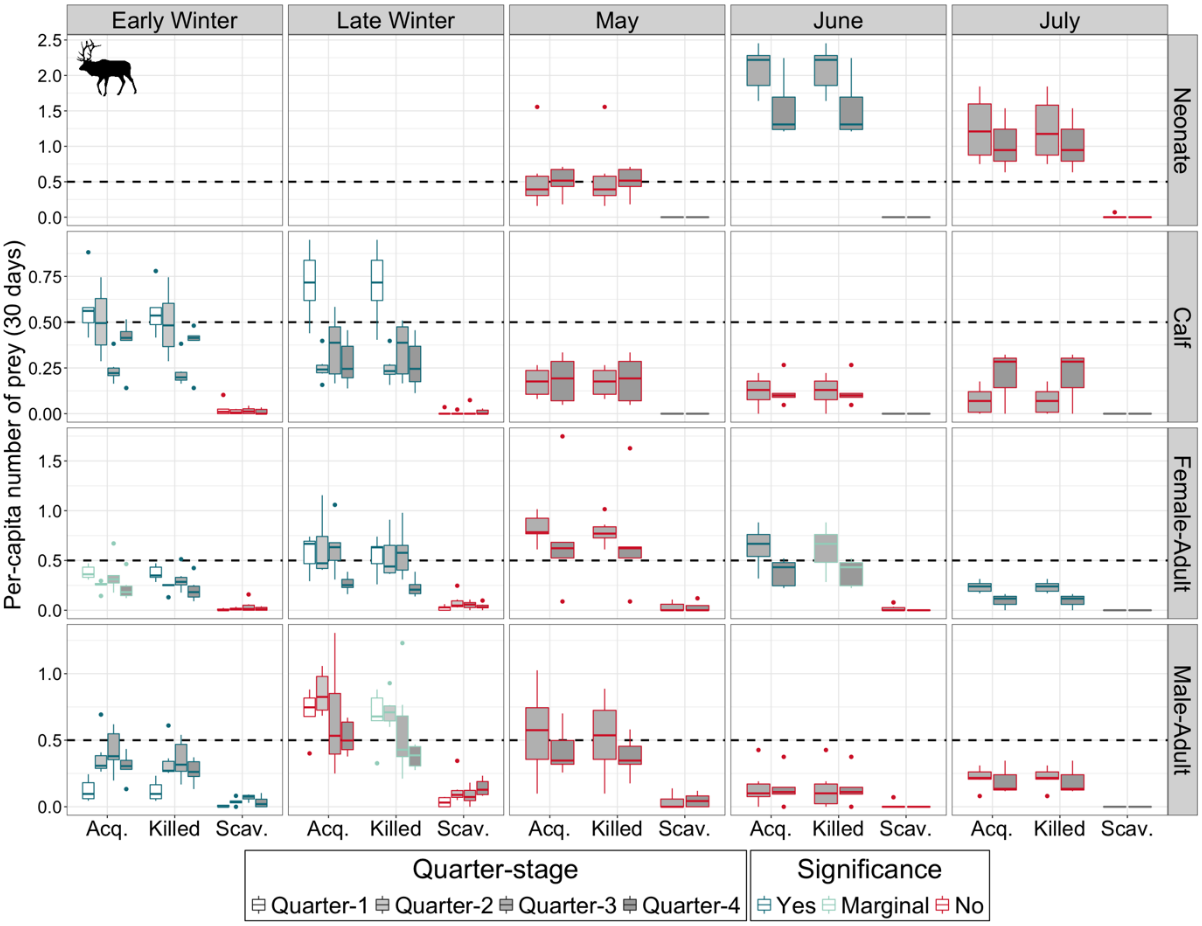

**Figure S4-E.31. Comparison of per-capita acquisition, kill, and scavenging rates (number-prey) for wolves on elk sex-age classes for all seasonal months across quarters in Northern YNP.** Dashed line is inserted at 0.5 in each panel to facilitate comparison. The winter season columns are the same as displayed in Fig. 4-33, and the meaning of all coloring is the same as Fig. 4-27.

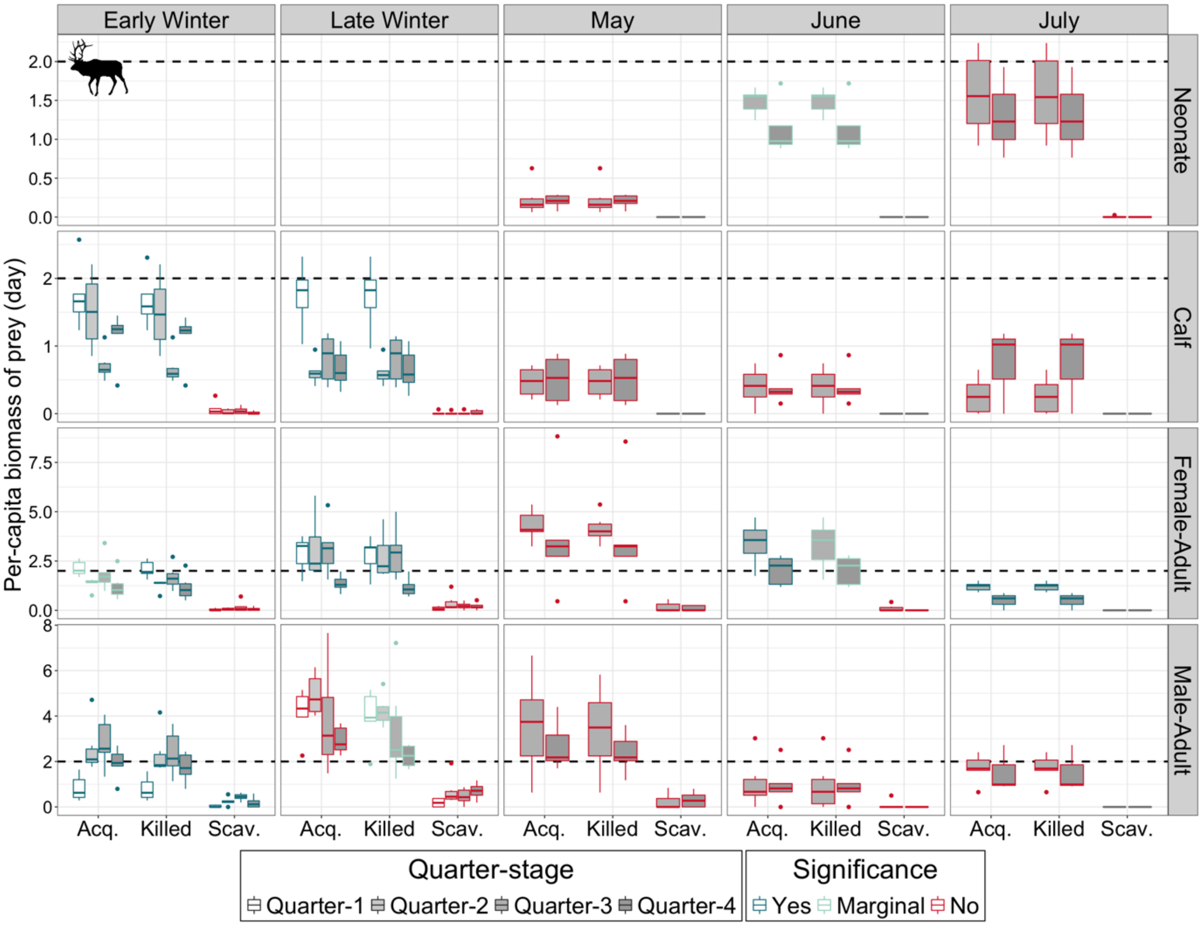

**Figure S4-E.32. Comparison of per-capita acquisition, kill, and scavenging rates (biomass-prey) for wolves on elk sex-age classes for all seasonal months across quarters in Northern YNP.** Same as Fig. S4-E.31, except expressed in biomass and dashed line is inserted at 2.0 in each panel to facilitate comparison.

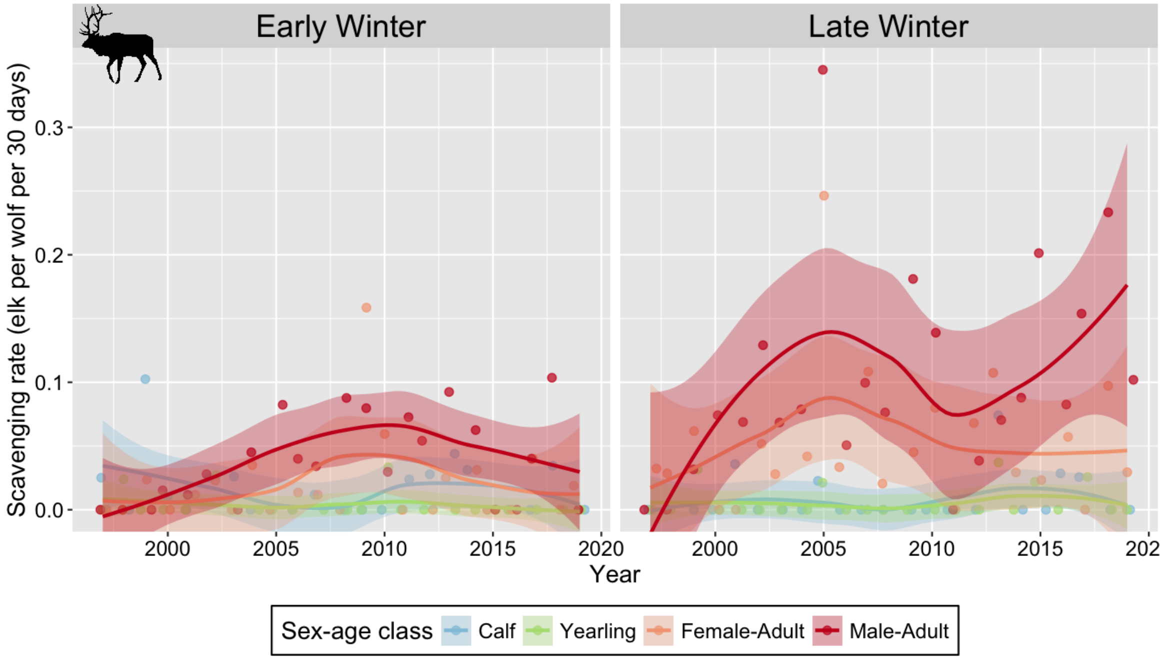

**Figure S4-E.33. Scavenging rates for wolves on elk sex-age class during the roaming period across time.** Lines display 'loess' fit to highlight longitudinal trends.

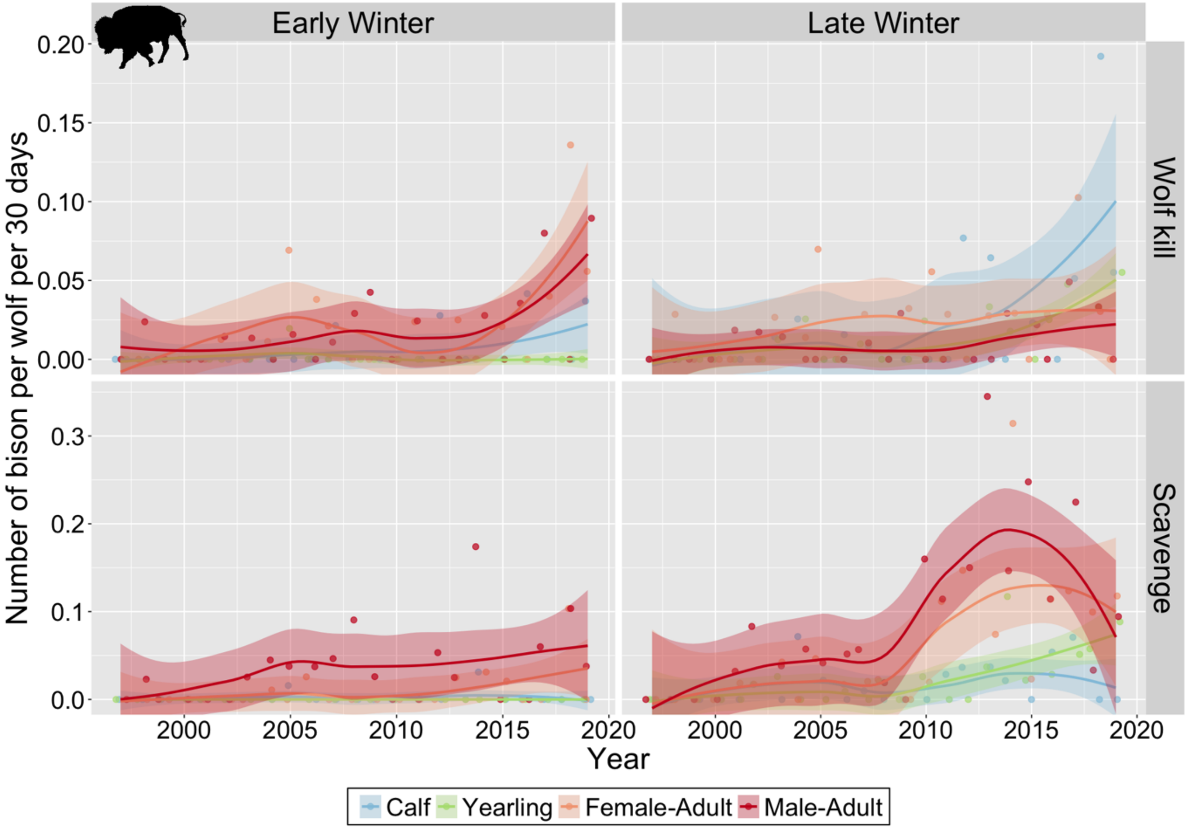

**Figure S4-E.34. Kill and scavenging rates for wolves on bison sex-age class during the roaming period across time.** Lines display 'loess' fit to highlight longitudinal trends.

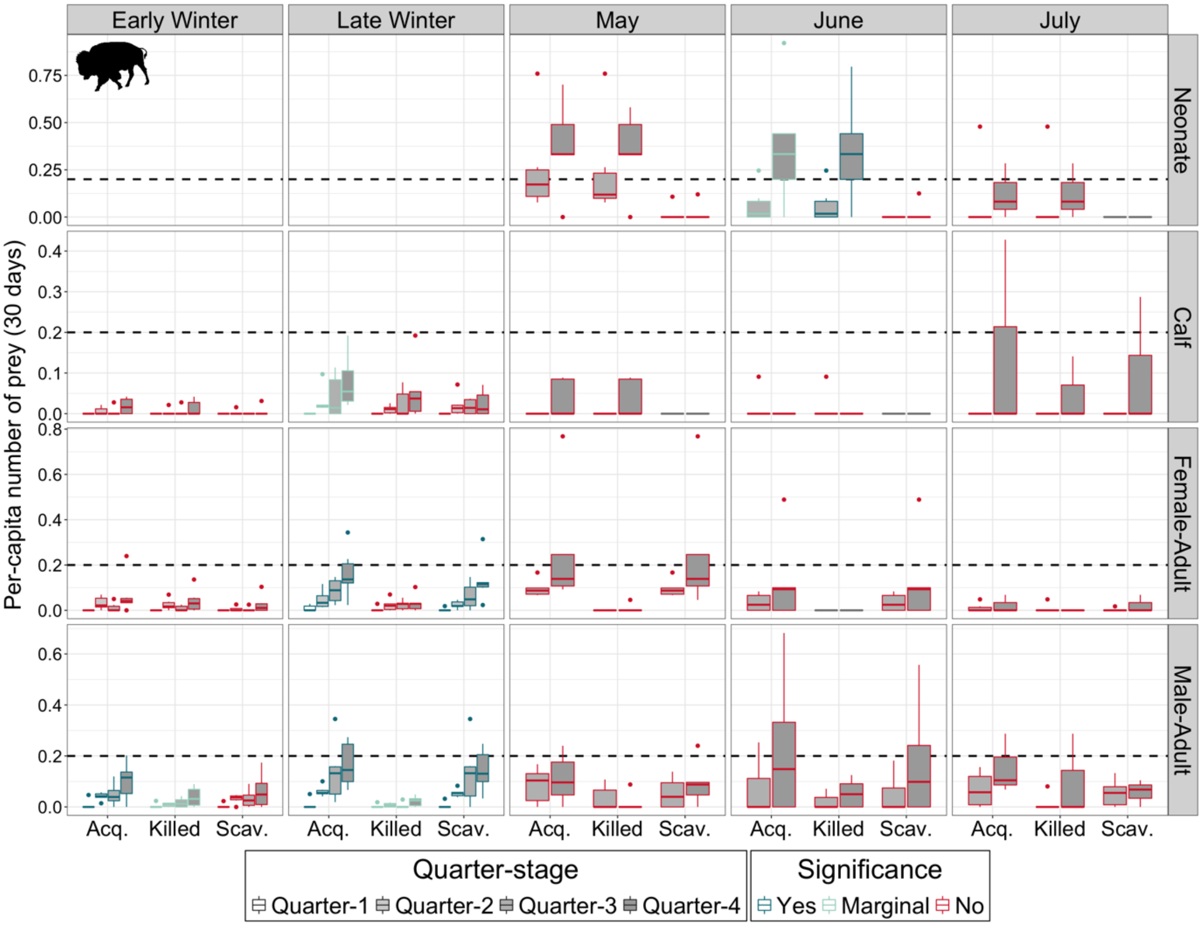

**Figure S4-E.35. Comparison of per-capita acquisition, kill, and scavenging rates (number-prey) for wolves on bison sex-age classes for all seasonal months across quarters in Northern YNP.** Dashed line is inserted at 0.2 in each panel to facilitate comparison. Data is the same as data presented in Fig. S4-E.36, except here is expressed in the number of prey. The meaning of all coloring is the same as Fig. 4-27.

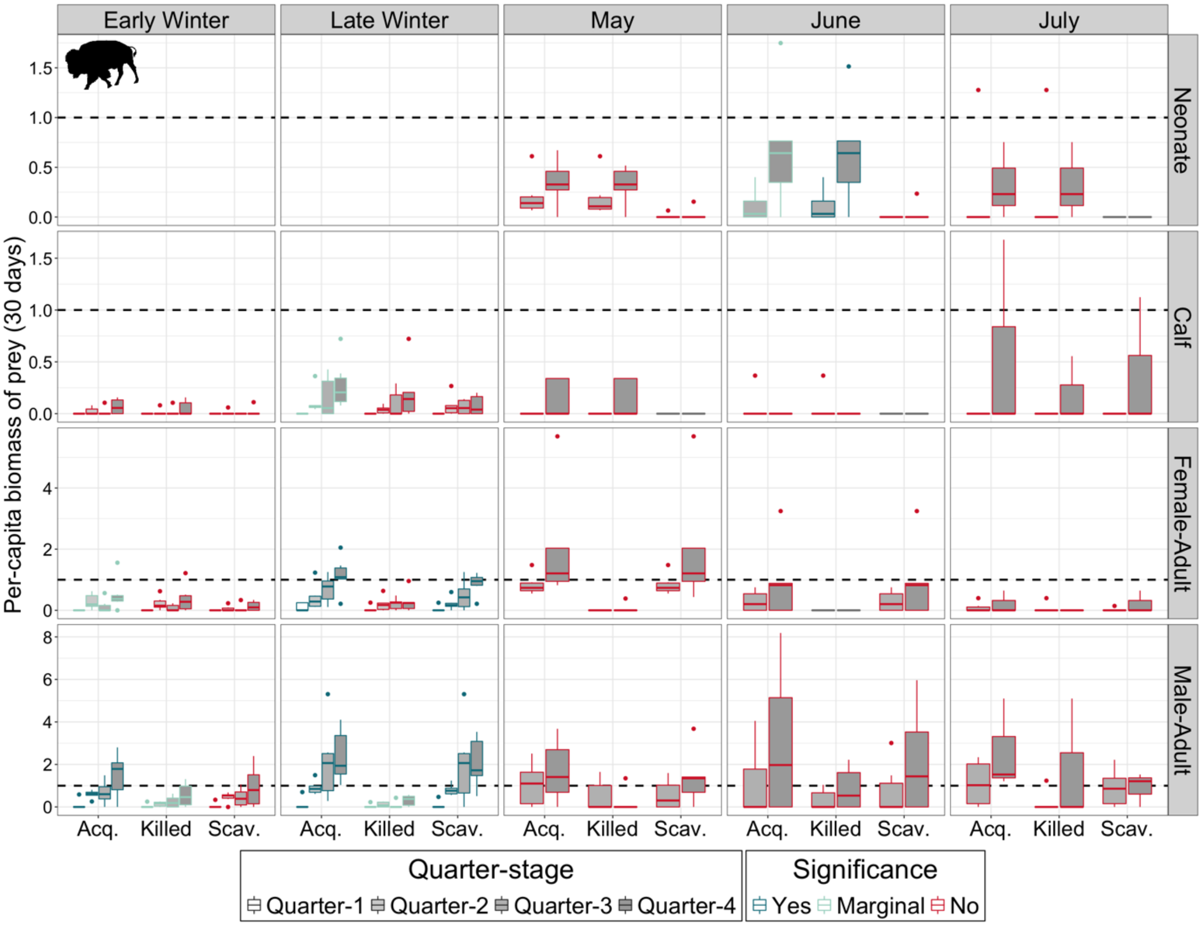

**Figure S4-E.36. Comparison of per-capita acquisition, kill, and scavenging rates (biomass-prey) for wolves on bison sex-age classes for all seasonal months across quarters in Northern YNP.** Dashed line is inserted at 1.0 in each panel to facilitate comparison. The winter season columns are the same as displayed in Fig. 4-34, and the meaning of all coloring is the same as Fig. 4-27.

## LITERATURE CITED

Beigy, M. 2019. cvcqv: Coefficient of variation (cv) with confidence intervals. R Package version 1.0.0.

## Chapter 5: Appendix S5-A. Supporting information for wolf-prey models.

**Table S5-A.1. AIC results obtained through the R package `AICcmodavg` (Mazerolle 2020) for functional response models fit to all-winter, population-level kill and scavenging rate estimates for Northern Yellowstone National Park (YNP) wolf packs.** Here, wolf packs were included only when they were deemed as 'strict' Northern YNP packs (i.e., 'Northern YNP' pack = Yes during the roaming period in Table 4-2). Fits of these models are displayed in Fig. S5-A.1.

| Species | Acquisition | Model | K | $AIC_c$ | $\Delta AIC_c$ | $w_i$ |
|---|---|---|---|---|---|---|
| Elk | Killed | Type II | 3 | 111.01 | 0.00 | 0.60 |
| Elk | Killed | Type III | 3 | 111.82 | 0.81 | 0.40 |
| Elk | Killed | Type I | 2 | 165.36 | 54.35 | 0.00 |
| Bison | Killed | Type I | 2 | 45.20 | 0.00 | 0.61 |
| Bison | Killed | Type II | 3 | 47.08 | 1.88 | 0.24 |
| Bison | Killed | Type III | 3 | 47.87 | 2.67 | 0.16 |
| Bison | Scavenged | Type I | 2 | 61.46 | 0.00 | 0.59 |
| Bison | Scavenged | Type II | 3 | 63.55 | 2.09 | 0.21 |
| Bison | Scavenged | Type III | 3 | 63.64 | 2.18 | 0.20 |

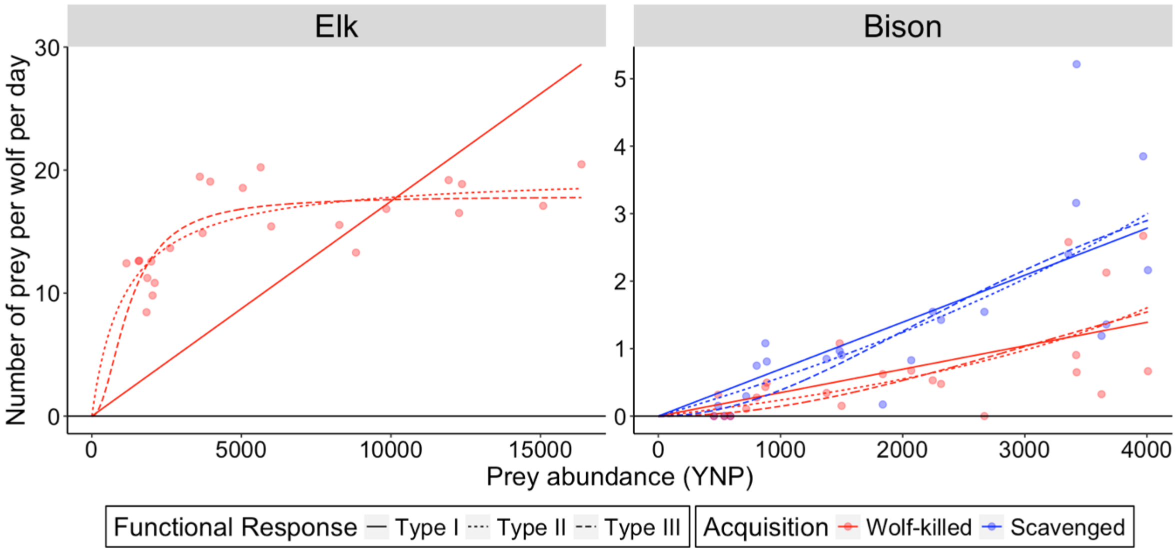

**Figure S5-A.1. Functional responses for wolf-killed elk, wolf-killed bison, and wolf-scavenged bison for 'strict' Northern YNP wolf packs.** The dotted lines for the Type II models were ultimately used as the motivation for the predator-prey models that we used to model wolf-prey dynamics. The type II model was the best supported for wolf-killed elk (Table S5-A.1), although the Type III model was also worthy of consideration (i.e., within 2 AIC units). Type II models were not the top-ranked model for wolf-bison relationships, but they described the rate that bison were killed or scavenged in the same general manner as the top-ranked Type I models over the range of bison abundances that were observed.

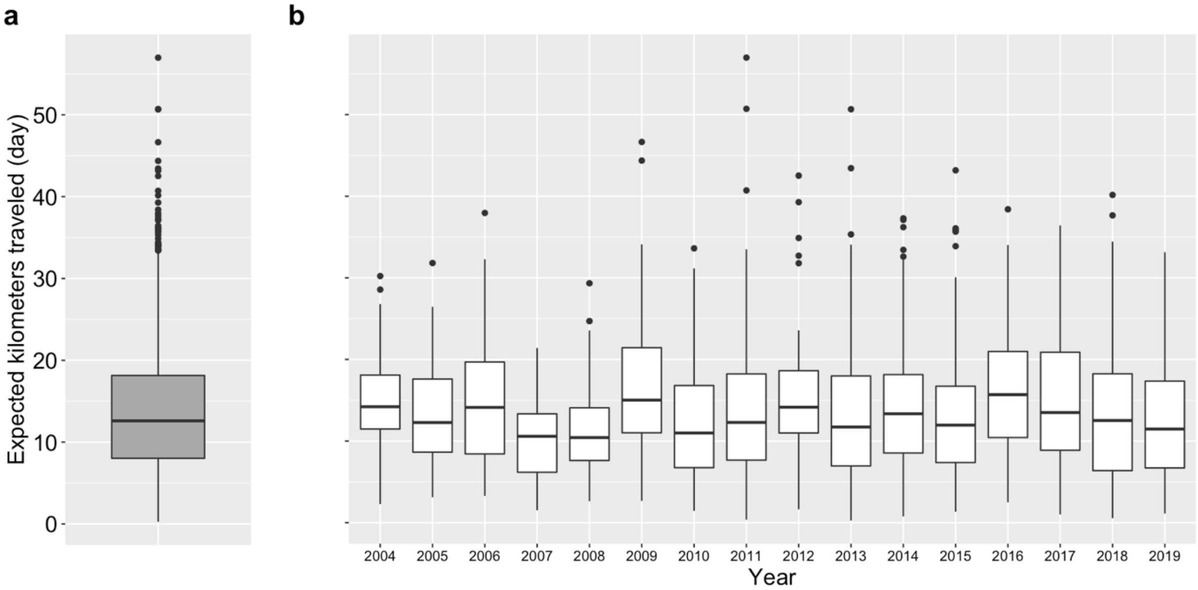

**Figure S5-A.2. Expected daily movement rate for GPS-collared wolves during winter across (a) all data and (b) annually.** The median value of 12.6 km displayed in panel (a) was the value that was used in functional response estimates; panel (b) is displayed only for context. Movement rate was estimated from 35 GPS-collared wolves during 90 unique 30-day sessions from 2004–2019. Data was censored to permit only one wolf in a pack during a 30-day session, randomly selecting an individual when necessary. Wolf days were censored if <66.67% of locations were successfully acquired. The 24-hour rate was calculated from the mean hourly movement rate of remaining locations, thereby filling in gaps from days when not all locations were acquired. For context, 80% of days acquired all 24 possible locations.

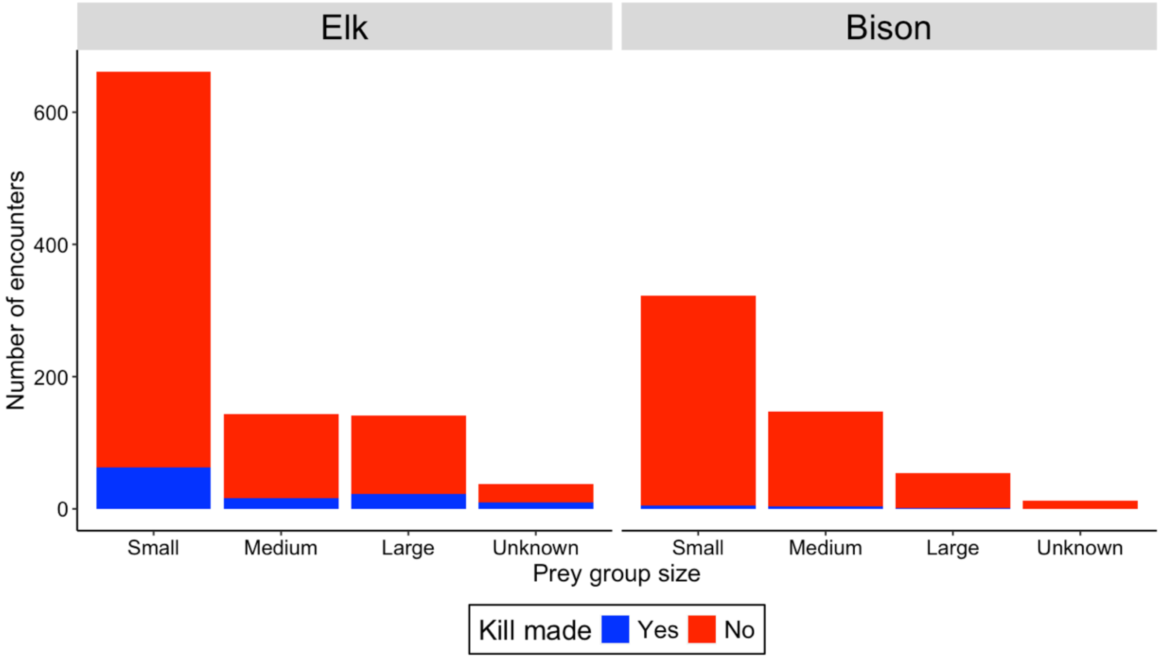

**Figure S5-A.3. Wolf-prey encounter data from Northern YNP, 2003–2021.** Groups are displayed here as small (1–10), medium (11–30), and large (>30) for display purposes but we used the associated raw data to estimate the per-capita risk of dying for an individual elk or bison. Data from 38 encounters for elk and 12 encounters for bison where group size was unknown were censored. We used data from throughout the year to maximize sample size, although 93% of observed encounters occurred between November and March. We estimated an overall per-capita risk of dying, which represented encounter success (*c*), by dividing the number of killed prey (*n* = 101 elk and n = *10* bison) by the total number of prey encountered (*n* = 19,247 elk and 7,776 bison) during 946 wolf-elk and 523 wolf-bison encounters. The resultant estimate for *c* was 0.00525 for elk and 0.00129 for bison.

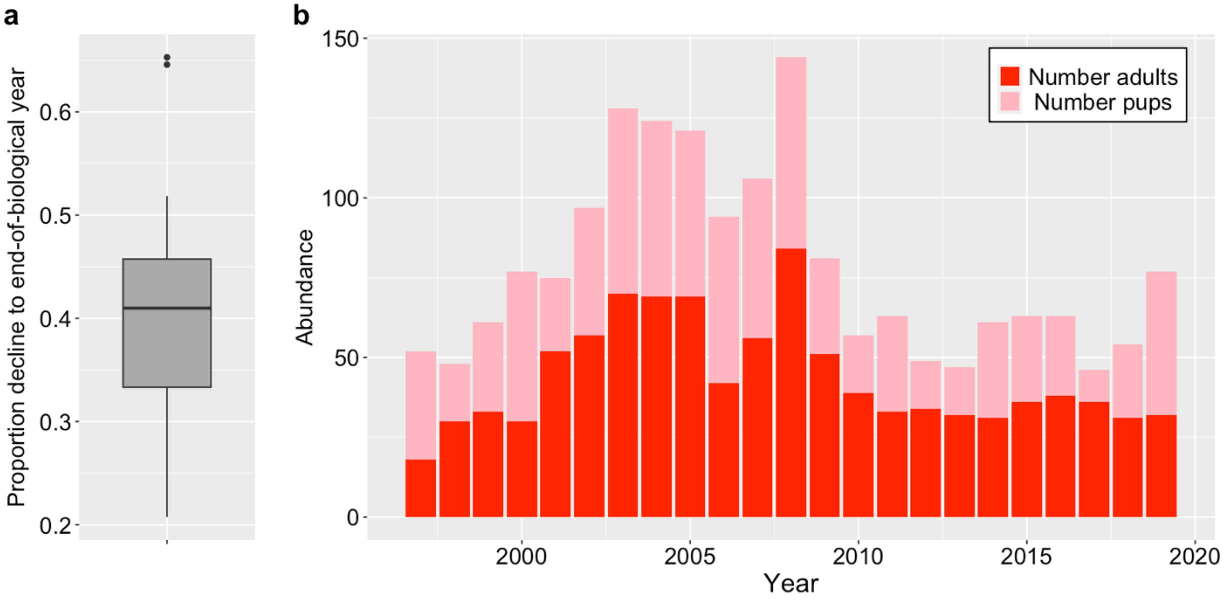

**Figure S5-A.4. Annual change in Northern YNP wolf abundance.** Panel (a) displays the proportional decline in the wolf population over the course of a wolf-year. This proportional decline was the result of changes in the wolf population displayed in panel (b). Panel (b) displays an annual abundance for wolves that is equal to the April 1 count for the number of wolves (i.e., any wolf present; red) and the number of newborn pups (pink) subsequently observed for that year. For all possible years, we estimated the proportional decline displayed in panel (a) as:

$$d_t = \frac{\left(W_t + W_{p_t}\right) - W_{t+1}}{W_t + W_{p_t}} \tag{1}$$

where $W_t$ represented red-filled wolves and $W_{p_t}$ represented pink-filled wolves.

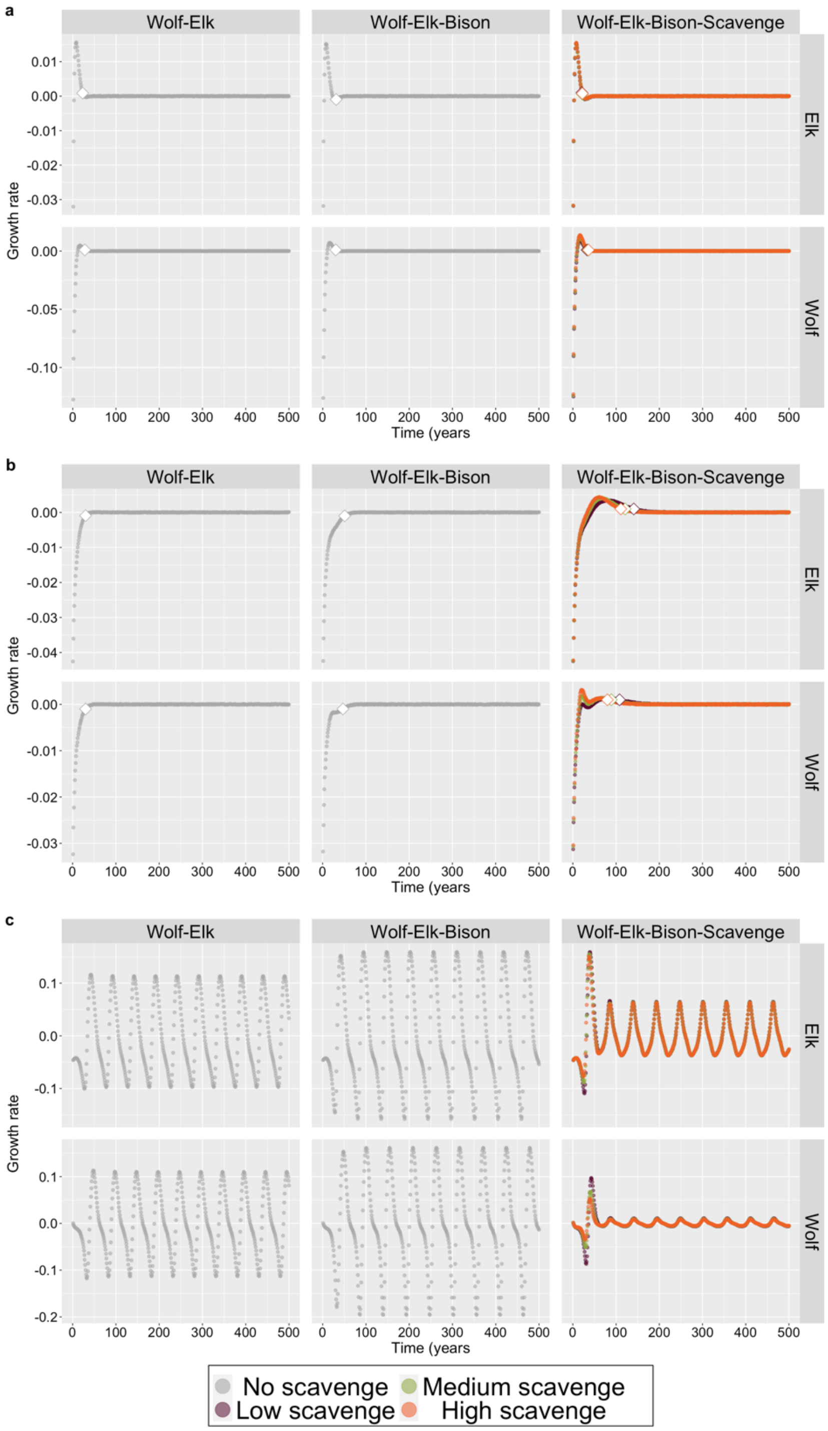

**Figure S5-A.5. Annual growth rate (*r*) over time for the wolf populations displayed in Figs. 5-5 and 5-6.** In all scenarios for populations that included scavenging (right-most column), the different colors display the associated dynamics. Diamonds display predicted stable equilibrium points where population growth rate (*r*) never again exceeded 0.001. Note the y-axis differs between panels a-c.

## LITERATURE CITED

Mazerolle, M. J. 2020. AICcmodavg: model selection and multimodel inference based on (Q) AIC (c). R package version 2.3-1.